

**Paleocene forests and climates of Antarctica: signals from
fossil wood**

Laura Jane Tilley

Submitted in accordance with the requirements for the degree of
Doctor of Philosophy

The University of Leeds
School of Earth and Environment

May 2016

The candidate confirms that the work submitted is his/her own and that appropriate credit has been given where reference has been made to the work of others.

This copy has been supplied on the understanding that it is copyright material and that no quotation from the thesis may be published without proper acknowledgement.

© 2016 The University of Leeds and Laura Jane Tilley

Acknowledgements

There are a number of people I would like to thank for their help and support during my PhD. My supervisors Jane Francis, Vanessa Bowman, Paul Wignall and Fiona Gill for their help and support especially during the last 2 years of my PhD. Thanks also to NERC for funding the PhD.

I would like to thank members of the PALEOPOLAR team: Jane Francis, Vanessa Bowman, Jon Ineson, James Witts, Rowan Whittle, Stuart Robinson, Jo Hall and Alistair Crame for their advice during annual research group meetings. In particular thank you to Jon Ineson for the sedimentary analysis and creating the sedimentary logs that are used in this project; it was a huge contribution that helped with interpretation of data obtained from the fossil wood.

I am grateful for the advice given by Roberto Pujana in the identification of wood. The Trans-Antarctic Association are thanked for the travel grant which enabled me to work with Roberto on Antarctic fossil wood housed at the Bernardino Rivadavia Natural Science Museum, Buenos Aires.

For technical support I would like to thank John Wyn Williams (Harri) for making excellent thin sections of the fossil wood specimens.

A special thank you to Gill Porter for giving support in writing this thesis.

To the best office mates and good friends that I have made during my time at Leeds: Tom, Rhian, James, Jo, Autumn, Ben, Edine, Ruza, Lauren. Thank you for the constant support, advice, encouragement and the good times outside work.

Finally and importantly I would to say thank you to my mum (Gyla Tilley) and brother (Alan Tilley) who have constantly supported me throughout my academic life and have encouraged me to keep going during the difficult times. Also thank you to my mum who has supported me financially during the last year, without this completion of the PhD would have been near impossible.

Abstract

During the green house world of the Paleocene, Antarctica was covered in extensive forests, even though the continent was situated over the South Pole. Fossil wood is abundant in the marine sequences of Seymour Island, Antarctica. Originating from forests that once grew on a volcanic arc now represented by the Antarctic Peninsula. This research presents a detailed study of the forests and climates of Antarctica primarily using a new assemblage of fossil wood and palynomorphs, directly tied to a sedimentary sequence (K/Pg boundary to Late Paleocene in age) on Seymour Island, which has allowed for a more rigorous interpretation of the composition and structure of the Antarctic Peninsula forests and the climates under which they grew. Tree types identified from fossil wood include: *Agathoxylon*, *Phyllocladoxylon*, *Protophyllocladoxylon*, *Podocarpoxyton/Cupressinoxyton*, *Nothofagoxyton*, *Weinmannioxyton*, *Myrceugenelloxyton* and *Antarctoxyton*. Their nearest living relatives (NLR) are found growing in warm to cool temperate Southern Hemisphere forests. Palynomorphs revealed diverse Podocarpaceae including *Lagarostrobus franklinii* (*Phyllocladidites mawsonii*) and shrubby angiosperm taxa such as Proteaceae, as well as ferns and mosses. Collective analysis of taxomomy, wood preservation, sedimentology and NLRs indicate that the lowland forests were similar to the cool temperate mixed *Nothofagus* forests of New Zealand and Thamnic/Implicate forests in Tasmania. Upland floras may have resembled *Araucaria* – *Nothofagus* woodlands found in cool temperate Chile today. Coexistence Analysis indicates marginally warm to cool temperate climates with sufficient rainfall for tree growth. Analysis of angiosperm anatomy suggests sufficient water availability. Mean growth ring analysis suggests a trend towards cooler climates from the Early to the Late Paleocene. However, the majority of trees suggest growth under a fluctuating climate. For the first time specific gravity (SG) has been calculated for fossil wood from Antarctica and has provided further insight into the ecology and growth conditions of the trees. Narrow values of SG (0.50 – 0.80) are indicative of a temperate climate in the Paleocene of Antarctica.

Table of Contents

Chapter 1 Introduction	1
1.1 Overview.....	1
1.2 Aims and objectives.....	3
1.3 Structure of this thesis.....	5
1.4 Paleocene climates.....	6
1.5 Forests of the Antarctic Peninsula.....	16
Chapter 2 Geological settings	21
2.1 Introduction.....	21
2.2 Geological evolution of the Antarctic Peninsula and the James Ross Basin.....	21
2.3 Geology of Seymour Island.....	26
2.4 The sedimentary sequence studied in this project.....	29
2.4.1 Sedimentology analysis.....	30
2.4.2 Age of the sedimentary section.....	35
2.5 Fossilwood.....	36
2.5.1 Depositional history of the fossil wood specimens.....	41
2.6 Summary.....	48
Chapter 3 Conifer wood	49
3.1 Introduction.....	49
3.2 Conifer wood anatomy and identification.....	49
3.3 Quantitative analysis of anatomical features of fossil conifer wood taxa identified in this project.....	56
3.4 Description of fossil conifer wood studied in this project.....	62
3.4.1 <i>Agathoxylon</i>	62
3.4.1.1 Description.....	62
3.4.1.2 Discussion.....	68

3.4.1.3 Comparison with other fossil wood of <i>Agathoxylon/Araucarioxylon</i>	70
3.4.1.4 Comparison with extant wood.....	72
3.4.1.5 Ecology of modern Araucariaceae.....	72
3.4.2 <i>Phyllocladoxylon</i>	73
3.4.2.1 Description.....	73
3.4.2.2 Discussion.....	78
3.4.2.3 Comparison with other fossil woods of <i>Phyllocladoxylon</i>	78
3.4.2.4 Comparison with extant wood.....	79
3.4.2.5 Ecology of <i>Phyllocladus</i>	79
3.4.3 <i>Protophyllocladoxylon</i>	80
3.4.3.1 Description.....	80
3.4.3.2 Discussion.....	85
3.4.3.3 Comparison with other fossil woods of <i>Protophyllocladoxylon</i>	86
3.4.3.4 Comparison with extant wood.....	87
3.4.4 <i>Podocarpoxyton</i>	87
3.4.4.1 Description.....	88
3.4.4.2 Discussion.....	90
3.4.4.3 Comparison with other fossil wood of <i>Podocarpoxyton</i>	90
3.4.4.4 Comparison with extant wood.....	90
3.4.4.5 Ecology of Podocarpaceae.....	91
3.4.5 Unidentified conifer wood.....	93
3.5 Summary.....	93

Chapter 4	95
4.1 Introduction.....	95
4.2 Wood anatomy and identification.....	95
4.3 Description of fossil angiosperm wood studied in this project.....	99
4.3.1 <i>Nothofagoxylon</i>	99
4.3.1.1 Description.....	99
4.3.1.2 Discussion.....	110
4.3.1.3 Comparison with other <i>Nothofagoxylon</i> wood.....	111
4.3.1.4 Comparison with modern <i>Nothofagus</i>	112
4.3.1.5 Ecology of modern <i>Nothofagus</i>	112
4.3.2 <i>Weinmannioxylon</i>	115
4.3.2.1 Description.....	115
4.3.2.2 Discussion.....	119
4.3.2.3 Comparison with other fossil wood of <i>Weinmannioxylon</i>	120
4.3.2.4 Ecology of modern <i>Weinmannia</i>	120
4.3.3 <i>Myrceugenelloxylon</i>	122
4.3.3.1 Description.....	122
4.3.3.2 Discussion.....	126
4.3.3.3 Comparison with other fossil wood of <i>Myrceugenelloxylon</i>	126
4.3.3.4 Comparison with extant wood.....	127
4.3.3.5 Modern ecology of <i>Luma</i>	127
4.3.4 <i>Antarctoxylon</i>	128
4.3.4.1 Description.....	128
4.3.4.2 Discussion.....	129
4.3.4.3 Comparison to other fossil wood of <i>Antarctoxylon</i>	130

4.3.4.4 Comparison to extant wood.....	131
4.4 Summary.....	131
Chapter 5	133
5.1 Introduction.....	133
5.2 Palynology.....	133
5.2.1 Methods.....	134
5.2.2 Results.....	135
5.2.2.1 Palynomorphs present through the stratigraphic section.....	142
5.3 Structure and composition of forests from fossil wood.....	145
5.3.1 Abundance of tree types.....	145
5.3.2 Structure and composition of the forest.....	155
5.4 Discussion on the composition and structure of forests and ecology of the trees.....	159
5.4.1 Comparison between fossil wood and palynomorph records.....	159
5.4.2 Palaeoecology of the Antarctic forests.....	161
Chapter 6	167
6.1 Introduction.....	167
6.2 Introduction to palaeoclimate analysis and techniques.....	167
6.2.1 Growth ring analysis.....	167
6.2.2 Palaeoclimate information from fossil angiosperm woods.....	171
6.2.3 Palaeoclimate analysis using Nearest Living Relative (NLR).....	176
6.2.4 Specific gravity of the conifers and angiosperms.....	178
6.3 Methods used in this project.....	181
6.3.1 Growth ring analysis.....	181
6.3.2 Palaeoclimate information from fossil angiosperm woods.....	183

6.3.3 Palaeoclimate analysis using Nearest Living Relative.....	184
6.3.3.1 Coexistence Analysis.....	184
6.3.3.2 Frost tolerance of NLRs growing on the Antarctic Peninsula.....	186
6.3.4 Specific gravity of the conifer and angiosperms.....	186
6.4 Results.....	187
6.4.1 Growth ring analysis.....	187
6.4.1.1 Mean growth ring width.....	194
6.4.1.2 Mean Sensitivity (MS).....	201
6.4.2 Growth ring discussion.....	205
6.4.3 Palaeoclimate information from fossil angiosperm woods.....	214
6.4.3.1 Vulnerability Index (VI) and Mesomorphy Index.....	220
6.4.4 Discussion-Palaeoclimate information from fossil angiosperm wood.....	226
6.4.5 Palaeoclimate analysis using nearest living relative (NLR).....	229
6.4.5.1 Coexistence Analysis.....	229
6.4.6 Discussion – Coexistence analysis.....	238
6.4.6.1 Frost tolerance of NLRs growing on the Antarctic Peninsula.....	241
6.4.7 Specific gravity of the conifer and angiosperms.....	244
6.5 Overall discussion/summary.....	250
Chapter 7 Discussion.....	253
7.1 Introduction.....	253
7.2 Paleocene forests of Antarctica.....	253
7.3 Comparison to published records.....	258
7.3.1 Macro-floral record (wood and leaves).....	258
7.3.2 Micro-flora (palynological record).....	263

7.3.3 Comparison with other Paleocene forests in the Southern Hemisphere.....	266
7.4 Comparison with modern Southern Hemisphere forests.....	267
7.4.1 Tasmanian forests.....	267
7.4.2 New Zealand forests.....	270
7.4.3 Forests of Chile.....	272
7.4.4 Antarctic forests compared to modern analogues.....	273
7.5 Climate of the Antarctic Peninsula during the Paleocene.....	279
Chapter 8	293
List of references	299
Appendix A Wood specimens	324
Appendix B Wood anatomy measurements	337
Appendix B.1 Conifer wood anatomy measurements.....	337
Appendix B.2 Angiosperm wood anatomy.....	391
Appendix C Climate data from wood	414

List of Figures

Chapter 1

Figure 1.1. Location maps.....	3
Figure 1.2. CO ₂ trend through the Cenozoic.....	6
Figure 1.3. Paleocene climate zones.....	7
Figure 1.4. Global benthic oxygen and carbon isotope records derived from foraminifera from the Cretaceous to present day.....	9
Figure 1.5. Climate curve compilation for the Antarctic Peninsula.....	11
Figure 1.6. Average mean growth ring width from conifer wood from Jurassic to Eocene strata on Antarctica.....	12
Figure 1.7. Abundances of selected pollen and spore taxa from the Maastrichtian to earliest Danian from Seymour Island.....	13
Figure 1.8. Palaeotemperature data through the Late Cretaceous to the Paleocene/Eocene boundary from multiple proxies.....	14
Figure 1.9. Summary of the Cretaceous and Early Paleogene stratigraphic units from the Antarctic Peninsula.....	16
Figure 1.10. Valdivian model for Eocene flora growing in high altitude areas close to the volcanic centres on the Antarctic Peninsula to lowland distal floras.....	19

Chapter 2

Figure 2.1. Palaeogeographic map showing the early stages of rifting between west and east Gondwana during the Late Jurassic.....	22
Figure 2.2. The extent of the Larsen Basin on the eastern side of the Antarctic Peninsula.....	23
Figure 2.3. The main stages in the geological evolution of the Antarctic Peninsula and the Larsen Basin.....	25
Figure 2.4. Geological map of Seymour Island.....	29
Figure 2.5. The sedimentary sequence studied in this project.....	32

Figure 2.6. The sedimentary sequence of the Cross Valley Formation studied in this project.....	33
Figure 2.7. The age model for the sedimentary sequence studied in this project.....	38
Figure 2.8. Field photos of the geology of Seymour Island and fossil wood in the field, on Seymour Island.....	39
Figure 2.9. Location of the wood specimens studied in this project on the sedimentary sequence.....	40
Figure 2.10. Varieties of wood preservation.....	43
Figure 2.11. Wood preservation variety seen in thin section.....	44
Figure 2.12. The types of preservation observed in the wood specimens throughout the sedimentary sequence.....	48
Chapter 3	
Figure 3.1. The three dimensional structure of conifer wood.....	50
Figure 3.2. Plate showing different types of tracheid and cross-field pitting defined by the IAWA Committee (2004) and Philippe and Bamford (2008).....	53
Figure 3.3. The distribution of conifer taxa when quantitative anatomical features are plotted against each other.....	55
Figure 3.4. Identification of conifer wood taxa based on quantification of anatomical features: mean ray height and percentage of touching tracheid pits.....	58
Figure 3.5. Identification of conifer wood taxa based on quantification of anatomical features: mean number of pits per cross-field and percentage of uniseriate pitting.....	59
Figure 3.6. Identification of conifer wood taxa based on quantification of anatomical features: percentage of uniseriate tracheid pitting and percentage of touching tracheid pits.....	60
Figure 3.7. Identification of conifer wood taxa based on quantification of anatomical features: mean number of pits per cross-field and mean ray height.....	61

Figure 3.8. <i>Agathoxylon</i>	64
Figure 3.9. <i>Agathoxylon</i>	65
Figure 3.10. <i>Araucaria araucana</i> tree near volcano Lanin, Chile.....	73
Figure 3.11. <i>Phyllocladoxylon</i>	75
Figure 3.12. <i>Phyllocladus alpinus</i>	80
Figure 3.13. <i>Protophyllocladoxylon</i>	82
Figure 3.14. <i>Podocarpoxyton</i>	89
Figure 3.15. Podocarp-broad-leaved forest in New Zealand.....	92
Figure 3.16. Abundance of the four conifer wood morphotypes identified in this study.....	94
Chapter 4	
Figure 4.1. The three dimensional structure of angiosperm wood.....	96
Figure 4.2. Main anatomical features of angiosperm wood.....	98
Figure 4.3. <i>Nothofagoxyton</i>	101
Figure 4.4. <i>Araucaria araucana</i> - <i>Nothofagus pumilio</i> open forest.....	114
Figure 4.5. <i>Nothofagus</i> forest in New Zealand.....	114
Figure 4.6. <i>Weinmannioxylon</i>	117
Figure 4.7. a) <i>Weinmannia racemose</i> in New Zealand. b) <i>Weinmannia trichosperma</i> in Chile.....	122
Figure 4.8. <i>Myrceugenelloxyton</i>	124
Figure 4.9. <i>Luma apiculata</i> tree.....	128
Figure 4.10. <i>Antarctoxyton</i>	130
Figure 4.11. Abundance of four angiosperm wood morphotypes identified in this study.....	132
Chapter 5	
Figure 5.1. Location of palynology samples on the sedimentary sequence.....	134
Figure 5.2. Pollen and spore types identified.....	135
Figure 5.3. Pollen and spore types identified.....	137

Figure 5.4. Distribution of conifer morphotypes on the sedimentary sequence.....	156
Figure 5.5. Distribution of angiosperm morphotypes on the sedimentary sequence.....	158
Chapter 6	
Figure 6.1. The relationship between mean growth ring width (MGRW) and mean annual rainfall (MAR) from a global dataset.....	169
Figure 6.2. The relationship between mean growth ring width (MGRW) and mean annual temperature (MAT) from a global dataset...	169
Figure 6.3. This diagram illustrates that tree growth becomes more sensitive to climatic factors from the forest interior to the forest border.	170
Figure 6.4. Anatomical features related to climate.....	175
Figure 6.5. An example of Coexistent Analysis.....	177
Figure 6.6. An example of how specific gravity is measured in fossil wood using the method developed by Wheeler <i>et al.</i> (2007a).....	180
Figure 6.7. The relationships between conifer mean sensitivity (MS) and climate from a global data.....	182
Figure 6.8. The relationship between angiosperm mean sensitivity (MS) and climate from a global dataset.....	183
Figure 6.9. Wood specimens with false rings.....	188
Figure 6.10. A plot of mean growth ring values for individual wood specimens through the sedimentary sequence on Seymour Island.....	196
Figure 6.11. Mean growth ring width of all conifer wood specimens, all angiosperm wood specimens and each morphotypes separately presented in the form of a bar chart.....	197
Figure 6.12. Individual bar charts presenting the MGRW in each formation of the sedimentary sequence for each morphotype.....	198
Figure 6.13. A bar chart of mean growth ring width taken from the wood specimens in the López de Bertodano, lower to middle Sobral Formation, upper Sobral Formation and Cross Valley Formation.....	199

Figure 6.14. A plot of mean growth ring width taken from the wood specimens in the López de Bertodano Formation, lower to middle Sobral Formation, upper Sobral Formation and Cross Valley.....	200
Figure 6.15. A plot of mean sensitivity data against the stratigraphic section on Seymour Island.....	203
Figure 6.16. Frequency (%) of wood specimens showing complacent and sensitive growth for each formation in the sedimentary sequence on Seymour Island.....	204
Figure 6.17. Average mean sensitivity for all the wood specimens within each formation on the sedimentary sequence of Seymour Island.....	204
Figure 6.18. The frequency (%) of wood specimens within each morphotype showing complacent or sensitive growth.....	205
Figure 6.19. Histograms presenting the frequency (%) of anatomical features that are related to climate and environmental conditions in the angiosperm wood specimens presented in Table 6.4.....	219
Figure 6.20. A plot of VI values for the individual wood specimens from the upper López de Bertodano Formation (K/Pg to Early Paleocene) and through the Sobral Formation (Early to Late Paleocene).....	221
Figure 6.21. A plot of MI values for individual wood specimens from the upper López de Bertodano Formation (K/Pg to Early Paleocene) and through the Sobral Formation (Early to Late Paleocene.....	222
Figure 6.22. MAT ranges for modern nearest living relatives of the fossil plants identified in this project.....	230
Figure 6.23. WMMT tolerances for modern Nearest Living Relatives of the fossil plants identified in this project.....	231
Figure 6.24. CMMT tolerances for modern nearest living relatives of the fossil plants identified in this project.....	231
Figure 6.25. MAP tolerances for modern Nearest Living Relatives of the fossil plants identified in this project.....	232

Figure 6.26. MPWM tolerances for modern Nearest Living Relatives of the fossil flora identified in this project.....	233
Figure 6.27. MPDM tolerances for modern Nearest Living Relatives of the fossil plants identified in this project.....	233
Figure 6.28. Summary of temperature (MAT, CMMT, WMMT) and precipitation (MAP, MPDM, MPWM) tolerances of modern Nearest Living Relatives of fossil plants identified in this project.....	238
Figure 6.29. The MAT and MAP ranges inferred for the Antarctic Peninsula during the Paleocen from the Coexistence Analysis study carried out in this project, plotted on to Holdridge's life zone classification system.....	240
Figure 6.30. Frost tolerances for the NLRs of the main fossil taxa identified in this project.....	243
Figure 6.31. Bars charts showing the range of specific gravity for wood specimens within each morphotype present in the study.....	248
Figure 6.32. A plot of specific gravity values for individual wood specimens from through the López de Bertodano Formation (K/Pg to Early Paleocene), Sobral Formation (Early to Late Paleocene) and Cross Valley (Late Paleocene).....	249
Chapter 7	
Figure 7.1. Reconstruction of the Antarctic Peninsula forests during the Maastrichtian (Late Cretaceous).....	257
Figure 7.2. Abundance of conifer genera identified through the Cretaceous and Early Paleocene from Cantrill and Poole (2005).....	259
Figure 7.3. Abundance of angiosperm genera identified through the Cretaceous and early Paleocene from Cantrill and Poole (2005).....	260
Figure 7.4. Alpine heathland of Tasmania, which consists of low lying shrubs.....	270
Figure 7.5. Mixed <i>Nothofagus</i> forests, New Zealand.....	272

Figure 7.6. Lowland Valdivian forest, Chile.....	274
Figure 7.7. Mixed <i>Nothofagus</i> forests in Chile. Open canopy consisting of large <i>Nothofagus dombeyi</i> trees.....	275
Figure 7.8. <i>Araucaria-Nothofagus</i> open woodland. <i>Araucaria araucana</i> trees projecting above a canopy of stunted <i>Nothofagus</i> trees.....	276
Figure 7.9. Results from Francis and Poole (2002) of average mean growth ring width (conifers and angiosperms) for each stratigraphic formation from the Maastrichtian (Cretaceous) to the Eocene in the Antarctic Peninsula region. Average mean growth ring width from this study is also presented.....	284
Figure 7.10. Palaeotemperature estimates derived from different proxies and sources for the Late Cretaceous to the Paleocene/Eocene boundary. Yellow squares represent the estimates of Kemp et al. (2014) based on MBT/CBT proxies.....	288
Figure 7.11. Model output of Early Paleogene latitudinal temperature curves for land and ocean (mean annual temperature and sea surface temperatures under three different CO ₂ scenarios.....	290
Figure 7.12. Model outputs of latitudinal temperature gradients over land showing winter temperatures in the Southern Hemisphere for three different CO ₂ scenarios.....	291
Figure 7.13. Mean annual temperature latitudinal gradients over land for 4 scenarios.....	292

List of Tables

Chapter 3

Table 3.1. List of conifer wood features and their definitions used in this thesis.....	51
Table 3.2. Summary of the anatomical characters of <i>Agathoxylon</i> wood identified in this project.....	66
Table 3.3. Summary of the anatomical characters of <i>Agathoxylon</i> wood identified in this project.....	67
Table 3.4. Summary of the anatomical characters of <i>Phyllocladoxylon</i> wood identified in this project.....	76
Table 3.5. Summary of the anatomical characters of <i>Phyllocladoxylon</i> wood identified in this project.....	77
Table 3.6. Summary of the anatomical characters of <i>Protophyllocladoxylon</i> wood identified in this project.....	83
Table 3.7. Summary of the anatomical characters of <i>Protophyllocladoxylon</i> wood identified in this project.....	84

Chapter 4

Table 4.1. A list of angiosperm features with definitions.....	97
Table 4.2. Summary of the anatomical characters of <i>Nothofagoxylon</i> wood (Species A) identified in this project.....	102
Table 4.3. Summary of the anatomical characters of <i>Nothofagoxylon</i> wood (Species A, B) identified in this project.....	104
Table 4.4. Summary of the anatomical characters of <i>Nothofagoxylon</i> wood (Species B) identified in this project.....	106
Table 4.5. Summary of the Anatomical characters of <i>Nothofagoxylon</i> wood (Species C and D) in this project.....	108
Table 4.6. Summary of anatomical characters of <i>Weinmannioxylon</i> wood identified in this project.....	118
Table 4.7. Summary of the anatomical characters of <i>Myrceugenelloxylon</i> wood identification in this project.....	125

Chapter 5

Table 5.1. Palynomorphs present in each palynology sample analysed and its position on the stratigraphic section.....	139
Table 5.2. Palynomorphs identified in this project, their nearest living relative and the ecology of that modern relative.....	147

Chapter 6

Table 6.1. Mean growth ring width (MGRW), mean sensitivity (MS) and standard deviation for 30 fossil wood specimens identified in this project.....	189
Table 6.2. Fossil wood specimens with false rings.....	193
Table 6.3. Average MGRW for each formation.....	199
Table 6.4. The occurrence of quantitative and qualitative anatomical features that are related to climate in the fossil angiosperm wood specimens in this study.....	216
Table 6.5. VI and MI results for 17 angiosperm wood specimens in this project.....	223
Table 6.6. The MAT, CMMT, MAP, MPDM and MPWM tolerances for the NLRs of the fossil flora identified in this project.....	235
Table 6.7. Summary of temperature and precipitation tolerances of modern Nearest Living Relatives of the fossil plants using Coexistence Analysis.....	241
Table 6.8. Frost tolerance of taxa that are found in Chile, Tasmania and New Zealand.....	242
Table 6.9. Specific gravity (SG) data measured from the fossil wood specimens.....	246

Chapter 7

Table 7.1. The main tree types found in the Antarctic forests and their presence in the modern temperate forests of Tasmania, New Zealand and southern South America.....	279
--	-----

Table 7.2. Results for the Coexistence Analysis undertaken by Poole *et al.* (2005) and this study for mean annual temperature (MAT), cold month mean temperature (CMMT), warm month mean temperature (WMMT), mean annual precipitation (MAP), mean precipitation dry month (MPDM), mean precipitation wet month (MPWM)..... 282

Table 7.3. The average mean growth ring widths (MGRW) calculated for the, Snow Hill Island, López de Bertodano Formation, Sobral Formation, Cross Valley, Formation and La Meseta Formation by Francis and Poole (2002). The average MGRW calculated for the López de Bertodano, Sobral (lower to middle and upper) and Cross Valley formations..... 285

Chapter 1

Introduction

1.1 Overview

The Paleocene epoch 66 – 56Ma (Gradstein *et al.*, 2012), the focus of the thesis, is considered to have been a greenhouse world (Zachos *et al.*, 2008). During this time the location of the Antarctic continent was similar to present day (Lawver *et al.*, 1992), situated in its current position over the South Pole; however, the continent was still attached to Australia by the South Tasman Rise, and South America by land masses (Lawver *et al.*, 1992). The Antarctic Circumpolar Current that flows around Antarctica today was not fully developed until the Miocene.

The southern polar regions had no or possibly only small ice caps (Miller *et al.*, 2005) but instead they were covered in extensive vegetation (Cantrill and Poole, 2012). From the Mesozoic to the early Paleogene the Antarctic Peninsula (palaeolatitude 65°S during the Paleocene, Lawver *et al.*, 1992) (Figure 1.1) was an active volcanic arc (Hathway, 2000) and was covered in temperate forests that resembled the cool and warm temperate forests of Australia, New Zealand and South America today (Cantrill and Poole, 2012). Today the remains of these Antarctic forests are present as fossil pollen, leaves and wood which are found on the islands that surround the Antarctic Peninsula (e.g. Seymour Island, James Ross Island, Alexander Island and King George Island) (see Figure 1.1) (Poole and Cantrill, 2012).

Previous research on the Cretaceous and early Paleogene fossil flora of Antarctica has helped to gain insight into the composition of these high latitude forests and also the climate under which they grew (e.g. Askin, 1988; 1989; 1990; 1992; Francis, 1986; Falcon-Lang and Cantrill, 2000; Falcon-Lang *et al.*, 2001; Poole *et al.*, 2001; Francis and Poole, 2002; Poole *et al.*, 2003; Eklund, 2003; Eklund *et al.*, 2004; Cantrill and Poole, 2005; Poole *et*

al., 2005; Poole and Cantrill, 2006; Tosolini *et al.*, 2013; Pujana *et al.*, 2014; Bowman *et al.*, 2014 ; Pujana *et al.*, 2015).

In particular, fossil wood has been a useful resource for reconstructing Antarctic forest composition and observing past climate records stored within its growth rings and cell anatomy.

Published research on using wood to reconstruct forest composition and paleoecology has mainly focused on the Cretaceous Period and Eocene Epoch (for example, Falcon-Lang and Cantrill, 2000; Falcon *et al.*, 2001; Poole *et al.*, 2001, Pujana *et al.*, 2014,). Less work has been done on reconstructing forest of Paleocene age from fossil wood. Poole *et al.*(2003) identified a small collection of Paleocene age wood from Seymour Island and suggested that the forest composition were similar to modern Valdivian forests (described in more detail in section 1.5). Francis (1986), Francis and Poole (2002), Poole *et al.* (2005) have used growth rings and cell anatomy of wood to reconstruct the terrestrial climates of Antarctica during the Cretaceous to the Eocene (described in more detail in section 1.4).

The research project presented here is a part of a larger NERC project called PALEOPOLAR, being part of the Co-Evolution of Life and the Planet programme, to investigate high latitude environments during the latest Cretaceous and Paleogene and the response to end Cretaceous events.

The project focused on Late Cretaceous to Eocene marine sequences on Seymour Island, which is situated on the north-eastern tip of the James Ross Basin (Figure 1.1). The strata there contain abundant and exceptionally preserved fossils.

Fossil wood was collected by Jane Francis in 2010 from Seymour Island along a measured stratigraphic section that included the latest Cretaceous (including the K/Pg) to Late Paleocene strata. The exact location of the wood was recorded on the sections to allow taxonomic and climate data derived from the wood to be placed in a detailed stratigraphic context for the first time. This had never been done with previous fossil wood collections from this sequence.

The Paleocene Epoch is an interesting time to study as it occurs immediately after the Cretaceous-Paleocene mass extinction (K/Pg) and thus it is important in terms of investigating the recovery of biodiversity after the K/Pg event. It was also a time of fluctuating climate because the end of the Paleocene was marked by a rapid warming event called the Paleocene-Eocene Thermal Maximum (Zachos *et al.*, 2001). A modernisation of plants occurred during the Paleocene (Cantrill and Poole, 2012), which means that comparisons can be made with modern analogues.

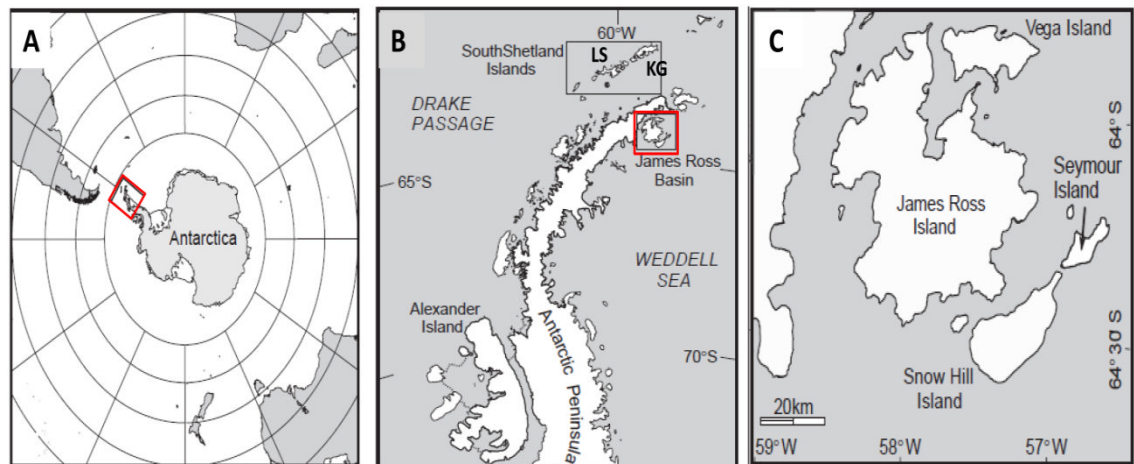


Figure 1. 1. Location maps of: a) The Antarctic Peninsula, outlined by a red box, b) Eastern islands surrounding the main land of the Antarctic Peninsula. Seymour Island is situated within the red square, c) Seymour Island. LS = Livingston Island and KG = King George Island. Modified from Poole *et al.* (2005).

1.2 Aims and objectives

The aim of this project was to reconstruct Paleocene forests and climates of the Antarctic Peninsula in order to understand how vegetation and climate evolved at high southern latitudes through this time period.

The objectives included:

Investigation of cell anatomy of fossil wood to:

- Identify wood types and reconstruct the composition of the Antarctic forests and their evolution over time.

- Reconstruct the climate in which the Antarctic forests grew using fossil wood.

In addition, palynomorph samples were investigated to gain further insight into forest composition with regards to non-woody plants.

Key questions that this research aims to answer:

- What was the composition of the forests that lived on the Antarctic Peninsula during the Paleocene and how did vegetation evolve through this Epoch?
- What is the climate record stored in the wood and how does that climate record correspond to other proxy records of Paleocene climates?
- How did the vegetation on land respond to fluctuating climates of the Paleocene?

All observations will allow a more detailed insight into the Antarctic forests than has been done before.

Seymour Island holds one of the highest latitude sedimentary records with abundant wood of latest Cretaceous and early Paleogene age and thus is an important location for understanding how polar regions responded to past greenhouse worlds, and how southern latitude vegetation might respond to future global warming.

This research also contributes to the accuracy of vegetation types represented in computer climate models. Previous research on modelling past greenhouse climates such as the Cretaceous and Eocene has outlined the importance of global vegetation type and distribution in reproducing low latitudinal temperature gradients which have been indicated from geological records. Otto-Bliesner and Upchurch (1997) examined the effects of adding vegetation to a climate model compared to a model where the landmasses were covered in bare soil and they found that global temperatures increased by 2.2°C and 4.1°C. High latitude vegetation has been found to be important in absorbing solar radiation and thus reducing the formation of ice (Upchurch *et al.*, 1998; Loptson *et al.*, 2014). Also, adding vegetation to models affects

climate sensitivity to increasing $p\text{CO}_2$ (temperature increasing, with doubling $p\text{CO}_2$) (Loftson *et al.* 2014).

1.3 Structure of this thesis

Chapter 1 presents an overview of the project and its aims and objectives. It also introduces climates of the Paleocene and the forests of the Antarctic Peninsula, which concerns the evolution of the forests from the Cretaceous to the Eocene and processes that controlled their floral composition.

The geological setting of the study area is presented in **Chapter 2** and includes information about the geological evolution of the eastern side of the Antarctic Peninsula, the geology of Seymour Island and the stratigraphy. A detailed description of the composition and depositional environment of sedimentary sequences studied in this project, as well as the age model. The location of the fossil wood specimens in the sedimentary section are presented and their preservation (e.g. permineralisation, size and shape) and from this their likely depositional history is discussed.

Chapter 3 presents the identification of the fossil conifer wood morphotypes studied and their nearest living relatives (NLRs) and **Chapter 4** presents the fossil angiosperm wood morphotypes identified and their NLRs.

Chapter 5 discusses the likely palaeoecology of the trees and forests growing on the Antarctic Peninsula from the NLRs of fossil wood types, information from the sedimentary sequence and their preservation. Palynology analyses were undertaken in this project to gain further insight into the flora of the Antarctic Peninsula with regards to non-woody plants.

Palaeoclimate reconstruction from the K/Pg boundary to the Late Paleocene using fossil wood is presented in **Chapter 6** using techniques such as growth ring analysis, palaeoclimate information from angiosperm wood anatomy, specific gravity and Coexistence Analysis (using nearest living relatives of fossil wood and palynomorphs).

Chapter 7 discusses the nature of the Paleocene forests and climates of the Antarctic Peninsula and how they compare with modern Southern Hemisphere forests, comparing this new data to previously published research on Paleocene forests and climates of Antarctica and other southern

high latitude regions during this time. Conclusions derived from this research are presented in **Chapter 8**.

1.4 Paleocene climates

This section discusses previous research on the climates of the Paleocene and particularly focuses on published climate records for Antarctica and southern high latitude regions.

The Paleocene is considered to have been a greenhouse world with $p\text{CO}_2$ levels similar or higher than today (300 to 800ppm) (Beerling and Royer 2011; Royer *et al.*, 2012) (Figure 1.2). The Earth's latitudinal temperature gradient was lower than today (Figure 1.3). Temperate forests occupied large areas of the high latitudes (Wolfe *et al.*, 1980; Spicer and Parrish, 1990; Poole *et al.*, 2006, Pancost *et al.*, 2013).

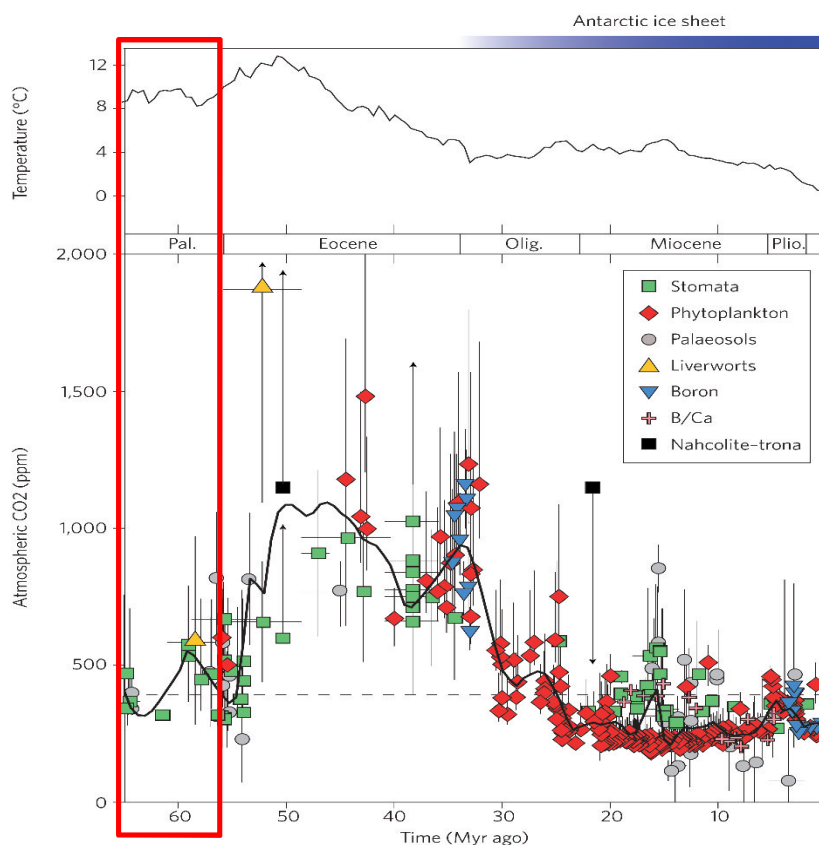
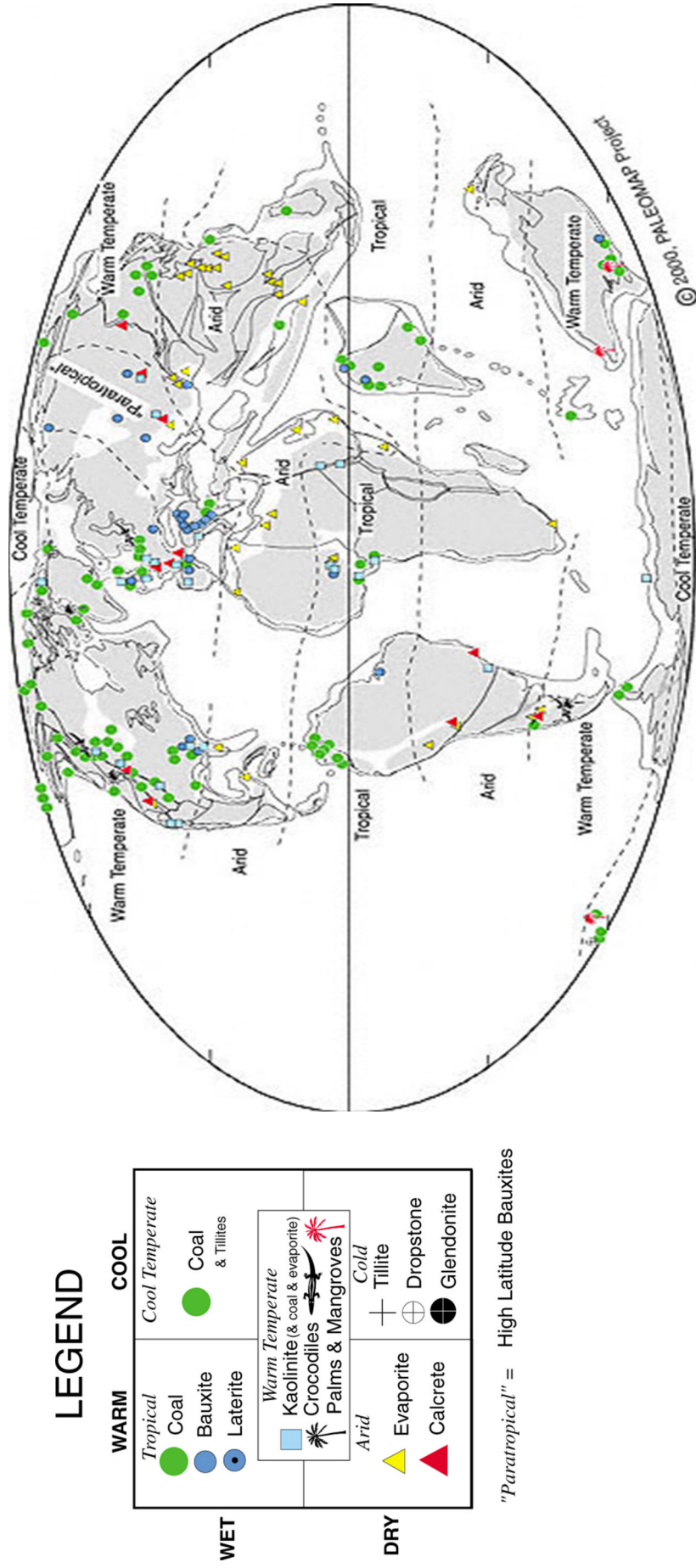


Figure 1. 2. Atmospheric CO₂ trend through the Cenozoic estimated from multiple proxies, which are shown on the key on the diagram. The horizontal dashed line represents modern CO₂ levels. Arrows on some proxies mark their upper or lower limit. The upper panel on the diagram presents deep sea temperature. The red box highlights the Paleocene Epoch. Diagram is taken from Beerling and Royer (2011).



Paleocene

Figure 1. 3. Paleocene climate zones. Legend on the left presents the different proxies that have been used to reconstruct the global climate zone. Diagram taken from <http://www.scotese.com>.

Within this greenhouse world climate fluctuated and evidence for this is best observed in the global oxygen and carbon isotope records derived from benthic foraminifera. Oxygen and carbon isotope compilation curves composed by Cramer *et al.* (2009) (see Figure 1.4) show a gradual trend towards increasing positive $\delta^{18}\text{O}$ from the latest Cretaceous to the early Late Paleocene, which suggests cooling during this time.

At 58.7Ma oxygen isotopes reach their most positive (0.5‰) in the Paleocene and this is coupled with a peak positive carbon, which is named the Paleocene carbon isotope maximum (PCIM) (Corfield, 1994, Cramer *et al.*, 2009, Westerhold *et al.*, 2011) and is thought to be caused by increased productivity and burial of $\delta^{12}\text{C}$. After the PCIM $\delta^{18}\text{O}$ values gradually decline into the Late Paleocene until the Paleocene/Eocene boundary where there was a rapid warming event (Paleocene Eocene Thermal Maximum PETM). This event is marked by a pronounced negative oxygen (- 1 to 1.5‰) and carbon isotope excursion (- 0.75‰) (Zachos *et al.*, 2001, Cramer *et al.*, 2009).

The PETM lasted for 100,000 to 250,000 years and within this time deep ocean temperatures warmed by 5 to 8°C (Zachos *et al.*, 2001; Sluijs *et al.*, 2007; Zachos *et al.*, 2008), sea surface temperatures (SSTs) at low latitudinal warmed by 5°C and high latitudinal areas warmed by 8 - 10°C (Zachos *et al.*, 2003).

The cause of the rapid warming and the associated negative carbon excursion is thought to have been the result of a large injection of methane and/or CO_2 into the atmosphere (Higgins and Schragg, 2006; Zachos *et al.*, 2008). The theories put forward for the cause of the release of the above mentioned greenhouse gases include: the destabilisation of methane hydrates along continental margins as a result of slope failure; the large scale burning of peatlands (Higgins and Schragg, 2006). Another possible cause is the oxidation of 5000 Gt of organic carbon as the result of the intrusion of a large sill complex into organic-rich sediments in the North Atlantic (Higgin and Schragg, 2006). The event is also associated with a extinction of benthic fauna which is likely to have been a consequence of low oxygen levels caused by stratification of the oceans (Zachos *et al.*, 2008).

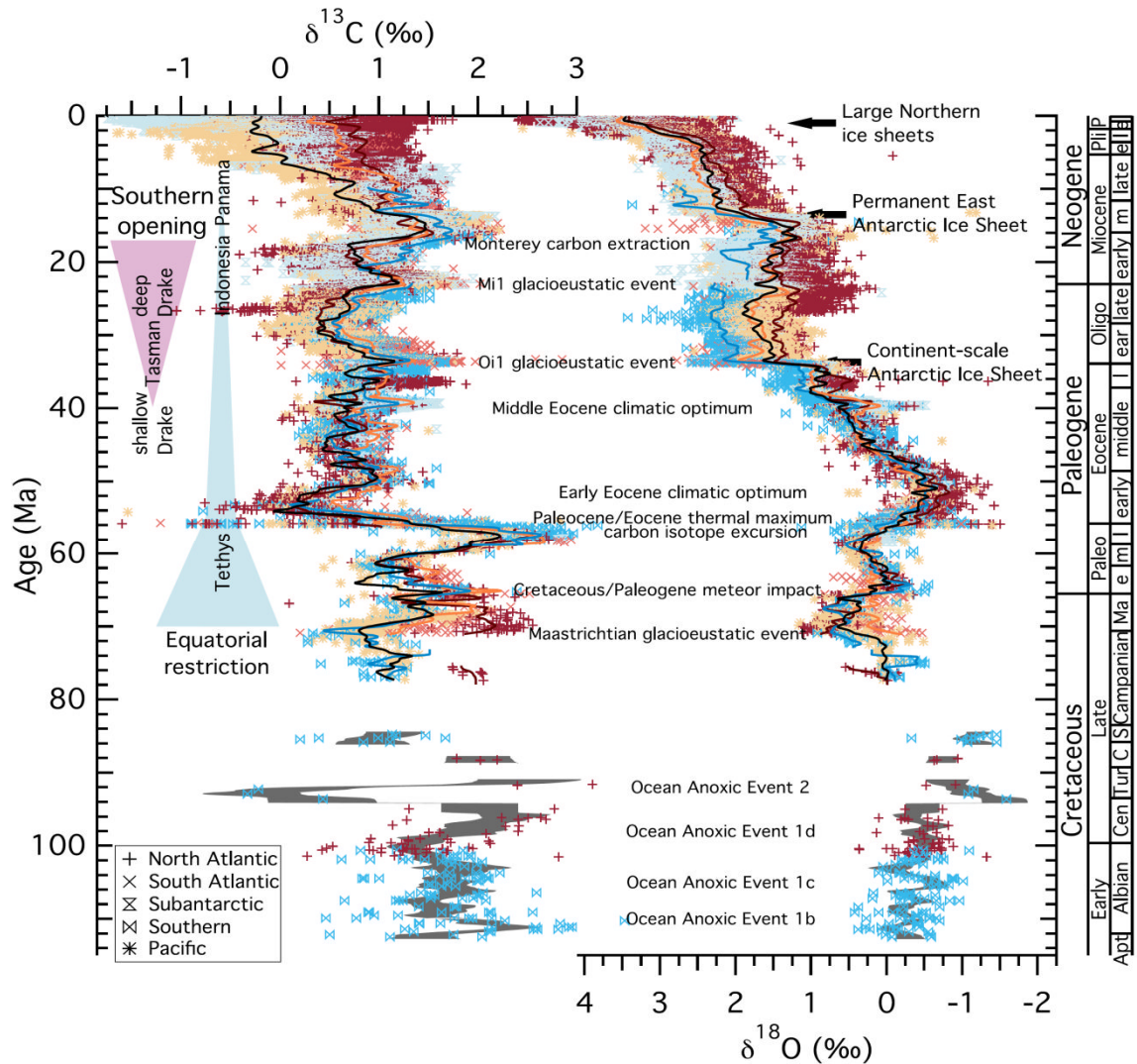


Figure 1. 4. Global benthic oxygen and carbon isotope records derived from foraminifera, from the Cretaceous to present day. The Paleocene is highlighted by a red box. Diagram is taken from Cramer *et al.* (2009).

Past climate research on the Antarctic Peninsula suggest that climates in this region were warm to cool temperate and seasonal from the latest Cretaceous to the early Paleogene. Evidence for this is indicated by the presence of fossil floras that are similar to vegetation found in modern southern temperate forests today (Askin 1992; Poole *et al.*, 2003; Cantrill and Poole, 2005; Poole and Cantrill, 2006). The presence of visible growth rings observed in fossil wood gives evidence for seasonal climates, and the growth ring widths suggest a growth rate similar to modern relatives growing in temperate New Zealand and Australia (Francis, 1986; Francis and Poole 2002).

Seasonality was also observed in fossil belemnites (late Maastrichtian) which show variation in $\delta^{18}\text{O}$ across annual growth bands, which yielded a mean annual temperature range of 6°C (Dutton *et al.*, 2007). Analysis of the weathering of clay minerals revealed an increase in smectite/kaolinite ratios in the Early Paleocene, which suggested pronounced seasonal rainfall during this time (Dingle and Lavelle, 2000).

Terrestrial and marine climate proxies reveal that climates of the Antarctic Peninsula fluctuated through the Paleocene, similar to the trends observed in the global benthic oxygen isotope records (as mentioned above). Proxies (refer to Figure 1.5, 1.6 and 1.8) reveal a cooling trend during through the Early Paleocene to the early-Late Paleocene, the climates then begin to warm to the Paleocene/Eocene boundary.

From the terrestrial realm, analysis of average mean growth ring widths of fossil wood from the Jurassic to the Eocene reveal that climate conditions became cooler and unfavourable for tree growth during the Late Cretaceous to the Early Paleocene, as indicated by narrowing of growth rings (Francis and Poole 2002) (Figure 1.6). An increase in growth ring width during the Late Paleocene to the Eocene revealed a possible change to warmer climates.

Mean annual temperatures derived from angiosperm anatomy and nearest living relatives (NLRs) of fossil flora suggest that mean annual temperatures (MAT) for the first part of Early Paleocene were between $9.9 - 13^\circ\text{C}$. Then temperatures increased to $11-18^\circ\text{C}$ during the latest Early Paleocene (Poole *et al.*, 2005). Mean annual precipitation from NLRs and wood physiognomy revealed that the Early Paleocene was relatively drier compared to the Cretaceous with mean annual precipitation around $652 - 4225\text{mm}$ per year as compared to $652 - 4944\text{mm}$ per year in the Cretaceous. The large ranges in mean annual precipitation values for both the Early Paleocene and the Cretaceous are due to the use of multi-techniques, which each have their own limitations. For example, techniques using wood physiognomy depend on the quality of preservation. In terms of the NLR approach, some nearest living relatives today have wide rainfall tolerances.

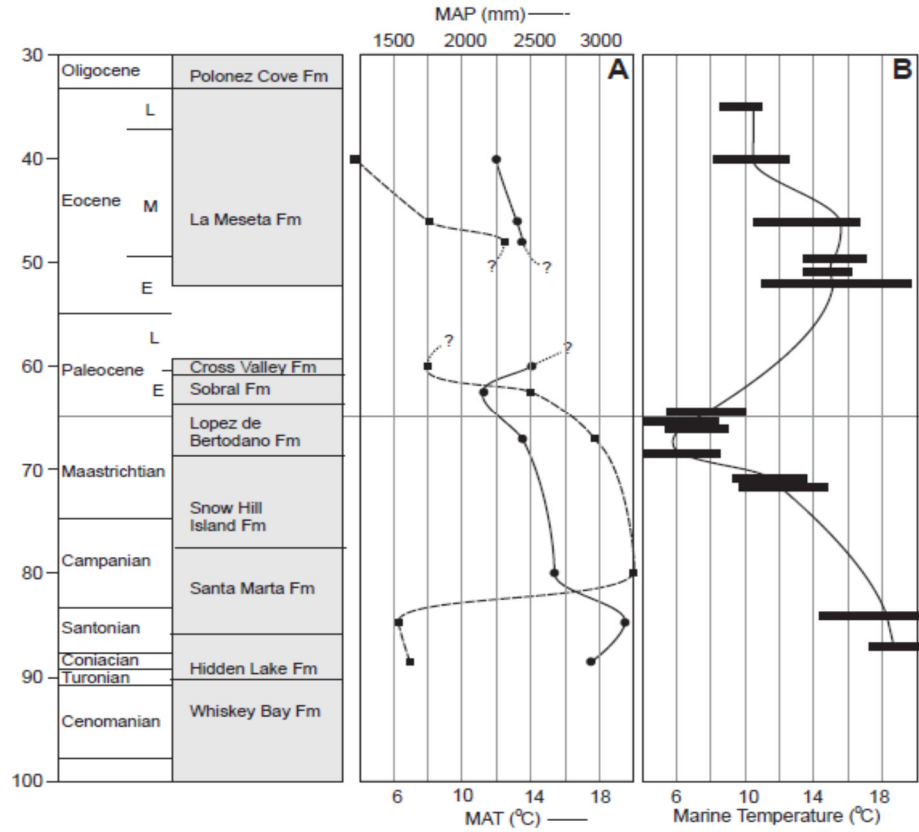


Figure 1. 5. Climate curve compilation for the Antarctic Peninsula taken from Poole *et al.* (2005), which includes the Cenomanian (Late Cretaceous) to the Oligocene. Graph A presents Mean annual temperature (MAT) (solid line) and Mean annual precipitation (MAP) (dotted line) from climate analysis on fossil flora (climate leaf analysis multivariate program, wood physiognomy and nearest living relative) undertaken by Poole *et al.* (2005). Graph presents mean sea surface temperatures, data collected from different sources: Barrera *et al.* (1987), Pirrie & Marshall (1990), Ditchfield *et al.* (1994).

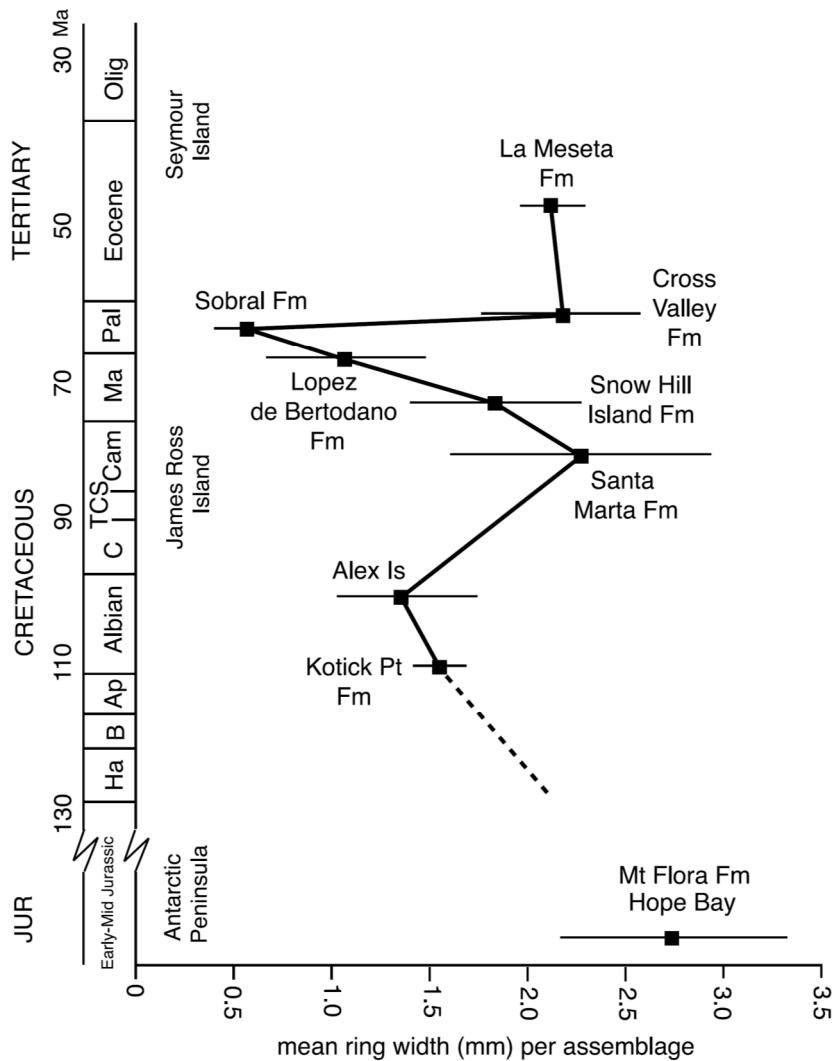


Figure 1. 6. Average mean growth ring width from fossil conifer wood from Jurassic to Eocene strata on Antarctica. The number of wood specimens per data point: Kotick Point Fm (=4), Santa Marta Fm (= 11), Snow Hill Fm (= 7), López de Bertodano (= 8), Sobral Fm (= 5), Cross Valley Fm (= 7), La Meseta Fm (= 8). Narrow growth rings = cooler/drier climates. Wider growth rings = warmer/wetter climates. Diagram taken from Francis and Poole (2002).

Cooling from the latest Cretaceous (Maastrichtian) into the Early Paleocene was further supported by the high resolution analysis of pollen abundances through the Maastrichtian and into the earliest Danian, which showed a decrease in plants that preferred warm and humid conditions, such as *Phyllocladites mawsonii* (nearest living relative of the conifer *Lagarostrobos franklinii*) (Bowman *et al.*, 2014) (Figure 1.7). Instead there was an increase in

cool temperate taxa, such as *Nothofagus*, podocarps conifers and *Araucaria* (Monkey Puzzle conifer), which had low abundances through much of the warm Cretaceous Period. Bowman *et al.* (2014) also found altitudinal temperature differences on the Antarctic Peninsula, revealed by floral differences. Lowland areas were likely to have been dominated by warm temperate floras that indicate mean annual temperatures between 10 – 15°C. Upland areas were likely to have been occupied by more cool temperate flora and suggest temperatures between 5 – 8°C. The temperatures produced for upland areas are based on the nearest living relative of pollen species *Araucariacites australis*, which is *Araucaria araucana* and today this species of tree grows in the cool temperate forests of southern Chile, at high altitude in the Andes.

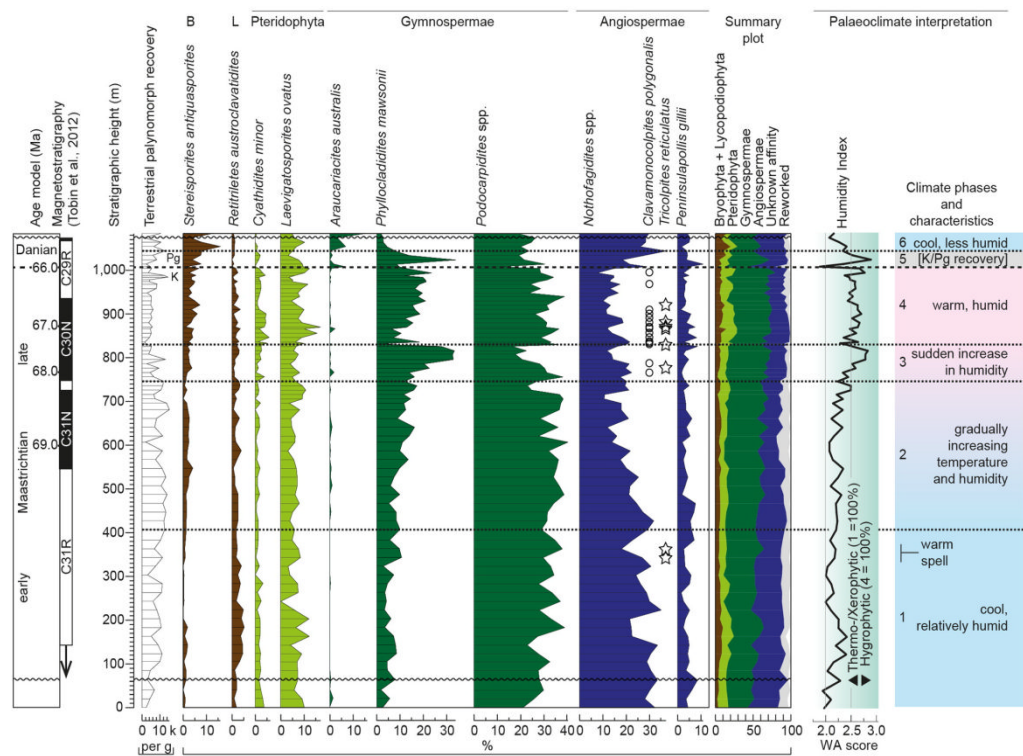


Figure 1. 7. Abundances of selected pollen and spore taxa from the Maastrichtian (latest Cretaceous) to the earliest Danian (earliest Paleocene), from Seymour Island. Climate phases for this period are presented on the left of the diagram. Diagram taken from Bowman *et al.* (2014).

Kemp *et al.* (2014) obtained palaeo-soil temperatures from the ratio of organic compounds (Methylation of Branched Tetraether and Cyclisation of branched Tetraether (MBT and CBT) (refer to Figure 1.8). They generally agree with temperatures indicated by the palaeo-flora and suggest mean annual temperatures around 12°C. However, MBT/CBT (methylation index of branched tetraethers/ cyclization ratio of branched tetraethers) mean annual temperatures for the Late Paleocene suggest cool temperate to sub-arctic (8°C) conditions and are therefore cooler than those obtained from fossil floras.

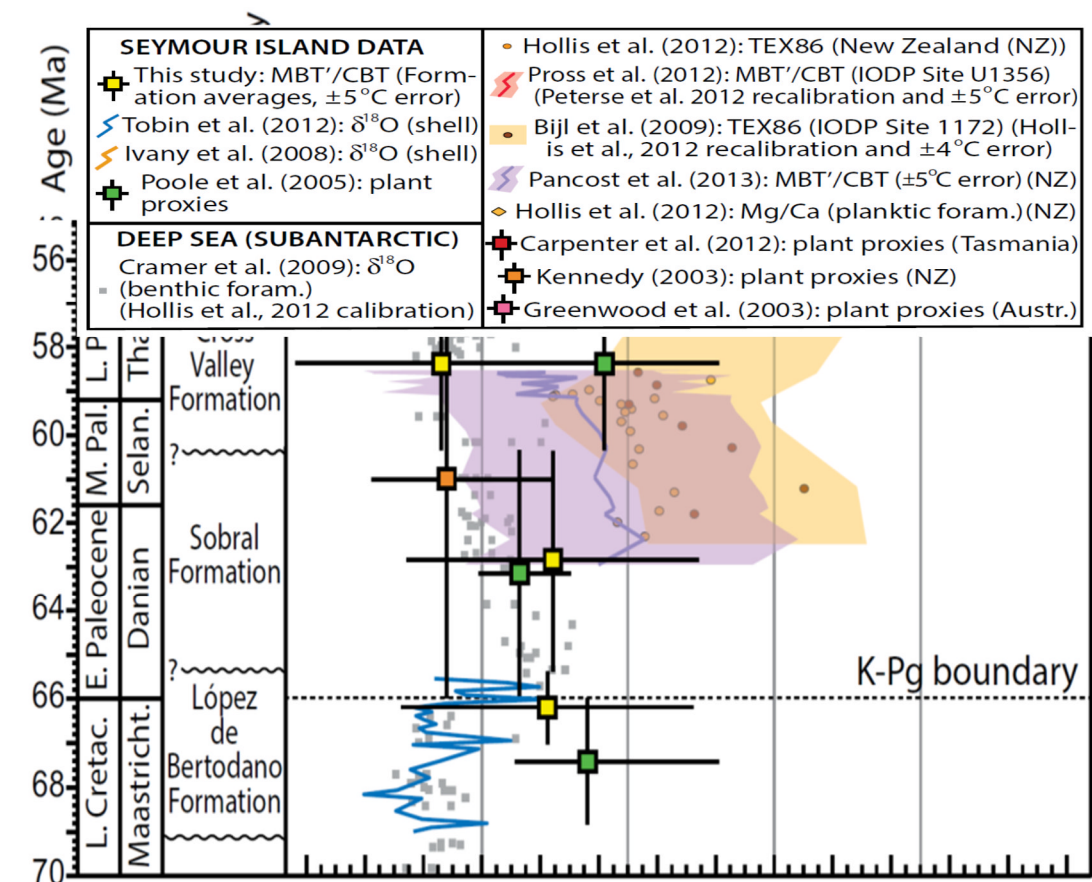


Figure 1. 8. Palaeotemperature data through the Late Cretaceous to the Paleocene/Eocene boundary from multiple proxies. The different proxies are presented in the key below the diagram. Diagram taken from Kemp *et al.* (2014).

Marine climate proxies are in general agreement with terrestrial proxies. Sea surface temperatures from oxygen isotopes derived from marine macro-fossils produced temperatures between 8 – 14°C for the Paleocene (Ditchfield *et al.*, 1994, Tobin *et al.*, 2012). Barrera *et al.* (1987) found that marine temperatures were 5 - 10°C from benthic foraminifera. Tobin *et al.* (2012) revealed that just after the K/Pg boundary in the earliest Danian there was a warming event where sea temperatures reached 14°C. This is not evident from the terrestrial proxies.

Evidence for the Paleocene – Eocene Thermal Maximum PETM appears to be absent from the Antarctic Peninsula because the Paleocene/Eocene boundary is missing from the rock record. Fossil floras from the early Eocene strata on Seymour Island (La Meseta Formation) and middle Eocene strata on King George Island suggest the cool to warm temperate climates continued in the early to middle Eocene (Poole *et al.*, 2001; Pujana *et al.*, 2014). However, research on palynomorphs and MBT/CBT analysis revealed sub-tropical conditions during the early Eocene (53.6 – 51.9 Myr ago) on the Wilkes Island Basin margin, East Antarctica (Pross *et al.*, 2012). The study of palynomorphs from this region revealed the presence of tropical plants such as Palm trees, Bombaceae and Proteaceae and other species with affinities to flora found in sub-tropical forests of Australia and New Guinea today. Soil temperatures of 16°C have been indicated from MBT/CBT analysis (Pross *et al.*, 2012).

Other southern high latitude regions during the Paleocene (e.g. southern Australia, New Zealand and southern South America) had similar climates as the Antarctic Peninsula indicated by the presence of similar fossil plants, such as *Araucaria*, *Nothofagus* and podocarps (Greenwood *et al.*, 2003; Pancost *et al.*, 2013). These regions were slightly warmer as a result of them being at slightly lower latitudes. For example, terrestrial climate proxies (palynomorphs and MBT/CBT) derived from the Canterbury Basin on the east coast of New Zealand produced temperatures of 15°C for the middle Paleocene which decreased to 10°C during the early Late Paleocene (58 – 59 Ma) (Pancost *et al.* 2013). Sea surface temperatures from TEX_{86}^L yield similar temperatures 16 – 19°C and also show cooling at 58.7 Ma (13 – 16°C) (Hollis *et al.*, 2012). This cooling relates to the Paleocene carbon isotope maximum (PCIM). During the

PETM terrestrial temperatures warmed to 20 – 22°C and SST temperatures warmed to 26 – 28°C in New Zealand (Hollis *et al.*, 2012; Pancost *et al.*, 2013). As a result there is an increase in sub-tropical floras. An increase in sub-tropical flora was also observed in micro and macro flora assemblages from south-eastern Australia, including palm trees and Proteaceae along with a decrease in temperate floras (Greenwood *et al.*, 2003).

1.5 Forests of the Antarctic Peninsula

Figure 1.9 shows the age and the stratigraphic distribution of the Cretaceous to Eocene fossil floras of the Antarctic Peninsula region. The units represent different palaeo-environments from the flood plain settings of Alexander Island (Figure 1.1), the intra arc settings of Livingston Island and the back arc basin settings of the Larsen Basin (Poole and Cantrill 2006).

This section will discuss the evolution of vegetation on the Antarctic Peninsula from the Cretaceous to the Eocene and then discuss how factors such as climate and volcanism affected forest composition.

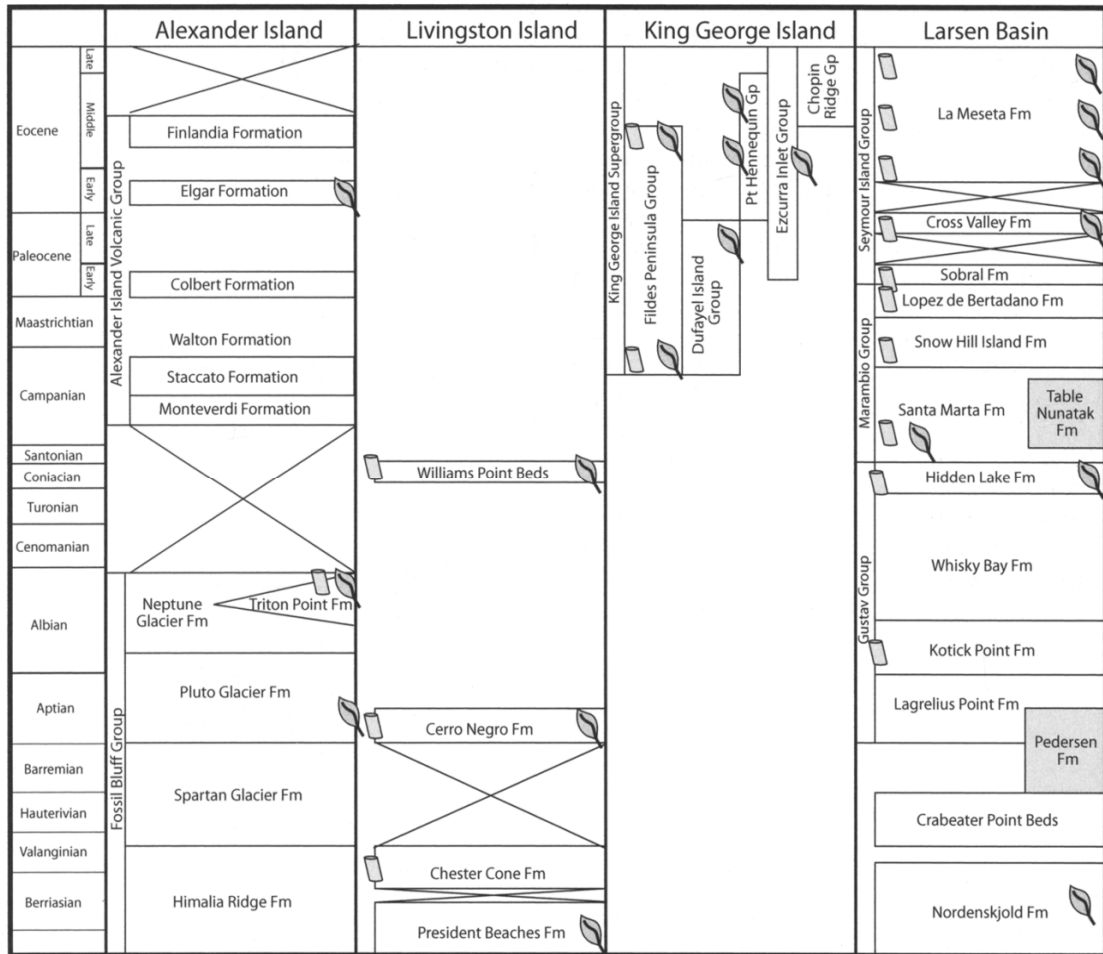


Figure 1. 9. Summary of the Cretaceous and Early Paleogene stratigraphic units from the Antarctic Peninsula. Units that contain fossil wood and leaves are marked by wood and leaf symbols. Taken from Poole and Cantrill (2006).

Past work on Antarctic Peninsula forests suggests four stages of evolution of forest vegetation from the Cretaceous to Eocene (Poole and Cantrill, 2006). The Early Cretaceous to early Late Cretaceous forests were warm temperate types, with the Early Cretaceous forests dominated by conifers of families such as Araucariaceae and Podocarpaceae (Cantrill and Poole, 2005; Poole and Cantrill, 2006). By the Albian (late Early Cretaceous) angiosperms had evolved but only occupied understory niches.

Diversification and modification of angiosperms occurred during the Late Cretaceous and is thought to have been triggered by the Cretaceous thermal maximum (100 to 80Ma), which allowed angiosperms from low latitudinal

regions to migrate to high latitudinal regions (Cantrill and Poole, 2012; Eklund 2003; Eklund *et al.*, 2004; Hayes *et al.*, 2006).

Late Cretaceous fossil leaf, wood and pollen assemblages of the James Ross Basin resemble those from extant families such as Lauraceae, Myrtaceae and Cunoniaceae, Gunneraceae, and Illiciaceae which are found living in temperate to sub-tropical forests of the Southern Hemisphere today (Askin *et al.*, 1992; Poole *et al.*, 2000a; Poole *et al.*, 2000b; Poole *et al.*, 2000c; Hayes *et al.*, 2006; Poole and Cantrill, 2006). The charcoalfied remains of flowers related to Myrtaceae, Winteraceae and Siparunaceae were recovered from units of late Santonian age, 85 Ma on Kenyon Peninsula, on the east coast of the Antarctic Peninsula in the Larsen Basin (Eklund, 2003). This provides further evidence for extensive modernisation of angiosperm floras on Antarctica.

During the latest Cretaceous (latest Maastrichtian) to the Eocene (early to middle) the forests had changed to cool temperate types with a diversification of Valdivian type floras (similar to forests that live in Patagonia today) and an increasing dominance of *Nothofagus*, podocarps and Araucariaceae (Poole *et al.*, 2003; Poole and Cantrill 2006; Pujana *et al.*, 2014; 2015; Bowman *et al.*, 2014).

Volcanic activity is a major factor controlling the floral composition in modern Valdivian forests that grow on the slopes of the Andes (Veblen *et al.*, 1995). Evidence from floral assemblages within Eocene volcanic sedimentary sequences on King George Island suggest that volcanic disturbances were also important in controlling floral composition on the Antarctic Peninsula (Poole *et al.*, 2001). Figure 1.10 presents a Valdivian model for the King George Island flora and it shows how volcanic vegetation changes from pre-eruption to post eruption and differences in the effects of eruptions with increasing distance from the volcanic centre (Poole *et al.*, 2001). Pre-eruption vegetation is diverse and consists of angiosperms and conifers, post-eruption floras have low diversity and density. On King George Island low diversity and low density floras (recovery/pioneer floras) consisting of mainly podocarps and *Nothofagus* overlie a debris flow and further up the sequence a high diversity and dense floral assemblage is found within tuffaceous sediments and indicate low volcanic disturbance.

Cantrill and Poole (2005) found that there are possible differences between floras on the west and east side of the Antarctic Peninsula with higher abundance of conifers and *Nothofagus* on the eastern side. Suggested reasons for this could be differences in precipitation from the west to the east, similar to the precipitation in the Andes and also distance from volcanic centres (Cantrill and Poole, 2005).

Overall it is clear that climate has broadly influenced the composition of the forest on the Antarctic Peninsula from the Cretaceous to the Eocene with a change from subtropical forests in the warm Cretaceous to cool temperate forests in the cooler Paleocene and Eocene. However, previous work on fossil flora have revealed that volcanic activity had an effect on composition, as well as regional climatic differences on the Antarctic Peninsula (east and west).

The results of this study of new floras from Seymour Island provides new and more detailed information about the vegetation that grew on the Antarctic Peninsula and the climates in which they lived during the Paleocene. This assemblage of fossil wood has been collected from measured stratigraphic sections so that it is possible to determine how vegetation and climate evolved through this interval. Also, it is possible to link the occurrence and preservation of the fossils to the sedimentary environment. In the past fossil wood has not been collected systematically on measured sections so this detailed information is missing and the accuracy of the stratigraphic occurrence is not as certain (J.Francis pers.comm 2015). Previous collections of Paleocene wood have not been properly stratigraphically constrained so this study presents a much better analysis of Paleocene floras and climates.

As part of the PALEOPOLAR project the results in this thesis have contributed and will contribute further to a broader analysis of Paleocene ecosystems and climates, derived from palaeoenvironmental analysis (Jonathan Ineson, sedimentologist at the Geological Survey of Denmark and Greenland), palynology and climate change (Bowman *et al.*, 2014, Francis, J.E, based at the British Antarctic Survey), marine invertebrate evolution (Crame, J.A., British Antarctic Survey; Joanne Hall.; Witts *et al.*, 2015, based at the University of Leeds) and climate modelling (Lunt, D, Loftson *et al.*, 2014, University of Bristol).

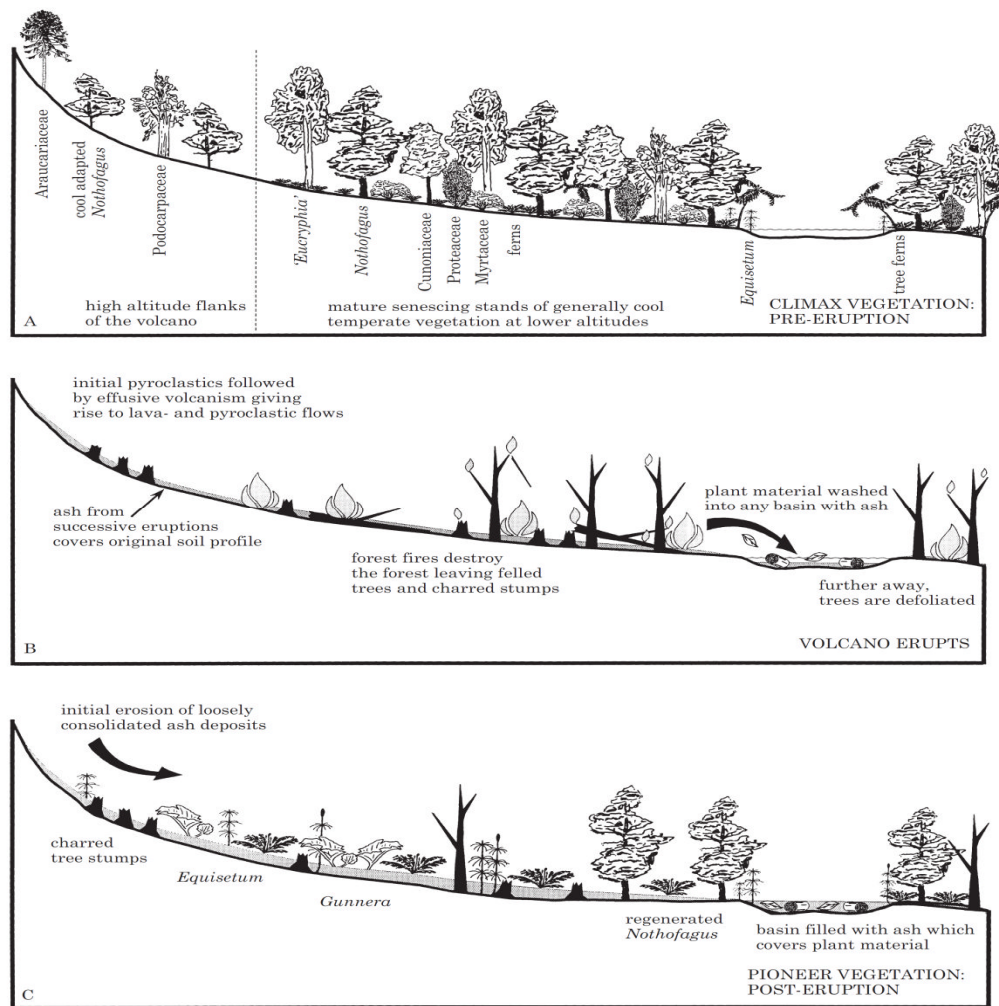


Figure 1. 10. Valdivian model for Eocene flora growing in high altitude areas close to the volcanic centres on the Antarctic Peninsula to lowland distal floras. A) Pre-eruption flora with diverse and dense vegetation. B) Post-eruption flora, high to mid altitude floras are destroyed by pyroclastic flows and forest fires; trees in more distal locations may be defoliated. C) low density and diversity flora consisting of *Nothofagus*, conifers and small shrubby plants. Diagram taken from Poole *et al.* (2001).

Chapter 2

Geological settings

2.1 Introduction

Chapter 2 presents the geological background to provide the context for the fossil wood and palaeoclimate studies in this project. Firstly, an overview of the evolution of the Antarctic Peninsula is provided, including information about the back-arc basin on its eastern side that includes Seymour Island. Secondly, an overview of the geology of Seymour Island is presented based on previously published work. The chapter will then focus on the sedimentary sequence from which fossil wood for this project was collected and will include a detailed discussion on the composition, depositional environment and the age model for the sequence. The final section will present the wood specimens studied in this project and discuss their location in the sedimentary and stratigraphic sequence, their preservation and their likely depositional history.

2.2 Geological evolution of the Antarctic Peninsula and the James Ross Basin

From the Jurassic to the Eocene period the Antarctic Peninsula was an evolving volcanic arc (Hathway, 2000). During this period Gondwana had started to break up, initially in an east to west direction. Antarctica, India and Australia formed the eastern part of Gondwana, and South America and Africa formed the western part (Lawver *et al.*, 1992; Hathway, 2000) (Figure 2.1). As a result of this extension oceanic crust formed on the eastern side of the Antarctic Peninsula and the eastern side of southern South America. Along the Antarctic Peninsula's western margin, the proto-Pacific plate was being subducted (Figure 2.1). Consequently a forearc basin developed on the western side of the volcanic arc and a back-arc basin developed on the eastern side, now called the Larsen Basin (Valle *et al.*, 1992) (Figure 2.2). Within the Larsen Basin is the James Ross Basin (Figure 2.2), which

encompasses James Ross Island, Cockburn Island, Snow Hill Island and Seymour Island (Valle *et al.*, 1992). The age of the James Ross Basin strata includes the Cretaceous to the Neogene (Valle *et al.*, 1992; Pirrie *et al.*, 1997; Hathway, 2000; Marensi, 2006; Marensi *et al.*, 2012).

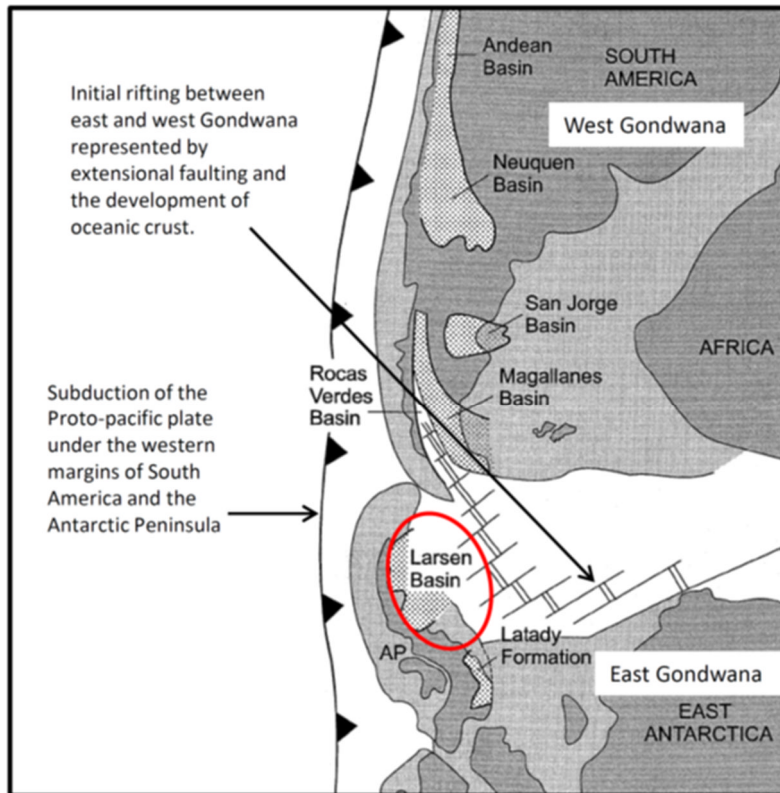


Figure 2. 1. Palaeogeographic map showing the early stages of rifting between west and east Gondwana during the Late Jurassic. The proto-Pacific plate at this time was being subducted under the western margin of the Antarctic Peninsula and South America. AP stands for Antarctic Peninsula. The Larsen Basin is circled in red. This diagram has been modified from Hathway (2000).

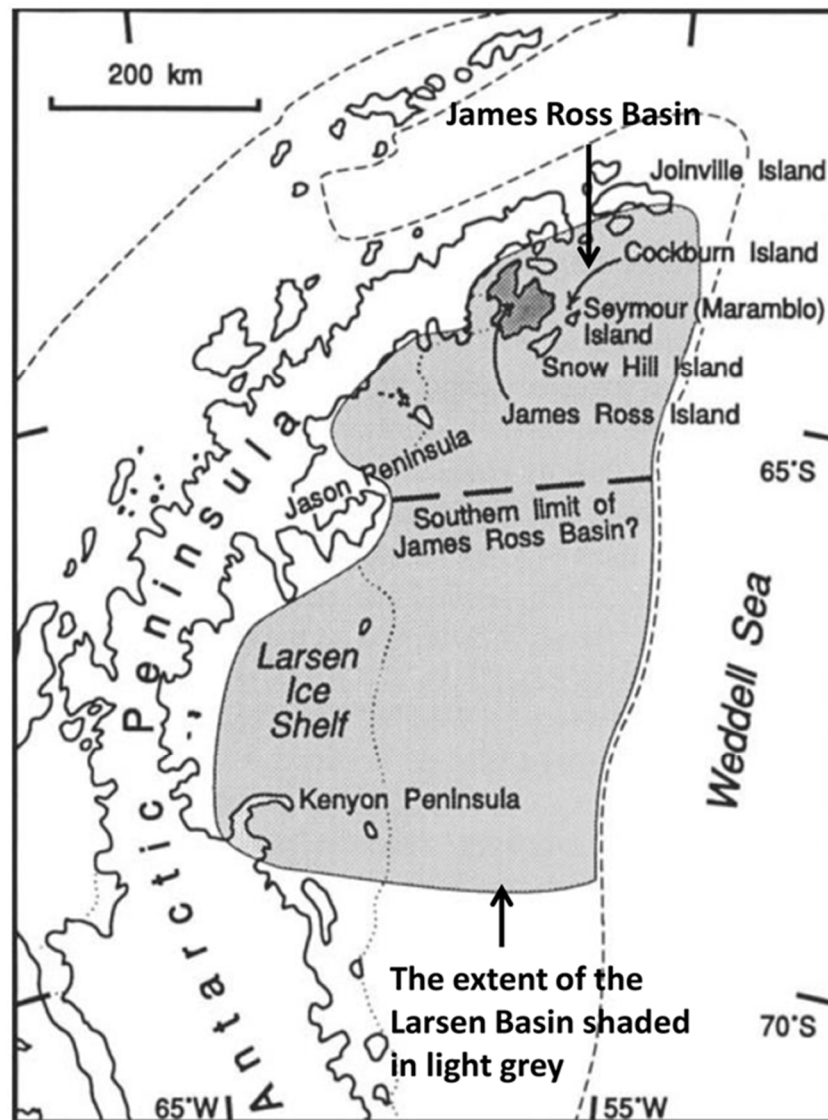


Figure 2. 2. The extent of the Larsen Basin on the eastern side of the Antarctic Peninsula, shaded in grey, and also the extent of the James Ross Basin that is within the Larsen Basin. The southern extent of the James Ross Basin is shown by a thick black dashed line. From Valle *et al.* (1992).

The initial development of the Larsen Basin during the Jurassic Period is likely to have been caused by extension due to continental stretching and subduction processes along the west side of the Antarctic Peninsula. These initial stages of development are represented by extensive normal faulting and silicic volcanic rock units (Hathway, 2000) (Figure 2.3).

The evolution of the Larsen Basin and the adjacent volcanic arc during the Late Cretaceous to Eocene is represented by three sedimentary megasequences that infill the Larsen Basin. From the oldest to the youngest these are the Gustav Group (Aptian – Coniacian age), Marambio Group (Santonian – Paleocene) and Seymour Island Group (Paleocene – Eocene) (Hathway, 2000). Each group is briefly described below in terms of its composition and depositional history:

Gustav Group: The Gustav Group consists of four stratigraphic formations: the Lagrelius Point Formation, Kotick Point Formation, Whiskey Bay Formation and Hidden Lake Formation seen on James Ross Island today (Hathway, 2000). The first three formations represent a deep marine depositional environment consisting of clastics including sandstones and mudstones, which formed as a sedimentary wedge against the eastern margin of the Antarctic Peninsula (Figure 2.3). They accumulated rapidly and have a cumulative thickness of 3000m. High sedimentation rates are linked to major subsidence of the basin and uplift of the volcanic arc, resulting in large amounts of material being eroded into the back-arc basin. The upper part of the Hidden Lake Formation (Coniacian age) is a 400m thick unit representing a volcanoclastic fan delta that includes material from pyroclastic flows, pumice, and volcanic bombs. It indicates that during this time there was a high frequency of volcanic activity (Hathway, 2000; Whitham *et al.*, 2006).

Marambio Group: During the Late Cretaceous there was a change from an extensional to a compressional stress regime on the eastern side of the volcanic arc, resulting in reverse faulting along the western side of the Larsen Basin (Figure 2.3; Hathway, 2000). This caused uplift of the basin and subsequently sedimentation started to outpace subsidence causing shallowing. This phase of basin inversion is represented by the Marambio Group, which represents an overall shallowing marine sequence and progradation of a marine shelf eastwards towards the Weddell Sea. The group consists of three formations: the Santa Marta Formation, seen on James Ross Island; the Snow Hill Formation, seen on both James Ross and Snow Hill islands; and the López de Bertodano Formation, exposed on Vega, Snow Hill and Seymour islands.

Seymour Island Group: The Seymour Island Group is confined to Seymour Island and Cockburn Island and consists of three formations: Sobral Formation, Cross Valley Formation and the La Meseta Formation. They represent further shallowing with alternating fluvial and shallow marine shelf sequences with inter-bedded volcanoclastic units. Sedimentation was influenced by eustatic sea-level changes as the basin was relatively stable during this time.

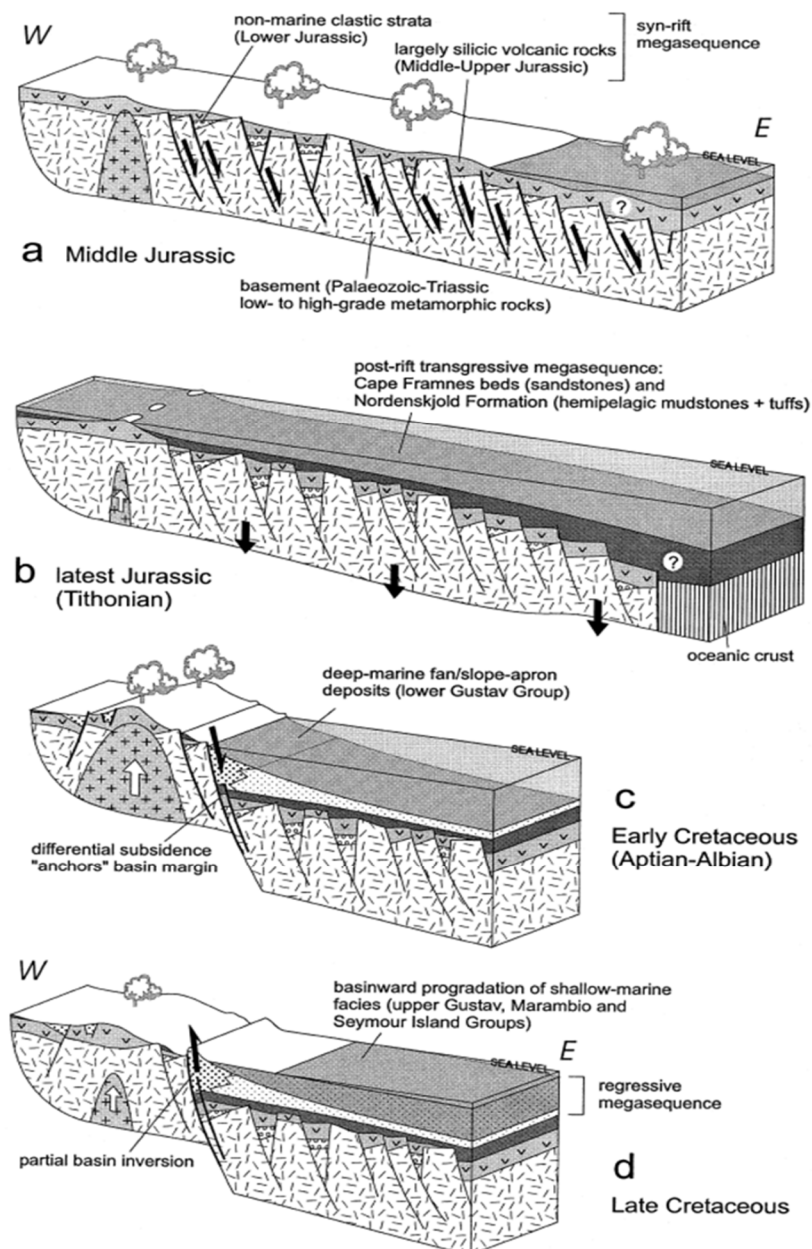


Figure 2. 3. The main stages in the geological evolution of the Antarctic Peninsula and the Larsen Basin. (From Hathway, 2000).

2.3 Geology of Seymour Island

This section presents an overview of the different geological units of Seymour Island, followed by a brief discussion of published interpretations of its depositional history and age. The following section (2.4) will then discuss the sedimentary sequence studied in this project.

The geology of Seymour Island consists of the upper part of the Marambio Group (Maastrichtian) and the Seymour Island Group (Paleocene – Eocene) (Figure 2.4). Seymour Island has a latest Cretaceous to Eocene stratigraphy with the K/Pg boundary well exposed (Crame *et al.*, 2004; Olivero, 2012). All of the strata on Seymour Island gently dips (9°) towards the south east. Five rock units are recognised on Seymour Island: the Haslum Crag Member of the Snow Hill Island Formation (Maastrichtian), the López de Bertodano Formation (latest Maastrichtian to earliest Paleocene), the Sobral Formation (Early Paleocene to Late Paleocene), the Cross Valley Formation (Late Paleocene) and La Meseta Formation (Early Eocene). Overall these units record an overall prograding palaeo-shoreline.

The upper part of Haslum Crag Member of the Snow Hill Island Formation (thickness of 68m) outcrops on the south western corner of Seymour Island (Crame *et al.*, 2004; Olivero, 2012) and it is the oldest rock unit. However, the majority of the Haslum Crag Member is on Snow Hill Island and it represents the development of deep marine channels that were infilled by coarse grained sandstones that grade into finer sandstones and mudstones (Olivero, 2012).

The Haslum Crag Member is unconformably overlain by the López de Bertodano Formation, which has a thickness of 1100m (Figure 2.4; Olivero, 2012) and extends over most of the southern half of Seymour Island. The López de Bertodano Formation is a continuous sedimentary sequence that consists of marine mudstones and silty sandstones that show a slight increase in grain size up section (Crame *et al.*, 2004). Concretionary and glauconite beds become increasingly common in the upper levels of the formation (Crame *et al.*, 2004). Overall the formation represents a shallowing-up sequence from an outer marine shelf setting to a mid-shelf depositional environment.

The K/Pg boundary is in the uppermost 59m of the López de Bertodano Formation, within a glauconite unit and is defined by a disappearance of many marine fauna, such as ammonites and bivalve and gastropod taxa (Crame *et al.*, 2004). It is also marked by an enrichment of iridium (Elliot *et al.*, 1994; Crame *et al.*, 2004). The K/Pg boundary on Seymour Island has been dated as 66Ma based on the magnetostratigraphy and correlation with dinoflagellate biozones (Bowman *et al.*, 2012; Tobin *et al.*, 2012; Bowman *et al.*, in revision). Below the K/Pg boundary the López de Bertodano Formation is highly fossiliferous and contains ammonites, bivalve, gastropods, marine reptile bones, as well as foraminiferas and dinoflagellates (Crame *et al.*, 2004). Fossil wood and fossil pollen derived from flora that were once living on the Antarctic Peninsula are also present throughout the formation, although wood is more abundant in the upper sections. The marine fauna is not very species-rich and many taxa are endemic to the Antarctic Peninsula; this and the fact the formation is relatively uniform has made the subdivision and accurate biostratigraphic dating of it difficult.

Macellari (1988) divided the formation into 10 informal units that were originally labelled Klb 1 to Klb 10. The basal unit (Klb 1) has now been re-assigned to the Haslum Crag Member (Crame *et al.*, 2004). The subdivisions of the bottom 6 units are based on the presence and abundance of *Rotularia*, a polychaete worm species. Klb 7 and Klb 10 are subdivided by the appearance and abundances of bivalve species and also changes in grain size and presence/abundance of glauconitic and concretionary beds. The uppermost unit Klb 10 is important as it contains the K/Pg boundary and the upper part of this unit is defined by a scarcity of marine macrofauna although fossil wood is abundant. The López de Bertodano Formation has been assigned a late Maastrichtian to Danian age using strontium isotope chemostratigraphy, magnetostratigraphy and dinoflagellates (Crame *et al.*, 2004; Bowman *et al.*, 2012; Tobin *et al.*, 2012).

The Sobral Formation unconformably overlies the López de Bertodano Formation and the contact is an erosional surface that records marine regression (Macellari, 1988; Sadler, 1988; Marensi *et al.*, 2012). Previously published work on the Sobral Formation have measured it as 238m thick (Marensi *et al.*, 2012). The formation outcrops on the south-eastern tip of

Seymour Island (Figure 2.4) and represents a shallowing sequence from a mid-shelf setting to a proximal delta front depositional environment (Macellari, 1988; Sadler, 1988; Marensi *et al.*, 2012). It consists of marine sandy mudstones that grade into sandstones with cross-bedding and coarse pebbly sandstones in the uppermost units. Glauconitic horizons are present at numerous levels, they are thought to represent transgressive surfaces and sedimentation starvation. Although gastropods are abundant in the lowermost units, overall the marine fauna is not as abundant compared to the López de Bertodano Formation (Macellari, 1988). Bioturbation is present in most of the units suggesting oxygenated conditions. Fossil wood and pollen are abundant throughout the Formation. Previously published work using foraminifera and dinoflagellates have dated the Sobral Formation as Early Paleocene (Danian) in age (Askin, 1988; Huber, 1988). However, this age has been revised and a Danian to Thanetian age has been allocated based on dinoflagellate biozones (Bowman *et al.*, in revision). This will be discussed in more detail in section 2.4.2.

The Cross Valley Formation sits unconformably on top of the Sobral Formation and it represents the infill of an incised valley that cuts into the Sobral Formation and López de Bertodano Formation (Marensi *et al.*, 2012) (Figure 2.4). The Cross Valley Formation is 195 – 214m thick (Marensi *et al.*, 2012; J Ineson 2015 pers. comm., 12 March) and it largely consists of pebbly sandstones with a high content of volcanoclastic material (pumice stones, volcanic glass) and charcoalified fossil wood (Marensi *et al.*, 2012). Previously published work has interpreted the depositional history of the Cross Valley Formation as being fluvio – deltaic facies embedded in an incised marine platform (Marensi *et al.*, 2012). Alternately, due to the presence of fossil log jams and volcanoclastic material, it has been suggested that the Cross Valley Formation was deposited rapidly by a high energy flow, such as a flash flood or a pyroclastic flow (J. Francis 2015, pers. comm., 1 Sep).

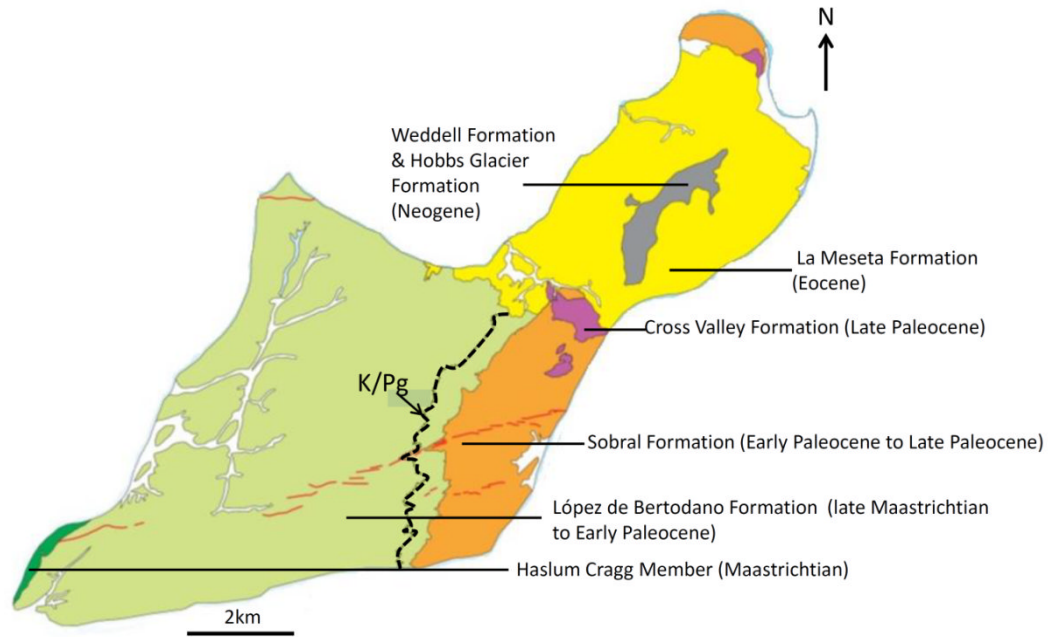


Figure 2. 4. Geological map of Seymour Island. All rock units gently dip towards the south east. The K/Pg boundary is shown by a dashed line. Diagram is modified from Marensi *et al.* (2012).

2.4 The sedimentary sequence studied in this project

The fossil wood specimens studied in this project were collected throughout a sedimentary succession that includes the upper part of the López de Bertodano Formation, the Sobral Formation, and the Cross Valley Formation. The age of the sequence ranges from the Late Cretaceous (Maastrichtian), just below the K/Pg boundary, to the Late Paleocene (Thanetian). The sequence was logged in detail along measured sections (see Figure 2.5 and 2.6) on Seymour Island during the 2009/2010 Antarctic field season (British Antarctic Survey) as part of the PALEOPOLAR project. The sections have been compiled into a composite log and the depositional environments of the sediments have been interpreted by Jon Ineson (J Ineson 2015, pers.comm., 13 March).

Figure 2.5 and 2.6 shows the composite log for the upper López de Bertodano Formation, the Sobral Formation, and the Cross Valley Formation. The cumulative thickness of the sedimentary log that includes the López de Bertodano Formation and the Sobral Formation is 400m. The Cross Valley Formation has a cumulative thickness of 300m.

This section of Chapter 2 has been divided into sub-sections 2.4.1 and 2.4.2 below. The first section will discuss the composition and depositional environments represented by the sedimentary sequence, and the second section will discuss the age model for the sedimentary sequence.

2.4.1 Sedimentology analysis

The sedimentary sequence in this project records an overall shallowing environment from a marine mid-shelf environment to a more shallow-marine fluvial environment (Figure 2.5 and 2.6). The sedimentology and depositional history of each formation are discussed separately below:-

López de Bertodano Formation: The top 80m of the López de Bertodano Formation consists of bioturbated sandy mudstones. The K/Pg boundary is at 17m on the sedimentary log (Figure 2.5) within a glauconitic horizon, which is approximately 2m thick. Another glauconitic horizon is present above this and is 4m thick. Above the K/Pg boundary concretion bearing horizons are scattered throughout the upper part of the formation and they are each approximately 1m thick. These horizons are also bioturbated with *Taenidium* and *Thalassinoides* burrows. A marine mid-shelf depositional environment has been interpreted for the upper part of the López de Bertodano Formation. This is because of the presence of structureless sandy mudstones, which suggests a low energy environment and the presence of trace fossils indicate a shore-face environment (J Ineson 2015, pers. comm., 13 March). The glauconitic horizons are thought to represent transgressive events that resulted in sediment starvation.

Sobral Formation: The Sobral Formation starts at 80m on the composite sedimentary log (Figure 2.5) and the boundary between it and the López de Bertodano Formation is an erosional unconformity that indicates a significant fall in sea level (J Ineson 2015, pers comm., 13 March). The unconformity has a relief of a few tens of metres (J Ineson 2015, pers. comm., 13 March). A conglomerate lag deposit is also found at the base of the Sobral Formation, which contains clasts of the underlying López de Bertodano Formation (Sadler, 1988). The Sobral Formation is 290m thick and has been divided into 7 depositional environments (J Ineson 2015, pers. comm., 13 March).

At the base of the Sobral Formation to a height of 195m on the sedimentary log the depositional setting has been interpreted as prodelta to delta front environments (J Ineson 2015, pers. comm., 13 March). The sedimentary deposits in this portion are muddy sandstones that grade into fine sandstones. Concretionary horizons and thin volcanic ash beds (5 – 10cm) are also frequent throughout this section (Figure 2.5). At 150–175m height there is a 15m thick unit that consists of glauconitic sands. The presence of the glauconite suggests sediment starvation and may have been caused by a transgression (J Ineson 2015, pers. comm., 13 March). All of the units from the base of the Sobral Formation to 195m are also heavily bioturbated with the following trace fossils: *Teichichnus*, *Helminthopsis*, *Diplocraterion*, *Chondrites*, *Taenidium* and *Thalassinoides*. The sediments generally reflect deposition in a low energy marine environment and the presence of the trace fossils indicate a shelf facies. The volcanic ash beds also suggest that the volcanic arc was active during this time but the volcanic source was likely to be distal.

The depositional environment then changed to a proximal delta front, represented by sedimentary deposits from 195m to 265m on the sedimentary log. This is represented by a lithological change to well-sorted sandstones and the presence of planar cross-bedding suggests a higher energy upper shore-face environment (J Ineson 2015, pers. comm., 13 March). The units are also bioturbated with trace fossils that include *Ophiomorpha nodosa* (dominant), *Skolithos*, *Arenicolites*, *Rhizocorallium* and *Thalassinoides*, all of which are associated with shore-face to fore-shore environments. In particular *Skolithos* and *Ophiomorpha* are normally associated with high energy sandy shore-face environments (Pemberton *et al.*, 1992; Gani *et al.*, 2009).

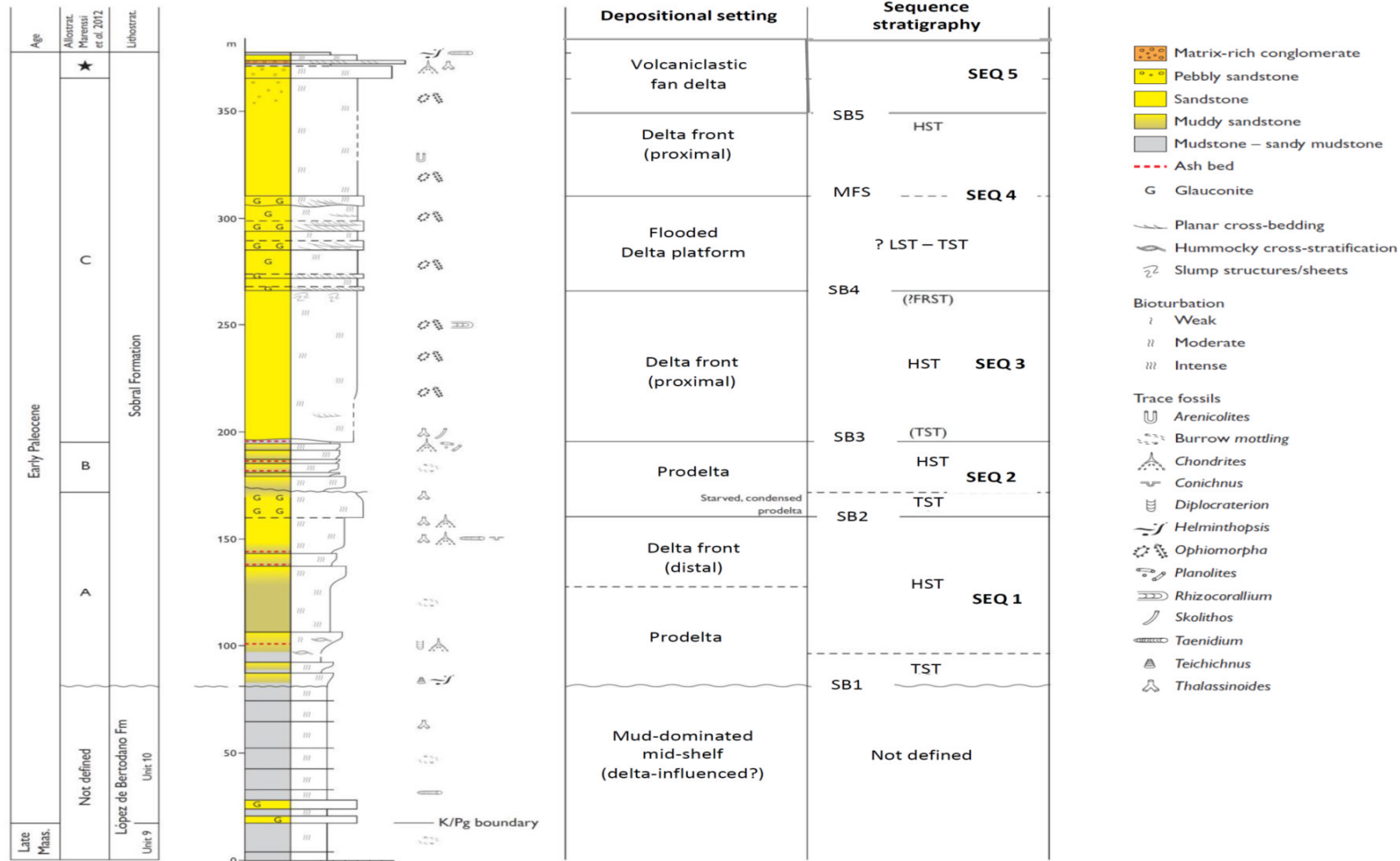


Figure 2. 5. The sedimentary sequence studied in this project, which includes the upper López de Bertodano Formation and the Sobral Formation. Depositional environments are indicated. LST= Low stand tract, HST = High stand tract, TST = Transgressive system tract, FRST = Forced regressive system tract. Courtesy of Jon Ineson.

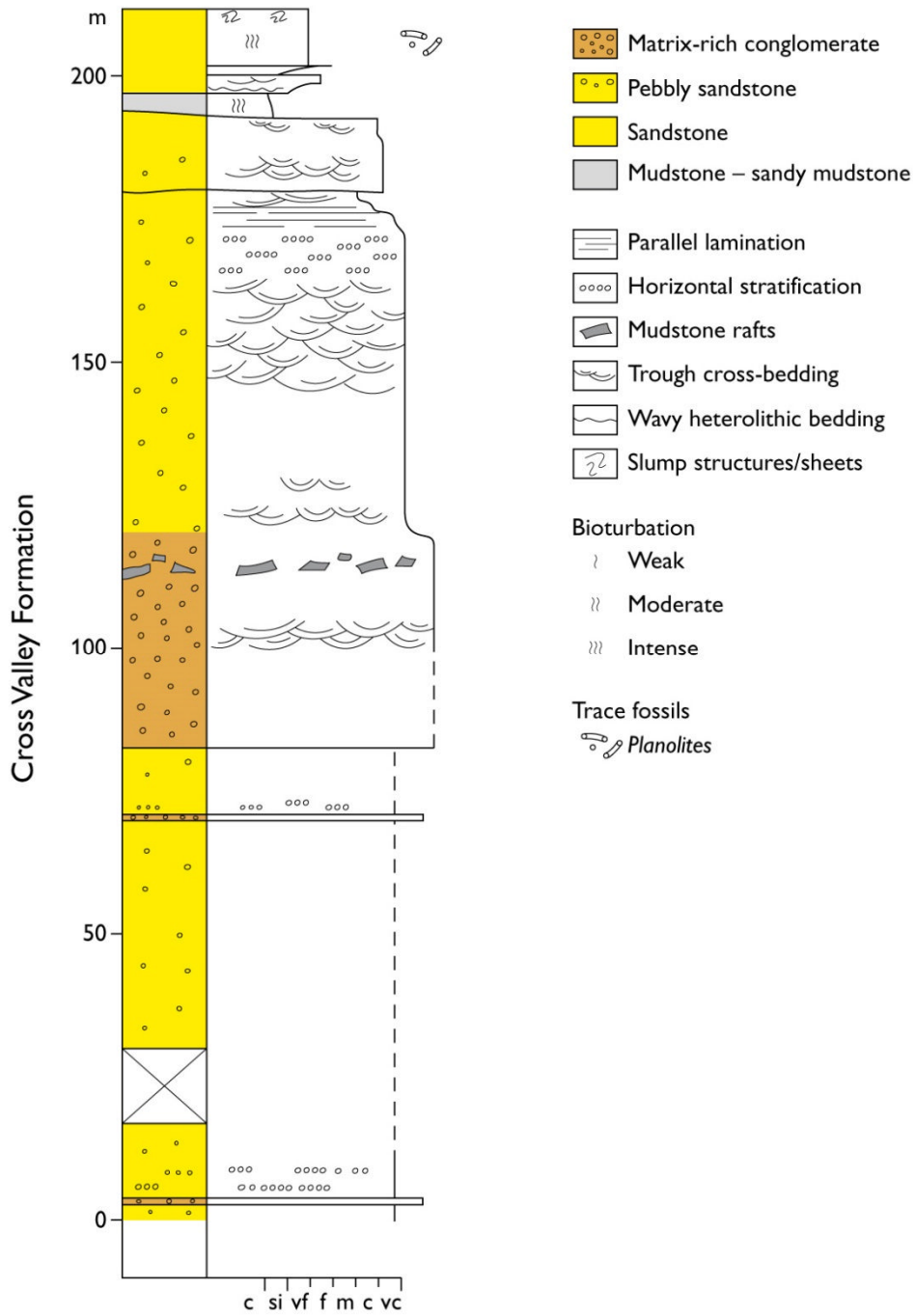


Figure 2. 6. The sedimentary sequence of the Cross Valley Formation studied in this project. Fossil wood occurs within the sandstone units and as clasts within the conglomerates. Courtesy of Jon Ineson.

The sedimentary deposits between 265 – 310m on the sedimentary log consist of fine to medium grained sands with alternating glauconitic sands, representing a flooded delta platform (J Ineson 2015, pers. comm., 13 March). They also have planar and trough cross-bedding, mud-drapes, tidal bundles and reactivation surfaces (J Ineson 2015, pers. comm., 13 March). The presence of glauconitic sands and mud-drapes suggest a high water level and low energy depositional setting, and the tidal bundles and reactivation surfaces represent ebb tidal-flow.

Higher in the succession (310 – 350m height) the Sobral Formation consists of well sorted, mud-poor sandstones which have planar and trough cross-bedding, with *Ophiomorpha* trace fossils. These sediments represent a return to a proximal delta front depositional setting.

From 350m height to the top of the Sobral Formation represents a volcanoclastic fan delta. It consists of sandstones that coarsen upwards into pebbly sandstones and conglomerates. Thin layers of alternating tuffaceous mudstones are also present. The coarse sandstones suggest an increasingly proximal setting but the presence of *Thalassinoides* and *Chondrites* indicates marine conditions persisted. The volcanoclastic nature of the units suggests that the volcanic source may have been closer to the depositional setting at that stage.

Cross Valley Formation: In agreement with previously published work (Askin *et al.* 1988; Wrenn and Hart, 1988; Marensi *et al.*, 2012) on the Cross Valley Formation has been interpreted as the infill of an incised valley (J Ineson 2015, pers. comm., 13 March). The majority of the formation consists of matrix-rich conglomerates and coarse sandstones that are poorly sorted (Figure 2.6). Mudstone rafts are present between 110 – 120m; volcanoclastic material such as pumice, ash and lapilli are present throughout the formation. Trough cross-bedding is present at 100m and also between 150 – 166m in sandstone units. Wood is frequently seen through the formation including charcoalfied logs and fragments. High concentrations of fossil logs (preserved as lignite) are also present with consistent orientations, suggestive of log jams (J. Francis 2015, pers. comm., 1 Sep). The presence of poorly sorted conglomerates and coarse sandstones and trough cross bedding suggests a high energy fluvial

depositional setting. In addition, the mudstone rafts also propose an erosive flow regime, possibly a flood event, where the mud clasts may have been eroded from flood plains of a river system. Today high concentrations of coarse woody debris are common features of river systems that flow through heavily forested areas in Chile (Andreoli *et al.*, 2007). Wood enters river systems by tree fall and erosion of vegetated flood plains. Also large influxes of wood usually occur after large disturbances, such as wildfires or earth quakes.

Volcanic clastic material in the formation suggests that the volcanic arc was active at least before or during the deposition of the formation. Modern day large explosive eruptive events in Chile (e.g. Chaiten volcanic eruption 2008) have caused large scale destruction of forested areas from pyroclastic flows and wildfires, and also deposited large quantities of volcanic tephra on the surrounding land (Umazano *et al.*, 2014). This loose material is removed from the land during periods of heavy rain into nearby river systems, increasing sediment load and thus the destructive power of the rivers. The increase influx of coarse wood debris causes log jams, which trap sediment and increase water level, eventually these jams can break and results in flooding and channel avulsion (the formation of a new river channel). The Cross Valley Formation may represent a similar event.

The top 20m of the Cross Valley Formation represents a return to a marine environment with the presence of mudstone units, slump structures, marine oyster fossils and *Skolithos* burrows (J Ineson 2015, pers. comm., 13 March). This unit is different from the underlying majority of the Cross Valley Formation, and more closely resembles the overlying La Meseta Formation, which represents an estuarine/shallow marine depositional setting (Marensi, 2006). However, the La Meseta Formation is considered a different formation because it is bound by an erosional unconformity.

2.4.2 Age of the sedimentary section

Figure 2.7 presents the most recent age model for the sedimentary sequence studied in this project. It has been assigned a late Maastrichtian to Thanetian age based on dinoflagellate biozones that correlate with dinoflagellate biozones in Late Cretaceous and Paleocene sequences on the east coast of New Zealand (Bowman *et al.*, in revision).

The lowermost 20m of the sequence is late Maastrichtian in age as indicated by the presence of *Manumiella druggii* dinocyst, which is also present in late Maastrichtian units of eastern New Zealand, southeastern Australia and the East Tasman Plateau. The K/Pg is present at the top of this biozone. The first 45m above the K/Pg boundary are defined by the *Hystrihospaeridium tubiferum* Acme Zone which is only found on Seymour Island and has been assigned as Danian age based on previous dating of the units (Bowman *et al.*, 2012). It correlates with the *Trithyrodinium evittii* Acme Zone in New Zealand (Figure 2.7). The *Trithyrodinium evittii* Acme Zone is present at the upper most 15 m part of the López de Bertodano Formation.

Most of the Sobral Formation has been assigned to the Danian age. This is based on the last occurrence of *Palaeoperidinium pyrophorum* at 350m, which also has its last occurrence at the end of the Danian in New Zealand (Crouch *et al.*, 2014). At 350m there is a hiatus and the Selandian is missing (Figure 2.7) (Bowman *et al.*, in revision). The top 25m of the Sobral Formation, after the hiatus, has been allocated to the Thanetian based on the presence of dinocyst genera *Apectodinium*, which first occurs in the Thanetian in New Zealand (Crouch *et al.*, 2014; Bowman *et al.* in revision).

The Cross Valley Formation has been allocated a Thanetian age, which is based on dinoflagellate cyst biostratigraphy undertaken by Askin (1988) and Wren and Hart (1988). Recent work on dating has suggested that the top of the Cross Valley Formation may only be a few hundred thousand years older than the top of the Sobral Formation (V Bowman 2015, pers. comm., 25 September). This is supported by evidence from sedimentology that suggests rapid deposition.

2.5 Fossil wood

Fossil wood is abundant throughout the sedimentary sequence on Seymour Island and the specimens are well preserved, maintaining their three dimensional structure and in some cases growth rings. The majority of the fossil wood is permineralised by calcite and occurs from hand-sized specimens to large fossilised logs (see Figure 2.8) which are found scattered across on the landscape of Seymour Island. Fragments of fossil wood preserved as lignite

are also commonly found throughout the sequence. During the 2009/2010 field season Jane Francis collected fossil wood systematically throughout the sedimentary sequence studied here, ensuring that the exact location of each piece of fossil wood was recorded on measured sections.

In this project 56 wood specimens have been studied and are distributed throughout the measured sedimentary sequence. Figure 2.9 presents the wood specimens studied in this project and their location on the sedimentary log.

A range of wood specimens throughout the section were studied so that possible patterns of wood types and climate regime could be determined through the latest Cretaceous and Paleocene. Some horizons in the sedimentary sequence are represented by more wood specimens than others, such as at 21m and 155m height. This is because at these horizons there are more well preserved large wood specimens that have a long growth ring series. A well preserved wood specimen is considered to be one that appears uncompressed and has growth rings that can be easily seen in hand specimen.

In order to make the presentation clear to the reader of the patterns observed in the data derived from the wood specimens (e.g. climate data) the Sobral Formation has been subdivided into the following sections: lower part, lower to middle part and upper part of the Sobral Formation (see Figure 2.9).

Wood specimens have also been allocated numbers, which are presented in Appendix A, Table A.1. This has been introduced to make the graphs that present climate data for individual wood specimens clear for the reader to interpret.

The following section (2.5.1) will discuss the depositional history of the wood specimens studied in this project. It will explain how the preservation type (e.g. type of mineralisation), size, shape of each wood specimen, and associated sedimentary deposits have been used to determine from where it was originally derived on the Antarctic Peninsula (e.g. upland or lowland areas).

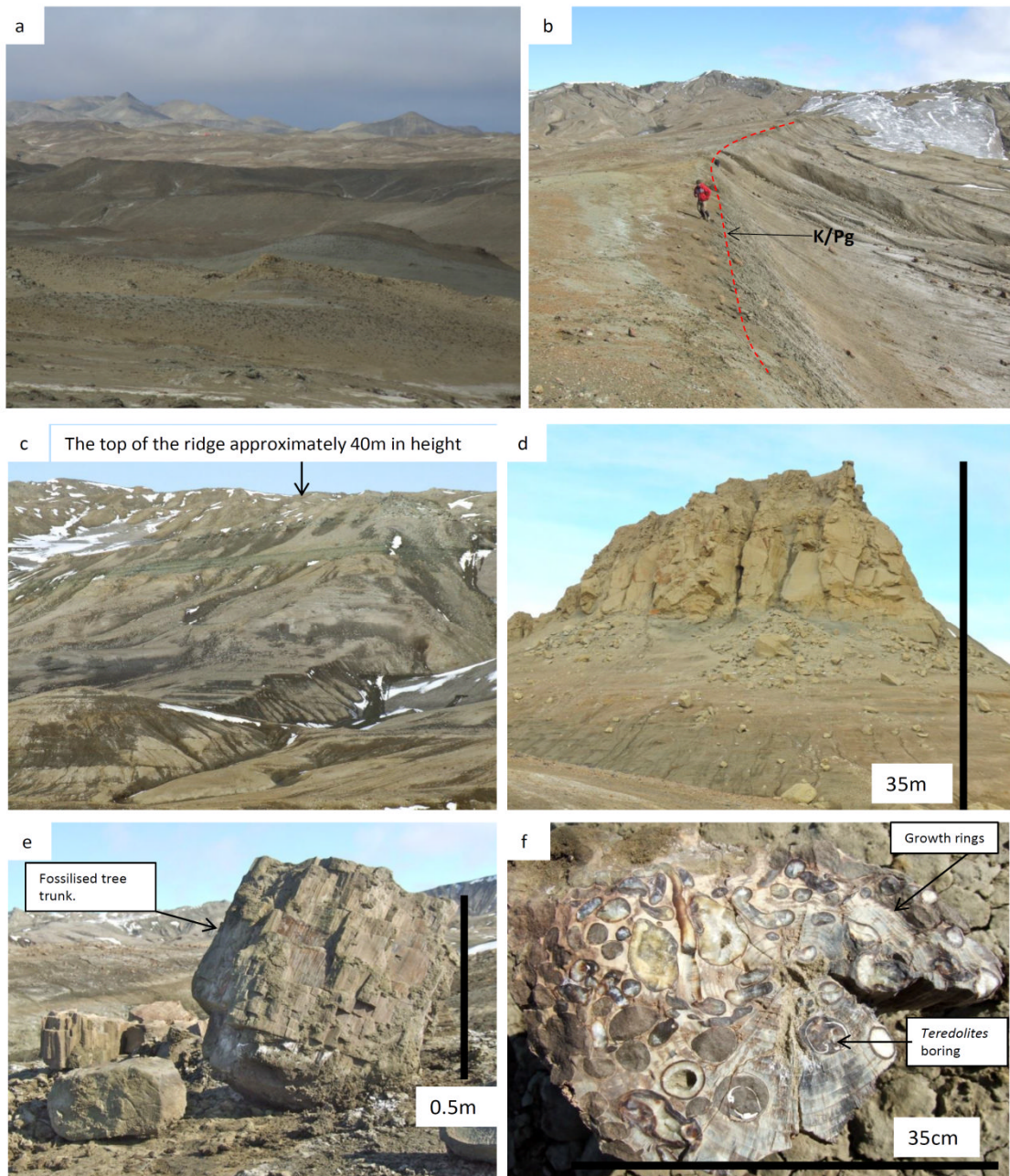


Figure 2. 8. Field photos of the geology of Seymour Island and fossil wood in the field, on Seymour Island. a) The barren landscape of Seymour Island, distance to far hills is 10km. b) The K/Pg boundary (red dashed line) within the López de Bertodano Formation. c) Sobral Formation. d) Cross Valley Formation. e) Fossilised tree trunk. f) Fossil wood with *Teredolites* burrows; growth rings are also visible. Photos are courtesy of Jane Francis.

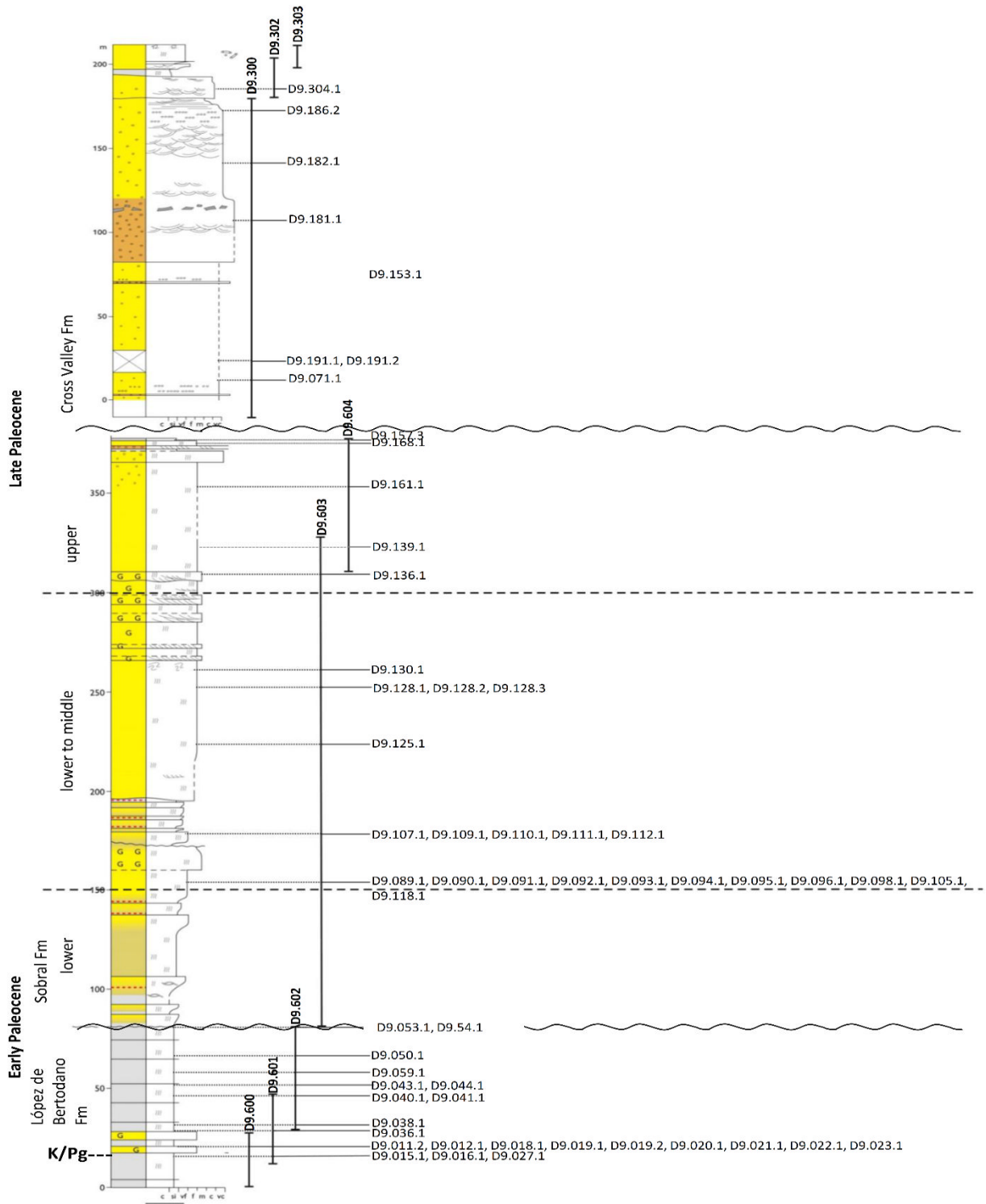


Figure 2. 9. Location of the wood specimens studied in this project on the sedimentary succession. The individual field section lines are represented by black vertical bars. Log courtesy of Jon Ineson.

2.5.1 Depositional history of the fossil wood specimens

The wood specimens here represent allochthonous pieces of wood that were derived from trees that grew on the terrestrial land of the Antarctic Peninsula during the Paleocene. When the trees died or were killed by disturbances the wood was eventually transported via river systems into the back-arc basin.

For each wood specimen its preservation type, size and shape have been catalogued (Appendix A, Table A.2). The uses of the above characteristics in terms of determining depositional history of the wood specimens will be explained in more detail below. Determination of the preservation type for each wood specimen was made from looking at the physical properties in hand specimen and also observing the mineralogy of wood specimens in thin section.

Preservation type: Different preservation types are associated with different environments and therefore are a useful indicator of depositional history/environments. The main preservation types observed in the wood sample here are permineralisation by calcite, permineralisation by haematite, preservation as lignite and charcoalification. Permineralisation by calcite is associated with marine or terrestrial depositional environments, where carbonate-rich waters are present (Buurman, 1972) (see Figure 2.10).

Permineralisation by calcite: In thin section, under cross polarised light, calcite crystals are observed within the lumen of the cells of the wood (see 2.11a,b) and are identified on the basis of having high birefringence and showing extinction to black when the microscope stage was turned (MacKenzie and Adams, 1994). Some of the wood specimens that are permineralised by calcite are also bored by *Teredolites* (Figure 2.10a).

Preservation as charcoal: In modern forests the charcoalification of wood can be caused by lightning, wildfires and volcanic activity (e.g. pyroclastic flows) (Scott, 2010). In the case of this study wood specimens that are charcoalified are interpreted as being derived from trees that were growing in on land areas that were prone to wildfires caused by either lightning or volcanic activity (likely to have affected upland areas). Some of the wood specimens

here are both charcoaled and permineralised by calcite, with a charcoaled outer coating and permineralised centre.

The wood specimens that are both charcoaled and permineralised are black in hand specimen (Figure 2.10e). They appear as petrified wood, although in some cases the wood still has fragments of charcoal on the outside, which have a vitreous lustre, and they leave a black streak on paper. In thin section the cell walls of the wood specimens are black and homogenised in transverse section (TS) (Figure 2.11c, d). Jones and Chaloner (1991) produced charcoal under experimental conditions in order to see how the physical properties of wood change. They found that in charcoaled wood the middle lamella between tracheids is missing and the cell walls between tracheids become homogenised.

Permineralisation by haematite is associated with terrestrial environments. Wood specimens that are permineralised by haematite are red in colour as hand specimens. In thin section, under plane polarised light they are also red and in cross polarized light the infill of the cell lumen is dark brown (Figure 2.10f, Figure 2.11h); these are common microscopic features of haematite (MacKenzie and Adams, 1994).

Shape and size of fossil wood: Wood specimens occur as sedimentary clasts. Those that have rounded and smooth edges are likely to have been transported long distances from their source (see Figure 2.10c). However, this does not mean that wood specimens that have angular edges can be interpreted as having been transported short distances, because wood can float as drift wood and does not necessarily have to be carried as bed load in a river (Braudrick and Grant, 2001). Small pieces are likely to have been transported further than large pieces of wood (Braudrick and Grant, 2001).

The likely depositional history for each wood specimen here is discussed in groups from the López de Bertodano Formation, Sobral Formation (80m to 300m), Upper Sobral Formation (300m onwards) and the Cross Valley Formation. The discussion is set out like this because the majority of wood specimens within each of these different sections have similar characteristics (e.g. permineralised by calcite or have rounded edges). Figure 2.12 shows

the main preservation types, shape and size of the wood specimens studied here, and their position in the sedimentary sequence.



Figure 2. 10. Varieties of wood preservation. a) D9.012.1, wood specimen that is permineralised by calcite. Growth rings and *Teredolites* borings can be seen. b) D9.012.1 wood specimen that is permineralised by calcite. c) D9.161.1 wood specimen that has a rounded edge. d) D9.050.1 wood that is heavily bored by *Teredolites*. e) D9.139.1 wood specimens that has a rounded edge. f) D9.191.1 wood specimen permineralised by haematite. Scale bars = 2cm.

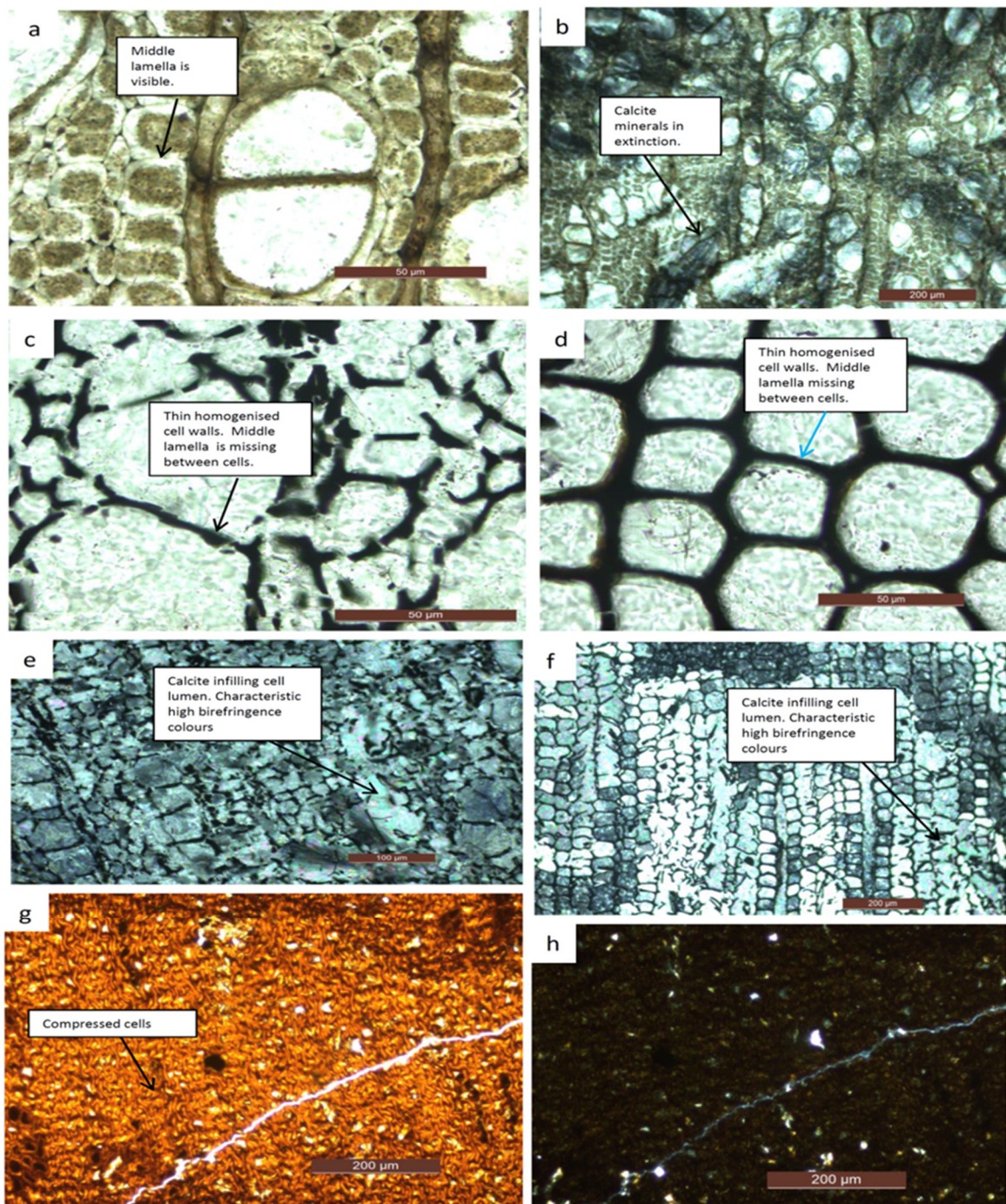


Figure 2. 11. Wood preservation variety seen in thin section. a) D9.012.1 plane polarized light, calcite permineralised; the layers of the fibre wall and also the middle lamella between neighbouring fibres can be seen; scale bar = 50 μ m. b) D9.012.1 calcite crystals in cross polarised light; scale bar = 200 μ m. c) D9.089.1 plane polarized light, charcoalified wood that has been permineralised by calcite, cell walls are homogenised; scale bar = 50 μ m. d) D9.161.1 plane polarised light, charcoalified wood that has been permineralised by calcite, cell walls are homogenised, scale bar = 50 μ m. e) D9.089.1, cross polarised light, calcite in lumen of the cells, scale bar = 100 μ m. f) D9.161.1 cross polarized light, calcite in the lumen of the cells, scale bar = 200 μ m. g) D9.191.1, plane polarised light, wood permineralised by haematite shown by the orange/red colour, also shows compression of cell walls, scale bar = 200 μ m. h) D9.191.1 cross polarised light, haematite observed as dark brown, scale bar = 200 μ m.

Depositional history of wood specimens from the López de Bertodano Formation lower, and lower to middle Sobral Formation (between 80 to 300m): The wood specimens from the López de Bertodano Formation and Sobral Formation are associated with marine mudstones and sandstones. At 21m on the sedimentary section 11 wood specimens are associated with a glauconitic horizon (Figure 2.12). Most of the wood specimens that are located within the López de Bertodano Formation and Sobral Formation (at 80 to 300m) are permineralised by calcite and are angular in shape. These characteristics and the associated sediments suggest that the wood specimens were likely to have been deposited in a marine environment. The fact that the wood specimens have angular edges suggests that they may have been transported short distances from their source, so they may have been derived from lowland areas on the Antarctic Peninsula. However, as mentioned in the previous section, angular shape is not a definite indicator of how far a wood specimen has been transported because it may have floated as driftwood or even deposited rapidly by a flash flood. In addition, many wood specimens are angular in shape because they have broken up while being weathered on the landscape today.

A number of the wood specimens also have *Teredolites* borings (see Figure 2.12a) (specimens D9.012.1, D9.021.1, D9.038.1, D9.041.1 D9.044.1, D9.050.1, D9.054.1, D9.091.1, D9.092.1, D9.093.1, D9.098.1, D9.107.1, D9.109.1, D9.110.1, D9.111.1, D9.112.1, D9.118.1, D9.125.1 and D9.153.1). *Teredolites* are tubular borings in wood substrates made by marine teredinid bivalves (see Figure 2.10d) (Savrda, 1991; Savrda *et al.*,1993). The wood substrates include drift wood and allocthonous wood pieces that have become saturated and deposited on the sea floor, as well as flooded coastal forests. The *Teredolites* ichnofacies is found in shallow marine and deep marine environmental settings (Savrda, 1991).

The wood specimens are associated with a glauconitic horizon at 21m. Glauconite is associated with shallow marine environments and low sedimentation rates (Nichols 1999). The glauconitic horizons in the sedimentary sequence here have a high concentration of wood (J Francis

2015, pers. comm. 1 September). Transgressions are sometimes represented by low sedimentation rate and this may be a possible reason for the formation of glauconite (Savrda, 1991; Savrda *et al.*, 1993). Also low sedimentation rate may mean that wood that has been gradually deposited on the basin floor may have been more concentrated. Also a high abundance of wood may have been caused by vegetated coastal areas being eroded by rising sea level. A transgression may have meant that wood from more inland areas was more likely to have been transported into the basin as well.

At 75m on the section two wood specimens (D9.090.1 and D9.089.1) have rounded edges and are charcoaled and permineralised by calcite. When observed in thin section the tracheid walls of each specimen, in transverse section, are black and homogenised. Calcite crystals have formed within the lumen of the cells. It is likely that these wood specimens were originally derived from trees living in upland areas on the volcanic arc, which were likely to be more prone to wildfires caused by volcanic activity. When the trees died or if they were destroyed by the wildfire, the wood specimens would have been transported into the back-arc basin via river systems where they may have floated for a while before becoming saturated by water and sinking to the bottom of the basin and then permineralised by calcite.

Upper Sobral Formation (from 300m to 390m): Five wood specimens were collected from the upper part of the Sobral Formation. Three of the wood specimens are associated with delta top facies (wood specimens D9.136.1, D9.139.1, D9.161.1) and two specimens are found in volcanoclastic fan delta facies (wood specimens D9.168.1 and D9.157.3). Three of the wood specimens are both charcoaled and permineralised by calcite (D9.139.1, D9.161.1, D9.157.3). Wood specimens D9.136.1 and D9.168.1 are permineralised by calcite. Wood specimens D9.136.1 and D9.161.1 also have rounded edges, which suggests that they may have undergone more transport. The charcoaled wood specimens are also likely to have originated from more inland areas close to the volcanic centres, in areas that were more at risk of wildfires caused by volcanic activity. The likely reason for the higher frequency of charcoaled wood specimens found in the upper Sobral Formation is due to the depositional setting being more proximal to the land of

the volcanic arc, resulting in more material from inland areas reaching the basin.

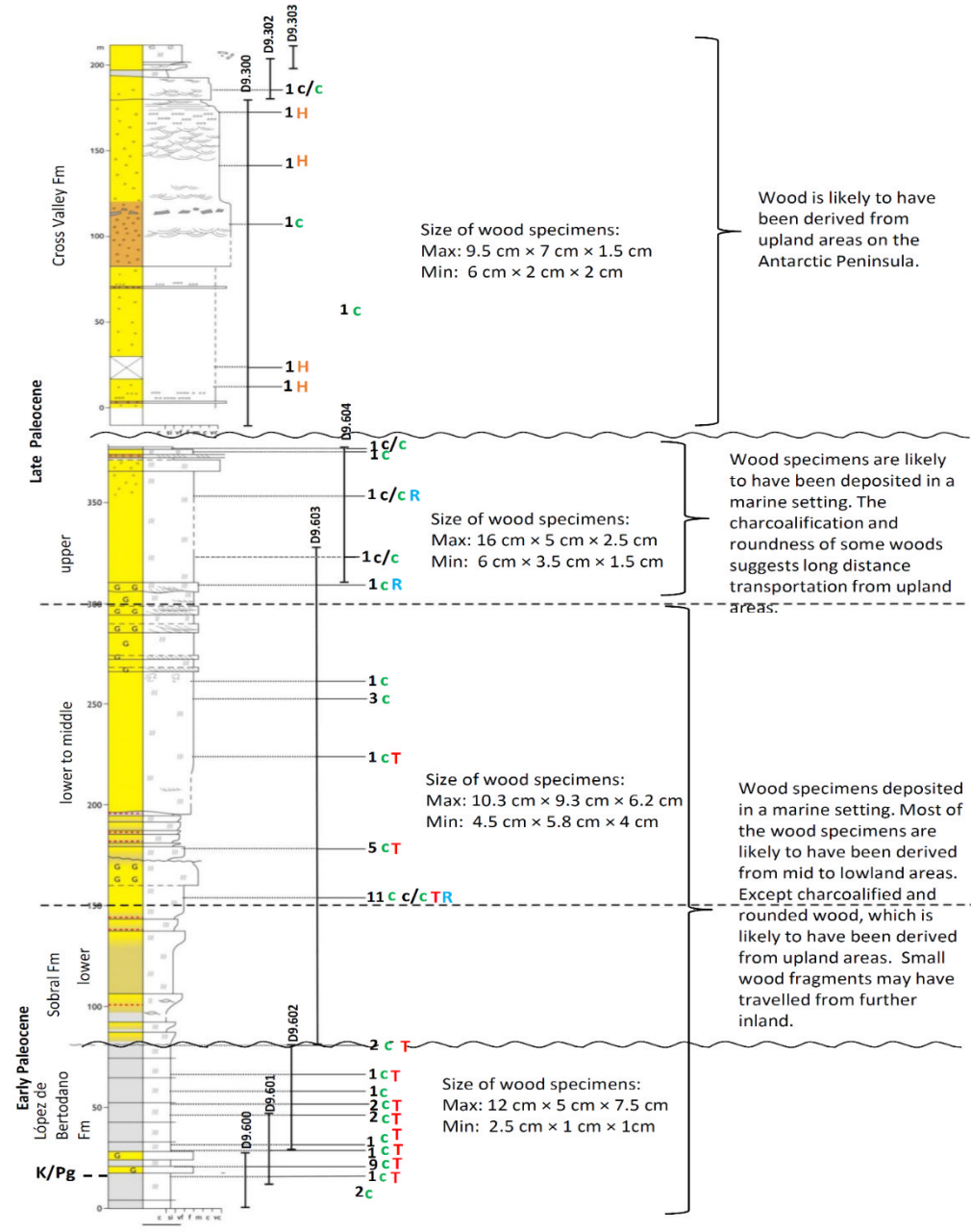
Cross Valley Formation: In this project 7 wood specimens (D9.071.1, D9.191.1, D9.191.2, D9.153.1, D9.181.1, D9.182.1, D9.186.1 and D9.304.1) have been studied from the Cross Valley Formation. Most of the fossil wood in this has been significantly compressed as lignite. Figure 2.11g,h presents a photo of wood specimens from the Cross Valley Formation in thin section; the cells are highly compressed making it difficult to distinguish any anatomical features. Some of wood specimens from the Cross Valley Formation are permineralised by calcite (D9.153.1 and D9.304.1), which supports the interpretation of a marine environment for the finer grained sedimentary deposits in the lower and upper parts of the formation. Some wood is permineralised by haematite (D9.071.1, D9.191.1, D9.191.2, D9.181.1, D9.182.1 and D9.186.1). This wood was probably preserved originally in a terrestrial setting but then eroded as clasts that were incorporated into the conglomeratic sandstones that were themselves the product of high-energy volcanoclastic flows into the basin. In addition, some wood was probably deposited very quickly by the high energy surge that deposited the Cross Valley Formation, causing them to be compressed during burial before they could be permineralised.

2.6 Summary

Fossil wood is present within the James Ross Basin on the eastern side of the Antarctic Peninsula. The fossils represent trees that were originally growing on the volcanic arc land areas to the west. When they died they were transported down rivers and floated out to sea as driftwood. Eventually they became waterlogged and were buried in the basin sediment, later to become permineralised.

Three types of preservation have been identified: i) preservation by calcite, relating to the marine environment, ii) preservation as logs which have been charcoalified (probably burnt in wildfires on the volcanic arc) and then permineralised by calcite in the marine environment, and iii) wood preserved by haematite-rich fluids while it was originally buried in terrestrial settings

before being eroded as clasts in the surge-like activity that formed the Cross Valley Formation deposits.



Key		
C Calcite permineralisation	c/c Charcoalification and permineralised by calcite	
H Haematite permineralisation	R Rounded edges	T Bored by <i>Teredolites</i>

Figure 2. 12. The types of preservation observed in the wood specimens throughout the sedimentary sequence. The numbers refer to the number of wood specimens studied at each horizon. Sedimentary log courtesy of Jon Ineson.

Chapter 3

Conifer wood

3.1 Introduction

This chapter presents morphological descriptions of conifer taxa found in Paleocene strata on Seymour Island section. The anatomical features and keys that are used to identify conifer types are discussed here followed by descriptions of the main conifer types in the fossil wood assemblage. Possible modern analogues are also considered and a brief summary of the possible palaeoecology of the Paleocene forests is presented.

3.2 Conifer wood anatomy and identification

Conifer wood consists of vertical tube-like structures called tracheids (Figure 3.1). The main purpose of tracheids is to transport water throughout the tree (Fritts, 1976). The radial walls of tracheids have bordered pits, which allow water to flow from one tracheid to the next. Running radially across the tracheids are rays, which store and transport nutrients throughout the tree. Areas where tracheids and ray cells intersect are called cross-fields and they contain cross-field pits. The arrangement of bordered pits and the type of cross-field pits are important features for identifying conifer wood, both modern and fossil. The nature of rays and the presence or absence of features, such as axial parenchyma, are also useful in the identification of conifer wood. Table 3.1 presents a glossary of anatomical features and wood terms used in this chapter.

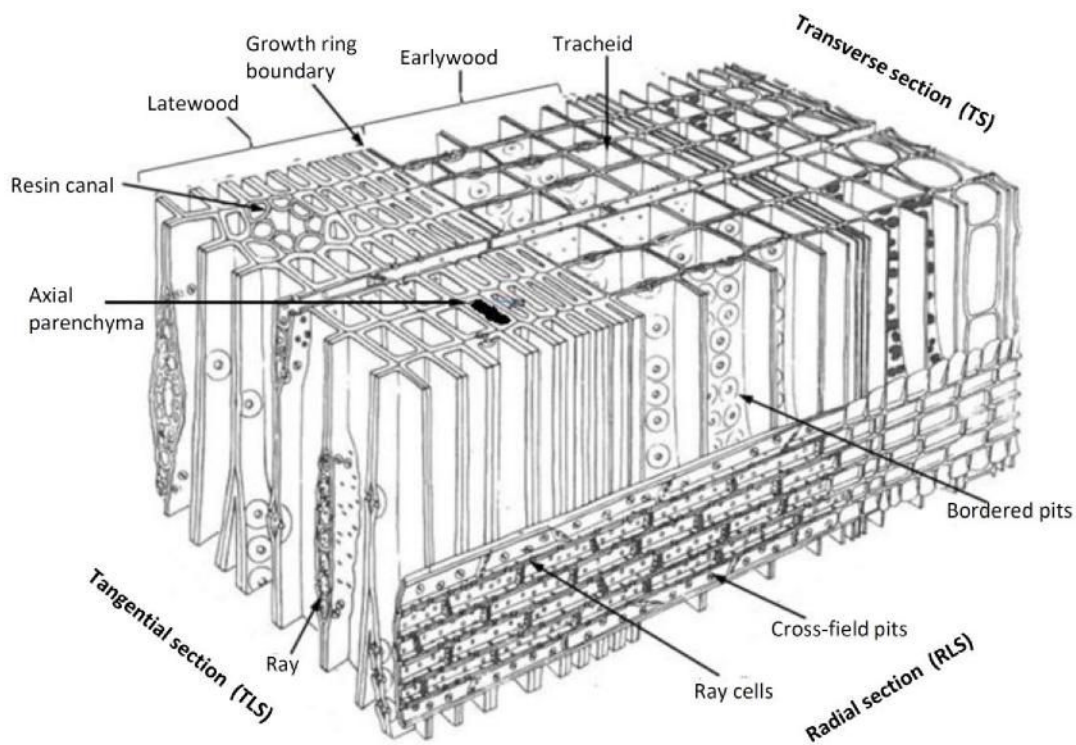


Figure 3. 1. The three dimensional structure of conifer wood. Modified from Schweingruber (1996).

In general, conifer wood is considered to be conservative, meaning that there is little difference in anatomical features between wood types. Some features, such as ray height, can vary within different parts of a single tree, such as in the root, branch or trunk wood (Chapman, 1994; Falcon-Lang, 2005a). In order to overcome these challenges when identifying modern conifer wood, identification keys have been developed (Greguss, 1955; IAWA Committee, 2004). Identification keys provide precise and detailed methods for measuring and describing anatomical features in conifer wood. They also give standard procedures for nomenclature, and a list of wood features that characterise different conifer taxa. These keys were used in this project.

Identification of fossil wood has been shown to be problematic because many fossil wood genera and species have been published based on poorly preserved and isolated specimens where the origin of the sample from within a tree has not been considered or was unknown (Philippe and Bamford, 2008; Philippe, 2011). There is also confusion over nomenclature

and miss-interpretation of fossil wood descriptions, which is a result of most wood types being described in the early 20th century when there was no universal standard procedure for description. Philippe and Bamford (2008) have attempted to reduce the ambiguity of fossil conifer wood taxonomy by revising original fossil wood descriptions and re-examining type specimens, and subsequently developing a new identification key.

Table 3. 1. List of conifer wood features and their definitions used in this thesis. IAWA committee (2004), Greguss (1955) and Fritts (1976).

Feature	Description
Bordered pits (Figure 3.2a, b, c)	Observed in radial section. Localised thickening of the tracheid walls with circular, rod-shaped, elliptical or slit-like apertures in the middle. Also referred to as tracheid pitting. The main purpose is to allow the flow of water from one tracheid to the next.
Compression wood	Forms on the lower side of leaning stems or branches to give mechanical support against gravitational pull. The features of compression wood include rounded and thick walled tracheids that have intercellular spaces between each other. In addition, growth rings tend to be wider than in the normal wood.
Cross-field (Figure 3.2g)	Observed in radial section. An area that is bound by the intersecting walls of a single tracheid and ray cell.
Cross-field pits (Figures 3.1 & 3.2d, e, f, g, h, i, j, k)	Observed in radial section. Found within cross-field areas. They occur in a number of forms: Oopores are cross-field pits with no borders; Oculipores are cross-field pits with borders.
Earlywood (Figure 3.1)	Observed in transverse section. The inner part of a growth ring that forms at the beginning of the growing season. Defined by larger tracheids with thin walls.

Table 3.1. continued

Features	Description
False rings	A band of narrow tracheids that resemble latewood cells within an annual growth ring, giving the appearance of multiple narrow rings. They are caused by inadequate conditions during the growing season, especially drought.
Growth rings (Figure 3.1)	Best observed in transverse section. Concentric layers representing an annual increment, formed of earlywood and latewood.
Latewood	Observed in transverse section. The outer part of a growth ring that forms towards the end of the growing season. Defined by smaller, radially flattened tracheids with thick walls.
Parenchyma (Figure 3.1)	Observed in transverse, radial and tangential sections. Cells with thin, pitted or smooth walls. The two main types are: 1) Axial parenchyma longitudinal cells that form parallel to the stem, which in transverse section can be diffuse or occur in tangential lines; 2) Ray parenchyma composed of horizontal cells that run radially through the wood.
Rays (Figure 3.1)	Best observed in radial and tangential section. Layers of parenchyma cells that run radially through the wood. In tangential view they can be uniseriate, biseriate or multiseriate. Their function is to store and transport nutrients.
Ray tracheid	Observed in radial section. They are found on the margins of rays and have bordered pits.
Resin spool (Figure 3.7)	Best observed in radial section. Organic matter (usually resin) found in tracheids. Usually "bow-tie" shaped
Tracheids (Figure 3.1)	Long unicellular wood element with a long axis parallel to the stem. Its function is water conduction and mechanical

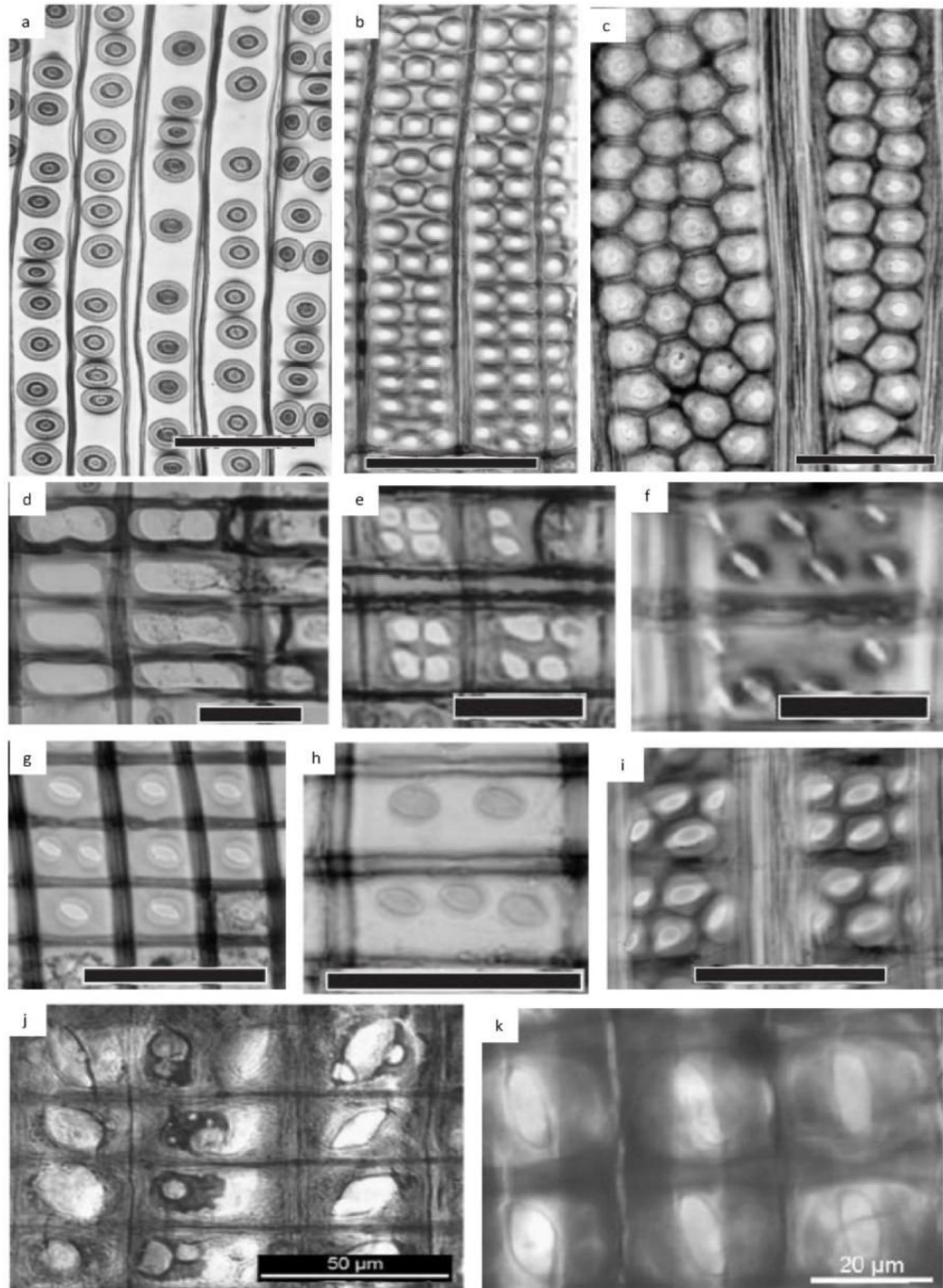


Figure 3. 2. Plate showing different types of tracheid and cross-field pitting defined by the IAWA Committee (2004) and Philippe and Bamford (2008). a) Uniseriate tracheid pitting, scale bar = 100 μ m. b) Biseriate and triseriate tracheid pitting, opposite arrangement, scale bar = 50 μ m. c) Multiseriate and biseriate tracheid pitting with arrangement alternate, scale bar = 50 μ m. d) Window-like cross-field pitting, scale bar = 50 μ m. e) Pinoid cross-field pits, scale bar = 50 μ m. f) Piceoid cross-field pits, scale bar = 20 μ m. g) Cupressoid cross-field pits, scale bar = 50 μ m. h) Taxodioid cross-field pits, scale bar = 50 μ m. i) Araucarioid cross-field pits, scale bar = 50 μ m. j) Phyllocladoid cross-field pits, scale bar = 50 μ m. k) Podocarpoid cross-field pits, scale bar = 20 μ m. Images a-i are from IAWA Committee (2004) and images j and k are from Philippe and Bamford (2008).

The fossil conifer wood in this project was described using features and measurements recommended by the IAWA committee (2004) wherever possible. Additional features considered to be useful for identification of fossil wood by Philippe and Bamford (2008) were also used. The terminology used to describe the different types of cross-field and tracheid pitting is shown in Figure 3.2. Other quantitative measurements that are routinely recorded in fossil wood descriptions, such as tracheid and pit diameter, have also been recorded here.

The Antarctic wood specimens were identified using the fossil conifer wood key developed by Philippe and Bamford (2008). The specimens were also compared to published descriptions of fossil wood from Antarctica and the Southern Hemisphere. Descriptions of extant wood have also been used for comparison, for example, those of Greguss (1955), Meylan and Butterfield (1978) and Patel (1968).

In an attempt to identify Antarctic fossil wood in a more precise and repeatable way, Falcon-Lang and Cantrill (2000) and Falcon-Lang and Cantrill (2001) developed a method to quantify the occurrence of certain features such as tracheid pitting. The percentage of uniseriate, biseriate and triseriate tracheid pitting; opposite versus alternately arranged multiseriate tracheid pitting; and touching versus spaced tracheid pitting. They used this method to separate fossil wood taxa into species. Figure 3.3 has been taken from Falcon-Lang and Cantrill (2001) and is used to demonstrate this method. Quantitative wood characteristics are plotted against each other and different wood genera should form distinct groups in different areas of the graph. Different species belonging to a genus will form groups within the same area of the graph.

In order to assist with identification in this project and to allow comparison with previous descriptions, tracheid, ray and cross-field pits characteristics were quantified here according to the method of Falcon-Lang and Cantrill (2000). Quantification was based on 50 random measurements for each of the above characteristics observed in earlywood. To comply with the IAWA committee (2004), the occasional presence of locally biseriate pitting was not included. See section 3.3.

Due to the problems with fossil wood taxonomy discussed above, the wood in this project was not assigned to published species. Different species identified in this project were assigned as letters (e.g. species A, B and C).

Twenty-five conifer wood specimens have been fully identified. The genera present are *Agathoxylon* (13 wood specimens), *Phyllocladoxylon* (6 wood specimens), *Protophyllocladoxylon* (5 wood specimens) and *Podocarpoxylon* (1 wood specimens). Wood specimens assigned to *Agathoxylon* have been separated into 4 species. Also *Protophyllocladoxylon* wood has been separated into 4 species. Two wood specimens could not be assigned a generic level but have similarity to *Cupressinoxylon* and *Podocarpoxylon*.

Section 3.4 presents each genus as summarised morphological descriptions and image plates illustrating the main anatomical features. In addition, where there is more than one specimen belonging to a genus, a summary table has been compiled of the anatomical features for each specimen. For each genus a brief description of the ecology of its nearest living relative is also given.

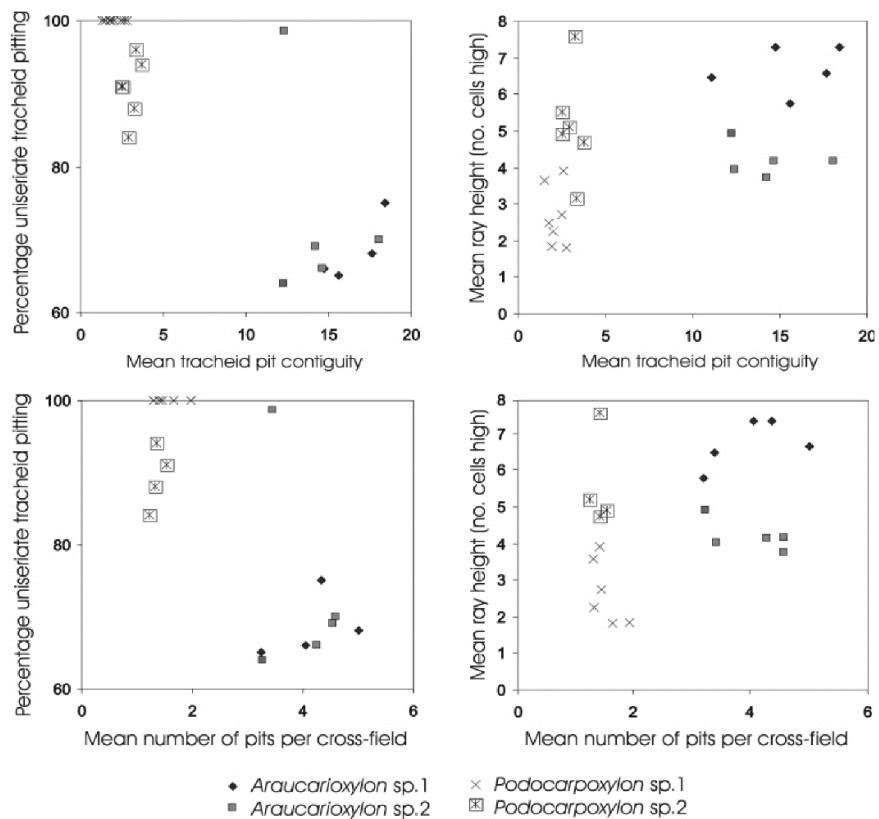


Figure 3. 3. The distribution of conifer taxa when quantitative anatomical features are plotted against each other. Different wood genera plot in different areas of the graphs. Different species within a genera will plot in the same area but will form discrete groups. Taken from Falcon-Lang and Cantrill (2001).

3.3 Quantitative analysis of anatomical features of fossil conifer wood taxa identified in this project.

In order to help distinguish different conifer wood taxa, anatomical characters were quantified for each specimen, and plotted against each other (Figure 3.4, 3.5, 3.6, 3.7), following the method used by Falcon-Lang and Cantrill (2000, 2001). The characters that were used are: percentage of uniseriate tracheid pitting, percentage of touching tracheid pitting, mean ray height (number of ray cells), and mean number of pits per cross-field. According to Falcon-Lang and Cantrill (2000, 2001) these characters have the highest variability between wood taxa. The method was developed so that fossil wood could be identified in a precise and repeatable way. When characters are plotted on to graphs different conifer taxa separate into different groups.

Qualitative anatomical features such as the presence of resin spools, tangential pitting and type of cross-field pitting (e.g. type of oopores in *Protophyllocladoxylon*) have also been considered when separating the wood specimens to species level. This is further discussed for each genera in section 3.4

The four conifer genera identified in this project form separate groups in at least three of the graphs (Figure 3.4, 3.5, 3.6). This shows that they represent different taxa. In Figure 3.7 *Phyllocladoxylon* and *Protophyllocladoxylon* cluster together, because both are characterised by having a low number of pits per cross-field.

Figure 3.7 exhibits high variability in mean ray height and mean number of cross-field pits among the specimens. A possible explanation is that ray height and the number of pits per cross-field has been proven to vary within different parts of a tree (e.g. branch or trunk wood) (Falcon-Lang, 2005a); the wood specimens here are most likely to represent wood from different parts of trees hence the wide scatter on the graphs.

The wood assigned to *Agathoxylon* separate into different species. Wood specimens D9.022.1, D9.044.1 and D9.168.1 are considered to be a separate *Agathoxylon* species. These specimens have a similar percentage of uniseriate tracheid pitting, and form a separate group in figures 3.5 and 3.6. Specimen D9.109.1 is also considered a separate species because it has no

uniseriate pitting, and plots in different regions from the other *Agathoxylon* woods in Figure 3.5 and 3.6. Specimen D9.139.1 is considered a separate species on the basis of having a lower percentage of uniseriate tracheid pitting, and a lower mean number of pits per cross-field compared to the other *Agathoxylon* wood (Figure 3.5, 3.6). The other *Agathoxylon* wood specimens are considered to be the same species because they all cluster closely together in all of the graphs (Figure 3.4, 3.5, 3.6 and 3.7).

Protophylocladoxylon wood specimens are spread out in Figure 3.4, 3.5 and 3.6. Specimens D9.093.1 and D9.112.1 are likely to be the same species, as they plot close together on all of the graphs. Wood specimens D9.071.1, D9.153.1 and D9.181.1 are considered to be three separate species. They have significantly different percentages of uniseriate tracheid pitting, and plot in different regions in figures 3.5 and 3.6.

All of the *Phyllocladoxylon* wood specimens, except specimen D9.125.1, cluster closely together in figures 3.4, 3.5, 3.6 and 3.7 and are therefore considered the same species. Specimen D9.125.1 plots separate from the other *Phyllocladoxylon* wood specimens in figures 3.4 and 3.7 because it has higher rays. It could be a separate species but other characteristics need to be considered and this is further discussed in section 3.4.2.

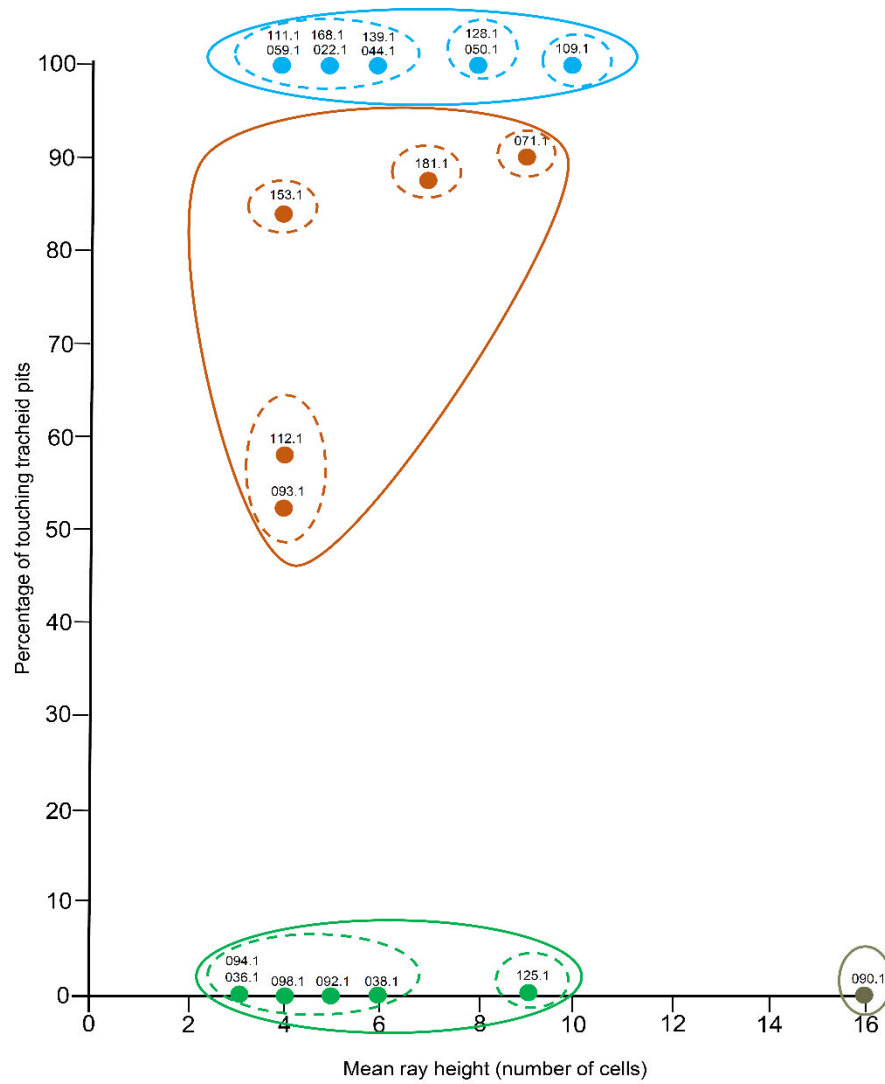


Figure 3. 4. Identification of conifer wood taxa based on quantification of anatomical features: mean ray height (number of cells) and percentage of touching tracheid pits. *Agathoxylon* = blue dots, *Phyllocladoxylon* = green dots, *Protophyllocladoxylon* = orange dots, and *Podocarpoxylon* = brown dots. The quantitative features chosen are the same as used by Falcon-Lang and Cantrill (2000, 2001).

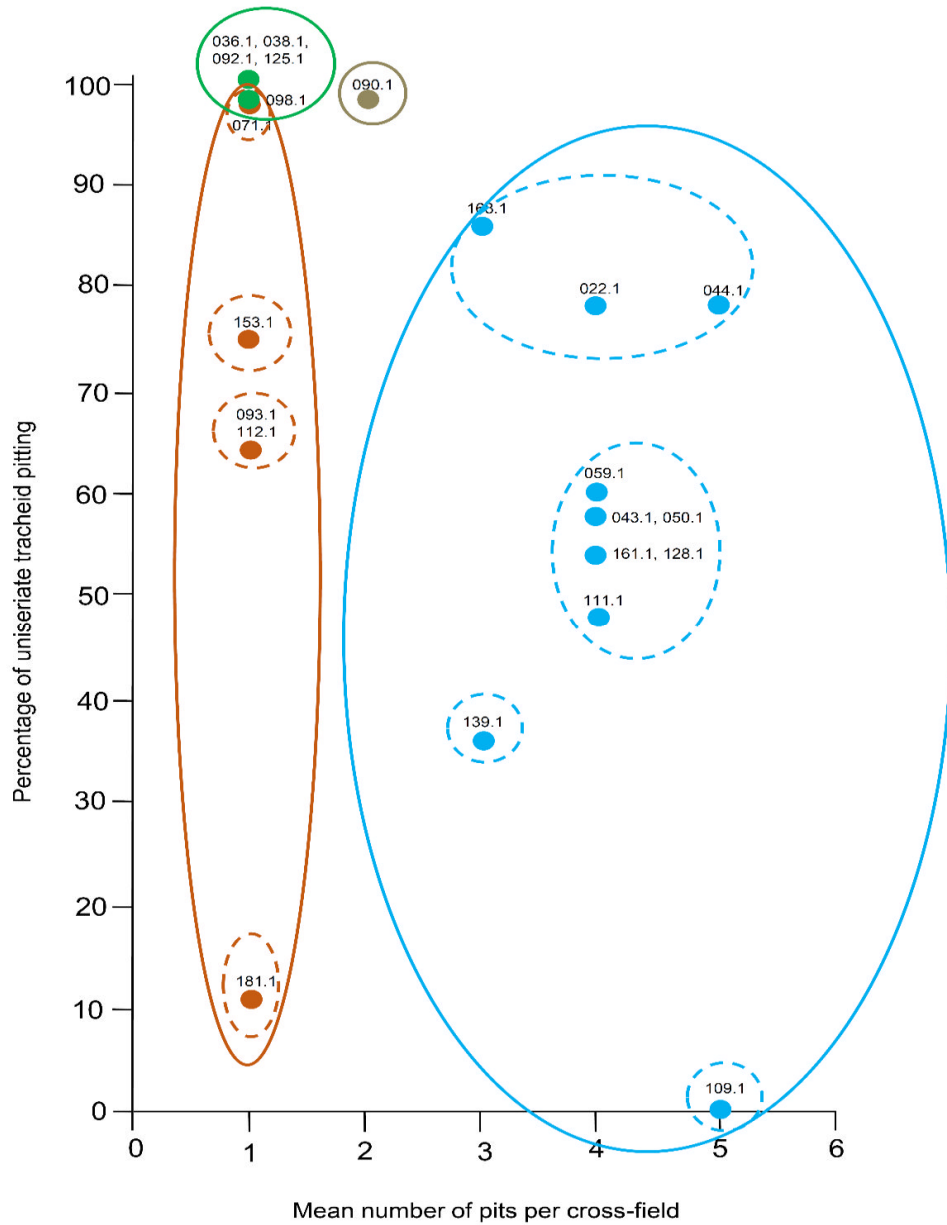


Figure 3. 5. Identification of conifer wood taxa based on quantification of anatomical features: mean number of pits per cross-field and percentage of uniseriate pitting. *Agathoxylon* = blue dots, *Phyllocladoxylon* = green dots, *Protophyllocladoxylon* = orange dots, and *Podocarpoxyton* = brown dots. The quantitative features chosen are the same as used by Falcon-Lang and Cantrill (2000, 2001).

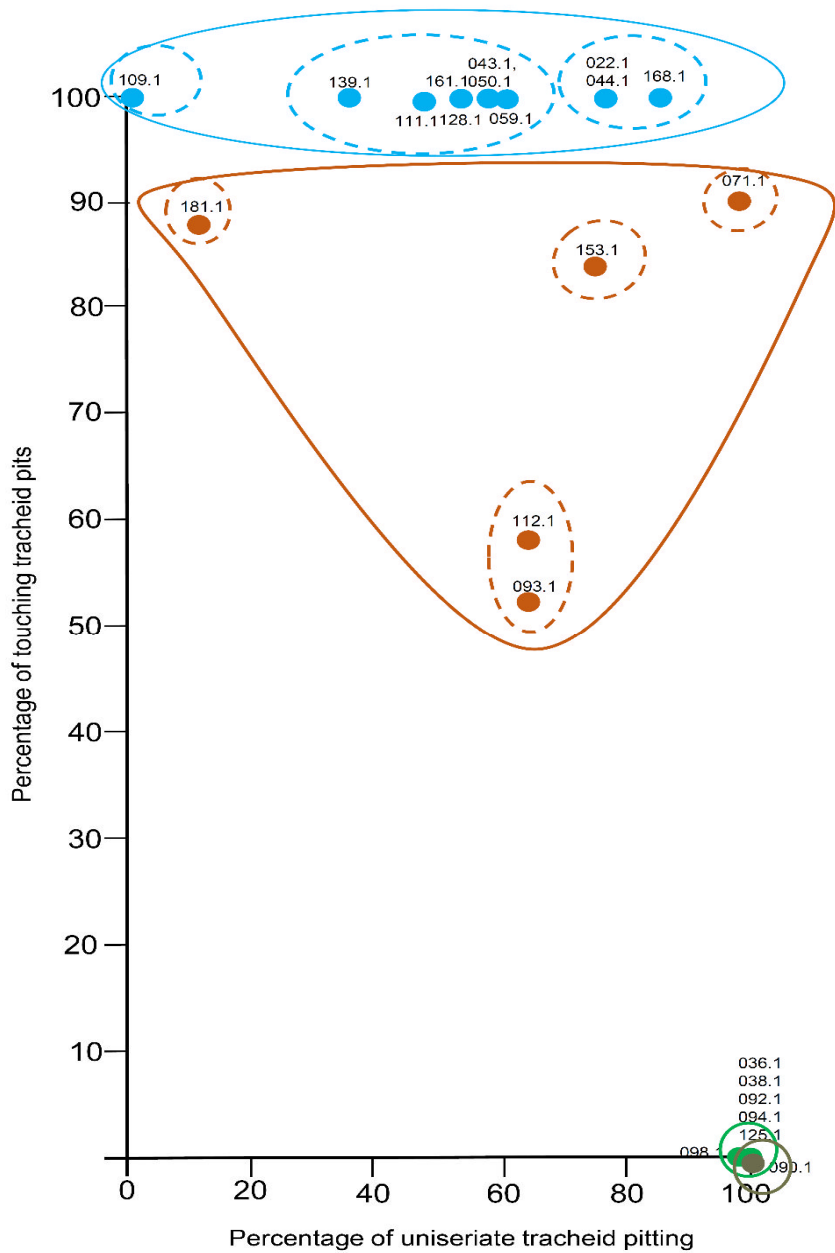


Figure 3. 6. Identification of conifer wood taxa based on quantification of anatomical features: percentage of uniseriate tracheid pitting and percentage of touching tracheid pits. *Agathoxylon* = blue dots, *Phyllocladoxylon* = green dots, *Protophyllocladoxylon* = orange dots, and *Podocarpoxyton* = brown dots. The quantitative features chosen are the same as used by Falcon-Lang and Cantrill (2000, 2001).

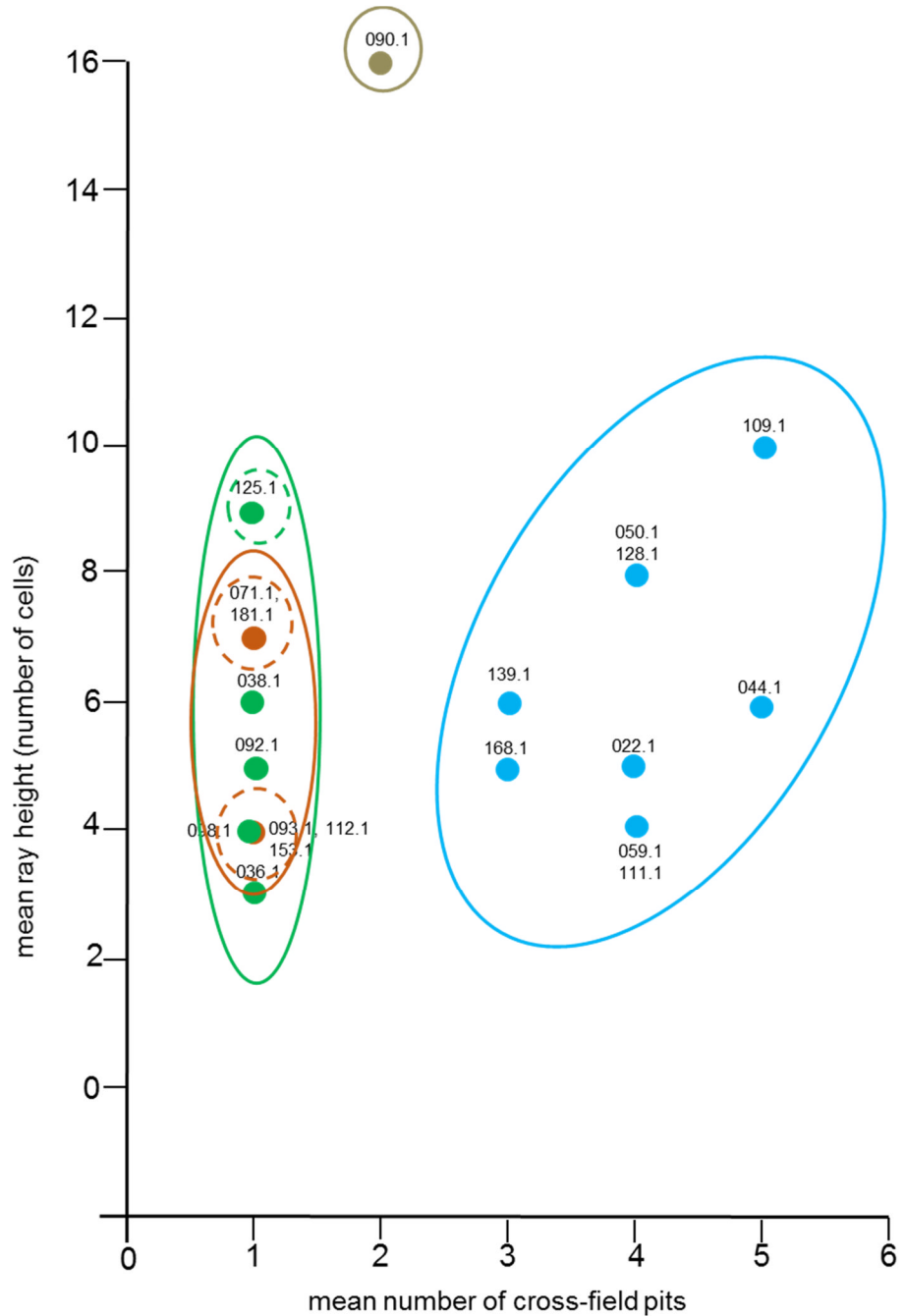


Figure 3. 7. Identification of conifer wood taxa based on quantification of anatomical features: mean number of pits per cross-field and mean ray height (number of cells). *Agathoxylon* = blue dots, *Phyllocladoxylon* = green dots, *Protophyllocladoxylon* = orange dots, and *Podocarpoxylon* = brown dots. The quantitative features chosen are the same as used by Falcon-Lang and Cantrill (2000, 2001).

3.4 Description of fossil conifer wood studied in this project

This section presents descriptions of each genus. In this section a general summary of each genus is presented. Measurements for individual genus are in Appendix B. Four conifer genera were identified in the Paleocene wood assemblage: *Agathoxylon*, *Phyllocladoxylon*, *Protophyllocladoxylon* and *Podocarpoxyton*.

3.4.1 *Agathoxylon*

Genus: Araucariaceae

Morphotype: *Agathoxylon* Hartig

3.4.1.1 Description

Specimen numbers: D9.022.1, D9.044.1, D9.043.1, D9.050.1, D9.059.1, D9.109.1, D9.111.1, D9.128.1 D9.136.1, D9.139.1, D9.161.1, D9.168.1, D9.304.1

Description: D9.109.1, D9.139.1 and D9.161.1 are likely to have been derived from mature stem wood due to the distinctiveness of growth ring boundaries, and low curvature of the growth rings. Other specimens (D9.043.1, D9.50.1, D9.059.1, D9.111.1, D9.128.1, D9.161.1) may have been derived from stem or branch wood, because their growth ring boundaries are distinct.

Specimens D9.022.1, D9.044.1 and D9.168.1 could have been derived from stem, branch or root wood because their growth rings are indistinct. The wood specimens also did not include a pith, and so a definite location in the tree could not be confirmed. False rings are present in D9.022.1, D9.050.1 and D9.059.1. Compression wood is absent in all specimens, except D9.043.1. Specimens D9.136.1 and D9.304.1 were studied as small fragments under SEM, and growth rings could not be seen, so their location within the tree is unknown.

Growth rings: Growth rings are distinct (D9.050.1, D9.059.1, D9.109.1, D9.111.1, D9.139.1, D9.128.1 D9.161.1) (Figure 3.8a) or indistinct (D9.022.1, D9.044.1, D9.168.1). The transition from earlywood to latewood is either

abrupt (Figure 3.8b) (D9.022.1, D9.043.1, D9.044.1, D9.050.1, D9.059.1, D9.139.1, D9.161.1, D9.168.1) or gradual (D9.111.1).

Tracheids: In TS earlywood tracheids are square, rectangular, hexagonal or rounded. Radial diameter ranges from 21.6 – 62.1µm, and tangential diameter ranges from 25.3 – 57.5µm. Latewood tracheids are generally rectangular in shape with radial diameter ranging from 9.8 – 25.3µm, and tangential diameter ranging from 30 – 44.1µm. Resin spools are present in wood specimens D9.043.1, D9.050.1, D9.059.1, D9.109.1 and D9.128.1 (Figure 3.8h).

Tracheid pitting: In RLS tracheid pitting is predominantly uniseriate and biseriate, sometimes triseriate (Figure 3.8c, d, e and Figure 3.9a,d). Specimen D9.109.1 has 4-seriate tracheid pitting. When tracheid pitting is multiseriate it has an alternate arrangement of pits (araucarian type pitting). Opposite or sub-opposite pitting is rare (D9.022.1 and D9.128.1). Pit outlines appear longitudinally flattened when in uniseriate rows and hexagonal when in multiseriate rows. Pit diameter ranges from 5 – 22.5µm. Pit apertures are round and have diameters that range from 3 – 12µm. Short rows of uniseriate and biseriate pitting are occasionally found on the tangential walls of tracheids in specimens D9.022.1, D9.044.1, D9.059.1, D9.109.1, D9.139.1 and D9.168.1 (Figure 3.8i).

Cross-field pitting: Most of the specimens have 2 - 5 pits per cross-field (Figure 3.8f, g and Figure 3.9c). Cross-fields with six pits were observed in D9.059.1 but they are infrequent. Specimen D9.109.1 has 3 – 8 cross-field pits (Figure 3.9b). Specimen D9.128.1 has 2 - 10 cross-field pits (Figure 3.9f). Cross-field pitting appears to be araucarioid in all specimens.

Rays: In TLS rays are predominantly uniseriate (Figure 3.8i). Biseriate rays are occasionally found in D9.050.1, D9.128.1 and D9.139.1. Mean ray height ranges from 4 – 10 cells high. Mean ray height in microns ranges from 85 – 273.4µm. In RLS ray walls are thin and smooth (Figure 3.9e) and ray cells can sometimes appear barrel shaped. In specimens D9.043.1, D9.050.1, D9.059.1, D9.109.1 and D9.128.1 rays are often filled with a dark resinous content. There are on average 2 – 6 rays per mm.

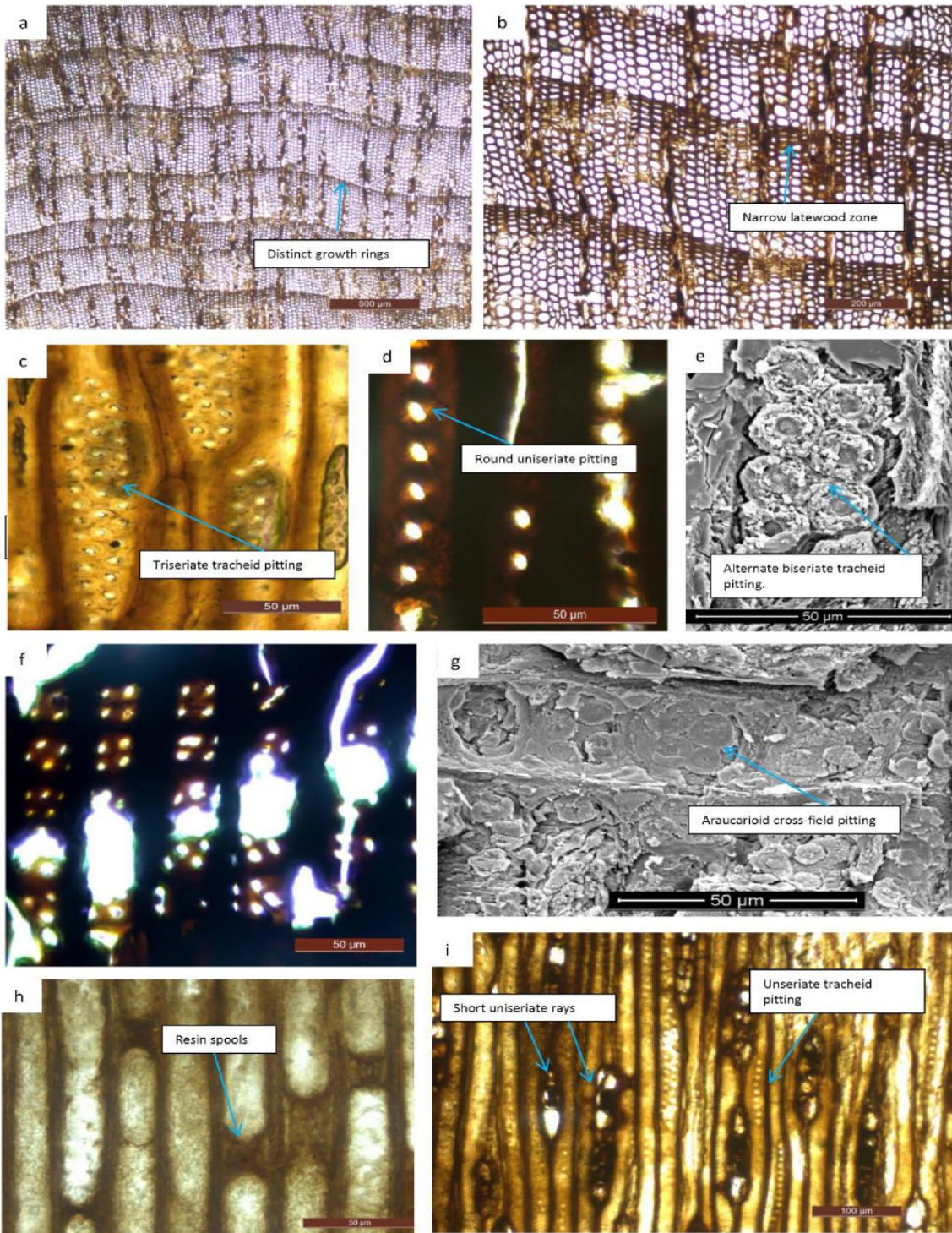


Figure 3. 8. *Agathoxylon* Species B (D9.059.1, D9.128.1, D9.161.1), Species D (D9.139.1) a) D9.059.1, TS showing distinct growth ring boundaries, scale bar = 500µm. b) D9.059.1, TS showing abrupt transition from earlywood to latewood, scale bar = 200µm. c) D9.128.1, RLS showing triseriate tracheid pitting, scale bar = 50µm. d) D9.139.1, RLS showing uniseriate tracheid pitting, scale bar = 50µm. e) D9.304.1 RLS showing biseriate tracheid pitting, scale bar = 50µm. f) D9.161.1 RLS showing araucarioid cross-field pitting, scale bar = 50µm. g) D9.304.1 RLS showing araucarioid cross-field pitting, scale bar = 50µm. h) D9.059.1 RLS showing resin spools, scale bar = 50µm. i) D9.059.1 TLS showing rays and tangential cross-field pitting, scale bar = 100µm. All images are from thin sections, except e and g, which are SEM micrographs.

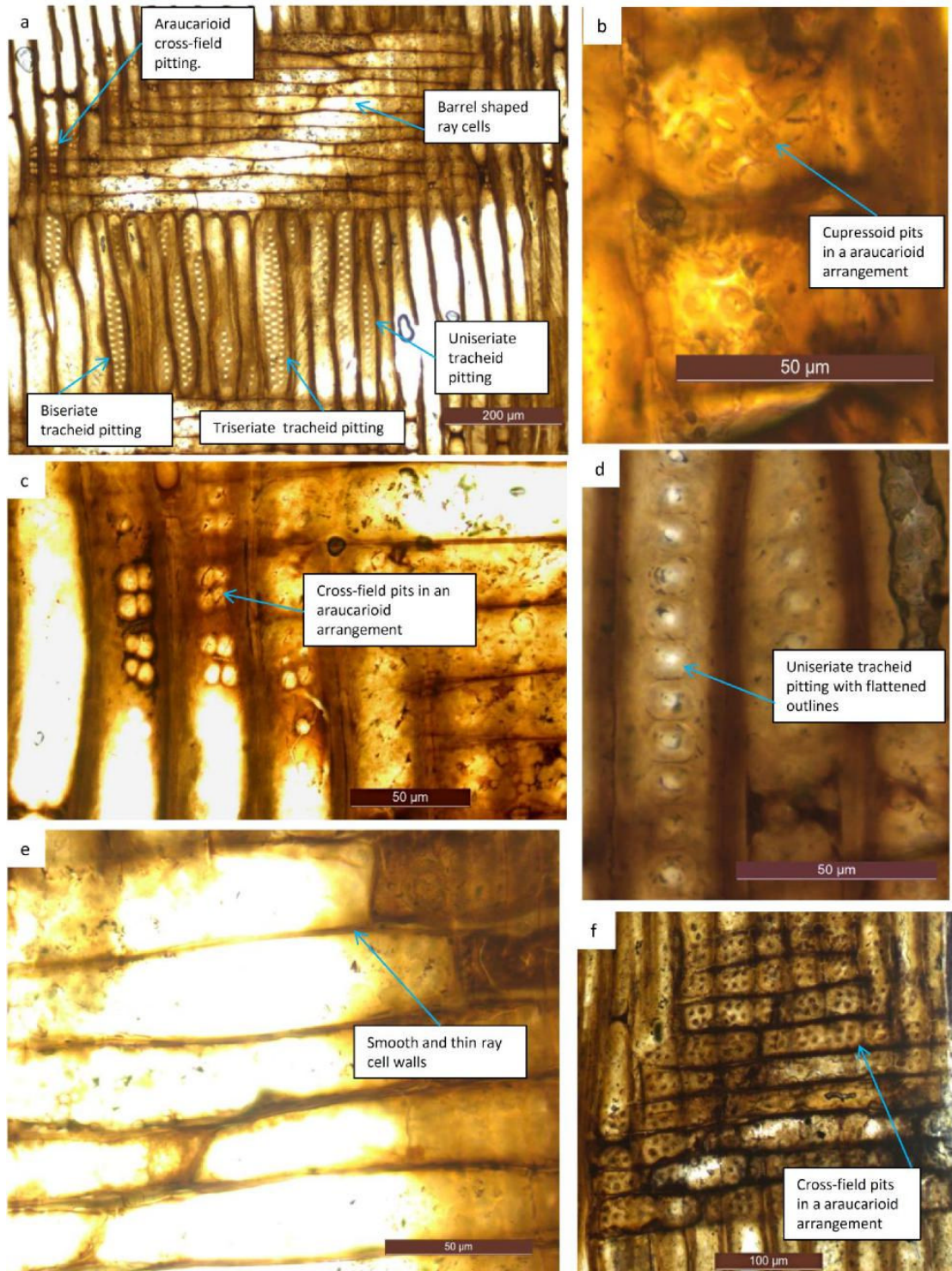


Figure 3. 9. *Agathoxylon* Species B (D9.043.1), Species C (D9.109.1), Species D (D9.128.1). a) D9.043.1 showing tracheid pitting, ray cells and cross-field pitting, scale bar = 200µm. b) D9.109.1 showing cross-field pits in a araucarioid arrangement, scale bar = 50µm. c) D9.043.1 showing cross-field pitting in a araucarioid arrangement, scale bar = 50µm. d) D9.043.1 showing uniseriate tracheid pitting, scale bar = 50µm. e) D9.043.1 showing ray walls, scale bar = 50µm. f) D9.128.1 Cross-field pitting in an araucarioid arrangement, scale bar = 100µm.

Table 3. 2. Summary of the anatomical characters of *Agathoxylon* wood identified in this project. Numbers in brackets are mean values.

Species	A			B		
Specimen number	D9.022.1	D9.044.1	D.168.1	D9.043.1	D9.050.1	D9.161.1
Growth rings	Indistinct	Indistinct	Indistinct	Distinct	Distinct	Distinct
Tracheid pitting						
Type	Araucarian	Araucarian	Araucarian	Araucarian	Araucarian	Araucarian
Uniseriate %	78	78	86	58	58	54
Biseriate %	22	18	14	38	36	38
Triseriate %	0	2	0	4	6	8
4- seriate %	0	0	0	0	0	0
Tangential pitting	Present	Present	Present	Absent	Absent	Uknown
Tracheid pit arrangement						
Opposite %	0	0	0	0	0	0
Sub opposite %	5	0	0	0	0	0
Alternate %	95	100	100	100	100	100
Touching pits %	100	100	100	100	100	100
Spaced pits %	0	0	0	0	0	0
Cross-field pitting						
Type	Araucarioi d	Araucarioi d	Araucarioi d	Araucarioi d	Araucarioi d	Araucarioi d
Number of pits per cross-field	2 to 7 (4)	2 to 7 (5)	2 to 4 (3)	2 to 6 (4)	3 to 5 (4)	2 to 5 (4)
Rays						
Height (number of cells)	1-13 (5)	1-16 (6)	2-7 (5)	n/a	2-16 (8)	n/a
Height (µm)	60 - 280 (138)	50-380 (175)	42.5 -165 (84.5)	n/a	100 - 410 (224)	n/a

Table 3. 3. Summary of the anatomical characters of *Agathoxylon* wood identified in this project. Numbers in brackets are mean values.

Species	B		C	D	
Specimen number	D9.059.1	D9.128.1	D9.109.1	D9.111.1	D9.139.1
Growth rings	Distinct	Distinct	Distinct	Distinct	Distinct
Tracheid pitting					
Type	Araucarian	Araucarian	Araucarian	Araucarian	Araucarian
Uniseriate %	60	54	0	48	36
Biseriate %	40	42	44	50	62
Triseriate %	0	4	46	2	2
4- seriate %	0	0	10	0	0
Tangential pitting	Present	Absent	Present	Absent	Present
Tracheid pit arrangement					
Opposite %	0	6	0	0	0
Sub opposite %	0	12	0	0	0
Alternate %	100	81	100	100	100
Touching pits %	100	100	100	100	100
Spaced pits %	0	0	0	0	0
Cross-field pitting					
Type	Araucarioid	Araucarioid	Araucarioid	Araucarioid	Araucarioid
Number of pits per cross-field	2 to 6 (4)	2 to 10 (4)	3 to 8 (5)	2 to 5 (4)	2 to 5 (3)
Rays					
Height (number of cells)	1 - 11 (4)	1 - 17 (8)	3 - 22 (10)	1 -7 (4)	3 - 11 (6)
Height (µm)	50 - 245 (129.2)	30 - 485 (210)	85 - 570 (273.4)	35 - 162.2 (90.7)	90 - 167.5 (145)

3.4.1.2 Discussion

According to Philippe and Bamford (2008) the wood specimens described here can be assigned to *Agathoxylon* on the basis of displaying araucarian tracheid pitting and araucarioid cross-field pitting. *Agathoxylon* is considered to be the legitimate name for woods possessing the above features (Philippe and Bamford, 2008; Philippe, 2011). However, the name *Araucarioxylon* has also been used for the same wood type, including wood previously identified from Antarctica, but the name is no longer legitimate according to International code of botanical nomenclature (ICBN) because it has been used previously for another type of wood (Philippe, 1993; 2011).

There is variability within the wood specimens described here, the most obvious being the presence of resin spools in D9.043.1, D9.059.1, D9.050.1, D9.109.1 and D9.128.1 but their absence in the other specimens. It is not possible to observe the presence of resin spools in D9.161.1 and D9.139.1 because the tracheids are dark in colour, making it difficult to see the contents within. It was also difficult to observe the presence of resin spools in specimens that were observed under the SEM (D9.304.1, D9.136.1). Specimens D9.022.1, D9.044.1 and D9.168.1 have indistinct growth rings boundaries.

There is variability in the percentage of uniseriate and multiseriate radial tracheid pitting between all of the wood specimens (Table 3.2 and Table 3.3). Tangential pitting is observed in D9.022.1, D9.044.1 and D9.059.1, D9.109.1, D9.136.1 and D9.168.1. The frequency of tangential pitting has been proven to be variable with ontogenetic age (Falcon-Lang, 2005a). As a result of preservation the nature of tracheids and rays could not be observed in D9.161.1. There is small variation in ray height and cross-field pitting between wood specimens, but these features can be variable within a single tree.

The *Agathoxylon* wood specimens described here have been separated into four species (A, B, C, and D) due to distinct features in each species, refer to Tables 3.2 and 3.3. The features that were considered when separating the wood to species level include the percentage of uniseriate, biseriate and multiseriate tracheid pitting; the presence or absence of resin spools; the

presence of tangential pitting; the number of cross-field pits, and distinctiveness of growth rings.

Four species are defined as follows:

- **Species A.** This species is defined by having indistinct growth rings, similar percentages of uniseriate and biseriate tracheid pitting and the presence of tangential tracheid pitting. Specimens D9.022.1, D9.044.1 and D9.168.1 have been identified as this species.
- **Species B.** This includes D9.043.1, D9.050.1, D9.059.1, D9.128.1 and D9.161.1. This species has distinct growth ring boundaries and similar percentages of uniseriate and biseriate pitting. Triseriate pitting is absent in specimen D9.059.1 but present in the other specimens, although it is infrequent. This species also has resin spools and a similar number of pits per cross-field. Specimen D9.059.1 has tangential tracheid pitting, but the other specimens do not. However, other features in D9.059.1 are similar to the other wood specimens in species B. In the quantitative analysis D9.059.1 grouped closely with other specimens within species B (section 3.3).
- **Species C.** This species has predominantly biseriate, triseriate and 4 – seriate tracheid pitting. Species C is also characterised as having resin spools and tangential pitting. This species includes wood specimen D9.109.1.
- **Species D.** This includes specimen D9.111.1 and D9.139.1. In the quantitative analysis (refer to section 3.3) these wood specimens did not form together as a separate group. They are considered separate from the other *Agathoxylon* wood specimen species on the basis that they do not have resin spools. They have similar proportions of uniseriate, biseriate and triseriate pitting.

It is difficult to identify specimens D9.136.1 and D9.304.1 because an adequate number of features could not be measured or observed. However, D9.136.1 appears similar to species A on the basis that only uniseriate and biseriate tracheid pitting was observed and it has tangential pitting, plus up to 4 pits per cross-field.

3.4.1.3 Comparison with other fossil wood of *Agathoxylon*

Agathoxylon wood is common in Cretaceous and Cenozoic sedimentary deposits in Antarctica. It has been documented and described from Early Cretaceous and Late Cretaceous Antarctic strata on Livingston Island (Torres and Lemoigne, 1989; Falcon-Lang and Cantrill, 2001; Poole and Cantrill, 2001), Alexander Island (Falcon-Lang and Cantrill, 2000) and James Ross Island (Ottone and Medina, 1998). *Agathoxylon* wood has also been documented from Paleocene and Eocene sedimentary sequences on Seymour Island (Torres *et al.*, 1994; Pujana *et al.* 2014; 2015).

Species A (D9.022.1, D9.043.1 and D9.168.1) has similarity to *Agathoxylon antarcticus* (Poole and Cantrill 2001; Pujana *et al.*, 2015) in terms of both having predominantly uniseriate pitting, absence of resin spools, ray height range of 1 -16 cells. *Agathoxylon antarcticus* is different because it has a higher a number of cross-field pitting (1 – 9 pits per cross-field) and does not have tangential pitting.

Specimen B (D9.043.1, D9.050.1, D9.059.1, D9.128.1 and D9.161.1) show similarity to *Agathoxylon pseudoparenchymatosum* identified by Pujana *et al.* (2014, 2015). The similarities in *Agathoxylon pseudoparenchymatosum* include distinct growth rings with an abrupt change from earlywood to latewood; uniseriate, biseriate and rare triseriate tracheid pitting; 1 – 7 cross-field pits (mean 3) and low ray height (1 – 7 cells high).

Other *Agathoxylon/Araucarioxylon* woods that have resin spools include *Araucarioxylon* sp. 2 and *Araucarioxylon chapmanae* identified by Falcon-Lang and Cantrill (2001) and Poole and Cantrill (2001). However, they are different in terms of proportions of uniseriate, biseriate and triseriate pitting and they also have higher number of cross-field pits.

Araucarioxylon novaezeelandii, first described from New Zealand by Stopes (1914) is also similar to Species B here on the basis of having resin spools, 5-6 pits per cross-field and low rays (1-7 cells high). *Araucarioxylon novaezeelandii* has also been reported from the Eocene of the Antarctic Peninsula (Torres *et al.*, 1994).

Species D (D9.111.1 and D9.139.1) are comparable to *Araucarioxylon* sp.1 (Falcon-Lang and Cantrill, 2000); the only difference being the higher proportion of biseriate pitting. *Araucarioxylon* sp.1 described in Falcon-Lang and Cantrill (2001) is also comparable but this has more cross-field pits and taller rays.

Agathoxylon type wood has also been described from the Cretaceous and Paleogene sedimentary sequences of Chile and Argentina. Specimen D9.109.1 is very similar to *Araucarioxylon pluriresinosum* described by Torres and Bagoczky (1986) from Late Cretaceous strata on Quirquina Island, Chile.

Similar wood types to those from the Antarctic Peninsula have also been documented from Chile (Ottone and Medina, 1998, Nishida *et al.*, 2006; Terada *et al.*, 2006). The fossil wood described here also shows some similarity to *Araucarioxylon pichasquense*, which has been documented from Paleogene sediments in southern Chile (Terada *et al.*, 2006a), which has 1-3 seriate tracheid pitting and low rays. The main difference is that it has a higher number of cross-field pits than the wood described here. *Agathoxylon* sp. described from Cretaceous sedimentary deposits in Argentina (Pujana *et al.*, 2007) has short rays, 2-5 cross-field pits but is different from the wood described here because it has predominantly uniseriate tracheid pitting.

3.4.1.4 Comparison with extant wood

Fossil wood identified as *Agathoxylon* shows close similarity to wood of living trees of the family Araucariaceae on the basis of having continuous tracheid pitting, which is always in an alternate arrangement when multiseriate; numerous cross-field pits (usually 1 – 12) and the general absence of axial parenchyma (Greguss, 1955). It is difficult to separate the modern genera *Araucaria* and *Agathis* based on wood features since they have many similarities. It is considered that the main difference is the distinctiveness of growth rings. For example *Agathis* has more clearly defined growth rings compared to *Araucaria*. *Agathis* also sometimes has axial parenchyma (Greguss, 1955).

3.4.1.5 Ecology of modern Araucariaceae

The nearest living relatives with wood similar to that of *Agathoxylon* are the modern conifers *Araucaria*, *Agathis* and *Wollemi*, which all belong to the family Araucariaceae (Kershaw and Wagstaff, 2001). This family occurs throughout cool temperate to tropical climate zones (Veblen *et al.*, 1995; Jaffré, 1995; Enright, 1995; Kershaw and Wagstaff, 2001). *Araucaria*-type conifers are found in north eastern Australia (*A.bidwillii* and *A.cunninghamii*), New Guinea (*A.cunninghamii* and *A.hunsteinii*), New Caledonia (e.g. *A.bernieri*, *A. biramulata*, *A. columnaris*, *A.hemorosa*, *A.schmidii*, *A.subulata*) and southern South America (*A.araucana* and *A.augustifolia*).

Agathis is found in New Zealand (*A. australis*), north eastern Australia (*A.atropupurea*, *A. microstachya* and *A.robusta*) and other western Pacific Islands (*A. labillardieri*, *A.macrophylla*, *A.microstachya*, *A. philippinensis* and *A.spathulata*) and extends northwards to the southern Asian islands (*A.borneensis*, *A.endertii* and *A.philippinensis*) (Ogden and Stewart, 1995; Enright, 1995; Kershaw and Wagstaff, 2001).

There is just one species belonging to *Wollemi* (*Wollemi nobilis*), which is found in eastern Australia (Kershaw and Wagstaff, 2001). *Araucaria* and *Agathis* are tall canopy trees that can reach up to 50m in height. They are slow-growing and have long-life spans up to 1000 years. *Araucaria* and *Agathis* are shade-intolerant and live at mid to high altitudes in montane areas that are susceptible to disturbances such as landslides, volcanic activity and wildfires; such disturbances create gaps in the forest canopy for regeneration. Wildfires are an important process for regeneration and both genera have developed thick barks that protect the trees from moderate fires that tend to kill other competing tree types in the surrounding area.

The warm temperate species *Agathis australis* from New Zealand and cool temperate *Araucaria araucana* (Figure 3.10) from the southern central Andes usually coexist with *Nothofagus* species. All are considered to be pioneer species that are the first to establish after a severe disturbance has wiped out most of the previous forest (Ogden and Stewart, 1995; Veblen *et al.* 1995; Veblen *et al.*, 1996). These tree taxa are shade-intolerant so grow at mid to high altitudes away from angiosperm-dominated ground cover, which causes shade.

Some of the *Agathoxylon* wood identified in this project are charcoaled or partly charred, so it is likely that the Araucarian type trees living on the Antarctic Peninsula occupied upland areas that were more susceptible to disturbances, such as wild fires triggered by volcanic activity.



Figure 3. 10. *Araucaria araucana* tree near volcano Lanin, Chile. *Araucaria araucana* tree is 30 – 40m in height. The undergrowth is composed of *Nothofagus* trees. Courtesy of Jane Francis.

3.4.2 *Phyllocladoxylon*

Family: Podocarpaceae

Genus: *Phyllocladoxylon* Gothan

3.4.2.1 Description

Specimens numbers: D9.036.1, D9.038.1, D9.092.1, D9.094.1, D9.098.1, D9.125.1

Description: D9.036.1, D9.038.1, D9.092.1, D9.094.1, D9.098.1 are likely to have been derived from either inner branch or stem wood because of high growth ring curvature. D9.098.1 also has compression wood. Wood specimen D9.125.1 is likely to have been derived from the outer part of a large branch or stem because its growth rings have low curvature.

Growth rings: Growth ring boundaries are distinct and the transition from earlywood to latewood is gradual (Figure 3.11a). Growth ring boundaries on D9.092.1 and D9.038.1 are undulating.

Tracheids: In TS earlywood tracheids are square or rounded. Radial diameter ranges from 21.6 – 43,5µm, and tangential diameter ranges from 30.7 – 41.5µm. Latewood tracheids are generally rectangular in shape with a radial diameter ranging from 14.7 – 19.1µm, and tangential diameter ranging from 25.8 – 31.5µm.

Tracheid pitting: In RLS tracheid pitting is predominantly uniseriate (Figure 3.11b, c) but is rarely biseriate in specimen D9.098.1. The arrangement of biseriate pitting is opposite. Tracheid pitting is abietinean. Pit outlines are circular with round apertures (Figure 3.11c). Mean pit diameter ranges from 13.5 - 15µm and mean pit aperture ranges from 5 - 8µm. Pitting is present only rarely on the tangential walls of tracheids in wood specimens D9.036.1 D9.038.1, D9.092.1 and D9.094.1 (Figure 3.11f). There may be pits on the tangential walls of specimen D9.125.1 but due to preservation they are difficult to make out. Tangential pitting is discontinuous and smaller than radial pitting. Tangential pitting is absent in D9.092.1.

Cross-field pitting: There is one large pit per cross-field, rarely two pits in specimen D9.094.1 (Figure 3.11d, e). Cross-field pits are phyllocladoid or round oopores and are very distinctive. Mean cross-field pit diameter ranges from 11.3 to 15µm.

Axial parenchyma: Absent.

Rays: In TLS rays are uniseriate (Figure 3.11g). Mean ray height ranges from 3 – 9 cells high. Mean ray height ranges from 65.5 – 194.8µm. In RLS ray walls are thin and smooth (Figure 3.11d). There are on average 3 – 4 rays per tangential mm.

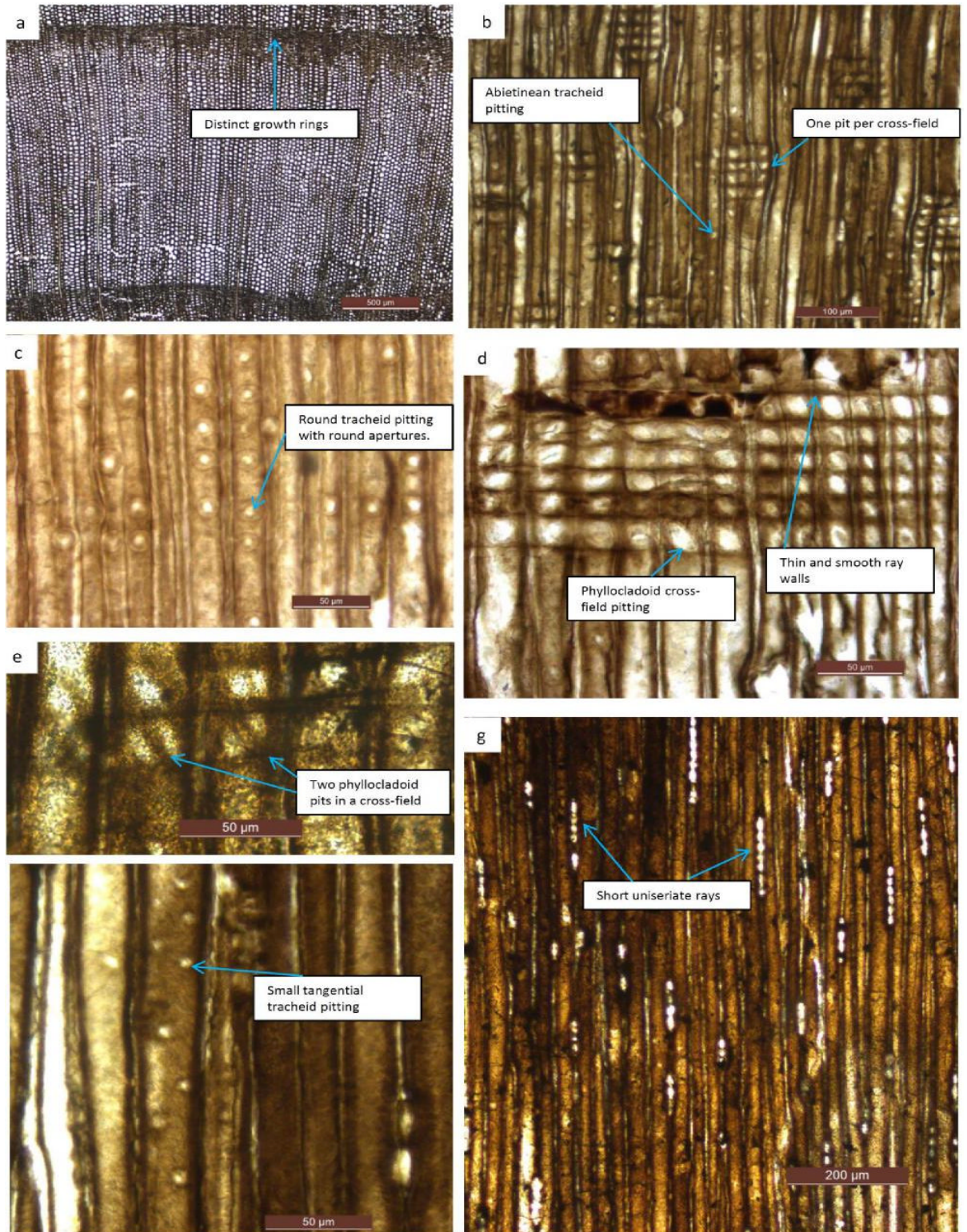


Figure 3. 11. *Phyllocladoxylon*, Species A a) D9.036.1, TS showing distinct growth ring boundaries, scale bar = 500 μ m. b) D9.092.1, RLS showing tracheid pitting and rays/cross-field pitting, scale bar = 100 μ m. c) D9.036.1 RLS showing uniseriate tracheid pitting, scale bar = 50 μ m. d) D9.036.1, RLS showing one oopore per cross-field, scale bar = 50 μ m. e) D9.094.1, RLS showing two oopores per cross-field, scale bar = 50 μ m. f) D9.036.1, TLS showing tangential tracheid pitting, scale bar = 50 μ m. g) D9.092.1, TLS showing uniseriate rays, scale bar = 200 μ m.

Table 3. 4. Summary of the anatomical characters of *Phyllocladoxylon* wood identified in this project. Numbers in brackets are mean values.

Specimen	D9.036.1	D9.038.1	D9.092.1
Growth rings	Distinct	Distinct	Distinct
Tracheid pitting			
Type	Abietinean	Abietinean	Abietinean
Uniseriate %	100	100	100
Biseriate %	0	0	0
Triseriate %	0	0	0
Tangential	Present	Present	Absent
Tracheid pitting arrangement			
Opposite %	0	0	0
Alternate %	0	0	0
Touching pits %	0	0	0
Spaced pits %	100	100	100
Cross-field pitting			
Type	Oopores: Phyllocladoid	Oopores: Phyllocladoid, round	Oopores: Phyllocladoid
Number of pits per cross-field	1 to 2	1 to 2	1 to 2
Rays			
Height (number of cells)	1-7(3)	2 - 13 (6)	1-13 (5)
Height (µm)	20-122 (65.5)	45 - 230 (101.30)	25 - 187.5 (95.6)

Table 3. 5. Summary of the anatomical characters of *Phyllocladoxylon* wood identified in this project. Numbers in brackets are mean values.

Specimen	D9.094.1	D9.098.1	D9.125.1
Growth rings	Distinct	Distinct	Distinct
Tracheid pitting			
Type	Abietinean	Abietinean	Abietinean
Uniseriate %	100	98	100
Biseriate %	0	2	0
Triseriate %	0	0	0
Tangential	Present	Present	Present
Tracheid pitting arrangement			
Opposite %	0	100	0
Alternate %	0	0	0
Touching pits %	0	0	0
Spaced pits %	100	100	100
Cross-field pitting			
Type	Oopores: Phyllocladoid	Oopores: Phyllocladoid	Oopores: Phyllocladoid
Number of pits per cross-field	1 to 2	1	1
Rays			
Height (number of cells)	1-7 (3)	2 - 8 (4)	3 - 21 (9)
Height (µm)	22.5 - 132.5 (70.6)	35-155 (85.3)	55 - 385 (194.8)

3.4.2.2 Discussion

According to Philippe and Bamford (2008), the wood specimens described here can be assigned to the genus *Phyllocladoxylon* because they have abietinean radial tracheid pitting and cross-fields that have one or two large oopores.

The wood specimens described here are all very similar in terms of cross-field pitting, radial tracheid pitting and the absence of axial parenchyma (see Table 3.4 and 3.5). Specimen D9.038.1 has occasional rounded oopores but is not considered to be a separate species because all other characteristics are similar to the other wood specimens in this genus. Specimen D9.092.1 has pronounced undulating growth rings and no pitting on tangential tracheid walls but it is considered that all other matching features warrant this specimen being placed in *Phyllocladoxylon*. There is small variation in ray height (Table 3.4 and Table 3.5) between wood specimens but this is considered insignificant because ray height has been shown to be variable within a single tree (Falcon-Lang, 2005a) (Figure 3.5).

3.4.2.3 Comparison of other fossil woods of *Phyllocladoxylon*

The wood specimens described here show close similarity to *Phyllocladoxylon antarcticum*, which was first described by Gothan (1908) from Seymour Island. *Phyllocladoxylon antarcticum* was later documented from King George Island (Torres and Lemoigne, 1988) and Eocene sedimentary sequences on Seymour Island (Pujana *et al.*, 2014).

Phyllocladoxylon pooleae is another species that has also been described from the Eocene sedimentary sequences of Seymour Island but is considered a different species from *Phyllocladoxylon antarcticum* because it has resin spools and rare biseriate pitting that is sub-opposite to alternate in arrangement (Pujana *et al.*, 2014).

Phyllocladoxylon has also been documented from Paleocene sediments in southern Patagonia and was considered to be similar to *Phyllocladoxylon antarcticum* (Nishida *et al.*, 2006).

3.4.2.4 Comparison with extant wood

The fossil wood described here shares characteristics with the wood of extant *Phyllocladus* of the family Podocarpaceae. The common features include distinct growth rings; 1–2 large pits per cross-field that can be oblique, ellipse, circular or window-like; scattered tracheid pitting and the absence of axial parenchyma (Greguss, 1955; Patel, 1968; Meylan and Butterfield, 1978). According to Patel (1967), the differences separating extant species of *Phyllocladus* are tracheid size, number of cross-field pits and ray height.

3.4.2.5 Ecology of *Phyllocladus*

Today *Phyllocladus* (Podocarpaceae) lives in warm, cool temperate and tropical climatic zones (Wagstaff, 2004). New Zealand has the highest diversity with three species, which are *Phyllocladus alpinus*, *Phyllocladus toatoa* and *Phyllocladus trichomanoides*. They live at elevations between sea level and 1900m. *Phyllocladus alpinus* (Figure 3.12) has the widest ecological niche as it is found at sea level in Westland and at altitudes of 1900m in montane areas of North Island and South Island where it occurs as shrubs (Wardle, 1969; Wagstaff, 2004). The other two species living in New Zealand do not exceed elevations of 800m. At low elevations *Phyllocladus* occurs as trees up to 15m in height and are associated with relatively infertile and poorly drained soils (Wardle, 1969; Molloy, 1996). They are generally shade-tolerant and occur in closed canopy settings along with broadleaved angiosperm species. In alpine zones *Phyllocladus alpinus* grows on well drained soils.

Phyllocladus apseniifolius, which is endemic to Tasmania, is closely related to *Phyllocladus alpinus* however it occurs at lower altitudes (Wagstaff, 2004) There is only one tropical species, which is called *Phyllocladus hypophyllus*

and lives in montane forests in Malaysia and New Guinea at elevations between 900m and 4000m (Enright, 1995; Coomes and Bellingham, 2011).

(Huon Pine) is also considered to be a nearest living relative of

Phyllocladoxylon (Cantrill and Poole, 2005; Bowman *et al.*, 2014).

Lagarostrobos franklinii is a tree species that belongs to the family Podocarpaceae and today it is endemic to the cool temperate forests of Tasmania (Gibson *et al.*, 1991; Gibson and Brown, 1991). It commonly occurs at low altitudes and grows on river banks.



Figure 3. 12. *Phyllocladus alpinus* (Celery Top Pine), New Zealand. Tree height is 1.5 – 2m. Taken from o2landscapes.com

3.4.3 *Protophyllocladoxylon*

Family: Podocarpaceae

Genus: *Protophyllocladoxylon* Kräusel

3.4.3.1 Description

Specimen numbers: D9.071.1, D9.093.1, D9.112.1, D9.153.1, D9.181.1

Description: The five specimens described here are likely to have been derived from the outer part of a branch or stem as growth rings show low curvature.

Growth rings: All specimens have distinct growth ring boundaries (Figure 3.13a, b). The transition from earlywood to latewood is abrupt.

Tracheids: In TS earlywood tracheids are square or hexagonal. Radial tracheid diameter ranges from 30 – 61.7 μ m and tangential tracheid diameter ranges from 32 – 52.5 μ m. Latewood tracheids are rectangular or square with a radial diameter of 17.6 – 38.5 μ m and a tangential diameter ranging from 31.8 – 38.9 μ m.

Tracheid pitting: In RLS tracheid pitting occurs predominantly as uniseriate or biseriate, rarely triseriate. Tracheid pitting arrangement is mixed and occurs as araucarian and abietinean (Figure 3.13c, d, g). Biseriate pitting in D9.093.1 and D9.112.1 is frequently opposite. Pits appear round when in an abietinean arrangement (Figure 3.13c), and horizontally flattened or hexagonal when they are in an araucarian arrangement. Pit apertures are round, but specimen D9.071.1 has tracheid pits that occasionally have elliptical apertures. Mean pit diameter ranges from 15 – 25 μ m, and pit aperture diameter ranges from 2 – 10 μ m. Specimen D9.181.1 has occasional pitting on the tangential walls of tracheids.

Cross-field pitting: There are 1 – 2 large oopores per cross-field (Figure 3.13e, f). Oopores are phyllocladioid, window-like or round. Mean pit diameter is 14 – 21 μ m. When there are two pits per cross-field, they are either arranged side-by-side or on top of each other.

Rays: In TLS rays are uniseriate (Figure 3.13h). Mean ray height ranges from 62 – 275 μ m. Mean ray height ranges from 4 – 7 cells high. In RLS ray walls are thin and smooth. There are on average 2–3 rays per tangential mm.

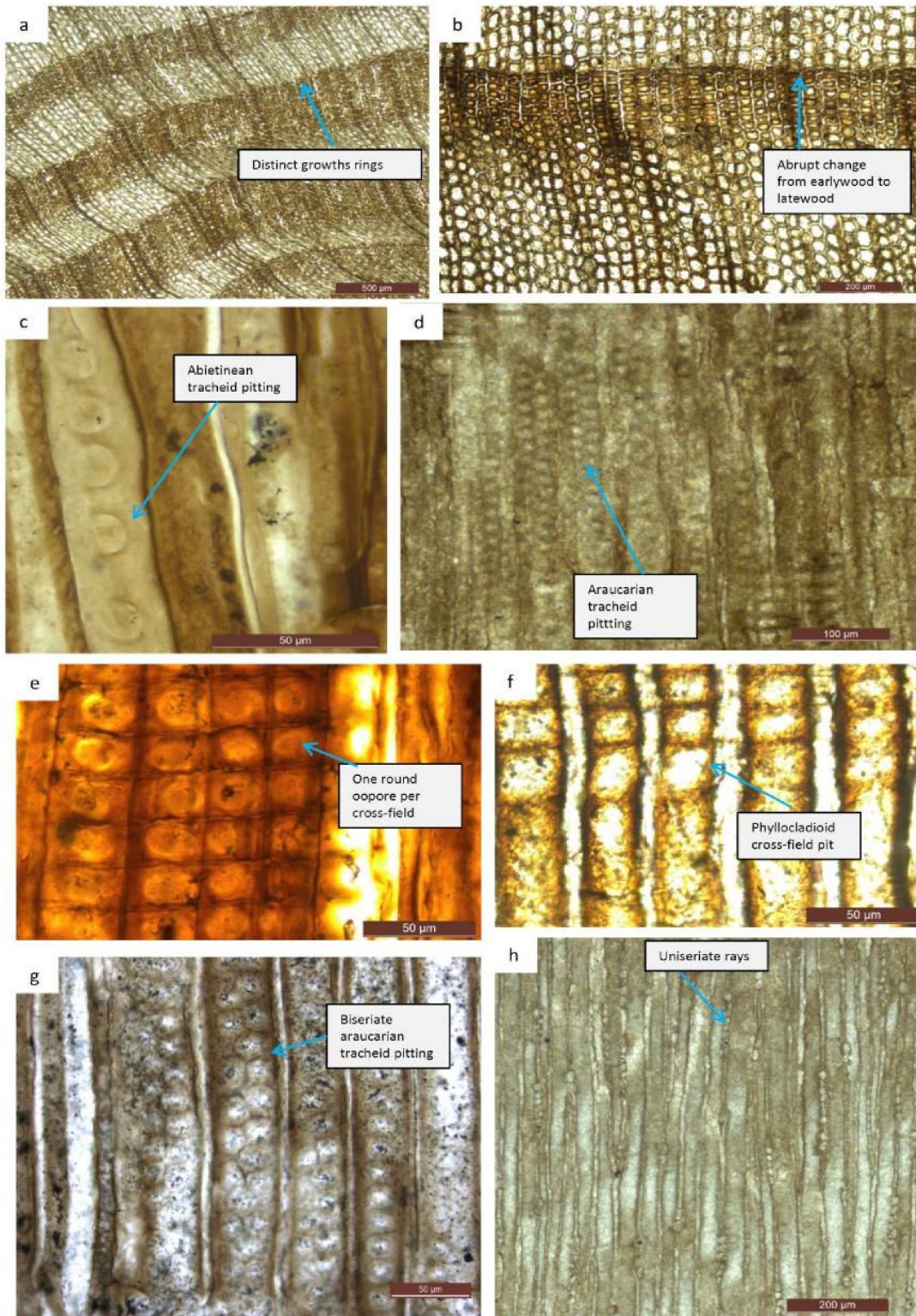


Figure 3. 13. *Protophyllocladoxylon*. Species A (D9.071.1), Species B (D9.093.1, D9.112.1), Species C (D9.153.1) a) D9.153.1, TS showing distinct growth ring boundaries, scale = 500μm. b) D9.093.1, TS showing abrupt change from earlywood to latewood, scale = 200μm. c) D9.071.1, RLS showing abietinean, scale = 50μm. d) D9.153.1, RLS showing araucarian tracheid pitting, scale = 100μm. e) D9.071.1, RLS showing one round oopore per cross-field, scale = 50μm. f) D9.093.1, RLS showing one phyllocladioid per cross-field; scale = 50μm. g) D9.112.1, RLS showing araucarian tracheid pitting, scale = 50μm. h) D9.112.1, TLS showing uniseriate rays, scale = 200μm.

Table 3. 6. Summary of the anatomical characters of *Protophylocladoxylon* wood identified in this project. Numbers in brackets are mean values.

Species	A		B	
Specimen number	D9.071.1		D9.093.1	D9.112.1
Growth rings	Distinct		Distinct	Distinct
Tracheid pitting				
Type	mixed		mixed	mixed
Uniseriate %	98		64	64
Biseriate %	2		36	36
Triseriate %	0		0	0
Tangential pitting	Absent		Absent	Absent
Tracheid pit arrangement				
Opposite %	0		94	88
sub opposite %	0		0	0
Alternate %	2		5	11
Touching pits %	90		52	58
Spaced pits %	10		48	42
Cross- field pitting				
Type	oopores: round		oopores: Phyllocladoid	oopores: Phyllocladoid, window-like
Number of pits per cross-field	1 to 2		1 to 2	1 to 2
Rays				
Height (number of cells)	2 to 23(7)		1 to 7 (4)	1 to 7 (4)
Height (μm)	60 - 550(118.5)		30 - 140(70)	35 - 130 (62.2)

Table 3. 7. Summary of the anatomical characters of *Protophylocladoxylon* wood identified in this project. Numbers in brackets are mean values.

Species	C	D
Specimen number	D9.153.1	D9.181.1
Growth rings	Distinct	Distinct
Tracheid pitting		
Tracheid pitting type	mixed	mixed
Uniseriate %	75	11
Biseriate %	25	82
Triseriate %	0	5
Tangential pitting	Absent	Present
Tracheid pit arrangement		
Oposite %	0	0
sub opposite %	0	0
Alternate	100	100
Touching pits %	84	88
Spaced pits %	16	11
Cross- field pitting		
Cross-field pits type	oopores: Phyllocladoid, window-like	oopores: Phyllocladoid, window-like
Number of pits per cross-field	1 to 2	1
Rays		
Height (number of cells)	2 to 8 (4)	3 to 18 (7)
Height (μm)	30 - 160(91.5)	65 - 275 (146)

*Due to poor preservation, characteristics of tracheid pitting were observed in less than 50 tracheids in specimens D9.153.1 and D9.181.1

3.4.3.2 Discussion

According to Philippe and Bamford (2008) the wood described here appears closest to the genus *Protophylocladoxylon*. *Protophylocladoxylon* can either have araucarian or mixed tracheid pitting or both, and is characterised by having 1 – 2 oopores per cross-field. The wood specimens described here have mixed tracheid pitting and 1 – 2 oopores.

There is significant variability (see figures 3.4, 3.5 and 3.6) within the *Protophylocladoxylon* wood described here, the most obvious being the percentages of uniseriate, biseriate and triseriate tracheid pitting (Table 3.6 and 3.7), and the percentage of tracheid pits that are touching or spaced. Due to poor preservation, tracheid pitting was observed in less than 50 tracheids in D9.153.1 and D9.181.1. This means that the percentages of different tracheid characteristics may not be fully representative of the wood specimens. There are also differences in the shape of oopores in cross-field areas (Table 3.6 and 3.7). Specimen D9.071.1 has round/ oval oopores; D9.093.1 has phyllocladoid oopores; specimens D9.112.1, D9.153.1 and D9.181.1 have oopores that are phyllocladoid and window-like in form.

The specimens have been separated into species based on the variability of the features mentioned above. The different species are as follows:

- **Species A.** Specimen D9.071.1 is considered a different species from the other wood specimens on the basis of having near exclusive uniseriate tracheid pitting and large round/oval oopores in cross-field areas.
- **Species B.** Specimens D9.093.1 and D9.112.1 have been grouped as species B. They both have the same proportion of uniseriate and biseriate tracheid pitting; similar proportions of biseriate tracheid pits that are opposite and alternate; and a similar percentage of spaced and touching tracheid pits. They also have the same mean ray height.
- **Species C and D.** Wood specimens D9.153.1 and D9.181.1 are considered separate species. Both specimens have a similar

percentage of touching and spaced pits and biseriate pitting that is exclusively in an alternate arrangement (araucarian), but they are considered different species based on having different oopores and different portions of uniseriate and biseriate pitting.

3.4.3.3 Comparison with other fossil woods of *Protophyllocladoxylon*

Protophyllocladoxylon has been reported from Paleocene and Eocene strata on Seymour Island (Pujana *et al.*, 2014; 2015). *Protophyllocladoxylon francisiae* described by Pujana *et al.* (2014; 2015) is taxonomically similar to specimen D9.181.1 and because it has predominantly araucarioid type tracheid pitting (biseriate and rarely triseriate pitting), window-like oopores in cross-fields and a mean ray height of 7 cells.

Wood specimen D9.071.1 shares anatomical characteristics with *Podocarpoxyton* sp. 1. described by Falcon-Lang and Cantrill (2000) from the Cretaceous of Alexander Island. These features are, exclusively uniseriate tracheid pitting that is dominantly touching and 1-2 large pits per cross-field, which are oval in shape. In *Podocarpoxyton* sp.1 the cross-field pits are described as podocarpoid with reduced borders. According to the identification key developed by Philippe and Bamford (2008) *Podocarpoxyton* sp.1 would be better placed in the morphotype *Protophyllocladoxylon* thus D9.071.1 is placed in *Protophyllocladoxylon*.

Wood with *Protophyllocladoxylon* type characters has been described from the Mesozoic localities indicating that some of the wood features are quite ancient. These woods are much older than those from Paleocene of Seymour Island, which, being younger, are more likely to be related to modern Podocarpaceae. At other locations in the Northern and Southern Hemispheres, *Protophyllocladoxylon* has only been described from Mesozoic sequences (Zhang *et al.* 2010 and references therein). The wood specimens described here have some similarity to the *Protophyllocladoxylon* species described from the Northern Hemisphere but are considerably younger in age.

Protophylocladoxylon szei described from the Late Triassic in China (Zhang *et al.*, 2010 and references therein) is taxonomically similar to D9.071.1 because it has exclusively uniseriate tracheid pitting that is continuous or sometimes spaced and large cross-field pits that are circular, broadly oval or elliptical. Ray height is also similar (1-10 cells high). *Protophylocladoxylon szei* is different because it only has 1 pit per cross-field and it is also considerably older in age younger.

Specimens D9.093.1 and D9.112.1 share anatomical characteristics with *Protophylocladoxylon quedlinburgense* described from the Early Jurassic in Germany. These characteristics are it has uniseriate pitting that is either continuous and spaced, and biseriate pitting that can be opposite or alternate (Zhang *et al.*, 2010 and references therein).

3.4.3.4 Comparison with extant wood

Protophylocladoxylon is closest to the wood of extant *Phyllocladus* of the family Podocarpaceae because it has distinct growth rings, large oopores, and no axial parenchyma. However, *Phyllocladus* is different because it has scattered tracheid pitting (Greguss, 1955; Meylan and Butterfield, 1978). It is assumed that *Protophylocladoxylon* possibly had a similar life habit to extant *Phyllocladus*. Today modern *Phyllocladus* is found in forests of the Southern Hemisphere. Species of *Phyllocladus* occur at all altitudes and prefer areas of high rainfall (see section 3.4.2.4).

3.4.4 *Podocarpoxyton*

Family Podocarpaceae

Genus: *Podocarpoxyton* Gothan

3.4.4.1 Description

Specimen number: D9.090.1

Description: This wood specimen is likely to have been derived from mature wood from either the outer part of a trunk or large branch due to low growth ring curvature.

Growth rings: Growth ring boundaries are indistinct (Figure 3.14a). The transition from earlywood to latewood is abrupt. Latewood is narrow and is only 5 cells wide. Growth ring width could not be measured due to poor preservation.

Tracheids: In TS earlywood tracheids are square or hexagonal. Earlywood tracheid tangential diameter ranges from 34.3 μm and radial diameter ranges from 30.7 μm . Latewood tracheids appear rectangular. Latewood tracheid tangential diameter ranges from 16 μm , radial diameter ranges from 13.6 μm .

Tracheid pitting: Tracheid pitting is uniseriate, sometimes part biseriate and are abietinean (Figure 3.14d). Pits are round and have round apertures. Mean pit diameter is 14 μm (range 10 – 17.5 μm). Pit aperture diameter ranges from 2.5 -7.5 μm . Tangential pitting is also present but is smaller in diameter 5 -10 μm (Figure 3.14f)

Cross-field pitting: Cross-field pits appear to be of cupressoid and taxiod type (Figure 3.14c, e). There are 1 to 2 pits per cross-field (Figure 3.14b). When two pits are present they are separate and either arranged side by side or oblique. Sometimes cross-field areas are blank. Mean cross-field pit diameter is 7 μm (range: 5 - 10 μm).

Axial parenchyma: none observed.

Rays: In TLS rays are uniseriate and long (Figure 3.14g). Mean ray height in microns is 255.7 μm (45 – 735 μm). Mean ray height in number of cells is 16 (range: 2 – 43). In radial section ray walls appear smooth and generally thin

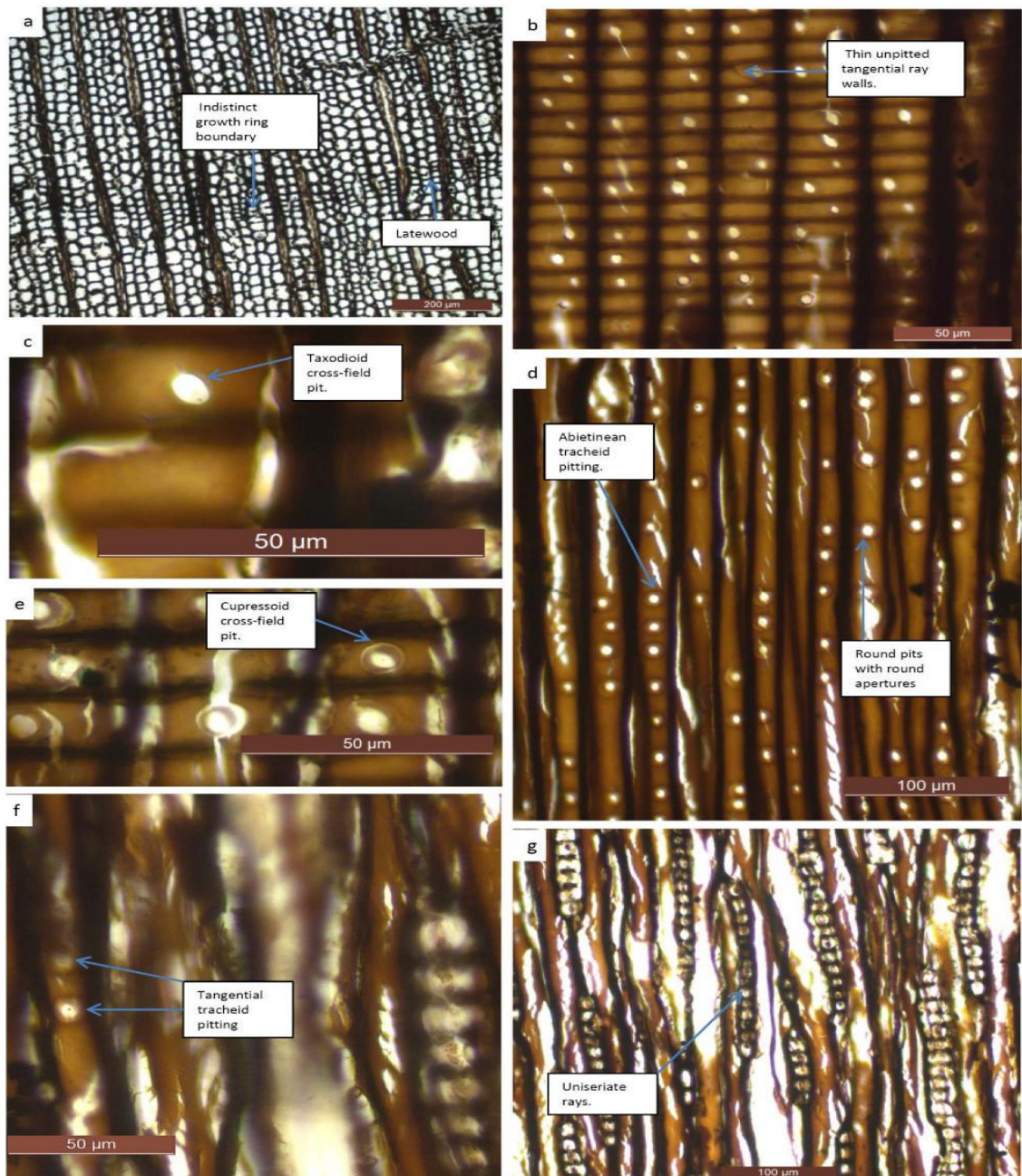


Figure 3. 14. *Podocarpoxylon*. a) TS showing indistinct growth ring boundaries, scale bar = 200 μm . b) RLS showing rays and cross-field pitting, scale bar = 50 μm . c) RLS showing taxodioid cross-field pit, scale bar = 50 μm . d) RLS showing tracheid pitting, scale bar = 100 μm . e) RLS showing cupressoid cross-field pits, scale bar = 50 μm . f) TLS showing tracheid pitting, scale bar = 50 μm . g) TLS showing uniseriate rays, scale bar = 100 μm .

3.4.4.2 Discussion

Since specimen D9.090.1 has abietinean tracheid pitting and cross-field pitting that is cupressoid to taxodioid the wood best fits the genus *Podocarpoxyton* (Philippe and Bamford, 2008). *Cupressinoxyton* wood also has abietinean pitting but is characterised as having exclusively cupressoid cross-field pitting. Determining the types of cross-field pitting can be difficult as sometimes pit outlines are difficult to see.

3.4.4.3 Comparison with other fossil wood of *Podocarpoxyton*

Podocarpoxyton has been reported from Early and Late Cretaceous sedimentary sequences on Livingston Island (Torres and Lemoigne, 1989; Falcon-Lang and Cantrill, 2001; Poole and Cantrill, 2001) and Alexander Island in Antarctica (Falcon-Lang and Cantrill, 2000). *Podocarpoxyton* wood has also been reported from Eocene sedimentary sequences on King George Island (Poole *et al.*, 2001) and Seymour Island (Pujana *et al.*, 2014). The wood identified in this project does not resemble the previously published *Podocarpoxyton* wood from the Antarctica Peninsula. The published *Podocarpoxyton* woods have exclusively podocarpoid cross-field pits and smaller rays compared to the wood described here.

Podocarpoxyton sp, which has been described from the mid-Eocene stratigraphy of southern- Chile (Terada *et al.*, 2006b) show similarity due to having 1-2 pits per cross-field, which are taxodioid and cupressoid. However, it is different because it has a gradual transition from earlywood to latewood and shorter rays.

3.4.4.4 Comparison with extant wood

The wood specimen described here has similarities to wood of both modern Podocarpaceae and Cupressaceae. Both families have cross-field pits that are podocarpoid, cupressoid and taxiod (Greguss, 1955; Meylan and Butterfield, 1978). The wood appears to be closest to Podocarpaceae

because most species of Cupressaceae have uneven or pitted marginal ray walls, which the specimen here does not have. Modern Podocarpaceae usually have abundant axial parenchyma, which the wood described here does not.

The wood described here shows some similarity to *Dacrycarpus dacrydioides* and *Prumnopitys ferruginea* from modern New Zealand (Meylan and Butterfield, 1978) as they are characterised as having indistinct to slightly distinct growth rings, tracheid pitting that is predominantly uniseriate, predominantly 1-2 pits per cross-field that are cupressoid and taxiod; and rays that can be 54 cells high.

3.4.4.5 Ecology of Podocarpaceae

Today podocarps are found living in the warm and cool temperate forests of New Zealand (e.g. *Podocarpaceae totora*, *Prumnopitys ferruginea*, *Prumnopitys taxifolia* and *Dacrycarpus dacrydioides*), the cool temperate forests of Tasmania (e.g. *Podocarpus drouynianus*, *Podocarpus lawrencei*), Chile and Argentina (e.g. *Lepidothamus fonkij*, *Podocarpus nubigena*, *Podocarpus saligna*, *Prumnopitys andina* and *Saxegothaea conspicua*) (Ogden and Veblen, 1995; Veblen *et al.*, 1995; Gibson *et al.*, 1995).

In general, temperate podocarps live in areas of high rainfall and occupy a wide range of altitudinal zones, but they are rarely found living at the treeline in temperate forests (Coomes and Bellingham, 2011). Most podocarp species occur as emergent canopy trees, although some do occur as shrubs, such as *Podocarpus lawrencei*, which lives in subalpine to alpine habitats in Tasmania (Gibson *et al.*, 1995).

Podocarps are slow growing and shade tolerant in varying degrees. In the forests of New Zealand and Valdivian forest in Chile podocarps can co-exist with broad-leaved trees, such as *Weinmannia* and *Nothofagus* species. However, they are most dominant on areas of infertile and poorly drained soils, where the competition from broad-leaved trees is less. On more fertile

soils in closed canopy settings, podocarps rely on disturbances, such as wind-throw down to create gaps for new growth (Ogden and Stewart, 1995; Lusk, 1996).

On North Island, New Zealand, podocarp species (*Prumnopitys ferrugina* & *Podocarpus halli*) are found living at mid-elevations on ridge tops that are prone to disturbances, such a wind-throw-down (Ogden and Stewart, 1995).

Podocarps are also found in the tropical forests of South America, Papua New Guinea, Australia, and Malaysia. Like temperate podocarps they are mainly found on poorly drained soils, but they are also found at high altitudes, living at the treeline in montane forests (Coomes and Bellingham, 2011).



Figure 3. 15. Podocarp-broad-leaved forest in New Zealand. Taken from www.nzpcn.org.nz

3.4.5 Unidentified conifer wood

Five specimens (D9.019.2, D9.182.1, D9.186.1, D9.191.1, D9.191.2 and D9.118.1) could not be identified. This is due to poor preservation preventing any defining features to be observed. The wood is definitely conifer wood because it has tracheids and no vessels.

Specimens D9.019.2 and D9.118.1 show similarity to *Podocarpoxyton* and *Cupressinoxyton* wood because they have abietinean pitting. Cross-field pits in Specimen D.019.2 cannot be distinguished. In specimen D9.118.1 cross-field pits can be seen, however the pit type (e.g. cupressoid and taxoid) cannot be distinguished due to poor preservation. There are 1 or 2 pits per cross-field in specimen D9.118.1. Axial parenchyma is present in both wood specimens. Modern Cupressaceae and Podocarpaceae trees are characterised as having spaced tracheid pitting and a low number of cross-field pits (Greguss, 1955; Meylan and Butterfield, 1978).

3.5 Summary

In summary, four types of conifer wood have been identified in the wood assemblage from Seymour Island. These include *Agathoxyton* (species: A, B, C and D), *Phyllocladoxyton*, *Protophyllocladoxyton* (species: A, B, C and D) and *Podocarpoxyton/Cupressinoxyton*. Although all morphotypes have been described previously from Seymour Island. The most common genus is *Agathoxyton*, followed by *Phyllocladoxyton*, *Protophyllocladoxyton* and *Podocarpoxyton/Cupressinoxyton*. Figure 3.16 presents a pie chart which illustrates the abundance of the different conifer genera identified.

Modern trees with woods of these types are common in the Southern Hemisphere forests in southern South America, New Zealand and Australia (including Tasmania). They live in a wide range of habitats from lowland to high altitude areas. Most of the tree types are shade-intolerant to varying degrees and have slow growth rates and they have different strategies in

order to avoid competition from faster growing broad-leaved angiosperm trees. These strategies include growing in sub-optimal conditions (e.g. poorly fertile soils), occupying areas that are prone to frequent large scale disturbances such as landslides, flooding and disturbances related to volcanic activity (e.g. wildfires and pyroclastic flows).

Abundance of the four conifer wood genera identified.

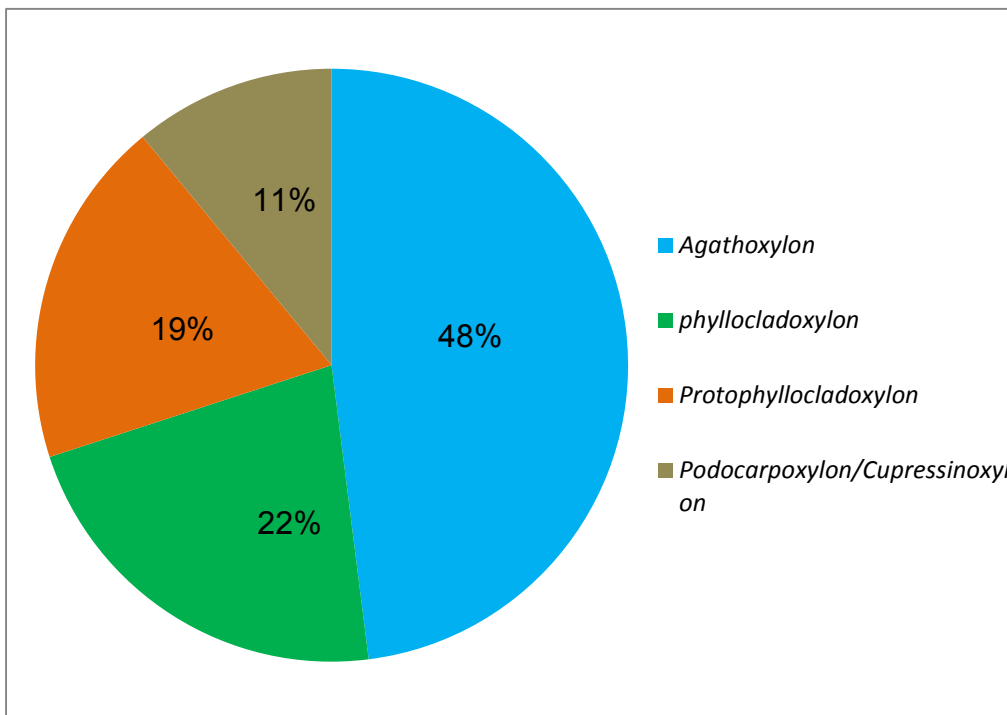


Figure 3. 16. Abundance of the four conifer wood genera identified in this study. Percentages are calculated out of the 27 conifer wood specimens that could be identified (including D9.118.1 and D9.019.2).

Chapter 4

Angiosperm wood

4.1 Introduction

This chapter presents descriptions of fossil angiosperm wood found in the Seymour Island section. Anatomical features and keys that were used to identify fossil angiosperm wood types are discussed in the next section. The bulk of the chapter contains descriptions of the main angiosperm wood types in the fossil wood assemblage. Possible modern analogues and ecology of nearest living relatives (NLRs) are also considered.

4.2 Wood anatomy and identification

Angiosperm wood is composed of vessels and fibres (Figure 4.1). The main purpose of vessels is to transport water throughout the tree (Fritts, 1976). The purpose of fibres is to mechanically support the vessels. Vessel ends have perforation plates, which control water flow through the vessels; perforation plates can be either simple or scalariform (Table 4.1). Vessel walls have pits and these aid the distribution of water through neighbouring vessels. Running radially across the vessels and the fibres are the rays, which store and transport nutrients throughout the tree. Pits are present where the vessels and ray cells intersect; these pits are called vessel-ray pitting. The arrangement of vessels, vessel-wall pitting, vessel-ray pitting, nature of rays and type of perforation plates are the main features used in the identification of angiosperm woods. Other features such as the presence and absence of axial parenchyma are also useful. Table 4.1 lists and briefly describes the anatomical features that were used for identification in this project.

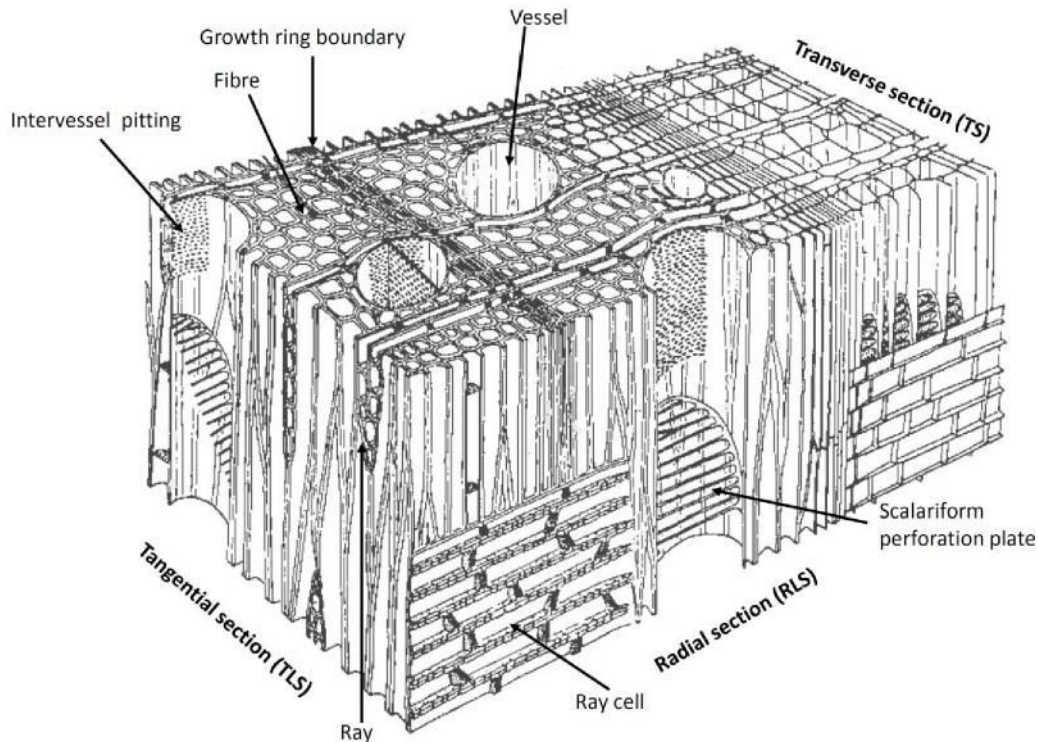


Figure 4. 1. The three dimensional structure of angiosperm wood. Modified from Schweingruber (1996).

The identification keys used for modern angiosperm wood are also widely used for fossil angiosperm wood. Angiosperm fossil wood in this project was described using the features and measurements recommended by the IAWA Committee (1989) except for vessel element length and ray classification. Vessel element length was measured in TLS from thin section and rays were classified using Kribs (1935)(within Carlquist, 2001) scheme. Some of the features used by the IAWA committee (1989) have been presented in Figure 4.2.

The angiosperm fossil wood was identified using the IAWA Insidewood database (2004) and comparisons with published descriptions of Cretaceous and Paleogene fossil angiosperm wood from Antarctica and South America. In addition, a modern wood atlas (Illic, 1991) and literature on modern angiosperm families were also consulted (Dickison, 1977; Meylan and Butterfield, 1978; Metcalfe, 1987; Patel, 1990; Cutler and Gregory, 1998).

Table 4. 1. A list of angiosperm features with definitions. Definitions adapted from IAWA committee (1989) and Carlquist (2001).

Anatomical feature	Definition
Diffuse porous (Figure 4.2c)	Observed in TS. Earlywood and latewood vessels are a similar size.
Fibre (Figure 4.1)	Long unicellular wood element with a long axis parallel to the stem. Its function is mechanical support of vessels.
Fibre-tracheid	A fibre that has pits on its radial and/or tangential walls.
Intervessel pitting (Figure 4.1 and 4.2d, e, f)	Best observed in TLS but can also be seen in RLS. Pitting on vessel walls. The purpose is to allow water to flow from one vessel to the next. Pitting can be simple or have borders.
Perforation plates (Figure 4.1 & 4.2g, h)	Best observed in RLS. Found on the end of vessels, they can be a simple round opening or have lateral bars (scalariform). They control the water flow between vessels.
Rays (Figure 4.1 & 4.2n)	Observed in TS, RLS and TLS. Layers of parenchyma cells that run radially through the wood. In tangential view they can be uniseriate, biseriate or multiseriate. Their function is to store and transport nutrients.
Ring-porous (Figure 4.2a)	Observed in TS. Where earlywood vessels are markedly larger than latewood vessels.
Semi-ring porous (Figure 4.2b)	Observed in TS. Gradual change to more narrow vessels in earlywood. Earlywood vessels are not distinctly larger than latewood vessels.
Septate fibres	Observed in RLS and TLS. Fibres with thin, unpitted lateral walls.
Tyloses (Figure 4.2l)	Best observed in RLS and TLS. Ballon-like structures that grow out from adjacent parenchyma cells. Formed as a result of wounding or loss of water pressure.
Vessels (Figure 4.1)	Long tube-like structure with long axis parallel to the stem. Its function is water conduction.
Vessel-ray pitting (Figure 4.2i, j, k)	Observed in RLS. Pits found in areas where vessel and rays intersect and occur in a number of forms. Vessel-ray pits can be simple or have borders.

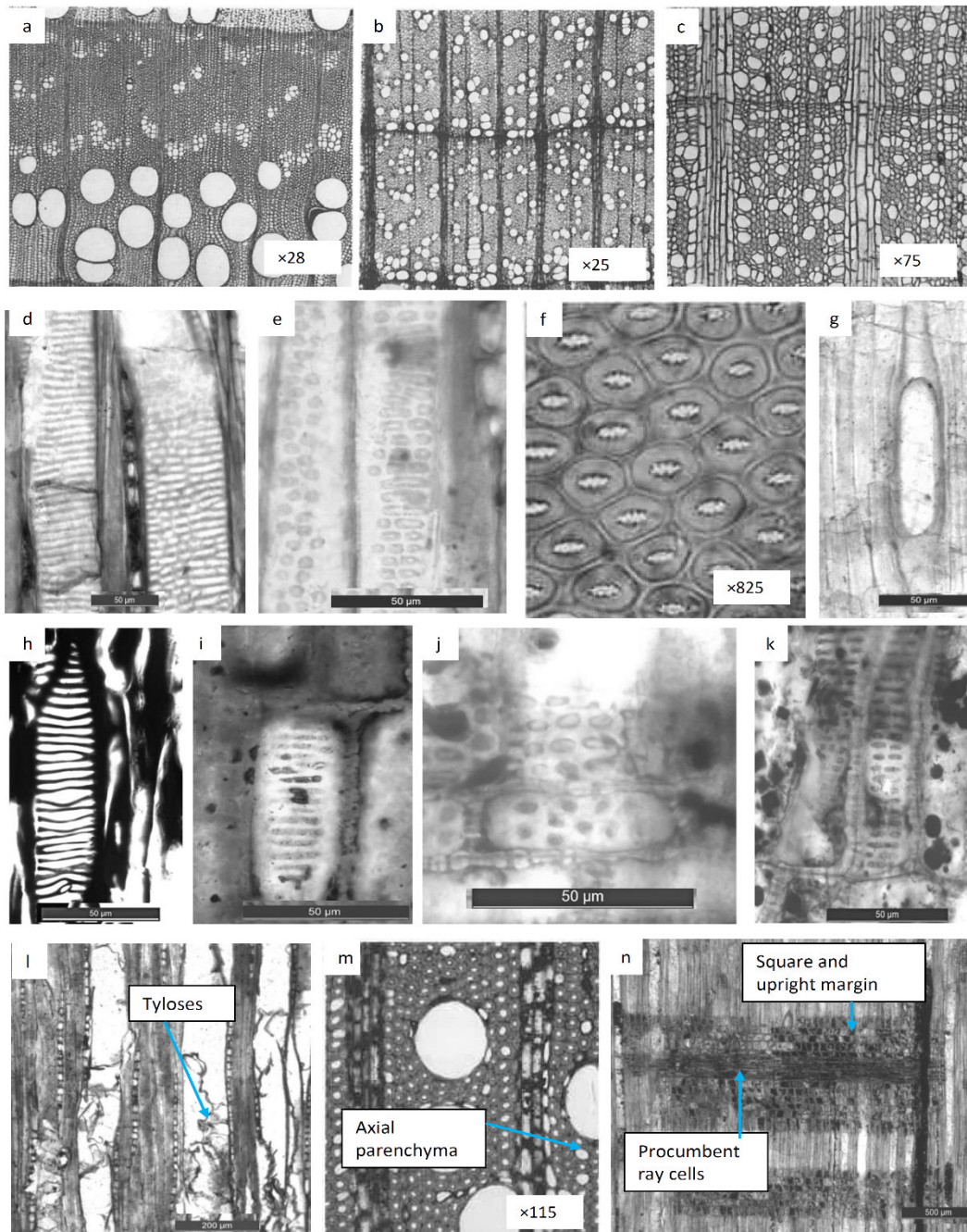


Figure 4. 2. Main anatomical features of angiosperm wood. a) TS showing ring-porous wood. b) TS showing semi-ring porous wood. c) TS showing diffuse porous wood. d) TLS showing scalariform intervessel pitting (left) and scalariform to opposite intervessel pitting (right). e) TLS showing opposite intervessel pitting. f) TLS/RLS showing alternate intervessel pits with borders. g) RLS showing simple perforation. h) RLS showing scalariform perforation plate. i) RLS scalariform vessel-ray pitting. j) RLS showing circular and oval-horizontally elongate vessel-ray pits with reduced borders. k) RLS showing horizontally-elongate vessel-ray pitting. l) TLS showing tyloses in vessels. m) TS showing diffuse axial parenchyma. n) RLS showing a ray with procumbent cells in the middle proportion and square to upright marginal cells. 28 Images a, b, c and f have been taken from IAWA committee (1989). Other images are of wood in this study.

Twenty-five angiosperm wood specimens have been identified in this project. The genus present are *Nothofagoxylon*, *Weinmannioxylon*, *Myrceugenelloxylon* and *Antarctoxylon*.

Section 4.3 presents each genus as summarised morphological descriptions and image plates illustrating the main anatomical features. In addition, where there is more than one specimen belonging to a genus, a summary table has been compiled of the anatomical features for each specimen. For each genus a brief ecology of its NLR (Nearest Living Relative) is also given.

4.3 Description of fossil angiosperm wood studied in this project.

This section presents descriptions of each genus. Anatomical measurements are given in Appendix B.2. Four angiosperm genera have been identified: *Nothofagoxylon*, *Weinmannioxylon*, *Myrceugenelloxylon* and *Antarctoxylon*.

4.3.1 *Nothofagoxylon*

Family: Nothofagaceae

Genus: *Nothofagoxylon* Gothan

4.3.1.1 Description

Specimen numbers: D9.011.2, D9.012.1, D9.015.1, D9.016.1, D9.018.1, D9.019.1, D9.021.1, D9.023.1, D9.027.1, D9.041.1, D9.053.1, D9.054.1, D9.089.1, D9.095.1, D9.096.1, D9.105.1, D9.110.1, D9.128.3, D9.130.1 and D9.157.3.

Description: Most of the wood specimens described here are likely to have come from either a branch or trunk wood. Wood Specimen D9.012.1 has pith present. Wood specimens D9.110.1 and D9.105.1 are likely to be mature wood since they are large specimens and the growth rings have low curvature. Specimen D9.054.1 has indistinct growth rings and therefore may be root wood.

Growth ring: Growth rings are distinct to indistinct (D9.054.1) (Figure 4.3a).

Vessels: Semi-ring porous arrangement (Figure 4.3a). The vessels appear as solitary and in radial files of 2 – 8, occasionally clusters of 4 – 6 vessels. In TS

vessels can be circular, angular and radially elongate in earlywood. Mean radial vessel diameter ranges from 52.9 – 108.1 μm and mean tangential vessel diameter ranges 45.7 – 78.8 μm . Mean vessel element length 327.4 – 1088.4 μm . There are on average 36 – 141 vessels per mm^2 . Tyloses are often present in vessels (Figure 4.3d).

Scalariform plates: Perforation plates are simple and scalariform (Figure 4.3c). Scalariform plates have numerous bars (>15 bars).

Intervessel pitting: Intervessel pitting is opposite, scalariform to opposite, and scalariform (Figure 4.3e, f). Sometimes pits have distinctive borders (Figure 4.3f). Pit diameter ranges from 5 – 47.5 μm .

Vessel-ray pitting: (RLS) Pitting occurs as scalariform, circular, oval-horizontally elongate, arrangement of pits is opposite (Figure 4.3g, h). Pit diameter ranges from 2 – 25 μm (horizontal diameter). Vessel- ray pitting have reduced borders (2 μm or less) in some specimens.

Axial parenchyma: Diffuse-rare (hard to determine).

Rays: (TLS) Rays are uniseriate, biseriate and part-biseriate (Figure 4.3i, j). Specimen D9.130.1 sometimes has rays that are 6-7 seriate. Mean ray height ranges from 235 - 504 μm . In TLS rays consist of both upright and procumbent cells and best fit into Kribs heterogeneous IIB. In RLS the main body of the rays are made of procumbent cells and the margins consist of one or two rows of square and upright cells (Figure 4.3b). Mean number of rays per tangential mm ranges from 5 – 15 rays.

Fibres: none-septate. Fibre-tracheid pitting only observed in D9.157.1. Fibre tangential diameter ranges from 12.5 – 42 μm and radial diameter ranges from 5 – 37 μm .

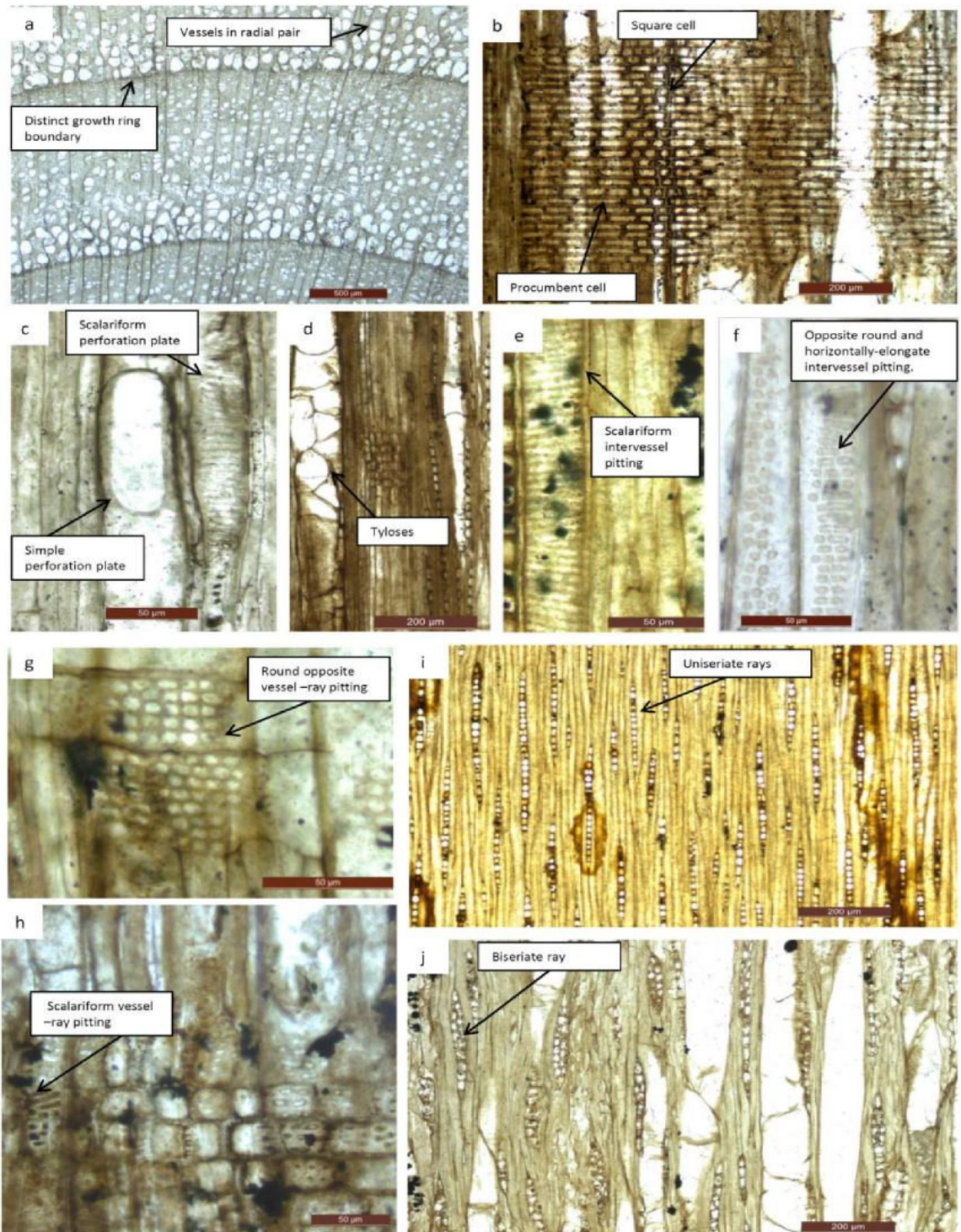


Figure 4. 3. *Nothofagoxylon*, Species A (D9.012.1, D9.095.1, D9.021.1, D9.018.1, D9.096.1), Species C (D9.054.1). a) D9.012.1, TS showing growth ring boundaries, scale bar = 500 μ m. b) D9.095.1, RLS showing ray cells, scale bar = 200 μ m. c) D9.012.1, RLS showing a simple and scalariform perforation plates, scale bar = 50 μ m. d) D9.021.1, RLS showing tyloses, scale bar = 200 μ m. e) D9.018.1 TLS showing scalariform intervessel pitting, scale bar = 50 μ m f) D9.096.1, showing circular, horizontally- elongate intervessel pitting in an opposite arrangement, scale bar = 50 μ m. g) D9.096.1, RLS showing circular opposite vessel-ray pitting, scale bar = 50 μ m. h) D9.096.1, RLS showing scalariform and horizontally elongate vessel-ray pitting, scale bar = 50 μ m. i) D9.018.1, TLS showing uniseriate rays, scale bar = 200 μ m. j) D9.054.1, RLS showing biseriate ray, scale bar = 200 μ m.

Table 4. 3. Summary of the anatomical characters of *Nothofagoxylon* wood (Species A, B) identified in this project. Numbers in brackets are mean values.

Species	A					B
	D9.023.1	D9.027.1	D9.089.1	D9.095.1	D9.096.1	D9.041.1
Growth rings	Distinct	Distinct	Distinct	Distinct	Distinct	n/a
Vessels						
Shape (TS)	Angular, radially elongate	Circular, angular, radially elongate	circular, angular	Circular, angular, radially elongate	Circular, angular, radially elongate	n/a
Porosity	Semi-ring	Semi-ring	diffuse - semi -ring	Semi-ring	Diffuse to semi-ring	n/a
Arrangement	Solitary, radial files (2 - 5), rarely clusters (5)	Solitary, radial file (2 -9), rarely clusters (6)	solitary, radial files (2 - 7) occasionally clusters (4)	Solitary, radial files (2 - 6)	Solitary, radial files (2 - 8)	Solitary, radial file (2 -3)
Number per mm-2	68 - 132 (105)	78 - 225 (141)	n/a	40 - 103 (68.2)	56 -165 (88.5)	n/a
Tangential diameter (µm) of vessels	25 - 90 (57.5)	17 - 105 (47.5)	20 - 75 (51.7)	42.5 – 122.9 (75.8)	42.5 - 110 (68)	n/a
Vessel element length	450-1035 (789.7)	500 - 950 (726.1)	n/a	680 - 1600 (940)	650 - 1400 (1088.4)	n/a
Perforation plates	Simple and scalariform	Simple and scalariform	scalariform, ?simple	Simple and scalariform	Simple and scalariform	Scalariform and simple

Table 4. 4. Summary of the anatomical characters of *Nothofagoxylon* wood (Species B) identified in this project. Numbers in brackets are mean values.

Species	B			
Specimen	D9.053.1	D9.110.1	D9.128.3	D9.157.3
Growth rings	Distinct	Distinct to Indistinct	Distinct	Distinct
Vessels				
Shape (Transverse)	Circular	Circular and radially-elongate	Circular , angular, radially elongate	Circular, radially-elongate
Porosity	Semi-ring	Semi-ring	Semi-ring	Semi-ring
Arrangement	Solitary, radial files (2 -5)	Solitary, radially (2 -3) sometimes 4, rarely clusters.	Solitary radial files m 2 -3 sometimes 6	Solitary radial files (2-3)
Number per mm-2	53 - 130 (96.1)	39 - 166 (103.9)	32 - 68 (49)	27 - 50 (36.8)
Tangential diameter (µm) of vessels	30 - 130 (65.9)	20 – 114.5 (49)	14.7 - 103.9 (48)	30 - 110 (78.8)
Vessel element length	240 - 1600 (720.7)	350 - 615 (490)	n/a	N/A
Perforation plates	Scalariform and simple	Scalariform and simple	Scalariform and simple	Scalariform
Intervessel pitting	Circular horizontally - elongate. Opposite, sometimes alternate	Horizontally-elongate. Opposite	Round, oval-elongate. Opposite	Circular, horizontally elongate. Opposite

Table 4.4. continued.

Species	B			
Specimen	D9.053.1	D9.110.1	D9.128.1	D9.157.1
Rays				
Width	Uniseriate	Uniseriate	Uniseriate	Uniseriate
Height (µm)	120 - 385 (291.8)	100 - 300 (242.8)	85-460 (220)	150 - 310 (236.1)
Marginal cells: rows, shape	1 or 2 upright	1 -2 upright	1-2 upright	n/a
Per tangential mm	5 to 10 (9)	3 – 7 (5)	8 - 12 (9)	n/a
Vessel - ray pitting	Circular, oval, horizontal- elongate	Circular, oval, horizontally-elongate	Circular, oval, elongate	Circular, oval elongate
Parenchyma	Diffuse -rare	Diffuse-rare	?	?
Fibres				
Septate	Absent	Absent	Absent	Absent
Pitting	Absent	Absent	Absent	Present

Table 4. 5. Summary of the Anatomical characters of *Nothofagoxylon* wood (Species C and D) in this project. Numbers in brackets are mean values.

Species	C		D
Specimen	D9.054.1	D9.105.1	D9.130.1
Growth rings	Indistinct	Distinct	Indistinct
Vessels			
Shape (Transverse)	Circular	circular and radially -elongate	Angular, radially-elongate
Porosity	Semi-ring	Semi-ring	Semi-ring
Arrangement	Solitary, radial groups of 2 -3 (rarely 4)	Solitary, radial files of 2 -7, clusters 3-6	Solitary, radial files (2-3), tangential pairs, sometimes clusters of 4
Number per mm-2	23 - 75 (45)	39 - 88 (62.7)	36 - 70 (53.6)
Tangential diameter (μm) of vessels	60 - 140 (87)	30.5 - 125 (72.7)	30 - 90 (61.9)
Vessel element length	625 - 1005 (750.8)	300 - 550 (421.3)	500 - 1825 (905)
Perforation plates	Scalariform and simple	Scalariform and simple	Scalariform and simple
Intervessel pitting	Scalariform, horizontally- elongate. Opposite	Scalariform, horizontally- elongate. Opposite	Round, oval elongate possibly scalariform. Opposite

Table 4.5. Continued.

Species	C		D
Specimen	D9.054.1	D9.105.1	D9.130.1
Rays			
Width	Uniseriate, part biseriata, biseriate	Uniseriate, biseriata, part -biseriate, occasionally triseriate	Uniseriate, biseriata, sometimes 6 - 7 seriate.
Height (μm)	100 - 722.5 (294.6)	65 - 725 (286)	150 - 700 (356.2)
Marginal cells: rows, shape	1 upright	1 upright	1-2 upright
Per tangential mm	3 - 8 (6)	11 to 17 (13)	2 - 6 (4)
Vessel - ray pitting	Oval, horizontally elongate, scalariform	Circular, oval, horizontally elongate	Circular, oval horizontally elongate
Parenchyma	?	Diffuse-rare	?
Fibres			
Septate	Absent	Absent	Absent
Pitting	Absent	Absent	Absent

4.3.1.2 Discussion

The wood specimens described here have been assigned to *Nothofagoxylon* because they share very Semi-ring porosity; vessels that are solitary and in radial rows; intervessel pits that are opposite, scalariform and sometimes alternate; perforation plates that are simple and scalariform, and also the presence of tyloses.

There is variability within the wood specimens described here. The most obvious differences include the type of vessel-ray pitting, intervessel pitting and ray width. Based on these differences the wood specimens have been separated into four species: A, B, C and D (Table 4.2; 4.3; 4.4 and 4.5). The four species are defined as follows:

- **Species A.** This species is characterised as having predominantly uniseriate rays and intervessel pitting and vessel-ray pitting that is scalariform, circular and horizontally elongate, which is oppositely arranged. Species A includes wood specimens D9.011.1, D9.012.1, D9.016.1, D9.018.1, D9.019.1, D9.021.1, D9.023.1, D9.027.1, D9.089.1, D9.095.1 and D9.096.1 (Table 4.2 and 4.3).
- **Species B.** Specimens D9.053.1, D9.110.1, D9.041.1, D9.128.3 and D9.157.1 have been grouped based on having predominantly uniseriate rays, intervessel pitting and vessel-ray pitting that is mainly elongate and oppositely arranged (Table 4.3 and 4.4).
- **Species C.** Specimens D9.054.1 and D9.105.1 have biseriate rays and sometimes triseriate rays (Table 4.5).
- **Species D.** Wood specimen D9.130.1 is considered a different species on the basis of having rays that are 1 - 7 seriate whereas the other wood specimens have ray widths that are between 1 – 3 seriate (Table 4.5).

Wood specimen D9.015.1 cannot be fully identified because a small number of features could be seen. The wood appears similar to *Nothofagoxylon* on the basis of scalariform perforation plates present; intervessel pitting that is circular and scalariform to opposite; vessel-ray pitting that is scalariform, circular and horizontally elongate.

4.3.1.3 Comparison of other *Nothofagoxylon* wood

Nothofagoxylon wood has been reported from Late Cretaceous strata on James Ross Island, Late Cretaceous and early Paleogene strata on Seymour Island, and Eocene strata on King George Island (Poole *et al.*, 2001; Poole, 2002).

Specimens A shows close similarity to *Nothofagoxylon scalariforme*, which has been reported from the Late Cretaceous strata on James Ross Island, Late Cretaceous and early Paleogene strata on Seymour Island, and Eocene strata on King George Island (Poole *et al.*, 2001; Poole, 2002). The common features include intervessel pitting that is scalariform and scalariform to opposite; vessel ray pitting that is circular, oval, horizontally-elongate and scalariform; and predominantly uniseriate rays. Quantitative feature values also recorded here are within the range of values for *Nothofagoxylon scalariforme*.

Species B D9.041.1, D9.053.1, D9.110.1, D9.128.3 and D9.157.3 show close similarity to *Nothofagoxylon ruei*, which has been reported from early Paleogene strata on Seymour Island (Poole, 2002). *Nothofagoxylon ruei* is characterised as having intervessel pitting that is opposite, occasionally alternate and circular to oval-horizontally elongate; vessel-ray pitting that is circular to horizontally elliptical and is opposite or sometimes alternate; and uniseriate rays.

Quantitative features (e.g. vessel diameter, number per mm², vessel element length) are also similar, except vessel element length in specimen D9.053.1, which is significantly higher than those recorded for *Nothofagoxylon ruei*.

Species C D9.054.1 and D9.105.1 are most similar to *Nothofagoxylon kraeusli*, which has been described from the Late Cretaceous and Paleocene strata on Seymour Island (Poole, 2002). *Nothofagoxylon kraeusli* is characterised as having uniseriate, biseriate and triseriate rays; intervessel pits that are mostly opposite, horizontally-elongate, scalariform or alternate; and vessel ray pits that are circular to elliptical, rarely scalariform.

Specimen D9.130.1 is generally similar to *Nothofagoxylon* wood, but it is different from previously described *Nothofagoxylon* species because it has rays that are up to 7- seriate.

Nothofagoxylon scalariforme, *Nothofagoxylon ruei* and *Nothofagoxylon kraeuseli* have also been reported from Palaeogene strata in southern Chile (Poole, 2002; Nishida *et al.*, 2006; Terada *et al.*, 2006a).

4.3.1.4 Comparison with modern *Nothofagus*

Modern genus *Nothofagus* of the family Nothofagaceae is split into genera *Nothofagus*, *Fuscospora*, *Lophozonia* and *Brassospora* (Poole, 2002). Fossil *Nothofagoxylon* wood described here shows similarity to wood of the modern genera *Nothofagus* and *Lophozonia*. Genus *Nothofagus* is characterised by having mostly uniseriate rays, and scalariform intervessel and vessel-ray pitting. Species belonging to the Genus *Lophozonia* is characterised as having intervessel pits that are circular to elongate and have an opposite or sometimes alternate arrangement, vessel-ray pits that are circular; and 1-3 seriate rays. Species B, C and D show similarity to *Lophozonia*.

4.3.1.5 Ecology of modern *Nothofagus*

Today genera *Lophozonia*, *Nothofagus* and *Fuscospora* of the genus *Nothofagus* are found living in warm to cool temperate forests in the Southern Hemisphere (Ogden *et al.*, 1996; McGlone *et al.*, 1996; Read and Brown, 1996; Veblen *et al.*, 1996; Poole, 2002).

Species of *Nothofagus* are found living in Chile and Argentina (*Nothofagus antarctica*, *Nothofagus betuloides*, *Nothofagus dombeyi* and *Nothofagus pumilio*). *Lophozonia* is found living in Australia (*Nothofagus cunninghamii*), and New Zealand (*Nothofagus menziessi*), Chile and Argentina (*Nothofagus alpine*, *Nothofagus glauca* and *Nothofagus obliqua*). *Fuscospora* is found living in Australia (*Nothofagus gunnii*) and New Zealand (*Nothofagus fusca*, *Nothofagus solandri* and *Nothofagus truncata*) (Ogden *et al.*, 1996; Read and Brown, 1996; Veblen *et al.*, 1996).

Species of *Nothofagus* living in New Zealand are evergreen trees and they are found living in a range of environments on North and South Island (Ogden

et al., 1996). In the mountainous regions of New Zealand, stands of *Nothofagus solandri* var *cliffortioides* and *Nothofagus menziessi* are found living near the timberline under a cool temperate climate. *Nothofagus menziessi* is also found living in southern areas of the South Island at low to mid altitudes, alongside other trees such as, *Weinmannia racemosa* and podocarp species. Figure 4.5 presents a photo of a *Nothofagus* forests in New Zealand. On North Island under a warm temperate climate *Nothofagus truncata* is found at mid-altitudes on ridge tops and steep slopes and is associated with *Agathis australis*.

In Chile and Argentina there are evergreen species (*Nothofagus betuloides*, *Nothofagus dombeyi*, *Nothofagus nitida*) and deciduous species (*Nothofagus alpina*, *Nothofagus antarctica*, *Nothofagus obliqua*, *Nothofagus pumilio*). *Nothofagus* is found living between latitudes of 37°S - 55°S in the cool temperate zone of Chile and Argentina. In the northern part of this latitudinal zone, *Nothofagus pumilio* and *Nothofagus antarctica* are found living at the alpine-timberline in the Andes in the form of krummholz. Krummholz are stunted trees that are deformed by wind (Veblen *et al.* 1995). At high altitudes in the Coastal Cordilla *Nothofagus pumilio* is associated with conifer *Araucaria Araucana* (Figure 4.4). At 55°S *Nothofagus antarctica* and *Nothofagus pumilio* are found living at sea level. *Nothofagus betuloides*, *Nothofagus dombeyi*, *Nothofagus nitida* are common components of the Valdivian forest where they occur as canopy trees and grow on waterlogged soils; they are associated with other tree types such as, *Weinmannia trichosperma*, *Aextoxicon punctatum* and podocarp species. At mid-elevation in the Andes *Nothofagus dombeyi* forms forests with *Nothofagus obliqua* and grows in areas of high moisture. *Nothofagus betuloides* and *Nothofagus dombeyi* also occurs at high altitudes (1200m) but *Nothofagus betuloides* prefers to live on more waterlogged soils (Veblen *et al.*, 1996).

All temperate *Nothofagus* species are shade-intolerant to varying degrees and as a result rely on large and small disturbances such as volcanic activity, earthquakes and wind-blowdown to remove the surrounding shade-casting vegetation (Veblen *et al.*, 1996).

Genus *Brassospora* is found in the tropical montane forests of New Guinea (e.g. *Nothofagus brassi*, *Nothofagus grandis* and *Nothofagus pullei*) and New Caledonia (e.g. *Nothofagus aequilateralis*, *Nothofagus balansae* and *Nothofagus discoidea*) (Read and Hope, 1996). The Antarctic wood is unlikely to be related to these types.

The fossil *Nothofagus* trees living on the Antarctic Peninsula may have occupied the same ecological niches as *Nothofagus* living in cool temperate forests today and may have also relied on disturbances such as, volcanic activity to regenerate (Poole *et al.*, 2001).



Figure 4. 4. *Araucaria araucana* – *Nothofagus pumilio* open forest. Height *Araucaria araucana* trees approximately 30m. *Nothofagus pumilio* are the small leafless trees.



Figure 4. 5. *Nothofagus* forest in New Zealand. www.lincolnecology.org.nz.

4.3.2 *Weinmannioxylon*

Family: Cunoniaceae

Genus: *Weinmannioxylon* Petriella

4.3.2.1 Description

Specimen numbers: D9.107.1, D9.128.2

Description: Wood specimens D9.107.1 and D9.128.2 are likely to have originated from the outer part of a tree trunk because they have low growth ring curvature.

Growth rings: Growth ring boundaries are indistinct (Figure 4.6a).

Vessels: Vessels are weakly diffuse (D9.107.1) to diffuse (D9.128.2). In TS vessels are circular and appear as mainly solitary and in tangential pairs; sometimes they are in groups of three in D9.107.1 (Figure 4.6a). Mean vessel wall thickness is less than 2 to 20 μ m. Mean vessel tangential diameter ranges from 49 – 53.1 μ m and mean vessel radial diameter ranges from 53.25 – 64.7 μ m. Vessel element length in specimen D9.107.1 ranges from 625 - 1080 μ m. Specimen D9.128.2 has on average 33 – 72 vessels per mm². Tyloses is abundant in specimen D9.107.1.

Perforation plates: (RLS) Perforation plates are scalariform (Figure 4.6g). There is one possible simple perforation plate in specimen D9.107.1 (Figure 4.6f).

Intervessel pitting: (TLS) Intervessel pitting is scalariform in specimen (D9.128.2).

Vessel- ray pitting: Vessel-ray pitting is scalariform, transitional and elongate in specimen D9.107.1. Pitting is exclusively scalariform in D9.128.1. Vessel-ray pitting is confined to upright marginal ray cells (Figure 4.6d, e). Pit diameter ranges from 10 - 30 μ m. Pits appear as simple or have reduced borders.

Fibres: None septate. Small pits with slit-like apertures are observed in D9.107.1 (Figure 4.6i). Mean fibre tangential diameter ranges from 23.5 – 32.58µm and mean fibre radial diameter ranges from 18.95 – 23.1µm. Fibre wall thickness ranges from 2 to 20µm.

Axial parenchyma:? Absent.

Rays: Rays are uniseriate, biseriate and triseriate (Figure 4.6h). In RLS the main body of the rays are made of procumbent cells, and margins are made of upright cells that can be 4 – 13 cells high (Figure 4.6b, c). In tangential view rays best fit the Kribs heterogeneous type I (D9.128.2) and IIA (D9.107.1). Rays are often axially joined (Figure 4.6h). Mean ray height ranges from 281.2 - 785µm. Mean number of rays per tangential millimetre is 4 to 16.

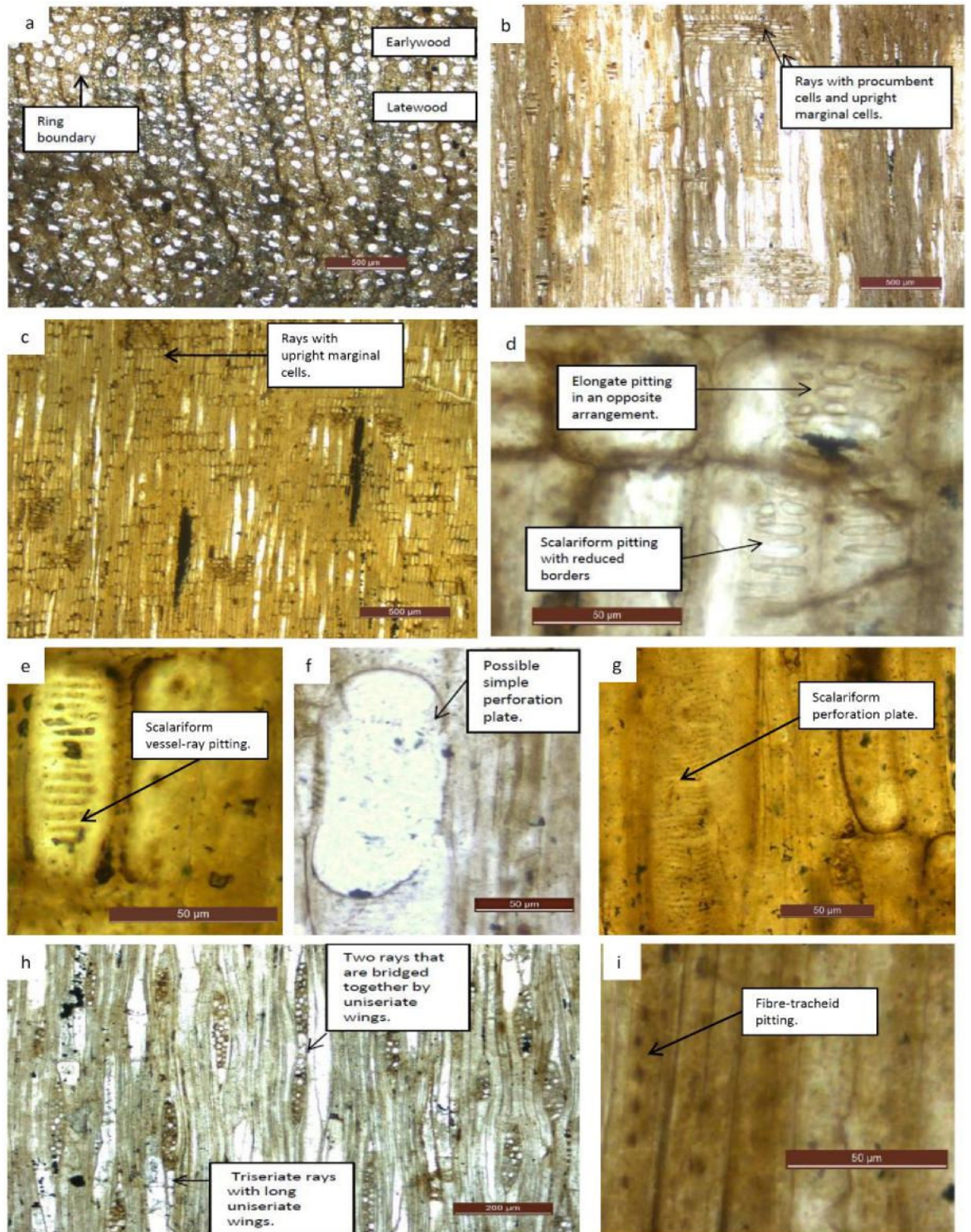


Figure 4. 6. *Weinmannioxylon*, Species A (D9.107.1) and B (D9.128.1). a) D9.107.1, TS showing growth ring boundary and vessel arrangement, scale bar = 100 μ m. b) D9.107.1, RLS showing rays, scale bar = 500 μ m. c) D9.128.2, RLS showing rays, scale bar = 500 μ m. d) D9.107.1, RLS showing vessel-ray pitting, scale bar = 50 μ m. d) D9.128.2, RLS showing vessel-ray pitting, scale bar = 50 μ m. f) D9.107.1, RLS showing possible simple perforation plate, scale bar = 50 μ m. g) D9.128.2, RLS showing scalariform perforation plate, scale bar = 50 μ m. h) D9.107.1, TLS showing rays, scale bar = 200 μ m. i) D9.107.1, RLS showing fibre-tracheid pitting, scale bar = 50 μ m.

Table 4. 6. Summary of anatomical characters of *Weinmannioxylon* wood identified in this project.

Species	A	B
Specimen number	D9.107.1	D9.128.2
growing rings	Indistinct	Indistinct
Vessels		
shape	Circular	Circular
porosity	Weakly diffuse	Diffuse
distribution	Solitary, tangential pairss, occasionally in groups of three.	Solitary, tangential pair
number per mm ²	N/a	33-72 (54.5)
tangential diameter	21 - 77.5 (53.1)	32.5 - 62.5 (49.4)
Vessel element length	N/a	N/a
perforation plates	Scalariform	Scalariform
intervessel pitting	N/a	Scalariform
Rays		
width	1-3 seriate	1-3 seriate
height	130 - 600 (281.2)	260 - 1525(785)
marginal cells, number of rows and shape	4 cells tall	4 - 13 cell tall
per tangential mm	3 - 6 (5)	8 - 16 (12)
Vessel-ray pitting	Scalariform, transitional, elongate	Scalariform
Parenchyma	n/a	? Diffuse
Fibres		
septate	absent	absent
pitting	present	absent

4.3.2.2 Discussion

Specimen D.107.1 has been assigned to *Weinmannioxylon*. Fossil wood assigned to *Weinmannioxylon* shares characteristics with wood of extant *Weinmannia*. These characteristics include mainly solitary vessels; vessel abundances that range from 40-100 mm²; scalariform perforation plates with numerous bars; vessel-ray pitting that is scalariform and opposite; tylose, rays that are heterocellular and are 1-4 cells wide; and fiber-tracheids with pits that have slit-like apertures (Dickison, 1977). The possible occurrence of simple perforation plates suggests that wood specimen D9.107.1 is also similar to *Eucryphia*, which is also of the family Cunoniaceae (Dickison, 1978). However, *Eucryphia* is characterised as having homogeneous rays and a high abundance of vessels >100 per mm², which is unlike D9.107.1. Thus D9.107.1 is closest to *Weinmannia*.

Specimen D9.128.2 shows similarity to Aextoxiceae, *Weinmannia* and *Caldcluvia* (Cunoniaceae), Gomortegaceae, Laurelieae (Monimiaceae), *Myrceugenella* (Myrtaceae) and Hamamelidaceae. All the wood belonging to these taxa have scalariform perforation plates, vessels that are predominantly solitary and vessel-ray pitting that is mostly scalariform. Specimen D9.128.2 is not likely to belong to taxa Aextoxiceae, *Myrceugenella* and *Laurelieae* because they have a higher abundance of vessels (>100 per mm²) (Rancusi *et al.* 1987; Nishida *et al.*, 1988). In addition, *Myrceugenella* has circular vessel-ray pitting and *Laurelieae* has wider rays with lower uniseriate wings. Gomortegaceae can also be dismissed due to having scalariform perforation plates with fewer bars and rays that best fit Kribs heterogeneous type IIA and B. Specimen D9.128.2 is close to Hamamelidaceae but is considered different because Hamamelidaceae mostly have biseriate rays, and species with vessel abundances over >100 per mm² (Wheeler *et al.*, 2010).

Specimen D9.128.2 is considered to be closest to *Weinmannia* because it has a similar range of vessel abundance, vessel tangential diameter and rays that can be 1-3 seriate (Dickison, 1977). Modern *Weinmannia sylvicola* wood has exclusively scalariform intervessel pitting and rays with over 4 marginal cells (Patel, 1990).

Specimens D9.107.1 and D9.128.2 are considered to be different species (Table 4.6) on the bases of specimen D9.128.2 having exclusively scalariform vessel-ray pitting, higher rays, more rays per tangential mm, and rays with more rows of upright marginal cells.

4.3.2.3 Comparison with other fossil wood of *Weinmannioxylon*

Antarctic wood assigned to *Weinmannioxylon* has been reported from the Late Cretaceous sequences of James Ross Island and Livingston Island (Poole *et al.* 2000b; Poole and Cantrill, 2001). *Weinmannioxylon* has also been reported from the Eocene sequences of King George Island (Poole *et al.* 2001).

Wood specimen D9.107.1 is very similar to *Weinmannioxylon nordenskjoldii* described by Poole *et al.* (2000b) from Late Cretaceous strata on James Ross Island. They both have indistinct growth rings, vessels that are arranged as solitary, tangentially paired and occasionally radially paired; scalariform perforation plates with numerous bars; and vessel-ray pitting that is usually opposite elongate and scalariform. They also both have similarities in terms of quantitative features such as mean vessel diameters and ray height. The main difference between the two is that the wood specimen described here has a lower abundance of vessels and is more diffuse to semi-ring porous.

Weinmannioxylon eucryphioides described by Poole *et al.* (2001) has simple perforation plates but it is different from the wood described here in having distinct growth rings, uniseriate and biseriate rays and no fibre-tracheid pitting.

Weinmannioxylon has also been described from Eocene sequences of Southern Chile (Terada *et al.* (2006b), which also shows similarity to the wood described here on the basis of having indistinct growth rings, and similar vessel-element lengths. However, it is different because it has rays that are only uniseriate and biseriate.

4.3.2.4 Ecology of modern *Weinmannia*

Today *Weinmannia* is found living in cool-temperate forests of New Zealand (*Weinmannia racemosa*, *Weinmannia sylvicola*) and Chile (*Weinmannia trichosperma*) (Dickison, 1977; Lusk, 1999).

Weinmannia racemosa (Figure 4.7a) from New Zealand is an evergreen canopy tree and is an important component of lowland podocarp-broadleaved forests in Westland, New Zealand, where it grows on infertile and poorly drained soil (Wardle and MacRae, 1966; Ogden and Stewart, 1995). It is also found living alongside *Nothofagus* species at low-mid altitudes on southern parts of South Island. On North Island *Weinmannia racemosa* lives in high altitudinal areas alongside *Quintinia actutifolia* and podocarp species. It has been suggested that *Weinmannia racemosa* is shade-tolerant because it is able to regenerate under a closed canopy (Coomes *et al.*, 2009).

Weinmannia sylvicola is only found on North Island, and is found living at high altitudes where it is associated with other trees such as *Dacrydium cupressinum* and *Ackama rosifolia* (Burns and Leathwick, 1996).

Weinmannia trichosperma (Figure 4.7b) is an evergreen tree and is found living at sea-level and mid-altitudes on the coastal range and the western slopes of the Andes, and grows on areas of moist soil and along river banks. It is commonly found in the Valdivian forests and grows alongside *Nothofagus* species and other broad-leaved trees such as, *Aextoxicon punctatum* and *Eucryphia cordifolia*. *Weinmannia trichosperma* is shade-intolerant, but is found living in old-growth forests where disturbances are infrequent (Lusk, 1999). A slow-growth rate and long-life span allows it to persist in these forests, unlike the faster growing and more short-lived *Nothofagus*, which struggles to regenerate under the shaded canopy of old-growth forests.

Weinmannia is also widely distributed in montane tropical forests of South America (e.g. *Weinmannia paulinnifolia* from Brazil), Madagascar (*Weinmannia rutenbergii*), Malaysia (*Weinmannia fraxinea*) (Dickison, 1977; Bradford, 1998) but these are unlikely related to Paleocene types in Antarctica.



Figure 4. 7. a) *Weinmannia racemosa* in New Zealand. **b)** *Weinmannia trichosperma* in Chile. Image a) is taken from www.forestflora.co.nz and image b) is taken from www.flickr.com/photos/cipsela/6034013373/ .

4.3.3 *Myrceugenelloxylon*

Family: Myrtaceae

Genus: *Myrceugenelloxylon* Nishida

4.3.3.1 Description

Specimen numbers: D9.020.1, D9.091.1

Description: This description is based on two wood specimens that are likely to have been derived from the inner part of a trunk or branch because their growth rings show high curvature. Specimen D9.091.1 also has a pith present.

Growth rings: Growth ring boundaries are indistinct (D9.020.1) (Figure 4.8a) to distinct (D9.091.1). Growth ring boundaries are defined by a change in fibre radial diameter and a small change in vessel diameter.

Vessel: Weakly diffuse porous (Figure 4.8a). Vessels appear as mainly solitary (80 – 90%) and are occasionally in tangential pairs and radial pairs. Vessels are sometimes in radial multiples of 3 – 5 in D9.091.1. Mean vessel tangential diameter ranges from 45.4 –56.9 μ m and vessel radial diameter ranges from 60 –56.9 μ m. Mean vessel element length ranges from 1062 –

1125 μ m. There are on average 57.9 – 73.7 vessel per mm². In specimen D9.091.1 there are fewer vessels in the earlywood.

Perforation plate: Perforation plates are scalariform with many fine bars (>30) (Figure 4.8c). Sometimes scalariform plates can appear reticulate. There is one possible occurrence of a simple perforation plate in specimen D9.091.1 (Figure 4.8f).

Intervessel pitting: Intervessel pitting is infrequent in both specimens and appears to be scalariform. However, it is difficult to distinguish between parts of scalariform plates and intervessel pitting.

Vessel- ray pitting: Pitting appears circular and horizontally-elongate and has an opposite arrangement (Figure 4.8e, h). Sometimes pitting is also scalariform. Pits are bordered. Vessel-ray pits are small (2.5 – 10 μ m) and are confined to marginal ray cells.

Rays: In TLS rays are uniseriate, biseriate, part-biseriate and triseriate (Figure 4.8g, i). Rays are usually axially joined together. In TLS rays best fit Kribs type I. In RLS rays are composed of 2 to 3 long procumbent cells with upright or square margin cells, which can be four or more cells high (Figure 4.8d). Mean ray height is 393 – 442 μ m and mean number of rays per tangential mm ranges from 7–12.

Fibres: Distinctly pitted in D9.020.1, but none observed in D9.091.1. Fibre tangential ranges from 15 – 27.5 μ m and radial diameter 15 – 25 μ m.

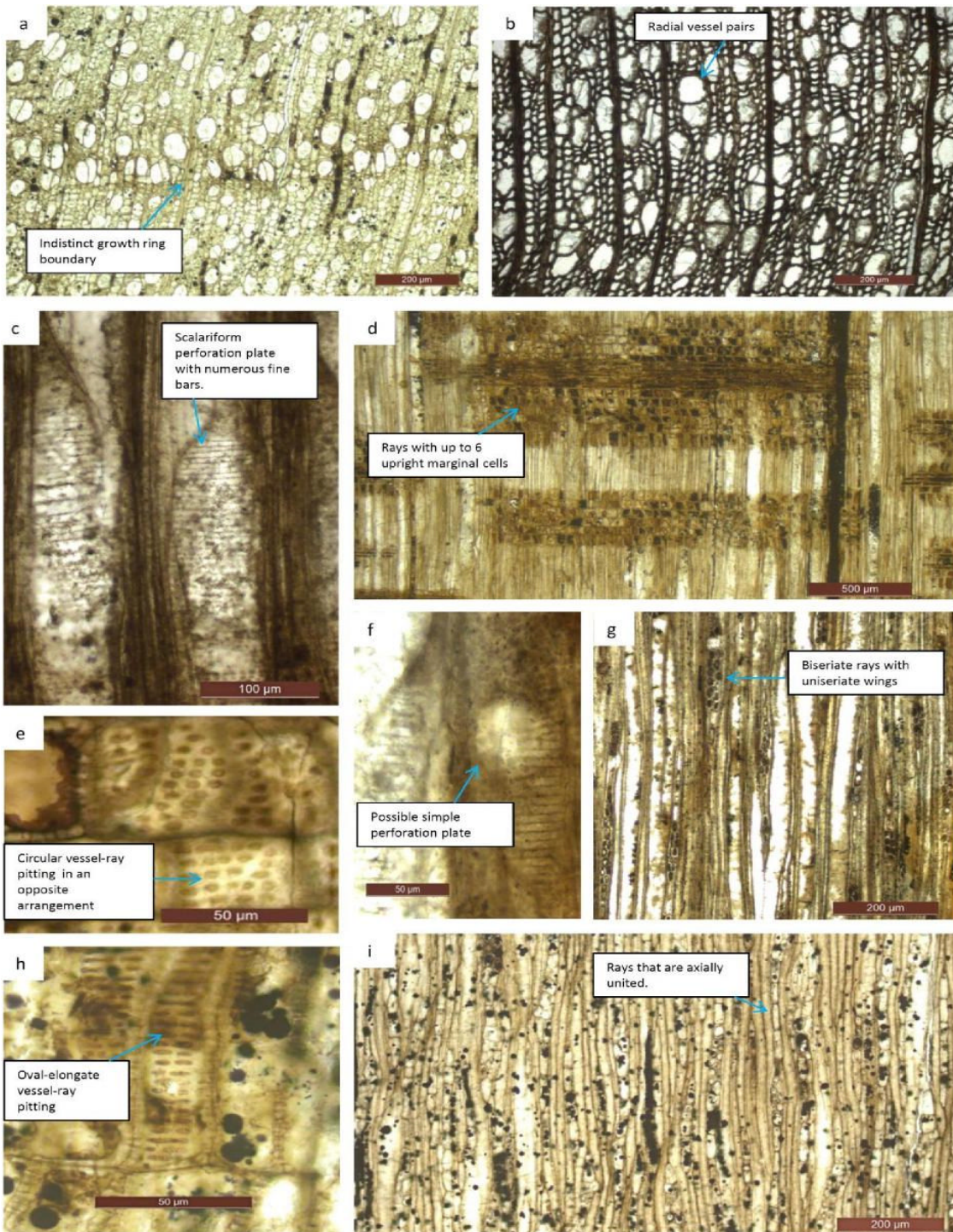


Figure 4. 8. *Myrceugenelloxylon* Species A a) D9.020.1, TS showing growth ring boundary and vessel arrangement, scale bar = 200 μm . b) D9.091.1, TS showing vessel arrangement, scale bar = 200 μm . c) D9.091.1, RLS showing scalariform perforation plates, scale bar = 100 μm . d) D9.020.1, RLS showing rays, scale bar = 500 μm . e) D9.091.1, RLS showing vessel-ray pitting, scale bar = 50 μm . f) D9.091.1, RLS showing possible simple perforation plate, scale bar = 50 μm . g) D9.091.1, TLS showing rays, scale bar = 200 μm . h) D9.020.1, RLS showing vessel-ray pitting, scale bar = 50 μm . i) D9.020.1, TLS, showing rays, scale bar = 200 μm .

Table 4. 7. Summary of the anatomical characters of *Myrceugenelloxylon* wood identification in this project. Number in brackets are mean values.

Specimen number	D9.020.1	D9.091.1
growth rings	indistinct	Fairly distinct
Vessels		
Shape	round, radially elongate, angular	round, radially elongate, angular
Porosity	diffuse-porous	diffuse-porous
Distribution	Mainly solitary, sometimes tangential and radial pairs.	Mainly solitary, sometimes tangential and radial pairs.
Number per mm ²	43-149 (73.7)	12 - 91 (57.9)
Tangential diameter	30 - 60 (45.9)	22.9 - 100 (56.9)
vessel element length	620 - 1300 (1062.85)	725 - 1700 (1125)
perforation plates	Scalariform	Scalariform
intervessel pitting	scalariform	opposite elongate and scalariform?
Rays		
Width	Predominantly biseriate, part-biseriate and uniseriate.	Predominantly biseriate or part biseriate. Sometime uniseriate. Rarely triseriate.
Height	165-895 (393)	140-665 (442)
Marginal cells, number of rows and shape	4 or more upright or square	4 or more upright and square
per tangential per mm	10 to 14 (12)	5 to 9 (7)
Vessel-ray pitting	Circular, horizontally elongate. Sometimes scalariform. Opposite arrangement	Circular, horizontally elongate. Some times scalariform. Opposite arrangement
Parenchyma	diffuse?	diffuse?
Fibres		
Septate	absent	absent
Pitting	present	present?

4.3.3.2 Discussion

The wood specimens described here have the closest resemblance to *Myrceugenelloxylon*. The genus *Myrceugenelloxylon* is characterised as having diffuse porous wood; vessels that are mostly solitary and sometimes in multiples of 2–3; scalariform perforation plates with few to many bars; intervessel pitting that is opposite and scalariform; and rays that are uniseriate, biseriate and triseriate. *Aextoxicoxylon harambouri* (Nishida *et al.*, 1988) also shows some similarity to the wood specimens described here, but differs in having mostly scalariform vessel-ray pitting, a higher proportion of triseriate rays and taller rays.

The two wood specimens here have some differences between them (Table 4.7). Specimen D9.020.1 has distinct pitting on fibre walls, on average smaller and more numerous vessels, and slightly more rays per tangential mm. Specimen D9.091.1 has vessels that are occasionally radial multiples 2 – 5, also it possibly has simple perforation plates. However, they have been classed as the same species because they share close similarity in majority of characteristics and these are vessel distribution, vessel tangential diameter, ray margin height and vessel ray pitting. The absence of fibre pitting in D9.091.1 could be due to poor preservation. There is only one possible simple perforation plate observed, so this feature is rare, and again its absence in D9.020.1 may be an artefact of preservation. The difference in ray frequency between the two specimens is small; this feature has been proven to change within different parts of a tree. Mean vessel diameter and vessels per mm² are similar between specimens and these features can change with environment.

4.3.3.3 Comparison with other fossil wood of *Myrceugenelloxylon*

Species A have close similarity to *Myrceugenelloxylon antarcticus* described from Maastrichtian and Paleocene strata on James Ross Island (Poole *et al.*, 2003), and Eocene strata on King George Island (Poole *et al.*, 2001). *Myrceugenelloxylon antarcticus* is characterised as having diffuse porosity; vessels that are mostly solitary; vessel-ray pitting that is circular to elongate; intervessel pitting that is scalariform and circular; and mainly biseriate and

uniseriate rays. Quantitative features such as vessel diameter are also similar to specimen D9.020.1. The specimens are different from *Myrceugenelloxylon antarcticus* in having the occasional presence of scalariform pitting. Another difference is that uniseriate portions of rays tend to be as wide as the biseriate portions in *Myrceugenelloxylon antarcticus* described by Poole *et al.* (2001).

Species A have some similar characteristics to *Myrceugenelloxylon maytenioides*, described by Nishida *et al.* (1988) and Terada *et al.* (2006a) from Late Oligocene –Early Miocene on the Chile/Argentina border. These include vessels that are mostly solitary and occasionally in radial multiples of 2 – 3, rarely 5; scalariform perforation plates with numerous bars; vessel-ray pitting that is circular and oval-horizontally elongate. However, the specimens described here are different because they have fewer vessels per mm², larger vessels, rare triseriate rays, less frequent rays per tangential mm, and the occasional presence of scalariform vessel-ray pitting.

4.3.3.4 Comparison with extant wood

Species A described here have the closest affinity to the genus *Luma* (previously called *Myrceugenella*) of the Myrtaceae family (Poole *et al.*, 2003). *Luma* shows some resemblance to the wood specimens described here on the basis of having simple and scalariform perforation plates with numerous bars; ray-vessel pits that are opposite to scalariform in arrangement; and rays that are uniseriate, biseriate, triseriate and fit Kribs heterogenous type I. However, it is different on the basis of having, on average, a smaller vessel diameter and significantly more vessels per mm² (Rancusi *et al.*, 1987).

4.3.3.5 Modern ecology of *Luma*

Today there are two species belonging to the genus *Luma* (*Luma apiculata* and *Luma chequen*) of the family Myrtaceae. *Luma apiculata* is a broad-leaved sub-canopy tree and is found living in the cool temperate Valdivian forests in Chile (Figure 4.9), at elevations below 700m a.b.s.l (Gut, 2008). It has an intermediate shade-tolerance and can grow and regenerate in old-growth forests (forests that have not undergone recent disturbance) (Gutiérrez *et al.*, 2009).

Luma chequen is a small shrub and is found growing in swamp habitats in central Chile under a Mediterranean type climate (Bascuñán-Godoy *et al.*, 2013).



Figure 4. 9. *Luma apiculata* tree. Image taken from www.studyblue.com.

4.3.4 *Antarctoxylon*

Family ?

Genus: *Antarctoxylon* Poole et Cantrill

4.3.4.1 Description

Specimen number: D9.040.1

Description: This description is based on one wood specimen that is likely to have been derived from the outer part of a trunk or branch because it has low growth ring curvature.

Growth rings: Growth rings are distinct and marked by a change in fibre diameter and vessel diameter (Figure 4.10a, b).

Vessels: Semi-ring porous arrangement (Figure 4.10a, b). Vessels have undergone compression so it is difficult to determine definite vessel shape in TS. They appear radially elongate in earlywood. Vessels are mainly arranged

in clusters of 3-9 and radial files of up to 4 vessels are also present (Figure 4.10a, b). Vessels are arranged in a diagonal pattern across the growth ring. Mean tangential vessel diameter is 44.5 μ m (range: 27.5 – 82.5 μ m). Mean radial vessel diameter is 53.9 μ m (range: 10 – 87.5 μ m). Mean vessel element length is 360 μ m (range: 160 - 525 μ m).

Perforation plates: Simple

Intervessel pitting: Circular to horizontally-elongate and in an alternate arrangement (Figure 4.10d, f). Horizontal diameter ranges from 5 - 20 μ m.

Vessel-ray pitting: Circular to horizontally elongate, the same as intervessel pitting (Figure 4.10c, d). Horizontal diameter ranges from 5 - 20 μ m.

Fibres: Non-septate. No pitting present. Due to poor preservation fibre diameter could not be measured.

Axial parenchyma: Present in RLS (Figure 4.10e).

Rays: In RLS the main body of the rays are made of long procumbent cells and margins are made of 1-3 rows of square and upright cells (Figure 4.10h). In TLS rays are 1-4 seriate (Figure 4.10i) and are best placed in Kribs heterogeneous IIB. Mean ray height is 284 μ m (range: 120 - 1220 μ m). Mean number of rays per tangential mm is 7 (range: 3 – 10 per tangential mm).

4.3.4.2 Discussion

The wood described here is closest to the fossil genus *Antarctoxylon*. *Antarctoxylon* is characterised by having diffuse or semi-ring porous wood; vessels that can be solitary and/or grouped; simple and/or scalariform perforation plates; and multiseriate rays (Poole and Cantrill, 2001).

4.3.4.3 Comparison to other fossil wood of *Antarctoxylon*

Antarctoxylon wood has been described from Late Cretaceous strata on Livingston Island and James Ross Island (Poole and Cantrill, 2001, Sakala and Vodrážka, 2014). It has also been described from Paleocene strata on Seymour Island (Poole *et al.*, 2003).

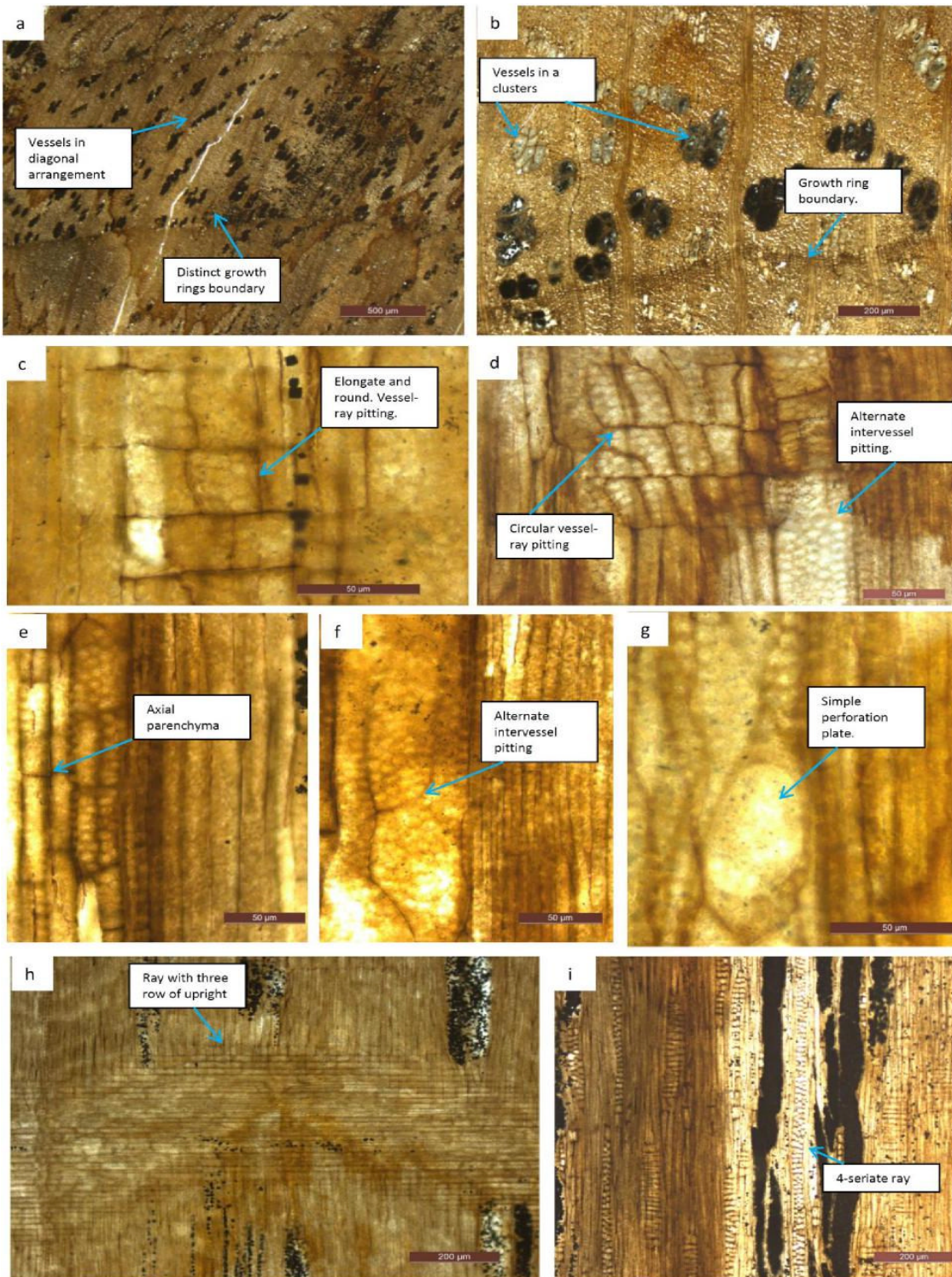


Figure 4. 10. *Antarctoxylon* a) TS showing growth rings and vessels, scale bar = 500μm. b) TS showing vessel arrangement, scale bar = 200μm c) RLS showing vessel-ray pitting, scale bar = 50μm. d) RLS showing vessel-ray pitting and intervessel pitting, scale bar = 50μm. e) RLS showing axial parenchyma, scale bar = 50μm. f) RLS showing intervessel pitting, scale bar = 50μm. g) RLS showing a simple perforation plate, scale bar = 50μm. h) RLS showing a ray, scale bar = 200μm. i) TLS showing rays, scale bar = 200μm.

The wood described here share characteristics with to *Antarctoxylon juglandoides* described by Poole *et al.* (2003) from Early Paleocene (López de Bertodano Formation) strata on Seymour Island. Anatomical characteristics include distinct growth rings; vessels that are in radial files of up to 6 and clusters of up to 10 vessels; small vessel size; intervessel pitting that is alternate and circular; rays that are 1-4 seriate; rays that have 1-3 rows of upright and square marginal cells; and simple perforation plates. However, there are anatomical differences between *Antarctoxylon juglandoides* and D9.040.1. *Antarctoxylon juglandoides* has diffuse porous wood, tyloses and vessel-ray pitting that is opposite, whereas D9.040.1 appears to have alternate pitting. Another difference is that D9.040.1 has a maximum ray height of 1220µm although, there is only one ray of that height. Specimen D9.040.1 has vessels that are arranged in diagonal linear patterns throughout the growth ring, whereas they do not in *Antarctoxylon juglandoides* in Poole *et al.* (2003).

The species *Antarctoxylon juglandoides* was given its name on the bases of having close similarity to modern Juglandaceae (Poole *et al.*, 2003), to which D9.040.1 also shows similarity. Juglandaceae has significantly larger vessels (>100µm) than the wood described here and that of *Antarctoxylon juglandoides* (IAWA Insidewood database, 2004).

4.3.4.4 Comparison to extant wood

Antarctoxylon does not have a modern living relative (Poole *et al.*, 2003).

4.4 Summary

In summary, four angiosperm wood types have been identified in the wood assemblages from the Paleocene strata on Seymour Island. These include *Nothofagoxylon* (species A, B, C and D), *Weinmannioxylon* (species A and B), *Myrceugenelloxylon* and *Antarctoxylon*. All of the morphotypes have been described previously from Seymour Island, some species are new such as *Nothofagoxylon* species D and *Myrceugenelloxylon* species B. Figure 4.11 presents the abundance of the above angiosperm morphotypes identified in this project in the form of a pie chart. The most common morphotype is

Nothofagoxylon followed by *Weinmannioxylon*, *Myrceugenelloxylon* and *Antarctoxylon*.

Nearest living relatives with similar wood to the above genera are common in Southern Hemisphere forests in southern South America, New Zealand and Australia (including Tasmania). The trees live in a wide range of habitats from low to high altitudes. Some of the nearest living relatives such as *Weinmannioxylon* and *Myrceugenelloxylon* live in closed canopy forests at low altitudes. Modern *Nothofagus* trees are shade-intolerant to varying degrees and thus live in sub-optimal sites such as poorly developed soils, at high altitudes near the treeline where temperatures are low, in areas that are prone to large scale disturbances.

Abundance of the four angiosperm wood genera identified

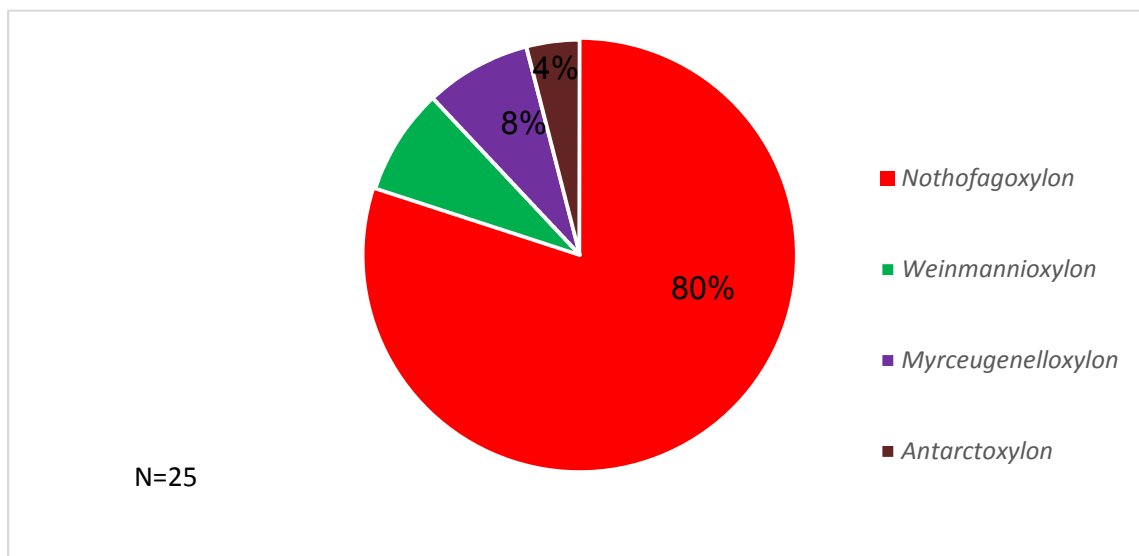


Figure 4. 11. Abundance of the four angiosperm wood genera identified in this study. Percentages are calculated out of the 25 angiosperm wood specimens that could be identified.

Chapter 5

Palaeoecology of the Antarctic forests

5.1 Introduction

This chapter discusses the composition and structure of the Antarctic forests during the Paleocene based on wood morphotypes identified in Chapters 3 and 4. New data from palynomorphs are presented to gain further insight into the composition and structure of the Antarctic forests. The identification of possible upland and lowland floras is determined by the preservation of the fossil wood, its location in the sedimentary sequence and comparisons with the ecology of nearest living relatives. This chapter firstly presents the new palynomorph data, and then discusses the composition and structure of the forests using information from the fossil wood. The fossil wood record and palynomorph record is compared and then the palaeoecology of the forests is discussed.

5.2 Palynology

Fossil wood data provides only a limited indication of the plant types in the forest, especially since the fossil wood only represents large forest trees. The non-woody shrubs and other plants that lived in the Paleocene forests of Antarctica are not represented in the wood record. In order to obtain a more complete record of the flora in the forests the pollen and the spores from the same sedimentary horizons were examined. This provides a much fuller and more detailed record of the flora from which the paleoecology of the forest could be deduced.

The palynology methods are described in section 5.2.1. The pollen and spore results are presented in section 5.2.2 as tables (Table 5.1 and 5.2) and image plates (Figure 5.2 and 5.3). Section 5.2.2.1 discusses the composition of the flora and possible structure of the forests living on the Antarctic Peninsula during the Paleocene.

5.2.1 Methods

In total 16 palynology samples were analysed from the same stratigraphic horizons in which the wood samples were obtained (Figure 5.1). The palynological samples were available as mounted slides prepared by Palytech Processing Ltd, Birkenhead, UK for the work of Bowman *et al.* (2014). The slides are housed at the British Antarctic Survey, Cambridge, UK. The presence or absence of different pollen types were recorded for each sample. Pollen and spore types and nearest living relatives were identified by consulting Bowman *et al.* (2014) and Raine *et al.* (2011).

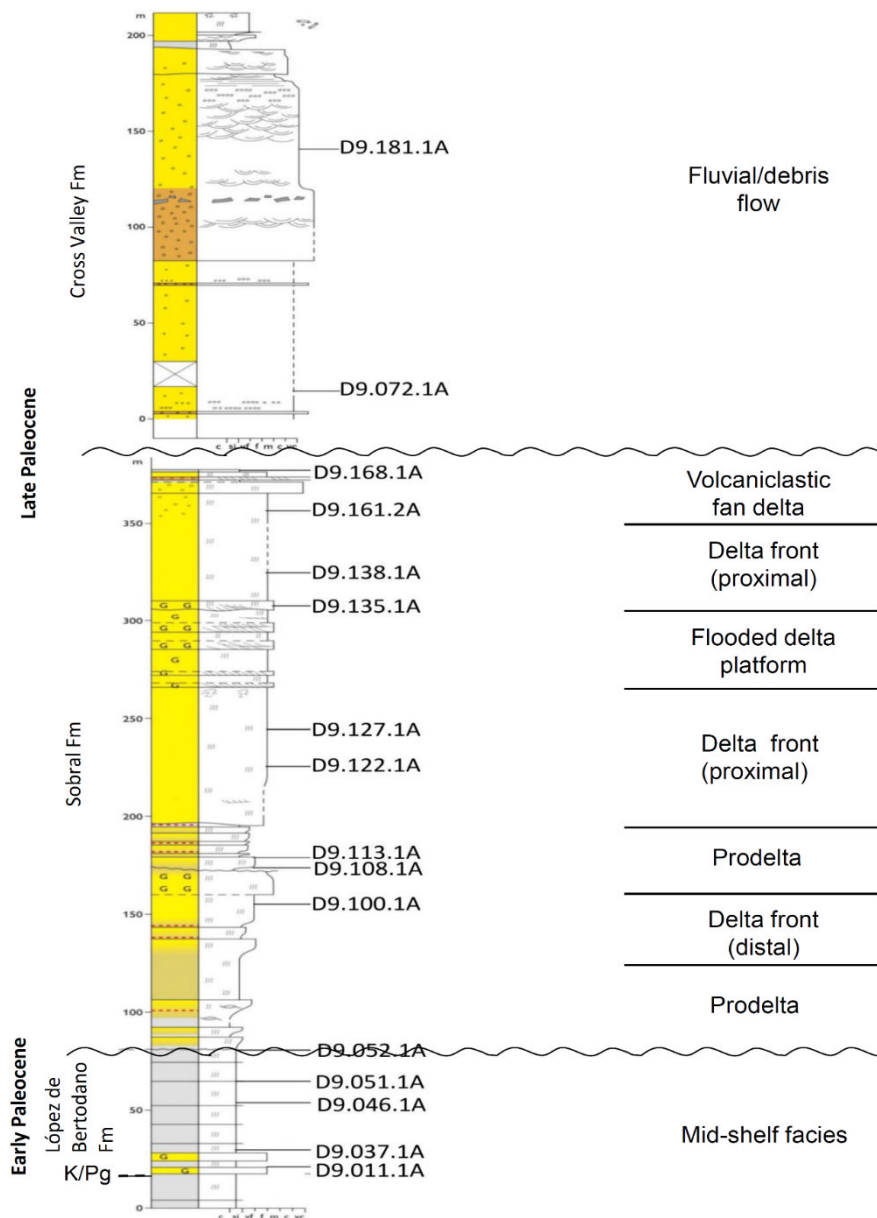


Figure 5.1. Location of palynology samples on the sedimentary sequence. Sedimentary long courtesy of Jon Ineson.

5.2.2 Results

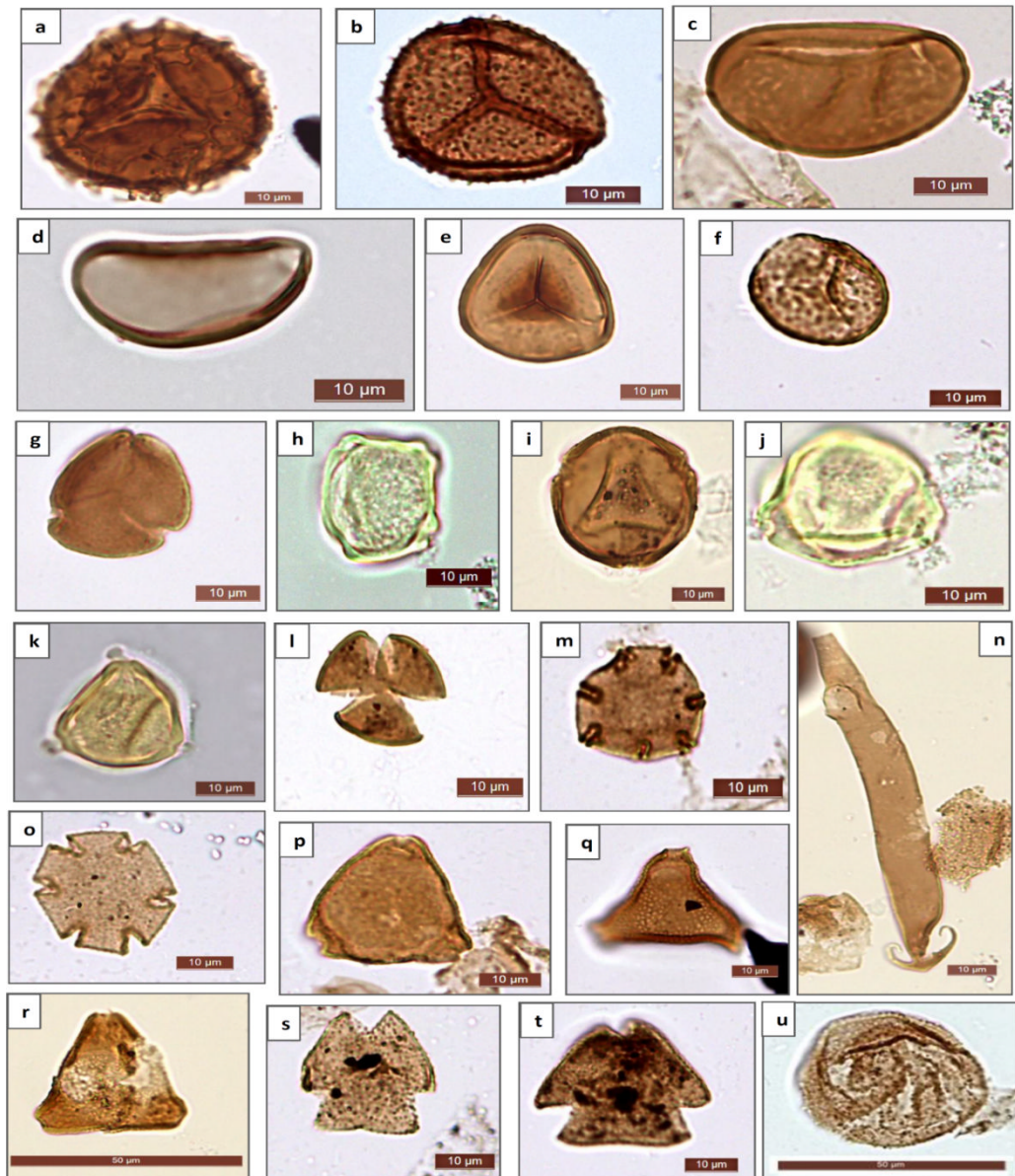


Figure 5.4. Pollen and spore types identified as part of this PhD research. a) *Retitriletes austroclavatidites*, scale bar = 10µm. b) *Osmundacidities wellmanii*, scale bar = 10µm. c) *Laevigatosporites major*, scale bar = 10µm. d) *Laevigatosporites ovatus*, scale bar = 10µm. e) *Stereisporites antiquasporites*, scale bar = 10µm. f) *Stereisporites regium*, scale bar = 10µm. g) *Tricolpites* sp.cf *T.phillipsii*, scale bar = 10µm. h) *Myrcipites harrisii*, scale bar = 10µm. i) *Triporopollenites* sp., scale bar = 10µm. j) *Myrcipites harrisii*, scale bar = 10µm. k) *Myrtaceidites* sp., scale bar = 10µm. l) *Tricolpites confessus*, scale bar = 10µm. m) *Nothofagidites flemingii*, scale bar = 10µm. n) Glochidia of *Azolla* sp., scale bar = 10µm. o) *Nothofagidites senectus*, scale bar = 10µm. p) *Proteacidites* sp. c.f. *P.scaboratus*, scale bar = 10µm. q) *Proteacidites* sp., scale bar = 10µm. r), *Proteacidites pseudomoides*, scale bar = 50µm. s) *Peninsulapollis askiniae*, scale bar = 10µm. t) *Peninsulapollis gillii*, scale bar = 10µm. u) *Araucariacites australis*, scale bar = 10µm.

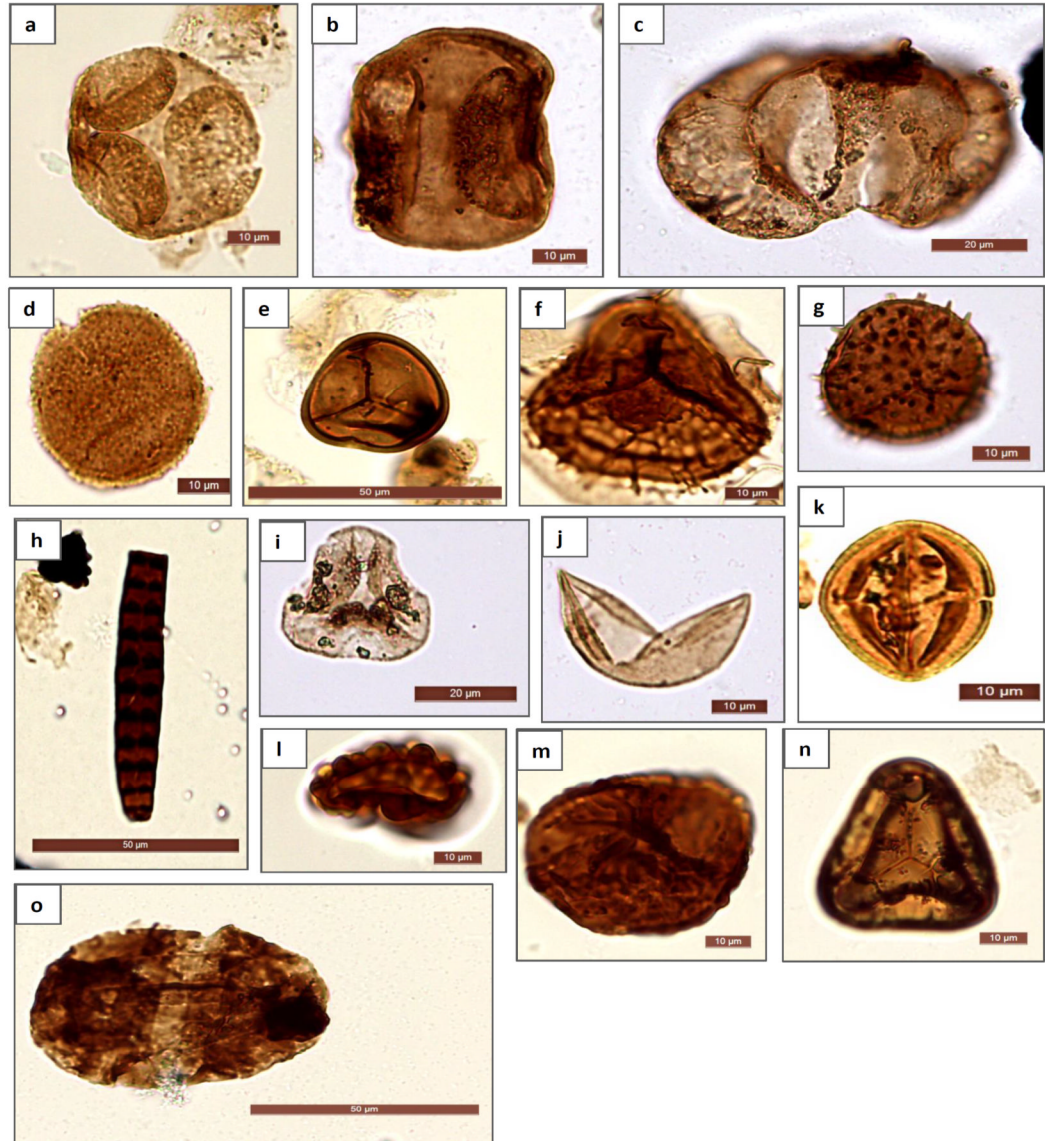


Figure 5.3. Pollen and spore types identified as part of this PhD project. a) *Microcachyidites antarcticus*, scale bar = 10µm. b) *Phyllocladidites mawsonii*, scale bar = 10µm. c) *Podocarpidites* sp., scale bar = 10µm. d) *Dacrydiiumites praecupressinoides*, scale bar = 10µm. e) *Cyathidites minor*, scale bar = 10µm. f) *Perotriletes majus*, scale bar = 10µm. g) *Ceratosporites equalis*, scale bar = 10µm. h) *Pluricellaesporites* sp., scale bar = 10µm. i) *Trichotomosulcites subgranulatus*, scale bar = 10µm. j) *Taxodiaceapollenites hiatus*, scale bar = 10µm. k) *Tricolporites* sp., scale bar = 10µm. l) *Polycolpites* sp. cf. *P. langstoni*, scale bar = 10µm. m) *Camarozonosporites ambigens*, scale bar = 10µm. n) *Cyathidites* sp. cf. *C. australis*, scale bar = 10µm. o) *Protohaploxypinus ?amplus*,

The location of the palynomorph samples on the sedimentary succession are presented in Figure 5.1. Figure 5.2 and Figure 5.3 presents an image plate of the different pollen types. Table 5.1 presents the pollen and spores recorded in each sample. Table 5.2 summarises the palynological type, its nearest living relative and the ecology of that modern relative.

Palynomorphs are abundant in all of the samples that were analysed. Common pollen types that are encountered in all or most of the samples include *Podocarpidites* spp. (absent from D9.167.1A), *Phyllocladidites mawsonii* (D9.051.1A, D9.113.1A), *Nothofagidites* spp., *Peninsulapollis gillii* and *Peninsulapollis askiniae* (Figure 5.2, 5.3 and Table 5.1).

The most diverse families present in the samples are Podocarpaceae, (e.g. *Podocarpidites* spp., *Microcachrydites antarcticus*, *Phyllocladidites mawsonii*, *Dacrydiumites praecupressinoides*), Proteaceae (*Peninsulapollis askiniae*, *Peninsulapollis gillii*, *Proteacidites scarboratus*, *Proteacidites pseudomoides*, *Triplopollenites* spp., *Proteacidites* sp.) and Nothofagaceae (*Nothofagidites flemingii*, *Nothofagidites senectus*). Some of the *Proteacidites* and *Nothofagidites* pollen were unable to be identified to species level due to preservation, specimens being folded over, or they could not be identified to species level.

Rare palynomorphs in the samples analysed here include *Myrtaceidites* spp., *Tripcolpites* sp. (D9.127.1A). *Myricipites harrissi* and similar types (e.g. *Myricipites* sp.1 and 2) are only found in sample D9.072.1A.

A diverse range of spores are also present. Frequently encountered taxa include *Stereisporites* spp., *Laevigatosporites* spp. and *Retitriletes austroclavatidites*. Other spore types are not as frequently present throughout the stratigraphic section. These include *Camarozonosporites abigens* (present in samples D9.011.1A, D9.037.1A), *Osmundacidities wellmanii* (D9.052.1A, D9.072.1A, D9.113.1A), *Ceratospores equalis* (D9.108.1A, D9.052.1A, D9.051.1A, D9.046.1A), *Cyathidites minor* D9.046.1A, D9.051.1A, D9.108.1A, D9.072.1A). Only isolated glochidiums of *Azolla* sp. were found in D9.037.1A.

Three spores have been reworked from older stratigraphic units of Permian and Triassic age because they are dark in colour, indicating thermal alteration (V.Bowman, pers. comm., November 2014). They include two *Cyathidites* sp. cf. *C. australis* (sample D9.113.1A & D9.138.1A) and one *Protohaploxylinus amplus* (D9.122.1A).

Table 5. 1. Palynomorphs present in each palynology sample analysed and its position on the stratigraphic section.

Height on section	Sample number	Pollen and spores encountered
105m on D9.300	D9.181.1A	<i>Araucariacites australis</i> , <i>Nothofagidites</i> sp., <i>Podocarpidites</i> sp., <i>Pluricellaesporites</i> sp., fungal spore, <i>Retitriletes austroclavatidites</i> , <i>Proteacidities</i> sp., <i>Laevigatosporites ovatus</i> , <i>Stereisporites antiquasporites</i>
15m on D9.300	D9.072.1A	<i>Podocarpidites</i> sp., <i>Laevigatosporites ovatus</i> , <i>Nothofagidites senectus</i> , <i>Peninsulapollis askiniae</i> , <i>Araucariacites australis</i> , <i>Stereisporites antiquasporites</i> , <i>Trichotomosulcites subgranulatus</i> , <i>Myricipites harissa</i> , <i>Myricipites</i> sp 1, <i>Myricipities</i> sp. 2, <i>Peninsulapollis gillii</i> , <i>Laevigatosporites major</i> , <i>Osmundacites wellmanii</i> , <i>Cyathodites minor</i> .
66m on D9.604	D9.167.1A	<i>Proteacidities</i> sp, ? <i>Araucariacites australis</i> , <i>Pluricellaesporites</i> sp., fungal spore, <i>Stereisporites antiquasporites</i> , <i>Tripoporollenites</i> sp., <i>Polycolpites</i> sp. cf. <i>P. langstonii</i>
48m on D9.604.1	D9.161.2A	<i>Podocarpidites</i> sp., <i>Nothofagidites senectus</i> , <i>Laevigatosporites ovatus</i> , <i>Stereisporites antiquasporites</i> , <i>Peninsulapollis gillii</i> , ? <i>Araucariacites australis</i> ,, ? <i>Phyllocladites mawsonii</i> , <i>Retitriletes austroclavatidites</i> .

Table 5.1. Continued.

Height on section	Sample number	Pollen and spores encountered
228m on D9.603	D9.135.1A	<i>Araucariacites australis</i> , <i>Podocarpidites</i> sp., <i>Phyllocladites mawsonii</i> , <i>Triporopollenites</i> sp. <i>Peninsulapollis askiniae</i>
246m on D9.603	D9.138.1A	<i>Araucariacites australis</i> , <i>Nothofagidites</i> sp., <i>Nothofagidites senectus</i> , <i>Podocarpidites</i> , <i>Stereisporites antiquasporites</i> , <i>Phyllocladites</i> <i>mawsonii</i> , <i>Peninsulapollis gilli</i> , <i>Retitriletes</i> <i>austrorivulidites</i> , <i>Cyathidites</i> sp. cf. <i>C.</i> <i>australis</i> (reworked).
165m on D9.603	D9.127.1A	<i>Phyllocladites mawsonii</i> , <i>Podocarpidites</i> sp, <i>Retitriletes austrorivulidites</i> , <i>Araucariacites</i> <i>australis</i> , <i>Microcachryidites antarcticus</i> , <i>Nothofagidites senectus</i> , <i>Stereisporites regium</i> , <i>Trichotomosulcites subgranulatus</i> , <i>Nothofagidites fleminigii</i> , <i>Laevigatosporites</i> <i>ovatus</i> , <i>Peninsulapollis gillii</i> , <i>Stereisporites</i> <i>antiquasporites</i> , <i>Proteacidites</i> sp, <i>Taxodiaceapollenites hiatus</i> , <i>Tripcolpites</i> sp, <i>Myrtaceidites</i> sp.
145.5m on D9.603	D9.122.1A	<i>Podocarpidites</i> sp., <i>Peninsulapollis gillii</i> , <i>Retitriletes austrorivulidites</i> , <i>Nothofagidites</i> <i>senectus</i> , <i>Araucariacites australis</i> , <i>Phyllocladites mawsonii</i> , <i>Laevigatosporites</i> <i>ovatus</i> , <i>Tricolpites confessus</i> , <i>Tricolpites</i> sp, <i>Proteacidites</i> sp, <i>Protohaploxypinus amplus</i> (reworked put on image plate), <i>Microcachryidites antarcticus</i> , <i>Stereisporites</i> <i>antiquasporites</i> .
98m on D9.603	D9.113.1A	<i>Stereisporites antiquasporites</i> , <i>Podocarpidites</i> sp., <i>Araucariacites australis</i> , <i>Laevigatosporites</i> <i>ovatus?</i> , <i>Peninsulapollis gilli</i> , <i>Nothofagites</i> <i>flemingii</i> , <i>Retriletes austrorivulidites</i> , <i>Proteacidites</i> sp., <i>Nothofagidites fleminigii</i> , <i>Osmundacidites wellmanii</i> , <i>Cyathidites</i> sp. cf. <i>C. australis</i> recycled (put into image plate). <i>Dacrydiumites praecupressinoides</i> ,

Table 5.1. Continued.

Height on section	Sample number	Pollen and spores encountered
93m on D9.603	D9.108.1A	<p><i>Podocarpidites</i> sp, <i>Nothofagidites senectus</i>, <i>Stereisporites antiquasporites</i>, <i>Retitriletes austroclavatidites</i>, <i>Stereisporites regium</i>, <i>Peninsulapollis gillii</i>, <i>Peninsulapollis askiniae</i>, <i>Araucariacites australis</i>, <i>Phyllocladidites mawsonii</i>, <i>Laevigatosporites ovatus</i>, <i>Pluricellaesporites</i> sp., fungal spore, <i>Cyathidites minor</i>, <i>Cerosporites equalis</i>, <i>Proteacidites</i> sp cf <i>P.scaboratus</i>, <i>Proteacidites Pseudomoides</i>, <i>Laevigatosporites major</i>, <i>Perotriletes majus</i></p>
75m on D9.603	D9.100.1A	<p><i>Stereisporites antiquasporites</i>, <i>Nothofagidites senectus</i>, <i>Phyllocladidites mawsonii</i>, <i>Stereisporites regium</i>, <i>Laevigatosporites ovatus</i>, <i>Peninsulapollis gillii</i>, ?<i>Araucariacites australis</i>, <i>Proteacidites</i> sp. cf. <i>P. scaboratus</i>, <i>Peninsulapollis askiniae</i>, <i>Retitriletes austroclavatidites</i>, <i>Podocarpidites</i> sp, <i>Taxodiaceapollenites hiatus</i>.</p>
48m on D9.602	D9. 052.1A	<p><i>Nothofagidites</i> sp., <i>Stereisporites antiquasporities</i>, <i>Proteacidites parvus</i>, <i>Retitriletes austroclavatidites</i>, <i>Podocarpidites</i> sp., <i>Araucarites australis</i>, <i>Peninsulapollis gillii</i>, <i>Laevigatosporities major</i>, <i>Proteacidites</i> sp, <i>Proteacidites</i> sp cf <i>scaboratus</i>, <i>Stereisporites regium</i>, <i>Tricolpites confessus</i>, <i>Peninsulapollis askiniae</i>, <i>Phyllocladidites mawsonii</i>, <i>Ceratosporites equalis</i>, <i>Triporopollenites</i> sp., <i>Osmundacidites wellmanii</i>, <i>Tricolpites/Proteacidite</i> sp?</p>
34m on D9.602	D9.051.1A	<p><i>Stereisporites antiquasporites</i>, <i>Nothofagidites</i> sp, <i>Nothofagidites senectus</i>, <i>Peninsulapollis askiniae</i>, <i>Araucariacites australis</i>, <i>Proteacidites pseudomoides</i>, <i>Retitriletes austroclavatidites</i>, <i>Proteacidites</i> sp, <i>Podocarpidites</i> sp., <i>Stereisporites regium</i>, <i>petrotriletes majus</i>, <i>Stereisporites</i> sp, <i>Ceratosporites equalis</i>, <i>Tricolporites</i> sp, <i>Cyathidites minor</i></p>

Table 5.1. Continued.

Height on section	Sample number	Pollen and spores encountered
22m on D9.602	D9.046.1A	<i>Nothofagidites flemingii</i> , <i>Araucariacites australis</i> , <i>Stereisporites antiquasporites</i> , <i>Peninsulapollis gillii</i> , <i>Retitriletes austroclavatidites</i> , <i>Proteacidites</i> sp., <i>Nothofagidites senectus</i> , <i>Laevigatosporites ovatus</i> , <i>Stereisporites regium</i> , <i>Cyathidites</i> sp ?, <i>Phyllocladidites mawsonii</i> , <i>Ceratosporites equalis</i> , <i>Tricolpites</i> sp.
14.8m on D9.601	D9.037.1A	<i>Peninsulapollis</i> sp, <i>Nothofagidites</i> sp, <i>Podocarpidites</i> sp, <i>Laevigatosporites ovatus</i> , <i>Araucariacites australis</i> , <i>Stereisporites antiquasporites</i> , <i>Phyllocladites mawsonii</i> , <i>Retitriletes austroclavacidites</i> , <i>Stereisporites regium</i> , <i>Dacrydiumites praecupressinioides</i> , <i>Peninsulapollis askiniae</i> , <i>Proteacidites</i> sp., <i>Microcachryidites antarcticus</i> , <i>Perotriletes majus</i> , <i>Camarozonosporites ambigens</i> , <i>Triporopollenites</i> sp.1, <i>Azolla</i> sp (glochidium), <i>Trichotomosulcites subgranulatus</i> <i>Triporopollenites</i> sp.
21m on D9.600	D9.011.1A	<i>Retitriletes austroclavatidites</i> , <i>Laevigatosporites ovatus</i> , <i>Proteacidites</i> spp, <i>Nothofagidites</i> , fungal spore, <i>Stereisporites antiquasporites</i> , <i>Camarozonosporites ambigens</i> , <i>Phyllocladites mawsonii</i> , <i>Araucariacites australis</i> , <i>Stereisporites regium</i> , <i>Tricolpites</i> cf <i>T.phillipsii</i> , <i>Pluricellaesporites</i> sp., fungal spore, , <i>Podocarpidites</i> sp.

5.2.2.1 Palynomorphs present through the stratigraphic section.

Terrestrial palynomorphs are normally transported by wind or by flowing water and can be transported long distances from their source. Lowland sourced palynomorphs can be transported to upland areas and vice versa. As a result it is difficult to speculate from where the palynomorphs originated. This is further made difficult in this project because only the presence of palynomorphs was recorded, not quantitative analysis, which would give a

better idea of the influx of pollen and help suggest if the source was close by. The palynomorphs as an indicator of the composition and structure of the forests on the Antarctic Peninsula is based on nearest living relatives, diversity of pollen within a sample and associated sedimentology. Each formation is discussed separately:

López de Bertodano Formation. This Formation (D9.011.1A, D9.037.1A, D9.046.1A, D9.051.1A, D9.052.1A) contain diverse pollen and spores (See Table 5.1, Figure 5.1). Most of the nearest living relatives of *Proteacidites* spp., *Peninsulapollis* spp., *Podocarpidites* spp., *Nothofagidites* spp., *Trichotomosulcites subgranulatus*, *Cyathidites* spp. and *Stereisporites* spp. grow in a wide range of habitats and altitudes (see Table 5.2). Nearest living relatives of *Araucariacites australis* and *Microcachrydites antarcticus* have more restricted ecological niches. Today the nearest living relative of *Microcachrydites antarcticus* is *Microcachrys tetragona* and is only found in alpine heathland and scrub in Tasmania. It is likely that the *Microcachrydites antarcticus* and *Araucariacites australis* pollen was derived from an upland flora because their NLRs (*Araucaria* and *Microcachrys tetragona*) occupy high altitudinal areas in modern Southern Hemisphere forests. *Dacrydiumites praecupressinioides* closest relative is *Dacrydium* in New Zealand, which occurs at low altitudes so it is likely that this tree type occurred at similar altitudes on the Antarctic Peninsula. The pollen type *Phyllocladidites mawsonii* is the same as the pollen of *Lagarostrobos franklinii*. Today *Lagarostrobos franklinii* is endemic to the cool temperate Tasmanian forests (see Table 5.2) and is restricted to low altitude areas, along river banks prone to flooding. It is likely that trees in the Antarctic forests had a similar ecology (see Table 5.2).

Sobral Formation. Samples D9.100.1A, D9.113.1A and D9.108.1A are associated with muddy sandstones that represent prodelta and distal delta front depositional environments. Samples from here contain the same pollen and spore types as those within the López de Bertodano Formation. Further up the section in a more proximal delta front setting samples D9.122.1A and D9.127.1A again show a similar composition but with the addition of *Microcachrys tetragona* being present in both samples. Pollen type *Taxodiaceapollenites hiatus* and *Myrtaceidites* sp. are also present in

D9.127.1A. The nearest living relative of *Taxodiaceapollenites hiatus* are trees within the family Cupressaceae. Today members of the family have a wide ecological and altitudinal range so these trees may have grown at all altitudes on the Antarctic Peninsula.

Sample D9.135.1A has a low diversity of taxa (see Table 5.1) despite its proximity to a terrestrial environment. One possibility is that the sample could represent a marginal or post volcanic setting, meaning that it is a recovery floral assemblage. It is associated with planar cross-bedding in a proximal delta front setting (more proximal to a terrestrial environment). Palynomorphs present include *Araucariacites australis*, *Podocarpidites* sp., *Phyllocladidites mawsonii*, *Triporopollenites* sp. and *Peninsulapollis askinaceae*. Samples D9.161.2A and D9.167.1A also contain possible *Podocarpidites* sp., *Nothofagidites* spp., *Proteacidites* spp., *Peninsulapollis gillii*, *Triporopollenites* sp. They contain a low abundance of Bryophytes and Pteridophytes. It is possible that these samples may represent a high altitude flora, because they are associated with volcanic clastic sediments, which suggests that they have originated from an upland area close to a volcanic centre. Samples D9.161.2A and D9.167.1A also have a lower diversity of taxa compared to those samples in the López de Bertodano Formation, which is as another indicator that they may represent an upland flora. Another reason for low diversity is that the depositional setting may not have been adequate for the preservation of palynomorphs. Bryophytes and Pteridophytes may have not survived the volcanic disturbances.

Cross Valley Formation. Palynomorph samples from this formation are not as diverse as from the López de Bertodano Formation and the lower Sobral Formation. Both samples contain *Araucariacites australis*, *Nothofagidites* sp., *Podocarpidites* sp., *Retitriletes austroclavities* (D9.181.1A), *Proteacidites* sp. (D9.181.1A), *Peninsulapollis* spp. (D9.072.1A), *Osmundacites wellmanii* (D9.072.1A), *Cyathodites minor* (D9.072.1A), *Trichotomsulcites sugranulatus* (D9.072.1A). In addition *Myrcipites harissa*, *Myrcipites* sp1., *Myrcipites* sp2. are only present in sample D9.072.1A and no other sample on the section. *Phyllocladidites mawsonii*, which is present in most of the samples in the López de Bertodano Formation and the Sobral Formation. It is absent in the Cross Valley Formation. The number of tree species tends to decline from low

to high altitude in modern Southern Hemisphere forests and therefore the low diversity of palynomorphs observed in the Cross Valley Formation may represent an upland flora, (Beadle, 1981; Jarman et al., 1991; Veblen *et al.*, 1996). Another interpretation is that the palynomorphs were destroyed during transportation by the high energy debris/pyroclastic flow that the Cross Valley Formation represents. The occurrence of *Myrcipites* spp. is not a good indicator of an upland flora since its nearest living relative is Casuarinaceae, which is found at all altitudes in Australian temperate forests today (see Table 5.2).

5.3 Structure and composition of forests from fossil wood

5.3.1 Abundance of tree types

Conifers: *Agathoxylon* is the most abundant genus and makes up 49% of the conifers identified, which suggests that this was a dominant conifer tree in the Antarctic forests. *Phyllocladoxylon* (22%) and *Protophyllocladoxylon* (18%) were also common tree types. *Podocarpoxyylon* or *Cupressinoxyylon* trees may have been less common as there are few wood specimens (11%) (Refer to Figure 3.16).

There is bias in the abundances of conifer tree types because some wood specimens could not be fully identified due to poor preservation. Some wood specimens could not be distinguished as either *Podocarpoxyylon* or *Cupressinoxyylon*. This may mean that *Podocarpoxyylon* may be under-represented and may have actually been a more abundant conifer type in the forest, or *Cupressinoxyylon* was actually present but misidentified as *Podocarpoxyylon*.

Angiosperms: *Nothofagoxyylon* is likely to have been the most important angiosperm tree type in the Antarctic forests because it makes up 79% of the angiosperm woods identified in this project. *Weinmannioxyylon* and *Myrceugenelloxyylon* wood specimens each make up 8% of the angiosperm assemblage and therefore were likely to have been minor components of the forests. One specimen of *Antarctoxyylon* suggests that it was likely to be a rare tree type (5%) (Refer to Figure 4.11).

Table 5. 2. Palynomorphs identified in this project, their nearest living relative and the ecology of that modern relative. The presence and absence of similar taxa within the wood record is also presented.

Species	Nearest Living Relative	Ecology	Presence/absence in wood record
Bryophyta			
<i>Stereisporites antiquasporites</i> , <i>Stereisporites regium</i>	Sphagnaceae	Moss, occurs under tropical to cool temperate climates. Sphagnum moss commonly occurs on the forest floors in temperate regions at low and high altitudes (Beadle, 1981; Wardle, 1991). Sphagnum bogs are a common feature of Magellanic moorlands in the cold temperate (Veblen <i>et al.</i> 1995). Sphagnum bogs are also present in waterlogged areas above the treeline in cool temperate western and central Tasmania (Beadle, 1981).	Absent
Lycopodiophyta			
<i>Retitriletes austroclavatidites</i>	Lycopodiaceae (Lycopodium)	Club mosses. Found living under tropical to cool temperate climates. In the Valdivian, Chile Lycopodium Paniculattum occurs as an epiphyte in the Valdivian forest of Chile and occur on trees in New Zealand (Wardle, 1991; Fernandez and Fontenla, 2010).	Absent
<i>Camarozonosporites ambigens</i>	Lycopodiaceae/Selaginellaceae	Lycopodium and Selaginella are also found in Magellanic woodland in Chile (Videl <i>et al.</i> , 2011). They are found above the treeline in Tasmania, in waterlogged conditions, where annual rainfall exceeds >1500mm.	
<i>Ceratosporites equali</i> , <i>Perotriletes majus</i>	Selaginellaceae	Species of Lycopodia are also commonly found in alpine regions, fell fields and the northern gumlands of New Zealand (Wardle, 1991).	

Table 5.2. Continued.

Species	Nearest Living Relative	Ecology	Presence/absence in wood record
Pteridophyta			
<i>Azolla sp.</i>	Salviniales, Salviniaceae	Aquatic fern that occurs on slow or still waterbodies in lowland and mountain areas (Brownsey and Smith-Dodsworth, 1989). <i>Azolla</i> is found in tropical and cool temperate climates and at all altitudes.	Absent
<i>Cyathidites minor</i>	Filicopsida, Cyatheaceae	Tree ferns, found growing in tropical to cool temperate climates. In the temperate zones they are found living in New Zealand, Australia, Tasmania (Beadle, 1981; Brownsey and Smith-Dodsworth, 1989, Wardle, 1991) and occurs at low to high altitudes. They prefer areas of high rainfall and damp soils. Common habitats include forests, open heathland, riverbanks and damp gullies (Beadle, 1981; Brownsey and Smith, 1989; Wardle, 1991).	Absent
<i>Osmundacidites wellmanii</i>	Filicopsida, Osmundaceae	Ferns, grows in tropical to cool temperate climates. Genera (<i>Leptopteris</i> , <i>Osmunda</i> , <i>Todea</i>) are found in temperate forests in Australia and New Zealand. They occur in low and montane areas. Common habitats include swamps, along streams and open scrub. Generally prefers damp environments but <i>Leptopteris hymenophylloides</i> grows on dryer sites on ridge tops (Brownsey and Smith-Dodsworth, 1989).	Absent

Table 5.2. Continued.

Species	Nearest Living Relative	Ecology	Presence/absence in wood record
<i>Laevigatosporites major</i> , <i>Laevigatosporites ovatus</i>	<i>Filicopsida</i> , ? <i>Blechnaceae</i>	Fern. Grows in tropical to cool temperate climate zones. Species are found in New Zealand, Australia, Tasmania and Chile, and occur at low to high altitudes (Beadle, 1981; Brownsey and Smith-Dodsworth, 1989; Wardle, 1991; Chamber and Farrant, 1996). They prefer damp environments and common habitats include open heath land, forest understory, river banks, damp gullies and coastal areas that are subject to salt spray.	Absent
Gymnosperm			
<i>Araucariacites australis</i>	Araucariaceae (<i>Agathis</i> & <i>Araucaria</i>)	Tall tree. Found in warm to cool temperate climate. Grows in well drained montane areas at mid to high altitudes (Ogden and Stewart, 1995; Veblen <i>et al.</i> , 1995). Shade-intolerant and relies on large scale disturbances for regeneration. See Chapter 3, section 3.4.1.4 for more detail.	Present (<i>Agathoxylon</i>)
<i>Dacrydiumites praecupressinoides</i>	Podocarpaceae, <i>Dacrydium</i> group	Tree. Found in tropical to cool temperate climates Temperate species <i>Dacrydium cupressium</i> is endemic to New Zealand and lives in a wide range of environments. It is most dominant in lowland podocarp-broadleaved forests on wet and infertile soils (Norton <i>et al.</i> , 1988; Lusk and Ogden, 1992). <i>Dacrydium cupressium</i> also occurs at mid-altitudes on well drained soils (Norton <i>et al.</i> , 1988). It prefers to live in areas where frosts are uncommon.	Present ? (<i>Podocarpoxyton</i>)

Table 5.2. Continued.

Species	Nearest Living Relative	Ecology	Presence/absence in wood record
<i>Microcachryidites antarcticus</i>	Podocarpaceae, <i>Microcachrys/Microstrobos</i>	Shrub, occupies cool and wet montane, open heathland, in Tasmania (Beadle, 1981).	Unlikely because it is a shrub
<i>Phyllocladites mawsonii</i>	Podocarpaceae (<i>Lagarostrobos franklinii</i>)	Tree, endemic to cool temperate forests of Tasmania. It has a wide range of climatic and environmental tolerances, living between 0 - 1000m.a.s.l, and found fertile and poorly fertile soils (Gibson <i>et al.</i> 1991). Although, it is mostly confined to lowland areas along riverbanks, which are prone large-scale flood events. It relies on these flood events to create gaps in the forest canopy so it can regenerate and also help the dispersal of seeds downstream (Gibson and Brown, 1991).	Present? (<i>Phyllocladoxylon</i>)
<i>Podocarpities</i> sp.	Podocarpaceae (<i>Podocarpus/Dacrydium</i>)	Tree or shrub. Today members of the family live in the Southern Hemisphere, in tropical and temperate climate zones (Coomes and Bellingham, 2011). In temperate forests they grow at all altitudes. Prefer soils that are poorly fertile or waterlogged (Ogden and Stewart, 1995; Coomes and Bellingham, 2011). See Chapter 3, section 3.4.1.5 for details.	Present? (<i>Phyllocladoxylon</i> , <i>Podocarpoxylon</i>)

Table 5.2. Continued.

Species	Nearest Living Relative	Ecology	Presence/absence in wood record
<i>Trichotomosulcites subgranulatus</i>	Podocarpaceae, <i>Phyllocladus</i> /extinct <i>Microcachrys</i>	Tree or Shrub. Found at all altitudes, prefers poorly drained and poorly fertile soils (Ogden and Stewart, 1995; Gibson <i>et al.</i> , 1995)	Present (<i>Phyllocladoxylon</i> , <i>Protophyllocladoxylon</i>)
<i>Taxodiaceapollenites hiatus</i>	?Cupressaceae/?Taxodiaceae	Tree. Cupressaceae is found living in tropical to cool temperate climates. A number of taxa are found in cool temperate parts of Tasmania, New Zealand and Chile/Argentina (Ogden and Stewart, 1995; Gibson <i>et al.</i> 1995; Veblen <i>et al.</i> , 1995). They occupy a wide variety of habitats, from dry areas to areas with high humidity and rainfall. Common habitats include montane (e.g <i>Fitzroya cupressoides</i> , <i>Athrotaxis cupressoides</i> , <i>Athrotaxis cupressoides</i> , <i>Libocedrus bidwillii</i>) (Veblen <i>et al.</i> 1995, Jarman <i>et al.</i> , 1991). Sphagnum bogland (e.g <i>Pilogerodendron uviferum</i>), areas that are poorly drained and have infertile soils (e.g <i>Pilogerodendron uviferum</i> and <i>Fitzroya cupressoides</i>). <i>Fitzroya cupressoides</i> is shade intolerant and grows in areas that are prone to large scale disturbances e.g from volcanism. It is usually the first to occupy sites after disturbances (Veblen <i>et al.</i> 1995).	Uncertain (<i>Cupressinoxylon</i> ?)

Table 5.2. Continued.

Species	Nearest Living Relative	Ecology	Presence/absence in wood record
Angiospermae			
<i>Myriciptes harrissii</i> , <i>Myricipites sp1</i> , <i>Myricipites sp 2</i>	Casuarinaceae	In the Southern Hemisphere Casuarinaceae is found in New Caledonia, New Guinea and Australia (Beadle, 1981). It commonly forms part of the understory in lowland and montane Eucalyptus woodlands in south-east Australia. They are also found in semi-arid western Australia in heathlands along with Proteaceae species (Beadle, 1981). Common substrates include poorly fertile soils, periodically waterlogged soils, rocky coastal areas, sand dunes and estuaries (Beadle, 1981).	Absent
<i>Myrtaceidites sp.</i>	Myrtaceae	Trees and shrubs. The Myrtaceae family is large and has a wide distribution throughout the Southern Hemisphere. Genera that live in the temperate regions include <i>Amomyrtus</i> , <i>Eucalyptus</i> , <i>Leptospermum</i> , <i>Luma</i> , <i>Metrosiderous</i> , <i>Myceugenia</i> and <i>Tequalis</i> Cook and Shore, 1980; Salmon, 1980; Landrum, 1981; Stewart and Veblen, 1982; Stephens <i>et al.</i> , 2005; Gutiérrez <i>et al.</i> , 2009; Gut 2008). The above genera have wide ecological niches and are found from lowland areas to mountainous regions. Habitats range from semi -arid to wet and include, shrublands, woodlands, open heath, lake margins; areas that have recently been disturbed; open and closed forests, and swamp forests. Substrates include waterlogged soils, fertile soils, low fertile soils (Beadle, 1981).	Present (<i>Myceugenelloxylon</i>)

Table 5.2. Continued.

Species	Nearest Living Relative	Ecology	Presence/absence in wood record
<i>Nothofagities senectus</i>	Dicotyledonae, Nothofagaceae, Nothofagus ancestral	Tree or shrub. The family is diverse in Chile, New Zealand, Australia, Tasmania, New Caledonia and New Guinea (Veblen <i>et al.</i> , 1996; Ogden <i>et al.</i> 1996; Read and Brown, 1996; Read and Hope, 1996). Most species are found living in cool temperate climates. Grow on a wide range of substrates, such as well drained soils, volcanic ash to poorly fertile and water-logged soils. Grow at all altitudes. They are shade-intolerant so most prefer environments that are less favourable for broad-leaved angiosperms. See Chapter 4, section 4.3.1.5.	Present (<i>Nothofagoxydon</i>)
<i>Nothofagities flemingii</i>	Dicotyledone, Nothofagaceae, <i>Nothofagus</i> (subgenus <i>Fuscospora/Nothofagus</i>)		
<i>Peninsulapollis askiniae</i> , <i>Peninsulapollis gillii</i> , <i>Proteacidites sp. cf. P. scaboratus</i> , <i>Proteacidites pseudomoides</i> , <i>Proteacidites sp.</i> , <i>Triporopollenites sp.</i>	Dicotyledone, Proteaceae	Most taxa occur as a sclerophyllous shrub (Johnson and Briggs, 1975). Today Proteaceae is diverse in Australia (e.g. <i>Banksia</i> , <i>Lomatia</i> , <i>Hakea</i> , <i>Embothrium</i> , <i>Grevillea</i>) and Southern South America (e.g. <i>Embothrium coccineum</i> , <i>Lomatia ferruginea</i> , <i>Gevuina avellana</i>) (Johnson and Briggs, 1975; Steubing <i>et al.</i> , 1983). Proteaceae occurs at sea level to alpine zones (Johnson and Briggs 1975; Beadle, 1981; Jarmen <i>et al.</i> , 1991; Castro-Arevalo <i>et al.</i> , 2008; Videl <i>et al.</i> , 2011). Habitats include heathlands, woodlands, forests and peatbogs.	Absent
<i>Tripocolpites sp. cf. T.phillipsi</i> , <i>Tricolpites confessus</i> ,	Dicotyledonae	Afinity unknown.	Absent
Polycolpites sp. cf. <i>P. langstonii</i> ,			Absent
Fungi			Absent

5.3.2 Structure and composition of the forests

The preservation and depositional history of the woods and ecology of their nearest living relatives have been used to interpret where tree types were growing on the Antarctic Peninsula. Figure 5.4 and 5.5 present the distribution of conifer and angiosperm genera on the sedimentary sequence. Each wood type has been discussed separately:

Phyllocladoxylon and *Protophyllocladoxylon*. *Phyllocladoxylon* wood (D9.036.1 and D9.038.1) was found in the López de Bertodano Formation at 30m and 31m on the sedimentary sequence associated with marine mudstones. In the Sobral Formation *Phyllocladoxylon* was associated with distal delta front facies at 155m (D9.094.1, D9.092.1 and D9.098.1) and proximal delta facies (D9.125.1) at 250m. *Protophyllocladoxylon* wood is found in the Sobral Formation (D9.093.1 and D9.112.1) and the Cross Valley Formation (D9.071.1, D9.153.1 and D9.181.1). The wood specimens in the Sobral Formation have been deposited delta front and prodelta facies.

The *Phyllocladoxylon* and *Protophyllocladoxylon* woods in the Sobral Formation are all permineralised by calcite and some have Teredolites borings, characteristic of a marine depositional environment. The nearest living relatives for both wood genus is the podocarp *Phyllocladus*. The nearest living relative of *Phyllocladoxylon* is also thought to include *Lagarostrobos franklinii* (Cantrill and Poole, 2005; Bowman *et al.*, 2014). In the Southern Hemisphere the majority of species of *Phyllocladus* are found at low altitudes (Wagstaff, 2004; Ogden and Stewart, 1995) (see Chapter 3). *Phyllocladus alpinus* occurs at high altitudes but is a small shrub. From the above evidence it is likely that the wood specimens in the López de Bertodano and Sobral formations are from trees that grew at low altitudes.

In the Cross Valley Formation *Protophyllocladoxylon* wood specimens are haematite stained suggesting original deposition in a terrestrial environment before being transported into the marine basin. The Cross Valley Formation represents a high energy debris flow and it is likely that the wood within the formation is from trees that grew at different altitudes (J.Francis 2015,

pers.comm., 1 September). Therefore the *Protophylocladoxylon* wood may have come from upland or lowland areas. Due to the size of the wood specimens and the low curvature of the growth rings it is likely that they were trees and not shrubs.

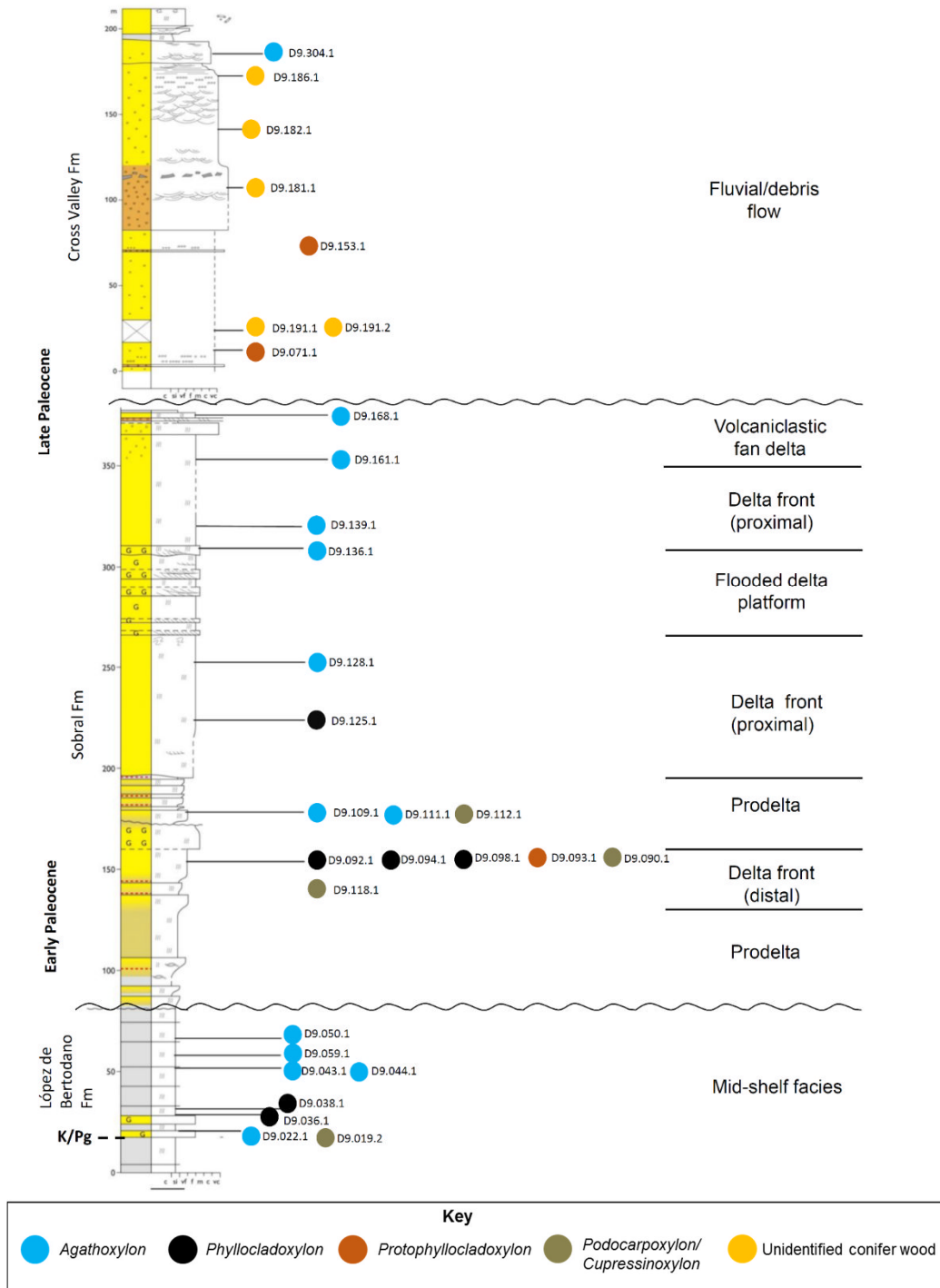


Figure 5.4. Distribution of conifer genera on the sedimentary succession. Sedimentary log courtesy of Jon Ineson.

Agathoxylon. This genera is found in the López de Bertodano Formation (D9.022.1, D9.043.1, D9.044.1, D9.050.1 and D9.059.1), Sobral Formation (D9.111.1 and D9.110.1, D9.128.1, D9.136.1, D9.139.1, D9.161.1 and D9.168.1) and Cross Valley Formation (D9.304.1). This morphotype has closest affinity to the family Araucariaceae. Modern trees in this family occupy mountainous regions prone to disturbances (see Chapter 3, section 3.4.1.5). Specifically, *Araucaria araucana* is found at high altitudes >1000m on the Andes (Veblen et al. 1995) and relies on disturbances for regeneration such as pyroclastic flows and wild fires. The wood from the López de Bertodano Formation and lower Sobral Formation show no evidence such as rounded edges that suggests they have been transported long distances from upland areas. In the upper Sobral Formation (D9.168.1, D9.161.1, D9.139.1 and D9.136.1) and Cross Valley Formation (D9.304.1). The fact that some of the wood specimens have been partly charred may suggest a similar ecology to modern *Araucaria araucana* which grows at high altitudes, in areas prone to wildfires caused by volcanic activity, in the Andes. Some of the partly charred wood is also rounded this maybe further evidence of long-distance transportation, however there is uncertainty because abrasion may have occurred in coastal areas also (Gonor et al., 1988). The wood specimens in the López de Bertodano Formation may have also been derived from upland areas and was transported as driftwood via river systems rather than bedload. Another possibility is that *Agathoxylon* trees grew at lower altitudes on the Antarctic Peninsula.

Podocarpoxyton/Cupressinoxyton. This one wood specimen (D9.090.1) has rounded edges and is partly charred. Similar to the partly charred Agathoxylon wood. This maybe evidence that the wood originated from upland areas, prone to wildfires caused by volcanic activity. Today podocarps and the Cupressaceae are found are found at all altitudes (see Table 5.2).

d)

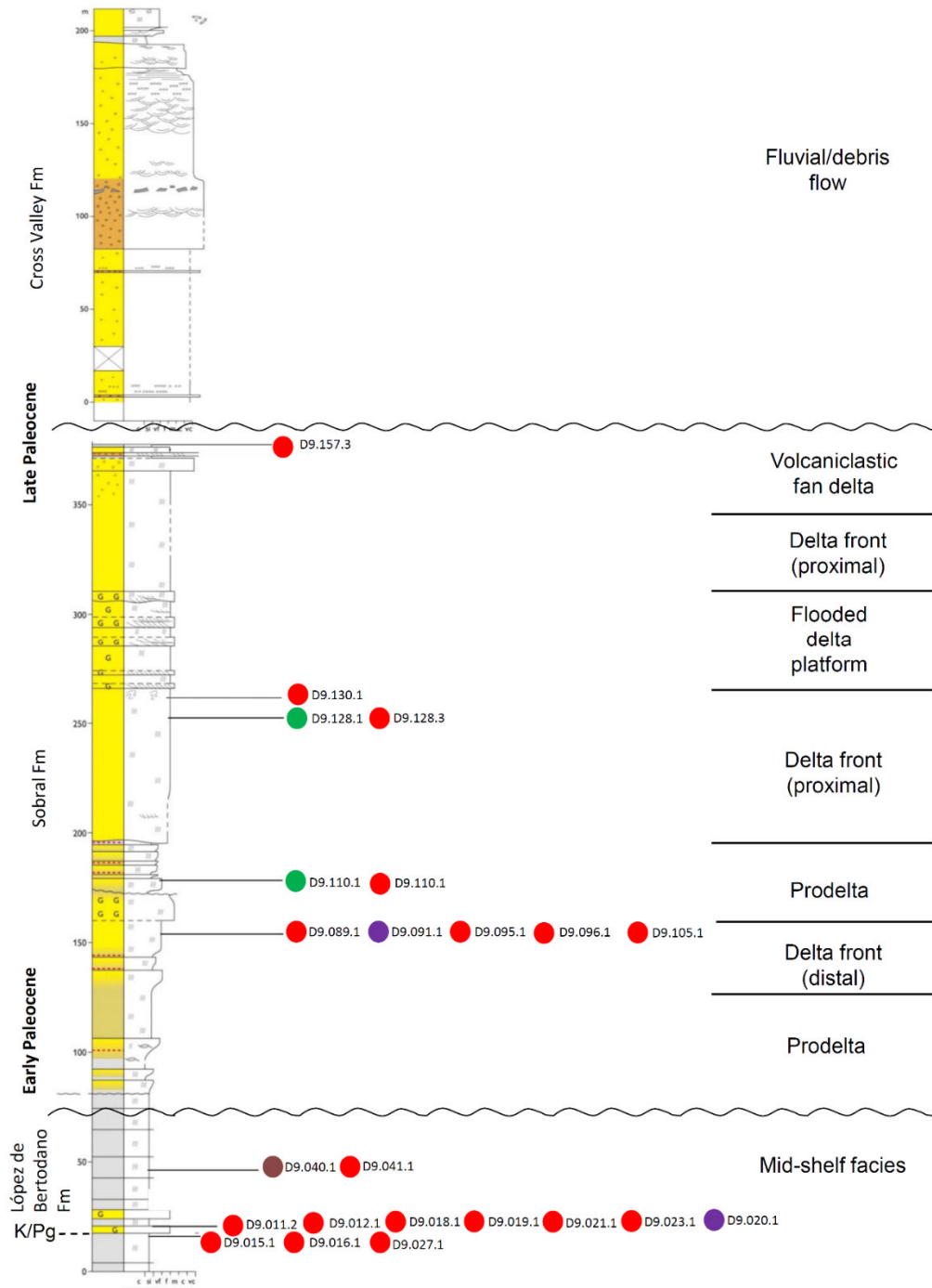


Figure 5.5. Distribution of angiosperm morphotypes on the sedimentary sequence. Sedimentary log courtesy of Jon Ineson.

Nothofagoxylon. *Nothofagoxylon* wood is located in the López de Bertodano Formation (D9.011.2, D9.012.1, D9.016.1, D9.018.1, D9.019.1, D9.021.1, D9.027.1, D9.041.1, D9.053.1 and D9.054.1) and Sobral Formation (D9.095.1, D9.096.1, D9.105.1, D9.110.1, D9.128.3, D9.130.1 and D9.157.3, D9.089.1). Wood specimen D9.089.1 located at 175m on the stratigraphic section is partly charred and rounded, and D9.157.3 in the uppermost units of the Sobral Formation is charred. It is possible that the wood specimens that are partly charred came from upland areas. Today in the Southern Hemisphere forests *Nothofagus* is found from sea-level, to 1000m in mountainous regions and it is likely that *Nothofagus* trees occurred at all altitudes on the Antarctic Peninsula (Veblen et al. 1996).

Weinmannioxylon, *Myrceugenelloxylon* and *Antarctoxylon*. *Weinmannioxylon* is found in the Sobral Formation where it is associated with prodelta (D9.107.1) and delta front (D9.128.1) facies. *Myrceugenelloxylon* is found in the López de Bertodano Formation (D9.020.1) where it is associated with marine mudstones. It is found in the Sobral Formation (D9.091.1) where it is associated with prodelta facies. All of the wood specimens are calcite permineralised. The nearest living relatives of *Weinmannioxylon* and *Myrceugenelloxylon* are today found in low to mid-altitude forests today. All of the evidence suggests that these tree types grew at similar altitudes on the Antarctic Peninsula. *Antarctoxylon* does not have a nearest living relative so it is difficult to suggest with confidence its ecology.

5.4 Discussion on the composition and structure of forests and ecology of the trees

5.4.1 Comparison between fossil wood and palynomorph records

Fossil wood identified in this project indicates that the following tree types lived in the Paleocene forests: *Araucaria/Agathis* (*Agathoxylon*), *Phyllocladus* (*Phyllocladoxylon* and *Protophyllocladoxylon*), *Podocarpoxyton/Cupressinoxylon*, *Nothofagus* (*Nothofagoxylon*), *Luma* (*Myrceugenelloxylon*), *Weinmannia* (*Weinmannioxylon*) and an extinct angiosperm tree type, *Antarctoxylon*.

Palynology analysis indicates the presence of trees of *Lagarostrobos franklinii*, *Nothofagus*, Myrtaceae, *Araucaria/Agathis*, *Phyllocladus* and *Podocarpus* spp. These tree types are also found in the wood record. The presence of palynomorphs belonging to Proteaceae, Casuarinaceae, Blechnaceae, Cyatheaceae, Lycopodiaceae, Sphagnaceae and *Azolla* sp. are not found in the wood record. The palynomorphs have thus given a better picture of the floral composition in the forests.

The absence of Proteaceae, Casuarinaceae, Pedaliaceae in the wood record is likely to be a result of them being shrubs or herbaceous plants and are therefore not usually preserved unlike the wood from large trees. Ferns will not be observed in the fossil wood record because they are mostly non-woody plants. It is uncertain whether *Antarctoxylon* is present in the pollen record because its affinity is unknown.

The pollen record shows a higher diversity of taxa within the family Podocarpaceae than the wood record. This is because the wood, especially conifer wood, is conservative, which makes it difficult to separate species (Falcon-Lang and Cantrill, 2000; Philippe and Bamford, 2009). As a result, in the published records many taxa within a family have been grouped into one morphotype. For example, *Phyllocladoxylon* and *Protophyllocladoxylon* includes wood that is similar to that of *Phyllocladus* and *Lagarostrobos* trees (Cantrill and Poole, 2005). *Podocarpoxyton* includes all fossil wood that is similar to that of all modern podocarps (Cantrill and Poole, 2005). Thus the range of tree species in the modern Southern Hemisphere forests is not represented in the range of wood types in the fossil assemblages.

Within the wood record the Nothofagaceae family wood types are similar to the modern sub-genus *Nothofagus* and *Lophonzia*. The *Nothofagus* that could be identified to species level include *Nothofagidites flemingii* and *Nothofagidites senectus* which belong to the sub-genera *Nothofagus* or *Fuscospora*.

Pollen belonging to the family Cunoniaceae are absent.

Trees have different pollen dispersal rates, and pollen can have different preservation potential. Possible reasons for the absence of Cunoniaceae include:

- Pollen size. Modern and fossil *Weinmannia* grains are observed as small (9 – 20µm) (Cranwell, 1959; APSA Members, 2007). Due to their small size the pollen grains may have been lost through the processing procedure. During analysis of the samples. There may have been a chance that pollen grains were overlooked.
- Preservation. Different pollen types have different preservation potentials thus determining whether the pollen type is present in the palynological record or not (Ferguson *et al.*, 2010).
- Pollen production, distribution and origin of trees. In this study only two wood specimens have been identified as *Weinmannioxylon* (*Weinmannia*), indicating that they may have been a minor component of the forests living on the Antarctic Peninsula. Research on modern pollen dispersal in New Zealand has shown that *Weinmannia racemosa* has very local pollen dispersal (Horrocks and Ogden, 1994). It is possible that *Weinmannia* type trees may have had a similar pollen dispersal and due to being minor components of the forest and depending on their location. This may have prevented them from being represented in the palynological record. Pollen dispersal from trees in forest settings can be inhibited due to lack of air circulation (Horrocks and Ogden, 1994). A possible combination of these factors could be the reason for why *Weinmannia* is not recorded here.

5.4.2 Palaeoecology of the Antarctic forests

The palaeoecology has been determined based on the nearest living relatives of wood morphotypes and palynomorphs. A possible upland and lowland flora has been distinguished and they are discussed separately below:

Lowland forests

The lowland floras of the Antarctic Peninsula are likely to have consisted of ancestors of the following conifer tree types: *Phyllocladus*, *Dacrydium*, *Lagarostrobos franklinii*, *Podocarpus* and possibly conifers of the Cupressaceae. Angiosperms include the Nothofagaceae, *Weinmannia*, *Luma*

and other Myrtaceae trees and Proteaceae. Other now extinct angiosperms were also present, such as *Antarctoxylon* (wood record), *Tripocolpites* sp. cf. *T.Phillipsi* and *Tricolpites confessus* (pollen record).

This interpretation is based on the interpretation that most of the wood that has been identified as *Nothofagoxylon*, *Phyllocladoxylon* and *Podocarpoxyton/Cupressinoxylon*, *Protophyllocladoxylon*, *Weinmannioxylon* and *Myrceugenelloxylon* are associated with marine sedimentary sequence and show no evidence of being transported long distances from source. The nearest living relatives of some of the palynomorphs grow in restricted low altitudinal areas (e.g. *Lagarostrobos franklinii* and *Dacrydium cupressinum*) (see Table 5.2). However, some have wide ecological ranges and grow at all altitudes, such as Proteaceae and Myrtaceae, which grow in heathland communities, woodlands and form the undergrowth in forests (Beadle, 1981; Wardle, 1991) (see Table 5.2).

The main canopy-forming trees in the Antarctic forests are likely to have been *Dacrydium*, *Lagarostrobos franklinii* and *Nothofagus* and other podocarp tree species. Today these trees are elements of the canopy in the cool temperate Valdivian forests of Patagonia, Tasmanian forests, and the cool and warm temperate forests of New Zealand (Jarman *et al.*, 1991; Veblen *et al.*, 1995; Ogden and Stewart, 1995; Veblen *et al.*, 1996). *Dacrydium* can reach heights of 35m and *Lagarostrobos franklinii* (endemic to Tasmania) can reach heights of 25m (Jarmen *et al.*, 1991; Norton *et al.*, 1988). *Nothofagus* is a common canopy tree at mid-altitudes on the slopes of the Andes, southern Chile. The tallest species is *Nothofagus dombeyi*, which can reach heights of 50m (Veblen *et al.*, 1996).

The sub-canopy is likely to have consisted of *Weinmannia*, *Luma*, other Myrtaceae trees and *Phyllocladus*. *Weinmannia* species today (e.g. *Weinmannia racemosa*, *Weinmannia sylvicola*, *Weinmannia trichosperma*) commonly form the sub-canopy in the Valdivian forests and cool and warm temperate closed and open canopy forests in New Zealand, along with Myrtaceae species (Ogden and Stewart, 1995, Veblen *et al.*, 1996; Gut 2008, Gutiérrez *et al.*, 2009). *Phyllocladus* species are also common as sub-canopy components in the New Zealand forests such as open podocarp forests in

lowland areas, mixed broad-leaved-conifer forests and closed-canopy warm temperate forests (Ogden and Stewart, 1995).

The wood record and palynomorph record suggests that the trees of the family Podocarpaceae and the genus *Nothofagus* were dominant tree types in the Antarctic forests, and broad-leaved angiosperm trees were likely to have been minor components. From this it is likely that the lowland Antarctic forests were likely to be open canopy forests. Firstly because the *Nothofagus* and podocarp trees generally have smaller leaves than other angiosperm trees and therefore are more likely to allow light to filter through the canopy (Ogden *et al.*, 1996; Read and Brown, 1996; Veblen *et al.* 1996). Another reason is that most Podocarpaceae and *Nothofagus* trees are shade-intolerant to various degrees and therefore are less common or absent in closed broad-leaved forests today and are more dominant in open forests or woodlands. Trees within these families prefer less optimum sites, such as poorly fertile soil or areas prone to major disturbances (see Table 5.2).

Today in cool temperate New Zealand, in areas of high rainfall, open canopy Podocarp forests (species include *Dacrydium cupressinoides*, *Prumnopitys ferruginea*, *Phyllocladus alpinus*) occur on poorly fertile and waterlogged soils on fluvio-glacial terraces (Ogden and Stewart, 1995). These terraces are also prone to major flooding which helps the regeneration of podocarp trees. *Nothofagus* forests occur at low altitude in southernmost South Island New Zealand where temperatures are too cold for broad-leaved trees and soils are too poor. Broad-leaved trees are minor components of these forests (main species being *Weinmannia racemosa*, *Quintinia acutifolia* and *Metrosideros umbellata*) (Ogden *et al.* 1996). These modern analogues suggest that the lowland Antarctic forests are likely to have grown on poorly fertile and or waterlogged soils. *Lagarostrobos franklinii* may have grown along river systems on the Antarctic Peninsula similar to its ecology today in Tasmania (see Table 5.2).

The undergrowth of the Antarctic forests may have consisted of shrubs of the families Proteaceae and Myrtaceae. The Proteaceae have a wide ecological niche, and can grow in most conditions and are common components of the Tasmanian forests and the Valdivian forests today (see Table 5.2). Some

Proteaceae may have grown in more open areas in the forests similar to *Embothrium coccineum* in Chile (Castro-Arevalo *et al.* 2008). Myrtaceae shrubs such as *Leptospermum* are found in the undergrowth in Tasmania and New Zealand (Beadle, 1981; Wardle, 1991; Jarmen *et al.*, 1991). The common occurrence of fern species belonging to the families Blechnaceae and Osmundaceae and tree ferns Cyatheaceae suggests that these plants were common components forming the undergrowth of the Antarctic forests. Epiphytic ferns e.g. *Lycopodium* probably grew on the trees. *Sphagnum* moss may have also growth on trees and on the forest floor.

The lowland forests on the Antarctic Peninsula are likely to have grown under moist and humid conditions because these are the conditions in which most trees belonging to Podocarpaceae prefer (Ogden and Stewart 1995; Lusk and Ogden, 1992). Also *Weinmannia* and *Luma* also prefer moist soils (Gut, 2008). More information on the climate in which the forests grew is presented in Chapter 6.

Upland forests

Tree types include *Araucaria*, *Nothofagus* and other conifers such as podocarps, the Cupressaceae and *Phyllocladus*. The interpretation is based on the nearest living relatives of the fossil genera *Agathoxylon* and *Nothofagoxylon*, which today are found living in high altitudes areas. *Podocarpoxyton* wood also show similar evidence of being transported long distances. *Protophyllocladoxylon* wood is found in the Cross Valley Formation which is thought to represent a more proximal setting to the volcanic arc. Podocarpaceae, Araucariaceae and *Nothofagus* pollen are found throughout the sedimentary sequence including the Cross Valley Formation. *Araucaria* is likely to have been the main canopy tree as *Agathoxylon* is the most abundant wood in the conifer wood record and its pollen *Araucariacites australis* is present in most of the palynomorph samples. *Nothofagus* trees and other conifer podocarps are likely to have been subcanopy trees.

Today modern *Araucaria araucana* grows above 1000m to the treeline in the southern Andes where it forms open woodlands with *Nothofagus* (Veblen *et al.* 1995; Veblen *et al.* 1996). The *Araucaria* trees can grow up to 50m in

height and *Nothofagus* grows as stunted trees or low lying shrubs at the treeline (Veblen *et al.*, 1996). On the drier eastern side of the Andes *Austrocedrus chilensis* (Cupressaceae) is also present. These woodlands grow in well drained soils and it is likely that trees on the Antarctic Peninsula, at high altitudes, grew in similar conditions. In montane areas of Tasmania conifer-dominated woodlands also occur (main species include *Athrotaxis* and *Podocarpus lawrencii*), although *Nothofagus* can commonly form stunted trees, and thus the high altitude forests may have also show some similarity to these also. In *Araucaria* woodlands of Chile the undergrowth is sparse, but in the Tasmanian montane woodlands ferns (e.g. *Blechnum*), *Sphagnum* moss and Myrtaceae shrubs are common (Jarman *et al.*, 1991). The fact that spores ferns and *Sphagnum* moss are present throughout the sedimentary sequence suggest that they may have been undergrowth components in the high altitude Antarctic forests also. Heathland may have formed above the tree line since *Microcachrys* pollen is present and this is a common shrub in the heathlands of Tasmania (Beadle, 1981). The heathlands in Tasmania also consists of Proteaceae spp., *Podocarpus lawrencii* and Myrtaceae spp. (Beadle, 1981). It is therefore possible that these taxa formed heathland on the Antarctic Peninsula.

Chapter 6

Palaeoclimate analysis

6.1 Introduction

This chapter concerns the relationship between wood morphology and climate parameters (e.g. seasonality, precipitation and temperature) to reconstruct Paleocene climates on the Antarctic Peninsula. The methods used include analyses of growth rings in both conifer and angiosperm wood, information from angiosperm wood morphology, and methods that have been adapted from work on modern wood to calculate specific gravity in fossil wood. In addition, the climate tolerances of nearest living relatives (NLR) of this fossil flora have been used to reconstruct climate parameters and frost tolerances.

Chapter 6 is divided into four main sections. These are: Introduction to the principles of the palaeoclimate analyses (section 6.2); methods of applying the above analyses to the fossil flora (section 6.3); and results, which are presented as tables, graphs and text (section 6.4). The implications of the results for each analysis are also discussed in section 6.4. Finally, an overall discussion discusses what the analyses indicate about the Paleocene climates of the Antarctic Peninsula (section 6.5).

6.2 Introduction to palaeoclimate analysis and techniques

6.2.1 Growth ring analysis

Growth rings develop in trees that grow under seasonal climates, where factors such as temperature, water availability and light are limiting during certain times of the year (Fritts, 1976; Schweingruber, 1996). During the start of the growing season (spring), when conditions are favourable, large and thin-walled cells are produced by cell division in the vascular cambium (a narrow layer of meristematic cells that occurs between the bark and wood) (Fritts, 1976). These large thin-walled cells comprise the earlywood within a growth ring. These cells are tracheids in conifers and fibres and vessels in

angiosperms (Figure 3.1 and 4.1). Late in the growing season (summer) cells in conifer wood and fibres in angiosperm wood become thicker walled and smaller in size, forming the latewood in a growth ring (Figure 3.1 and 4.1). However, the size of vessels does not decrease in angiosperm wood that is diffuse porous. In simple terms, long growing seasons result in wide growth rings and short growing seasons result in narrow growth rings (Fritts, 1976).

Sometimes there are interruptions in growth during the growing season, which can be a result of late frosts, drought or insect attack (Fritts, 1976; Schweingruber, 1996). The trees react to these events by producing a false ring within the true annual growth ring. False rings caused by drought are formed a narrow layer of small cells (even just 1 or 2 cells thick) that resemble late wood. A false ring caused by frost damage or insect attack can usually be distinguished from drought rings because there is usually a layer of distorted or exploded cells or insect-damaged cells.

In a study of ring widths in modern trees from across the world, Falcon-Lang (2005b) has shown that, at a global level, mean growth ring width (MGRW) increases with increasing mean annual temperature (MAT) (Figure 6.2). However, relatively narrow growth rings are still produced in some trees despite temperature. The wide range in MGRW with increasing MAT (Figure 6.2) is because the relationship between tree growth and climate is complicated with a number of variables involved, which will be discussed further.

The overall relationship between MGRW and mean annual rainfall (MAR) is not as strong (Figure 6.1) as that of MAT. MGRW initially shows an increase with increasing MAR values between 0 and 1000mm but, as with MAT, the range of MGRW is still wide and other variables are involved.

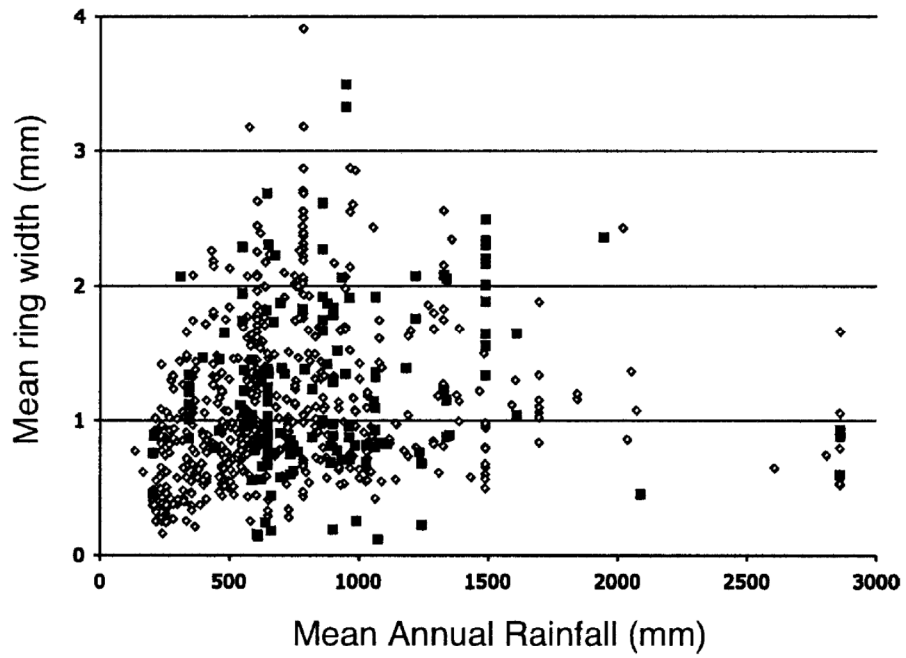


Figure 6. 1. The relationship between mean growth ring width (MGRW) and mean annual rainfall (MAR) from a global dataset. Open diamonds = conifers, closed squares = angiosperms. From Falcon-Lang (2005b).

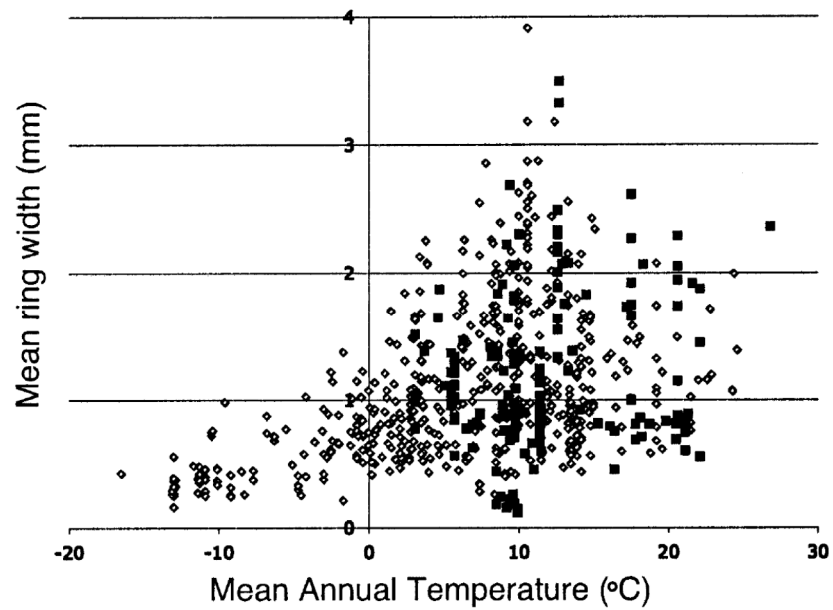


Figure 6. 2. The relationship between mean growth ring width (MGRW) and mean annual temperature (MAT) from a global dataset. Open diamonds = conifers, closed squares = angiosperms. From Falcon-Lang (2005b).

In modern forests the effects of climatic parameters on tree growth can vary depending on site factors. These factors include: altitude, whether a tree is found in the interior or at the margins of a forest, soil quality (depends on how much moisture it can hold), and slope aspect (Fritts, 1976). Figure 6.3 demonstrates that tree growth is more sensitive to climatic factors when a tree is living at its ecological threshold (e.g. forest margins). This is because with increasing distance from the forest interior the forest stand becomes less dense and trees become more exposed. The decrease in precipitation effectiveness and moisture availability is due to the increased effect of temperature, wind and solar radiation on transpiration, and evaporation of moisture from soil. As a result, this causes a decrease in growth ring width and also variability in ring width from one year to the next. Growth ring width can also decrease with increasing altitude as result of shorter growing seasons caused by lower temperatures.

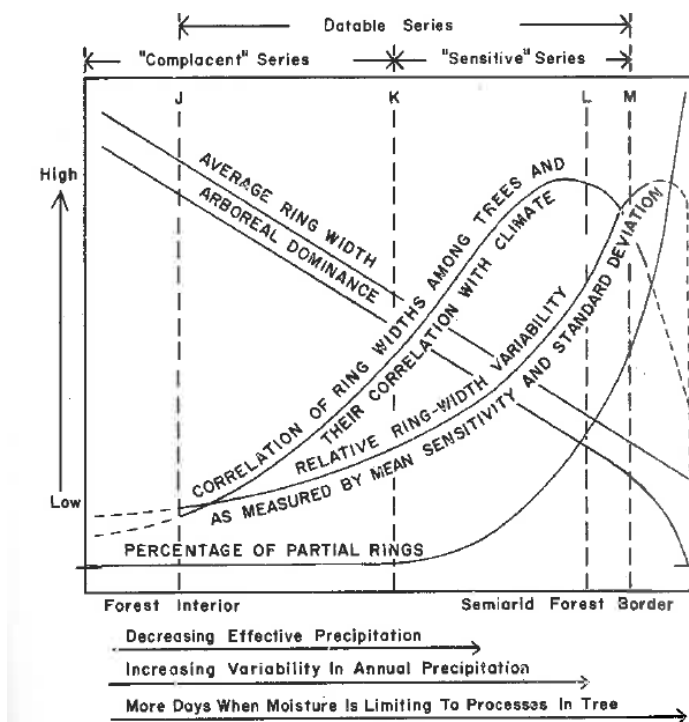


Figure 6. 3. This graph illustrates that tree growth becomes more sensitive to climatic factors from the forest interior to the semi-arid forest border. Taken from Fritts (1976).

Growth ring width can also vary within a tree as a result of internal factors. These include ontogeny, life habit and origin within a tree (e.g. branch or stem). For example, trees have different life spans they may be long-lived and slow growing (narrow growth rings) or short-lived and fast growing (wider growth rings) (Schweingruber, 1996). Falcon-Lang (2005a) found that growth ring width and growth variability decreased with increasing age. Branch wood has narrower growth rings than stem wood because the cells are smaller (Chapman, 1994).

Different parts of a tree have different stresses exerted on them. This can be mechanical stress such as gravitational pull on leaning stems or branches that leads to the formation of reaction wood. Reaction wood forms on either the underside or upper side (depending on whether a conifer or angiosperm respectively) of the branch or stem and holds it in place, stopping further leaning. Reaction wood has thicker walled cells and the growth rings tend to be wider compared to the normal wood (Fritts, 1976; Schweingruber, 1996). Branches also often tend to be more exposed than stems and as a result tend to show higher year to year variability in growth. They are also more prone to frost damage (Falcon-Lang, 2005a).

6.2.2 Palaeoclimate information from fossil angiosperm woods

Previous research on extant angiosperm wood has suggested that the characteristics of some anatomical features are controlled by climatic parameters (e.g. seasonality, water availability and temperature) (Carlquist, 1977; Carlquist and Hockman, 1985; Wheeler and Baas, 1993; Carlquist, 2001; Wheeler *et al.*, 2007). These features include vessel diameter, and vessel length and vessel density; ring porosity and, perforation plate type (see Chapter 4 for Figure 4.1 and 4.2 demonstrating these anatomical features). The anatomical features and their relationship to climate are discussed below.

a) Vessel diameter, frequency and element length. Carlquist (1977) made an observation that with increasing aridity woody angiosperm plants have a higher frequency of short vessels with small diameters (Figure 6.4 illustrates these features). This is a survival strategy that reduces the effect of air

embolisms (air pockets), a process whereby air replaces water in vessels and affects conductivity. This can be caused by drought or freezing of water in vessels. Increasing the number of vessels reduces the impact of air embolisms because there is back-up if some vessels do get impaired (Carlquist, 1977). Wider vessels are more efficient at conducting water; however they are more prone to air embolisms than narrow vessels (Carlquist, 1977). Shorter vessel elements are structurally stronger than longer vessels and are also better at localising air embolisms.

Using these observations, Carlquist (1977) developed the Vulnerability Index (VI) and Mesomorphy Index (MI) to quantify a plant's adaption to the availability of water within its environment:

$VI = \text{mean vessel diameter } (\mu\text{m}) \div \text{mean vessels per square mm}$

$MI = VI \times \text{mean vessel element length } (\mu\text{m})$

The VI is an indicator of how well a plant is adapted (hydraulic safety versus efficiency) to withstand water stress (e.g. drought). VI values below 1.0 suggest xeromorphy (adaption to arid environments) and values greater than this indicate mesomorphy (adaption to environments with sufficient water availability).

MI values are indicators of plants that either live in xeric (arid environments) or mesic conditions (environments with sufficient water availability). MI values of 75 and below indicate xeromorphy and values of more than 200 indicate mesomorphy.

The findings from Carlquist (1977) are supported by more recent studies (Wheeler and Baas, 1993; Wheeler *et al.*, 2007) that have analysed the presence of anatomical features on a global scale across regions with different climate zones. These studies have found that woods that have large vessel diameters ($>100\mu\text{m}$) and, low vessel density ($< 5 \text{ mm}$ or $5 - 20 \text{ mm}^2$) are most common in tropical areas of India, South East Asia, Africa and Australia. Short vessel lengths are most common in the dry Mediterranean regions.

The variability of vessels is also dependant on internal factors within a woody angiosperm plant, such as ontogeny and, wood organ type (branch, trunk or root). Vessel diameter increases and vessel density decreases from juvenile to mature wood (Poole, 1994, Carlquist, 2001 and references therein). Poole (1994) found that there was a significant increase in vessel diameter and longer vessel element length from branch to trunk to root wood in three different tree species. Root wood had significantly larger vessel diameters and element length than the other organs. As a result, this causes considerable differences in VI and MI values within a tree. Poole (1994) suggested overcoming this problem in fossil wood by identifying and recording the likely location of a fossil wood specimen from within the tree structure.

Relationships between plant size and vessel density, diameter and length have also been found in other studies. Olson and Rosell (2013) conducted a study to find whether stem diameter or water availability controlled vessel characteristics in angiosperms with different habits (e.g shrub or tree) from a range of different environments such as wet to dry habitats. They found that trees with the same stem diameters and stem lengths had similar vessel diameters. They suggested that vessel size has an indirect relationship to climate because small plants with narrow vessels are mostly found in dry conditions. Wheeler *et al.* (2007b) also found that vessels with diameter <50 μm are more common in shrubs but vessels >200 μm are virtually absent in shrubs from dry habitats.

b) Vessel grouping. Wood with large groups of vessels tend to be associated with arid conditions where the risk of air embolism (air pockets) is high (Figure 6.4). Having more and larger groups of vessels allows for higher conductivity potential and is considered to increase safety against air embolisms because it creates more alternative pathways for water flow if neighbouring vessels are damaged (Carlquist, 1984). In order to quantify the average vessel grouping in woods, the Vessel Group Index (VGI) was developed. This involves counting how many vessels are in a group (solitary vessels = a group of 1) and calculating the average for the number of groups observed (Carlquist, 1984; 2001). An experimental study by Lens *et al.* (2011), which evaluated different traits that plants develop to increase resistance to air embolism found that vessel grouping had a strong relationship with a higher resistance to negative

pressures caused by embolisms. This suggests that VGI is a good indicator of a water availability.

c) Ring porosity. Ring porous and semi-ring porous woods have been suggested to be an indicator of seasonal climates because they are most abundant in trees that grow in temperate zones with well-defined seasons (Wheeler *et al.*, 2007b) (see Chapter 4 for Table 4.1 and Figure 4.2 which demonstrates the different porosity types available in angiosperm wood). However, ring porosity is most abundant in the Northern Hemisphere and rare in the Southern Hemisphere temperate zones. This has led to the suggestion that porosity is also related to deciduousness and length of the growing season. The rarity of ring porous woods in the Southern Hemisphere at present is attributed to the majority of trees being evergreen.

d) Perforation plates. Globally there is a higher incidence of woods with simple perforation plates because they are considered to be more efficient at conducting water compared to the more primitive scalariform type (Wheeler and Baas, 1993; Carlquist, 2001; Wheeler *et al.*, 2007b) (see Chapter 4 for Table 4.1 and Figure 6.4 which demonstrate the different perforation plate types). However, there are climatic constraints to their global distribution. For example, scalariform perforation plates are most abundant in temperate regions, where there is sufficient water availability. Exclusively simple perforation plates are most abundant in woody angiosperms that grow in arid climates (Figure 6.4).

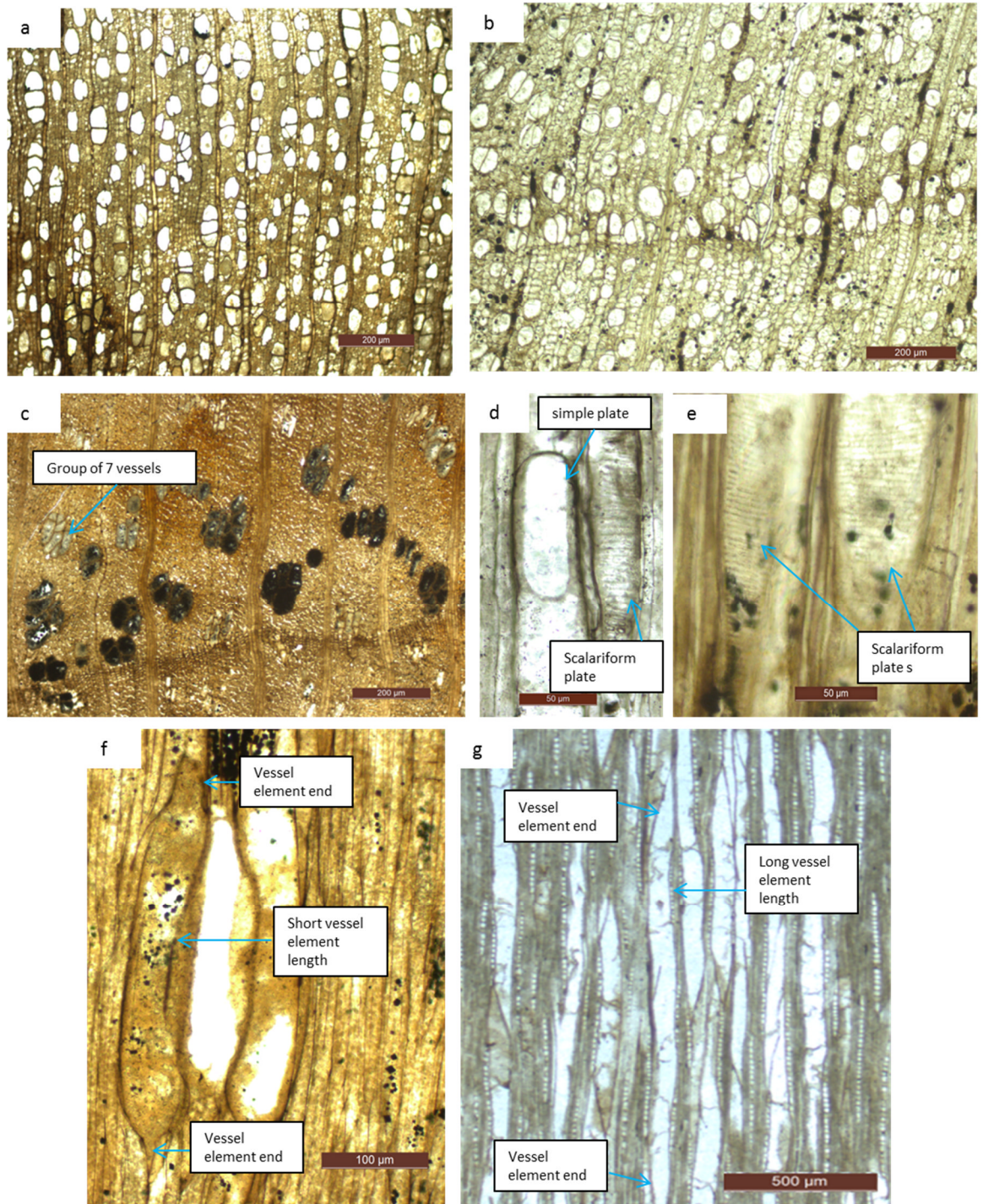


Figure 6. 4. Anatomical features related to climate. a) D9.027.1, TS presenting the highest vessel frequencies amongst the wood specimens here, scale bar = 200 μm . b) D9.020.1, TS showing predominantly solitary vessels, scale bar = 200 μm . c) D9.040.1, TS showing predominantly vessels in groups, scale bar = 200 μm . d) D9.012.1, RLS showing co-existing scalariform and simple perforation plates, scale bar = 50 μm . e) D9.020.1, RLS showing exclusively scalariform perforation plates, scale bar = 50 μm . f) D9.040.1, TLS short vessel length, scale bar = 100 μm . g) D9.096.1, TLS showing long vessel length, scale bar = 500 μm .

6.2.3 Palaeoclimate analysis using Nearest Living Relative (NLR)

Using the Nearest Living Relative (NLR) approach to reconstruct past climate conditions assumes that fossil flora had the same climate tolerances as their modern relatives (Mosbrugger and Utescher, 1997).

Based on this assumption Mosbrugger and Utescher (1997) developed Coexistence Analysis, which uses the NLRs of a fossil floral assemblage (fossil wood, leaves and pollen) to reconstruct past climate variables in a quantitative and systematic way. In this approach the tolerance ranges for each NLR for a given climate variable (e.g. MAT) are plotted against each other, and the range in which all of the NLRs coexist is the likely range for the fossil flora assemblage (see Figure 6.5 for an example).

In order for the Coexistence Analysis to give the most accurate range for past climate parameters the identification of the fossil flora with its NLR has to be correct; the more precise the identification of NLR (e.g. to species level), and the higher the number of NLRs present, the more accurate the climate range output will be. It also has to be considered that Coexistence Analysis was developed for relatively young fossil plant assemblages (e.g. Miocene) with plant types that have relatives that are probably still living today. To apply this technique to Paleocene plant assemblages is less robust because the climate tolerances of plants growing under higher CO₂ levels than during the late Cenozoic may mean that their climate tolerances may have been somewhat different.

In terms of climate controls on modern plant distribution, previous studies have found that minimum temperatures and the cold tolerance/frost resistance of a plants are important (Sakai and Wardle, 1978; Sakai *et al.*, 1981). Frost tolerance is measured as the minimum temperature that a plant can withstand before 50% of its leaves or shoots are damaged by frost (Bannister and Neuner, 2001; Bannister and Lord, 2006).

Previous studies have found that with increasing temperature-related gradients such as latitude, altitude and distance from the sea, the cold tolerance of plants increases. Studies over wide latitudinal scales in the

Southern Hemisphere have found that plants living in South Africa have on average a lower frost tolerance (mean frost tolerance -4°C) than plants growing at higher latitudes in South America where mean annual temperatures (MATs) and cold month mean temperature (CMMT) are cooler (mean frost tolerance -8°C) (Bannister and Lord, 2006). Sakai and Wardle (1978) found that the frost tolerance of plants in New Zealand correlated well with their latitudinal and altitudinal distribution. For instance, trees such as *Agathis australis* and *Nothofagus fusca*, which are found on North Island in low to mid montane environments where climates are warm temperate (MATs 15°C and coldest month daily minimum 7°C), have relatively low leaf frost tolerances (frost tolerance of -7°C , and -8°C). Trees that are found at high altitudes on South Island (MAT is 12°C and coldest month daily minimum is -4°C) such as *Phyllocladus alpinus* have a high frost resistance of -20°C .

Recording the frost tolerance of NLRs here is useful for giving an estimation of how harsh winter frosts were on the Antarctic Peninsula during the Paleocene (although there is no evidence of frost, such as frost rings in the wood, in the fossil plant record).

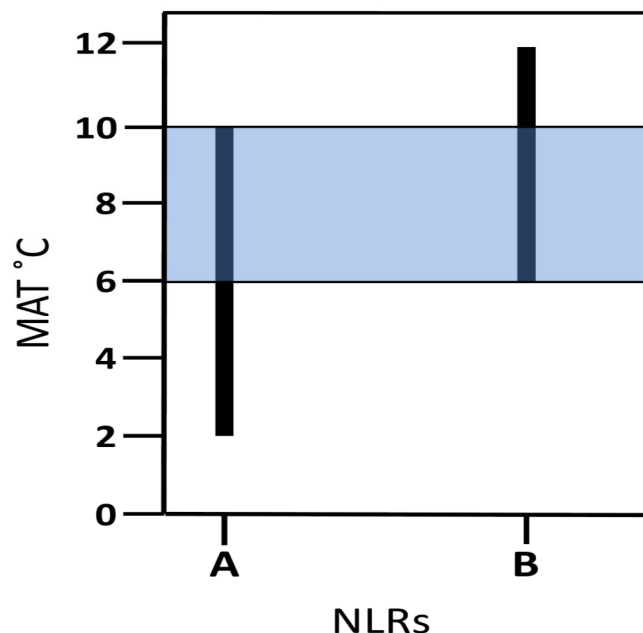


Figure 6. 5. An example of Coexistent Analysis. The graph shows the mean annual temperature (MAT) ranges for NLR's of fossil flora A and B. The interval in which the ranges coexist is shown by the blue box so this is the likely MAT range ($6 - 10^{\circ}\text{C}$) of the fossil floras. Figure modified from Mosbrugger and Utescher (1997).

6.2.4 Specific gravity of the conifers and angiosperms

Specific gravity is a measure of the density of the wood and can provide information about ecology and growth conditions in living trees. The method has been adapted for use on fossil wood and has been used in this project.

In this study the specific gravity of the fossil conifer and angiosperm woods were calculated in order to gain further insight into the ecology and life habit of the trees from which they were derived, as well as indicating the palaeoenvironment in which these trees grew on the Antarctic Peninsula during the Paleocene.

The specific gravity (SG) of modern wood is measured as the ratio of oven-dried weight of wood to the weight of water displaced by green (undried) wood (Wiemann and Williamson, 2002). The specific gravity of wood is closely related to wood density as both are determined by the proportion of wood that is made of cell tissue, except that wood density is measured as the mass of wood per unit volume (e.g. Kg. m^{-3}) (Swenson and Enquist, 2007; Williamson and Wiemann, 2010). Thus wood with thick cell walls has a high density and high SG (Hacke *et al.*, 2001; Chave *et al.*, 2009; Lens *et al.*, 2011). In conifers this relates to the ratio of tracheid wall thickness to lumen diameter (Hacke *et al.*, 2001; Chave *et al.*, 2009). In angiosperms wood density is determined by the size and frequency of vessels, as well as fibre frequency and wall thickness.

Wood density is considered to be related to woody plant traits and functions. These include mechanical strength, hydraulic efficiency, resistance to air embolism (air bubbles) caused by freezing or drought conditions; growth rate; life span/mortality; shade tolerance and also leaf traits. (leaf size, density and deciduousness) (Chave *et al.*, 2009; Zhang *et al.*, 2013). Within woody plants there is a trade-off between some of these traits. For example, to reduce the risk of air embolism some plants build thicker cell walls, and thus have a relatively high wood density/specific gravity. Having more mechanically strong wood means less risk of cell implosion or distortion caused by negative pressures resulting from trapped air (Hacke *et al.*, 2001; Lens *et al.*, 2011).

Trees that have a higher density of wood have also been linked to a longer life span but building more high density wood comes at a cost to the plant, such as a slower growth rate and being less hydraulically efficient, which has also been linked to the plant having smaller leaves and less photosynthetic capacity (Chave *et al.*, 2009; Lens *et al.*, 2011). High density wood is found in trees that are shade tolerant and grow in environments that are prone to drought or freezing conditions, and grow in nutrient poor soils (Pittermann *et al.*, 2006; Chave *et al.*, 2009; Poorter *et al.*, 2010).

In contrast, plants that have low density wood are more hydraulically-efficient and fast growing but they are more at risk of air embolism and have relatively shorter life spans (Chave *et al.*, 2009, Lens *et al.*, 2011). Shade intolerant and pioneer species usually have low wood density, as they are usually fast growing so that they can benefit from light gaps in the canopy. Trees that have low density also live in environments that have plenty of water and fertile soils (Hacke *et al.*, 2001; Wienmann and Williamson, 2002; Chave *et al.*, 2009; Pittermann *et al.*, 2006). Therefore wood density is an indicator of the ecological requirements of a tree.

Specific gravity/ wood density and climate parameters (e.g. Mean Annual Temperature MAT and mean annual Precipitation MAP) have been studied across latitudinal and altitudinal gradients (Wiemann and Williamson, 2002; Swenson and Enquist, 2007). Both studies found that values of SG values in forest stands increased with increasing MAT. Wiemann & Williamson (2002) found that mean specific gravity increased by 0.0049 per °C. In this study they also found that there was a weak negative trend between specific gravity and MAP. However, Swenson and Enquist (2007) did not find any trend between wood density and MAP. Both studies found that wood from tropical zones have a wider and more extreme range of wood density/specific gravities than from temperate zones, perhaps due to diversity (Swenson and Enquist, 2007).

Also, trees that grow in tropical environments are not as constrained by limiting climate factors, such as temperature and precipitation, but instead competition between other plants is more important, therefore plants will develop different and diverse ways of competing with each other, whereas in temperate zones trees are more limited by climate conditions (e.g.

temperature or precipitation) which results in a limited range in specific gravity (Swenson and Enquist, 2007).

Since wood specific gravity has been shown to be an indicator of modern plant ecology and the climates that they grow in, methods have been developed to try and calculate specific gravity of fossil wood. Wheeler *et al.* (2007a) developed a method of estimating the specific gravity of fossil wood mathematically by calculating the percentage occupied by cell walls in fossil wood. This is done by placing a point grid (e.g. 100 points) over a transverse image of the wood using image J software (<https://imagej.nih.gov/ij/>) (see Figure 6.6) and counting the points that are on the cell wall. This percentage is then multiplied by 1.05 which is the specific gravity of the swollen cell wall substance of all woods. This is done because it is assumed that during the permineralisation process wood is usually saturated with water.

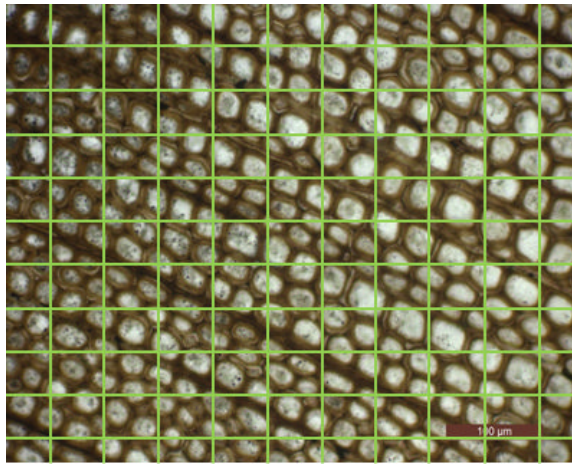


Figure 6. 6. An example of how specific gravity is measured in fossil wood using the method developed by Wheeler *et al.* (2007a). A grid is placed over a photograph of the fossil wood and the number of points that fall on a cell wall are counted.

6.3 Methods used in this project

6.3.1 Growth ring analysis

In this project growth ring series were measured on 30 specimens of fossil wood from Antarctica. From these data mean growth ring width (MGRW) was calculated for each specimen in order to give an indication of overall climate change through the stratigraphic section. Mean sensitivity (MS) was also calculated for each wood specimen.

$$MS = \frac{1}{n-1} \sum_{t=1}^{t=n-1} \left| \frac{2(x_{t+1} - x_t)}{x_{t+1} + x_t} \right|$$

Equation for mean sensitivity. (X = ring width, t = year number of the ring, n = the number of rings in the sequence).

This is an indication of variation in growth from one growing season to the next (Fritts, 1976). Values greater than 0.3 indicate growth under a fluctuating climate (sensitive growth), and values below indicate growth under an equable climate (complacent growth). Falcon-Lang (2005b) has shown a relationship between climate and growth in conifers, with higher values of mean sensitivity found in trees living under cold cold/dry climates (Figure 6.7). Trees that grow in areas prone to disturbances also have high mean sensitivity values. The relationship between MS and climate for angiosperm wood is much weaker, resulting in a large range in values under different climatic conditions (Figure 6.8).

The fossil wood specimens in this project occur as isolated fragments and so it was necessary to assess the origin of the fossil specimen from within a tree (branch, trunk etc). The likely origin of each wood specimen within a tree was estimated by looking at the distinctiveness and curvature of the growth rings (e.g. wood with rings of a small radius of curvature was considered as originating from a small branch or young stem, as opposed to wood with rings of a large radius of curvature that most likely came from a large trunk).

As mentioned in the introduction, a tree's response to climate can differ depending on site and ecology. The field record of the exact location of the fossil wood specimens on the stratigraphic section allows for a better refined interpretation of climate signals from the wood because the palaeoenvironment could be assessed (although this is more closely related to depositional environment than direct growth environment). Sedimentary information has also been taken into account when considering the individual fossil wood specimens because the nearest living relatives (NLR) can help understand the importance of limiting factors to growth such as climate can change with elevation. Nearest living relatives and their ecologies have also been taken into account.

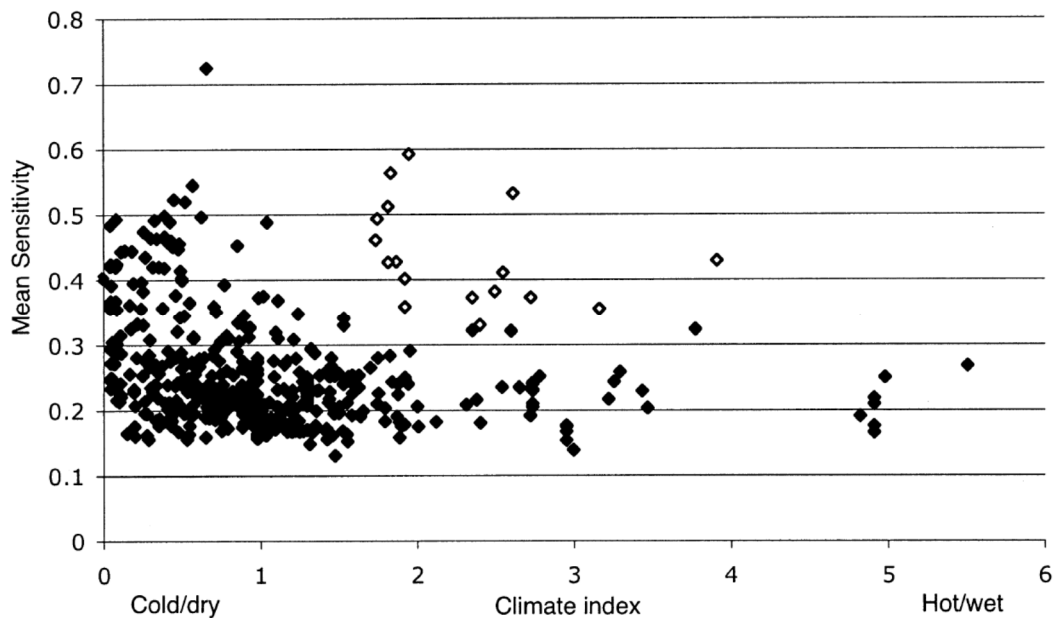


Figure 6. 7. The relationships between conifer mean sensitivity (MS) and climate from a global data. Open diamonds represent conifers that grew in flood disturbed areas such as streamside settings. Taken from Falcon-Lang (2005b).

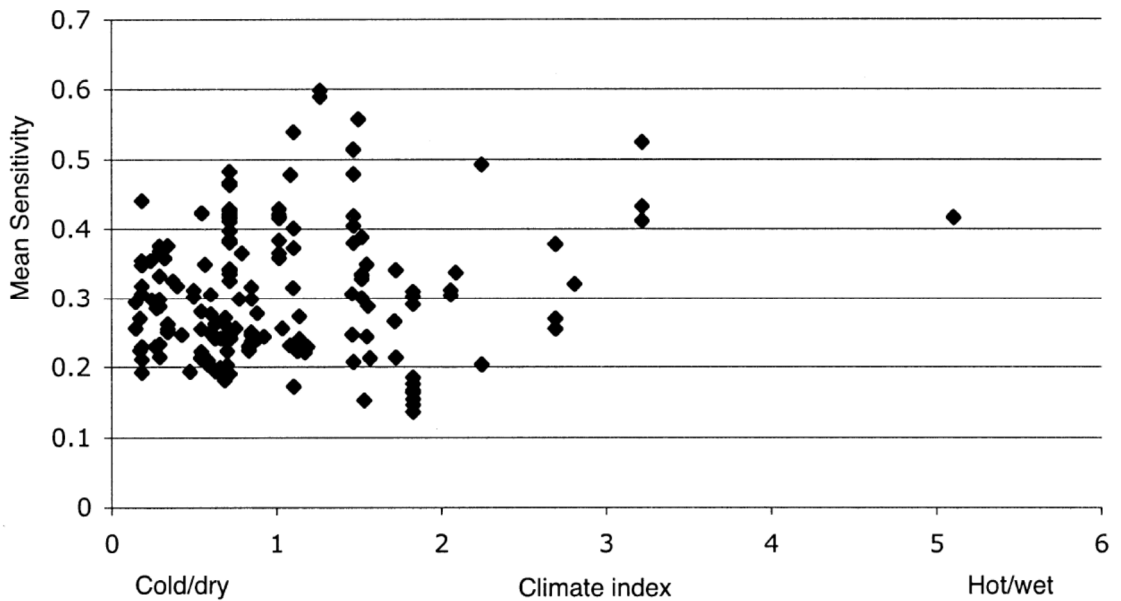


Figure 6. 8. The relationship between angiosperm mean sensitivity (MS) and climate from a global dataset. Taken from Falcon-Lang (2005b).

6.3.2 Palaeoclimate information from fossil angiosperm woods

In this project the incidence of climate-related anatomical features was recorded in the angiosperm wood specimens that were well preserved enough for the features to be observed. These are:

- Ring porosity (ring porous, semi-ring porous, diffuse porous)
- Perforation type (exclusively simple, scalariform and simple, or exclusively scalariform)
- Vessel Group Index; average vessel diameter (μm) (<50, 50 - 100 and >100)
- Average vessel frequency (mm^2) (<5, 5 – 20, 20 – 40, 40 – 100 and >100)
- Average vessel element length (μm) (<350, 350 – 800 and >850)

The quantitative measurements were carried out following the procedures advised by the IAWA Committee (1989) (see Chapter 4). The different size categories used for vessel diameter, vessel density and vessel element length were taken from Wheeler *et al.* (2007b), to make it easier to compare with

their records. The Vessel Group Index was calculated from counting 25 random groups of vessels across the transverse thin section.

In this project Vulnerability Index (VI) and Mesomorphy Index (MI) were calculated from the fossil angiosperm wood as indicators of water availability for angiosperm trees living on the Antarctic Peninsula during the Paleocene.

Fifty vessel diameter (tangential diameter) measurements were taken for each wood specimen. Twenty-five measurements were taken for vessel frequency per mm² and vessel element length per wood specimen. The data are presented in (Appendix B.2) and the mean values are presented in Table 6.4.

To overcome the bias that could result from making quantitative measurements of vessel variables in different wood organs (e.g. branch, trunk), the likely origin of the wood specimens within a tree were determined by looking at the distinctiveness and curvature of the growth rings.

6.3.3 Palaeoclimate analysis using Nearest Living Relative

6.3.3.1 Coexistence Analysis

In this study Coexistence Analysis was carried out using the NLRs of the wood specimens and palynomorphs identified in this project in order to reconstruct the likely climate conditions for the Antarctic Peninsula during the Paleocene.

The climate variables that were analysed are mean annual temperature (MAT), cold month mean temperature (CMMT), warm month mean temperature (WMMT), mean annual precipitation (MAP), mean precipitation of the driest month (MPDM) and mean precipitation of the wettest month (MPWM).

Climate data were obtained from the Palaeoflora database (<http://www.geologie.unibonn.de/Palaeoflora>; T. Utescher 2014, pers. comm., 2 January; T. Utescher 2015, pers. comm., 27 July), and the Atlas of Living Australia (ALA, <http://www.ala.org.au>). Mean annual precipitation tolerance for *Lagarostrobos franklinii* was taken from Gibson *et al.* (1991a).

The Palaeoflora database is an online resource that provides NLR climate tolerances for Cenozoic plant taxa. The identification of the fossil flora NLRs were gathered from scientific literature. The climate tolerances of the NLRs were gathered from climate station data or from Worldclim (<http://www.worldclim.org>, after Hijmans *et al.*, 2005). Worldclim is an online climate database that uses existing climate data from global climate stations to create interpolated climate grids, which have a resolution of 1 km². The interpolations were developed using algorithm software packages that account for the effects of variables such as elevation, latitude and longitude on climate parameters (Hijmans *et al.*, 2005). It uses monthly average climate data and the climate records used are from 1950 – 2000.

The Atlas of Living Australia (ALA) is an online resource that includes information on the distribution of modern species and climate data for mainly Australia and surrounding islands, but it also includes data from other parts of the world such as Africa, New Zealand and also South America. The data used by the ALA is obtained from a number of resources including literature, field observations and online resources such as Worldclim and GBIF (biodiversity database). In this study only Worldclim data was collected from ALA because it has the most comprehensive dataset out of the sources that were available.

The majority of NLRs for the fossil wood morphotypes are confined to the Southern Hemisphere. However, for taxa that are found in both hemispheres, such as the family Cupressaceae, only the climate data for Southern Hemisphere taxa were included. Most of the NLRs of the fossil flora here are only known at genus or family level.

The data for the climate variable MAT were mostly obtained from the Atlas of Living Australia. Mean precipitation dry month and mean precipitation wet month data for *Lagarostrobos franklinii* was collected from Atlas of Living Australia. The climate data for CMMT, WMMT, MAP, MPDM and MPWM was exclusively obtained from the Palaeoflora database because these variables were not available from the Atlas of Living Australia. Some of the climate parameter data for nine NLRs (see Table 6.6) could not be obtained due to

the dataset being incomplete or the data was not available from the above sources. This will be further discussed in the result section (6.4.3.1).

Araucaria araucana has been chosen as the likely NLR of the fossil wood type *Agathoxylon* and the pollen type *Araucariacites australis*. The interpretation is based on the interpretation by Bowman *et al.* (2014) who suggested that the *Araucariacites australis* pollen grain was most taxonomically similar to *Araucaria araucana*. Not all of the climate variables could be obtained for *Araucaria araucana*, so instead the climate range for genus *Araucaria* was used.

The results for Coexistence Analysis for the NLR identified here are presented in section 6.4.5.1 in the form of a table (Table 6.6), which includes all the values for the different climate variables for each NLR, and the sources from where the climate data was obtained. The NLR tolerance ranges for each climate variable are also illustrated as graphs (Figures 6.22 to 6.27).

6.3.3.2 Frost tolerance of NLRs growing on the Antarctic Peninsula

In order to investigate how harsh the minimum temperatures and the severity of frost may have been like on the Antarctic Peninsula during the Paleocene, the frost tolerances of the NLRs were obtained from a number of sources: Sakai and Wardle (1978), Sakai *et al.*, (1981), Bannister and Neuner (2001), Bannister and Lord (2006). The data were only obtained for taxa that lived under similar climates to the ones inferred by the Coexistence Analysis, which will be discussed in more detail in section 6.4.3.2. The data are presented in Table 6.8 and Figure 6.29.

6.3.4 Specific gravity of the conifers and angiosperms

The method developed by Wheeler *et al.* (2007a) was used. A 100 point grid was placed over a transverse image of the wood specimens using Image J, in order to calculate the cell wall percentage (Figure 6.6). This was done 7 times for each wood specimen. From this a mean specific gravity value was calculated. Only the best preserved wood specimens were used, which had

no signs of compression, had intact cell walls and clear cell wall and lumen boundaries.

The value ranges that distinguish between low, medium and high specific gravity are in accordance with IAWA Committee (1989): low specific gravity is 0.40 and below, medium specific gravity is between 0.40 – 0.75 and high specific gravity is >0.75 .

The results from the specific gravity analysis are presented in the section 6.4.4, Tables 6.9. Figure 6.31 presents the variation of specific gravity between each morphotype and between individual wood specimens within them. The SG of individual wood specimens was plotted against the stratigraphic section of Seymour Island (Figure 6.32), in order to see if there was a trend from the K/Pg boundary to the Late Paleocene.

6.4 Results

6.4.1 Growth ring analysis

The number of wood specimens from which growth ring data could be derived varies throughout the stratigraphic section. Wood specimens are abundant in the López de Bertodano Formation ($n = 15$) and the lower and middle parts of the Sobral Formation (between 150 and 200m on the stratigraphic section) ($n = 12$). Wood specimens are sparse at the top of the Sobral Formation ($n = 3$) and in the Cross Valley Formation ($n = 2$).

Growth rings are visible on all of the wood specimens. The number of growth rings in a series ranges from 3 – 110 rings (Table 6.1). The quality of preservation varied within seven wood specimens and growth rings measurements had to be missed out in areas of poor preservation. Wood that is poorly preserved has undergone compression or a large area of cells are ruptured.

Mean growth ring width (MGRW) and Mean Sensitivity (MS) results for the 30 wood specimens are presented in Table 6.1 and Figures 6.10 to 6.18. The results for MGRW and MS are described separately in sections 6.4.1.1 and 6.4.1.2. Individual ring measurements for each wood specimen are presented in the Appendix C.1.

False rings are present in wood specimens D9.059.1, D9.050.1, D9.022.1 and D9.092.1 (Table 6.2 and Figure 6.9). Three of the wood specimens that have false rings are of *Agathoxylon* wood type, and one of *Phyllocladoxylon* type (D9.092.1). Ten false rings are present in wood specimen D9.059.1 (*Agathoxylon*). The false rings present in all of the specimens mostly occur in the early wood, which suggests that they formed in spring as a result of problems with water supply during the spring (see Table 6.2).

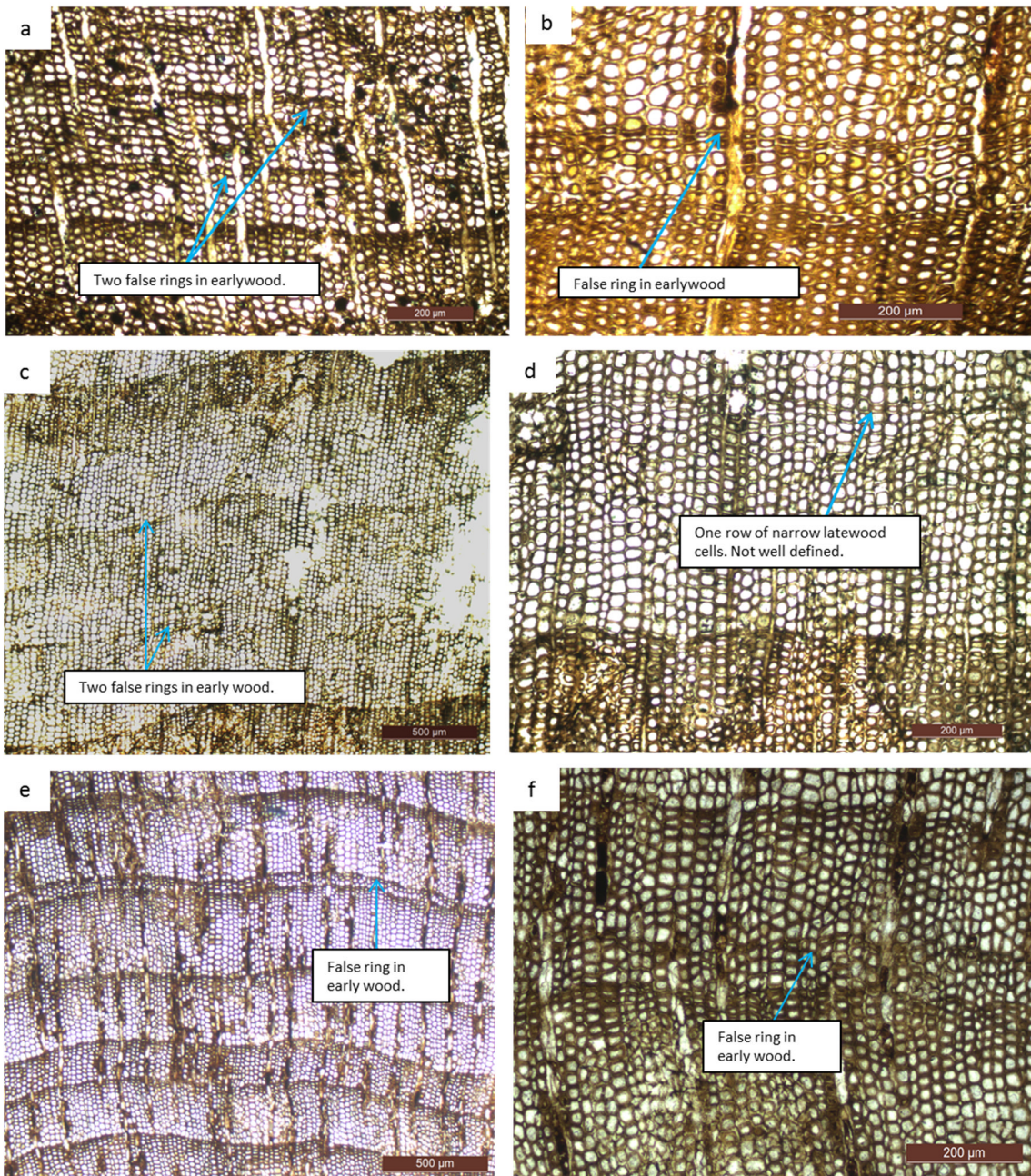


Figure 6. 9. Wood specimens with false rings. a) D9.022.1, scale bar = 200µm. b) D9.050.1, scale bar = 200 µm. c) D9.092.1, scale bar = 500 µm. d) magnification of the first false ring in photo c, scale bar = 200 µm. e) D9.059.1, scale bar = 500 µm. f) D9.059.1, scale bar = 200 µm.

Table 6. 1. Mean growth ring width (MGRW), mean sensitivity (MS) and standard deviation for 30 fossil wood specimens identified in this project. Tree numbers and wood types are also given. Wood type include angiosperm (A) or conifer (C).

Tree number	Wood Type (A or C)	Morphotype	Number of growth rings	Ring width minimum (mm)	Ring width maximum (mm)	Mean ring width (mm)	Standard deviation	Mean Sensitivity	Complacent or sensitive growth (C or S)
2	A	<i>Nothofagoxylon</i>	5	3.26	6.7	4.69	1.19	0.32	S
3	A	<i>Nothofagoxylon</i>	7	3.2	7.9	5.84	1.41	0.37	S
5	C	<i>Nothofagoxylon</i>	18	1.24	5.05	1.97	0.95	0.34	S
8	C	<i>Podocarpoxyton/Cupresinoxylon</i>	59	0.22	2.5	0.63	0.37	0.2	C
9	A	<i>Myrceugenelloxylon</i>	12	0.5	3.44	2.11	0.82	0.41	S
11*	C	<i>Agathoxylon</i>	26	0.1	0.7	0.37	0.15	0.41	S
12	A	<i>Nothofagoxylon</i>	3	1.42	3.83	2.51	0.99	0.7	S
13	C	<i>Phyllocladoxylon</i>	13	0.98	1.8	1.38	0.28	0.25	C

Wood specimens with growth rings series that were interrupted due to poor preservation are shown with an *.

Table 6.1. continued

Tree number	Wood Type (A or C)	Morphotype	Number of growth rings	Ring width minimum (mm)	Ring width maximum (mm)	Mean ring width (mm)	Standard deviation	Mean Sensitivity	Complacent or sensitive growth (C or S)
14	C	<i>Phyllocladoxylon</i>	10	0.38	5.65	2.03	1.51	0.406	S
15	A	<i>Antarctoxylon</i>	6	0.35	4.87	2.4	1.6	0.489	S
19	C	<i>Agathoxylon</i>	55	0.12	0.53	0.28	0.11	0.4	S
20*	C	<i>Agathoxylon</i>	110	0.1	1.61	0.44	0.29	0.38	S
21	A	<i>Nothofagoxylon</i>	15	0.605	1.675	1.09	0.30	0.22	C
23	A	<i>Nothofagoxylon</i>	11	0.76	2.5	1.54	0.50	0.3	C
26*	C	<i>Phyllocladoxylon</i>	18	0.8	2.15	1.51	0.36	0.16	C
27	C	<i>Protophyllocladoxylon</i>	30	0.17	1.57	0.65	0.43	0.282	C

Table 6.1. continued

Tree number	Wood Type (A or C)	Morphotype	Number of growth rings	Ring width minimum (mm)	Ring width maximum (mm)	Mean ring width (mm)	Standard Deviation	Mean Sensitivity	Complacent or sensitive growth (C or S)
28	C	<i>Phyllocladoxylon</i>	26	0.77	2.3	1.34	0.35	0.19	C
30*	A	<i>Nothofagoxylon</i>	7	2.6	5.95	4.45	1.22	0.26	C
31	C	<i>Phyllocladoxylon</i>	42	0.28	2.18	1.16	0.44	0.28	C
33	C	<i>Podocarpoxylo</i> <i>n</i> / <i>Cupressinoxylo</i> <i>n</i>	25	1	4.08	2.43	0.9	0.23	C
34	A	<i>Weinmannioxylon</i>	10	1.6	2.8	1.97	0.32	0.17	C
35*	C	<i>Agathoxylon</i>	18	0.16	1.2	0.5	0.32	0.617	S
36	A	<i>Nothofagoxylon</i>	18	0.88	2.71	1.54	0.55	0.31	S
37	C	<i>Agathoxylon</i>	65	0.06	1.1	0.31	0.20	0.389	S

Table 6.1. continued

Tree number	Wood Type (A or C)	Morphotype	Number of growth rings	Ring width minimum (mm)	Ring width maximum (mm)	Mean ring width (mm)	Standard Deviation	Mean Sensitivity	Complacent or sensitive growth (C or S)
38	C	<i>Protophylocladoxylon</i>	44	0.34	1.7	0.91	0.37	0.31	S
45	C	<i>Agathoxylon</i>	31	0.1	1.5	0.79	0.36	0.57	S
46*	C	<i>Agathoxylon</i>	13	1.53	2.5	1.96	0.3	0.2	C
47*	C	<i>Agathoxylon</i>	22	0.25	2.4	0.91	0.54	0.7	S
50	C	<i>Protophylocladoxylon</i>	49	0.14	0.93	0.43	0.19	0.27	C
53*	C	<i>Protophylocladoxylon</i>	6	0.3	0.62	0.48	0.2	0.199	C

Table 6. 2. Fossil wood specimens with false rings. The number of false rings and where they occur within a ring are given.

Specimen number	Wood type	Number of false	Total number of rings	Where false rings occur (EW = Earlywood LW=Late wood)	Season in which false rings may have occurred
D9.022.1	<i>Agathoxylon</i>	2	26	EW /LW	Early spring/ late summer
D9.050.1	<i>Agathoxylon</i>	3	110	EW	Early spring
D9.059.1	<i>Agathoxylon</i>	10	55	EW to LW	Early spring -Late summer
D9.092.1	<i>Phyllocladoxylon</i>	2	18	EW	Early spring to mid spring

6.4.1.1 Mean growth ring width (MGRW)

Mean growth ring widths (MGRW) (Figure 6.10, Table 6.1 for individual wood specimens) show a wide range in values (0.28 – 5.84mm). The data is scattered, although there appears to be a trend towards narrower growth rings from the Early Paleocene into the Late Paleocene (Figures 6.10, 6.14). The widest range in values is found in the López de Bertodano Formation (0.28mm to 5.84mm) (Figure 6.10). MGRW values for wood specimens located in the lower to middle Sobral Formation also show a wide range of values between 0.31 – 4.45mm. However, the values are narrower in range compared to the López de Bertodano Formation. At the top of the Sobral Formation all the wood specimens are *Agathoxylon* type wood and their mean growth rings range in values from 0.79 – 1.96mm. The two *Protophyllocladoxylon* woods D9.153.1 and D9.181.1 (tree number 50 and 53 On Figure 6.10) from the Cross Valley Formation have narrow mean growth ring widths of 0.43mm and 0.48mm.

Figure 6.12 presents average MGRW for each morphotype and how it varies within each Formation. *Nothofagoxylon* and *Phyllocladoxylon* MGRW decreases from the López de Bertodano Formation to the lower to middle Sobral Formation. *Protophyllocladoxylon* MGRW decreases from the lower to middle part of the Sobral Formation into the Cross Valley Formation. The *Agathoxylon* and *Podocarpoxylon/Cupressinoxylon* woods show an opposite trend with an increase in MGRW from the López de Bertodano Formation to the lower to middle Sobral Formation. The MGRW trends seen for the individual form-genera are described in more detail below:

***Agathoxylon*:** *Agathoxylon* wood in the López de Bertodano Formation has growth rings that are less than 0.50 mm (0.28 mm – 0.44 mm) (Figure 6.10). In the lower to middle Sobral Formation the MGRW range slightly increases (0.37 – 0.5mm) and further increases to 0.79 to 1.96 mm in the upper Sobral Formation. Average MGRW for the López de Bertodano Formation and the lower to middle Sobral Formation is 0.36 mm and 0.40 mm (Figure 6.12), a difference of only 0.04 mm.). The difference between the lower to middle part of Sobral Formation and the upper Sobral Formation is larger (difference of 0.82mm).

Nothofagoxylon: *Nothofagoxylon* has the widest range in MGRW in the López de Bertodano Formation (1.09 – 5.84 mm) (Figure 6.10). The range then decreases to 1.54 – 4.45mm in the lower to middle Sobral Formation. The average MGRWs also show a decrease of 0.71mm in MGRW from the López de Bertodano Formation to the lower to middle Sobral Formation (Figure 6.12).

Phyllocladoxylon: The MGRW range for the López de Bertodano Formation is 1.38 – 2.03mm and then it decreases to 1.16 – 1.51mm in the lower to middle part of the Sobral Formation (Figure 6.10). Average MGRW between two formations for this morphotype 1.7mm and 1.33mm (Figure 6.12).

Protophyllocladoxylon: *Protophyllocladoxylon* wood specimens in the lower to middle Sobral have a narrow MGRW range of 0.65 to 0.91mm (Figure 6.10). The range in the Cross Valley Formation decreases to 0.43 – 0.48mm. Average MGRWs for the lower to middle part of Sobral Formation and the Cross Valley Formation is 0.78 and 0.45 so there is a small decrease of 0.33mm (Figure 6.12).

In terms of differences in MGRW values between wood types, in general the conifer wood specimens tend to have narrower growth rings than the angiosperm wood specimens (Figure 6.11). However, the total sample size is rather small and some angiosperm wood types are represented by only one specimen so it is difficult to make definitive conclusions about this.

The average mean growth ring width values for the López de Bertodano Formation, lower to middle part of Sobral Formation and the Cross Valley Formation are presented in Table 6.3 and Figures 6.13 and 6.14. Figures 6.13 and 6.14 show a decrease in MGRW from the Early Paleocene to the Late Paleocene. There is a decrease from 1.98 mm MGRW in the López de Bertodano Formation to 1.52 mm MGRW in the lower to middle Sobral Formation (150 – 200m). A further small decrease to 1.22 mm MGRW occurs in the upper part of the Sobral Formation, which further decreases to 0.45mm in the Cross Valley Formation. The significance of this is discussed in section 6.5.

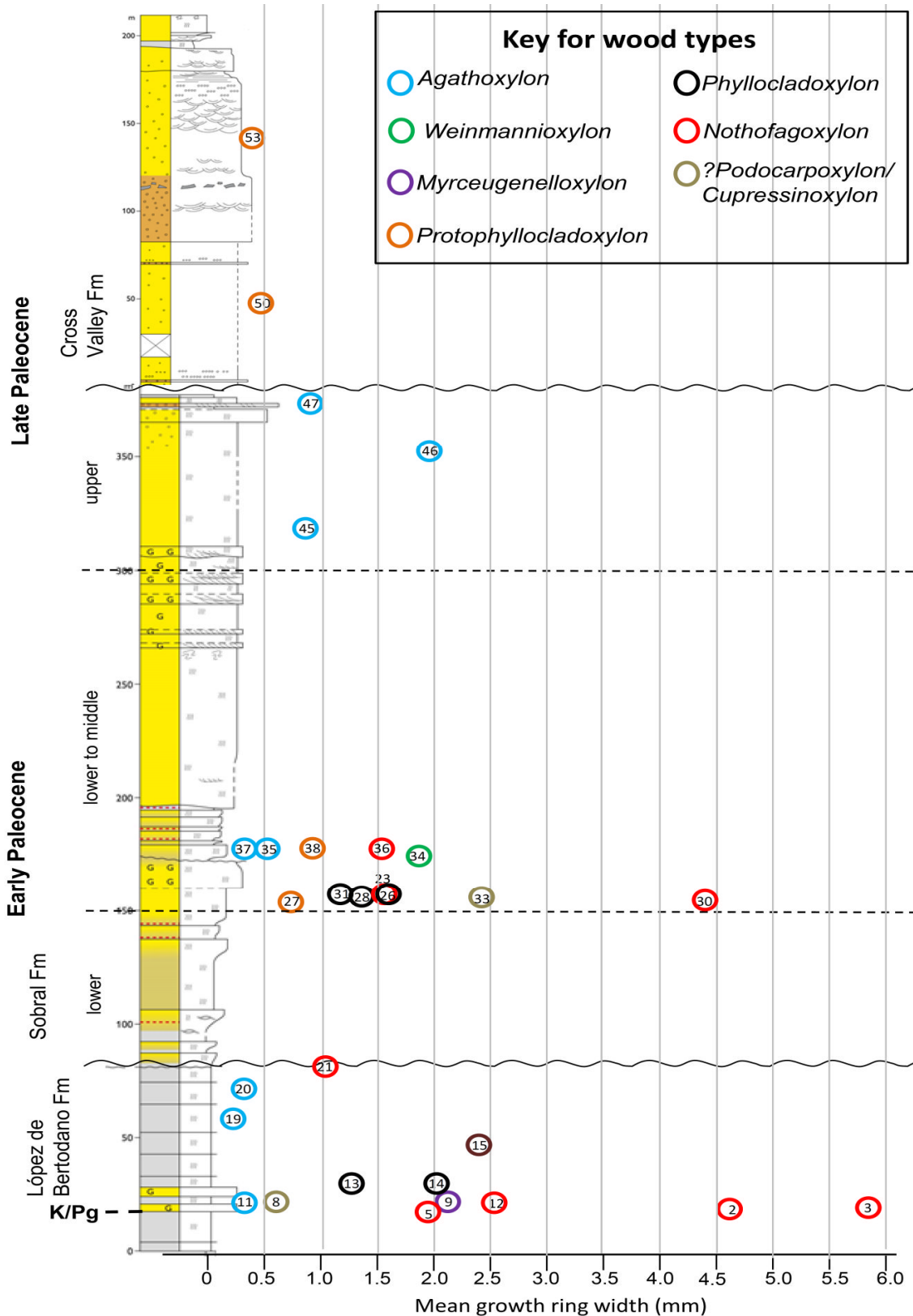


Figure 6. 10. A plot of mean growth ring values for individual wood specimens through the sedimentary sequence on Seymour Island. Stratigraphic log courtesy of Jon Ineson.

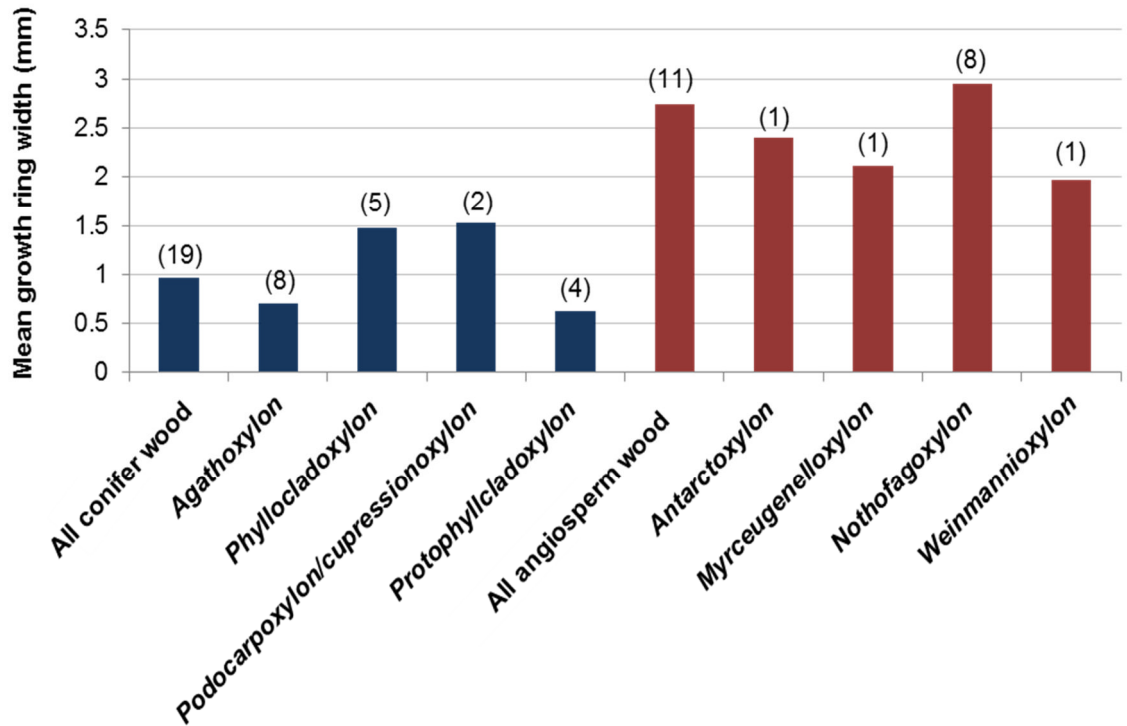


Figure 6. 11. Mean growth ring width of all conifer wood specimens, all angiosperm wood specimens and each genus separately presented in the form of a bar chart. Conifer genera are in blue and angiosperm form genera are in red. The numbers in brackets above each bar are the number of wood specimens within each genus.

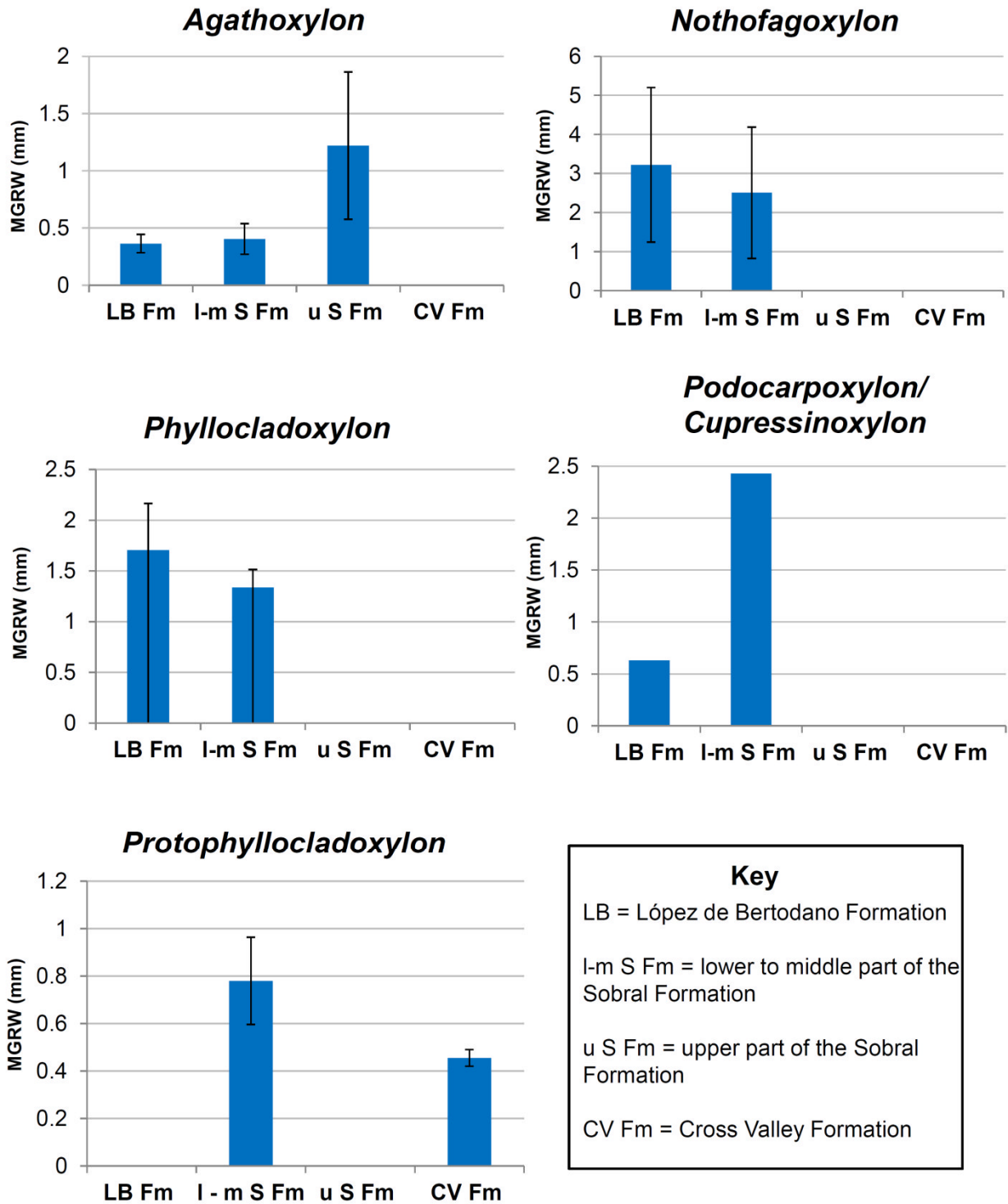


Figure 6. 12. Individual bar charts presenting the MGRW in each formation of the sedimentary sequence for each genus. Formations are along the x axis and MGRW is along the y axis. LB = López de Bertodano Formation I – m S FM = lower to middle part of the Sobral Formation U S Fm = upper part of the Sobral Formation CV Fm = Cross Valley Formation. Standard deviation is shown by the black lines.

Table 6. 3. Average MGRW for each formation

Formation	MGRW mm	Standard deviation
López de Bertodano Formation	1.98	1.67
lower to middle part of the Sobral Formation	1.52	1.1
upper part of the Sobral Formation	1.22	0.64
Cross Valley Formation	0.45	0.03

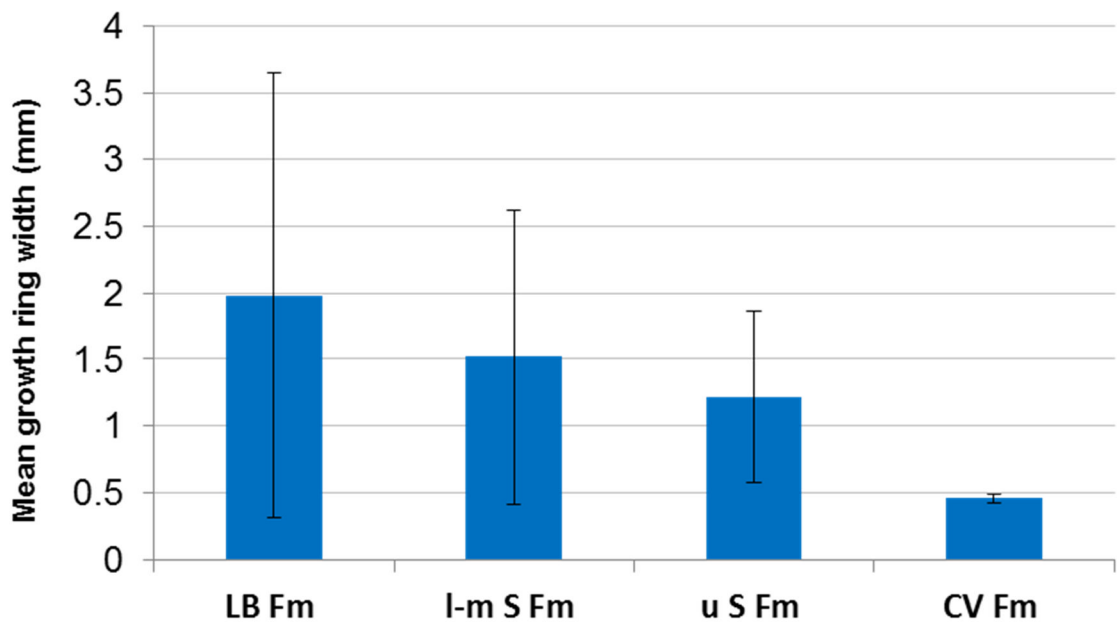


Figure 6. 13. A bar chart of mean growth ring width taken from the wood specimens in the López de Bertodano (wood specimens = 14), lower to middle Sobral Formation (wood specimens = 12), upper Sobral Formation (wood specimens = 3) and Cross Valley Formation (wood specimens = 2). Black lines represent standard deviation.

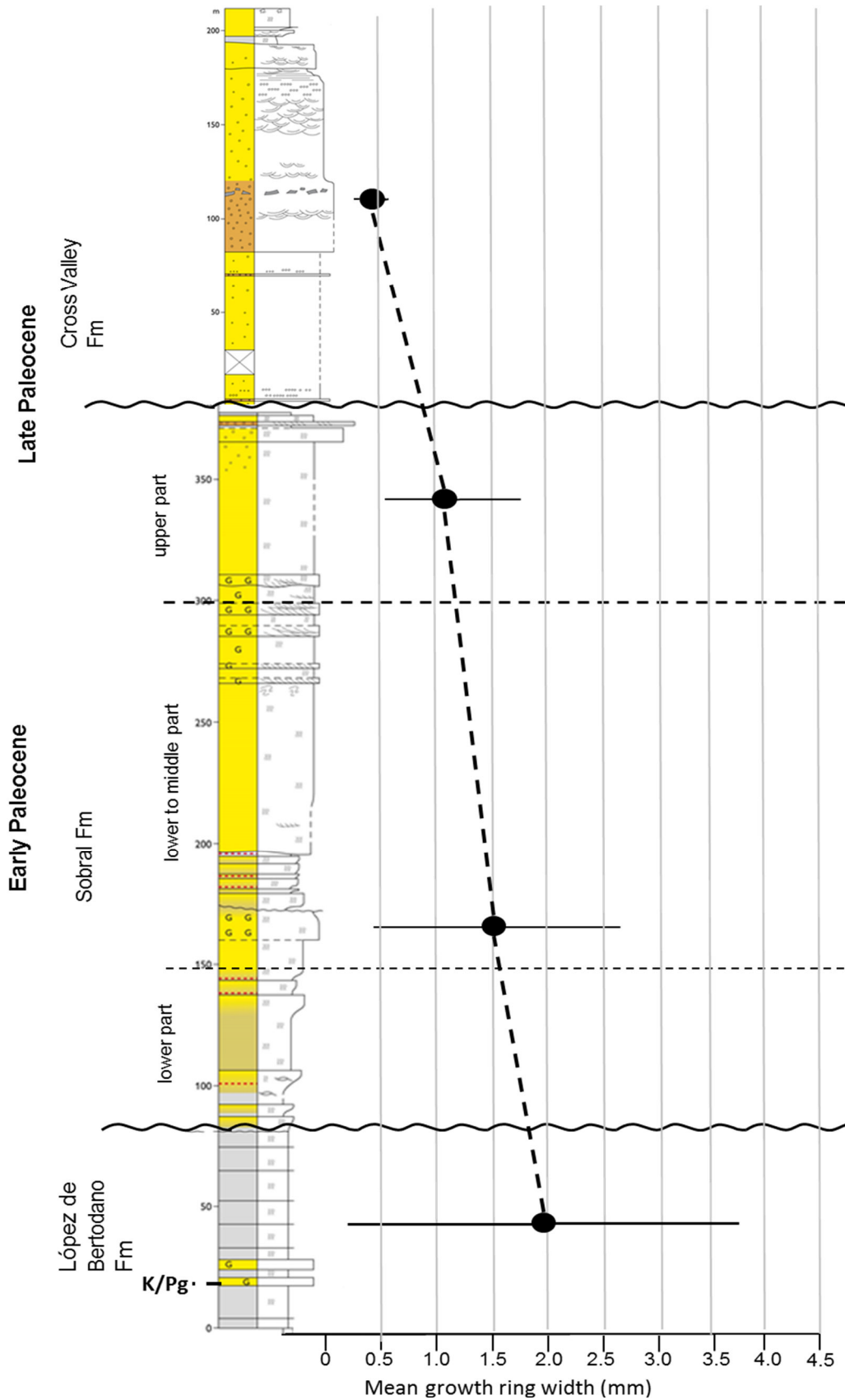


Figure 6. 14. A summation mean growth ring width taken from the wood specimens in the López de Bertodano Formation (wood specimens = 13), lower to middle Sobral Formation (wood specimens = 12), upper Sobral Formation (wood specimens = 3) and Cross Valley (wood specimens = 2). Log courtesy of Jon Ineson. The circles are located at the horizon where most of the wood specimens are present. The horizontal line on each data point represents the standard deviation.

6.4.1.2 Mean Sensitivity (MS)

MS values for individual wood specimens are plotted against the stratigraphic section (Figure 6.15) (Table 6.1). Values range from 0.20 to 0.7 and there are approximately an equal number of wood specimens that show complacent growth (n = 14) and sensitive growth (n = 16). There is no distinct trend of MS values through the stratigraphic section. Figure 6.16 presents the frequency of complacent and sensitive growth for each formation and it shows that sensitive and complacent growth fluctuated throughout the Paleocene. The majority of wood specimens in the López de Bertodano Formation show sensitive growth (76 %). There is a change in the lower to middle Sobral Formation with the majority of wood specimens showing complacent growth (75%). A return to a high frequency of sensitive growth in the upper Sobral Formation is observed. The two wood specimens in the Cross Valley Formation show complacent growth. Figure 6.17, which presents average MS for each formation shows the same variation in MS as Figure 6.15. The upper part of the Sobral Formation has the highest MS (0.5) and the Cross Valley has the lowest (0.23).

In the López de Bertodano Formation most the wood specimens show sensitive growth have values between 0.32 and 0.7 (Figure 6.15). Four wood specimens show complacent growth and their values range from 0.20 – 0.25. The trees located in the lower to middle part of the Sobral Formation (150 m and 200 m) have complacent MS values that range from 0.16 – 0.28; and the four wood specimens that show sensitive growth have values between 0.31 and 0.61. Two of the *Agathoxylon* wood specimens (D9.139.1 and D9.168.1) at the top of the Sobral Formation show sensitive growth and have values of 0.36 and 0.54. In the Cross Valley Formation, two *Protophylocladoxylon* have MS values between 0.10 and 0.27. Specimens D9.092.1 (*Phyllocladoxylon*) and D9.054.1 (*Nothofagoxylon*) show the lowest values (0.16) of MS. Specimens D9.023.1 and D9.168.1 show the highest values of MS (0.7).

Figure 6.18 presents the frequency of complacent growth vs sensitive growth for each morphotype to examine whether the MS values are linked to tree type. The majority of *Agathoxylon* woods show sensitive growth (87%) and values have a wide range from 0.36 – 0.7. *Nothofagoxylon* wood specimens

also show sensitive growth (62.5%), and values range from 0.3 – 0.4. Most of the *Phyllocladoxylon* and *Protophylocladoxylon* woods show complacent growth (80% and 75% retrospectively). *Phyllocladoxylon* and *Protophylocladoxylon* wood specimens that show complacent growth have values that range from 0.16 – 0.28 and 0.20 – 0.28. Both specimens of *Podocarpoxyton/Cupressinoxyton* show complacent growth (0.2 – 0.23). *Antarctoxyton* and *Myceugenelloxyton* wood specimens complacent growth (0.2 – 0.23). *Antarctoxyton* and *Myceugenelloxyton* wood specimens show sensitive growth (0.49 and 0.41 retrospectively). The *Weinmannioxyton* wood specimen shows complacent growth (0.17).

Figures 6.15 and 6.18 demonstrate that the mean sensitive values are not biased towards specific tree types, which is what would be expected if MS is a measure of sensitivity of the growth to climate.

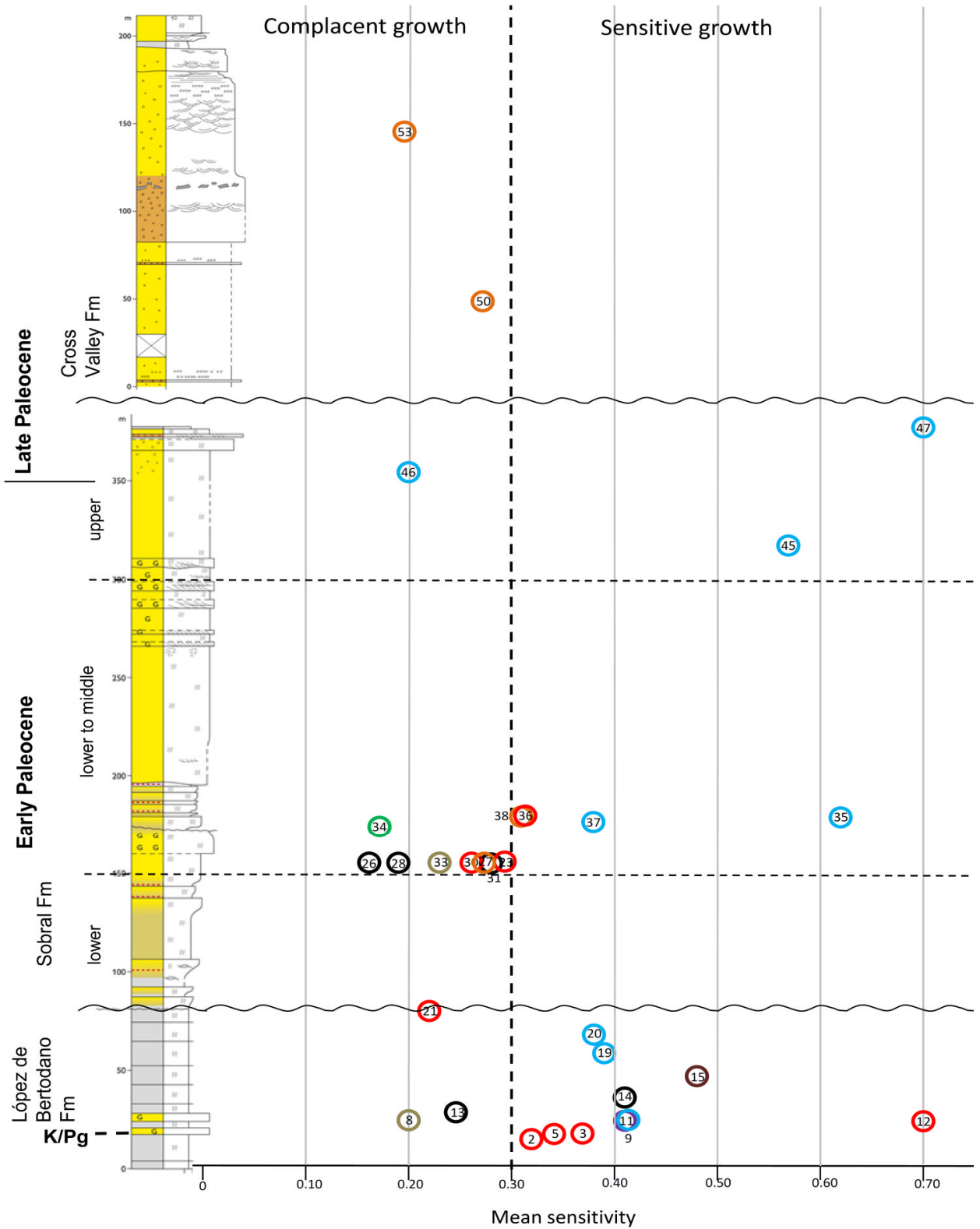


Figure 6. 15. A plot of mean sensitivity data against the stratigraphic section on Seymour Island. The numbers inside the coloured rings indicate the tree number. Sedimentary log courtesy of Jon Ineson.

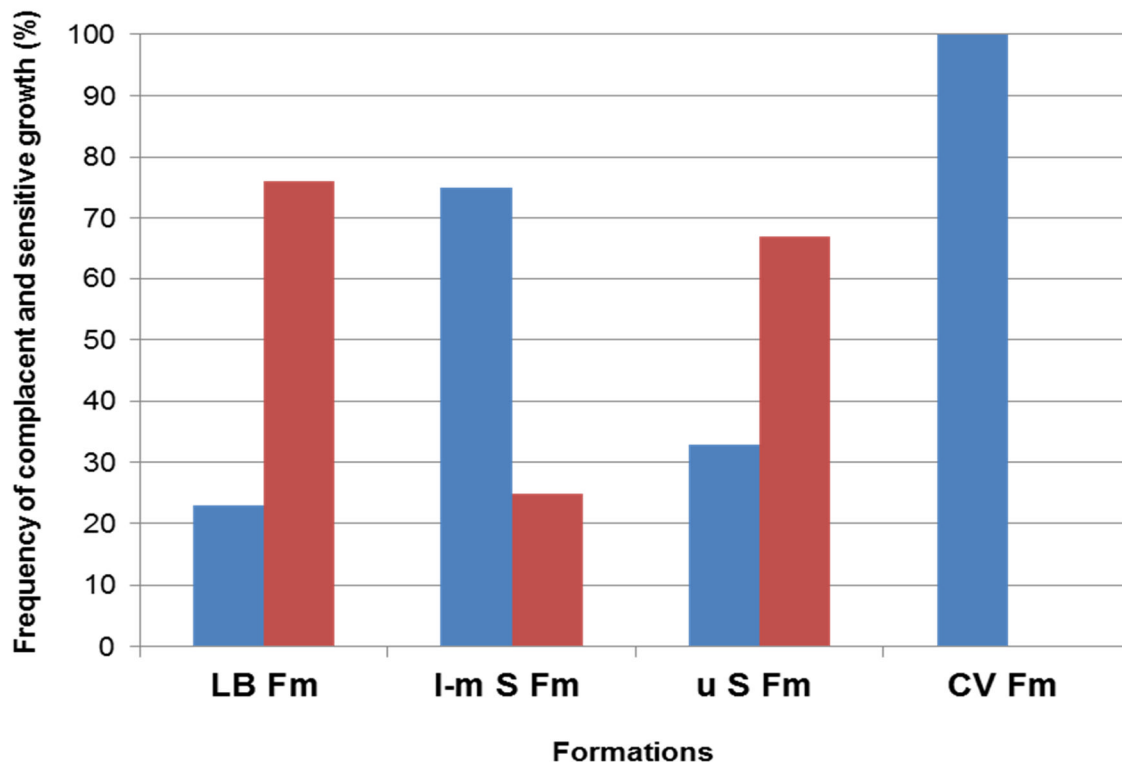


Figure 6. 16. Frequency (%) of wood specimens showing complacent and sensitive growth for each formation in the sedimentary sequence on Seymour Island. LB = López de Bertodano Fm, I–m S Fm = lower to middle part of the Sobral Formation, U S Fm = upper part of the Sobral Formation, CV Fm = Cross Valley Formation. Blue bars = complacent growth and red bars = sensitive growth.

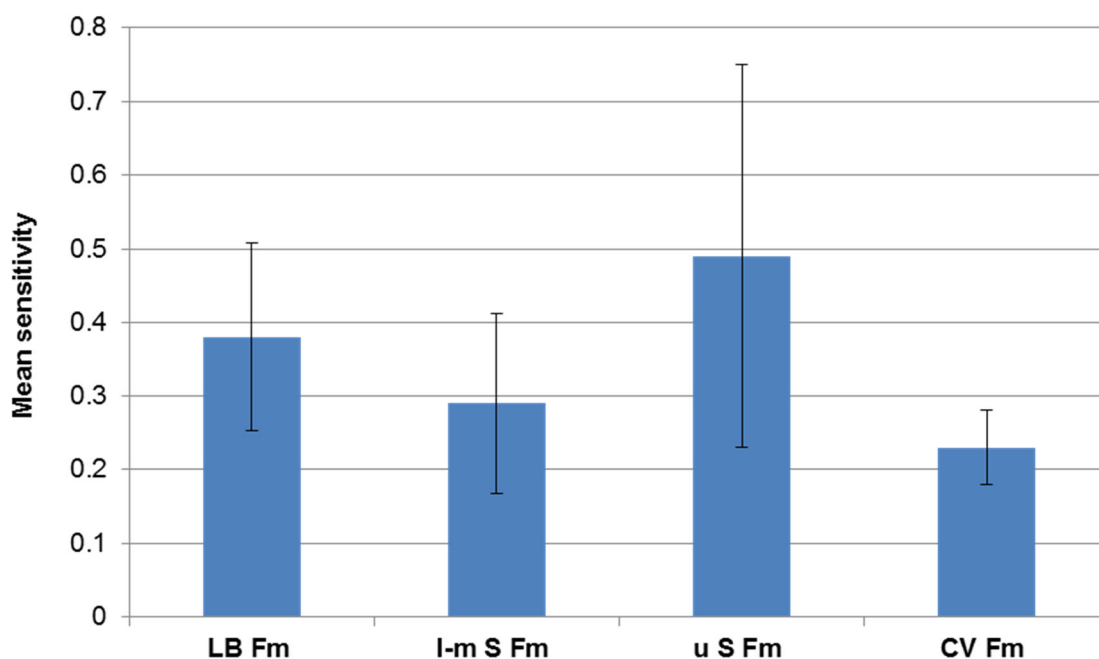


Figure 6. 17. Average mean sensitivity for all the wood specimens within each formation on the sedimentary sequence of Seymour Island. LB = López de Bertodano Fm, I–m S Fm = lower to middle part of the Sobral Formation, U S Fm = upper part of the Sobral Formation, CV Fm = Cross Valley Formation. Blue bars = complacent growth and red bars = sensitive growth.

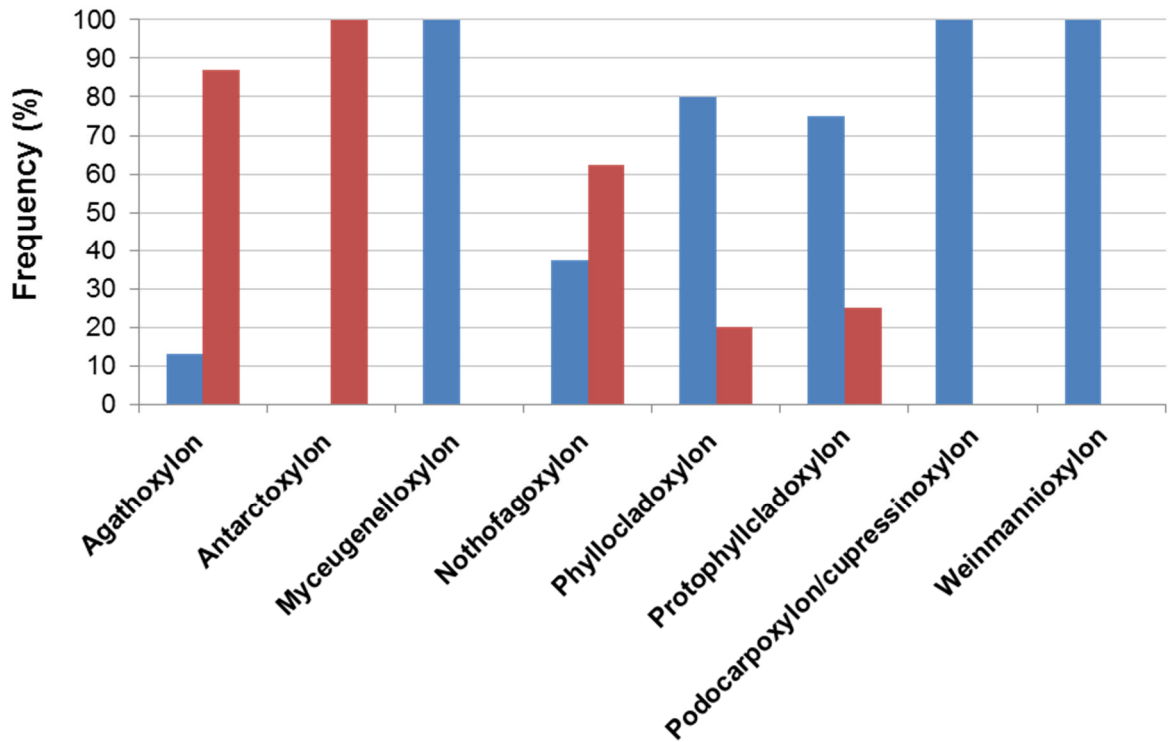


Figure 6. 18. The frequency (%) of wood specimens within each morphotype showing complacent or sensitive growth. Blue bars = complacent growth and red bars = sensitive growth.

6.4.2 Growth ring discussion

The presence of clearly visible growth rings in the wood specimens suggests that the trees grew under a seasonal climate on the Antarctic Peninsula during the interval of the latest Cretaceous to the Late Paleocene. The seasonality shown by the growth rings in the wood may be due largely to growth ceasing during the prolonged dark polar winters (Francis, 1986; Francis and Poole, 2002; Poole *et al.*, 2005).

The false rings found in the wood specimens (D9.022.1, D9.050.1, D9.059.1 and D9.092.1) are likely to be due to droughts because there is no damage to the cells, which would suggest frost damage instead. Some of the false rings occur in the summer wood, which may suggest that precipitation was seasonal, with summer seasons being drier. The fact that there are few wood specimens with false rings and infrequent occurrence of false rings within a wood specimen suggests that drought was not common on the Antarctic Peninsula. However, the fact that most of the wood specimens with false rings are *Agathoxylon* suggests false rings and dry conditions may have been

related to conditions at the growth site of these trees. Modern members of the family Araucariaceae grow in open areas on slopes, and on thin soils or in rocky areas, on which soils do not hold much moisture (Ogden and Stewart, 1995; Veblen *et al.*, 1995; Jaffré, 1995).

The trend towards narrower mean growth ring widths from the latest Cretaceous to the Late Paleocene (Figure 6.10, 6.13, 6.14) suggests that there may have been a general trend towards less favourable growth conditions for the trees living on the Antarctic Peninsula during this time. This may reflect a trend towards cooler climates. This trend is also observed for average MGRW in *Nothofagoxylon*, *Phyllocladoxylon* and *Protophyllocladoxylon* for each formation (Figure 6.12). However, *Agathoxylon* and *Podocarpoxyton/Cupressinoxylon* wood specimens did not show a trend towards cooler climates.

Overall mean sensitivity values show no clear trend from the latest Cretaceous to the Late Paleocene. The frequency of wood specimens with complacent and sensitive growth varies throughout the sedimentary sequence. The majority of wood in the López de Bertodano Formation show sensitive growth (Figure 6.15, 6.16) suggesting variability in one or more limiting factors from one year to the next. In the lower to middle Sobral Formation the majority of wood specimens show less variable (complacent) growth and probably grew under a stable climate where no single limiting factor affected growth. Two of the three wood specimens in the upper Sobral Formation indicate growth under a fluctuating climate. Both wood specimens in the Cross Valley Formation suggest a return to a stable climate (complacent MS values).

The wide range in values observed for MGRW and MS could be a result of other factors that are not related to climate, such as ontogeny of the wood, different tree types having different ecologies, the wood being derived from different areas on the Antarctic Peninsula (e.g. upland or lowland areas) or preservation bias. The above-mentioned factors will be discussed separately in terms of what they mean for unravelling the story of what climates and environments were like for trees living on the Antarctic Peninsula during the Paleocene.

a) Preservation bias. There is bias in the dataset here, as a result of the differences in abundance of well-preserved wood specimens through the section. Most of the wood from the top of the Sobral Formation and Cross Valley Formation was too poorly preserved to provide growth ring data.

The trend towards narrower MGRW observed in figures 6.10, 6.13 and 6.14 may not be a true climate signal but instead it may be the result of a small number of wood specimens that only belong to two tree types (*Agathoxylon* and *Protophylocladoxylon*) that had a specific ecology and life habitat on the Antarctic Peninsula. For instance, the modern relatives of *Agathoxylon* (Araucariaceae) and *Protophylocladoxylon* (*Phyllocladus*) are naturally slow-growing (Ogden and Stewart, 1995; Veblen *et al.*, 1995) and as a result have narrow growth rings. However, *Nothofagoxylon*, *Phyllocladoxylon* and *Protophylocladoxylon* do show a trend towards more narrow growth rings, which may be a climate signal.

The wide range in values for MGRW and MS may be partly due to some wood specimens providing only short growth ring series, which do not represent a complete picture of the regional growth environment (Falcon-Lang, 2005b). Falcon-Lang (2005b) suggested wood specimens that have growth ring series with over 50 rings are best for recording regional climate signal.

The wood specimens here are also likely to have been derived from different parts of trees so, as discussed in section 6.2.1, this could also be another reason for the wide range in values.

b) Tree types and ecological differences. The data recorded for MGRW and MS through the sedimentary succession could be a reflection of individual ecologies of the different tree types living on the Antarctic Peninsula. Mean growth ring width values for individual wood types will be interpreted separately in terms of information they provide about the environment and climates in which they lived on the Antarctic Peninsula. This will be interpreted by looking at the life habits and ecologies of nearest living relatives and the likely origin of trees on the on the Antarctic Peninsula from which the wood specimens were derived.

Agathoxylon: *Agathoxylon* wood specimens had some of the narrowest MGRWs. The majority of the *Agathoxylon* woods also show sensitive growth except for D9.161.1. The mean growth ring widths are similar to those recorded for modern *Araucaria araucana* (MGRW range: 0.5 – 3.33mm, the majority are below <1.5mm) living at latitudes between 36°S and 40°S in the Andes (Chile/Argentina), altitudes > 500 m a.s.l and situated on the western more mesic side of the Andes (Chile side) and drier eastern side (Argentinian side) (LaMarche *et al.*, 1979a,b; Mundo *et al.*, 2012; Muñoz *et al.*, 2013). Mean annual temperatures (MAT) are roughly around 5 – 8°C in these regions and precipitation from west to east decreases from 2000 to 500 mm per year. Growth rings in *Araucaria araucana* have been found to decrease slightly with increasing elevation (Mundo *et al.*, 2012). *Araucaria araucana* MGRWs collected from Chile and Argentina by LaMarche *et al.* (1979a,b) did not show any pattern with latitude (north to south of distribution) or longitude (west to east). Muñoz *et al.* (2013) also found no clear trend in MGRW from the more mesic western side of the Andes and the drier eastern side. Although, they did find a significant decrease in MGRW (0.51mm) in the Patagonian steppe (71°W - 70°W). The majority of wood specimens in the López de Bertodano Formation and the lower/middle Sobral Formation (D9.022.1, D9.059.1, D9.050.1, D9.111.1) have narrower growth rings than modern *Araucaria araucana*. This means that climate conditions may have been less favourable for the *Agathoxylon* trees growing on the Antarctic Peninsula compared to their modern relatives in Chile and Argentina.

MS values are a lot higher than those recorded for modern relatives of the family Araucariaceae that are found in New Zealand and Southern Chile (*Agathis australis* and *Araucaria araucana*), which have values between 1.5 and 3.0 (Ahmed and Ogden, 1985; Mundo *et al.*, 2012; Muñoz *et al.*, 2013). This is due to these modern relatives living in year-round mild climates with high seasonal rainfall. MS values for *Araucaria araucana* trees living on the drier eastern side of the Andes (Argentina side) are higher (>2.0) compared to the more mesic west side (Chile) because is more prone to droughts during the summer period (Muñoz *et al.*, 2013).

Mean growth ring width values from *Agathoxylon* woods in the López de Bertodano Formation and lower to middle part of the Sobral Formation suggest growth conditions less favourable than those from the upper Sobral Formation. The MS values suggest that they grew under fluctuating climate conditions, where it is likely that water was the growth limiting factor, which is also further suggested by the presence of false rings found in specimens in the Lopez de Bertodano Formation and lower to middle Sobral Formation.

Agathoxylon trees are likely to have lived at high altitudes like modern *Araucaria* (see Chapter 5). The trees may have lived at the forest borders in more open areas where precipitation was less effective and water availability was more variable (Fritts, 1976).

Nothofagoxylon: Modern members of the Nothofagaceae family have wide ecological niches (see Chapter 4 and 5) so it is likely that the large variation in MGRWs of the wood specimens here is due to *Nothofagus* trees living on the Antarctic Peninsula during the Paleocene in a large range of environments, such as upland and lowland areas, forest interior and margins; with different soil types and quality. This is likely to have caused differences in growth rates of the trees and their growth response to climate conditions. Wood specimens D9.012.1, D9.023.1, D9.053.1, D9.089.1 and D9.110.1 have MGRWs that are similar to those recorded from modern *Nothofagus* species living in alpine zones, under the cool temperate climates of New Zealand (*N.solandri* and *N.menzessi*) and southern Chile (*N.pumilio*), which have a range of MGRWs between 0.5 – 2mm (Norton 1983a,b; Lara *et al.*, 2001; 2005; Massaccesi *et al.*, 2007). These modern species grow on poorly fertile soils, under cool temperatures (New Zealand: 8 -10°C, Chile 11 - 5°C) and seasonal precipitation (> 1000mm per year), with most of the precipitation falling in winter as snow.

None of the wood specimens have MGRWs as narrow as those recorded for *N.pumilio* in southern most Chile (55°S), which are < 1 mm. They usually form as stunted trees (Lara *et al.*, 2001; 2005; Massaccesi *et al.*, 2007). The slow growth due to the year-round cold climates and high precipitation (>3000mm). The *Nothofagus* species living on the Antarctic Peninsula may have lived under more favourable climates with warmer temperatures. Wood specimens

D9.016.1, D9.027.1 and D9.096.1 have wider growth rings (>2mm) in comparison to those recorded by the modern species mentioned above. The wood specimens with the wide MGRW >2mm may be a response to their local environment as well. For example, they may have lived in more favourable conditions, in the forest interior and grew on more fertile soils. The wood specimens that show narrower growth rings may have been derived from different environments e.g. cooler upland areas and forest borders. Wood specimen D9.089.1 has rounded edges and is partly charred which is evidence that it may have been derived from upland areas (Chapter 2 and 5). The narrowing of average MGRW for *Nothofagoxylon* from the López de Bertodano Formation to the lower to middle Sobral Formation may suggest a change to less favourable conditions.

Four *Nothofagoxylon* wood specimens show definite sensitive growth (D9.016.1, D9.012.1, D9.027.1 and D9.023.1). However, it is uncertain whether their MS values are a reflection of fluctuating climate, or individual responses to their local environment, as they only have a small number of growth rings present. In particular, specimen D9.023.1, which has a high MS value (0.70), only has three growth rings. Specimen D9.012 has a longer growth ring series (18 rings) and therefore its climate signal may be more reliable. Modern species *N.pumilio*, found at 35 - 55°S in Chile, where it forms the treeline, have MS values ranging from 0.17 – 0.37. The highest MS values are recorded at its most southern distribution, where temperatures are limiting to growth (Lara *et al.*, 2001; 2005; Massaccesi *et al.*, 2007). *Nothofagus* species (*N.solandri* & *N.menziessi*) living in southern New Zealand at the alpine timberline also have similar MS values, between 0.04 – 0.40 (Norton, 1983a,b). In modern relatives MS can vary within an area, depending on slope aspect, soil conditions and altitude. Most of the wood specimens that show sensitive growth are from the López de Bertodano Formation and some of these wood specimens also have wide MGRWs. The high MS observed indicate growth under a fluctuating climate, possibly where water was the limiting factor rather than temperature. The trees from which the wood specimens were derived may have also been situated at the forest borders. This may also be true for D9.110.1 which is the only *Nothofagoxylon* specimen that shows sensitive growth from the lower to middle Sobral

Formation. The *Nothofagoxylon* wood specimens that show more complacent growth may have grown in the forest interior where climatic factors were less limiting.

Other conifers (*Phyllocladoxylon*, *Protophyllocladoxylon* and *Podocarpoxyylon/Cupressinoxylon*): The nearest living relatives of the form genera *Phyllocladoxylon* and *Protophyllocladoxylon* include, *Phyllocladus* and *Lagarostrobos franklinii*. Wood specimens D9.019.1 and D9.118.1 are either *Podocarpoxyylon* or *Cupressinoxylon* so their nearest living relative are Podocarps or Cupressaceae. Modern members of the families Podocarpaceae and Cupressaceae are slow growing < 2mm per year (diameter breast height) (Dunwiddie, 1979; Dunwiddie and LaMarche, 1980, Enright and Ogden, 1995). Their slow growth rate is likely attributed to growing in areas of high rainfall and on infertile and poorly drained soils. The *Phyllocladoxylon*, *Protophyllocladoxylon* and *Podocarpoxyylon/Cupressinoxylon* MGRWs here suggest similar growth rates and thus a similar ecology to their modern relatives and possibly similar climate conditions. The narrower MGRWs observed in *Protophyllocladoxylon* specimens (D9.153.1 and D9.181.1) found in the Cross Valley Formation, compared to those found in the Sobral Formation, may indicate a change to less favourable conditions in the Late Paleocene. Also, the change to narrow growth ring widths could be due to differences in where the trees were living on the Antarctic Peninsula (e.g. local environmental factors, upland or lowland sites). For example, the *Protophyllocladoxylon* wood specimens in the Sobral Formation are likely to be derived from trees living in mid-altitudinal to lowland areas (see Chapter 2 and 5), whereas wood specimens from the Cross Valley Formation may have been derived from upland areas, where temperatures may have been cooler (Fritts 1976). The decrease of MGRW in *Phyllocladoxylon* wood specimens from the Lopez de Bertodano Formation to the lower to middle Sobral Formation (Figure 6.10 and 6.12) also suggests a change to less favourable climates. The fact that D9.019.1 has significantly narrow MGRW (0.63mm) than wood specimen D9.118.1 (2.43mm) could be due to a number of reasons such as, they may actually be different wood types, and/or lived in different local environmental conditions.

Modern members of the family Podocarpaceae and Cupressaceae have a wide range in MS values (LaMarche, 1979c; Dunwiddie, 1979). *Phyllocladus* and Podocarps can have high mean sensitivities of > 0.4. This is likely due to the fact that *Phyllocladus* and podocarps are frequently disturbed or live in more stressed conditions, to avoid competition, such as poorly fertile and waterlogged soil. As a result this may cause them to be more sensitive to changes in climate conditions (LaMarche, 1979c, Dunwiddie, 1979). Modern *Lagarostrobos franklinii* has very complacent growth even though it grows along river banks, prone to flood disturbance (Dunwiddie and LaMarche, 1980). Its complacent growth has been attributed to high water availability in these environments, under mild climates. The majority of the *Phyllocladoxylon*, *Protophyllocladoxylon* and *Podocarpoxylon/Cupressinoxylon* specimens show complacent growth suggesting that no single factor was limiting to the growth of these trees. The *Phyllocladus* and *Podocarp/Cupressaceae* type trees may have grown in more favourable environments (e.g. better soil quality) on the Antarctic Peninsula, which were less prone to disturbances, compared to many of their NLRs, such as in the interior of the forests where conditions would have been more stable, and water availability was not as limiting. Specimen D9.038.1 show clear sensitive growth and D9.112.1 show slight sensitivity growth conditions so these wood types may have been derived from more trees living at the forest border.

Other angiosperms (*Weinmannioxylon*, *Antarctoxylon* and

***Myrceugenelloxylon*):** *Weinmannia* is thought to be the NLR of *Weinmannioxylon*, and it is considered a long-lived pioneer species, and has a fairly slow growth-rate (Lusk, 1999; Coomes *et al.*, 2005). *Weinmannia racemosa* is common in podocarp forests in cool temperate New Zealand, where rainfall is high and mean temperatures range from 12°C (summer) and 5°C (winter). In these areas it grows on a variety of soils (Coomes *et al.*, 2005). Mean growth rates of 3.18 mm per year (radial growth) have been recorded for *Weinmannia racemosa* growing on good fertile and well drained soils; and 1.06mm per year (radial growth) on waterlogged and poorly fertile soils (Coomes *et al.*, 2005).

Weinmannia trichosperma trees found in old growth forests at high altitudes in the Andes (southern Chile) have growth rates recorded of 0.82mm per year (Lusk, 1999). The MGRWs of the *Weinmannioxylon* wood specimen here resemble the growth rates of *Weinmannia racemosa* growing in New Zealand on waterlogged soils. Although it is not possible to say exactly what conditions the *Weinmannia* type tree on the Antarctic Peninsula was living in, it suggests growth under similar climate conditions to those found growing in New Zealand.

There is little information in the growth rates and MGRW for the NRL of *Myrceugenelloxylon*. *Antarctoxylon* does not have a NLR. This makes it difficult to make comparison with their growth rates. However, the two wood specimens here have MGRW of >2mm, which suggests fast growth rates.

The *Myrceugenelloxylon* and *Antarctoxylon* wood specimens found in the López de Bertodano Formation suggest growth under a fluctuating climate. Today the NRL of *Myrceugenelloxylon*, *Luma* grows at mid-low altitudes on under moist conditions in the Andes (Gut, 2008), so it is possible that water was the limiting factor for the *Luma* type tree on the Antarctic Peninsula. *Weinmannioxylon* wood specimens have MS value suggests it lived in equable conditions in the Antarctic Peninsula forests.

6.4.3 Palaeoclimate information from fossil angiosperm woods

Table 6.4 presents all data from angiosperm wood specimens identified in this project in which anatomical features related to climate could be observed. The frequencies (%) of the different anatomical features in the wood specimens are presented as histograms in Figure 6.19.

a) Vessel Group Index (VGI). VGI was calculated for 22 wood specimens (Table 6.4). Figure 6.19a illustrates that all of the wood specimens have a low VGI with the majority (55%) having groups of two vessels or less. None of the wood specimens had exclusively solitary vessels (VGI of 1). Only 4% (one wood specimen) had a VGI of 4.5, but this is still considered low.

b) Vessel Porosity. Vessel porosity was observed in 20 wood specimens. Figure 6.19b presents the frequency (%) of ring, semi-ring and diffuse porosity and shows that the majority (80%) of the wood specimens are semi-ring porous and only 20% are diffuse porous. None of the wood specimens are ring porous.

c) Perforation plates. Figure 6.19c presents the frequency (%) of simple and scalariform vessel perforation plates in the wood specimens. Perforation plates were observed in 20 wood specimens. (Wood specimens D9.157.1 and D9.089.1 were not included because it was uncertain whether they had exclusively scalariform or simple perforation plates due to the vessel being broken and fragmented see Chapter 4). Figure 6.19c shows that the majority (75%) of wood specimens have a combination of simple and scalariform perforation plates. Exclusively scalariform perforation plates are present in 20% of the wood specimens. Only 5% of the wood specimens have exclusively simple perforation plates. All of the specimens that had co-occurrence of simple and scalariform perforation plates belonged to the morphotype *Nothofagoxylon*.

d) Vessel diameter. Figure 6.19d shows the frequency (%) of wood specimens with vessels of <50, 50 – 100 and >50 μm diameter. Mean vessel diameter was measured for 22 wood specimens. The majority (72%) of the wood specimens have vessel diameters between 50 - 100 μm .

e) Vessel density. Figure 6.19e shows the incidence of wood specimens that have vessel densities of <5, 5 – 20, 20 – 40, 40 – 100, >100 per mm^2 . Vessel density could be measured for 17 of the wood specimens. The majority (82%) of wood specimens had a vessel density of 40 – 100 mm^2 . The minority (6%) of wood specimens have vessel densities between 5 – 20 mm^2 , and 12% percent of the wood specimens had a vessel > 100 mm^2 .

f) Vessel element length. The incidence of wood specimens with <350 μm , 350 – 800, >800 μm vessel lengths are shown in Figure 6.19f. Vessel element length (μm) was measured in 16 of the wood specimens. The majority (56%) of wood specimens have vessel element lengths between 350 - 800 μm . The

high incidence of vessel element length >350 suggests that there was sufficient water available on the Antarctic Peninsula.

Table 6. 4. The occurrence of quantitative and qualitative anatomical features that are related to climate in the fossil angiosperm wood specimens in this study.

Specimens numbers	Genus	Porosity	Perforation plate type	Vessel Group Index	Vessel diameter (µm)	Vessel density (mm ²)	Vessel element length (µm)
D9.011.2	<i>Nothofagoxylon</i>	Semi-ring	Simple & Scalariform	1.68	78.32	59	N/A
D9.012.1	<i>Nothofagoxylon</i>	Semi-ring	Simple & Scalariform	1.88	54.5	71	692.4
D9.016.1	<i>Nothofagoxylon</i>	Semi-ring	Simple & Scalariform	1.92	80.07	65	848.8
D9.018.1	<i>Nothofagoxylon</i>	Semi-ring	Simple & Scalariform	1.36	72.15	56	327.4
D9.019.1	<i>Nothofagoxylon</i>	Semi-ring	Simple & Scalariform	1.6	59.44	N/A	670.4
D9.020.1	<i>Myrceugenelloxylon</i>	Diffuse	Scalariform	1.32	45.4	74	1062.85
D9.021.1	<i>Nothofagoxylon</i>	N/A	Simple & Scalariform	1.56	55	N/A	361
D9.023.1	<i>Nothofagoxylon</i>	Semi-ring	Simple & Scalariform	2.12	55.94	99	789.7
D9.027.1	<i>Nothofagoxylon</i>	Semi-ring	Simple & Scalariform	2.2	45.73	141	717.2
D9.040.1	<i>Antarctoxylon</i>	Semi-ring	Simple	4.4	44.5	N/A	360

Table 6.4.

Specimens numbers	Genus	Porosity	Perforation plate type	Vessel Group Index	Vessel diameter (µm)	Vessel density (mm²)	Vessel element length (µm)
D9.053.1	<i>Nothofagoxylon</i>	Semi-ring	Simple & Scalariform	2.2	66	96	720.72
D9.089.1	<i>Nothofagoxylon</i>	N/A	Scalariform ?simple	2.04	51.7	N/A	N/A
D9.091.1	<i>Myrceugenelloxylon</i>	Diffuse	Scalariform	1.4	56.94	58	1120
D9.095.1	<i>Nothofagoxylon</i>	Semi-ring	Simple & Scalariform	1.84	76.85	68	940
D9.096.1	<i>Nothofagoxylon</i>	Semi-ring	Simple & Scalariform	1.96	68	88	1088.4
D9.105.1	<i>Nothofagoxylon</i>	Semi-ring	Simple & Scalariform	1.8	72.73	63	416.8

Table 6.4.

Specimens numbers	Genus	Porosity	Perforation plate type	Vessel Group Index	Vessel diameter (µm)	Vessel density (mm²)	Vessel element length (µm)
D9.107.1	<i>Weinmannioxylon</i>	Diffuse	Scalariform	1.6	53.13	N/A	N/A
D9.110.1	<i>Nothofagoxylon</i>	Semi-ring	Simple & Scalariform	1.64	49.03	104	490.55
D9.128.2	<i>Weinmannioxylon</i>	Diffuse	Scalariform	1.12	49.4	54	N/A
D9.128.3	<i>Nothofagoxylon</i>	Semi-ring	Simple & Scalariform	1.52	48.08	49	N/A
D9.130.1	<i>Nothofagoxylon</i>	Semi-ring	Simple & Scalariform	2.16	61.9	53	905
D9.157.3	<i>Nothofagoxylon</i>	Semi-ring	Scalariform ?simple	1.6	78.85	37	N/A

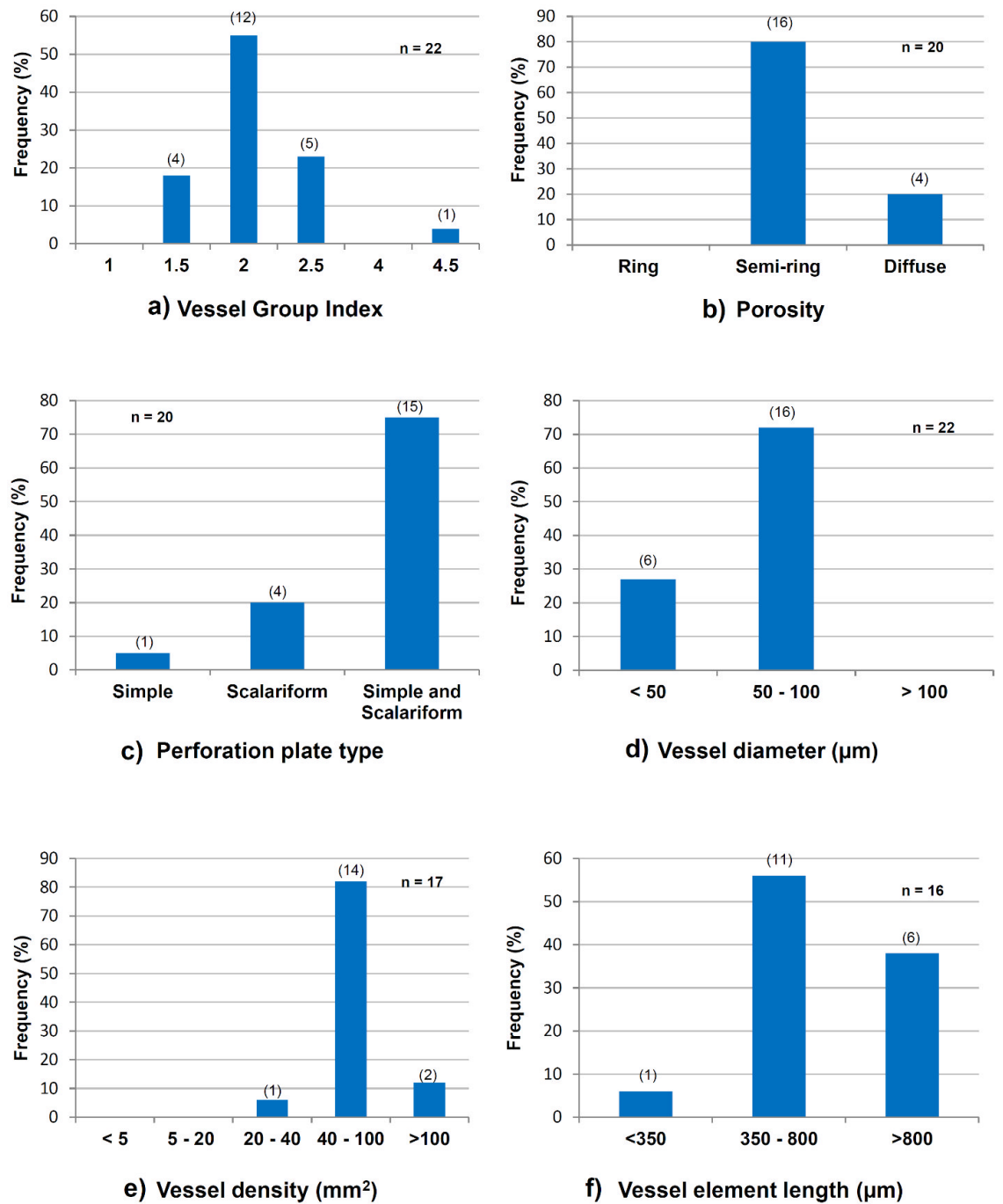


Figure 6. 19. Histograms presenting the frequency (%) of anatomical features that are related to climate and environmental conditions in the angiosperm wood specimens presented in Table 6.4: a) Vessel Group Index, b) Porosity, c) perforation plate type, d) Vessel diameter (e) vessel density (mm^2), and f) Vessel element length (μm). The numbers in brackets above each column are the number of specimens that possess that feature type; n = the total number of specimens used.

6.4.3.1 Vulnerability Index (VI) and Mesomorphy Index (MI)

The VI and MI results for the angiosperm wood specimens in this project are presented in Table 6.5. The VI was calculated for 17 of the angiosperm wood specimens. MI was calculated for 13 wood specimens (some of the wood specimens did not have intact vessel elements preserved). The actual number of measurements that could be made is presented in Table 6.5, plus mean values. The recommended number of measurements (25) could not be made on two wood specimens for vessel density mm^2 and on four specimens for vessel element length (μm) because these wood specimens were not as well preserved. For example, some areas in the woods were compressed and not enough vessel elements were preserved.

VI and MI values are also plotted separately against the stratigraphic section for Seymour Island (Figure 6.20 and 6.21). However, the Cross Valley Formation is absent in figures 6.20 and 6.21 because angiosperms were not found in this Formation.

Most of the angiosperm wood types are *Nothofagoxylon*. Only two specimens of *Myrceugenelloxylon* and one specimen of *Weinmannioxylon* could be used for VI and just one *Myrceugenelloxylon* could be used for MI calculations (refer to Table 6.5).

Vulnerability Index (VI). The VI shows a wide range in values. The majority of the wood specimens have values below 1.0 (range: 0.33 – 0.99) (Figure 6.20). The wood specimens that show values below 1.0 are *Nothofagoxylon* (D9.027.1, D9.023.1, D9.012.1, D9.053.1 and D9.110.1), *Myrceugenelloxylon* (D9.020.1 and D9.091.1) and *Weinmannioxylon* (D9.128.2). Seven wood specimens, which are all *Nothofagoxylon* have values above 1.0 (values range from 1.0 to 2.14). There is a narrowing in the range of values from López de Bertodano Formation (0.33 – 1.33) to the middle of the Sobral Formation at 250m on the section (most values range from 0.78 – 1.16), although there are more wood specimens in the López de Bertodano Formation ($n = 8$) than at different heights through the Sobral Formation. There is just one specimen at the top of the Sobral Formation and that has a high value of 2.14.

Mesomorphy Index (MI). The MI values show no distinct pattern through the stratigraphic section (Figure 6.21). A wide range of values were obtained, which are all above 200. The lowest values recorded are 231.29 (D9.110.1) and 232.64 (D9.027.1) and the highest value recorded is 1062.41 (D9.095.1).

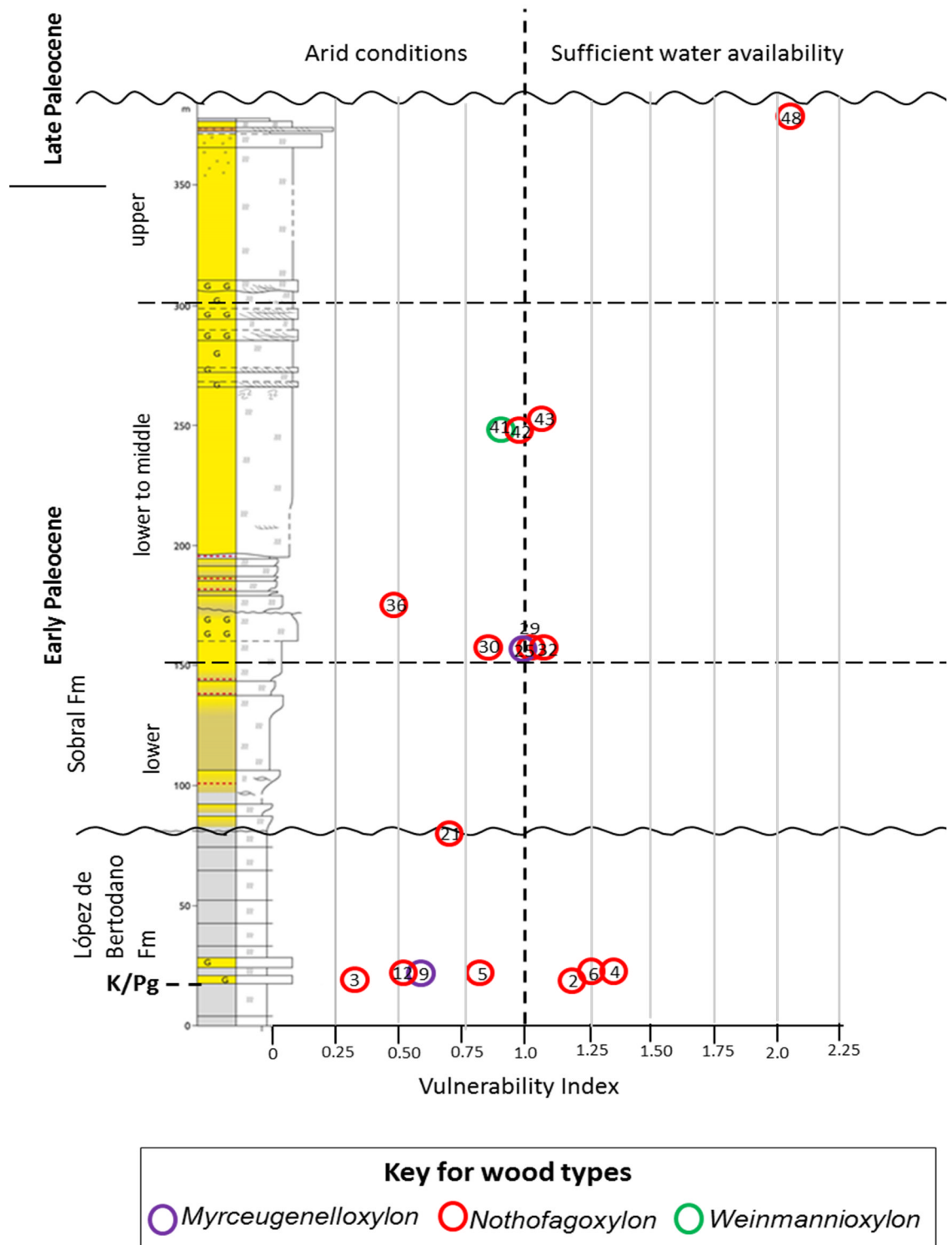


Figure 6. 20. A plot of VI values for the individual wood specimens from the upper López de Bertodano Formation (K/Pg to Early Paleocene) and through the Sobral Formation (Early to Late Paleocene). Numbers within circles are Tree Numbers. Stratigraphic log courtesy of Jon Ineson.

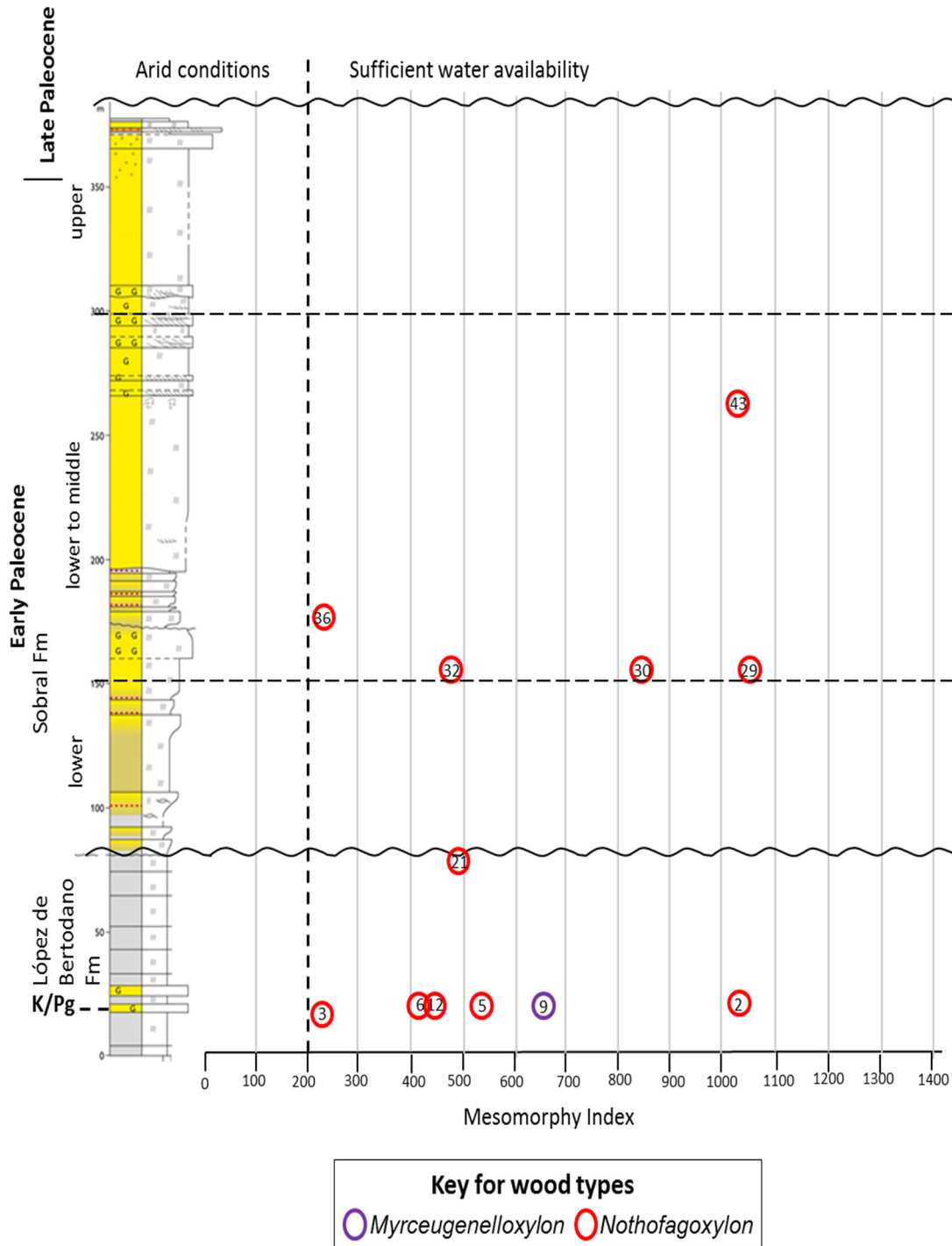


Figure 6. 21. A plot of MI values for individual wood specimens from the upper López de Bertodano Formation (K/Pg to Early Paleocene) and through the Sobral Formation (Early to Late Paleocene). Number within the circles are tree numbers. Stratigraphic log courtesy of Jon Ineson.

Table 6. 5. VI and MI results for 17 angiosperm wood specimens in this project.

Tree number	Genus	Wood organ	Mean vessel diameter (μm)	Mean vessels per mm^2	Mean vessel element length (μm)	Vulnerability Index	Mesomorphy Index
2	<i>Nothofagoxylon</i>	Large branch or trunk	80.07	65	848.8	1.24	1045.6
3	<i>Nothofagoxylon</i>	Branch or trunk	45.73	141	717.2 (17)	0.33	232.64
4	<i>Nothofagoxylon</i>	Branch or trunk	78.32	59	N/A	1.33	N/A
5	<i>Nothofagoxylon</i>	Inner part of large branch or trunk	54.5	71	692.4	0.77	531.57
6	<i>Nothofagoxylon</i>	Inner part of trunk or branch	72.15	56	327.4	1.29	421.82
9	<i>Myrceugenelloxylon</i>	Branch or inner part of trunk	45.4	74	1063 (7)	0.62	652.08
12	<i>Nothofagoxylon</i>	Outer part of trunk or large branch	55.94	99	789.7	0.57	446.2

Table 6.5.

Tree number	Genus	Wood organ	Mean vessel diameter (μm)	Mean vessels per mm^2	Mean vessel element length (μm)	Vulnerability Index	Mesomorphy Index
21	<i>Nothofagoxylon</i>	Branch or trunk	65.99	96	720.7	0.69	495.4
25	<i>Myrceugenelloxylon</i>	Inner part of trunk or branch	56.94	58	N/A	0.99	N/A
29	<i>Nothofagoxylon</i>	Outer part of large branch or trunk	76.85	68	940	1.14	1062.41
30	<i>Nothofagoxylon</i>	Outer part of trunk or large branch	68	88	1088.4	0.78	841.04
32	<i>Nothofagoxylon</i>	Outer part of large trunk or branch	72.73	63	417	1.16	481.23

Table 6.5.

Tree number	Genus	Wood organ	Mean vessel diameter (μm)	Mean vessels per mm²	Mean vessel element length (μm)	Vulnerability Index	Mesomorphy Index
36	<i>Nothofagoxylon</i>	Branch or trunk	49.03	104	490 (9)	0.48	231.29
41	<i>Weinmannioxylon</i>	Outer part of trunk	49.4	54	N/A	0.92	N/A
42	<i>Nothofagoxylon</i>	Branch or trunk	48.07	50 (15)	N/A	0.97	N/A
43	<i>Nothofagoxylon</i>	Branch or trunk	61.9	54	905 (21)	1.15	1037.4
48	<i>Nothofagoxylon</i>	Outer part of trunk	78.85	37 (8)	N/A	2.14	N/A

6.4.4 Discussion – Palaeoclimate information from fossil angiosperm wood

The analysis of the occurrence and frequency of anatomical features in the fossil angiosperm wood suggests that the climate on the Antarctic Peninsula was a seasonal climate with sufficient water availability.

All of the wood features suggest sufficient water availability. A seasonal climate is indicated by the majority of wood specimens having semi-ring porous woods. This compares well with the high abundance of semi-ring porous woods found in temperate areas of the Southern Hemisphere today (Wheeler *et al.*, 2007b). The majority of wood specimens have vessel densities between 40 – 100 mm²; vessel diameters between 50 – 100µm and vessel elements lengths >350µm. This indicates a temperate climate because these features are most common in temperate zones today (Wheeler *et al.*, 2007b).

The combination of scalariform and simple perforation plates is the most common type and are only present in the *Nothofagoxylon* woods. It is uncertain from the literature what the high incidence of co-occurring scalariform and simple perforation plates in wood means in terms of climate conditions. This was suggested to be an evolutionary trend towards more efficient conductivity (Carlquist, 2001, Oskolski and Jansen, 2009). Oskolski and Jansen (2009) found that the distribution pattern of simple and scalariform perforation plates in vessels of modern woody angiosperm plants indicates that simple perforation plates are most abundant in large vessels and scalariform perforation plates mostly occur in small vessels. This is seen in woods with distinctive growth rings (e.g. ring porous woods), where it appears that conductive efficiency is favoured at the start of the growing season (simple perforation plates) and safety at the end of the growing season (scalariform perforation plates). Today the occurrence of this feature is uncommon (Wheeler *et al.* 2007b). Woods from New Zealand and temperate Europe have the highest abundance of mixed perforation plates. Therefore, from these findings it could be suggested that this feature is related to seasonal climates.

The co-occurrence of simple and scalariform perforation plates is also present in a number of modern *Nothofagus* species (Poole, 2002): *N.cunninghamii* (Tasmania), *N.dombeyi* (southern Chile), *N.alpina* (southern Chile), *N. menzessi* (New Zealand), *N.solandri* (New Zealand) and *N.fusca* (New Zealand). Today these tree types live under seasonal climates in cool temperate forests. Most live in moist montane areas (except for *N.solandri*, which prefers drier areas). Therefore the presence of wood with the co-occurrence of scalariform and simple perforation plates is likely to indicate a cool temperate climate during the Paleocene. In addition the higher abundance of wood specimens with exclusively scalariform perforation plates compared to simple perforation plates imply sufficient water availability.

VI and MI. The VI results show that the majority (n = 10) of angiosperm wood specimens that were analysed here are derived from trees that grew in water stressed conditions on the Antarctic Peninsula during the Paleocene. However, a significant number of wood specimens (n = 7) also grew in an environment with sufficient water availability. The MI results, however, indicate that the trees that were growing in mesic conditions with sufficient water availability. Therefore the two indices appear to contradict each other in some cases.

Lens *et al.* (2011) has questioned the usefulness of the Vulnerability Index and Mesomorphy Index as indicators of a plants adaption to the availability of water in its environment because they appear to be too simplistic in terms of the variables involved. Additional xylem features other than the ones included in VI and MI have been shown to have a strong relationship with the cavitation resistance and hydraulic conductivity. These include the presence of thicker inter-vessel pit membranes between connecting vessels, which are less likely to rupture under the negative pressure caused by cavitation and cause leakage of air into neighbouring vessels (Lens *et al.*, 2011 and references therein). The smaller number of inter-vessel pits per vessel wall reduces the chance of a faulty pit rupturing and causing air leakage into neighbouring vessels. Wood density also has a strong relationship to cavitation resistance because thicker walled cells are less likely to implode under negative pressure caused by air embolism.

MI has shown to be a more reliable indicator of cavitation resistance as it includes more variables, one of them being vessel element length, which has a relationship (although weak) with cavitation resistance, in terms of decreasing size and increasing cavitation resistance Lens *et al.* (2011). Vessel element length is also linked to vessel length, which is considered the most important feature in the resistance to cavitation because it controls other variables that also show a strong relationship to cavitation, such as the number of inter-vessel pits per vessel and the numbers of vessels that are connected in groups.

VI was shown to be a weak indicator of cavitation resistance because vessel density and vessel diameter have been shown to have no relationship to cavitation resistance (Lens *et al.* 2011). However, the study conducted by Lens *et al.* (2011) is based on woods from one genus and therefore is biased to how a single genus adapts to resist cavitation. The relationship between these two vessel variables and water availability discovered by Carlquist (1977) was based on a wider range of angiosperm types.

Poole (1994) also showed contradictory results when reconstructing the palaeoenvironment around South East England during the Eocene, with VI suggesting arid conditions and MI suggesting mesic conditions. However, the two indices were still considered useful methods for giving a general indication of the availability of water in past climates. The variables used are also easily measured in fossil wood, whereas features such as intervessel pit membrane thickness cannot be measured.

When comparing the VI and MI results for the wood specimens here, specimens that have particularly low VI values also have lower MI values, which were near the 200 borderline for mesic environments (e.g. D9.027.1 and D9.110.1). Most of the wood specimens that did show adaptation to more arid conditions in VI had values that were close to the borderline value of 1.0 that separates adaptation to arid conditions from sufficient water availability. This suggests water stress was not that high for those trees.

The nearest living relative (NLR) of all the fossil form genera (*Nothofagoxylon*, *Myrceugenelloxylon* and *Weinmannioxylon*) live in warm to

cool temperate forests in the Southern Hemisphere with high seasonal rainfall > 1000 mm per year. The MI analyses gives values that are expected for environments in which the NLR's inhabit.

The large variation in values within the two indices may be partly due to the wood specimen being derived from different wood organs.

The MI results do not show any distinct changes in water availability up through the stratigraphic section. The narrowing in the range of values from the latest Cretaceous through to the mid-early Paleocene is not likely to be a climatic signal because of the potential bias caused by the smaller number of wood specimens present in the Sobral Formation compared to the López de Bertodano Formation. Similarly, specimen D9.157.3 in the upper Sobral Formation may suggest a return to conditions with sufficient water but without more data points this is uncertain.

6.4.5 Palaeoclimate analysis using nearest living relative (NLR)

6.4.5.1 Coexistence Analysis

The data for the different climate variables that could be acquired for each NLR are presented in Table 6.6. Altogether, there are 22 NLRs that could be identified in this project. The data source used for each of the climate variables are also given for each of the NLR and presented in Table 6.6.

For all of the climate variables most of the data could be obtained for the main tree types. However, for MAP, CMMT, WMMT, MPDM and MPWM data could not be used for *Microcachrys*, Cupressaceae because the published dataset was incomplete. MPDM and MPWM could not be obtained for *Dacrydium*. Also data could not be obtained for the following fern and clubmosses: Cyatheaceae, Osmundaceae, Lycopodiaceae and Selaginellaceae. These fern types have a wide spread distribution (T Utescher, pers comm., 2 January).

The results for each climate variable are presented below along with individual graphs that show the coexistence interval for each variable.

MAT: Figure 6.22 presents the MAT tolerances for the NLRs. The range in which most of trees coexist today is between 7.7– 13°C. The lower and upper limits are defined by *Luma* (Myrtaceae) and *Lagarostrobus franklinii* (Podocarpaceae).

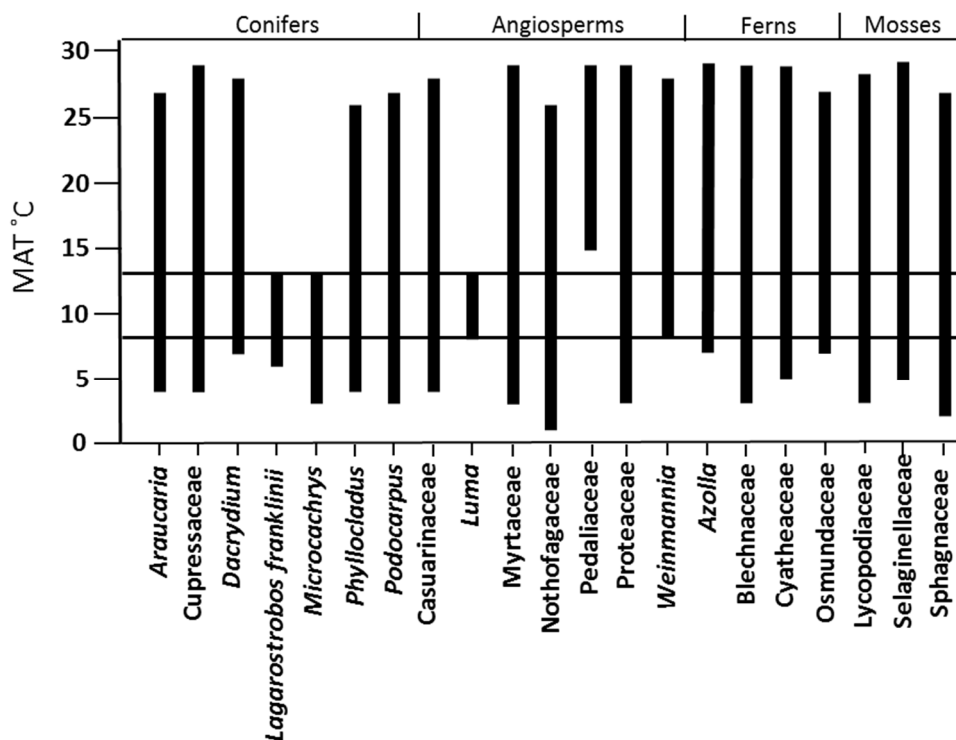


Figure 6. 22. MAT ranges for modern nearest living relatives of the fossil plants identified in this project.

WMMT: Figure 6.23 shows that the WMMT range in which the majority of the NLRs coexist today ranges from 18 – 19.6°C. The lower and upper limit is determined by *Luma* and *Lagarostrobus franklinii*.

CMMT: Figure 6.24 shows that the CMMT range in which the majority of the NLR coexist is between 6.6 – 9.1°C. The lower and upper limit of coexistent range is defined by *Araucaria* and *Luma*.

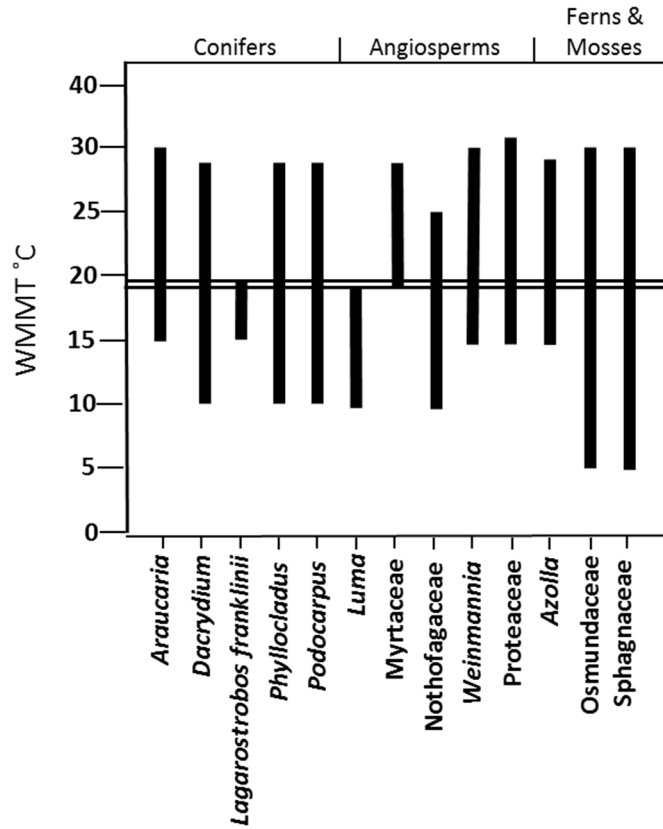


Figure 6. 23. WMMT tolerances for modern Nearest Living Relatives of the fossil plants identified in this project.

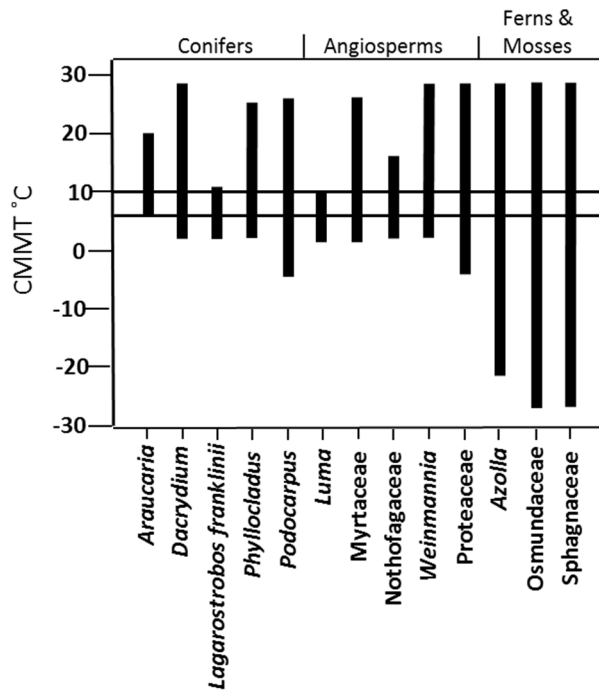


Figure 6. 24. CMMT tolerances for modern nearest living relatives of the fossil plants identified in this project.

MAP: The MAP ranges for the NLRs are illustrated in Figure 6.25. The range in which they coexist is between 1000 – 2489mm per year. The lower and upper limit is determined by *Lagarostrobos franklinii* and Nothofagaceae.

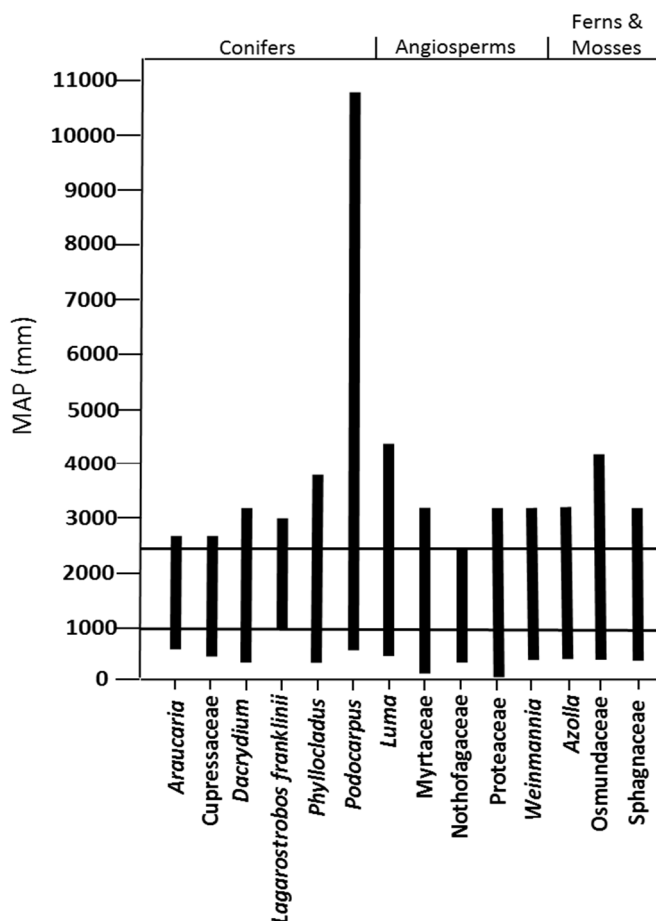


Figure 6. 25. MAP tolerances for modern Nearest Living Relatives of the fossil plants identified in this project.

MPWM: Figure 6.26 shows that the range in which most of the NLRs coexist is between 107 and 321mm of precipitation. The lower range is defined by *Araucaria* and the upper range is determined by *Lagarostrobos franklinii*.

MPDM: Figure 6.27 presents the tolerance ranges of MPDM for each NLR. The range in which they coexist is between 38 – 90mm. The lower range is defined by *Lagarostrobos franklinii* and the upper range is defined by *Araucaria* and Nothofagaceae.

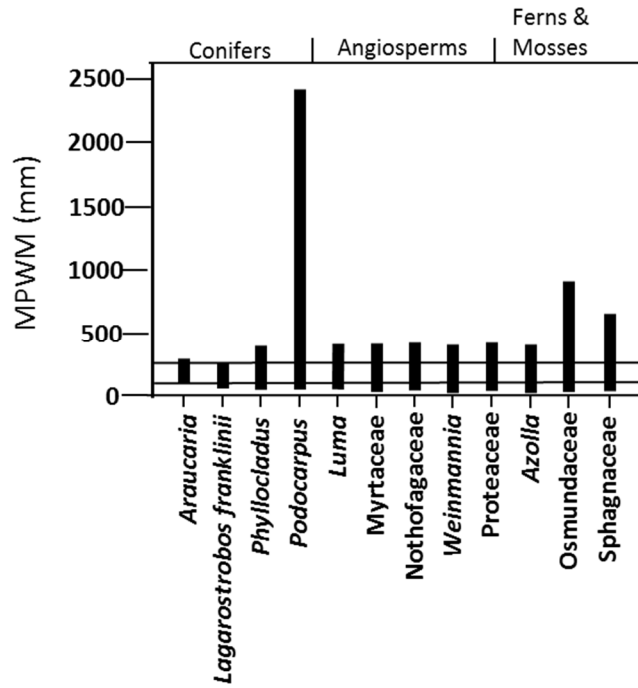


Figure 6. 26. MPWM tolerances for modern Nearest Living Relatives of the fossil flora identified in this project.

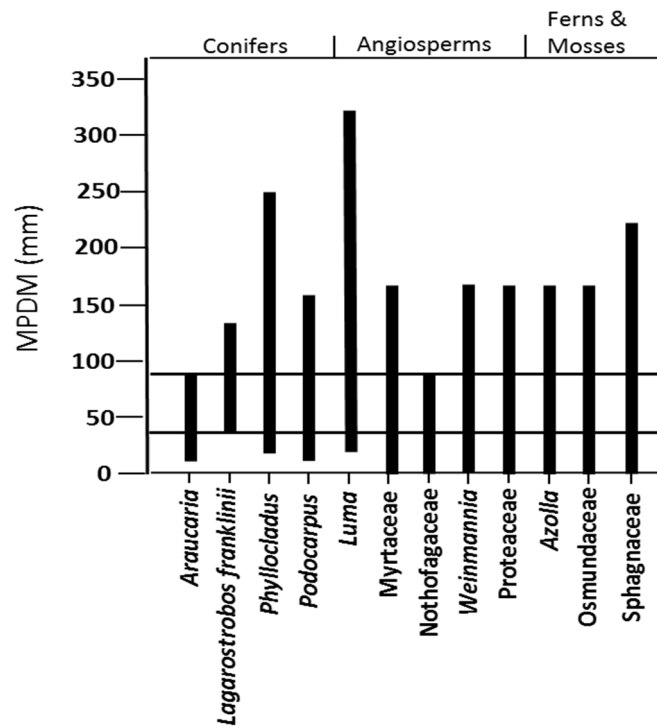


Figure 6. 27. MPDM tolerances for modern Nearest Living Relatives of the fossil plants identified in this project.

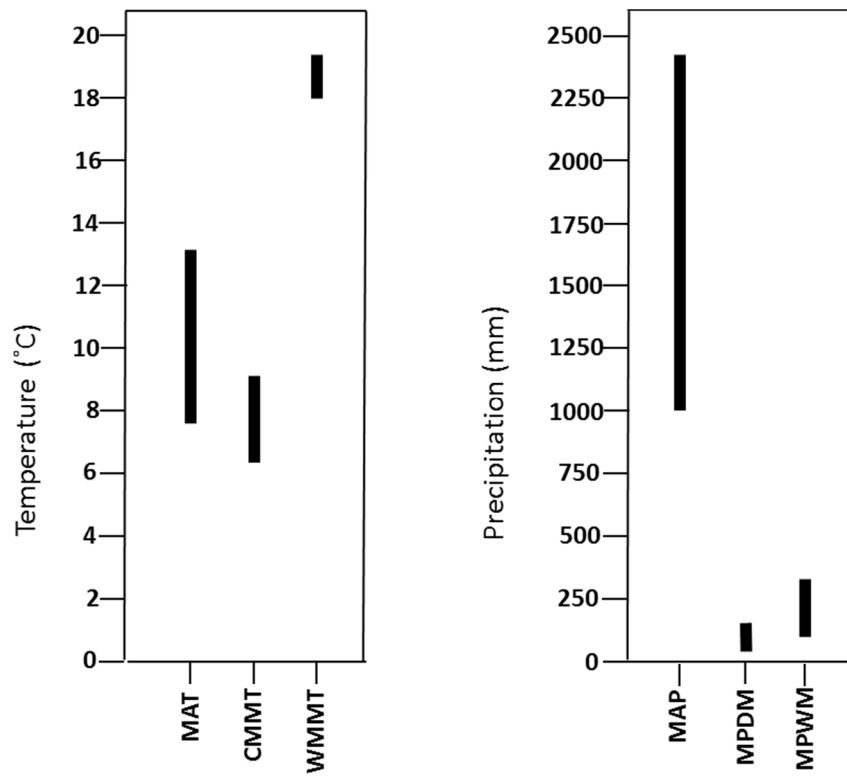


Figure 6. 28. Summary of temperature (MAT, CMMT, WMMT) and precipitation (MAP, MPDM, MPWM) tolerances of modern Nearest Living Relatives of fossil plants identified in this project.

Table 6. 6. The MAT, CMMT, MAP, MPDM and MPWM tolerances for the NLRs of the fossil flora identified in this project. *Lagarostrobos franklinii* MPWM and MPDM data was collected from Atlas of living Australia (these are shown with ‡ next to the values). Most of the MAT data was obtained from the Atlas of Living Australia but for some NLRs data was obtained from the Palaeoflora database (these are shown with * next to the values). Data for CMMT, WMMT, MAP, MPDM and MPWM was obtained from the Palaeoflora database. Data from Gibson *et al.*(1991) is marked with an †.

NLR	MAT (°C)		CMMT (°C)		WMMT (°C)		MAP (mm)		MPDM (mm)		MPWM (mm)	
	Min	Max	min	max	Min	Max	Min	Max	Min	Max	Min	Max
Conifers												
<i>Araucaria</i>	3.7	26.9	6.6	21.8	15.2	30.6	790	2700	1	90	107	350
Cupressaceae	3.8	28.8	N/A	N/A	N/A	N/A	447	2756	N/A	N/A	N/A	N/A
<i>Dacrydium</i>	6.7 *	27.7 *	2.5	27	11.7	28.1	N/A	N/A	N/A	N/A	N/A	N/A
<i>Lagarostrobos franklinii</i>	5.8	13	1.9	10.8	16.3	19.6	1000†	3000†	38‡	139‡	64‡	321‡
<i>Microcachrys</i>	3.8	13	N/A	N/A	N/A	N/A	N/A	N/A	N/A	N/A	N/A	N/A
<i>Phyllocladus</i>	4.2	26.5	2	26.1	9.8	28.5	389	3869	18	256	68	386
<i>Podocarpus</i>	3.3	27.2	-0.6	27	10.6	28.8	652	10798	13	165	68	2446

Table 6.6. Continued.

NLR	MAT (°C)		CMMT (°C)		WMMT (°C)		MAP (mm)		MPDM (mm)		MPWM (mm)	
	Min	Max	min	max	Min	Max	Min	Max	Min	Max	Min	Max
Angiosperms												
Causarinaceae	4.5	27.7	N/A	N/A	N/A	N/A	N/A	N/A	N/A	N/A	N/A	N/A
<i>Luma</i>	7.7 *	13 *	1.6	9.1	9.2	18	574	4486	17	326	58	409
Myrtaceae	3.3	29.5	0.1	27	18.8	28.1	250	3151	0	165	30	389
Nothofagaceae	1.7	24.6	1.6	15	9.2	25	447	2489	2	90	50	414
Proteaceae	3.3	29.5	-2.7	27	14.3	32.9	24	3151	0	165	8	389
Pedaliaceae	14.9	29.1	N/A	N/A	N/A	N/A	N/A	N/A	N/A	N/A	N/A	N/A
<i>Weinmannia</i>	8.5 *	27.7 *	1.8	27	14.3	31.2	200	3151	0	165	25	389

Table 6.6. Continued.

NLR	MAT (°C)		CMMT (°C)		WMMT (°C)		MAP (mm)		MPDM (mm)		MPWM (mm)	
	Min	Max	min	max	Min	Max	Min	Max	Min	Max	Min	Max
Ferns												
<i>Azolla</i>	6.8	28.8	-22.2	27	15.1	28.1	201	3151	3	165	33	389
Blechnaceae	32	28.9	N/A	N/A	N/A	N/A	N/A	N/A	N/A	N/A	N/A	N/A
Cyatheaceae	4.7	27.2	N/A	N/A	N/A	N/A	N/A	N/A	N/A	N/A	N/A	N/A
Osmundaceae	6.8	26.8	-27.8	27	4.9	30.6	184	4150	0	165	30	914
Mosses/club mosses												
Lycopodiaceae	3.3	28.5	N/A	N/A	N/A	N/A	N/A	N/A	N/A	N/A	N/A	N/A
Selaginellaceae	50	294	N/A	N/A	N/A	N/A	N/A	N/A	N/A	N/A	N/A	N/A
Sphagnaceae	2.1	26.9	-27.8	27	4.9	31	184	3151	0	225	30	605

6.4.6 Discussion – Coexistence analysis

This section discusses the results of the climate variables resulting from the Coexistence Analysis for the NLRs of the fossil flora identified in this project. The results from Coexistence Analysis suggests that the climate of the Antarctic Peninsula region during the Paleocene experienced a mean annual temperature of 7.7 – 13°C, with cold month mean above freezing (6.6 – 9.1°C) and average summer temperatures of 18 – 19.6°C (Table 6.7 and Figure 6.28).

The annual precipitation ranged from 1000 – 2489 mm per year, with low rainfall during the driest month (38 – 90 mm) and 107 – 321 mm during the wettest month.

The results for MAT and MAP using Coexistence Analysis presented above suggests that the climate of the Antarctic Peninsula during the Paleocene was cool temperate to marginally warm temperate, and the forests were likely to have been moist to wet rainforests according to the Holdridge life zone classification system (see Figure 6.29) (Emanuel *et al.*, 1985).

A CMMT range (6.6 – 9.1°C) suggests that winter periods were mild and the WMMT range (18 – 19.6°C) suggests that summer periods were warm. This suggests that winters were generally frost-free (as indicated by lack of frost rings in the wood). Therefore, climates were likely to be equable all year around.

The majority of the NLRs of the fossil flora occur in a wide range of climate zones, from sub-tropical to cool temperate and have wide mean annual precipitation ranges, for example, *Nothofagaceae*, *Araucaria*, *Phyllocladus*, *Podocarpaceae*, *Proteaceae*, *Weinmannia* and *Myrtaceae* (refer to Chapter 5). All the fern and moss families also have a wide ecological niche and are found under most climatic conditions.

For most of the climatic variables (MAP, MAT, CMMT, WMMT and MPDM) the ranges in which most of the NLRs coexist were predominantly determined by *Luma*, *Microcachrys* (MAT only) and *Lagarostrobos franklinii*, which have

short ranges for the different climate variables. Today *Lagarostrobos franklinii* is confined to the moist forests of Tasmania. *Microcachrys* is endemic to the cool, wet sub-alpine zones of Tasmania, and *Luma* is endemic to the cool temperate Valdivian forests and prefers to grow in moist conditions.

The climate conditions inferred from this Coexistence Analysis are comparable to those of four regions: Valdivian Andes, Chile (39 – 41°S); Central/western Tasmania; and New Zealand (South Island). These regions have wide spread rainforests, with taxa similar to those found in the forests of the Antarctic Peninsula. Mean annual temperature for these regions are within or close to the range deduced for the Paleocene (Chile: 11 °C, Tasmania: 7 – 12°C, and New Zealand: 10 – 15 °C) and temperatures are mild during the coldest months (Tasmania: 1.5 – 4 °C, Chile 5 °C, New Zealand: 6 – 8 °C) (Veblen and Ashton, 1978; Hill *et al.*, 1988; Ogden and Stewart, 1995; Wardle, 2001). Today these regions are also have high mean annual rainfall that ranges from 500 – 5000 mm and rainfall is sufficient throughout the year, exceeding 50 mm during the driest months (summer months: January and February) (Veblen and Ashton, 1978; Jarman *et al.*, 1991; Enright and Ogden, 1995; Wardle, 2001; Sanguinetti and Kitzberger, 2008).

In this study it was not possible to define separate climate conditions for upland and lowland areas on the Antarctic Peninsula for the Paleocene. This is because the fossil wood and pollen in this study are allochthonous and for some of the fossil wood their definite origin on Antarctic Peninsula cannot be determined based on their physical features. The definite origin of the pollen could not be determined in this study. Also, some of the fossil flora in this study that are related to modern Podocarpaceae, *Phyllocladus* and Nothofagaceae (e.g. *Phyllocladoxylon*, *Podocarpoxyton* and *Podocarpidites* sp.) have been interpreted as occupying upland and lowland areas because modern members of these families are found at high and low altitudes today (e.g. *Phyllocladus alpinus*, *Nothofagus pumilio* and *Nothofagus antarctica*) (Ogden and Stewart, 1995; Veblen *et al.*, 1996). The exact affinities of the fossil flora to modern relatives are unknown.

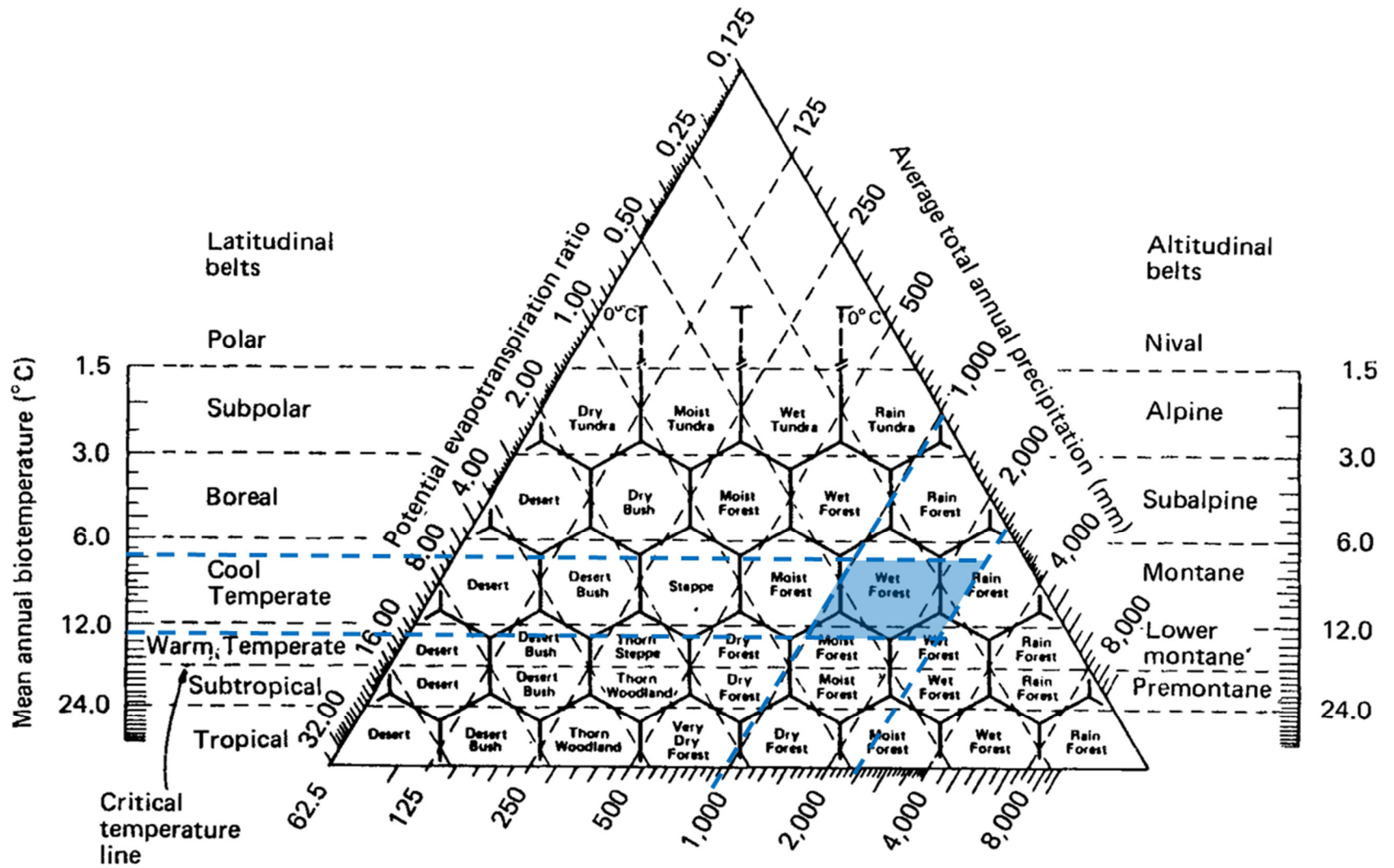


Figure 6. 29. The MAT and MAP ranges inferred for the Antarctic Peninsula during the Paleocene (blue zone) from the Coexistence Analysis study carried out here, plotted on to Holdridge's life zone classification system. Diagram of Holdridge's life zone system was taken from Emanuel *et al.* (1985).

Table 6.7. Summary of temperature and precipitation tolerances of modern Nearest Living Relatives of the fossil plants using Coexistence Analysis.

Climate variables	Values	
	Min	Max
Temperature variables (°C)		
MAT	7.7	13
CMMT	6.6	9.1
WMMT	18	19.6
Precipitation variables (mm)		
MAP	1000	2489
MPDM	107	321
MPWM	38	90

6.4.6.1 Frost tolerance of NLRs growing on the Antarctic Peninsula

The results for the frost tolerance of the NLRs are presented in Table 6.8 and Figure 6.30. A number of the NLRs are only distinguished at family or genus level, such as *Podocarpus*, *Nothofagaceae*, *Cupressaceae* and *Phyllocladus*. They have a large range of frost tolerances.

The presence of the presence of *Dacrydium*, *Lagarostrobos franklinii*, *Luma* and *Weinmannia*, which have specific or narrow ranges of cold tolerance, suggests that minimum temperatures on the Antarctic Peninsula are likely to have been no lower than -7°C to -8°C because this is the lowest temperature that *Lagarostrobos franklinii* and *Weinmannia* can tolerate today.

Table 6. 8. Frost tolerance of taxa that are found in Chile, Tasmania and New Zealand. Data sources: 1) Sakai and Wardle (1978), 2) Sakai *et al.* (1981), 3) Bannister and Neuner (2001), 4) Bannister and Lord (2006)

NLR	Cold Hardness °C	Data Source
Conifers		
<i>Araucaria araucana</i>	-6 to -12	3
<i>Dacrydium cupressinum</i>	-8	2
Cupressaceae	-8 to -20	1, 2, 3, 4
<i>Lagarostrobos franklinii</i>	-8	3
<i>Microcachrys tetragona</i>	-17	2
<i>Phyllocladus</i>	-10 to -22	1
Podocarps	-7 to -22	1, 2, 3, 4
Angiosperms		
<i>Luma apiculata</i>	-8.6	4
Myrtaceae	-8 to -14	1, 2, 4
<i>Nothofagus</i>	-5 to -22	1, 2, 4
Proteaceae	-7 to -14	2, 4
<i>Weinmannia</i>	-7.4 to -8.5	1, 4

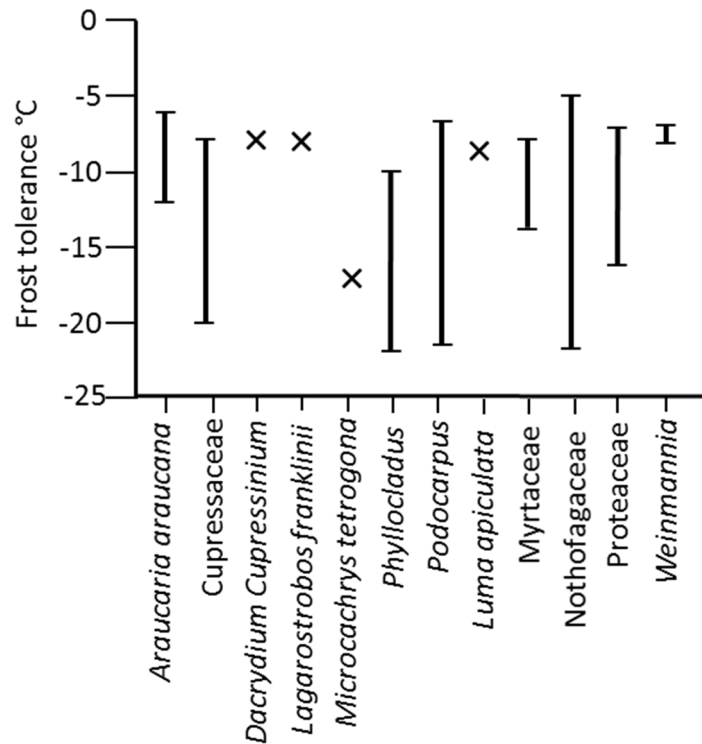


Figure 6. 30. Frost tolerances for the NLRs of the main fossil taxa identified in this project. Data sources: Sakai and Wardle (1978), Sakai *et al.* (1981), Bannister and Neuner (2001) and Bannister and Lord (2006).

The large range in frost tolerances reflects the wide latitudinal and altitudinal ranges in which the species that belong to these families and genera occur today. For example, within the genus *Phyllocladus*, *Phyllocladus trichomanoides* and *Phyllocladus asplenifolius* have the lowest frost tolerance of -10°C compared to *Phyllocladus alpinus*; the former two species are found in low to mid-montane areas of Tasmania and New Zealand, where minimum temperatures are not very low and the occurrences of frosts are infrequent, whereas *Phyllocladus* is found in alpine zones where temperatures are a lot lower and often occupy frost valley floors (Sakai and Wardle, 1978). Similarly, within the family Nothofagaceae, species such as *Nothofagus fusca* and *Nothofagus truncata* which grow in warm temperate to cool temperate forests in North Island, New Zealand have a lower frost tolerance compared to *Nothofagus antarctica* which grows in sub-alpine areas of southern Chile and

at lower altitudes where it occupies frosty valley floors that are prone to cold air drainage (Sakai *et al.*, 1981; Veblen *et al.*, 1996). Minimum temperatures on the Antarctic Peninsula are not likely to have been lower than -7 to -8 °C because these are the lowest temperature that *Lagarostrobos franklinii* and *Weinmannia* can tolerate today. These tree types are mostly found in mid to low montane areas in the rainforests of Tasmania and New Zealand (Wardle and Macrae, 1966; Gibson and Brown, 1991) and from the interpretation of the paleoecology (see Chapter 5) similar trees types are likely to have occupied similar niches on the Antarctic Peninsula during the Paleocene.

Upland areas on the Antarctic Peninsula are likely to have been subject to colder minimum temperatures. *Araucaria* type trees growing on the Antarctic Peninsula in the past have been interpreted as occupying upland areas (Chapter 5). Today *Araucaria araucana* has a maximum cold tolerance of -12°C which suggests that coldest winter temperatures during the Paleocene are not likely to have commonly exceeded this.

Temperatures may have been harsher above the treeline in heathland communities on the Antarctic Peninsula which was likely dominated by small shrubs such as *Microcachrys tetragona* (Bowman *et al.*, 2014). Modern *Microcachrys tetragona* has a frost tolerance of -17 °C and grows in alpine heathland communities in central Tasmania where winter temperatures can reach as low as -13 °C and frosts occur frequently throughout the year.

6.4.7 Specific gravity of the conifers and angiosperms

The range in specific gravity of the fossil wood specimens is small (0.50 to 0.8), considered as medium to high specific gravity by (IAWA Committee, 1989) (Figure 6.31 and 6.32). In general, conifer wood types (*Agathoxylon*, *Phyllocladoxylon* and *Protophyllocladoxylon*) have higher specific gravities than the angiosperm wood types.

In terms of trends through the stratigraphic section Figure 6.32 wood from the López de Bertodano Formation has the greatest number of specimen range in specific gravity values (0.5 – 0.78) and wood from the Sobral Formation has narrower range and slightly higher values (range: 0.59 – 0.8) (IAWA

Committee, 1989). This slight change could be due to a greater number of the conifer species being present in the lower part of the Sobral Formation in particular *Phyllocladoxylon*, *Protophyllocladoxylon* which have high specific gravity.

The fossil conifer wood types *Phyllocladoxylon*, *Protophyllocladoxylon* and *Agathoxylon* have relatively high specific gravities compared to the angiosperms. Wood of modern relatives such as *Phyllocladus* and *Araucaria* also have high wood densities (Pittermann *et al.* 2006). Pittermann *et al.* (2006) suggested the reason for this is that they have a very slow growth rate and tend to grow on nutrient-poor soils, in particular *Phyllocladus*. It is likely that the wood specimens here had a similar life habit. Modern *Araucaria araucana* has an estimated specific gravity range of 0.40 – 0.52 (<http://www.wood-database.com>). The fossil *Araucaria* type trees here have a slightly higher specific gravity, possibly due to adaption to different environments e.g. drier conditions.

The specific gravity values for *Nothofagoxylon* fossil wood specimens fall into the range of specific gravity values for modern *Nothofagus* species that are found in warm to cool temperate zones of the Southern Hemisphere (0.45 – 0.75) (<http://insidewood.lib.ncsu.edu>). The traits of modern *Nothofagus* is that they are usually pioneer species after major disturbances, are shade intolerant and mostly occupy soils of low fertility (except *N.cunninghamii*) and grow under seasonal rainfall (Ogden *et al.*, 1996; Read and Brown, 1996; Veblen *et al.*, 1996). Fossil *Nothofagus* may have had similar traits.

Fossil *Myrceugenelloxylon* wood has a lower specific gravity (0.61 and 0.63) than what would be expected compared to its nearest living relative *Luma*, which has a specific gravity higher than > 0.75 (<http://insidewood.lib.ncsu.edu>). *Luma* is a shade tolerant tree and grows in areas of high rainfall and likes moist conditions. It is possible that the fossil tree type had a different life strategy or environmental conditions were different on the Antarctic Peninsula.

The range of values of specific gravity recorded here suggest a temperate climate for the Antarctic Peninsula during the latest Cretaceous to Late

Paleocene. In addition, *Nothofagoxylon*, *Phyllocladoxylon* and *Protophyllocladoxylon* have similar specific gravities to their nearest living relatives, suggesting that the Paleocene trees also lived under cool temperate climates with seasonal rainfall.

Table 6. 9. Specific gravity (SG) data measured from the fossil wood specimens.

Specimen number	Morphotype	SG (mean)
D9.027.1	<i>Nothofagoxylon</i>	0.62
D9.012.1	<i>Nothofagoxylon</i>	0.56
D9.018.1	<i>Nothofagoxylon</i>	0.5
D9.019.1	<i>Nothofagoxylon</i>	0.51
D9.019.2	<i>Podocarpoxylo</i> <i>n/Cupressinoxylo</i> <i>n</i>	0.75
D9.020.1	<i>Myrceugenelloxylon</i>	0.63
D9.022.1	<i>Agathoxylon</i>	0.68
D9.023.1	<i>Nothofagoxylon</i>	0.59
D9.036.1	<i>Phyllocladoxylon</i>	0.77
D9.038.1	<i>Phyllocladoxylon</i>	0.78
D9.043.1	<i>Agathoxylon</i>	0.56
D9.059.1	<i>Agathoxylon</i>	0.68
D9.050.1	<i>Agathoxylon</i>	0.67
D9.090.1	<i>Podocarpoxylo</i> <i>n</i>	0.63
D9.091.1	<i>Myrceugenelloxylon</i>	0.61
D9.093.1	<i>Protophyllocladoxylon</i>	0.76
D9.094.1	<i>Phyllocladoxylon</i>	0.8

Table 6.9. Continued.

Specimen number	Morphotype	SG (mean)
D9.096.1	<i>Nothofagoxylon</i>	0.63
D9.098.1	<i>Phyllocladoxylon</i>	0.72
D9.105.1	<i>Nothofagoxylon</i>	0.71
D9.118.1	<i>Podocarpoxyton/Cupressinoxyton</i>	0.67
D9.110.1	<i>Nothofagoxylon</i>	0.59
D9.111.1	<i>Agathoxyton</i>	0.75
D9.112.1	<i>Protophyllocladoxyton</i>	0.8
D9.153.1	<i>Protophyllocladoxyton</i>	0.6

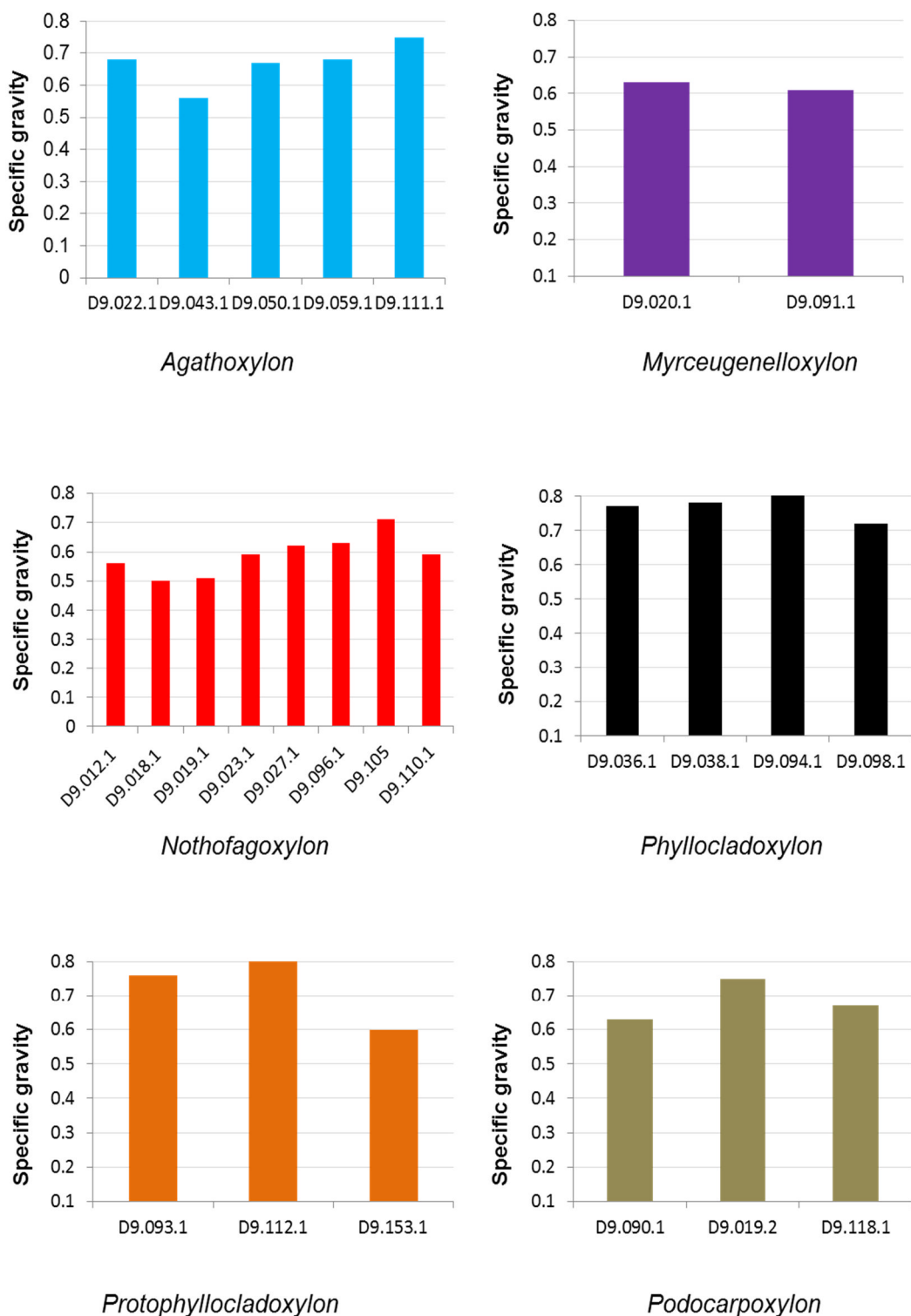


Figure 6. 31. Bars charts showing the range of specific gravity for wood specimens within each morphotype present in the study. Specimen numbers are shown along the X axis and specific gravity is shown on the y axis.

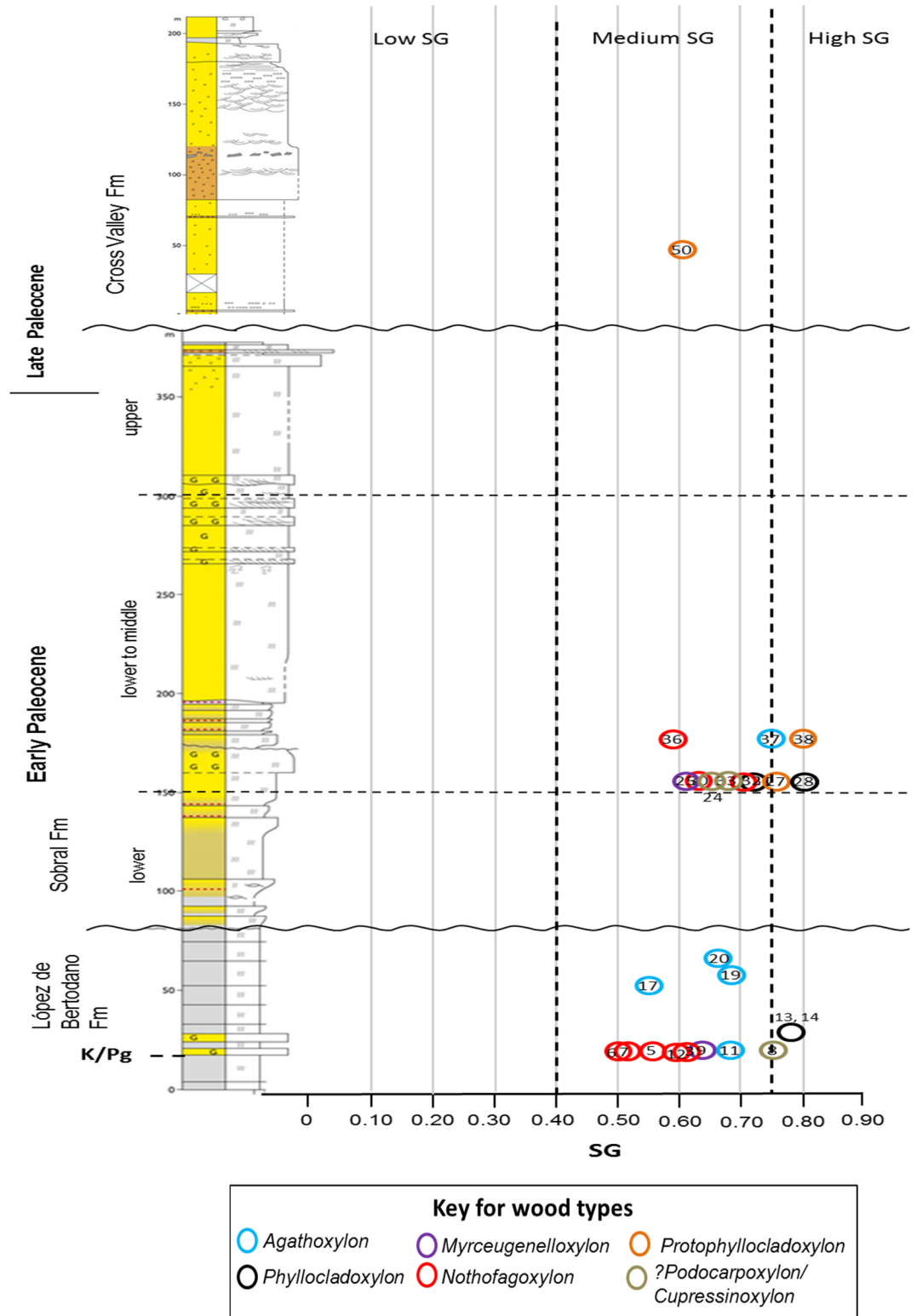


Figure 6. 32. A plot of specific gravity values for individual wood specimens from through the López de Bertodano Formation (K/Pg to Early Paleocene), Sobral Formation (Early to Late Paleocene) and Cross Valley (Late Paleocene). Stratigraphic log courtesy of Jon Ineson.

6.5 Overall discussion/ summary

The palaeoclimate analyses conducted on fossil wood and palynomorphs as described above indicate a temperate climate on the Antarctic Peninsula during the Paleocene. similar to modern climates of New Zealand, Chile and Tasmania. Seasonality

A cool to warm temperate climate with mean annual temperature of 7.7 - 13°C has been estimated from Coexistence Analysis, climates similar to those of southern Chile (39 - 41°S), western/central Tasmania and New Zealand. It also indicates that temperature were mild all year-round, with warm month mean temperatures of 18 – 19.6°C and cold month mean temperature of 6.6 – 9.1°C.

The strong growth rings in all of the wood specimens indicate seasonal climates. This is supported by the majority of angiosperm wood specimens being semi-ring porous, which is a feature that is most common in temperate regions (Wheeler *et al.*, 2007b).

The decrease in mean growth ring width from the Early Paleocene to the Late Paleocene suggests a change to less favourable growth conditions, for example, cooler climates.

The narrow range in wood specific gravity values observed in wood specimens is also indicative of a temperate climate and the absence of frost rings in the wood is further evidence for mild climates. Although, this evidence suggests that climates are likely to have been mild on the Antarctic Peninsula, occasional frosts may have occurred as they do in southern temperate regions today. The frosts tolerances of nearest living relatives today in southern Chile, Tasmania and New Zealand suggest that winter frosts on the Antarctic Peninsula in lowland areas were not likely to have been severe, and with temperatures around -7 to -8°C. The severity of winter frosts is likely to have been harsher in upland forests probably around -12 °C and possibly up to -17 °C. However, the lack of frost rings indicate that the trees did not suffer from freezing temperatures, probably because the cold conditions occurred during periods in which the trees were dormant and thus freezing temperatures did not affect cell growth.

Data from Coexistence Analysis suggests that there was sufficient year-round rainfall, but with higher rainfall in the winter months compared to the summer months. The Mesomorphy Index results, which are considered to be more reliable than the VI Index, also suggest that the trees on the Antarctic Peninsula grew under sufficient water conditions. However, the presence of false rings in *Agathoxylon* and *Phyllocladoxylon* wood suggests that there may have been periods of water shortage.

This is further supported by high mean sensitivity values in the majority of the *Agathoxylon* wood specimens, some *Nothofagoxyton* and one *Phyllocladoxylon* wood specimens, which imply growth under a fluctuating climate. It is possible that the limiting growth factor was water availability. Since not all wood specimens show sensitive growth or have false rings it is probable that the wood specimens came from different areas of the Antarctic Peninsula. For example, the *Agathoxylon* woods were likely to have been derived from trees in upland areas, or in open forests where they were more exposed

Chapter 7

Discussion

7.1 Introduction

This research presents a detailed study of the Paleocene forests and climates of the Antarctic Peninsula, primarily using a new assemblage of fossil wood and palynomorphs. The fossil wood specimens are tied to a new measured sedimentary sequence on Seymour Island which has allowed for a more rigorous interpretation of the composition and structure of the Antarctic Peninsula forests and the climates under which they grew. This chapter discusses the outcomes of this research and the findings will be compared to previous research on the Paleocene flora of Antarctica and those of the Southern Hemisphere. Information about the Paleocene forests will also be compared to modern temperate forests in the Southern Hemisphere in order to see if there was similarity in structure and processes that controlled forest composition. The findings from the climate analysis will be discussed and compared to published climate records from the terrestrial and the marine realm to see if they are in agreement. The climate results here will also be compared to the global Paleocene climate proxies to see how they fit the global trend.

7.2 Paleocene forests of Antarctica

During the Paleocene the Antarctic Peninsula was an active volcanic arc, which was covered in cool temperate forests. Wood from trees that once grew in these forests was transported from the arc via river systems into a back-arc basin, now called the Larsen Basin, where they floated as drift wood before sinking to the basin floor and becoming permineralised. Today Seymour Island holds the highest latitude Paleocene sedimentary deposits which contain abundant fossil wood. Fossil wood studied in this project was collected from a measured sedimentary sequence of K/Pg to Late Paleocene

in age that includes the following formations: upper part of the López de Bertodano Formation, Sobral Formation and Cross Valley Formation. The temporal range of the sedimentary succession includes the Danian and late Thanetian, the Selandian is missing. The succession represents a shallowing depositional environment from a marine mid-shelf setting to a deltaic environment to a fluvial environment (Chapter 2). A combined analysis of the fossil wood specimens in terms of its preservation, identification, the ecology of nearest living relatives, and associated sediments has allowed a detailed insight into the composition and structure of the Antarctic forests.

The identification of fossil wood in this project has revealed that the forests of Antarctica during the Paleocene consisted of angiosperm and conifer trees similar to modern types found in Australia, New Zealand and South America today. From the fossil wood assemblage, conifer tree types that grew in the forests included: *Agathoxylon*, *Phyllocladoxylon*, *Protophyllocladoxylon* and *Podocarpoxyton* and/or *Cupressinoxylon* (Chapter 3). Angiosperm tree types included: *Nothofagoxyton*, *Weinmannioxylon*, *Myrceugenelloxyton* and *Antarctoxyton* (Chapter 4). All together 52 wood specimens could be identified plus four wood types that could be only identified as conifers.

The majority of wood assemblages in this study are conifers (55%) (Chapter 5), which suggests that conifers were important components of the Antarctic forests during the Paleocene. *Agathoxylon* and *Nothofagoxyton* are likely to have been the most dominant tree types in the forests as they compose 25% and 38% of the wood specimens that could be identified. *Phyllocladoxylon* (11%) and *Protophyllocladoxylon* (10%) tree types are likely to have been common. *Podocarpoxyton* and/or *Cupressinoxylon* (6%) trees, and the other angiosperms (*Weinmannioxylon* (4%), *Myrceugenelloxyton* (4%) and *Antarctoxyton* (2%)) may have been minor components.

In addition analysis of palynomorphs revealed the presence of diverse podocarpaceae including *Lagarostrobus franklinii* (pollen type: *Phyllocladidites mawsonii*), *Microcachrys* (small shrub) (Pollen type: *Microcachryidites antarcticus*), shrubby angiosperm taxa such as Proteaceae and Casuarinaceae, as well as ferns and sphagnum mosses.

Lowland floras on the Antarctic Peninsula are likely to have consisted of an overstorey dominated by *Nothofagus* and podocarp trees (e.g. types similar to living *Lagarostrobos franklinii*, *Phyllocladus* and *Dacrydium*) (see Figure 7.1). Other broad-leaved angiosperms such as *Weinmannia*, Myrtaceae (e.g. *Luma*) and ancient *Antarctoxylon* are likely to have been minor components in the overstorey (see Chapter 5).

The trees growing in these lowland forests are likely to have occupied moist conditions possibly on poorly drained soils by comparison to modern analogues (Veblen *et al.*, 1995; Ogden and Stewart, 1995; Veblen *et al.*, 1996). *Phyllocladus* and *Weinmannia* are found growing on poorly drained and poorly fertile soils on river terraces in lowland podocarp forests in New Zealand (Ogden and Stewart, 1995). *Lagarostrobos franklinii* grows along riverbanks in lowland cool temperate forests of Tasmania (Gibson *et al.*, 1991). Understorey niches were likely occupied by Proteaceae shrubs, Myrtaceae shrubs, ferns and tree ferns (e.g. Osmundaceae, Cyatheaceae, Blechnaceae) and mosses (e.g. Sphagnaceae, Lycopodiaceae and Selaginellaceae).

Upland forests were likely composed of conifer tree types, in particular *Araucaria* (fossil wood type *Agathoxylon*) would have been dominant growing in open forests on well drained soils (see Figure 7.1). *Nothofagus* trees may have also been present. Above the treeline there may have been heathland communities that consisted of podocarp shrubs, including *Microcachrys*, ferns species, Proteaceae, Casuarinaceae and sphagnum moss mounds. Today *Microcachrys* grows in heathland communities above the treeline in Tasmania (Beadle, 1981).

Evidence for the possible composition of upland forests on the Antarctic Peninsula is mainly based on the ecology of nearest living relatives. The nearest living relatives of *Agathoxylon* and *Nothofagoxylon* are mainly found in montane environments at high-altitudes (Veblen *et al.*, 1995; Ogden and Stewart, 1995). Partly charred *Agathoxylon* and *Nothofagoxylon* wood found in the upper Sobral Formation gives further evidence that these ancient tree types may have had a similar ecology to their modern relatives growing at high altitudes in Chile, which rely on large scale disturbances including

disturbances from volcanic activity such as pyroclastic flows and wild fires (Veblen *et al.*, 1995;1996). Some of wood specimens are also rounded and this may suggest abrasion from being transported long distances as bed-load (Chapter 2). No definite conclusion can be made about distance of transport from rounded edges alone since abrasion could have also occurred in a marine influenced depositional environment through wave action (Gonor *et al.*, 1988). Thus the abrasion may have occurred after deposition of the wood.

The Cross Valley Formation contains *Protophyllocladoxylon*, *Agathoxylon* and unidentified conifer wood. The formation represents deposition from a debris flow (see Chapter 2) as it contains volcanic clasts, large logs and mud-rafts. The fact that all the wood specimens are conifers could suggests that they have been transported from high altitude sources because in modern Southern Hemisphere forests conifers become more abundant at higher altitudes as they can grow in harsh conditions, unlike broadleaved trees that prefer well developed soils and warm climates (Veblen *et al.*, 1995; Ogden and Stewart, 1995; Lusk 1996; Coomes *et al.*, 2005). The pollen assemblages are less diverse at the top of the Sobral Formation compared to the lower part of the formation and consists mostly of ferns, *Araucaria*, podocarps, Proteaceae and *Nothofagus*. Proteaceae and Podocarpeaceae and mosses and ferns are found at all altitudes in Southern Hemisphere forests today (see Chapter 5) so it is possible that they may have grown at all altitudes on the Antarctic Peninsula.

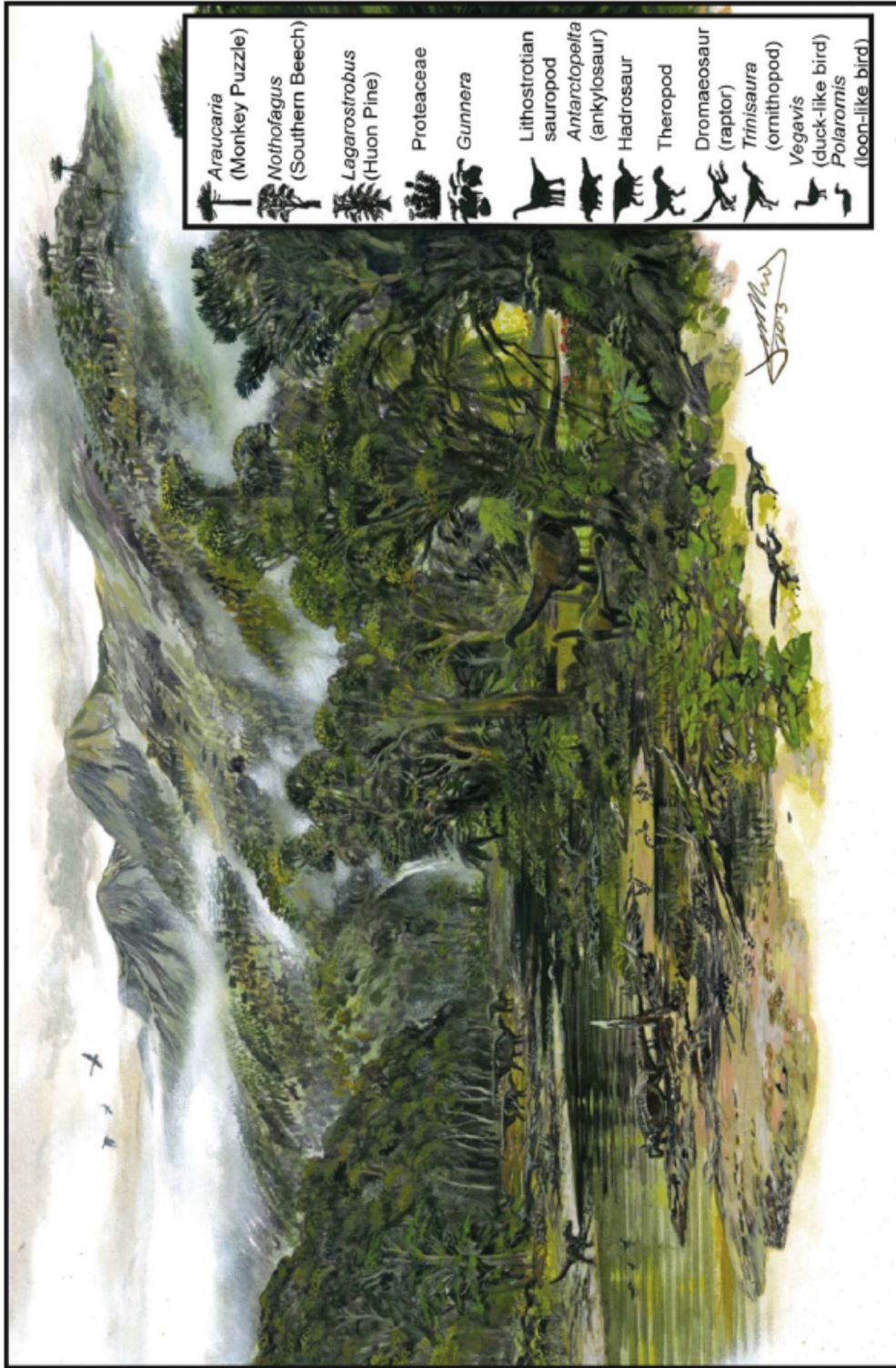


Figure 7. 1. Reconstruction of the Antarctic Peninsula forests during the Maastrichtian (Late Cretaceous). The Paleocene forests would have been similar to the forests presented in this painting. However, dinosaurs were extinct during the Paleocene. *Gunnera* would have also been absent from the forests. *Nothofagus* and podocarp trees would have been the main canopy trees forming the lowland forests. The undergrowth would have consisted of Proteaceae, and other angiosperm shrubs (Myrtaceae) and ferns. Upland areas would have consisted of open woodland with *Araucaria* forming the main canopy trees. Taken from Bowman *et al.* (2014). Painted by James McKay.

7.3 Comparison to published records

Fossil wood, leaves and palynomorphs have previously been documented throughout the Paleocene strata on Seymour Island (Askin, 1988; Askin, 1989; Askin, 1990; Askin, 1992, Poole *et al.*, 2003; Cantrill and Poole, 2005; Cantrill *et al.*, 2011; Tosolini *et al.*, 2013; Bowman *et al.*, 2014; Pujana *et al.*, 2015). The published fossil flora records all suggest warm to cool temperate forests on the Antarctic Peninsula with common components such as Nothofagaceae, Podocarpaceae and Araucariaceae, although, the published palynomorph and leaf records reveal a higher diversity of plant taxa present. A detailed comparison between the published macro-floral (leaves and wood) and micro-floral (palynomorphs) records and the fossil floral record here is discussed below.

7.3.1 Macro-floral record (wood and leaves)

Previous research on Paleocene fossil wood supports the evidence from this project that conifers were important in the forests during this time. The families Podocarpaceae and Araucariaceae were particularly important (Cantrill and Poole, 2005). Cantrill and Poole (2005) compiled a large database of all the fossil wood that had been identified up to that time and found that *Phyllocladoxylon* was the most abundant type out of all the conifer woods identified (45%) (see Figure 7.2). *Agathoxylon* and *Podocarpoxyton* consisted of 30% each of conifer types identified. The Cupressaceae had a minor presence in the forests with *Cupressinoxylon* consisting of 2% of the conifer identified. In addition to this Pujana *et al.* (2015) identified *Protophylocladoxylon* wood from the Cross Valley Formation (Late Paleocene), which is the first documentation of this genus in the Paleocene strata of Antarctica.

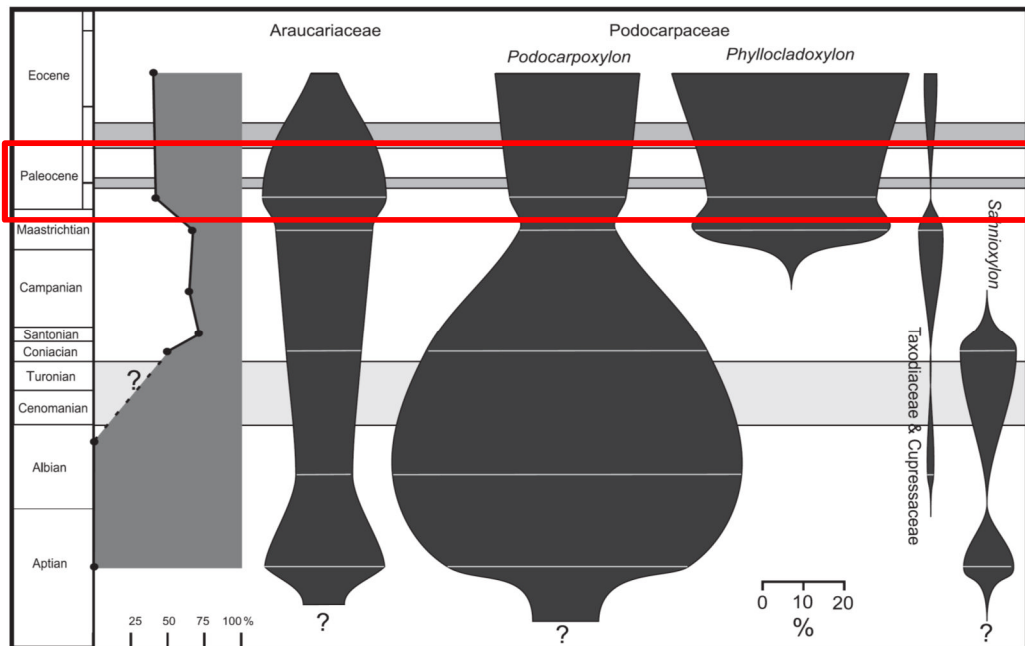


Figure 7. 2. Abundance of conifer genera and families identified through the Cretaceous and Early Paleocene from Cantrill and Poole (2005). Graph to the left presents the abundance of conifer wood relative to angiosperm wood. Dark grey balloon diagrams represent the abundance of conifer genera. Thin white lines represent where data was collected. Dark grey horizontal shaded areas represent non-deposition. Light grey horizontal shaded bands show where no flora has been collected. The red box highlights the Paleocene. Diagram taken from Cantrill and Poole (2005).

In both the wood and leaf record the Nothofagaceae is the most abundant and diverse family. The genus *Lophozonia* has been noted to be the main sub-genus of the family Nothofagaceae documented in the wood record (Cantrill and Poole, 2005). *Nothofagoxyton* wood species present include: *N. scalariforme*, *N. ruei*, *N. kraeuseli*, *N. aconcaguaense*, *N. triseriatum* and *N. corrugatus* (Poole, 2002; Cantrill and Poole, 2005). Other angiosperms were present in the Paleocene forests, although they were less important (Cantrill and Poole, 2005). They include: *Antarctoxyton*, *Weinmannioxyton*, *Illicioxyton*, *Atherospermoxyton*, *Eucryphioxyton* and *Myrceugenelloxyton* (see Figure 7.3).

The conifer types identified in this study are the same as those recorded in the published record and *Agathoxyton* and *Phyllocladoxyton* were also found to be the most abundant taxa. This gives further evidence that conifers were major components of the Paleocene forests. Similar to the published records (Cantrill and Poole, 2005). Cupressaceae is also considered to be a rare

component in this study. The fact that *Protophylocladoxylon* wood is found in this study supports the findings of Pujana *et al.* (2015) but also provides new evidence that it was present throughout the Paleocene.

This project has added to the knowledge of the composition of the Antarctic forests because it is the first to formally identify and record different wood types in detail through the Paleocene period. There has been little work done identifying and formally describing fossil wood for the Paleocene (e.g. Poole, 2002; Poole *et al.*, 2003; Pujana *et al.*, 2015). *Agathoxylon*, *Phyllocladoxylon* and *Protophylocladoxylon* have not previously been documented from Early Paleocene strata on Antarctica (see Chapter 3 and 4).

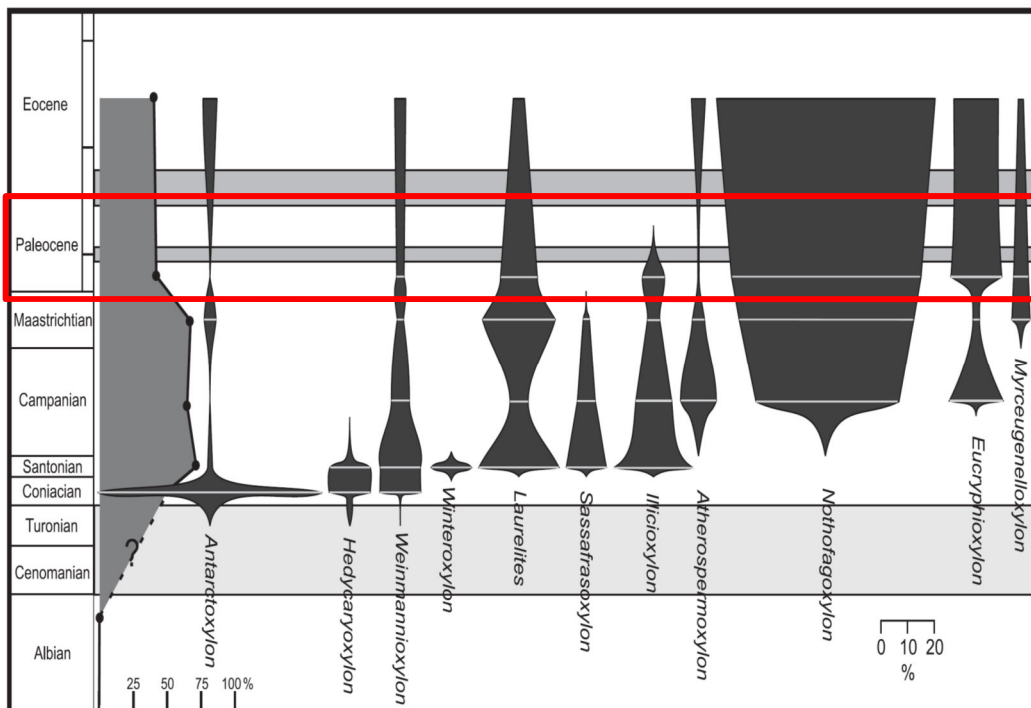


Figure 7. 3. Abundance of angiosperm genera identified through the Cretaceous and early Paleocene from Cantrill and Poole (2005). Graph to the left presents the abundance of conifer wood relative to angiosperm wood. Dark grey balloon diagrams represent the abundance of angiosperm genera. Thin white lines represent where data was collected. Dark grey horizontal shaded areas represent non-deposition. Light grey horizontal shaded bands show where no flora has been collected. The red box highlights the Paleocene. Diagram taken from Cantrill and Poole (2005).

Fossil leaves have been previously documented from mudstone layers at the top of the Cross Valley Formation (Cantrill *et al.*, 2011; Tosolini *et al.*, 2013). Leaves belonging to the conifer families Araucariaceae and Podocarpaceae have been documented which agrees with the wood record. The leaf record supports the proposal that *Nothofagus* was an important component of the Antarctic forests. Fossil *Nothofagus* leaves have been found with close taxonomic affinities to modern leaves of *Nothofagus alessandri* (genus: *Fuscospora*) and *Nothofagus obliqua* (genus: *Lophozonia*) from Chile, *N.gunnii* (genus: *Fuscospora*) from Tasmania. The leaf record from Seymour Island produces a higher diversity of angiosperm taxa compared to the wood record. Leaf taxa include: Caldcluvia (Cunoniaceae), Proteaceae, Leguminosae, Winteraceae, Lauraceae, Moraceae, Myricaceae, Illiciaceae and Atherospermaceae (Tosolini *et al.*, 2013).

Also tree ferns are present belonging to the family Osmundaceae (Cantrill *et al.* 2011). Leaf assemblages from the Dufayel Island flora and the Barton Peninsula, King George Island (Late Paleocene to Early Eocene) also show angiosperms with affinities to Lauraceae, Atherospermaceae, Sterculiaceae, Bixaceae and Cochlospermaceae, Myricaceae, Illiciaceae (Cantrill and Poole, 2012 references therein).

The collection of wood throughout the measured sedimentary succession in this study provides the most detailed study so far about the evolution of Antarctic plants and climates through the Paleocene. In terms of compositional changes, there is a change from angiosperm and conifer wood being both common in the López de Bertodano Formation and lower Sobral Formation to predominantly conifer wood at the top of the Sobral Formation (350m and above) and Cross Valley Formation. This could be related to a change in depositional environments. For instance, the upper part of the Sobral Formation is likely to represent a proximal setting due to the presence of volcanoclastic sediments. The Cross Valley Formation has been interpreted as a debris flow that carried wood from more inland areas on the volcanic arc (J Francis 2015, pers.comm., 1 September). Therefore there may have been more wood sourced from upland areas.

These findings are in agreement with the broad observations previously recorded in the fossil flora record through the sedimentary succession on Seymour Island (Cantrill and Poole, 2005; Pujana *et al.*, 2015).

Cantrill and Poole (2005) found a general trend that conifer wood becomes more abundant at the top of the Sobral Formation (80% abundance compared to angiosperm wood). They suggested the change in composition was linked to volcanic activity, although they do not state what that exact link is. A possible interpretation put forward in this current study is that the link between an increase in conifer wood and volcanic material is due to the upper Sobral Formation representing a more proximal depositional setting, or a closer volcanic source. Therefore more material including wood may have been transported from upland areas.

Conifers may have been more abundant in upland areas close to a volcanic source because they may have preferred to live in environments that undergo frequent disturbance (e.g. from volcanic activity), similar to many conifer species growing in the Southern Hemisphere today. Cantrill and Poole (2005) do not state what conifer wood types were present, and therefore it is difficult to make a stronger link between the change in the composition of the forest and volcanic activity from their study.

Cantrill and Poole (2005) also noted an influx in angiosperm wood associated with glauconitic horizons that are thought to represent transgressive events. It is thought that during these transgressional phases coastal areas were eroded including the vegetation living on them, thus a large influx of wood was input into the basin. In this current study a high abundance of wood is found at a glauconitic horizon in the López de Bertodano Formation (at 21m level on section) but there is no significant pattern in angiosperm wood and conifer wood abundances.

Recently published research on the identification of wood from volcanoclastic sedimentary units of the Cross Valley Formation (Late Paleocene) has revealed that conifer wood is dominant and angiosperm wood is rare (Pujana *et al.*, 2015) agreeing with the results in this project. Pujana *et al.* (2015) found that *Agathoxylon* was the most abundant wood type present, consisting

of 56% of the wood types identified. Other conifer wood types identified by Pujana *et al.* (2015) included *Podocarpoxyton*, *Phyllocladoxyton*, and *Cupressinoxyton*. Only one angiosperm was identified and this has been assigned to subclass Magnoliidae. *Agathoxyton* was not found to be abundant in the Cross Valley Formation in this project, instead *Protophyllocladoxyton* was more abundant. However, most of the wood was poorly preserved making it impossible to identify them, so there may actually be a higher abundance of Araucariaceae in this study.

The dominance of conifer wood and in particular *Agathoxyton* wood found by Pujana *et al.* (2015) further supports the theory put forward here that the wood from the Cross Valley Formation may have been derived from upland areas because modern trees of the family Araucariaceae are found in montane areas today. If the wood assemblage was sourced from more lowland areas it would be expected that more angiosperm wood would be present.

At the top of the Cross Valley Formation in the marine mudstone unit there is a mixed leaf assemblage which includes diverse angiosperm, conifer and ferns (Tosolini *et al.*, 2013). This may represent a return to more lowland coastal environment because in modern lowland forests in the Southern Hemisphere have higher diversity of plant species compared to upland areas (Veblen *et al.*, 1996)

7.3.2 Micro-flora (palynological record)

There is general agreement in the plant types found in the palynological records here and the published records (Askin, 1988; 1989; 1990; 1992; Bowman *et al.*, 2014). The same conifer families are present: Podocarpaceae, Araucariaceae and Cupressinaceae. In the record here and the published record Podocarpaceae is the most diverse family. Podocarpaceae pollen with affinities close to modern *Dacrydium*, *Phyllocladus*, *Lagarostrobos franklinii*, *Microcachrys/Microstrobos* and *Podocarpus* are present (Askin, 1988; 1989; 1990; Bowman *et al.*, 2014). Cupressaceae is rare in the palynological record in this study and the published records and thus suggests that these trees were uncommon in the Antarctic forests.

Bowman *et al.* (2014) recorded a sharp increase in *Phyllocladidites mawsonii* (NLR: *Lagarostrobos franklinii*) at the K/Pg followed by a rapid decrease in the

early Danian as a result of a change to cooler, less humid climates. Although abundance counts of palynomorphs were not carried out in this project, *Phyllocladidites mawsonii* is found in most of the samples analysed here through the section, suggesting it was a common component in the Antarctic forests.

Araucariacites australis (NLR: *Araucaria/Agathis*) is common in the Paleocene sedimentary deposits (Askin, 1988; 1989; 1990; Bowman *et al.*, 2014). A sharp increase of *Araucariacites australis* is recorded in the earliest Danian (50m above the K/Pg in the López de Bertodano Formation), as a result of a change to cooler climates (Bowman *et al.*, 2014). Bowman *et al.* (2014) suggested that the pollen type *Araucariacites australis* has the closest affinity to modern cool temperate *Araucaria araucana* (Monkey Puzzle tree) and is interpreted as growing at high altitudes on the Antarctic Peninsula.

Araucariacites australis is found in most of the palynomorph samples here and thus agrees that this was an important tree type in the Paleocene forests.

Previous research on palynomorphs reveal angiosperms were present within the Paleocene forests and these include: Nothofagaceae, Proteaceae, Cunoniaceae, Myrtaceae, Ericales, Liliaceae, Ranunculaceae and Casuarinaceae, Loranthaceae, Sapindaceae and Stericuliaceae (Askin, 1988; 1990; 1992; Bowman *et al.*, 2014).

Nothofagaceae is the most dominant angiosperm present during the Paleocene and all sub-genera of the family are present (e.g. *Nothofagus*, *Fuscospora*, *Lophozia* and *Brassii*) (Askin, 1989; 1990; Bowman *et al.*, 2014). The family Proteaceae is common during the Late Cretaceous and earliest Paleocene. However, Bowman *et al.* (2014) recorded that most species in the Late Cretaceous and earliest Paleocene are rare with the exception of *Peninsulapollis gillii*. This species is also common in the palynomorph assemblage in this study. Cunoniaceae is rare in the pollen record and only mentioned in Askin (1992). Cranwell (1959) documented small grains of possible affinity to Cunoniaceae (cf *Weinmannia*) from Seymour Island.

Most of the angiosperm taxa mentioned above are present in the pollen record in this study, however, Ericales, Liliaceae, Ranunculaceae,

Aquifoliaceae, Loranthaceae, Sapindaceae and Stericuliaceae are absent. Nothofagaceae is commonly found in all the palynology samples analysed here. Although only two types of *Nothofagus* pollen were fully identified (*Nothofagidites senectus* and *Nothofagidites flemingi*), it is likely that more types are present but due to them being folded over or poor preservation it was difficult to identify all of the *Nothofagus* pollen to species level.

Similar to the published record Proteaceae also appears to be diverse here with four taxa present (*Peninsulapollis askinae*, *Peninsulapollis gillii*, *Proteacidities pseudomoides*, Proteaceae sp.cf *P.scaboratus*). Possibly more species were present, but some were just identified to genus level because their identity was uncertain. *Peninsulapollis askinae* and *Peninsulapollis gillii* are the most common types.

Pteridophytas and Bryophyta have previously been documented and most of the same taxa are found in the palynology samples here: *Azolla* sp., Blechnaceae, *Microsorium*, Selaginellaceae, Lycopodiaceae, Cyatheaceae, Sphagnaceae and Osmundaceae (Askin, 1988; 1990; 1992 references therein, Bowman *et al.*, 2014). *Steirosporites* spp. (Sphagnaceae) and *Laevigatosporites* spp. (Filicospsida, Blechnaceae) are the most abundant taxa present (Askin, 1990). Bowman *et al.* (2014) recorded a major increase in these two species at the K/Pg and 50m above. *Cyathidites minor*, *Osmundacidites wellmanii*, *Retriletes austroclavatidites* are minor components in the Danian (Bowman *et al.*, 2014). The high abundance of *Steirosporites* spp. and *Laevigatosporites* spp. is also reflected in this study because they are found in every sample. *Retriletes austroclavatidites* was more infrequently present.

The reconstruction of the Late Cretaceous and earliest Danian Antarctic forests by Bowman *et al.* (2014) based on detailed analyses of palynomorphs show close similarities to the forest reconstruction in this study based on wood and palynomorphs samples. Bowman *et al.* (2014) indicates that the lowland forests on the Antarctic Peninsula were warm temperate and humid. Overstorey niches were dominated by *Nothofagus* and Podocarpaceae (e.g. *Lagarostrobos franklinii*, *Dacrydium*, *Phyllocladus* and other Podocarp trees). Understorey niches and the floors of the forests were occupied by ferns, tree

ferns and sphagnum moss. In more open and well drained areas Proteaceae are likely to have grown. Upland floras were dominated by *Araucaria* trees that grew in open forests on well drained soils in cool temperate and less humid conditions. Above the treeline heathland may have been present composed of *Microcachrys* and Ericaceae. Some of the plant taxa such as Ericaceae are not recorded in this project. The tree type *Weinmannia*, which is recorded in the wood assemblage in this study, is not recorded by Bowman *et al.* (2014) in the pollen record.

Bowman *et al.* (2014) noted an increase in *Araucariacites australis* pollen in the Danian and suggested that *Araucaria* may have extended to slightly lower altitudes during this time of cooling. In this project *Agathoxylon* wood is common in the López de Bertodano Formation (Danian) at the same stratigraphic level mentioned by Bowman *et al.* (2014) and may suggest further support for the possible extension of *Araucaria* trees to lower altitudes.

7.3.3 Comparison with other Paleocene forests in the Southern Hemisphere

Fossil flora assemblages of Paleocene age have been documented from Argentina (Salamanca Formation, San Jorge Basin. Palaeo-latitude 50°S) Palaeo-latitude 50°S, Chile (Chorrillo Chico Formation, present day latitude 55°S) New Zealand (Canturbury Basin palaeo-latitude 55°S) and Australia (Gibson Basin, palaeo-latitude 60°S), (Greenwood, 2003; Nishida *et al.*, 2006; Brea *et al.*, 2011; Pancost *et al.*, 2013). The above fossil flora assemblages have the same families present as in this study. These include Nothofagaceae, Araucariaceae, Podocarpaceae, Proteaceae, Myrtaceae and Cunoniaceae.

Fossil pollen and leaves in the Gibson Basin (Australia) reveal that conifer trees and *Nothofagus* dominated south eastern Australian forests in the Late Paleocene (Greenwood, 2003). This is comparable to the reconstruction of the Antarctic forests in this project. Petrified forests in southern Argentina of Danian age indicate dense warm temperate podocarp forests (Brea *et al.*, 2011). Palm trees which are found in tropical to sub-tropical forests today were also present in the Paleocene forests of Argentina and southern Australia (Greenwood, 2003; Brea *et al.*, 2011). The absence of sub-tropical

flora in the Antarctic forests is due to the continent being at higher latitudes compared to the above mentioned sites and thus had a cooler climate.

Podocarps were diverse in New Zealand similar to this study (Pole and Vajda, 2009; Pancost *et al.*, 2013). However *Araucaria* macro-flora and pollen become rare in the Paleocene stratigraphy on New Zealand and is instead replaced by *Agathis* (Pole and Vajda, 2009). In southern Chile fossil wood assemblages taxa including *Nothofagoxylon*, *Weinmannioxylon* and *Podocarpoxyton* and *Phyllocladoxylon* are present and reveal a cool temperate forest very similar to the Antarctic Peninsula (Nishida *et al.*, 2006).

7.4 Comparison with modern Southern Hemisphere forests

The Paleocene forests of Antarctica that have been reconstructed in this project share a taxonomic floral composition with modern warm and cool temperate forests of Tasmania, New Zealand and the Valdivian forests that occur in southern Chile and Argentina. These regions have mild all year climates with high rainfall (Veblen and Ashton, 1978; Hill *et al.*, 1988; Jarman *et al.*, 1991; Veblen *et al.*, 1995; Ogden and Stewart, 1995; Wardle *et al.* 2001) and share the same plant families including Nothofagaceae, Podocarpaceae, Cupressinaceae and Araucariaceae (not found in Tasmania) (Dettmann, 1989; McLoughlin, 2001). This is due to the fact that these landmasses were joined together forming the super-continent Gondwana in the Mesozoic. Provincialism of species occurred during the break-up of Gondwana and as a result these regions also have endemic species and differences in forest composition.

This section will discuss how the Paleocene forests of Antarctica compare to the modern forests of Tasmania, New Zealand and southern South America with regards to composition, structure and forest processes. The section will finish with an overall discussion to summarise which of these modern forests the Paleocene fossil Antarctic forests most resemble.

7.4.1 Tasmanian forests

The cool temperate rainforests of Tasmania are located in the western and central areas of the Island where mean annual rain fall is high (>1500 mm per year) (Jarman *et al.*, 1991). The dominant tree types that characterise the

Tasmanian forests are similar to those found in the fossil pollen and wood record here. These include *Lagarostrobos franklinii*, Nothofagaceae, *Phyllocladus*, Cupressaceae (e.g. *Athrotaxis*, *Diselma*) and Myrtaceae (Eucalyptus) (Beadle, 1981; Jarman *et al.* 1991). All the trees in the Tasmanian forests are evergreen, except *Nothofagus gunnii* (Brown and Read, 1996). Other dominant tree types that are found in the Tasmanian forests are not found in the fossil record in this study, are *Eucryphia* and *Atherosperma* (Beadle, 1981; Jarman *et al.*, 1991). However, Poole *et al.* (2003) have previously found Eucryphiaceous fossil wood in the Sobral Formation on Seymour Island.

Tree types *Araucaria*, *Luma*, *Dacrydium* and *Weinmannia* that are found in the fossil floral record in this study are not found in Tasmania today. The family Casuarinaceae, which is found in the fossil pollen record in this study, is only found on the drier eastern side of Tasmania, usually forming the undergrowth in Eucalyptus woodlands or in rocky coastal areas (Beadle, 1981). The Tasmanian forests also have a diverse understorey flora which consists of ferns, mosses, conifers and angiosperms (Jarman *et al.*, 1991). Some taxa are present in the pollen record in this study such as Proteaceae, Myrtaceae, Podocarps (*Microcachrys* and *Podocarpus lawrencei*), Blechnum (fern) and Cyatheaceae (fern).

The forests of Tasmania are split into four main types: Callidendrous, Thamnic, Implicate, and montane forests (Jarman *et al.*, 1991). The first three forests types are widespread over western and central Tasmania and occur from sea level to 1000m and contain most of the dominant tree types (e.g. *Lagarostrobos franklinii*, *Phyllocladus*, *Nothofagus*, *Atherosperma* and *Eucryphia*) in different proportions. The main differences between the forests are tree height and complexity of the undergrowth.

Unlike the forests of New Zealand and South America, most of the trees in the Tasmanian forests can re-generate without frequent large scale disturbances (Read and Hill, 1985; Read and Hill, 1988; Brown and Read, 1996). The montane forests are confined to the montane areas of central Tasmania (above 900m) and are dominated by conifers, in particular Cupressaceae (*Athrotaxis*). *Nothofagus cunninghamii* and *Nothofagus gunnii* also occur as

stunted trees with multiple stems (Jarmen *et al.*, 1991). Above the treeline, alpine heathland and scrub is present and consists of small shrubs of Podocarpaceae (*Microcachrys* and *Podocarpus lawrencei*), ferns and angiosperms (Beadle 1981). The main controls on these forests are soil type, altitude and disturbance such as forest fires. Most species within these rainforests do not regenerate well after forest fires and instead are replaced by Eucalyptus forests (Ogden and Powell, 1979).

The lowland forests on the Antarctic Peninsula are likely to have had a similar overstorey composition to the closed canopy Thamnic and Implicate forests because the main tree types in these forests are *Lagarostrobos franklinii*, *Phyllocladus* and *Nothofagus*. These forests grow on intermediate to poorly fertile soils and tree height ranges from 8 – 20m tall (Jarman *et al.*, 1991). It is possible that the Antarctic forests grew on similar soil types and trees were of similar height to those of the above mentioned forests. The obvious differences between the Antarctic forests and Thamnic and Implicate forests is the absence of *Eucryphia* and *Atherosperma* in this study. *Dacrydium* is present in the Antarctic forest but absent in the modern Tasmanian forests. From the pollen record in this study the understorey layer in the Antarctic forests were likely to have had a lower diversity of plants compared to the modern Thamnic and Implicate forests.

The high-altitude forest reconstructed for the Antarctic Peninsula does have some similarity to the montane forest in Tasmania with regards to conifers being the main canopy forming trees. They are also likely to have had the same open canopy structure with a sparse understorey as evidenced by the low diversity of shrub and fern taxa present in the palynology record in this study.

Similar to the Tasmanian forests, the Antarctic upland forest understorey is likely to have included *Nothofagus* spp., Proteaceae spp. and ferns. Sphagnum moss may have formed on trees and on the ground because these are present in the palynological samples throughout the sedimentary sequence. Above the Antarctic forest tree-line, heathland and scrub may have also been present and is likely to have consisted of *Microcachrys* and other Podocarps in the form of low shrubs (Figure 7.4).



Figure 7. 4. Alpine heathland of Tasmania, which consists of low lying shrubs. The heathlands above the treeline on the Antarctic Peninsula are thought to have been similar to this. Taken from <https://farm6.static.flickr.com>.

7.4.2 New Zealand Forests

New Zealand has both warm and cool temperate forests and they are evergreen (Ogden and Stewart, 1995). The warm temperate forests occupy low to mid altitudinal (sea level to 600m.a.b.s.l) areas on North Island and they are mixed conifer and broad-leaved forests and are characterised by *Agathis australis* (north of 38°S) (Ogden and Stewart, 1995). Cool temperate forests mainly occupy South Island, but they also occur at high altitudes on North Island (south of 38°S). They are less diverse than the warm temperate forests.

The forests most similar to the Paleocene forests of the Antarctic Peninsula are those of the cool temperate mixed *Nothofagus* forests present in North Island and northern South Island in montane areas, and southern South Island at low altitudes (Figure 7.5). Common tree types other than *Nothofagus* include Podocarpaceae (*Dacrydium*, *Phyllocladus*, *Halocarpus*) and Cupressaceae (*Libocedrus*) (Ogden *et al.*, 1996). Broad-leaved angiosperms trees form the sub-canopy such as *Weinmannia*, *Myrtaceae* spp., *Quintinia*,

Ixerba and *Elaeocarpus*. However, in southern South Island there is less diversity in broad-leaved trees compared to the northern mixed *Nothofagus* forests. Tree-ferns and ferns form (e.g. *Cyathea* and *Blechnum*) the understorey of the mixed *Nothofagus* forests (Figure 7.5). These forests occupy poorly fertile soils and have open canopies (Ogden *et al.*, 1996). In montane areas they grow on slopes prone to disturbances because *Nothofagus* species in New Zealand are shade-intolerant and rely on disturbances to regenerate. Due to similarities in composition it is possible that the Antarctic forests lived under similar cool temperate climates and on poorly fertile soils.

The warm temperate conifer-broad leaved forests of New Zealand from sea level to 600 m do have similar taxa to the Antarctic forests such as, *Dacrydium* (*Dacrydium cupressinum*), *Phyllocladus* (*Phyllocladus trichosperma*), Cupressaceae (*Libocedrus plumose*) and a number of podocarp species, *Weinmannia* and Proteaceae (only *Knightia*) (Wardle, 1991, Ogden and Stewart, 1995). *Agathis australis* is the canopy dominant in these forests and usually forms a closed canopy. The fossil Araucariaceae trees that once lived on the Antarctic Peninsula are thought to be more like the cool temperate *Araucaria araucana* that live at high altitudes on the slopes of the southern Andes, Chile. Evidence for this is based the presence of *Agathoxylon* wood that is charcoalified suggesting that it had a similar life strategy; the fossil wood also has growth ring widths that resemble those of *Araucaria araucana* (further discussed in section 7.6). Further evidence for this is derived from palynological research conducted by Bowman *et al.* (2014) who found that *Araucariacites australis* is most abundant in the cool temperate and less humid climates during the latest Cretaceous and earliest Paleocene.

The modern warm temperate forests of New Zealand are different from the Antarctic forests because they have a higher diversity of angiosperm families which are not present in the fossil record in this study.



Figure 7. 5. Mixed *Nothofagus* forests, New Zealand. The lowland Antarctic forests are considered to have had a similar open canopy structure and an understorey consisting of ferns. Photo taken from www.landcareresearch.co.nz

7.4.3 Forests of Chile

The Valdivian forests occur between latitudes between 37°45' to 43°20' °S and they predominantly occupy the western slopes of the Andes (Chilean side) but they are also found on the eastern side (Argentina) (Veblen *et al.*, 1995). The northern Patagonian forests (43°S to 47°S) and the temperate southern *Nothofagus* forests and wood land (37°S to 55°S) occupy higher latitudes. These forests occur predominantly on the western side (Chile) of the Andes, but they do also occur on the eastern side (Argentina).

The western side of the Andes has higher rainfall than the east (western side >1500 mm per year, eastern side 500 mm per year) (Veblen *et al.*, 1995). As a result the forests on the eastern side are less diverse and are dominated by conifers (e.g. *Araucaria araucana* and Cupressaceae) and *Nothofagus pumilio* and *Nothofagus antarctica*, which can tolerate dry conditions (Veblen *et al.*, 1995; Veblen *et al.* 1996). The east and west forests share a number of species but the Valdivian forests are the most diverse. The *Nothofagus* forests and woodlands are the least diverse. In the northern part of the distribution they occur at high altitudes and are found at low altitudes in the most southern distribution (Veblen *et al.*, 1995; Veblen *et al.* 1996).

This section is going to focus on the wetter western side of the Andes because it has common species with the Antarctic forests. In addition the coexistence analysis suggests wet rainforests (discussed further in section 7.6).

Large scale disturbances such as volcanic activity and earthquakes have a major effect on the composition of these forests. For instance, the lowland Valdivian forests (sea level to 400m altitude) are rarely affected by large-scale disturbances and they consist of shade-tolerant broad-leaved trees (e.g. the species including *Luma apiculata* and other Myrtaceae trees), which can continuously regenerate in the absence of disturbance (Gutiérrez *et al.*, 2009) (Figure 7.6). Shade-intolerant *Nothofagus* species, which rely on disturbances to regenerate, are minor components or absent in these forests (Gutiérrez *et al.*, 2004). However, some long-lived shade-intolerant trees such as *Weinmannia trichosperma* and two podocarps species (e.g. *Saxegothea conspicua* and *Podocarpus nubigena*) can persist in these forests (Lusk 1996; 1999).

The Antarctic forests do have similar flora to the modern lowland Valdivian forests such as Myrtaceae trees, in particular *Luma apiculata* which is similar, the fossil wood type *Myrceugenelloxylon*. Despite this there are obvious differences between these modern forests and the Antarctic forests. For example, the near absence of *Nothofagus* in the lowland Valdivian forest, whereas the fossil record in this study suggests that *Nothofagus* was a common component at all altitudes in the Antarctic forests.



Figure 7. 6. Lowland Valdivian forest, Chile, with dense closed canopy and undergrowth. Taken from www.wikimedia.org.

The lowland forests on the Antarctic Peninsula would have had a similar composition of taxa to the mixed *Nothofagus* forests in Chile in terms of the dominance of *Nothofagus* and the presence of broad-leaved tree types such as Myrtaceae and *Weinmannia*, as well as conifers (Podocarpaceae and Cupressaceae) (Figure 7.7). The differences between the forests include less diversity of angiosperm trees in the Antarctic forests. For example the absence of *Eucryphia*, *Aextoxicon punctatum* and *Drimys winteri* in the wood and palynological record in this study. The Antarctic forests have a higher diversity of Podocarpaceae compared to the Valdivian forests. *Phyllocladus*, *Lagarostrobos* and *Dacrydium* are absent in the Valdivian forests. Another difference is the absence of tree ferns and the low diversity in ferns in the Valdivian forests. Bamboo is absent from the Antarctic fossil record. From the palynological record there is a higher diversity of Proteaceae compared to the modern Chilean forests.

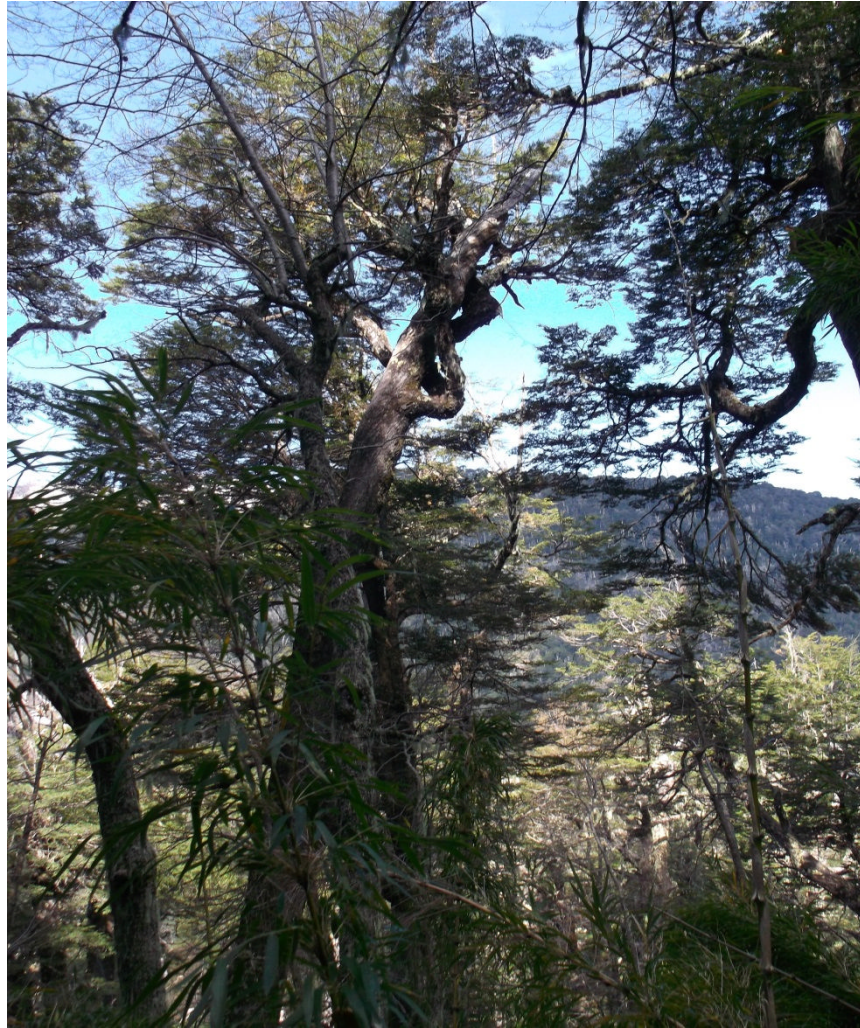


Figure 7. 7. Mixed *Nothofagus* forests in Chile. Open canopy consisting of large *Nothofagus dombeyi* trees. The main undergrowth component is bamboo (present at the bottom of the photo). Tree height approximately 30m.

The high altitude *Araucaria-Nothofagus* forests do show close similarity in terms of taxa high altitude forests reconstructed for the Antarctic Peninsula (Figure 7.8). The interpretation of fossil *Agathoxylon* and *Nothofagoxylon* tree types growing at high altitudes is mainly based on their nearest living relatives (see chapter 5). Some wood specimens at the top of the Sobral Formation are partly charred, which gives evidence that these wood specimens may have had a similar life strategy to *Araucaria araucana* and southern South American *Nothofagus* spp., such as growing in areas prone to large scale disturbances such as wild-fires caused by volcanic activity. Most of the wood specimens that have rounded edges are also *Agathoxylon* and therefore this

could be interpreted as further evidence that the wood has been transported long distances.



Figure 7. 8. *Araucaria-Nothofagus* open woodland. *Araucaria araucana* trees projecting above a canopy of stunted *Nothofagus* trees (deciduous *Nothofagus pumilio*). The undergrowth is sparse. The high altitude forests on the Antarctic Peninsula are thought to have been similar, maybe stunted trees of *Phyllocladus*, and other trees belonging to Podocarpaceae and Cupressaceae may have also been present.

7.4.4 Antarctic forests compared to modern analogues

The collective analysis of taxonomy and preservation of the fossil wood and palynomorphs and associated sediments has revealed that the Antarctic forests have a mixed resemblance to the modern forests of Tasmania, New Zealand and southern Chile. Table 7.1 presents the main trees types that grew in Paleocene Antarctic forests from this study and those present in the modern temperate forests in the above regions.

Lowland forests on the Antarctic Peninsula were likely to be most similar to the modern mixed cool *Nothofagus* forests found on South Island, New

Zealand and the lowland mixed *Thamnic/Implicate* forests of Tasmania. The forests in these regions have the highest number of tree taxa in common with the Paleocene Antarctic forests (see Table 7.1). *Nothofagus* and Podocarpaceae trees are important components in these forests. The frequent occurrence of *Nothofagus* and Podocarpaceae type fossil wood and pollen throughout the sedimentary sequence in this study suggests that they were important in the Antarctic forests.

Dacrydium spp. and *Lagarostrobos franklinii* are present in the Antarctic fossil pollen record and the former is also present in the New Zealand forests and the latter is endemic to the Tasmanian forests. The Antarctic forests are most similar to the New Zealand mixed *Nothofagus* forest in terms of broad-leaved angiosperms trees present, specifically *Weinmannia*, which is the most important broad-leaved tree in the *Nothofagus* forests have a low diversity over other angiosperm trees.

The undergrowth in the Antarctic forests is likely to have been similar to the Tasmanian and New Zealand forests because of the presence of tree ferns and ferns. However they may have been more similar to the Tasmanian forest because, these forest have a higher diversity of Proteaceae, whereas Proteaceae is uncommon in New Zealand, with just one species *Knightia*.

The main difference is that the New Zealand and Tasmanian forests have a higher diversity of plant taxa than the Antarctic forests. The only similarity between the lowland Valdivian forests and the Antarctic forests is the presence of *Luma apiculata* in the Valdivian forests which is thought to be similar to the fossil wood type *Myrceugenelloxylon*, as well as the presence of *Weinmannioxylon*.

Poole *et al.* (2003) described fossil eucryphiaceous wood from Paleocene strata on Seymour Island and *Atherospermoxylon* is present in Paleocene flora although this has not been formally described (Cantrill and Poole, 2005). This may give further evidence that the lowland forests shared similarity to the Tasmanian forests since *Eucryphia* and *Atherosperma* is a common component of these forests.

The upland forests of Antarctica were most similar to the open canopy *Araucaria* and *Nothofagus* forests at high-altitudes in the Andes. This is primarily based on the presence of *Araucaria* and *Nothofagus* wood being found in the record in this study. In the Antarctic forests *Phyllocladus* and other podocarps and possibly Cupressaceae may have also been present in these high altitude forests because nearest living relatives grow at high altitudes in Chile, New Zealand and Tasmania. *Protophyllocladoxylon* and other conifer wood is present in the Cross Valley Formation and lithology suggests that wood within it may have been carried from upland areas. This is supported by the findings of Pujana *et al.* (2015) (refer to section 7.3.1). Most of the *Agathoxylon* wood in the study by Pujanas *et al.* (2015) is also reported to be charcoalfied giving further support that it had a similar life strategy to its nearest living relative *Araucaria araucana* in Chile.

Above the tree-line heathland similar to the heathland of Tasmania may have been present, consisting of low lying shrubs of podocarps, *Microcachrys*, Proteaceae and Casuarinaceae and Sphagnum moss.

Large scale disturbances such as explosive volcanic activity and earthquakes were likely to be important processes in the Antarctic Peninsula forest, similar to southern South America because it would have had a similar geological setting (Lawver *et al.*, 1992). Poole *et al.* (2001) presented a Valdivian model for King George Island, Antarctic Peninsula (see Chapter 1, section 1.5) because there is evidence on the island that volcanic activity played an important part in the Antarctic forest composition with low diversity fossil floral assemblages (mainly podocarps and *Nothofagus* leaves and wood) overlying debris flow deposits with volcanic clastic material. Further up the sequence a high diversity and dense floral assemblage associated with little volcanic clastic material is present and therefore suggests low disturbance flora. Therefore the trees in the Antarctic forest are likely to have had similar habitats, such as *Nothofagus* being shade-intolerant similar to the types in Chile and New Zealand that rely on large scale disturbances to persist in the forest. The more shade tolerant trees are likely to have grown in lowland areas. Table 7.1 shows that the Paleocene forests of Antarctica contained components of all three modern forests in Tasmania, New Zealand and

southern South America. The Antarctic forests can thus be considered as the ancestors of the modern Southern Hemisphere vegetation.

Table 7. 1. The main tree types found in the Antarctic forests and their presence in the modern temperate forests of Tasmania, New Zealand and southern South America. ✓ = tree taxa is present and ✗ = tree taxa is absent.

Main tree types present in this study.	Modern forests		
	Tasmania	New Zealand	southern South America
Araucariaceae	✗	✓ <i>Agathis australis</i>	✓ <i>Araucaria araucana</i>
Podocarpaceae	✓	✓	✓
Podocarpus	✓	✓	✓
<i>Lagarostrobos franklinii</i>	✓	✗	✗
<i>Phyllocladus</i>	✓	✓	✗
<i>Dacrydium</i>	✗	✓	✗
<i>Microcachrys</i>	✓	✗	✗
Cupressaceae	✓	✓	✓
Weinmannia	✗	✓	✓
Myrtaceae	✓	✓	✓
Proteaceae	✓	✓	✓
Nothofagaceae	✓	✓	✓
Causaurinaceae	✓	✗	✗
Total common taxa	10	10	8

7.5 Climate of the Antarctic Peninsula during the Paleocene

Multiple techniques using fossil wood and palynomorphs have been conducted to reconstruct climate conditions on the Antarctic Peninsula during the Paleocene. These analyses are more detailed than has previously been undertaken using fossil wood. The exact location of individual specimens on a sedimentary succession has allowed insight into climate trends through this time, as well as considerations about possible environments that the wood

has originated from. Knowing the identity of the wood has allowed comparisons with modern relatives which has revealed possible reasons for the climate signals recorded in the wood. Furthermore, for the first time specific gravity has been calculated for fossil wood from Antarctica. This has allowed new insight of the ecology and growth conditions of trees that lived on the Antarctic Peninsula through comparison with the specific gravity values of nearest living relatives. It has also given further support to the interpretation of climate data derived from growth rings and angiosperms.

Overall the climate results in this study reveal that climate conditions on the Antarctic Peninsula were seasonal, cool to marginally warm temperate with sufficient rainfall. The Coexistence Analysis, using the nearest living relatives of fossil wood and palynomorphs, indicates that mean annual temperatures (MAT) were between 7 - 13°C and mean annual precipitation (MAP) was between 1000 – 2489mm per year. Although climates are likely to have been mild all year around, winters are likely to have been cool and wet (cold month mean temperature: 6.6 – 9.1°C and mean precipitation wet month: 107 – 321mm) and summers warm and drier (warm month mean temperature: 18 – 19.6°C and mean precipitation dry month: 38 – 90mm per year).

The climate conditions are within the range of modern climates of New Zealand, western/central Tasmania and southern Chile which have a combined mean annual temperature range between 7 - 15°C and mean annual precipitation range between 500 – 5000mm per year (Veblen and Ashton, 1978; Hill *et al.*, 1988; Ogden and Stewart, 1995; Wardle *et al.*, 2001). Previous results from Coexistence Analysis undertaken by Poole *et al.* (2005) is in general agreement with results here as they indicate a warm to cool temperate climate. The Coexistence Analysis conducted by Poole *et al.* (2005) included 600 wood specimens collected by the authors, plus wood specimens collected by other researchers. In addition, nearest living relatives of published palynomorph and leaf types from Antarctica were also included. Poole *et al.* (2005) results are presented in Table 7.2 alongside the Coexistence Analysis results in this study. The Coexistence Analysis results by Poole *et al.* (2005) also propose a cool to warm temperate climate and the results in this study generally fit into their ranges. However, their mean annual

temperatures and warm month mean temperatures for the latest Early Paleocene are warmer with maximum temperatures of 18°C and 23°C.

Mean annual precipitations ranges by Poole *et al.* (2005) are lower than those recorded here, suggesting drier conditions, although when Poole *et al.* (2005) calculated average MAP values that included results from other techniques using leaf morphology (e.g. Leaf Margin Analysis (LMA) and Climate Leaf Analysis Multivariate Program (CLAMP)) and wood physiognomy (e.g. multivariate anatomical analysis) they yielded values of 2448mm per year and 1721mm per year for the Early Paleocene to the latest Early Paleocene. This is closer to the range in this study. The difference between the two records is likely to be due to different taxa being included in the two studies.

The results here are also in close agreement with the MAT produced by Bowman *et al.* (2014) for lowland floras (10 – 15°C) and upland floras (5 – 8°C) on the Antarctic Peninsula for the earliest Danian. A cool temperate climate is supported by an increase in the importance of Nothofagaceae, Podocarpaceae and Araucariaceae as observed here and in previously published fossil wood and palynomorphs records (Cantrill and Poole, 2005; Bowman *et al.*, 2014).

Growth ring analysis reveals that all of the wood specimens had visible growth rings, giving further support for a seasonal climate. Plotting mean growth ring width (MGRW) and mean sensitivity (MS) for both individual wood specimens and as average values for each formation has revealed that climates became less favourable for tree growth from the Early Paleocene (López de Bertodano Formation average MGRW = 1.98mm) to the Late Paleocene (Cross Valley Formation average MGRW = 0.45mm).

Table 7. 2. Results for the Coexistence Analysis undertaken by Poole *et al.* (2005) and this study for mean annual temperature (MAT), cold month mean temperature (CMMT), warm month mean temperature (WMMT), mean annual precipitation (MAP), mean precipitation dry month (MPDM), mean precipitation wet month (MPWM).

Climate parameters	Poole <i>et al.</i> (2005) Early Paleocene	Poole <i>et al.</i> (2005) latest Early Paleocene	This study (Paleocene)
MAT (°C)	12.2 - 13	11.1 - 18.1	7 -13
CMMT (°C)	7.6 - 11.8	7.6 - 7.7	6.6 - 9.1
WMMT (°C)	16 - 18	15.2 - 23.9	18 - 19.6
MAP (mm)	652 - 691	574 - 1215	1000 - 2489
MPDM (mm)	17 - 29	25 - 37	38 - 90
MPWM (mm)	58 - 183	148 - 183	107 - 321

Previous research on growth rings in Paleocene wood has been undertaken by Francis (1986) and Francis and Poole (2002). Francis and Poole (2002) calculated average MGRW for each stratigraphic formation for the Paleocene (López de Bertodano, Sobral and Cross Valley formations). They calculated average MGRW for conifer and angiosperm wood together and just conifer wood. Their results for average MGRWs for each formation that includes both conifer and angiosperm wood are presented in Figure 7.9 and Table 7.3 and average MGRW results from this current study are also plotted in the same figure for comparison. The results by Francis and Poole (2002) that included conifer and angiosperm wood was plotted in Figure 7.9 because both wood types are included in the average MGRW results in this study. The average MGRW results by Francis and Poole (2002) using just conifer wood are presented in Table 7.3 for further comparison.

Overall the average MGRW results by Francis and Poole (2002) and the MGRW results in this study show a similar trend with cooling from the latest Cretaceous to the mid-Paleocene. However, Francis and Poole (2002) results show a dramatic increase in MGRW from in the Sobral Formation to the Cross Valley Formation (Figure 7.9, Table 7.3). Their study is at a lower resolution

then here as they used fewer samples in the Sobral Formation (5 specimens), only one mean value is taken for each formation and the exact location of the specimens on the formations is unknown. Francis (1986) produced a single number for the Tertiary based on 6 wood specimens (2.25mm) which is within the range here.

The wood morphotypes here have growth rings that are comparable to their nearest living relatives in cool temperate Chile and Australasia (see Chapter 6, section 6.4.4). In particular, *Agathoxylon* has growth ring widths similar to those of *Araucaria araucana* and *Nothofagoxylon* woods have similar growth ring widths to modern *Nothofagus* that grow at high altitudes in Chile and New Zealand (Norton, 1983a,b; Lara *et al.*, 2001; 2005; Massaccesi *et al.*, 2007; Mundo *et al.*, 2012; Muñoz *et al.*, 2013). This contrasts with the findings of Francis (1986) who found that *Agathoxylon* and *Nothofagoxylon* growth rings were wider than their modern relatives in Chile.

In the present study the majority of wood specimens show sensitive growth suggesting the trees grew under a fluctuating climate where water was likely to be the limiting factor. Francis (1986) and Francis and Poole (2002) recorded values below 3 for MS, suggesting growth under equable climates, opposite to what is found here. Interestingly the wood specimens that show sensitive growth here are mostly *Agathoxylon* and *Nothofagoxylon*. Today these trees live in open woodlands and well drained poorly fertile soil and it is likely that the fossil tree types grew in similar environments. In these more exposed areas trees may have been more sensitive to climate factors such as low moisture availability due to the increased effect of temperature and wind on the evaporation of water from soil (Fritts, 1976). The wood morphotypes are not mentioned in the published studies so it is difficult to make any direct comparisons.

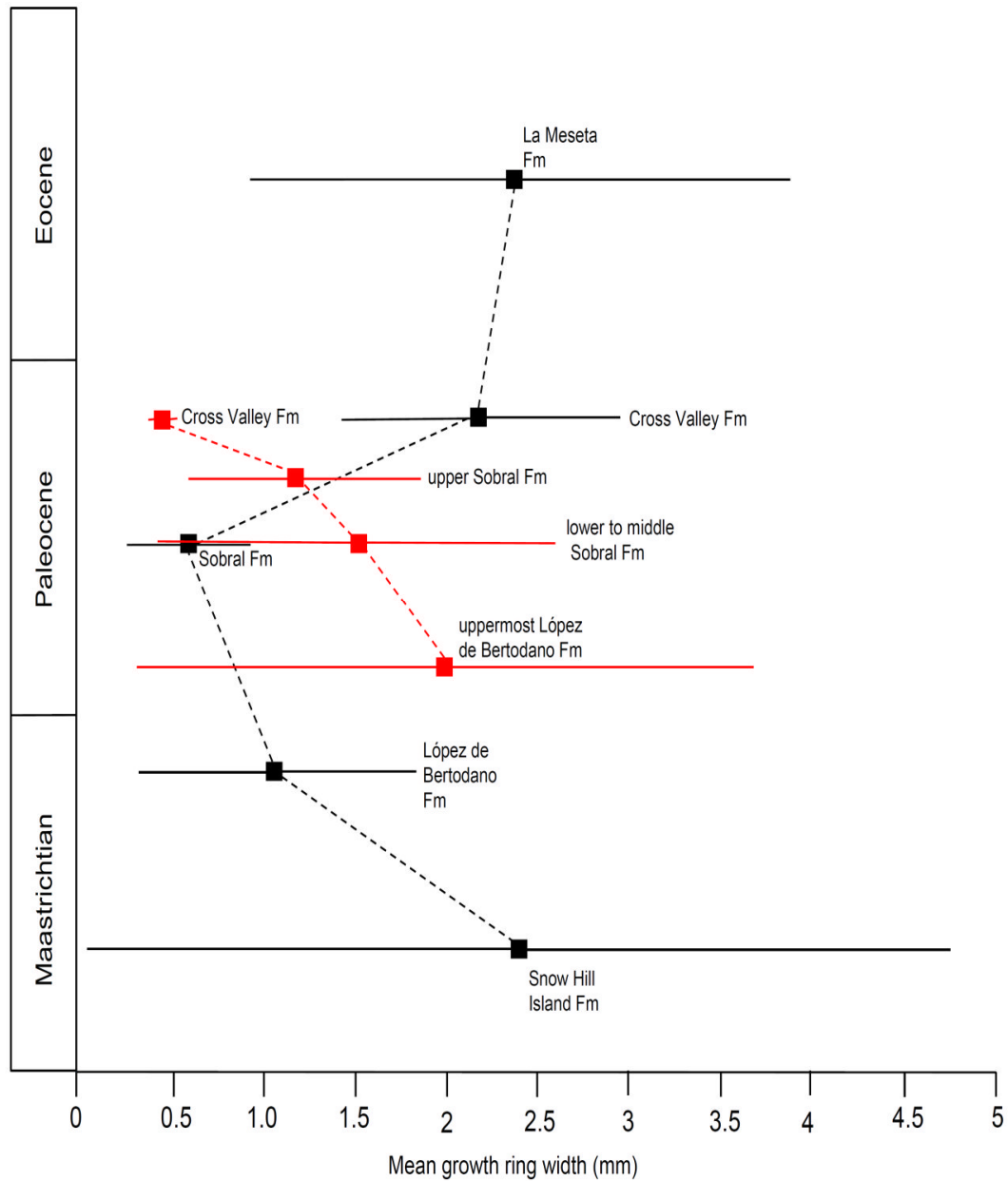


Figure 7. 9. Results from Francis and Poole (2002) (Black) of average mean growth ring width (conifers and angiosperms) for each stratigraphic formation from the Maastrichtian (Cretaceous) to the Eocene in the Antarctic Peninsula region. Data in red represents the results recorded here for average mean growth ring widths for the upper Lopez de Bertodano Formation, Sobral Formation (lower to middle and upper) and Cross Valley Formation. Horizontal lines in both red and black represent standard deviation.

Table 7. 3. The average mean growth ring widths (MGRW) calculated for the, Snow Hill Island, López de Bertodano Formation, Sobral Formation, Cross Valley, Formation and La Meseta Formation by Francis and Poole (2002). C = conifer and A = angiosperm. The average MGRW calculated for the López de Bertodano, Sobral (lower to middle and upper) and Cross Valley formations.

Formations and their age range	Francis and Poole (2002)				This study	
	MGRW (C & A)	Standard deviation	MGRW (C only)	Standard deviation	MGRW	Standard deviation
Snow Hill Island (Maastrichtian)	2.43	2.33	1.58	0.91	N/A	N/A
López de Bertodano (Late Maastrichtian to Early Paleocene)	1.08	0.74	1.09	0.8	N/A	N/A
uppermost López de Bertodano	N/A	N/A	N/A	N/A	1.98	1.67
Sobral Formation (Early to Late Paleocene)	0.57	0.32	0.57	0.32	N/A	N/A
lower to middle Sobral	N/A	N/A	N/A	N/A	1.52	1.1
upper Sobral	N/A	N/A	N/A	N/A	1.22	0.64
Cross Valley (Late Paleocene)	2.22	0.76	2.16	0.82	0.45	0.03
La Meseta (Eocene)	2.42	1.45	2.11	0.82	N/A	1.67

False rings are found in four wood specimens in this study, three of them are *Agathoxylon*. Poole *et al.* (2005) also found false rings in Early Paleocene wood suggesting that water availability may have been poor at certain times, although they do not say how many specimens had false rings or how often they occurred within each specimen.

The majority of angiosperm wood specimens in this study have characteristics indicative of temperate climates. Francis and Poole (2002) and Poole *et al.* (2005) also found that the majority of angiosperm wood specimens that are Paleocene in age also had anatomical features characteristic of temperate climates. These include: ring porous or semi-ring porous, scalariform perforation plates, low number of grouped vessels and vessel abundance $>100\text{mm}^2$.

The Mesomorphy and Vulnerability Index are indicators of water availability. Here the Mesomorphy Index was considered to a better indicator of water availability than the Vulnerability Index here based on more consistent results and also previous findings of experimental work on modern angiosperm wood (Lens *et al.*, 2011). The results suggest that water was sufficient on the Antarctic Peninsula with all values above 300. Poole *et al.* (2005) recorded results over 300 for the Mesomorphy Index for wood of Early Paleocene (value of 341) and latest Paleocene age (value of 321), which also suggests sufficient water availability.

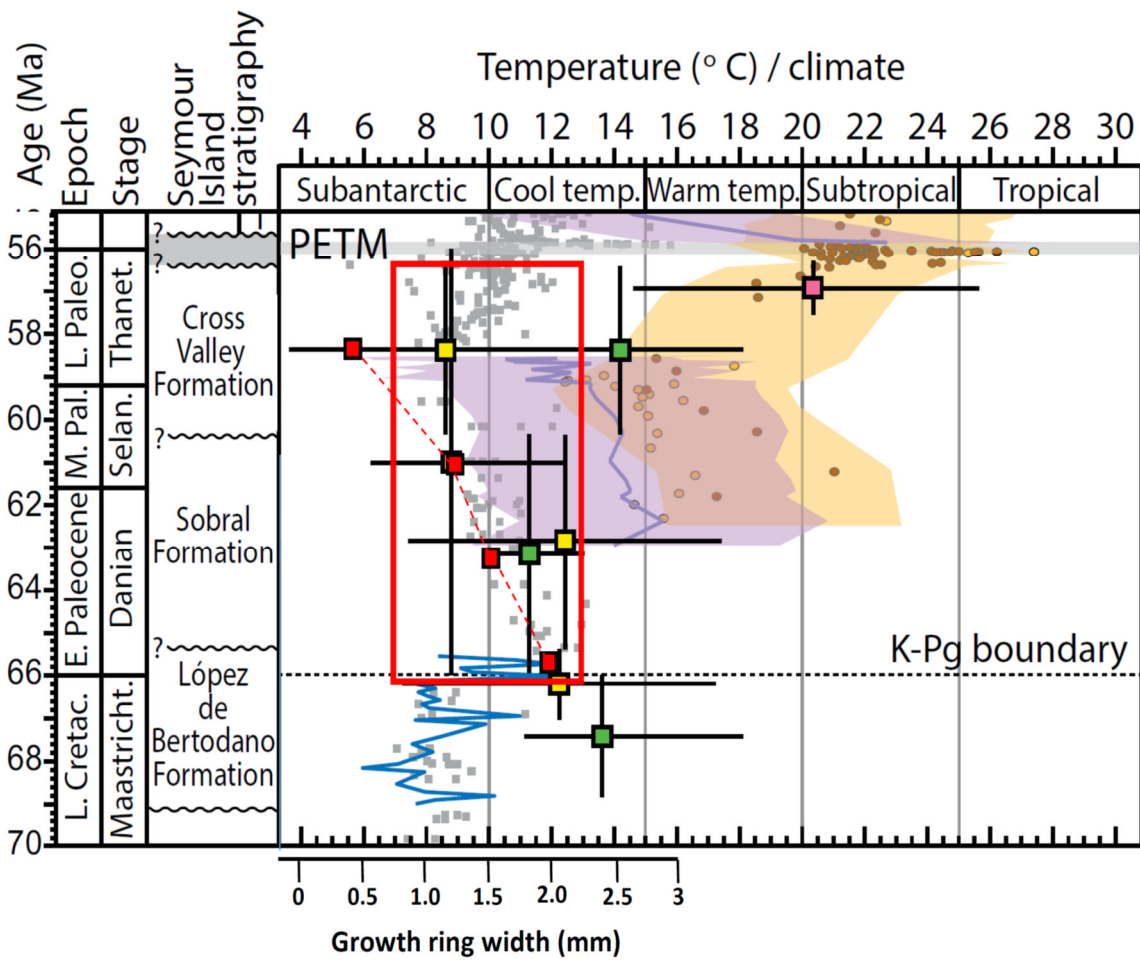
Specific gravity gives further evidence that the trees on the Antarctic Peninsula are likely to have grown under similar conditions and had similar ecologies to their NLRs growing in the Southern Hemisphere today. This is because specific gravity values for wood morphotypes *Agathoxylon*, *Phyllocladoxylon* and *Nothofagoxylon* are similar to the values of their modern relatives (*Araucaria*, *Nothofagus* and *Phyllocladus*) which grow in New Zealand, Chile and Tasmania today where climates are mild and water availability is sufficient. A narrow range of specific gravity values were recorded here (0.50 – 0.80) for the fossil wood specimens. This is further evidence of a temperate climate because modern temperate forests have less variation in wood specific gravity compared to tropical forests which contain trees that have wood with very low and very high specific gravity.

Mean annual temperatures here are within close range of those produced from MBT/CBT proxies for the same sedimentary succession by Kemp *et al.* (2014). Their results are shown in Figure 7.10 with the MATs recorded for Seymour wood also plotted. They produced MATs of 15°C for the Early Paleocene and 8°C for the Late Paleocene. This cooling trend is also in agreement with a decrease in mean growth ring widths from the Early to Late Paleocene observed in the fossil wood in this study, suggesting that this could be a true climate signal. The MATs here are also in agreement with the seas surface temperatures, which are suggested to have been around 8 - 14°C.

In terms of a wider context, the Paleocene climate reconstructions for Antarctica undertaken in this study fit well with previous studies that have investigated Paleocene climates in other high latitude regions in the Southern Hemisphere.

Mean annual temperatures recorded in this study fit well with the MATs and SSTs recorded from Paleocene stratigraphy in the Canterbury Basin, off the east coast of New Zealand. Pancost *et al.* (2013) recorded MATs of 15°C for the Early Paleocene and 10°C for the Late Paleocene (58 – 59Ma) from MBT/CBT proxies. Hollis *et al.* (2012) recorded SST temperatures from TEX₈₆^L of 16°C for the Early Paleocene and 13°C for the Late Paleocene. Overall the results from the above published records and in this study agree give further support for a small latitudinal temperature gradient during the Paleocene.

The decrease in temperatures observed in New Zealand from the Early and Late Paleocene also agrees with the decrease in mean growth ring width recorded from Early to the Late Paleocene in this study. The cooling trend is also observed in the global benthic oxygen signal (Zachos *et al.*, 2001; Cramer *et al.*, 2009) which gives support that this maybe a global change in climate and that the growth ring data here is a climate signal.



SEYMOUR ISLAND DATA	
<ul style="list-style-type: none"> ■ This study: MBT/CBT (Formation averages, $\pm 5^\circ\text{C}$ error) ⚡ Tobin et al. (2012): $\delta^{18}\text{O}$ (shell) ⚡ Ivany et al. (2008): $\delta^{18}\text{O}$ (shell) ■ Poole et al. (2005): plant proxies 	<ul style="list-style-type: none"> ● Hollis et al. (2012): TEX86 (New Zealand (NZ)) ⚡ Pross et al. (2012): MBT/CBT (IODP Site U1356) (Peterse et al. 2012 recalibration and $\pm 5^\circ\text{C}$ error) ● Bijl et al. (2009): TEX86 (IODP Site 1172) (Hollis et al., 2012 recalibration and $\pm 4^\circ\text{C}$ error) ⚡ Pancost et al. (2013): MBT/CBT ($\pm 5^\circ\text{C}$ error) (NZ) ● Hollis et al. (2012): Mg/Ca (planktic foram.) (NZ)
DEEP SEA (SUBANTARCTIC)	
<ul style="list-style-type: none"> ■ Cramer et al. (2009): $\delta^{18}\text{O}$ (benthic foram.) (Hollis et al., 2012 calibration) 	<ul style="list-style-type: none"> ■ Carpenter et al. (2012): plant proxies (Tasmania) ■ Kennedy (2003): plant proxies (NZ) ■ Greenwood et al. (2003): plant proxies (Austr.)

Figure 7. 10. Palaeotemperature estimates derived from different proxies and sources for the Late Cretaceous to the Paleocene/Eocene boundary. Yellow squares represent the estimates of Kemp *et al.* (2014) based on MBT/CBT proxies. The mean annual temperature estimates recorded in this study from Coexistence Analysis is represented by a red box. The mean growth ring width values calculated in this study for the López de Bertodano, Sobral and Cross Valley formations are also presented in this figure (red squares with black outline) in order to compare the climate trend from growth rings with the previously published temperature data. Diagram taken from Kemp *et al.* (2014)

There are no studies that have focused on modelling climate for the Paleocene Epoch. Instead most research has concentrated on the Late Paleocene and Early Eocene (Shellito *et al.*, 2003; Sewall *et al.*, 2004; Loptson *et al.*, 2014). These models focus mainly on the discrepancy between surface temperatures recorded from proxies and those reconstructed using models. Models cannot accurately recreate the small latitudinal temperature gradient that the proxies indicate and instead produce temperatures too high for low latitude regions and too low for high latitude regions.

Shellito *et al.* (2003) looked at the effects of different CO₂ scenarios (500ppm, 1000ppm and 2000ppm). Temperature outputs under the CO₂ levels of 1000ppm and 2000ppm were the most agreeable with proxy data and were the only scenarios in which polar coastal regions were ice free (Figure 7.11 and 7.12). The mean annual temperatures produced in this study also are in agreement with the middle and high CO₂ scenarios (Figure 7.11). The highest CO₂ scenario is the only scenario that could reconstruct cold mean month temperatures that were in line with the polar fossil flora records (8°C). The cold month mean temperature range produced in this study is warmer than southern high latitude temperatures produced by the models in Shellito *et al.* (2003). Recent studies using a number of proxies such as leaf stomata have indicated that CO₂ levels of 2000ppm are too high for the Late Paleocene and Early Eocene (Beerling and Royer, 2011 and Royer *et al.* 2012). These recent studies suggest CO₂ levels for the Paleocene were between 300 and 800ppm.

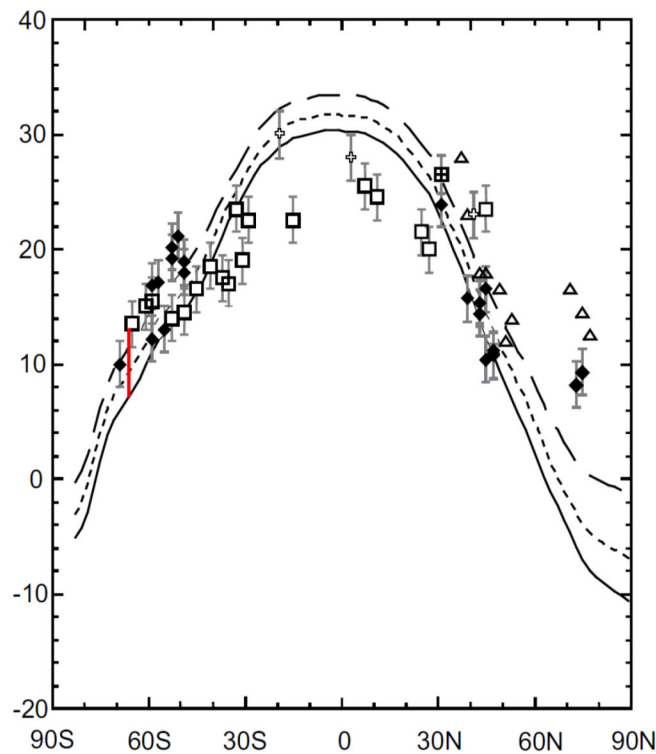


Figure 7. 11. Model output of Early Paleogene latitudinal temperature curves for land and ocean (mean annual temperature and sea surface temperatures under three different CO₂ scenarios: 500ppm (solid line), 1000ppm (short dashed line), 2000ppm (long dashed line)). Temperature data from proxies are also plotted for comparison: Open squares, ocean temperature data; diamonds, Eocene flora temperature estimates; hatched squares and markers, open surface temperatures. The red line presents mean annual temperature results from Coexistence Analysis conducted in this study. This diagram has been modified from Shellito *et al.* (2003) references for proxy data are within this publication.

Research by Lopton *et al.* (2014) found that adding dynamic vegetation rather than homogenous vegetation in to a global climate model increases climate sensitivity meaning that higher temperatures can be produced with lower CO₂ levels. It also reduced the temperature differences between proxies and modelled climate for the Eocene. Figure 7.13 presents mean annual latitudinal temperature curves for model outputs under different CO₂ scenarios: fixed global vegetation (shrubs) under 2 x pre-industrial CO₂ and under 4x pre industrial CO₂; dynamic vegetation (TRIFFID model) under 2 x preindustrial CO₂ and 4 x pre-industrial CO₂. The figure shows that there is less discrepancy between the model simulations with dynamic vegetation and

4 x preindustrial CO₂ and data from proxies. The discrepancy between the proxy data and dynamic vegetation at 4 x pre-industrial CO₂ had a root mean square error of 9.5°C compared to the root mean square error of 16°C and 17.7°C for the fixed vegetation at 2 x pre-industrial and 4 x pre-industrial CO₂. Therefore adding dynamic vegetation to a model decreases the discrepancy between the models and climate data from proxies. The authors noted that adding accurate vegetation types on landmasses may further reduce discrepancies between proxy and modelled temperatures results. The results in this study allow for a more accurate and detailed reconstruction of vegetation types at southern high latitudes to be input into climate models, providing more accurate model simulations for the Paleocene period.

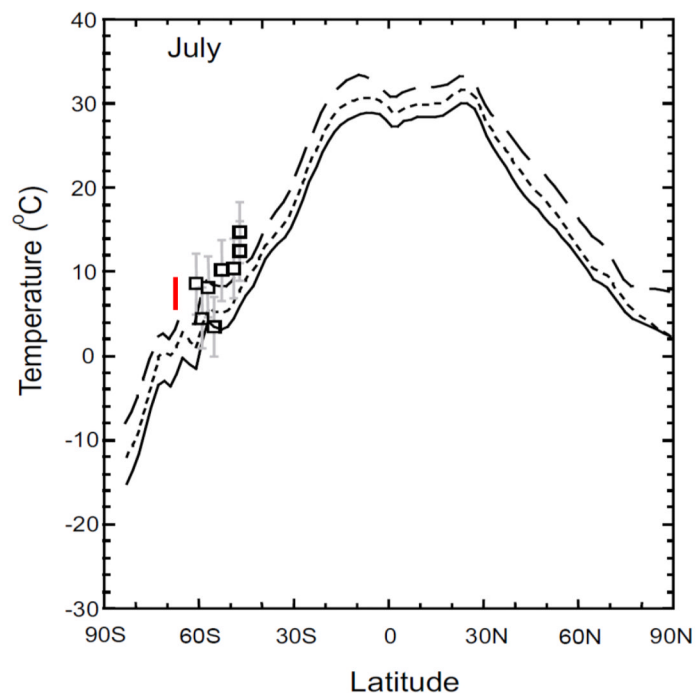


Figure 7. 12. Model outputs of latitudinal temperature gradients over land showing winter temperatures in the Southern Hemisphere for three different CO₂ scenarios: 500ppm, 1000ppm, 2000ppm. Cold month mean temperatures from Eocene flora is also presented in order to make comparisons between the proxy data and the model outputs. The red line represents the cold month mean temperature range produced from Coexistence Analysis in this study for Seymour Island. Diagram taken from Shellito *et al.* (2003), references for proxies are within this publication.

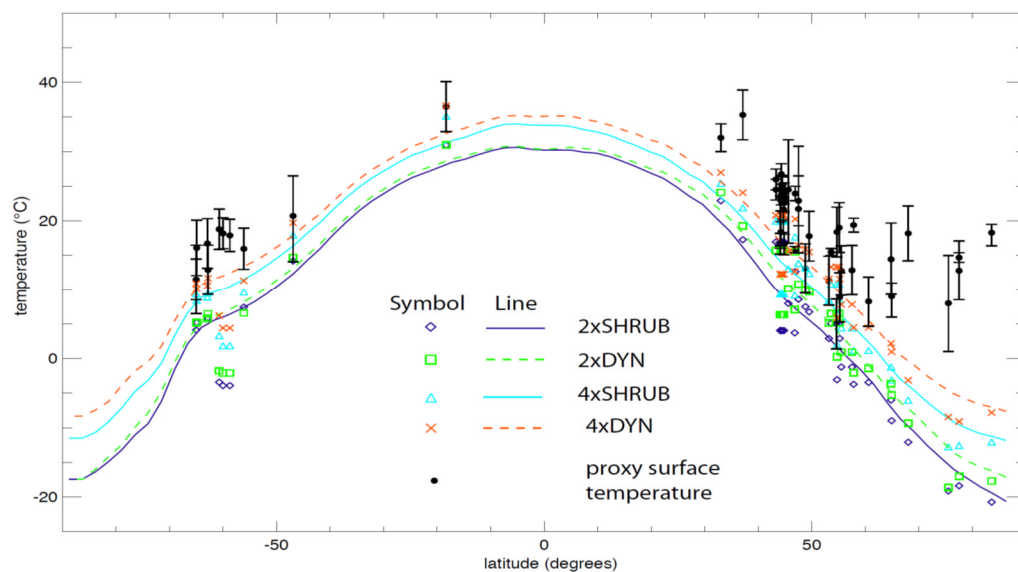


Figure 7. 13. Mean annual temperature latitudinal gradients over land for 4 scenarios: fixed vegetation at 2 x preindustrial CO₂ (2x SHRUB, purple line), fixed vegetation at 4 x pre industrial CO₂ (4x SHRUB, blue line), dynamic vegetation at 2 x preindustrial CO₂ (2x DYN, green dashed line), dynamic vegetation at 4 x pre-industrial CO₂ (4x DYN, orange dashed line). Black circles are surface temperature proxies. Diagram is taken from Loftson *et al.* (2014).

Chapter 8

Conclusions

Fossil wood is abundant in the Paleocene marine sedimentary sequences of Seymour Island. The wood originated from forests that once grew on a volcanic island arc now represented by the Antarctic Peninsula. To the east of the volcanic arc was a back arc basin, now called the Larsen Basin. When the trees in these forests died their wood was transported via river systems into the back-arc basin where they floated as drift wood, before eventually sinking to the basin floor and then were permineralised.

A new fossil wood assemblage which was collected along a new measured stratigraphic section on Seymour Island has been investigated in order to reconstruct the Paleocene forests and climates of the Antarctic Peninsula. The stratigraphic section is latest Cretaceous (K/Pg) to Late Paleocene in age. It includes the uppermost López de Bertodano Formation, Sobral Formation and the Cross Valley Formation. The sequence represents a shallowing depositional environment from a marine mid-shelf, deltaic environment and a fluvial environment.

The exact location of the wood on the section was recorded so that data derived from the wood could be put into a stratigraphical context. Also, sedimentological data could be used to interpret where the wood originated on the Antarctic Peninsula (e.g. upland or lowland areas).

Composition and reconstruction of the Antarctic Peninsula Forests

- Altogether 56 fossil wood specimens were studied. The size, shape and preservation type of the wood was recorded in order to help interpret their likely origin on the Antarctic Peninsula. The type of preservation included calcite permineralisation (associated with marine depositional environments), partly charred (charred from wildfires or lightning) and haematite (associated with terrestrial depositional environments) (Chapter 2).

- Wood that had been permineralised by calcite was most common in the marine sediments of the López de Bertodano Formation and most of the Sobral Formation. Partly charred and rounded wood was present in the upper Sobral Formation and was associated with volcanoclastic material; this sedimentary facies is suggestive of a more proximal setting close to a volcanic source. Wood that had haematite permineralisation was most common in the Cross Valley Formation which represents a fluvial depositional environment.
- Both conifer and angiosperm genera were identified in this study. Conifer genera include: *Agathoxylon*, *Phyllocladoxylon*, *Protophyllocladoxylon* and *Podocarpoxyton/Cupressinoxylon*. Angiosperm wood types include: *Nothofagoxyton*, *Weinmannioxylon*, *Myrceugenelloxyton* and *Antarctoxyton*.
- The nearest living relatives (NLRs) of the identified wood genera are found in the Southern Hemisphere temperate forests today. They grow in a wide range of habitats and altitudes. They have different ecologies, for example, modern *Araucaria* (fossil wood genera : *Agathoxylon*) and *Nothofagus* (morphotype: *Nothofagoxyton*) are shade-intolerant to varying degrees so they grow in sub-optimal environments (e.g. poorly fertile soils), at high altitude locations in harsh environments, or in areas prone to large scale disturbances. This is to avoid competition from faster growing broad-leaved trees. It is likely that the fossil tree types in the Antarctic forests had a similar ecology.
- The most abundant wood genera identified in the wood assemblage was *Nothofagoxyton* (38%) and *Agathoxylon* (25%) which suggests that these were dominant tree types in the Paleocene Antarctic forests. *Phyllocladus* type trees (*Phyllocladoxylon*, 11% and *Protophyllocladoxylon* , 10%) were also likely to be common tree types. Other tree types *Weinmannioxylon*, *Myrceugenelloxyton*, *Antarctoxyton* and *Podocarpoxyton/Cupressinoxylon* are likely to have been minor components.
- Palynological work carried out in this study gave a more detailed insight into the Paleocene Antarctic forests with regards to non-woody plants. The same trees identified in the wood assemblage were also found in the palynological samples such as *Araucaria/Agathis* (pollen type:

Araucariacites australis), *Phyllocladus* (*Trichotomosulcites subgranulatus*), *Nothofagus* (*Nothofagities*) and *Myrtaceae* (*Myrtaceidites* sp.). In addition, palynological samples indicated trees of *Lagarostrobos franklinii* (*Phyllocladites mawsonii*) *Podocarps* spp., *Microcachrys* (*Microcachryidites antarcticus*), *Proteaceae* (*Proteacidites* sp, *Peninsulapollis* sp.), *Casuarinaceae*, *Blechnaceae*, *Cyatheaceae*, *Lycopodiaceae*, *Sphagniaceae* and *Azolla* sp.

- The reconstruction of the composition and structure of the Antarctic forests are mainly based on the ecology of nearest living relatives (NLRs) of the fossil wood and palynomorphs. Sedimentary data and preservation type were also taken into consideration.
- The lowland forests on the Antarctic Peninsula are likely to have been dominated by *Nothofagus*, *Phyllocladus*, *Lagarostrobos franklinii* trees and other *Podocarpus* spp, which would have formed the canopy. *Myrtaceae* trees and *Weinmannia* may have formed the sub-canopy trees. The undergrowth are likely to have consisted of ferns (*Blechnum* and *Cyatheaceae*), *Proteaceae*, and *Myrtaceae* shrubs. These lowland forests are thought to have been most similar to the modern cool temperate mixed *Nothofagus* forests in Tasmania and New Zealand because these forests both contain, *Nothofagus*, *Phyllocladus*, ferns and tree ferns. *Weinmannia* is only present in the New Zealand forests. *Lagarostrobos franklinii* is endemic to the Tasmanian forests and mainly occupies riverbanks. It is possible that it had the same ecology on the Antarctic Peninsula. Most of the trees in these modern forests (e.g. *Weinmannia*, *Nothofagus* and *Phyllocladus*) grow on poorly fertile and poorly drained soils. The forests also have an open canopy, so it is likely that the forests on the Antarctic Peninsula grew under similar conditions.
- The upland forests are likely to have been similar to the *Araucaria* and *Nothofagus* woodlands on growing at high altitudes in Chile today. Partly charred *Agathoxylon* and *Nothofagoxylon* wood is found at the top of the Sobral Formation and is associated with volcanic clastic material. This suggests that the *Nothofagus* and *Araucaria* trees on the Antarctic Peninsula may have had a similar ecology to their modern relatives. Today their modern relatives in Chile are found growing at

high altitudes in areas that are prone to disturbances which they rely on to regenerate, such as close to active volcanic centres where wildfires and pyroclastic flows are frequent. Other conifers may have been present in these upland forests such as *Phyllocladus*, Cupressaceae and podocarps because wood and pollen of these types are found in the Cross Valley Formation, which is interpreted as being derived from upland areas because its sedimentology resembles a debris flow caused by either a flash flood or pyroclastic flow, as it contains a large wooden logs that are in the arrangement of log jams, rip-up clasts and volcaniclastic material. Above the treeline on the Antarctic Peninsula heathland may have occurred consisting of ferns, *Microcachrys* and Proteaceae. *Microcachrys* is a common component of the Tasmanian forests today.

Paleocene climates of Antarctica

- Multiple techniques using fossil wood and palynomorphs have been conducted to reconstruct climate conditions on the Antarctic Peninsula during the Paleocene. These include growth ring analysis, climate analysis of angiosperm wood anatomy, Coexistence Analysis and specific gravity of fossil wood.
- The climate results reveal that climate conditions on the Antarctic Peninsula were seasonal, cool to marginally warm temperate with sufficient water availability for the trees to grow on the Antarctic Peninsula to grow. .
- Coexistence Analysis indicated that temperatures and precipitation on the Antarctic Peninsula during the Paleocene are comparable to the cool temperate climates of Chile, Tasmania and New Zealand with mean annual temperatures ranging from 7 - 13°C and mean annual precipitation ranging from 1000 – 2489mm per year. Climates were mild all year around with cooler wetter winters, cold mean month temperatures from 6.6 – 9.1°C, wet month mean precipitation from 107 – 321mm per year. Summers were warm and drier, warm month mean temperature (18 -19.6°C) and dry month precipitation (38 – 90mm per year).

- Growth ring analysis was undertaken to observe how climates changed through the Paleocene. It determined that climates of the Antarctic Peninsula were seasonal because all of the wood specimens had distinct growth rings. Calculating mean growth ring width for each wood specimens through the stratigraphic section shows a trend towards narrow rings from the Early Paleocene to the Late Paleocene suggesting a change to cooler climates. Average mean growth ring width decreases from 1.98mm in the López de Bertodano Formation (Early Paleocene) to 0.45mm in the Cross Valley Formation (Late Paleocene).
- The majority of high mean sensitivity values were from *Agathoxylon*, *Nothofagoxylon* and *Phyllocladoxylon* woods which implies that they grew under a fluctuating climate where water may have been the limiting factor. This is further supported by the presence of false rings in *Agathoxylon* and *Phyllocladoxylon* wood which indicates there may have been periods of water shortage. Since not all of the wood specimens had high mean sensitivities it may be possible that the ones that did originated from trees growing in different areas on the island arc, for example more exposed areas where precipitation was less effective.
- Specific gravity analysis of fossil wood allowed new insight into the ecology and growth conditions of the trees growing on the Antarctic Peninsula during the Paleocene and also gave further support to the interpretation of climate data derived from growth rings and angiosperms. A narrow range of specific gravity values were recorded (0.50 – 0.80) for fossil wood specimens. A narrow range in values is what would be expected for trees growing in a temperate forest. Specific gravity values for wood morphotypes *Agathoxylon*, *Phyllocladoxylon* and *Nothofagoxylon* had similar values to their modern relatives and thus suggests they grew under similar conditions.
- Climate analysis of angiosperm woods found that they had characteristics that are associated with modern angiosperm trees growing in temperate regions.
- Mesomorphy and Vulnerability was calculated for indicators of water availability. The Mesomorphy index was considered to be a better

indicator of water availability and it revealed that there was sufficient water availability in the Antarctic forests during the Paleocene because all of the wood values were above 300.

- The climate data in this study agrees with previously published mean annual temperatures for the Paleocene from Antarctica. For example, MBT/CBT proxies (8 - 13°C), Coexistence Analysis (11 – 18°C).
- The growth ring analysis in this study generally agrees with the narrowing of growth rings in the Early Paleocene. However, in this study growth ring widths continue to narrow into the Late Paleocene, whereas in previously published studies growth ring width steeply increases. The growth ring data in this study is more robust because the exact stratigraphic location for each data point is known.
- The climate data in this study also agrees with Paleocene mean annual temperatures (MAT) and sea surface temperatures (SST) from New Zealand (MAT: 10 - 15°C and SST: 15 - 16°C). Also fossil flora assemblages of Paleocene age from New Zealand, southern Australia and southern South America have similar plant types to those found on Seymour Island (e.g. *Nothofagus*, podocarps and *Araucaria*) suggesting a similar climate. The growth ring data in this study agrees with the global increase in $\delta^{18}\text{O}$ values observed through the Early Paleocene to Late Paleocene and thus supports that the growth ring signal in this study is likely to be a climate signal.
- This project gives a more detailed insight into the composition and structure of the Antarctic forests during the Paleocene than has been previously done before. It has also given a detailed insight into the climates of Antarctica during this time because having the data tied to a stratigraphic section allows future research to make more direct comparisons. This research is important in contributing to reconstructing more accurate vegetation cover at high latitudes, as well as contributing to high latitude climate for the Paleocene. This will help improve the accuracy of boundary conditions in palaeoclimate models.

List of References

- Andreoli, A., Comiti, F. and Lenzi, M.A. 2007. Characteristic, distribution and geomorphic role of large woody debris in a mountain stream of the Chilean Andes. *Earth Surface Processes and Landforms*. **32**(11), pp.1675–1692.
- Ahmed, M. and Ogden, J. 1985. Modern New Zealand tree-ring chronologies III. *Agathis australis*(Salisb.) - Kauri. *Tree-ring bulletin*. **45**, pp. 12-24.
- Askin, R.A. 1988. Campanian to Paleocene palynological succession of Seymour and adjacent islands, north eastern Antarctic Peninsula. In: Feldmann, R.M. and Woodburne, M.O. eds. *Geology and Paleontology of Seymour Island, Antarctic Peninsula*. Boulder: Geological Society of America Memoirs, **169**, pp.131-154.
- Askin, R.A. 1989. Endemism and heterochroneity in the Late Cretaceous (Campanian) to Paleocene Palynofloras of Seymour Island, Antarctica: implications for origins, dispersal and palaeoclimates of southern floras. In: Crame, J.A. ed. *Origins and Evolution of the Antarctic Biota*. London: Geological Society Special Publication. **47**, pp.107-119.
- Askin, R.A. 1990. Campanian to Paleocene spore and pollen assemblages of Seymour Island, Antarctica. *Review of Palaeobotany and Palynology*. **65**, pp.105-113.
- Askin, R.A. 1992. Late Cretaceous-Early Tertiary Antarctic outcrop evidence for past vegetation and climates. *Antarctic research series*. **56**, pp.61-73.
- Atlas of living Australia. *Atlas of living Australia website*. [online]. [Accessed January - May 2015]. Available from: <http://www.ala.org.au>
- Bannister, P. and Neuner, G. 2001. Frost resistance and the distribution of conifers. In: Bigras, F.J. and Colombo, S.J. (eds). *Conifer cold hardiness*. Dordrecht: Kluwer Academic Publishers, pp. 3-21.
- Bannister, P. and Lord, J.M. 2006. Comparative winter frost resistance of plant species from southern Africa, Australia, New Zealand, and South America grown in a common environment (Dunedin, New Zealand). *New Zealand Journal of Botany*. **44**(2), pp.109–119.

- Barrera, E., Huber, B.T., Savin, S.M. and Webb, P.N. 1987. Antarctic marine temperatures: late Campanian through Early Paleocene. *Paleoceanography*. **2**(1), pp.21-47.
- Bascuñán-Godoy, L., Alcaíno, C., Carvajal, D.E., Sanhueza, C., Montecinos, S. and Maldonado, A. 2013. Diferentes respuestas fotoprotectoras bajo condiciones de sequía en dos especies predominantes del bosque pantanoso de Chile. *Gayana. Botánica*. **70**(2), pp.267-274.
- Beadle, N.C.W. 1981. *The vegetation of Australia*. Stuttgart: Gustav Fischer Verlag.
- Beerling, D.J. and Royer, D.L. 2011. Convergent Cenozoic CO₂ history. *Nature Geoscience*. **4**(7), pp.418-420.
- Bowman, V.C., Francis, J.E., Riding, J.B., Hunter, S.J. and Haywood, A.M. 2012. A latest Cretaceous to earliest Paleogene dinoflagellate cyst zonation from Antarctica, and implications for phytoprovincialism in the high southern latitudes. *Review of Palaeobotany and Palynology*. **171**, pp.40–56.
- Bowman, V.C., Francis, J.E., Askin, R.A., Riding, J.B. and Swindles, G.T. 2014. Latest Cretaceous-earliest Paleogene vegetation and climate change at the high southern latitudes: palynological evidence from Seymour Island, Antarctic Peninsula. *Palaeogeography, Palaeoclimatology, Palaeoecology*. **408**, pp.26-47.
- Bowman, V.C., Ineson, J., Riding, J., Crame, J., Francis, J., Condon, D., Whittle, R. and Ferraccioli, F. in revision. The Paleocene of Antarctica: dinoflagellate cyst biostratigraphy, chronostratigraphy and implications for the palaeo-Pacific margin of Gondwana. *Gondwana Research*.
- Bradford, J.C. 1998. A cladistic analysis of species groups in *Weinmannia* (Cunoniaceae) based on morphology and inflorescence architecture. *Annals of the Missouri Botanical Garden*. **84**(4), pp.565-593.
- Braudrick, C.A. and Grant, G.E. 2001. Transport and deposition of large woody debris in streams: a flume experiment. *Geomorphology*. **41**(4), pp.263-283.

- Brea, M., Matheos, S.D., Raigemborn, M.S., Iglesias, A., Zucol, A.F. and Práparo, M. 2011. Paleoecology and Paleoenvironments of Podocarp trees in the Ameghino Petrified forest (Golfo San Jorge Basin, Patagonia, Argentina): Constraints for Early Paleogene paleoclimate. *Geologica Acta*. **9**(1), pp.12-28.
- Brown, M.J. and Jennifer, R. 1996. A comparison of the ecology and conservation management of cool temperate rainforests in Tasmania and Americas. In: Lawford, R.G., Fuentes, E. and Alaback, P.B. eds. *High-latitude rainforests and associated ecosystems of the west coast of the americas: climate, hydrology, ecology and conservation*. New York: Springer, **116**, pp.320-341.
- Brownsey, P.J. and Smith-Dodsworth, J.C. 1989. *New Zealand ferns and allied plants*. Auckland: Bateman.
- Burns, B.R. and Leathwick, J.R. 1996. Vegetation-environment relationships at Waipoua Forest, Northland, New Zealand. *New Zealand Journal of Botany*. **34**(1), pp.79-92.
- Buurman, P. 1972. Mineralization of fossil wood. *Rijksmuseum van Geologie en Mineralogie*. **12**, pp.1–43.
- Cantrill, D.J. and Poole, I. 2005. Taxonomic turnover and abundance in Cretaceous to Tertiary wood floras of Antarctica: implications for changes in forest ecology. *Palaeogeography, Palaeoclimatology, Palaeoecology*. **215**(3), pp.205-219.
- Cantrill, D.J., Tosolini, A.M. and Francis, J.E. 2011. Paleocene flora from Seymour Island, Antarctica: revision of Dusén's (1908) pteridophyte and conifer taxa. *Alcheringa*. **35**(3), pp.309-328.
- Cantrill, D.J. and Poole, I. 2012. *The vegetation of Antarctica through geological time*. New York: Cambridge University Press.
- Carlquist, S. 1977. Ecological Factors in Wood Evolution: A Floristic Approach. *American Journal of Botany*. **64**(7), pp.887-896.
- Carlquist, S. 1984. Vessel grouping in dicotyledon wood: significance and relationship to imperforate tracheary elements. *ALISO*. **10**(4), pp.505–525.

Carlquist, S. and Hoekman, D.A. 1985. Ecological wood anatomy of the woody southern Californian flora. *IAWA Bulletin n.s.* **6**(4), pp.319–347.

Carlquist, S. 2001. *Comparative wood anatomy: Systematic, ecological, and evolutionary aspects of dicotyledon wood*. 2nd edition. Berlin, Heidelberg, New York: Springer Verlag.

Castro-arévalo, M., Reyes-Díaz, M., Alberdi, M., Jara-Rodríguez, V., Sanhueza, C., Corcuera, L.J. and Bravo, L.A. 2008. Effects of low temperature acclimation on photosynthesis in three Chilean Proteaceae. *Revista Chilena de Historia Natural*. **81**, pp. 321-333.

Chambers, T.C. and Farrant, P.A. 1996. *Blechnum blechnoides* (Bory) Keys, (Blechnaceae), formerly *B.banksii* (Hook. F.) mett. Ex diels, a fern from salt-spray habitats of New Zealand and Chile. *New Zealand Journal of Botany*. **34**(4), pp.441-445.

Chapman, J.L. 1994. Distinguishing internal developmental characteristics from external palaeoenvironmental effects in fossil wood. *Review of Palaeobotany and Palynology*. **81**(1), pp.19-32.

Chave, J., Coomes, D. Jansen, S., Lewis, S.L., Swenson, N.G. and Zanne, A.E. 2009. Towards a worldwide wood economics spectrum. *Ecology letters*. **12**(4), pp.351-366.

Cook, J.M., Mark, A.F. and Shore, B.F. 1980. Responses of *Leptospermum scoparium* and *L. ericoides* (Myrtaceae) to waterlogging. *New Zealand Journal of Botany*. **18**(2), pp.233 - 246.

Coomes, D.A., Allen, R.B., Bentley, W.A., Burrows, L.E., Canham, C.D., Fagan, L., Forsyth, D.M., Gaxiola-Alcantar, A., Parfitt, R.L., Ruscoe, W.A., Wardle, D.A., Wilson, D.J. and Wright, E.F. 2005. The hare, the tortoise and the crocodile: the ecology of angiosperm dominance, conifer persistence and fern filtering. *Journal of Ecology*. **93**(5), pp.918-935.

Coomes, D.A., Kunstler, G., Canham, C.D. and Wright, E. 2009. A greater range of shade-tolerance niches in nutrient-rich forests: an explanation for positive richness-productivity relationships?. *Journal of Ecology*. **97**(4), pp.705-717.

- Coomes, D.A. and Bellingham, P.J. 2011. Temperate and tropical podocarps: How ecologically alike are they?. *Smithsonian Contributions to Botany*. **95**, pp.119-140.
- Corfield, R.M. 1994. Palaeocene oceans and climate: An isotopic perspective. *Earth-Science Reviews*. **37**(3), pp.225-252.
- Crame, J.A., Francis, J.E., Cantrill, D.J. and Pirrie, D. 2004. Maastrichtian stratigraphy of Antarctica. *Cretaceous Research*. **25**(3), pp.411–423.
- Cramer, B.S., Toggweiler, J.R., Wright, J.D., Katz, M.E. and Miller, K.G. 2009. Ocean overturning since the Late Cretaceous: Inferences from a new benthic foraminiferal isotope compilation. *Paleoceanography*. **24**(4), pp.1-14.
- Cranwell, L.M. 1959. Fossil pollen from Seymour Island, Antarctica. *Nature*. **184**, pp.1782-1785.
- Crouch, E.M., Willumsen, P.S., Kulhanek, D.K. and Gibbs, S.J. 2014. A revised Paleocene (Teurian) dinoflagellate cyst zonation from eastern New Zealand. *Review of Palaeobotany and Palynology*. **202**, pp.47-79.
- Cutler, D.F. and Gregory, M. 1998. *Anatomy of the dicotyledons. Volume IV. Saxifragales*. Oxford: Clarendon Press.
- Dettman, M.E. 1989. Antarctica: Cretaceous cradle of austral temperate rainforests?. In: Crame, J.A. eds. *Origins and Evolution of the Antarctic Biota*. London: Geological Society Special Publication, **47**(1), pp.89-105.
- Dickison, W.C. 1977. Wood anatomy of *Weinmannia* (Cunoniaceae). *Torrey Botanical Society*. **104**(1), pp.12-23.
- Dickison, W.C. 1978. Comparative anatomy of Eucryphiaceae. *American Journal of Botany*. **65**(7), pp.722-735.
- Dingle, R.V. and Lavelle, M. 2000. Antarctic Peninsula Late Cretaceous-Early Cenozoic palaeoenvironments and Gondwana palaeogeographies. *Journal of African Earth sciences*. **31**(1), pp.91-105.
- Ditchfield, P.W., Marshall, J.D. and Pirrie, D. 1994. High latitude palaeotemperature variation: new data from the Tithonian to Eocene of James

Ross Island, Antarctica. *Palaeogeography, Palaeoclimatology, Palaeoecology*. **107**, pp.79-101.

Dunwiddie, P.W. 1979. Dendrochronological studies of indigenous New Zealand trees. *New Zealand Journal of Botany*. **17**(3), pp.251-266.

Dunwiddie, P.W. and LaMarche, V.C. 1980. Dendrochronological characteristics of some native Australian trees. *Australian Forestry*. **43**(2), pp.124-135.

Dutton, A., Huber, B.T., Lohmann, K.C. and Zinsmeister, W.J. 2007. High-resolution stable isotope profiles of a Dimitobelid belemnite: implications for paleodepth habitat and late Maastrichtian climate seasonality. *Palaios*. **22**(6), pp.642-650.

Ecology at Lincoln University, Canterbury, New Zealand. 2010. *Questioning the drowning*. [online]. [Accessed 11 February 2016]. Available from: www.lincolnecology.org.nz

Eklund, H. 2003. First Cretaceous flowers from Antarctica. *Review of Palaeobotany and Palynology*. **127**(3), pp.187-217.

Eklund, H., Cantrill, D.J. and Francis, J.E. 2004. Late Cretaceous plant mesofossils from Table Nunatak, Antarctica. *Cretaceous Research*. **25**(2), pp.211-228.

Elliot, D.H., Askin, R.A., Kyte, F.T. and Zinsmeister, W.J. 1994. Iridium and dinocysts at the Cretaceous-Tertiary boundary on Seymour Island, Antarctica: implications for K-T event. *Geology*. **22**(8), pp.675–678.

Emanuel, W.R., Shugart, H.H. and Stevenson, M.P. 1985. Climatic change and the broad-scale distribution of terrestrial, ecosystem complexes. *Climate Change*, **7**(1), pp.29–43.

Enright, N.J. 1995a. Conifers of Tropical Australasia. In: Enright, N.J. and Hill, R.S. eds. *Ecology of the Southern Conifers*. Carlton: Melbourne University Press, pp.197-222.

Enright, N.J. and Odgen, J. 1995b. The southern conifers - a synthesis. In: Enright, N.J. and Hill, R.S. eds. *Ecology of the southern conifers*. Calton: Melbourne University Press, pp.271-287.

Falcon-Lang, H.J. and Cantrill, D.J. 2000. Cretaceous (Late Albian) coniferales of Alexander Island, Antarctica. 1: Wood taxonomy: a quantitative approach. *Review of Palaeobotany and Palynology*. **111**(1), pp.1-17.

Falcon-Lang, H.J. and Cantrill, D.J. 2001. Gymnosperm woods from the Cretaceous (mid-Aptian) Cerro Negro Formation, Byers Peninsula, Livingston Island, Antarctica: the arborescent vegetation of a volcanic arc. *Cretaceous Research*. **22**(3), pp.277-293.

Falcon-Lang, H.J. 2005a. Intra-tree variability in wood anatomy and its implications for fossil wood systematics and palaeoclimatic studies. *Palaeontology*. **48**(1), pp.171-183.

Falcon-Lang, H.J. 2005b. Global climate analysis of growth rings in woods, and its implications for deep-time paleoclimate studies. *The Paleontological Society*. **31**(3), pp.434-444.

Ferguson, D.K., Lee, D.E., Bannister, J.M., Zetter, R., Jordan, G.J., Vavra, N. and Mildenhall, D.C. 2010. The taphonomy of a remarkable leaf bed assemblage from the Late Oligocene-Early Miocene gorge lignite measures, southern New Zealand. *International Journal of Coal Geology*. **84**(2), pp.173-181.

Fernández, N. and Fontenla, S. 2010. Mycorrhizal status of obligate and facultative epiphytic ferns in a Valdivian temperate of Patagonia, Argentina. *American Fern Journal*. **100**(1), pp.16-26.

Forest Flora. 2016. *Weinmannia racemosa* Kamahi. [online]. [Accessed 20 November 2014]. Available from: <http://www.forestflora.co.nz>

Francis, J.E. 1986. Growth rings in Cretaceous and Tertiary wood from Antarctica and their Palaeoclimatic Implications. *Palaeontology*. **29**(4), pp. 665-684.

Francis, J.E. and Poole, I. 2002. Cretaceous and early Tertiary climates of Antarctica: evidence from fossil wood. *Palaeogeography, Palaeoclimatology, Palaeoecology*. **182**(1), pp.47-64.

Fritts, H.C. 1976. *Trees rings and climates*. London: Academic Press.

Gani, R.M., Bhattacharya, J.P. and MacEachern, J.A. 2009. Using Ichnology to determine the relative influence of waves, storms, tides, and rivers in deltaic deposits: Examples from Cretaceous western interior seaway, U.S.A. *Society of Sedimentary Geology and Applied Ichnofacies*. pp 209 – 225.

Gibson, N., Davies, J. and Brown, M.J. 1991. The ecology of *Lagarostrobos franklinii* (Hook.f.) Quinn (Podocarpaceae) in Tasmania. 1. Distribution, floristics and environmental correlates. *Australian Journal of Ecology*. **16**(2), pp.215-222.

Gibson, N. and Brown, M.J. 1991. The ecology of *Lagarostrobos franklinii* (Hook.f.) Quinn (Podocarpaceae) in Tasmania. 2. Population structure and spatial pattern. *Australian Journal of Ecology*. **16**(2), pp.223-229.

Gibson, N., Barker, P.C.J., Cullen, P.J. and Shapcott, A. 1995. Conifers of Southern Australia. In: Enright, N.J. and Hill, R.S. eds. *Ecology of the southern conifers*. Carlton: Melbourne University Press, pp.223-251.

Gonor, J.J., Sedell, J.R. and Benner, P.A. 1988. What we know about large trees in estuaries, in the sea and on coastal beaches. In: Maser, C., Tarrent, R.F., Trappe, J.M. and Franklin, J.F. eds. *From the forest to the sea: a story of fallen trees*. Oregon: Bureau of Land Management U.S. Department of the interior, pp. 83-112.

Gothan, W., 1908. Die fossilen Hölzer von der Seymour und Snow Hill Insel. Wissenschaftliche Ergebnisse der Schwedischen Südpolar Expedition 1901–1903. **3**(8), pp.1-33.

Gradstein, F.M., Ogg, J.G., Schmitz, M.D. and Ogg, G.M. 2012. *The geological time scale 2 volume set*. Oxford, Amsterdam, Waltham: Elsevier.

Greenwood, D.R. 2003. Plant communities and climate change in southeastern Australia during the early Paleogene. In: Wing, S.L., Gingerich,

P.D., Schmitz, B. and Thomas, E. eds. *Causes and consequences of globally warm climates in the early Paleogene*. Boulder: The Geological Society of America, Special paper, **369**, pp.365-380.

Greguss, P. 1955. *Identification of living gymnosperms on the basis of xylotomy*. Budapest: Akadémiai Kiadó.

Gustavo. 2011. *Weinmannia trichosperma*. [online] [Accessed 20 November 2014] Available from: www.flickr.com

Gut, B. 2008. *Trees in Patagonia*. Basel: Birkhäuser.

Gutiérrez, A.G., Armesto, J.J. and Aravena, J.C. 2004. Disturbance and regeneration dynamics of an old-growth North Patagonian rain forest in Chiloé Island, Chile. *Journal of Ecology*. **92**, pp.598-608.

Gutiérrez, A.G., Armesto, J.J., Aravena, J.C., Carmona, M., Carrasco, N.V., Christie, D.A., Peña, M., Pérez, C. and Huth, A. 2009. Structural and environment characterization of old-growth temperate rainforests of northern Chiloé Island, Chile: Regional and global relevance. *Forest Ecology and Management*. **258**(4), pp.376-388.

Hacke, U.G., Sperry, J.S., Pockman, W.T., Davis, S.D and McCulloh, K.A. 2001. Trends in wood density and structure are linked to prevention of xylem implosion by negative pressure. *Oecologia*. **126**(4), pp.457-461.

Hathway, B. 2000. Continental rift to back-arc basin: Jurassic-Cretaceous stratigraphical and structural evolution of the Larsen Basin, Antarctic Peninsula. *Journal of the Geological Society, London*. **157**(2), pp.417–432.

Hayes, P.A., Francis, J.E., Cantrill, D.J. and Crame, J.A. 2006. Palaeoclimate analysis of Late Cretaceous angiosperm leaf floras, James Ross Island, Antarctica. In: Francis, J.E., Pirrie, D. and Crame, J.A. eds. *Cretaceous-Tertiary High-Latitude Palaeoenvironments, James Ross Basin, Antarctica*. London: Geological Society, London, Special Publications, **258**, pp.49-62.

Hijmans, R.J., Cameron, S.E., Parra, J.L., Jones P.G., and Jarvis. A. 2005. Very high resolution interpolated climate surfaces for global land areas. *International Journal of Climatology*. **25**, pp.1965-1978.

- Hill, R.S., Read, J. and Busby, J.R. 1988. The temperature-dependence of photosynthesis of some Australian temperate rainforest trees and its biogeographical significance. *Journal of Biogeography*, **15**(3), pp.431–449.
- Hollis, C.J., Taylor, K.W.R., Handley, L., Pancost, R.D., Huber, M., Creech, J.B., Hines, B.R., Crouch, E.M., Morgans, H.E.G., Crampton, J.S., Gibbs, S., Pearson, P.N. and Zachos, J.C. 2012. Early Paleogene temperature history of the Southwest Pacific Ocean: Reconciling proxies and models. *Earth and Planetary Science Letters*. **349**, pp.53-66.
- Horrocks, M. and Ogden, J. 1994. Modern pollen spectra and vegetation of Mt Hauhungatahi, central North Island, New Zealand. *Journal of Biogeography*. **21**(6), pp.637-649.
- Huber, B.T. 1988. Upper Campanian-Paleocene foraminifera from the James Ross Island region, Antarctic Peninsula. In: Feldmann, R.M. and Woodburne, M.O. eds. *Geology and Paleontology of Seymour Island, Antarctic Peninsula*. Boulder: Geological Society of America Memoirs, **169**, pp.163-252.
- IAWA Committee. 1989. IAWA list of microscopic features for hardwood identification. *IAWA Bulletin*. **10**(3), pp.219-332.
- IAWA Committee. 2004. IAWA list of microscopic features for softwood identification. *IAWA Journal*. **25**(1), pp.1-70.
- Ilic, J. 1991. *CSIRO Atlas of hardwoods*. Berlin: Springer-Verlag.
- Insidewood. 2004. *Insidewood database* [online]. [Accessed January 2012 - September 2014]. Available from: <http://insidewood.lib.ncsu.edu/search>
- Jaffré, T. 1995. Distribution and ecology of the conifers of New Caledonia. In: Enright, N.J. and Hill, R.S. eds. *Ecology of the southern conifers*. Calton: Melbourne University Press, pp. 171-196.
- Jagniecki, E.A., Lowenstein, T.K., Jenkins, D.M. and Demicco, R.V. 2015. Eocene atmospheric CO₂ from the nahcolite proxy. *Geology*. **43**(12), pp.1075-1078.
- Jarman, S.J., Kantvilas, G. and Brown, M.J. 1991. *Floristic and ecological studies in Tasmanian rainforest*. *Tasmanian NRCP Technical Report No.3*.

Hobart: The Tasmanian component of the National Rainforest Conservation Program C/- Forestry Commission.

Johnson, L.A.S and Briggs, B.G. 1975. On the Proteaceae - the evolution and classification of a southern family. *Botanical Journal of the Linnean Society*. **70**(2), pp.83-182.

Jones, T.P. and Chaloner, W.G. 1991. Fossil charcoal, its recognition and palaeoatmospheric significance. *Palaeogeography, Palaeoclimatology, Palaeoecology*. **97**(1), pp.39-50.

Kemp, D.B., Robinson, S.A. Crame, J.A., Francis, J.E., Ineson, J., Whittle, R.J., Bowman, V. and O'Brien, C. 2014. A cool temperate climate on the Antarctic Peninsula through the latest Cretaceous to early Paleogene. *Geology*. **42**(7), pp.583-586.

Kershaw, P. and Wagstaff, B. 2001. The southern conifer family Araucariaceae: history, status, and value for paleoenvironmental reconstruction. *Annual Review of Ecology and Systematics*. **32**, pp.397-414.

LaMarche, V.C., Holmes, R.L., Dunwiddie, P.W. and Drew, L.G. 1979a. Tree-ring chronologies of the Southern Hemisphere: 1. Argentina. Chronology series V. *Laboratory of Tree-ring research, Arizona*, pp. 3-69.

LaMarche, V.C., Holmes, R.L., Dunwiddie, P.W. and Drew, L.G. 1979b. Tree-ring chronologies of the Southern Hemisphere: 2: Chile. Chronology series V. *Laboratory of Tree-ring research, Arizona*, pp. 3-43.

LaMarche, V.C., Holmes, R.L., Dunwiddie, P.W. and Drew, L.G. 1979c. Tree-ring chronologies of the Southern Hemisphere: 3. New Zealand. Chronology series V. *Laboratory of Tree-ring research, Arizona*, pp. 3-59.

Landcare Research. 2016. *Nothofagus menziessi* -*Weinmannia racemosa*-*N.fusca*/*Blechnum discolor* forest. [online]. [Accessed 11 February 2016]. Available from: www.landcareresearch.co.nz

Landrum, L.R. 1981. The phylogeny and geography of Myrceugenia (Myrtaceae). *Brittonia*. **33**(1), pp.105-129.

- Lara, A., Aravena, J.C., Villalba, R., Wolodarsky-Franke, A., Luckman, B. and Wilson, R. 2001. Dendroclimatology of high-elevation *Nothofagus pumilio* forests at their northern distribution limit in the central Andes of Chile. *Canadian Journal of Forest Research*. **31**(6), pp.925-936.
- Lara, A., Villalba, R., Wolodarsky-Franke, A., Aravena, J.C., Luckman, B.H. and Emilio, C. 2005. Spatial and temporal variation in *Nothofagus pumilio* growth at tree line along its latitudinal range (35°40'-55°S) in the Chilean Andes. *Journal of Biogeography*. **32**(5), pp.879-893.
- Lawver, L.A., Gahagan, L.M. and Coffin, M.F. 1992. The development of paleoseaways around Antarctica. *Antarctic research series*. **56**, pp.7–30.
- Lens, F., Sperry, J.S., Christman, M.A., Choat, B., Rabaey, D. and Jansen, S. 2011. Testing hypotheses that link wood anatomy to cavitation resistance and hydraulic conductivity in the genus *Acer*. *New Phytologist*. **190**(3), pp.709 – 723.
- Loptson, C.A., Lunt, D.J. and Francis, J.E. 2014. Investigating vegetation-climate feedbacks during the early Eocene. *Climate of the past*. **10**(2), pp.419-436.
- Lusk, C. and Ogden, J. 1992. Age structure and dynamics of a Podocarp-broadleaf forest in Tongariro National Park, New Zealand. *Journal of Ecology*. **80**, pp.379-393.
- Lusk, C.H. 1996. Stand dynamics of the shade-tolerant conifers *Podocarpus nubigena* and *Saxegothaea conspicua* in Chilean temperate rain forest. *Journal of Vegetation Science*. **7**(4), pp.549-558.
- Lusk, C.H. 1999. Long-lived light-demanding emergents in southern temperate forests: the case of *Weinmannia trichosperma* (Cunoniaceae) in Chile. *Plant Ecology*. **140**(1), pp.111-115.
- Macellari C.E. 1988. Stratigraphy, sedimentology, and paleoecology of Upper Cretaceous/Paleocene shelf-deltaic sediments of Seymour Island. In: Feldmann, R.M. and Woodburne, M.O. eds. *Geology and Paleontology of Seymour Island, Antarctic Peninsula*. Boulder: Geological Society of America Memoirs, **169**, pp.25-54.

- MacKenzie, W.S. and Adams, A.E. 1994. *A colour atlas of rocks and minerals in thin section*. London: Manson.
- Marenssi, S., Santillana, S. and Bauer, M. 2012. Estratigrafía, petrografía sedimentaria y procedencia de las formaciones Sobral y Cross Valley (Paleoceno), isla Marambio (Seymour), Antártica. *Andean Geology*. **39**(1), pp. 67-91.
- Marenssi, S.A. 2006. Eustatically controlled sedimentation recorded by Eocene strata of the James Ross Basin, Antarctica. In: Francis, J.E., Pirrie, D. and Crame, J.A. eds. *Cretaceous-Tertiary high-latitude palaeoenvironments, James Ross Basin, Antarctica*. London: Geological Society, London, Special Publications. **258**, pp.125-133.
- Massaccesi, G. Roig, F.A., Martínez Pastur, G.J. and Barrera, M.D. 2007. Growth patterns of *Nothofagus pumilio* trees along altitudinal gradients in Tierra del Fuego, Argentina. *Trees*. **22**(2), pp. 245-255.
- McLoughlin, S. 2001. The breakup history of Gondwana and its impact on pre-Cenozoic floristic provincialism. *Australian Journal of Botany*. **49**(3), pp.271-300.
- Metcalf, C.R. 1987. *Anatomy of the dicotyledons: Volume III. Magnoliales, Illiciales and Laurales*. 2nd edition. Oxford: Clarendon Press.
- Meylan, B.A. and Butterfield, B.G. 1978. *The structure of New Zealand woods*. Wellington: Science Information Division, DSIR.
- Miller, K.G., Wright, J.D. and Browning, J.V. 2005. Visions of ice sheets in a greenhouse world. *Marine Geology*. **217**(3), pp.215-231.
- Molloy, B.P.J. 1996. A new species name in *Phyllocladus* (Phyllocladaceae) from New Zealand. *New Zealand Journal of Botany*. **34**(3), pp.287-297.
- Mosbrugger, V. and Utescher, T. 1997. The coexistence approach - a method for quantitative reconstructions of Tertiary terrestrial palaeoclimate data using plant fossils. *Palaeogeography, Palaeoclimatology, Palaeoecology*. **134**(1), pp.61-86.

- Mundo, I.A., Juñent, F.A.R., Villalba, R., Kitzberger, T. and Barrera, M.D. 2012. Araucaria araucana tree-ring chronologies in Argentina: spatial growth variations and climate influences. *Trees*. **26**(2), pp.443-458.
- Muñoz, A.A., Barichivich, J. Christie, D.A., Dorigo, W., Sauchyn, D., González-Reyes, A., Villalba, R., Lara, A. Riquelme, N. and González, M.E. 2013. Patterns and drivers of Araucaria araucana forest growth along a biospherical gradient in the northern Patagonian Andes: Linking tree rings with satellite observations of soil moisture. *Austral Ecology*. **39**(2), pp.158-169.
- New Zealand plant conservation network. 2016. *Podocarp broadleaved forest*. [online]. [Accessed 10 March 2016]. Available from: <http://www.nzpcn.org.nz>
- Nichols, G. 1999. *Sedimentary and Stratigraphy*. Oxford: Blackwell Publishing company.
- Nishida, M., Nishida, H. and Nasa, T. 1988. Anatomy and affinities of the petrified plants from the Tertiary of Chile V. *The Botanical Magazine, Tokyo*. **101**(3), pp.293-309.
- Nishida, H., Uemura, K., Tereda, K., Yamada, T., Herrera, M.R. and Hinojosa, L.F. 2006. Preliminary report on permineralized plant remains possibly from the Paleocene Chorrillo Chico Formation, Magallanes region, Chile. In: Nishida, H. ed. *Post-Cretaceous floristic changes in Southern Patagonia Chile*. Tokyo: Taisei Printing Co Ltd, pp.11-27.
- Norton, D.A. 1983a. Modern New Zealand Tree-ring Chronologies I. *Nothofagus solandri*. *Tree-bulletin*. **43**, pp.1-17.
- Norton, D.A. 1983b. Modern New Zealand Tree-ring chronologies II. *Nothofagus menziesii*. *Tree-bulletin*. **43**, pp.39-49.
- Norton, D.A., Herbert, J.W. and Beveridge, A.E. 1988. The ecology of *Dacrydium cupressinum*: a review. *New Zealand Journal of Botany*. **26**(1), pp.37-62.
- Ogden, J. and Powell, J.A. 1979. A quantitative description of the forest vegetation on an altitudinal gradient in the Mount Field National Park,

- Tasmania, and a discussion of its history and dynamics. *Australian journal of ecology*. **4**(3), pp.293-325.
- Ogden, J. and Stewart, G.H. 1995. Community dynamics of the New Zealand conifers. In: Enright, N.J. and Hill, R.S. eds. *Ecology of the southern conifers*. Calton: Melbourne University Press, pp.81-119.
- Ogden, J. Stewart, G.H. and Allen, R.B. 1996. Ecology of New Zealand Nothofagus forests. In: Veblen, T.T., Hill, R.S. and Read, J. eds. *The ecology and biogeography of Nothofagus forests*. New Haven: Yale University Press, pp.25-82.
- Olivero, E.B. 2012. Sedimentary cycles, ammonite diversity and palaeoenvironmental changes in the upper Cretaceous Marambio Group, Antarctica. *Cretaceous Research*. **34**, pp.348-366.
- Olson, M.E. and Rosell, J.A. 2013. Vessel diameter-stem diameter scaling across woody angiosperms and the ecological causes of xylem vessel diameter variation. *New Phytologist*. **197**(4), pp.1204 -1213.
- Oskolski, A.A. and Jansen, S. 2009. Distribution of scalariform and simple perforation plates within the vessel network in secondary xylem of Araliaceae and its implications for wood evolution. *Plant Systematics and Evolution*. **278**(1), pp.43–51.
- Otto-Bliesner, B.L. and Upchurch, G.R. 1997. Vegetation-induced warming of high-latitude regions during the Late Cretaceous period. *Nature*.**385**, pp. 805-807.
- Ottone, E.G. and Medina, F.A. 1998. A wood from the Early Cretaceous of James Ross Island, Antarctica. *Ameghiniana*.**35**(3), pp.291-289.
- Pancost, R.D., Taylor, K.W.R., Inglis, G.N., Handley, L., Hollis, C.J., Crouch, E.M., Pross, J., Huber, M., Schouten, S., Pearson, P.N., Morgans, H.E.G. and Raine, J.I. 2013. Early Paleogene evolution of terrestrial climate in the SW Pacific, southern New Zealand. *Geochemistry. Geophysics. Geosystems*.**14**, pp.1-17.

- Patel, R.N. 1968. Wood anatomy of Podocarpaceae indigenous to New Zealand: 3. *Phyllocladus*. *New Zealand Journal of Botany*. **6**(1), pp.3-8.
- Patel, R.N. 1990. Wood anatomy of the dicotyledons indigenous to New Zealand 20. Cunoniaceae. *New Zealand Journal of Botany*. **28**(3), pp.347-355.
- Pemberton, S., MacEachern, J.A. and Frey, R.W. 1992. Trace fossil facies models: environment and allostratigraphic significance. *Facies models: response to sea level change: Geological Association of Canada*. pp.47-72
- Philippe, M. 1993. Nomenclature générique des trachéidoxyles fossiles mésozoïques á champs araucarioïdes. *Taxon*. **42**(1), pp.74-80.
- Philippe, M. and Bamford, M.K. 2008. A key to morphogenera used for Mesozoic conifer-like woods. *Review of Palaeobotany and Palynology*. **148**(2), pp.184-207.
- Philippe, M. 2011. How many species of *Araucarioxylon*?. *Comptes Rendus Palevol*. **10**(2), pp.201-208.
- Pirrie, D. and Marshall, J.D. 1990. Diagenesis of Inoceramus and Late Cretaceous paleoenvironmental geochemistry: a case study from James Ross Island, Antarctica. *Palaios*. **5**(4), pp.336-345.
- Pirrie, D., Crame, J.A., Riding, J.B., Butcher, A.R. and Taylor, P.D. 1997. Miocene glaciomarine sedimentation in the northern Antarctic Peninsula region: the stratigraphy and sedimentology of the Hobbs Glacier Formation, James Ross Island. *Geological Magazine*. **134**(6), pp.745-762.
- Pittermann, J., Sperry, J.S., Wheeler, J.K., Hacke, U.G. and Sikkema, E.H. 2006. Mechanical reinforcement of tracheids comprises the hydraulic efficiency of conifer xylem. *Plant, Cell and Environment*. **29**(8), pp.1618-1628.
- Plants of NW Pichincha. 2012. *Study Blue*. [online]. [Accessed 20 November 2014]. Available from: www.studyblue.com
- Pole, M. and Vajda, V. 2009. A new terrestrial Cretaceous-Paleogene site in New Zealand - turnover in macroflora confirmed by palynology. *Cretaceous Research*. **30**(4), pp.917-938.

- Poole, I. 1994. Twig - Wood Anatomical Characters as paleoecological Indicators. *Review of Palaeobotany and Palynology*. **81**(1), pp.33–52.
- Poole, I., Richter, H.G. and Francis, J.E. 2000a. Evidence for Gondwanan origins for Sassafras (Lauraceae)? Late Cretaceous fossil wood of Antarctica. *IAWA Journal*. **21**(4), pp.463-475.
- Poole, I., Cantrill, D.J., Hayes, P. and Francis, J. 2000b. The fossil record of Cunoniaceae: new evidence from the Late Cretaceous wood of Antarctica?. *Review of Palaeobotany and Palynology*. **111**(1), pp.127-144.
- Poole, I., Gottwald, H. and Francis, J.E. 2000c. Illicioxylon, an element of Gondwanan polar forests? Late Cretaceous and Early Tertiary woods of Antarctica. *Annals of Botany*. **86**(2), pp.421-432.
- Poole, I. and Cantrill, D. 2001. Fossil woods from Williams Point beds Livingston Island, Antarctica: a Late Cretaceous southern high latitude flora. *Palaeontology*. **44**(6), pp.1081-1112.
- Poole, I., Hunt, R.J. and Cantrill, D.J. 2001. A fossil wood flora from King George Island: ecological implications for an Antarctic Eocene vegetation. *Annals of Botany*. **88**(1), pp. 33-54.
- Poole, I. 2002. Systematics of Cretaceous and Tertiary Nothofagoxylon: implications for Southern Hemisphere biogeography and evolution of the Nothofagaceae. *Australian Systematic Botany*. **15**(2), pp.247–276.
- Poole, I., Mennega, A.M.W. and Cantrill, D.J. 2003. Valdivian ecosystems in the Late Cretaceous and Early Tertiary of Antarctica: further evidence from myrtaceous and eucryphiaceous fossil wood. *Review of Palaeobotany and Palynology*. **124**(1), pp.2-27.
- Poole, I., Cantrill, D. and Utescher, T. 2005. A multi-proxy approach to determine Antarctic terrestrial palaeoclimate during the Late Cretaceous and Early Tertiary. *Palaeogeography, Palaeoclimatology, Palaeoecology*. **222**(1), pp.95-121.
- Poole, I. and Cantrill, D.J. 2006. Cretaceous and Cenozoic vegetation of Antarctica integrating the fossil wood record. In: Francis, J.E., Pirrie, D. and

- Crame, J.A. eds. *Cretaceous-Tertiary High-Latitude Palaeoenvironments, James Ross Basin, Antarctica*. London: Geological Society, London, Special Publications, **258**, pp.63-81.
- Poorter, L. McDonald, I. Alarcón, A. Fichtler, E. Licona, J.C., Peña-Claros, M., Sterck, F., Villegas, Z. and Sass-Klaassen, U. 2010. The importance of wood traits and hydraulic conductance for the performance and life history strategies of 42 rainforest tree species. *New Phytologist*. **185**(2), pp.481-492.
- Pross, J. Contreras, L., Bijl, P.K., Greenwood, D.R., Bohaty, S.M., Schouten, S., Bendle, J.A., Röhl, U., Tauxe, L., Raine, I., Huck, C.E., Fliedert, T., Jamieson, S.S.R., Stickley, C.E., Schoutbrugg, B., Escutia, C., Brinkhuis, H. and IODP expedition 318 scientists. 2012. Persistent near-tropical warmth on the Antarctic continent during the early Eocene epoch. *Nature*. **488**, pp.73-77.
- Pujana, R.R., Umazono, A.M. and Bellosi, E.S. 2007. Maderas fósiles afines a Araucariaceae de la Formación Bajo Barreal, Cretácico Tardío de Patagonia central (Argentina). *Revista del Museo Argentino de Ciencias Naturales nueva serie*. **9**(2), pp.161-167.
- Pujana, R.R., Santillana, S.N. and Marensi, S.A. 2014. Conifer fossil woods from La Meseta Formation (Eocene of Western Antarctica): Evidence of Podocarpaceae-dominated forests. *Review of Palaeobotany and Palynology*. **200**, pp.122-137.
- Pujana, R.R., Marensi, S.A. and Santillana, S.N. 2015. Fossil woods from the Cross Valley Formation (Paleocene of Western Antarctica): Araucariaceae-dominated forests. *Review of Palaeobotany and Palynology*. **222**, pp.56-66.
- Raine, J.I., Mildenhall, D.C. and Kennedy, E.M. 2011. *New Zealand fossil spores and pollen: an illustrated catalogue*. 4th edition. [Online] [1 December 2014]. Available from: <http://data.gns.cri.nz/sporepollen/index.htm>
- Rancusi, M.H., Nishida, M. and Nishida, H. 1987. Xylotomy of Important Chilean woods. In: Nishida, M. ed. *Contributions to the Botany in the Andes II*. Tokyo: Academia Scientific Book INC, pp.68-153.
- Read, J. and Hill, R.S. 1985. Dynamics of *Nothofagus*-dominated rainforest on mainland Australia and lowland Tasmania. *Vegetatio*. **63**(2), pp.67-78.

- Read, J. and Hill, R.S. 1988. The dynamics of some rainforest associations in Tasmania. *Journal of Ecology*. **76**(2), pp.558-584.
- Read, J. and Brown, M.J. 1996. Ecology of Australian *Nothofagus* forests. In: Veblen, T.T., Hill, R.S. and Read, J. eds. *The ecology and biogeography of Nothofagus forests*. New Haven: Yale University Press, pp. 131-181.
- Read, J. and Hope, G.S. 1996. Ecology of *Nothofagus* forests of New Guinea and New Caledonia. In: Veblen, T.T., Hill, R.S. and Read, J. eds. *The ecology and biogeography of Nothofagus forests*. New Haven: Yale University Press, pp. 201-256.
- Royer, D.L., Pagani, M. and Beerling, D.J. 2012. Geobiological constraints on Earth system sensitivity to CO₂ during the Cretaceous and Cenozoic. *Geobiology*.**10**(4), pp.298-310.
- Sadler, P.M. 1988. Geometry and stratification of uppermost Cretaceous and Paleogene units on Seymour Island, northern Antarctic Peninsula. In: Feldmann, R.M. and Woodburne, M.O. eds. *Geology and Paleontology of Seymour Island, Antarctic Peninsula*. Boulder: Geological Society of America Memoirs, **169**, pp.303-320.
- Sakai, A. and Wardle, P. 1978. Freezing resistance of New Zealand trees and shrubs. *New Zealand Journal of Ecology*. **1**, pp.51–61.
- Sakai, A., Paton, D.M. and Wardle, P. 1981. Freezing resistance of trees of the South Temperate Zone, especially subalpine species of Australasia. *Ecology*. **62**(3), pp.563–570.
- Sakala, J. and Vodrážka, R. 2014. A new species of *Antarctoxylon*: a contribution to the early angiosperm ecosystem of Antarctica during the late Cretaceous. *Antarctic Science*. **26**(04), pp.371-376.
- Salmon, J.T. 1980. *The native trees of New Zealand*. Auckland: Reed books.
- Sanguinetti, J. and Kitzberger, T. 2008. Patterns and mechanisms of masting in the large-seeded southern hemisphere conifer *Araucaria araucana*. *Austral Ecology*. **33**(1), pp.78–87.

- Savrda, C.E. 1991. Teredolites, wood substrates, and sea-level dynamics. *Geology*. **19**(9), pp.905-908.
- Savrda, C.E., Ozalas, K., Demko, T.H., Huchison, R.A. and Scheiwe, T.D. 1993. Log-grounds and the ichnofossil Teredolites in transgressive deposits of the Clayton Formation (Lower Paleocene), western Alabama. *Palaios*. **8**(4), pp.311-324.
- Schweingruber, F.H. 1996. *Tree rings and environment: dendroecology*. Berne: Paul Haupt.
- Scotese, C.R. 2002. *Paleomap website*. [online]. [Accessed 18 April 2016]. Available from: <http://www.scotese.com>.
- Scott, A.C. 2010. Charcoal recognition, taphonomy and uses in palaeoenvironmental analysis. *Palaeogeography, Palaeoclimatology, Palaeoecology*. **291**(1), pp.11–39.
- Sewall, J.O., Huber, M. and Sloan, L.C. 2004. A method for using a fully coupled climate system model to generate detailed surface boundary conditions for paleoclimate modeling investigations: an early Paleogene example. *Global and Planetary Change*. **43**(3), pp.173-182.
- Shellito, C.J., Sloan, L.C. and Huber, M. 2003. Climate model sensitivity to atmospheric CO₂ levels the Early-Middle Paleogene. *Palaeogeography, Palaeoclimatology, Palaeoecology*. **193**(1), pp.113-123.
- Spicer, R.A. and Parrish, J.T. 1990. Late Cretaceous-early Tertiary palaeoclimates of northern high latitudes: a quantitative view. *Journal of the Geological Society*. **147**(2), pp.329-341.
- Stephens, J.M.C., Molan, P.C. and Clarkson, B.D. 2005. A review of *Leptosperum scoparium* (Myrtaceae) in New Zealand. *New Zealand Journal of Botany*. **43**(2), pp.431-449.
- Steubing, L., Alberdi, M. and Wenzel, H. 1983. Seasonal changes of cold resistance of Proteaceae of the South Chilean laurel forest. *Vegetatio*. **52**(1), pp.35-44.

Stewart, G.H. and Veblen, T.T. 1982. Regeneration patterns in southern rata (*Metrosideros umbellata*) - Kamahi (*Weinmannia racemosa*) forests in central Westland, New Zealand. *New Zealand Journal of Botany*. **20**(1), pp. 55-72.

Stopes, M.C. 1914. A new Araucarioxylon from New Zealand. *Annals of Botany*. **2**, pp.341-350.

Swenson, N.G. and Enquist, B.J. 2007. Ecological and evolutionary determinants of a key plant functional trait: wood density and its community-wide variation across latitude and elevation. *American Journal of Botany*. **93**(3), pp.451-459.

Terada, K., Nishida, H., Asakawa, T.O. and Herrera, M.R. 2006a. Fossil wood assemblage from Cerro Dorotea, Ultima Esperanza, Magallanes (XII) region, Chile. In: Nishida, H. ed. *Post-Cretaceous floristic changes in Southern Patagonia Chile*. Tokyo: Taisei Printing Co Ltd, pp.67-89.

Terada, K., Asakawa, T.O. and Nishida, H. 2006b. Fossil woods from Arroyo Cardenio, Chile Chico province, Aisen (XI) region, Chile. In: Nishida, H. ed. *Post-Cretaceous floristic changes in Southern Patagonia Chile*. Tokyo: Taisei Printing Co Ltd, pp.57-65.

The wood database. The wood database. [Online]. [Accessed 15 July 2015]. Available from: <http://www.wood-database.com>.

The world's best photos of orites. 2016. *Heathland with orites revoluta, Cradle Mountain*. [online]. [Accessed 11 February 2016]. Available from: <https://farm6.static.flickr.com>

Tobin, T.S., Ward, P.D., Steig, E.J., Olivero, E.B., Hilburn, I.A., Mitchell, R.N., Diamond, M.R., Raub, T.D. and Kirschvink, J.L. 2012. Extinction patterns $\delta^{18}O$ trends, and magnetostratigraphy from a southern high-latitude Cretaceous-Paleogene section: Links with Deccan volcanism. *Palaeogeography, Palaeoclimatology, Palaeoecology*. **350**, pp.180-188.

Torres, T. and Bagoczky, L.B. 1986. Xilotomy of fossil conifers from the Quiriquina Island, Chile. *Comunicaciones*. **37**, pp.65-80.

- Torres, T. and Lemoigne, Y. 1988. Tertiary fossil wood from the Arctowski Cove Formation, King George Island, Antarctica. *Serie Científica del Instituto Antártico Chileno*. **37**, pp.69-107.
- Torres, T. and Lemoigne, Y. 1989. Fossil wood findings of angiosperm and gymnosperms of the upper Cretaceous at Williams Point, Livingston Island, South Shetland Islands, Antarctica. *Serie Científica del Instituto Antártico Chileno*. **38**, pp.10-29.
- Torres, T. Marensi, S. and Santillana, S. 1994. Fossil wood of Seymour Island, La Meseta Formation, Antarctica. *Serie Científica del Instituto Antártico Chileno*. **44**, pp.17-38.
- Tosolini, A.M.P., Cantrill, D.J. and Francis, J.E. 2013. Paleocene flora from Seymour Island, Antarctica: revision of Dusén's (1908) angiosperm taxa. *Alcheringa: An Australasian Journal of Palaeontology*. **37**(3), pp.366-391.
- Umazano, A.M., Melchor, R.N., Bedatou, E., Bellosi, E.S. and Krause, J.M. 2014. Fluvial response to sudden input of pyroclastic sediments during the 2008-2009 eruption of the Chaitén Volcano (Chile): The role of logjams. *Journal of South American Earth Sciences*. **54**, pp. 140–157.
- Upchurch, G.R., Otto-Bliesner, B.L. and Scotese, C. 1998. Vegetation-atmosphere interactions and their role in global warming during the latest Cretaceous. *Philosophical Transactions of the Royal Society of London B: Biological Sciences*. **353**(1365), pp.97-112.
- Utescher, T. and Mosbrugger, V. 2015. *The Palaeoflora Database*. [online]. [Accessed January - March 2015]. Available from: <http://www.geologie.unibonn.de/Palaeoflora>.
- Valle, R.A.D., Elliot, D.H. and Macdonald, D.I.M. 1992. Sedimentary basins on the east flank of the Antarctic Peninsula: proposed nomenclature. *Antarctic Science*. **4**(4), pp.477–478.
- Veblen, T.T. and Ashton, D.H. 1978. Catastrophic influences on the vegetation of the Valdivian Andes, Chile. *Vegetatio*. **36**(3), pp.149–167.

- Veblen, T.T., Burns, B.R., Kitzberger, T., Lara, A. and Villalba, R. 1995. The ecology of the conifers of southern South America. In: Enright, N.J. and Hill, R.S. *Ecology of the southern conifers*. Carlton: Melbourne University Press, pp.120-170.
- Veblen, T.T., Donoso, C., Kitzberger, T. and Rebertus, A.J. 1996. Ecology of southern Chilean and Argentinean *Nothofagus* forests. In: Veblen, T.T., Hill, R.S. and Read, J. eds. *The ecology and biogeography of Nothofagus forests*. New Haven: Yale University Press, pp. 293-353.
- Videl, O.J., Bannister, J.R., Sandoval, V., Pérez, Y. and Ramírez, C. 2011. Woodland communities in the Chilean cold-temperate zone (Baker and Pascua basins): Floristic composition and morpho-ecological transition. *Gayana. Botanica*. **68**(2), pp.141-154.
- Wagstaff, S.J. 2004. Evolution and biogeography of the austral genus *Phyllocladus* (Podocarpaceae). *Journal of Biogeography*. **31**(10), pp.1569-1577.
- Wardle, P. and MacRae, A.H. 1966. Biological flora of New Zealand: 1. *Weinmannia Racemosa* Linn.F.(Cunoniaceae). Kamahi. *New Zealand Journal of Botany*. **4**(1), pp.114–131.
- Wardle, P. 1969. Biological flora of New Zealand: 4. *Phyllocladus alpinus* Hook F. (Podocarpaceae), Mountain Toatoa, Celery Pine. *New Zealand Journal of Botany*. **7**(1), pp.76-95.
- Wardle, P. 1991. *Vegetation of New Zealand*. Cambridge: Cambridge University Press.
- Wardle, P., Ezcurra, C., Ramirez, C. and Wagstaff, S. 2001. Comparison of the flora and vegetation of the southern Andes and New Zealand, *New Zealand Journal of Botany*. **39**(1), pp.69-108.
- Westerhold, T., Röhl, U., Donner, B., McCarren, H.K. and Zachos, J.C. 2011. A complete high-resolution Paleocene benthic stable isotope record for the central Pacific (ODP Site 1209). *Paleoceanography*. **26**(2), pp.1-13.

- Wheeler, E.A. and Baas, P. 1993. The potentials and limitations of dicotyledonous wood anatomy for climatic reconstructions. *Paleobiology*. **19**(4), pp.487–498.
- Wheeler, E.A., Wiemann, M.C. and Fleagle, J.G. 2007a. Wood from the Miocene Bakate Formation, Ethiopia Anatomical characteristics, estimates of original specific gravity and ecological inferences. *Review of Palaeobotany and Palynology*. **146**(1), pp.193-207.
- Wheeler, E.A., Baas, P. and Rodgers, S. 2007b. Variations in dicot wood anatomy: A global analysis based on the Insidewood Database. *IAWA Journal*. **28**(3), pp.229–258.
- Wheeler, E.A., Sung, J.L. and Baas, P. 2010. Wood anatomy of the Altingiaceae and Hamamelidaceae. *IAWA Journal*. **31**(4), pp.399-423.
- Whitham, A.G., Ineson, J.R. and Pirrie, D. 2006. Marine volcanoclastics of the Hidden Lake Formation (Coniacian) of James Ross Island, Antarctica: an enigmatic element in the history of a back-arc basin. In: Francis, J.E., Pirrie, D. and Crame, J.A. eds. *Cretaceous - Tertiary high-latitude palaeoenvironments, James Ross Basin, Antarctica*. London: Geological Society, London, Special Publications, **258**, pp. 21–47.
- Wiemann, M.C. and Williamson, G.B. 2002. Geographic variation in wood specific gravity: effects of latitude, temperature, and precipitation. *Wood and fibre science*. **31**(1), pp.96-107.
- Wikipedia. 2016. *Valdivian temperate rain forest*. [online]. [Accessed 11 February]. Available from: www.wikimedia.org.
- Williamson, B.G. and Wiemann, M.C. 2010. Measuring wood specific gravity correctly. *American Journal of Botany*. **97**(3), pp.519-524.
- Witts, J.D., Bowman, V.C., Wignall, P.B., Crame, J.A., Francis, J.E. and Newton, R.J. 2015. Evolution and extinction of Maastrichtian (Late Cretaceous) cephalopods from the López de Bertodano Formation, Seymour Island, Antarctica. *Palaeogeography, Palaeoclimatology, Palaeoecology*. **418**, pp.193-212.

- Wolfe, J.A. 1980. Tertiary climates and floristic relationships at high latitudes in the Northern Hemisphere. *Palaeogeography, Palaeoclimatology, Palaeoecology*. **30**, pp.313-323.
- Wren, J.H. and Hart, G.F. 1988. Paleogene dinoflagellate cyst biostratigraphy of Seymour Island, Antarctica. In: Feldmann, R.M. and Woodburne, M.O. eds. *Geology and Paleontology of Seymour Island, Antarctic Peninsula*. Boulder: Geological Society of America Memoirs, **169**, pp. 163-252.
- Zachos, J., Pagani, M., Sloan, L., Thomas, E. and Billups, K. 2001. Trends, rhythms, and aberrations in global climate 65Ma to present. *Science*. **292**, pp. 686-693.
- Zachos, J.C., Wara, M.W., Bohaty, S. Delaney, M.L., Petrizzo, M.R., Brill, A., Bralower, T.J. and Premoli-Silva, I. 2003. A transient rise in tropical sea surface temperature during the Paleocene-Eocene thermal maximum. *Science*. **302**, pp.1551-1554.
- Zachos, J.C., Dickens, G.R. and Zeebe, R.E. 2008. An early Cenozoic perspective on greenhouse warming and carbon-cycle dynamics. *Nature*. **451**, pp.279-283.
- Zhang, S.B., Cao, K.F., Fan, Z.X. and Zhang, J.L. 2013. Potential hydraulic efficiency in angiosperm trees increases with growth-site temperate but has no trade-off with mechanical strength. *Global Ecology and Biogeography*. **22**(8), pp.971-981.
- Zhang, Y., Wang, J. and Lujun, L. 2010. *Protophylocladoxylon jingyuanense* sp. nov., a gymnospermous wood of the Serpukhovian (Late Mississippian) from Gansu, Northwest China. *Acta geologica sinica*. **84**(2), pp.257-268.
- 2 Landscapes. 2016. *Plant profiles > Phyllocladus*. [online]. [10 March 2016]. Available from: <http://www.o2landscapes.com>

Appendix A. Wood specimens.

Table A.1 New numbers allocated to wood specimens.

Specimen numbers	numbers allocated in this project
D9.015.1	1
D9.016.1	2
D9.027.1	3
D9.011.1	4
D9.012.1	5
D9.018.1	6
D9.019.1	7
D9.019.2	8
D9.020.1	9
D9.021.1	10
D9.022.1	11
D9.023.1	12
D9.036.1	13
D9.038.1	14
D9.040.1	15
D9.041.1	16
D9.043.1	17
D9.044.1	18
D9.059.1	19
D9.050.1	20
D9.053.1	21
D9.054.1	22
D9.089.1	23
D9.090.1	24
D9.091.1	25
D9.092.1	26
D9.093.1	27
D9.094.1	28
D9.095.1	29
D9.096.1	30

Table A.1 Continued.

Specimen number	New numbers allocated in this project
D9.098.1	31
D9.105.1	32
D9.118.1	33
D9.107.1	34
D9.109.1	35
D9.110.1	36
D9.111.1	37
d9.112.1	38
D9.125.1	39
D9.128.1	40
D9.128.2	41
D9.128.3	42
D9.130.1	43
D9.136.1	44
D9.139.1	45
D9.161.1	46
D9.168.1	47
D9.157.3	48
D9.071.1	49
D9.153.1	50
D9.191.1	51
D9.191.1	52
D9.181.1	53
D9.182.1	54
D9.186.1	55
D9.304.1	56

Specimen	D9.015.1	D9.016.1	D9.027.1	D9.011.1	D9.012.1	D9.018.1	D9.019.2
Location on section	lopes below K-T layer	Slopes below K-T layer	At 3m on line D9.601	At 21m level on D9.600	At 21m level on D9.600	at 21m on D9.600(bag says k2)	at 21m on D9.600
remarks	Fragments of wood held together by masking tape and attached to rock	2 thin pieces of wood, that look like they fit together.	1 large piece of wood within a piece of rock. 1 smaller piece in rock and a separate piece. They all look like they are from the same piece.	Wood fragments are stuck together with masking tape.	2 pieces of wood possibly of a large branch.	2 pieces (don't know how they fit together Look like the quarter of a small branch or the inner part of a trunk. Angular edges, broken up pieces, so possibly high energy regime, but they would have travelled very far.	Small branch or the inside of a log
Preservation type hand specimen	Calcite mineralisation	It has a weathered look to it fragmented sharp edges, broken into two. Premineralised. Calcite. Black weathered look on inside.	Calcareous permineralisation. Light brown woody colour. And woody texture. The inside is a dark purply grey colour.	Calcite mineralisation	Calcite mineralisation	Looks like it has undergone calcite premineralisation . Weathered, with angular edges, light (woody colour) the out side.	light woody colour on outside, very dark grey on inside
Boreholes	N/A	N/A	N/A	N/A	2 on a, 1 on b (3 altogether)	n/a	n/a
Length	Largest fragment (4cm)	8.5cm (2 pieces stuck together)	largest piece: 3.5cm other pieces 4.5cm-3cm pieces	4cm	(a) 8.5cm. B) 6.3cm	Large piece: 6.2cm Small piece: 6.9cm	7cm
Width	Largest Fragment(2cm)	4.2cm (two pieces stuck together)	largest piece: 6.5cm other pieces 2.5cm	5cm	(a,6cm) b)5cm	7.5cm	6.2cm
Thickness	5mm (largest fragment)	7mm (two pieces stuck together)	Largest piece 5cm. Other piece s 3cm-1.5cm	3cm	(a6cm) b) 5cm	4.1cm	3.5cm

Specimen	D9.036.1	D9.038.1	D9.040.1	D9.041.1	D9.043.1	D9.044.1
Location on section	at 15m on D9.601	17m on D9.601	at 31m on D9.601 328	at 31m on D9.601	19.5m level on section line D9.602	19.5m level on section line D9.602
remarks	2 small pieces of wood that look to be from the inner part of a trunk or branch.	1 piece of wood possibly the inner part of the trunk or large branch. Rings have high curvature. Angular edges.	3 pieces of wood just fragments	fragment of wood broken piece from the inside of trunk or branch. Rings have high curvature, looks like there is a pith present.	small fragments of black wood. Can smell sulphur	1 piece
Preservation type hand specimen	Calcareous permineralisation.	calcareous permineralisation.	Calcareous permineralisation. Show an orange brown rusty colour in some areas suggesting hemetite. The outside of the wood pieces is a light woody colour, the inside is a dark grey black.	petrified. Iron hemite (pink colouring) mineralisation, along with calcite	Lignified, reason because black and possibly calcite mineralisation.	calcarous mineralisation. Looks as though there is a bit of iron in there as well.
Boreholes	N/A	13 (1cm x 1cm) (7mm x 5mm)	n/a	4 borings. size 2cm to 7mm	n/a	21 visible bore holes 1.3-2cm
Length	largest piece 3.5cm. Smaller piece 4cm	4.5cm	wood pieces range from: 5.5cm-4.5cm	8.5cm	range 2.5-3cm	6.5cm
Width	largest piece 2cm Smaller piece: 1.5cm	6.2cm	range: 3.5cm-3cm	4.3cm	1cm	7.8cm
Thickness	largest piece 1.8cm. Smaller piece 1.3cm	4.3cm	1.3cm-1cm	2.3cm	1cm-2mm	5cm

Specimen	D9.019.1	D9.020.1	D9.021.1	D9.022.1	D9.023.1
Location on section	at 21m on D9.600(bag says k1 layer near kT)	at 21m on D9.600	At 21 m on D9.600	At 21m on D9.600.(bag says wood k1)	At 21m on D9.600.(bag says wood near k1)
remarks	Bag full of small shards and 1 larger piece. All shards are angular. Lare piece broken fragments can,t tell which piece of a tree it came from. It has angular edge possibly transported in a high energy regime, but hasn't travelled very far.	contains 2 pieces. One piece is attached to rock. Glauconite minerals are resent in rock. Medium grained sandstone.	there are three fragments: 1 attached to rock and 2 separate pieces.	There are three pieces the in bag and they are attached to them.	8 small pieces. 5 are thin shards. Are slightly larger thicker pieces. Some are attached to rock.
Preservation type hand specimen	This is just a fragment of wood, can tell which part of the tree it would have come from. Sharp jagged edges The outside is a light woody colour inside is darker. Looks like calcite premineralisation.	weathered a light woody colour on outside. Dark on inside. Calcite preservation.	Calcareous mineral preservation. All pieces have a light brown woody texture and colour on the outside, but this dark grey on the inside. The two sperate fragments have a more smooth feel to them.	The preservation looks calcareous. All three pieces have a woody colour and texture on the out side. On the inside they are a dark purply grey colour. They are just broken up fragments that have jagged edges.	Calcareous permineralisation. Light brown woody colour. And woody texture. The inside is a dark purply grey colour.
Boreholes	n/a	n/a	There appears to be 1 in the piece of wood that is attached to the rock.	n/a	n/a
Length	7.5cm	Largest piece: 4.2cm. Small piece: 7.2cm	Wood attached to rock: 5cm. The other pieces range from 3 and 4 cm	6cm, 4.7cm, 5.3cm	thin shards range from 4.7cm-2.4cm. Three larger blocks 4.5cm-3cm
Width	4.1cm	Largest piece:4.4cm. Small piece: 2.2cm	Wood attached to rock: 2.5cm. The other pieces around 2 cm	3cm, 3.5cm, 2.5cm	Thin shards range from 1.5cm-7mm. Three large blocks: 2.5cm-1.3cm
Thickness	1.8cm	Largest piece 3cm. Small piece:2cm	wood attached to rock: 8mm. The other pieces are 8mm and 1.2mm	1.3cm, 1.2cm, 1.5cm	Thin shards 2mm Three Large blocks: 1.7cm-9mm

Specimen	D9.059.1	D9.050.1	D9.053.1	D9.054.1	D9.089.1	D9.090.1
Location on section	at 27.5 on D9.602	at 34.5 on D9.602	at 48m on D9.602	at 48m on D9.602	at 75m on D9.603	at 75m on D9.603
remarks	2 pieces	1 large piece	2 pieces	1 piece	1 pieces	1 piece with a rounded end smooth out side . Yellow on the outside, dark grey on the inside, possibly slightly charred. Growth rings are a little wavy, maybe it has undergone some compression. Possible from the outer part of a tree since growth rings have low curvature.
Preservation type hand specimen	Calcareous perminerlisation. Its has a slight pink haze on the cut surface and outside of wood suggesting hemitite.	Calcareous perminerlisation.dark grey but appear to have a very slight pink ting to it, suggesting hemitite is present. There is a bit of shell that looks as though it has undergone pyrotite minerlisation.	Calcarous minerlisation. Light brown woody colour on the outside. Dark grey on the inside. On the bottom of one of the pieces, there is a slight orangy red colour, suggesting hemitite.	Calcate minerlisation. Some area have red and yellow minerals.	Black in colour Soft flakey outside look charcoalified and mineralised in the middle.	Calcite perminerlisation.
Boreholes	n/a	over 50 size range 1cm-5mm	n/a	1	n/a	n/a
Length	7.4cm	12cm	3.5cm	4.8cm	3.5cm	7.5cm
Width	2.5cm	5cm	4.5cm	5cm	4.5cm	6cm
Thickness	3.5cm	7.5cm	2.2cm	5cm	3cm	4.2cm

Specimen	D9.118.1	D9.107.1	D9.109.1	D9.110.1
Location on section	at 75m on D9.603	at 95m on D9.603	at 96m on D9.603	at 96m on D9.603
remarks	1 piece of wood, angular in sides/edges. Looks like it is from the outer part of trunk.	1 piece of wood, angular in shape	1 piece of wood, angular in shape	piece of wood it has a curved edge, looks like it comes from a branch. Look half in tack.
Preservation type hand specimen	Petrified calcite permineralisation. Dark grey on the inside.	petrified calcite, as it is grainy under the microscope. Colour is dark grey on inside, suggesting organic matter is still present.	Calcified dark bluey grey inside.	pertrified calcified, however under the normal microscope one of the bore holes had elongate crystals. Small area on the outside that has red-yellow staining.
Boreholes	3 (1cm x 3mm to 1.5cmx 1.3cm	10 1x 1.5cm to 2mm x 2mm	1(1x1cm)	9 (1cm x 7mm) to (5mm x 2mm)
Length) 10.3cm	6.7cm	7cm	4.5cm
Width	9.3cm	8cm	10.2cm	5.8cm
Thickness	6.2cm	5.7cm	4cm	4cm

Specimen	D9.111.1	D9.112.1	D9.125.1	D9.128.1	D9.128.2
Location on section	at 96m on D9.603	at 96m on D9.603	doesn't say, could possibly be 145.5m on D9.603	173m at D9.603	173m at D9.603
remarks	1 full round piece possibly branch or inner part of a trunk. Angular edges	1 large piece, full ring series.	2pieces look to be part of a branch or trunk. They are angular shaped.	3 pieces of wood just fragments angular edges. Dark grey colour. No growth rings are present.	1 piece fragment angular edges.
Preservation type hand specimen	Calcite permineralisation	calcite permineralisation	Appear to be Calcite permineralisation. Dark grey almost black on the inside. Light grey-wood brown on the outside.	calcite permineralisation. Dark grey.	Calcite permineralisation dark grey
Boreholes	heavily bored 70> size ranging from 8mm x 6mm) to 2mmx2mm)	42> 1cm x 8mm)	2 (7mm)	3	n/a
Length	9.5cm	9.5cm	7.5cm. 7cm	n/a	5.6cm
Width	7.5cm	6.5cm	5.5cm. 6cm	5.5cm, 6cm, 6cm	4.5cm
Thickness	7.2cm	8.5cm	3.1cm. 3.3cm	3cm, 3.5cm,1.5cm	3cm

Specimen	D9.128.3	D9.130.1	D9.136.1	D9.139/1	D9.161.1
Location on section	173m at D9.603	183m on D9.603	230m on D9.603	239m on D9.603	48m on D9.604
remarks	1 piece of wood attached to sediment and 1 piece by it self. Anguler sided pieced, can tell which part of a tree it came from.	14 small pieces. Angular pieces	lots of thin fragments that have one egde that is rounded.	a bag with lots of small fragment. A separate bag with a larger piece of wood that has a rounded shape. The outside feels like it has been charred, but the inside has been permineralised	1 piece of wood. Rounded end
Preservation type hand specimen	calcite permineralisation with a bit of iron in there.	Calcite permineralisation	calciter permineralisation, due to grainy texture,calcite crystals. However it is black suggesting a lot of organic matter.	large piece in separate bag:Calcite permineralisation and slight charred outside. Small fragments Calcite permineralisation.	calcite permineralisation. It has hemitite staining. I think that it has some sulphate minerals in there as well.
Boreholes	n/a	n/a	n/a	n/a	n/a
Length	6cm. 3cm	range from 4.5cm to 2cm	10cm	Large piece in separate bag. 8cm	7.3cm
Width	2cm. 4cm	1.8cm to 5mm	1.7mm	large piece in separate bag 4.3cm	4.6cm
Thickness	2cm. 3cm	1cm to 5mm	1cm-5mm	large piece in separate bag: 2cm	3cm

Specimen	D9.168.1	D9.157.3	D9.071.1	D9.153.1	D9.191.1
Location on section	66.6m on D9.604	top of sobral mudstone layer	9m on D9.300	From bluff in Cross Valley	at 25.5m D9.300
remarks	1 fragment, looks like branch. Orange-yellow colour on the outside. Dark grey on the inside.	fragment of wood (lignite) angular	contains a number of pieces all are angular	3 fragment angular don't know which part of a tree they wood come from	very angular broken up piece of wood, from tree rings it looks like it has undergone compression. It is very angular. Can't tell what part of a tree it could possibly come from.
Preservation type hand specimen	Calcite permineralisation, might have some iron oxide in their.	Lignified it is dark grey, black on the inside	one piece is brown inside, possibly organic matter, could be lignite. Looks like the original wood is still present.	1 piece is calcified , there the two other pieces are red suggesting iron oxide.	Looks to be calcium carbonate. It is very light in colour. On a fresh cut surface it is a very dark colour suggesting a lot of organic material.
Boreholes	n/a	n/a	n/a	white piece: 11 (1cmx8mm to 4mmx 4mm) red piece: 4mm x 2mm)	n/a
Length	16cm	6cm	range 9cm-7cm	White piece:4.3cm Red piece: 6cm	5.8cm
Width	5cm	3.5cm	6cm to 2.5cm	white piece 6cmRed piece: 3.5cm	4.5cm
Thickness	2.5cm	1.5cm	2.2cm to 6mm	white piece 3cm Red piece: 1.3cm	5.4cm

Specimen	D9.191.2	D9.181.1	D9.182.1	D9.186.1	D9.304.1
Location on section	at 21m on D9.302	1	142m on D9.300	At 145 on D9.300	5m on D9.302
remarks	flat angular piece. Looks like it has undergone compression.	Woody texture, compressed, reddish colour. Flat shard.	1 piece stuck together with masking tape. Rounded edges. Inside of large branch or trunk. High curvature of rings. Rings are really wide.	Slim piece of wood with haematite staining.	1 thin piece
Preservation type hand specimen	calcite permineralisation. iron oxide present	Haematite	iron oxide. Reddy-brown in colour	Haematite	calcite permineralisation/charcoalified
Boreholes	n/a	n/a	n/a	n/a	n/a
Length	10.3cm	10cm	9.5cm	9.5	9.3cm
Width	10.5cm	3	5.5cm	7cm	4.7cm
Thickness	2.7cm	1.1	6cm	1.5cm	1cm

Specimen	D9.091.1	D9.092.1	D9.093.1	D9.094.1
Location on section	at 75m on D9.603	75m near cairn on D9.603	at 75m on D9.603	at 75m on D9.603
remarks	bit of the inner part of a branch or trunk, it hasn't got a full ring series. Tree ringd present show high ring curvature.	1 piece of wood. Its a large piece of wood. Due to low ring curvature. Angular sides.	1 piece of wood with masking tape around. It's a bit crumbly. Either part of a large branch or the inside of a trunk. Not fully all their. Its has an angular shape.	1 piece inner part of a tree or branch. It stills has curvature to the wood.
Preservation type hand specimen	Calcite permineralisation	Calcite permineralisation	Calcified it is dark grey on the cut surface. There is also a pink-brown ting to it. Petrified calcite permineralisation.	it is permineralised. Calcite.
Boreholes	2 (9mm)	8 all over (1.6cm x(1.4cm) all appear to be around that size.	28 on one surface and the side(1cmx1cm) (-7mmx7mm)	n/a
Length	8cm	10.5cm	8cm	3.5cm
Width	3cm	8cm	7cm	8cm
Thickness	4.5cm	5.2cm	4.9cm	3cm

Appendix B Wood anatomy measurements

Appendix B.1 Conifer wood anatomy measurements

Ray height μm

	D9.019.2	D9.193	D9.036.1	D9.112.1	D9.059.1	D9.111	D9.098.1	D9.153.1	D9.071	D9.022.1
1	30	105	95	65	140	110	155	95	275	122.5
2	20	35	20	35	135	65	75	70	200	140
3	10	235	45	70	75	35	55	160	380	170
4	25	125	60	80	235	90	125	55	80	97.5
5	27.5	245	52	35	115	85	125	65	160	122.5
6	35	62	57	35	75	85	50	70	145	145
7	50	125	90	55	90	90	50	135	115	140
8	32	220	65	110	120	162.5	75	70	275	72.5
9	40	230	50	40	110	50	110	125	125	67.5
10	37	215	40	40	245	115	50	30	150	200
11	77	295	25	65	105	75	85	70	70	60
12	35	75	75	100	110	110	35	155	175	87.5
13	25	96	75	50	140	80	100	87	200	127.5
14	80	230	75	20	130	75	82.5	120	147	100
15	27	165	85	70	235	90	100	130	550	215
16	12	155	80	55	75	80	110	145	275	162
17	37	175	30	60	75	90	120	120	380	100
18	57	35	110	90	100	85	45	145	85	155
19	30	180	65	70	90	125	60	75	110	135
20	27	56	40	35	175	120	70	30	165	207.5
21	40	56	30	35	50	90	95	40	70	105
22	35	195	75	50	175	50	80	60	140	280
23	40	100	122	70	75	100	80	100	110	110
24	12	200	100	90	175	100	100	60	60	130
25	12	80	77	130	180	110	100	75	270	205

D9.094.1	D9.139.1	D9.050.1	D9.118.1	D9.092.1	D9.109.1	D9.168.1	D9.038.1
95	110	167	60	115	392.5	122.5	50
40	167.5	410	92.5	75	530	50	145
115	175	150	55	77.5	140	35	90
55	132.5	232	127.5	187.5	115	42.5	112.5
90	140	270	100	130	320	75	97.5
90	100	262.5	160	110	85	92.5	45
45	160	362.5	92.5	32.5	155	50	140
65	125	262.5	200	75	365	117.5	65
45	90	115	90	107.5	375	95	200
100	125	197.5	352.5	100	235	135	75
47.5	100	360	170	62.5	125	90	70
80	330	250	175	37.5	360	100	180
60	130	105	75	150	162	77.5	110
132.5	preservation	135	45	25	275	65	57.5
62.5	145	160	15	90	95	60	75
42.5		125	45	100	375	112.5	45
77.5		215	147.5	115	200	75	112.5
90		150	100	50	360	145	140
40		395	30	77.5	225	75	62.5
67.5		150	120	42.5	250	50	77.5
82.5		325	37.5	140	410	105	137.5
22.5		100	95	75	105	65	50
40		245	90	150	570	50	80
105		225	100	165	435	165	230
75		250	255	100	175	62.5	85

D9.093.1	D9.044.1	D9.128.1	D9.090.1	D9.181.1	D9.125.1
85	220	135	165	130	62.5
57.5	75	255	325	115	112.5
60	125	110	90	117.5	160
47.5	265	275	300	180	140
70	205	100	135	65	130
110	75	300	135	75	150
75	325	140	45	185	95
42.5	150	300	275	90	80
92.5	352	365	225	240	260
140	180	87.5	55	137.5	150
35	310	225	115	155	255
60	140	150	450	60	195
105	65	275	137.5	180	185
75	55	195	210	130	190
40	50	260	100	135	925
110	110	485	210	140	180
55	115	475	735	175	385
100	380	270	275	122.5	125
115	105	85	675	125	65
37.5	190	75	75	275	120
40	70	300	185	250	135
70	132	175	140	130	250
30	275	150	255	230	140
45	265	30	405	150	325
62.5	150	35	675	75	55

Rays per tangential mm

D9.019.2	D9.112.1	D9.036.1	D9.193	D9.059.1	D9.111	D9.098
2	2	3	4	4	2	3
3	1	1	4	4	4	3
4	2	4	5	7	2	2
2	3	2	4	4	2	4
4	1	3	6	4	1	2
1	1	3	6	5	1	4
5	4	3	8	9	3	2
1	4	3	6	5	3	2
3	5	4	7	5	3	5
3	1	4	4	6	3	5

D9.153.1	D9.071	D9.022	D9.094.1	D9.139.1	D9.050.1	D9.118.1
5	N/a	5	3	3	4	5
4		5	1	4	3	5
3		5	3	3	5	4
4		5	3	4	4	7
5		6	2	2	5	5
3		3	1	4	5	2
5		8	3	2	3	3
2		4	2	3	4	5
2		5	4	2	5	4
6		6	2	2	7	3

D9.109.1	D9.168.1	D9.093.1	D9.044.1	D9.090.1	D9.181.1	D9.125.1
4	2	1	6	6	7	7
4	3	3	4	5	4	6
3	1	2	7	5	7	4
1	2	1	7	8	7	5
6	4	1	4	5	n/a	6
3	4	3	5	12		4
5	1	2	6	13		n/a
4	2	1	4	8		
3	3	5	5	8		
3	1	1	7	7		

Ray height number of cells

D9.036.1	D9.112.1	D9.193	D9.019.2	D9.059.1	D9.111	D9.098
5	4	5	N/A		4	8
1	2	2		4	2	4
2	4	11		2	1	3
3	5	3		8	3	8
2	2	9		3	3	7
3	2	2		1	3	3
5	3	3		2	4	2
3	7	10		3	7	4
2	2	5		3	2	7
2	3	9		7	6	2
1	4	13		3	3	4
4	6	3		3	4	2
4	3	4		5	3	6
4	1	6		4	4	4
4	4	8		9	2	6
2	3	6		2	4	6
1	4	7		2	3	7
6	5	1		3	6	2
3	4	7		2	5	3
1	3	2		6	5	3
1	2	2		1	3	4
3	3	10		11	2	4
7	5	4		2	5	4
4	6	10		4	5	5
4	7	3		6	4	6

D9.153	D9.071	D9.022	D9.094	D9.139.1	D9.050.1	D9.118	D9.092.1	D9.109.1
6	9	4	5	5	6	4	6	15
3	7	5	2	10	16	6	3	22
8	15	7	5	6	5	3	4	4
2	3	3	3	3	8	6	8	3
3	7	4	5	6	11	6	6	12
3	5	5	4	4	10	12	13	2
preservation problems	4	8	2	6	12	6	2	6
	10	2	3	5	8	10	3	11
	4	7	2	4	2	4	5	19
	5	9	5	4	3	23	6	10
	2	2	1	11	15	11	3	4
	5	3	4	6	11	11	2	17
	7	4	3	preservation	8	4	7	6
	5	2	6		10	3	1	10
	23	8	3		7	1	5	3
	9	6	2		8	2	5	15
	15	3	3		8	11	7	6
	3	6	5		5	7	3	16
	4	5	2		15	2	4	8
	7	9	3		4	8	2	9
	2	3	3		13	2	7	17
	5	13	1		3	6	4	4
	4	4	2		10	5	7	21
	2	5	7		7	6	4	19
	10	7	3		10	18	6	6

D9.168.1	D9.038.1	D9.093.1	D9.044.1	D9.128.1	D9.090.1	D9.181.1	D9.125.1
6	2	5	7	4	10	9	3
2	6	3	2	8	19	6	13
5	5	5	4	3	5	7	9
6	9	2	10	12	17	10	8
3	6	3	7	2	9	3	7
4	2	6	2	12	8	3	4
2	8	4	12	5	2	11	5
5	3	2	5	11	20	4	4
4	12	5	13	13	15	12	13
5	4	7	5	3	3	4	9
4	4	2	11	4	6	8	13
5	10	2	4	5	30	4	11
3	7	7	2	12	9	12	10
3	3	4	2	7	15	7	10
6	4	2	1	8	6	6	5
4	2	6	4	17	13	6	12
3	7	2	4	16	44	9	21
7	7	6	16	11	16	5	6
3	3	7	3	3	40	6	4
2	4	2	7	3	3	18	6
5	8	2	2	11	12	15	9
3	3	3	7	7	9	6	15
2	4	1	10	5	18	15	9
7	13	2	10	1	24	7	18
3	3	3	5	1	43	5	3

Tracheid aperture diameter μm

D9.161.1	D.112.1	D9.059.1	D9.098	D9.153	D9.071	D9.036.1
10	10	Borders are not clear	preservation	can't due to preservation	3.5	7.5
10	5				3	5
10	10				3.5	7.5
10	10				3.5	10
12	5				3.5	7.5
12	10				2.5	7.5
5	7				N/a preservation	7.5
10	5					10
5	5					7.5
5	5					5
10	7					10
5	5					5
5	5					5
10	5					7.5
7	7					5
3	5					5
7	10					7.5
7	5					5
10	5					5
7	10					5
7	10					5
7	10					5
12	10					5
12	5					5
7	5					5

D9.161.1	D.112.1	D9.059.1	D9.098	D9.153	D9.071	D9.036.1
5	5	n/a	n/a	n/a	n/a	5
5	5					5
5	5					5
5	10					5
10	10					5
10	10					5
10	5					7.5
5	5					7.5
5	5					7.5
7	5					7.5
5	5					7.5
5	5					7.5
5	5					7.5
5	5					5
10	5					5
10	5					5
5	5					5
5	10					7.5
5	5					5
5	10					5
5	10					5
5	10					5
10	5					5
10	5					5

D9.022	D9.094.1	D9.139.1	D9.050.1	D9.111.1	D9.118.1	D9.092.1
5	10	5	5	N/A	7.5	7.5
5	10	5	10		7.5	7.5
6	10	5	7.5		x	7.5
5	10	5	10		7.5	7.5
5	7.5	5	7.5		10	x
7	7.5	5	7.5		7.5	5
7	7.5	5	10		10	5
7	10	5	5		10	5
5	7.5	5	5		10	5
7	7.5	5	7.5		10	x
6	7.5	7.5	5		5	x
7	7.5	5	5		5	5
7	7.5	5	7.5		7.5	x
7	7.5	7.5	8		7.5	x
5	10	5	10		5	x
6	5	5	7.5		5	5
8	7.5	5	10		x	7.5
7	12.5	3.25	5		7.5	5
5	10	2.5	5		x	5
7	7.5	5	7.5		x	x
5	5	5	10		5	5
7	7.5	5	10		10	x
5	7.5	5	7.5		x	x
7	10	2.5	10		x	x
5	7.5	5	10		12.5	5

D9.022	D9.094.1	D9.139.1	D9.050.1	D9.111.1	D9.118.1	D9.092.1
5	7.5		5	10		12.5
7	7.5		5	10		x
10	7.5		7.5	7.5		10
8	7.5		10	10		15
10	10		7.5	12.5		10
5	7.5		7.5	5		15
7.5	10		5	5		10
8	5		5	5		10
7	10		5	10		12.5
7	25		5	10		12.5
7	7.5		6.25	10		15
7	7.5		7.5	7.5		12.5
8	7.5		5	10		x
5	10		5	5		10
8	7.5		3.75	5		x
5	7.5		2.5	7.5		x
8	7.5		5	5		x
7	10		5	7.5		x
7	7.5		5	5		7.5
7	5		5	5		15
7.5	7.5		5	7.5		12.5
8	5		5	10		5
7	7.5		5	10		x
6	10		5	7.5		x
3	10		5	7.5		x

D9.109.1	D9.168.1	D9.038.1		D9.044.1	D9.128.1	D9.090.1	D9.181.1	D9.043.1
x	2.5	5		5	x	5	x	7.5
2.5	2.5	5		5	x	5	x	7.5
5	2.5	5		7.5	x	5	7.5	5
5	2.5	2.5		7.5	x	5	5	5
5	5	2.5		5	x	5	5	5
2.5	5	5		5	x	5	5	5
2.5	2.5	5		10	x	5	5	5
6.75	2.5	2.5		10	x	7.5	2.5	2.5
10	2.5	2.5		10	x	5	2.5	7.5
5	2.5	2.5		10	2.5	5	5	2.5
2.5	2.5	2.5		7.5	5	5	2.5	5
12.5	2.5	2.5		5	5	5	2.5	5
6.75	2.5	2.5		7.5	2.5	7.5	2.5	7.5
5	2.5	2.5		10	5	2.5	2.5	5
2.5	2.5	7.5		10	2.5	2.5	2.5	2.5
7.5	2.5	5		7.5	5	5	2.5	5
2.5	2.5	2.5		7.5	5	5	2.5	5
5	2.5	2.5		10	5	2.5	x	7.5
2.5	2.5	5		7.5	2.5	5	x	5
3.75	2.763158	5		7.5	2.5	5	x	5
5		5		5	2.5	5	x	5
7.5		5		7.5	2.5	5	x	5
2.5		5		7.5	5	5	x	2.5
2.5		5		7.5	2.5	5	x	10
2.5		10		7.5	2.5	5		

Tracheid pit diameter μm

D9.036.1	D9.112.1	D9.059.1	D9.111	D9.098	D9.153.1	D9.071
20	20	10	7.5	10	15	20
17.5	20	10	5	15	15	22
20	20	10	10	15	10	20
15	20	10	10	10	12.5	22
12	22.5	5	10	10	12.5	20
12.5	20	5	10	10	12.5	20
15	20	5	5	10	17.5	20
17.5	20	10	5	15	12.5	20
15	20	7	10	15	15	20
15	15	10	10	15	12.5	20
10	15	15	10	15	12.5	20
12.5	15	10	5	15	15	15
12.5	22	10	5	15	12.5	15
12.5	20	10	7.5	20	n/a	15
16	22	10	5	20		15
15	20	10	7.5	15		17.5
15	20	10	7.5	10		17.5
15	20	10	7.5	10		15
15	20	10	7.5	20		15
15	20	10	5	12		15
12.5	15	5	7.5	15		15
17.5	20	5	5	15		15
12.5	20	15	5	20		15
12.5	20	15	7.5	20		15
15	20	5	7.5	15		20

D9.036.1	D9.112.1	D9.059.1	D9.111	D9.098	D9.153.1	D9.071
15	20	5	7.5	10		20
12.5	25	10	7.5	15		20
15	20	5	5	10		20
20	20	5	7.5	15		22.5
15	15	5	7.5	15		20
12.5	25	10	10	15		17.5
12.5	15	10	5	15		20
15	10	10	7.5	15		20
12.5	15	10	7.5	15		20
12.5	25	10	5	10		22.5
15	15	10	5	10		20
16.25	10	7	5	10		15
15	15	5	5	12		15
15	25	5	5	10		20
15	15	10	5	15		20
15	15	7	5	15		20
15	20	5	7.5	10		17.5
15	20	5	7.5	10		22.5
17.5	20	15	7.5	10		17.5
12.5	20	10	7.5	20		17.5
12.5	15	10	5	10		15
15	20	10	10	10		20
17.5	25	10	7.5	10		15
15	25	10	7.5	10		15
15	25	10	5	10		12.5

D9.022	D9.193.1	D9.094.1	D9.139.1	D9.050.1	D9.118.1
10	N/A	20	15	bad preservation	15
10		15	15		15
12.5		15	10		15
11		15	10		20
10		15	10		12.5
10		15	10		20
10		15	10		20
10		13.75	10		20
10		15	10		15
12.5		15	12.5		15
10		17.5	12.5		15
10		15	12.5		12.5
10		15	10		15
10		17.5	10		20
12.5		15	12.5		15
10		12.5	7.5		20
12.5		12.5	10		20
15		15	7.5		20
12		12.5	12.5		15
12		12.5	12.5		15
10		12.5	12.5		12.5
10		12.5	10		15
10		15	12.5		15
12		12.5	12.5		20

D9.022	D9.193.1	D9.094.1	D9.139.1	D9.050.1	D9.118.1
7		12.5	12.5		
10		12.5	15		
15		5	15		
12.5		15	15		
12		15	22.5		
15		15	20		
12		15	20		
10		15	20		
12		12.5	22.5		
12		12.5	15		
12.5		15	12.5		
10		15	17.5		
11		15	17.5		
15		15	12.5		
8		10	10		
10		17.5	10		
8		20	10		
10		17.5	12.5		
10		17.5	10		
10		15	12.5		
8		20	12.5		
12		12.5	10		
10		12.5	12.5		
10		15	12.5		
8		10	12.5		
8		15	12.5		

D9.092.1	D9.109	D9.168.1	D9.038.1	D9.093.1	D9.044.1
15	15	12.5	15	15	10
17.5	12	12.5	15	12.5	12.5
20	12.5	12.5	15	12.5	12.5
15	12.5	10	15	17.5	12.5
15	12.5	10	15	15	10
15	15	10	17.5	15	10
15	15	10	15	17.5	12.5
12.5	12.5	12.5	17.5	15	12.5
20	20	12.5	15	17.5	12.5
15	20	10	12.5	17.5	10
12.5	15	12.5	15	15	10
12.5	15	10	15	17.5	12.5
15	20	7.5	12.5	17.5	12.5
12.5	15	8.75	15	17.5	12.5
15	12.5	10	15	12.5	12.5
12.5	12.5	10	15	15	10
12.5	15	7.5	17.5	15	12.5
15.5	15	15	17.5	17.5	12.5
12.5	15	12.5	17.5	15	10
15	12.5	12.5	17.5	15	12.5
12.5	15	preservation	17.5	15	10
15	12.5	10.9375	15	12.5	10
12.5	15		15	17.5	12.5
15	15		15	17.5	10

D9.092.1	D9.109	D9.168.1	D9.038.1	D9.093.1	D9.044.1
12.5	12.5		15	17.5	10
15	12.5		15	17.5	10
10	12.5		15	15	10
17.5	10		15	12.5	10
15	12.5		12.5	12.5	10
12.5	15		15	15	10
12.5	12.5		15	17.5	12.5
15	13.75		15	20	10
15	15		12.5	15	10
15	12.5		17.5	15	10
20	15		15	15	12.5
15	15		12.5	12.5	12.5
12	12.5		10	12.5	12.5
15	12.5		12.5	17.5	12.5
15	15		12.5	15	12.5
15	15		10	12.5	12.5
17.5	15		12.5	12.5	12.5
17.5	15		12.5	15	10
15	15		12.5	15	10
15	20		12.5	12.5	7.5
15	15		10	15	12.5
17.5	15		12.5	17.5	10
15	12.5		12.5	15	10
15	12.5		10	15	10
12.5	20		12.5	15	10
15	10		10	17.5	12.5

D9.128.1	D9.090.1	D9.181.1	D9.043.1
10	15	15	12.5
10	17.5	25	15
10	12.5	20	15
10	15	20	10
10	17.5	25	12.5
10	12.5	15	10
10	12.5	15	12.5
10	12.5	15	10
7.5	12.5	17.5	12.5
10	17.5	20	15
10	12.5	15	10
12.5	17.5	22.5	15
12.5	15	20	10
12.5	10	22.5	15
7.5	15	15	10
10	15	15	10
10	15	20	15
10	12.5	20	17.5
12.5	15	25	12.5
12.5	15	25	15
7.5	15	17.5	15
10	15	17.5	15
10	15	17.5	10
10	15	15	15
7.5	15	15	15

D9.128.1	D9.090.1	D9.181.1	D9.043.1
10	12.5	20	15
7.5	10	12.5	10
7.5	12.5	22.5	12.5
10	15	17.5	12.5
7.5	12.5	15	12.5
10	15	17.5	10
10	15	20	10
12.5	15	22.5	12.5
10	15	20	12.5
10	12.5	15	10
10	15	22.5	12.5
10	12.5	22.5	12.5
7.5	12.5	12.5	12.5
7.5	12.5	17.5	15
7.5	12.5	20	5
7.5	15	20	15
10	12.5	25	10
10	12.5	25	15
10	15	25	15
10	12.5	15	15
7.5	12.5	25	15
10	12.5	25	15
10	15	20	15
10	15	20	15
10	15	20	15

Number of pits per Cross Field

D9.022	D9.071	D9.94.1	D9.161	D9.139.1	D9.036.1	D9.050.1
4	1	1	2	4	1	5
4	1	1	3	4	1	4
5	1	1	4	3	1	4
3	1	1	3	2	1	4
6	1	1	4	2	1	3
4	1	1	3	2	1	3
6	1	1	3	2	1	3
3	1	1	4	2	1	N/A
3	1	1	2	5	1	
2	1	1	4	5	1	
2	1	1	3	4	1	
2	1	1	4	3	1	
3	1	1	5	6	1	
3	1	1	5	4	1	
3	1	1	4	4	1	
2	1	1	4	4	1	
4	1	1	3	4	1	
8	1	1	3	3	1	
2	1	1	5	3	1	
2	1	1	4	4	1	
4	1	1	4	3	1	
4	1	1	4	5	1	
5	1	1	2	3	1	
3	1	1	4	3	1	
4	1	1	2	3	1	

D9.022	D9.071	D9.94.1	D9.161	D9.139.1	D9.036.1	D9.050.1
5		1	4	2	1	
2		1	3	3	1	
5		1	2	4	1	
4		1	2	5	1	
5		1	2	3	1	
5		1	2	2	1	
5		1	4	2	1	
5		1	2	2	1	
5		1	2	4	1	
2		1	3	3	1	
4		1	5	3	1	
2		1	5	3	1	
4		1	3	2	1	
3		1	4	2	1	
3		1	4	5	1	
3		1	4	3	1	
4		1	4	4	1	
3		1	3	5	1	
3		1	4	4	1	
4		1	4	4	1	
3		1	4	2	1	
2		1	4	3	1	
2		1	5	3	1	
4		2	3	2	1	
2		2	3	2	1	

D9.111.1	D9.059.1	D9.118.1	D9.092.1	D9.112.1	D9.098.1	D9.153.1	D9.109.1	D9.168.1
2	4	n/a	1	2	1	1	8	2
2	2		1	2	1	1	4	2
4	3		1	2	1	1	4	2
4	3		1	1	1	1	3	4
5	3		1	1	1	1	4	2
n/a	4		1	1	1	1	6	2
	4		1	1	1	1	5	2
	5		1	1	1	1	5	2
	5		1	1	1	1	5	4
	5		1	1	1	1	4	3
	4		1	1	1	1	5	2
	4		1	1	1	1	5	2
	3		1	1	1	1	7	3
	4		1	1	1	1	5	2
	4		1	1	1	1	5	3
	6		1	1	1	1	4	5
	6		1	1	1	1	5	2
	4		2	1	1	1	4	2
	4		2	1	1	1	3	3
	3		1	1	1	1	4	3
	N/A		1	1	1	1	4	4
			1	1	1	1	7	4
			1	1	1	1	5	3
			1	1	1	1	8	3
			1	1	1	1	4	3

D9.111.1	D9.059.1	D9.118.1	D9.092.1	D9.112.1	D9.098.1	D9.153.1	D9.109.1	D9.168.1
			1	1	1	1	5	3
			1	1	1	1	4	2
			1	1	1	1	5	6
			1	1	1	1	8	2
			1	1	1	1	8	2
			1	1	1	1	5	4
			1	1	1	1	7	2
			1	1	1	1	4	3
			1	1	1	1	6	4
			1	1	1	1	4	2
			1	1	1	1	4	preservation
			1	1	1	1	5	
			1	1	1	1	5	
			1	1	1	1	6	
			1	1	1	1	5	
			1	1	1	1	6	
			1	1	1	1	7	
			1	1	1	1	4	
			1	1	1	1	4	
			1	1	1	1	4	
			1	1	1	1	7	
			1	1	1	1	5	
			1	1	1	1	6	
			1	1	1	1	6	
			1	1	1	1	4	

D9.038.1	D9.093.1	D9.044.1	D9.128.1	D9.043.1
1	1	4	10	5
1	1	2	8	4
1	1	2	4	4
1	2	2	2	4
1	2	4	2	2
1	2	5	2	3
1	1	5	4	2
1	1	5	3	2
1	1	5	4	4
2	1	4	3	4
2	1	4	4	3
2	1	5	7	2
1	1	5	7	2
1	1	6	4	2
1	2	5	4	4
1	1	4	3	6
1	1	6	5	4
1	1	4	5	4
1	1	6	8	4
1	1	6	2	2
1	1	4	2	6
1	1	4	3	6
1	1	4	4	4
1	1	4	5	3

D9.038.1	D9.093.1	D9.044.1	D9.128.1	D9.043.1
1	1	4	5	3
1	1	7	6	2
1	1	4	5	4
1	1	4	6	4
1	1	5	5	4
1	1	6	3	3
1	1	4	4	2
1	1	5	6	3
1	1	6	7	2
1	1	6	3	2
1	1	5	7	2
1	1	4	4	6
1	1	7	3	4
1	1	7	4	3
1	1	4	5	3
1	1	4	4	4
1	1	3	4	5
1	1	preservation	7	1
1	1		3	1
1	1		2	3
1	1		3	2
1	1		2	2
1	1		4	2
1	1		5	2
1	1		6	3
1	1		4	3

Tracheid tangential diameter μm . Early wood

D9.112.1	D9.036	D9.111	D9.153.1	D9.022	D9.059	D9.094.1
40	35	22.5	35	32.5	23.8	32.5
30	45	25	35	30	26.1	32.5
32.5	30	17.5	40	22.5	25.3	32.5
32.5	40	25	45	22.5	25.4	32.5
37.5	25	25	37.5	17.5	31.5	37.5
30	30	25	40	20	26.16	25
35	32.5	25	37.5	20	28.4	35
37.5	35	25	40	22.5	34.7	32.5
40	37.5	25	40	20	24.7	35
40	42.5	25	40	25	27.2	35
35	30	22.5	40	20	25.9	32.5
42.5	30	25	37.5	25	31.8	37.5
27.5	30	25	37.5	20	25.045	42.5
27.5	42.5	35	32.5	22.5	28.1	35
25	37.5	30	35	25	25.7	25
30	35	25	35	30	25.8	32.5
30	35	30	35	27.5	26.4	40
25	35	30	37.5	25	24.9	40
25	25	35	40	20	31	25
32.5	25	37.5	45	25	25.8	30
25	20	37.5	40	27.5	24.1	32.5
25	25	32.5	40	30	22.4	35
35	30	37.5	40	32.5	25.4	30
25	30	37.5	45	32.5	24.6	35

D9.139.1	D9.050.1	D9.109.1	D9.168.1	D9.038.1	D9.093.1	D9.181.1
37.5	23.3	55	30	30	50	55
35	20.9	50	35	30	45	55
31.25	28.1	75	35	25	42.5	50
42.5	28.13	62.5	37.5	45	42.5	55
42.5	24.15	60	30	35	45	60
35	34.7	52.5	42.5	20	47.5	45
45	28.8	65	45	30	50	52.5
35	27	62.5	45	30	45	75
47.5	28.4	52.5	40	27.5	50	57.5
47.5	25.5	60	37.5	27.5	40	60
35	27.4	60	37.5	27.5	52.5	40
47.5	24.3	40	35	32.5	40	40
40	30.6	52.5	35	30	40	50
40	31.5	50	37.5	32.5	42.5	55
47.5	31.9	62.5	42.5	30	35	62.5
40	31.4	60	35	30	32.5	50
37.5	27.3	55	40	35	45	37.5
32.5	22.15	55	42.5	32.5	47.5	50
35	29.7	65	47.5	27.5	35	50
37.5	31.2	60	37.5	32.5	40	60
27.5	26.5	52.5	40	25	47.5	55
35	23.7	52.5	37.5	30	37.5	55
35	28.07	57.5	37.5	32.5	45	55
50	30.7	62.5	37.5	35	45	47.5

D9.043. 1	D9.044. 1	D9.128. 1	D9.136. 1	D9.304. 1	D9.019. 2	D9.092. 1	D9.098. 1	D9.090. 1
70	N/A	N/A	N/A	N/A	23.4	33.7	42.4	26,9
70					21.9	42.5	43	32.5
37.5					20.3	55.6	41.6	33.25
55					20.2	44.4	52.2	36.8
55					21.9	55.96	51.2	41.6
55					22.7	50.74	46.5	44.4
55					22.4	36.1	36.6	43.2
52.5					29.4	36.8	44.6	38.5
45					21.3	30.4	49	44.3
60					21.4	27.7	34.1	36.5
45					20	30.8	37.4	37.6
35					23.1	45.1	44.7	24.9
47.5					22	23.8	39.7	47.5
50					23.1	25.1	44.6	32.7
55					22.1	32.9	42.8	42.2
42.5					20.8	37.9	34.1	43.6
52.5					25.8	22.6	39.7	28.3
55					24.2	27.3	45.2	28.9
45					26.8	38.5	31.1	27.2
35					27	40.9	39.8	28.7
47.5					36	22.35	42.1	29.5
45					35.7	24.2	49	22.6
40					31.3	45.3	35.9	33.2
45					29.5	44.5	38.2	25.5

Tracheid radial diameter μm Latewood

D9.112.1	D9.036	D9.111	D9.153.1	D9.022	D9.059	D9.094.1	D9.139.1
35	35	40	35	37.5	25.8	30	27.5
32.5	15	45	35	35	32.2	25	27.5
30	25	40	32.5	35	26.9	32.5	32.5
30	15	45	25	35	28.4	30	25
30	30	30	27.5	40	18.9	30	25
30	32.5	32.5	35	45	28.8	40	30
25	27.5	37.5	32.5	37.5	31.9	32.5	40
30	20	37.5	32.5	40	30.9	25	25
30	27.5	35	35	42.5	25.6	30	32.5
25	30	35	32.5	37.5	30.1	35	30
25	32.5	35	32.5	37.5	31.5	35	22.5
25	17.5	35	37.5	32.5	24.1	45	30
25	15	35	35	30	23.6	15	30
30	25	35	35	32.5	27.4	30	25
25	30	27.5	30	35	27.1	27.5	32.5
30	30	30	35	43.75	19.8	30	50
40	32.5	25	32.5	45	23.4	35	25
40	30	25	30	27.5	20.2	30	32.5
37.5	25	25	35	20	28.8	32.5	30
45	25	35	30	25	21.8	27.5	27.5
32.5	22.5	35	32.5	20	17.6	30	30
32.5	25	35	30	25	28	32.5	27.5
35	25	40	35	25	29.1	35	40
35	25	30	40	25	23.6	35	22.5
37.5	30	35	32.5	25	30.5	27.5	32.5
35	32.5	30	32.5	22.5	22.1	35	30

D9.050.1	D9.109.1	D9.168.1	D9.038.1	D9.093.1	D9.181.1	D9.043.1
30.48	57.5	35	35	42.5	40	40
28.84	50	27.5	32.5	32.5	55	45
25.87	40	32.5	30	35	50	35
28.3	55	40	27.5	42.5	47.5	32.5
31.5	55	30	20	20	50	55
30.4	40	32.5	30	35	20	60
25	55	preservation	32.5	35	35	60
22.2	50		17.5	40	50	50
25	45		20	32.5	25	30
26	50		25	37.5	50	45
38	40		30	35	30	30
30.5	40		22.5	40	50	32.5
33.3	50		25	37.5	30	45
24.1	40		30	40	45	45
28.2	50		17.5	42.5	50	35
26	20		30	30	50	40
35.6	40		25	35	45	35
30.7	47.5		25	35	25	30
35.3	42.5		30	25	20	40
35.8	50		22.5	40	50	45
36.8	27.5		20	32.5	50	35
29.3	42.5		32.5	35	30	47.5
29.7	32.5		30	35	50	35
21.8	40		37.5	35	20	30
40.13	50		35	15	20	35
32.3	50		27.5	35	25	40

D9.044.1	D9.128.1	D9.136.1	D9.304.1	D9.019.2	D9.092.1	D9.098.1	D9.090.1
				27.4	39.8	33	19.8
				19.4	30.1	37.1	25.6
				19.1	25.5	34.1	25.3
				22.5	27.9	26.8	25.5
				20.9	27.4	24.3	25.3
				23.3	31.8	18.4	17.7
				23	27.3	38.4	21.2
				20.3	30.22	35.9	14.35
				22.1	28.9	37.8	15.4
				23.3	30.5	32.9	13.25
				24.2	34.3	26.6	17.7
				24.17	32.4	25.6	12.5
				25	48.6	34.1	14.6
				24	42.9	31.2	12.3
				23	37.6	37.8	16.7
				22.9	26.3	26.21	13.9
				22.4	34.2	32.3	15.5
				23.3	34.17	23.7	17.6
				19.8	28.5	33	17.6
				20.5	32.3	42	17.4
				25.3	26.6	29.2	11.2
				27.6	26.6	28.4	19.9
				22.1	35.8	21.3	13.39
				25.7	15.8	17	12.1
				22.5	33.2	42	10.4
				24.1	38.7	42.5	12.3

Tracheid radial diameter early wood μm

D9.112.1	D9.036.1	D9.111	D9.153.1	D9.022.1	D9.094.1	D9.059.1	D9.139.1
45	27.5	30	55	15.9	32.5	30.7	47.5
40	50	32.5	55	20.6	30	27.6	42.5
30	35	45	52.5	21.8	45	29.2	35
30	43.75	50	52.5	20.6	30	27.8	35
40	32.5	35	50	19.6	27.5	31	35
37.5	35	37.5	37.5	18.7	25	27.4	30
35	50	32.5	37.5	15.8	45	24.5	35
32.5	40	32.5	35	26.9	32.5	29	35
40	40	30	37.5	30.2	37.5	30.5	40
30	35	25	45	22	32.5	28.8	62.5
45	30	12.5	25	23	30	31.3	75
45	25	25	30	23.3	37.5	24.7	37.5
27.5	27.5	30	22.5	23.9	37.5	23.7	35
22.5	32.5	30	25	24.3	25	22.8	35
22.5	32.5	12.5	25	17.7	25	20.6	37.5
20	35	12.5	12.5	24.4	27.5	25.2	35
32.5	30	17.5	50	23.2	30	23	35
15	25	20	45	16.2	20	17.7	32.5
17.5	27.5	12.5	55	23.2	25	24.6	42.5
17.5	32.5	10	52.5	22.4	20	24.6	37.5
12.5	25	17.5	50	18.8	30	22.3	35
10	20	20	45	19.6	35	19.5	25
45	20	15	22.5	26.6	25	29	30
35	37.5	17.5	17.5	22.8	30	21	42.5
35	25	20	50	20.3	32.5	22.5	35

D9.050.1	D9.109	D9.168.1	D9.038.1	D9.093.1	D9.181.1	D9.043.1
30.5	65	32.5	30	50	70	55
27.3	60	35	27.5	50	50	37.5
26.6	65	32.5	30	50	55	37.5
24.2	75	35	37.5	50	65	45
28.3	70	32.5	30	50	65	52.5
24.7	70	32.5	30	45	52.5	40
30.1	60	42.5	30	45	65	57.5
34.7	45	30	30	55	65	42.5
29.3	77.5	40	25	60	67.5	37.5
32.4	45	35	25	37.5	60	35
24.2	55	37.5	25	50	62.5	40
26.6	50	37.5	40	52.5	60	25
29.3	62.5	30	22.5	40	80	50
25.6	65	35	37.5	50	62.5	30
31.8	65	35	30	45	60	32.5
29.6	75	35	25	40	55	50
33.6	55	40	27.5	50	55	25
21.7	62.5	30	32.5	50	55	45
21.3	50	35	25	40	75	37.5
25	65	25	25	50	70	40
26.4	62.5	27.5	35	45	60	42.5
29.9	75	32.5	25	40	55	40
31.6	62.5	35	35	40	60	55
28.8	65	35	27.5	42.5	55	30
19.5	50	25	37.5	40	62.5	35

D9.044.1	D9.128.1	D9.136.1	D9.304.1	D9.019.2	D9.092.1	D9.125.1	D9.098.1	D9.090.1
				25.7	46.33	N/A	40.3	23.7
				22.9	37.6		52.3	28.2
				24.2	35.8		54.5	25.1
				16.6	35.3		52.1	22.5
				17.4	31.5		46.8	28.8
				19.5	28.6		50.8	30
				17	40.26		40.3	27.6
				26.2	31.36		35	34.4
				22.9	29.3		37.4	33.8
				19.6	29.3		45	31.9
				27.9	29.2		52	29.4
				26.8	24.5		36.3	36.9
				21.1	37.8		42.1	35.2
				14.2	31.2		42.4	30.2
				14.2	31.6		49.4	27
				19.5	30.1		32.8	38.1
				29	26		35.5	30.2
				24.7	22		39.7	29.4
				17	24.5		37	34.2
				21.5	26.3		49	34.7
				33.18	27.1		32.8	30.837
				34.3	38.4		40.7	33.7
				30.6	32.4		38.9	36.9
				31.5	36.3		55.7	38.4
				27.6	35.8		49.8	17.4

D9.112.1	D9.036.1	D9.111	D9.153.1	D9.022.1	D9.094.1	D9.059.1	D9.139.1	D9.050.1
27.5	30	30	52.5	9.67	20	22.6	15	24
30	25	35	50	8	25	12	12.5	17.4
25	20	30	55	8.6	10	14.7	10	11.7
30	17.5	35	47.5	15	7.5	9.5	12.5	17.9
25	22.5	30	27.5	6.8	25	17.7	22.5	13.8
25	12.5	30	20	10.8	15	13.1	15	12.5
22.5	17.5	25	25	9.5	15	12.1	15	13.3
20	17.5	27.5	55	10.2	12.5	12.4	7.5	14.6
20	12.5	27.5	57.5	11.9	15	16.3	12.5	13.7
15	22.5	30	47.5	9.3	20	14.3	10	17.9
20	17.5	30	50	7.6	10	11.9	12.5	10.1
20	20	22.5	40	8.1	20	10.2	15	13.1
15	10	20	37.5	9.2	20	14.3	10	15.5
15	12.5	25	30	16.5	15	15.7	10	19.4
20	10	32.5	25	11	15	12.7	12.5	17.4
45	18.75	30	25	9.8	25	12.3	15	18.7
45	10	25	25	7.9	30	12	10	17.4
40	17.5	25	22.5	9.8	15	15.9	15	15.9
40	20	17.5	22.5	11.3	30	16.2	10	19.4
40	17.5	20	17.5	12.5	15	14.6	12.5	19.1
30	17.5	25	17.5	8.7	17.5	18	12.5	12.2
30	20	25	42.5	11	25	16.6	12.5	14.1
25	17.5	15	55	9.3	30	11.5	10	14.2
32.5	15	12.5	62.5	6.5	25	13.7	15	15
35	17.5	7.5	52.5	6.9	15	16.6	22.5	14.3

D9.109	D9.168.1	D9.038.1	D9.093.1	D9.181.1	D9.043.1
27.5	12.5	15	15	25	17.5
22.5	12.5	15	17.5	20	20
20	25	20	20	22.5	20
25	15	17.5	17.5	30	17.5
20	20	20	15	20	15
27.5	N/A	30	17.5	25	7.5
25		17.5	15	30	20
20		12.5	20	17.5	12.5
12.5		12.5	25	25	15
30		15	25	20	12.5
15		15	10	25	17.5
22.5		15	17.5	17.5	20
25		20	20	10	12.5
25		15	12.5	25	10
22.5		12.5	20	17.5	15
30		15	12.5	20	25
15		17.5	15	15	10
25		25	17.5	10	10
25		25	20	15	15
25		15	20	20	10
17.5		15	30	25	15
20		10	20	25	15
25		12.5	15	10	15
25		12.5	15	15	15
25		12.5	7.5	25	15

D9.019.2	D9.092.1	D9.125.1	D9.098.1	D9.090.1
27.6	35.8		49.8	17.4
12.8	14.8		11	9.9
9.6	18		16.5	13.2
9.2	11.5		20.1	19.8
13.3	9.1		18.28	15.4
11.6	15.8		20.8	17.9
14.7	13		17.7	13.2
16.7	12.1		25.6	12.1
20.1	13.5		15.2	9.4
9.9	14.6		20.3	14.9
13.9	12.25		23.7	17.2
13.7	10.57		15.3	16.6
16.7	18.04		16.7	13.2
9.9	15.7		14.6	15.4
12.4	18.04		19.5	17.9
18.3	15.2		18.3	11
11.9	14.1		23.9	8.8
13.1	13.12		18.9	11
12.3	13.5		25.1	15.5
14.7	12.3		28.3	13.3
13.3	14.1		13.4	13.9
15.1	16.65		16.5	11.2
13	21		22	6.6
13.6	14.1		16.6	13.2
13.8	23.7		18.6	16.7
16.7	14.9		21.73	14.2

Uniseriate (u) vs Biseriate (b) vs Triseriate (t) tracheid pitting

D9.022	D9.071	D9.153	D9.036	D9.112	D9.050	D9.059	D9.098
u	u	b	u	b	u	u	u
b	u	b	u	b	b	b	u
u	u	u	u	b	b	b	u
u	u	u	u	u	u	u	u
u	u	u	u	u	b	u	u
u	u	u	u	b	b	u	u
u	u	u	u	b	b	u	u
u	u	u	u	u	u	u	u
u	u	u	u	u	b	b	u
b	u	u	u	u	t	b	u
b	u	u	u	b	b	b	u
u	u	b	u	u	u	b	u
u	u	preservation	u	u	b	b	u
u	u		u	b	u	u	u
u	u		u	b	u	u	u
b	u		u	b	b	u	u
u	u		u	u	t	u	u
b	u		u	b	u	b	u
u	u		u	b	u	u	u
u	u		u	u	u	b	u
u	u		u	u	u	b	u
u	u		u	u	u	b	u
u	u		u	u	u	b	u
u	u		u	b	b	b	u
b	u		u	u	u	b	b
b	u		u	b	b	u	u

D9.022	D9.071	D9.153	D9.036	D9.112	D9.050	D9.059	D9.098
u	u		u	u		u	u
u	u		u	b		u	u
b	b		u	u		u	u
b	u		u	u		u	u
u	u		u	u		u	u
u	u		u	u		u	u
u	u		u	u		b	u
u	u		u	u		u	u
u	u		u	u		u	u
b	u		u	u		u	u
u	u		u	u		b	u
u	u		u	b		b	u
u	u		u	u		b	u
u	u		u	u		b	u
b	u		u	u		u	u
b	u		u	u		u	u
u	u		u	u		u	u
u	u		u	u		u	u
u	u		u	b		u	u
u	u		u	b		b	u
b	u		u	u		b	u
u	u		u	b		u	u
u	u		u	u		u	u
u	u		u	u		u	u
u	u		u	u		u	u
b	u		u	u		u	u

D9.111	D9.094.1	D9.161.1	D9.139.1	D9.050.1	D9.118.1	D9.092.1	D9.109
u	u	u	u	b	u	u	t
u	u	u	u	b	u	u	b
u	u	u	b	b	u	u	t
u	u	u	b	b	u	u	t
b	u	u	b	b	u	u	b
b	u	u	u	b	u	u	b
b	u	u	u	u	u	u	b
u	u	u	u	b	u	u	t
u	u	b	u	u	u	u	b
u	u	u	b	u	u	u	t
b	u	b	b	u	u	u	t
b	u	b	b	u	u	u	t
b	u	t	b	u	u	u	b
b	u	b	b	b	u	u	t
u	u	b	b	u	u	u	b
u	u	b	b	u	u	u	t
b	u	u	b	b	u	u	t
b	u	u	t	b	u	u	b
u	u	u	b	u	u	u	b
u	u	b	u	u	u	u	b
u	u	b	u	u	u	u	4
b	u	u	u	b	u	u	4
b	u	u	u	b	u	u	4
b	u	u	b	u	u	u	4
b	u	u	b	u	u	u	4

D9.168.1	D9.038.1	D9.093.1	D9.044.1	D9.128.1	D9.181.1	D9.043.1
b	u	u	u	u	t	b
u	u	u	u	b	b	b
b	u	u	u	u	b	b
u	u	u	u	u	b	b
u	u	u	u	u	b	u
b	u	b	b	u	b	u
b	u	b	u	b	b	u
b	u	u	u	b	b	u
u	u	u	u	b	b	u
u	u	u	u	t	u	u
u	u	u	u	b	u	u
u	u	u	b	b	b	u
u	u	u	u	b	b	u
u	u	b	u	u	b	u
u	u	b	b	u	b	u
u	u	u	u	b	b	b
u	u	u	u	b	b	b
u	u	u	b	u		u
u	u	u	u	b		b
u	u	b	u	b		b
b	u	u	u	u		b
u	u	u	u	b		b
u	u	u	u	u		b
u	u	u	u	u		b
u	u	u	u	u		b
u	u	u	u	b		b

D9.168.1	D9.038.1	D9.093.1	D9.044.1	D9.128.1	D9.181.1	D9.043.1
u	u	u	b	b		u
u	u	u	b	u		u
u	u	u	u	b		u
u	u	u	u	b		u
u	u	u	u	u		u
u	u	u	b	u		t
u	u	u	u	b		b
u	u	u	u	b		b
u	u	b	u	t		u
u	u	u	b	u		t
u	u	u	b	u		b
u	u	u	b	u		u
u	u	u	u	b		u
u	u	u	u	b		u
b	u	u	u	u		u
u	u	u	u	u		b
u	u	u	u	u		b
u	u	u	u	b		u
u	u	u	u	u		u
u	u	u	u	u		u
u	u	u	u	u		u
u	u	u	u	u		u
u	u	u	u	u		u
u	u	u	u	u		u
u	u	u	u	u		b
u	u	b	t	u		u

Touching pits 1 = touching 0= separate.

D9.022	D9.071	D9.153	D9.036	D9.112	D9.050	D9.059	D9.098
1	1	1	1	1	1	1	apitean
1	1	1	0	1	1	1	
1	1	1	0	1	1	1	
1	1	1	0	1	1	1	
1	1	1	0	1	1	1	
1	1	1	0	0	1	1	
1	1	1	0	1	1	1	
1	1	1	0	0	1	1	
1	1	1	0	0	1	1	
1	1	1	1	1	1	1	
1	1	1	1	1	1	1	
1	1	1	0	1	1	1	
1	1	1	0	1	1	1	
1	1	0	0	0	1	1	
1	1	0	0	1	1	1	
1	1	0	o	1	1	1	
1	1	0	0	1	1	1	
1	1	1	0	1	1	1	
1	1	1	0	1	1	1	
1	1	1	0	1	1	1	
1	1	1	0	0	1	1	
1	0	1	0	1	1	1	
1	1	1	0	0	1	1	
1	1	1	0	1	1	1	
1	1	1	0	1	1	1	

D9.022	D9.071	D9.153	D9.036	D9.112	D9.050	D9.059	D9.098
1	1		0	1		1	
1	1, 0		0	0		1	
1	1		0	0		1	
1	1		0	0		1	
1	1		0	0		1	
1	1		0	1		1	
1	1		0	1		1	
1	1		0	0		1	
1	1, 0		0	1		1	
1	1		0	1		1	
1	1		0	1		1	
1	0, 1		0	1		1	
1	1		0	0		1	
1	1		1	0		1	
1	1		0	1		1	
1	1		0	1		1	
1	1		0	1		1	
1	1		0	1		1	
1	1		0	1		1	
1	1		0	1		1	
1	1		0	1		1	
1	1		0	0		1	
1	1		0	0		1	
1	1		0	1		1	
1	1		0	1		1	

D9.093.1	D9.181.1	D9.043.1
1	1	1
1	1	1
0	1	1
1	1	1
1	1	1
1	1	1
1	1	1
0	1	1
0	1	1
0	0	1
0	0	1
1	1	1
1	1	1
1	1	1
1	1	1
0	1	1
0	1	1
1		1
1		1
1		1
0		1
0		1
0		1

D9.093.1	D9.181.1	D9.043.1
0		1
0		1
0		1
0		1
0		1
0		1
0		1
0		1
0		1
0		1
0		1
0		1
1		1
1		1
1		1
1		1
1		1
0		1
0		1
0		1
1		1
1		1
1		1
1		1
1		1
0		1
0		1
0		1
1		1
1		1

Opposite vs Alternate tracheid pitting

D9.022	D9.071	D9.153	D9.036	D9.112	D9.050	D9.059
x	all uniseriate	a	x	o	x	x
a		a	x	o	a	a
x		x	x	o	a	a
x		x	x	x	x	x
x		x	x	x	a	x
x		x	x	o	a	x
x		x	x	o	a	x
x		x	x	x	x	x
x		x	x	x	a	a
a		x	x	x	a	a
a		x	x	o	a	a
x		a	x	x	x	a
x			a	x	a	a
x			x	o	x	x
x			x	o	x	x
a			x	o	a	x
x			x	x	a	x
o			x	o	x	a
x			x	o	x	x
x			x	x	x	a
x			x	x	x	a
x			x	o	a	a
a			x	x	x	a
x			x	a	a	x

D9.022	D9.071	D9.153	D9.036	D9.112	D9.050	D9.059
x				x		x
x				a		x
a				x		x
a				x		x
x				x		x
x				x		x
x				x		a
x				x		x
x				x		x
a				x		x
x				x		a
x				o		a
x				x		a
x				x		a
x				x		x
a				x		x
o				x		x
x				o		x
x				o		x
x				x		a
x				o		a
a				x		x
x				x		x
x				x		x
a				x		x

D9.098	D9.111	D9.161	D9.139	D9.050.1	D9.118.1	D9.92.1	D9.109.1
x	a	a	a	a	n/a	x	a
x	a	a	a	a			a
x	a	a	a	a			a
x	x	a	a	a			a
x	x	a	a	a			a
x	100% alternate	a	x	a			a
x		a	a	a			a
x		a	a	a			a
x		a	a	a			a
x		a	x	a			a
x		a	a	a			a
x		a	a	a			a
x		a	a	a			a
x		a	a	a			a
x		a	a	a			a
x		a	a	a			a
x		a	x	a			a
x		a	x	a			a
x		a	a	a			a
x		a	a	a			a
x		a	a	a			a
x		a	a	a			a
x		a	x	a			a
x		a	a	a			a
x		a	a	a			a
O		a	a	a			a
x		a	x	a			a

D9.168. 1	D9.038.1	D9.093.1	D9.044. 1	D9.128. 1	D9.181. 1	D9.043.1
a	x	x	x	x	a	a
x		x	x	a	a	a
a		x	x	x	a	a
x		x	x	x	a	a
x		x	x	x	a	x
a		o	a	x	a	x
a		o	x	a	a	x
a		a	x	a	a	x
x			x	o	a	x
x			x	a	x	x
x			x	a	x	x
x			x	a	a	x
x			x	a	a	x
x			x	o	a	x
x			so	x	a	x
x			x	x	a	a
x			x	o	a	a
x			so	a		x
x			x	x		a
x			x	a		a
a			x	a		a
x			x	o		a
x			x	x		a
x			x	x		a
x			x	o		a

D9.168. 1	D9.038.1	D9.093.1	D9.044. 1	D9.128. 1	D9.181. 1	D9.043.1
x			so	o		x
x			a	o		x
x			x	o		x
x			x	o		x
x			x	o		x
x			a	a		a
x			x	x		a
x			x	x		a
x			x	x		x
x			a	o		a
x			o	o		a
x			o	x		x
x			so	x		x
x			u	x		x
x			x	o		x
x			x	x		x
x			x	x		a
x			x	x		a
x			x	x		x
x			x	x		x
x			x	x		x
x			x	x		x
x			x	x		x
x			x	x		x
x			x	x		b
x			a	x		x

Appendix B.2 Angiosperm wood anatomy measurements

Ray height μm

D9.053.1	D9.096.1	D9.012	D9.089.1	D9.107	D9.016	D9.020	D9.095.1	D9.023	D9.128.2
260	650	490	560	350	262.5	445	800	525	925
300	295	330	520	165	400	895	300	425	510
368	375	250	400	280	405	820	735	315	902.5
260	645	135	600	370	245	445	450	375	960
220	510	325	700	225	345	510	800	515	1525
240	300	115	230	275	300	230	430	360	305
380	565	385	200	400	385	430	555	375	1050
240	530	350	595	130	325	250	555	420	475
200	300	268	155	400	145	185	585	445	885
360	485	270	235	325	395	190	450	235	1000
218	85	360	320	300	460	575	425	310	1095
375	265	485	325	350	475	165	200	230	845
320	585	215	200	225	420	400	340	360	620
325	410	220	585	300	415	280	475	240	905
160	515	295	300	275	320	690	700	175	812
220	340	490	225	305	270	300	415	580	535
333	350	120	545	200	155	290	525	565	760
340	385	200	400	155	270	250	350	695	347
300	585	190	300	200	260	275	450	710	1080
360	475	280	210	250	230	285	630	475	855
350	545	305	350	185	375	410	545	400	810
281	480	250	375	175	220	565	565	375	985
120	225	255	375	600	320	265	620	355	260
380	300	335	462	325	310	1495	205	350	575
385	325	385	475	265	270	260	525	410	605

D9.018	D9.027	D9.110	D9.019.1	D9.054.1	D9.105.1	D9.040.1	D9.041.1	D9.021.1	D9.197.2
125	400	272.5	300	307.5	315	130	235	340	225
340	495	275	435	295	155	1220a	225	300	250
517	145	265	110	195	290	120	285	700	115
520	760	150	325	700	440	230	290	150	200
185	380	185	250	235	125	155	240	125	350
175	395	270	295	235	507.5	250	240	100	375
130	195	270	330	420	272	220	105	385	235
433	435	275	225	117.5	100	175	135	500	405
410	230	140	275	292.5	290	170	115	460	350
195	370	260	200	340	200	360	340	225	300
320	610	240	275	315	445	255	225	125	350
415	320	205	290	285	65	780	275	150	350
95	490	100	285	100	300	235	260	275	315
170	175	375	160	130	305	117.5	185	510	200
420	500	165	125	200	152.5	145	130	350	225
225	250	250	325	500	257.5	250	360	265	217.5
187	112	265	145	160	272.5	300	300	385	260
220	200	125	235	375	150	245	210	500	240
290	105	295	260	325	275	160	200	425	205
375	325	295	375	335	220	400	210	330	390
295	195	270	290	165	235	150	322.5	450	255
495	450	300	300	722.5	152.5	265	202.5	300	200
395	260	280	250	305	525	485	225	1125 j	155
175	67	300	300	135	725	350	325	250	160
160				175	395	875	255	250	265

D9.091.1	D9.011.2	D9.128.3	D9.130.1	D9.157.3
665	350	150	300	260
250	425	295	330	265
225	235	130	350	255
420	142.5	460	700	205
175	400	310	385	215
212.5	180	260	500	310
695	210	135	150	300
750	520	95	255	165
390	200	285	525	150
270	235	175	515	
465	300	450	525	
140	475	365	250	
475	360	365	515	
710	200	170	235	
485	305	190	150	
415	250	180	320	
235	325	85	400	
925	300	100	300	
190	350	165	340	
435	410	85	500	
565	165	135	285	
610	180	315	275	
575	265	225	400	
340	260	260.5	150	
450	250	110	250	

Vessel element length um

D9.053.1	D9.096.1	D9.012	D9.095.1	D9.107	D9.016	D9.020	D9.023	D9.019.1
380	1080	680	800	preservation	1180	1300	975	1290
558	650	760	1200		940	780	780	585
660	1000	770	1160		900	1200	885	600
760	960	580	1000		980	620	700	700
240	980	700	880		1100	1200	875	650
1600	1300	640	1460		700	1140	930	550
600	1400	500	700		780	1200	945	1275
700	1140	280	800		920	only dat due to preservation problems	600	800
1760	1000	800	900		600		350	675
400	1300	650	720		820		950	710
600	900	660	980		760		635	650
700	1040	800	960		600		655	550
800	1060	780	800		960		790	480
680	1160	860	680		620		845	500
700	1060	760	1000		840		625	475
600	1020	720	800		880		1035	820
720	1180	700	840		900		660	650
700	1000	760	1000		1000		1020	475
800	1000	700	820		880		872.5	475
860	1360	660	780		1200		450	425
480	1120	690	900		800		800	500
600	1180	560	1600		320		635	750
680	1080	800	1020		720		1030	800
720	1100	900	900		800		800	700
720	1140	600	800		1020		900	675

D9.128.2	D9.018	D9.027	D9.110	D9.054.1	D9.105.1	D9.040.1	D9.041.1	D9.021.1
N/A	625	725	575	1005	500	250	n/a	310
	825	915	615	757.5	515	340		290
	395	730	350	900	327.5	160		365
	520	615	475	700	500	410		450
	175	525	450	550	400	350		600
	330	585	395	830	435	475		preservation
	380	680	500	650	450	375		275
	300	890	510	625	457.5	525		400
	265	755	545	740	360	405		375
	335	815	Preservation	preservation	300	400		325
	120	600			275	355		325
	255	500			355	380		175
	280	950			300	355		350
	175	775			412.5	260		225
	315	570			507.5			400
	195	670			550			preservation
	260	900			570			550
	250	590			475			
	250	815			285			
	405	650			425			
	270	860			335			
	325	700			550			
	285	600			425			
	355	735			300			
	295	780			410			

D9.197.2	D9.091.1	D9.011.2	D9.130.1
715	1250	1025	1000
n/a preservation	1100	N/A	1000
	1250		1070
	1250		1825
	1110		950
	1025		850
	920		850
	1060		1000
	725		500
	1000		750
	850		550
	1260		1000
	700		1000
	1500		1110
	1000		950
	1150		750
	850		525
	1225		950
	1450		500
	1300		750
	1700		1125
	1000		
	1125		
	1350		
	850		

Number of rays per tangential mm.

D9.053.1	D9.096.1	D9.012	D9.89.1	D9.107	D9.95.1	D9.016	D9.020	D9.023
7	8	7	5	5	5	12	11	12
8	7	7	6	5	7	8	13	14
9	9	6	7	6	7	13	13	12
9	8	7	7	4	6	10	14	13
5	7	6	6	4	6	8	11	12
10	9	4	7	4	6	13	10	12
10	7	7	4	5	4	9	12	10
9	8	7	7	3	4	13	14	14
10	6	10	5	5	5	13	13	10
10	7	10	8	6	8	8	14	11

D9.019.1	D9.128.2	D9.018	D9.027	D9.110	D9.054.1	D9.105.1	D9.040.1
8	10	9	11	3	5	14	6
10	14	10	11	5	8	17	6
9	16	13	13	7	6	17	7
12	9	9	13	9	6	14	9
9	15	11	10	3	6	14	8
8	14	8	15	4	8	13	10
9	13	6	17	4	7	11	6
9	13	10	14	7	3	11	3
9	8	11	14	6	7	13	6
9	12	12	9	7	7	11	5

D9.041.1	D9.021.1	D9.091.1	D9.011.2	D9.128.3	D9.130.1
9	17	5	4	10	5
7	12	6	5	10	2
12	9	6	5	12	4
8	8	6	6	9	5
8	15	9	4	9	2
8	16	8	6	8	5
5	20	7	5	11	4
8	19	9	4	6	3
8	20	7	6	11	4
7	20	5	2	8	6

Number of vessels per mm squared.

D9.053.1	D9.096.1	D9.012	D9.107	D9.095.1	D9.016	D9.020	D9.023	D9.128.2
90	121	55	N/A	65	59	54	132	64
130	116	79		79	57	50	113	43
118	165	70		60	60	149	130	45
111	76	67		55	53	60	104	50
122	68	68		64	47	51	121	64
105	73	55		57	60	66	92	54
99	106	79		56	50	68	68	43
107	125	85		52	60	58	86	44
70	73	59		67	48	80	92	63
120	82	67		70	74	89	118	72
120	62	58		69	81	62	119	56
99	82	53		71	61	129	98	67
57	124	46		90	64	107	71	70
95	108	87		96	66	79	70	57
85	94	94		96	60	50	74	33
95	71	103		103	69	89	108	34
100	121	80		40	79	70	100	57
112	94	73		60	85	77	119	65
93	70	98		63	75	75	117	64
119	60	83		63	64	98	108	63
88	56	75		65	66	57	93	52
68	67	66		62	76	60	96	51
53	69	68		59	78	43	88	47
76	68	51		73	76	61	77	49
71	62	60		70	63	61	93	56

D9.018	D9.027	D9.089.1	D9.110.1	D9.054.1	D9.105.1	D9.041.1	D9.091.1	D9.011.2
76	140	N/A	39	49	65	n/a	66	62
41	85		55	41	67		83	97
68	104		65	49	81		12	103
63	85		88	38	69		70	67
52	127		83	43	88		57	77
71	115		91	47	63		64	55
48	117		100	43	81		57	14
80	118		86	64	72		86	49
84	123		76	65	71		91	48
62	225		65	56	75		85	44
107	120		111	23	75		58	65
63	125		118	49	51		51	73
47	168		102	78	65		56	60
52	78		130	60	62		44	21
51	132		127	33	66		62	55
47	218		149	27	73		51	55
39	223		105	49	48		43	62
38	102		105	56	69		31	42
37	194		166	36	52		35	62
38	120		124	39	46		41	55
68	109		97	46	41		55	69
48	167		93	37	46		64	50
56	185		139	43	50		59	51
33	189		144	43	54		66	80
30	158		140	35	39		61	65

D9.128.3	D9.130.1	D9.157.3	D9.021.1	D9.019.1
55	65	34	n/a	n/a
40	50	37		
46	56	32		
44	52	50		
45	44	46		
53	55	27		
45	67	28		
59	63	41		
37	59			
50	44			
62	58			
59	52			
68	40			
42	48			
32	63			
n/a	56			
	70			
	54			
	40			
	36			
	57			
	67			
	38			
	45			
	61			

Vessel lumen diameter tangential μm

D9.128.2	D9.012	D9.016	D9.096	D9.053.1	D9.020	D9.018	D9.027	D9.023
52.5	50	122	85	112	50	67.5	78	60
45	45	127.5	90	32.5	55	62.5	49	72
60	32.5	95	60	30	50	90	83	70
52.5	43	85	70	60	30	95	105	85
47.5	45	92.5	70	65	35	70	96	88
55	42.4	95	100	67.5	52.5	70	45	77
60	37.5	57.5	87.5	72.5	42.5	42.5	46	90
45	40	62.5	95	62.5	55	80	47	60
47.5	30	50	87.5	65	47.5	62.5	46	62
57.5	27.5	47.5	75	60	60	70	34	68
57.5	80	55	42.5	60	47.5	92.5	35	41.25
47.5	70	85	50	52.5	30	90	35	46
52.5	62.5	75	110	55	55	82.5	35	51.25
47.5	62.5	95	60	37.5	60	57.5	36	51
55	45	87.5	50	130	47.5	55	37.5	60
55	47.5	40	52.5	42.5	45	90	25	36
55	30	70	55	35	35	12.5	32.5	50
45	100	30	82.5	35	50	80	31.75	32
50	77.5	32.5	77.5	35	50	77.5	29	45
60	45	110	70	70	40	70	25	60
55	45	112	105	95	50	77.5	26	50
40	62.5	92.5	52.5	77.5	40	90	22	56
45	50	87.5	45	70	37.5	100	22	53
47.5	37.5	92.5	65	42.5	42.5	35	17	72
40	30	105	62.5	32.5	40	72.5	17.5	63

D9.128.2	D9.012	D9.016	D9.096	D9.053.1	D9.020	D9.018	D9.027	D9.023
52.5	50	90	55	65	52.5	62.5	78	50
62.5	70	115	65	80	40	95	85	43
55	45	110	67.5	95	52.5	62.5	57	56.25
52.5	55	100	70	85	40	110	66	80
40	32.5	85	70	77.5	45	42.5	35	47
45	45	95	70	97.5	57.5	55	40	45
40	77.5	95	70	95	37.5	92.5	44	60
52.5	62.5	87.5	50	105	30	92.5	48	48
55	52.5	70	85	75	42.5	82.5	87	25
50	45	77.5	62.5	42.5	35	82.5	42	57.5
45	55	67.5	90	90	32.5	87.5	42	67.5
57.5	52.5	65	45	87.5	55	95	67.5	67.7
45	32.5	70	60	70	40	95	29	53.25
47.5	30	102	67.5	72.5	52.5	80	27	55
40	110	90	57.5	30	40	107.5	27	47.5
52.5	70	70	55	32.5	42.5	87.5	26.7	41.9
50	60	55	65	65	42.5	47.5	32.7	41.4
35	90	72.5	60	67.5	45	45	21.4	49.8
32.5	55	72.5	65	52.5	52.5	82.5	45.9	68.4
55	30	55	75	100	42.5	50	61.4	61
47.5	72.5	72.5	60	70	42.5	107.5	51.5	48.02
42.5	72.5	90	57.5	65	60	45	40.5	46.6
55	65	65	52.5	60	52.5	42.5	81.5	56
35	95	45	70	52.5	47.5	35	59.8	47.4
50	62.5	82.5	55	70	42.5	30	35.6	35.1

D9.019.1	D9.095.1	D9.89.1	D9.107	D9.110.1	D9.054.1	D9.105.1	D9.040.1
75	105	55	72.5	95	75	72.5	40
102.5	82.5	62.5	72.5	37.5	60	95	50
83.75	57.5	37	65	45	60	75	47.5
52.5	57.5	60	55	35	105	77.5	47.5
52.5	77.5	40	55	82.5	80	75	55
37.5	110	50	50	40	57.5	75	37.5
105	70	55	60	50	105	97.5	32.5
115	87.5	52	52.5	32.5	95	90	30
62.5	70	48	42.5	25	75	92.5	82.5
35	42.5	40	42.5	37.5	90	87.5	62.5
42.5	50	32	70	75	140	67.5	55
92.5	82.5	42	72.5	55	75	85	30
90	75	37	70	35	105	62.5	40
85	55	50	55	80	100	70	40
30	62.5	42	60	37.5	75	70	30
87.5	85	20	37.5	57.5	87.5	60	35
57.5	72.5	55	60	37.5	67.5	60	27.5
55	55	75	62.5	40	117.5	125	32.5
45	102.5	65	62.5	20	120	117.5	32.5
47.5	90	65	70	62.5	92.5	97.5	55
67.5	60	58	72.5	45	115	82.5	55
62.5	100	62	42.5	30	100	62.5	60
57.5	57.5	65	75	30	85	90	60
57.5	95	60	77.5	32.5	70	122.5	40
55	95	65	72.5	35	75	72.5	35

D9.019.1	D9.095.1	D9.89.1	D9.107	D9.110.1	D9.054.1	D9.105.1	D9.040.1
70.45	83.4	Just diameter was taken because vessels are not well preserved	58.32	25	97.5	69.45	
56.829	61.8		62.39	105	77.5	63.38	
72.7	49.3		52.05	62.5	100	63.4	
42.6	82.5		45.3	50	105	70.62	
47.1	66.3		35.2	33.75	90	72.63	
46.02	120.6		46.6	45	115	70.6	
76.13	115.4		63.56	35	60	72.45	
68	89.1		35.57	37.5	70	61.67	
75	93.1		55.1	75	80	33.4	
60.2	70.25		51.93	77.5	100	72.45	
77	92.74		47.7	50	60	77.72	
64.17	67.66		35.43	52.5	70	84.16	
53.31	84.7		50.6	92.5	60	65.23	
48.32	59.9		29.7	57.5	67.5	62.5	
52.85	59.97		42.59	40	100	32.19	
57.64	59.21		44.2	42.49	77.6	30.58	
60.11	100.9		31.8	23.81	88.6	77.69	
49.5	67.46		35.77	63.33	75.1	79.5	
41.6	97.66		29	58.42	74	68.84	
30.6	122.97		21	43.26	77.7	57.14	
40.9	72.22		30.5	40.71	83.8	64.32	
34	61.6		24.5	114.52	75.6	66.7	
35.007	46.4		71.7	37.37	81.4	61.7	
31.8	56.7		58.4	46.3	83.2	37.67	
26.7	63.4		70.5	24.001	88.36	38.4	

D9.021.1	D9.091.1	D9.011.2	D9.128.3	D9.130.1	D9.157.3
65	65	55	80.2	30	100
50	55	50	74.1	70	80
52.5	60	55	51	50	100
65	65	55	67	50	85
85	50	60	67	82.5	100
60	100	50	36	85	65
60	75	40	21.38	60	75
60	90	40	25	75	50
55	65	35	87	55	105
50	50	110	14.76	82.5	105
47.5	55	130	74.87	55	90
42.5	60	75	16.8	60	85
50	55	55	27.6	57.5	105
75	55	85	103.89	40	100
50	75	85	52.5	60	100
70	65	167	25	55	100
45	65	150	32	65	95
75	60	75	35	30	85
55	62.5	65	30	55	75
65	80	75	45	65	30
40	50	65	55	75	75
50	45	75	50	40	60
40	75	50	40	75	80
37.5	60	130	40	60	100
50	60	55	37.5	65	57.5

D9.021.1	D9.091.1	D9.011.2	D9.128.3	D9.130.1	D9.157.3
72.04	63.9	55	60	65	55
42.8	43.8	80	85	62.5	75
53.03	53.4	50	22.5	65	110
20.17	47.16	55	35	70	90
76.43	23.8	72.5	40	70	40
49.87	78.3	185	30	50	45
78.49	69.4	325	52.5	55	75
49.57	56.2	70	57.7	55	65
40.29	47.12	55	60	75	75
84.45	75.5	125	57.5	75	100
60.43	45	65	37.5	90	65
70.29	64.8	50	27	80	70
58.1	38.7	57.5	27.5	75	65
46.84	38.4	25	22.5	67.5	60
50.45	58.5	25	30	65	90
55.97	38.3	25	35	57.5	50
55.38	81.6	125	82.5	55	80
48.41	69.9	145	75	40	55
75.62	42.2	100	70	75	90
39.87	48.8	100	65	75	90
25.56	47.2	35	65.5	62.5	75
61.57	35.6	55	50	52.5	90
46.56	31	52	30	70	65
30.56	22.9	40	47.5	50	90
62.37	28.1	57	50	40	75

Vessel lumen diameter radial μm

D9.128.2	D9.012	D9.016	D9.096	D9.053.1	D9.020	D9.018	D9.027	D9.023	D9.019.1
50	70	110	75	125	75	130	105	123	70
35	47.5	142.5	55	27.5	62.5	120	102	97.5	127.5
60	42.5	185	100	32.5	65	147.5	97.5	43	82.5
47.5	57.5	145	40	102	50	95	110	80	70
50	45	140	87.5	85	62.5	120	66	77	72.5
47.5	47.5	112.5	135	112	80	70	46	87.5	42.5
47.5	45	60	115	112.5	65	67.5	87.5	83	85
50	45	67.5	107.5	65	70	80	46	73	87.5
55	35	75	85	40	70	150	46	67.5	42.5
57.5	35	82.5	95	40	50	120	47.5	105	50
52.5	90	47.5	35	40	55	155	43	62	40
62.5	77.7	147	35	55	45	155	42.5	45	137.5
62.5	45	140	175	55	80	150	42.5	49	115
55	77.5	120	75	40	100	95	32	50	125
55	50	140	57.5	177.5	70	100	26	80	35
52.5	55	60	45	42.5	42.5	130	35	62	82.5
60	27.5	67.5	35	25	35	115	25	57	60
70	110	55	117.5	20	65	117.5	46	47	75
55	125	45	140	25	75	105	29	61	32.5
47.5	55	145	125	107.5	45	107.5	17.5	56	47.5
52.5	87.5	87.5	95	82.5	75	82.5	25	80	127.5
47.5	82.5	130	55	80	65	117.5	29	100	52.5
57.5	75	87.5	35	85	72.5	120	30	65	90
60	50	115	80	130	52.5	45	20	93.25	67.5
60	32.5	100	62.5	27.5	60	162.5	12	87.5	57.5

D9.128.2	D9.012	D9.016	D9.096	D9.053.1	D9.020	D9.018	D9.027	D9.023	D9.019.1
80	67.5	182.5	40	90	65	90	120	60	80.112
57.5	97.5	125	85	130	55	145	122	62	38.06
65	45	100	77.5	140	65	50	90	82	85.2
55	60	150	92.5	112	45	117.5	87	62	39.7
42.5	32.5	140	87.5	57.5	50	45	37	65	32.1
50	45	165	102.5	55	62.5	155	35	67	81.8
40	75	155	85	62.5	70	135	100	32.5	73.2
50	72.5	65	65	105	40	130	98	40	95.2
45	52.5	120	142.5	62.5	52.5	105	165	15	104.3
47.5	27.5	80	105	45	42.5	77.5	60	95	82.7
55	55	75	155	122.5	35	145	60	87.5	68
57.5	50	107.5	102	72.5	75	127.5	76.5	87.5	53.018
47.5	32.5	135	45	105	35	125	42	87.5	55.84
45	25	85	52.5	67.5	65	117.5	37	60	50
45	35	112	72.5	37.5	47.5	172.5	29	58.25	39.3
60	100	102.5	80	40	57.5	105	165	52.5	20.8
62.5	52.5	125	105	120	67.5	65	30.2	32	49.45
60	120	130	87.5	67.5	62.5	45	26	39.26	57.6
50	65	65	80	95	62.5	115	26.3	82.3	42.3
55	60	65	95	92.5	40	82.5	90.3	40.6	25.56
40	60	137.5	80	97.5	55	110	94.7	95.3	32.5
40	47.5	140	95	87.5	70	105	78.5	53.6	27.3
55	62.5	80	52.5	72.5	70	75	62.5	47	26.8
45	125	37.5	90	35	77.5	45	67.6	81.12	25.02
62.5	85	120	65	45	45	62.5	37.8	33.7	32.99

D9.095.1	D9.089	D9.107	D9.110	D9.054.1	D9.105.1	D9.040.1	D9.021.1
157.5	55	77.5	115	72.5	105	50	90
115	62.5	85	55	80	120	52.5	65
170	62.5	92.5	45	60	115	37.5	55
70	67	52.5	52.5	150	110	10	95
102.5	57	72.5	65	125	80	75	85
105	55	57.5	35	90	75	47.5	105
50	55	60	30	85	130	70	95
60	50	60	40	72.5	120	55	70
75	52	60	30	115	137	62.5	55
52.5	50	60	40	97.5	112.5	50	70
82.5	32	90	105	52.5	65	60	40
172.5	35	90	105	87.5	125	42.5	60
115	37	82.5	32.5	85	82.5	35	55
62.5	30	82.5	105	82.5	72.5	45	55
57.5	35	30	35	80	50	50	75
62.5	15	102.5	57.5	100	52.5	87.5	55
90	47	80	35	157.5	90	57.5	115
47.5	57	87.5	35	142.5	80	40	85
100	75	77.5	30	110	120	60	90
135	75	90	87.5	115	117.5	75	50
77.5	67	55	60	110	70	55	55
165	80	50	40	77.5	80	70	50
140	67	105	27.5	75	70	70	70
162.5	50	67.5	44	60	182.5	65	72.5
120	55	82.5	52.5	140	82.5	25	70
60.32		80.6	27.5	110	63.61		85.68

D9.095.1	D9.089	D9.107	D9.110	D9.054.1	D9.105.1	D9.040.1	D9.021.1
49.3		77.8	142.5	77.5	41.8		81.06
41.7		86.6	90	75	62.23		77.1
91.7		87.2	70	125	85.8		96.57
84.64		21.5	52.5	110	65.41		87.99
165.8		59.4	55	115	48.89		59.89
146.1		86.2	45	85	61.67		103.14
122.1		33.8	27.5	100	72.52		87.4
149.2		40.7	62.5	105	83.47		94.79
67.65		54.6	110	130	74.44		71.73
52.06		83.4	70	75	126.9		61.18
83.95		56.7	60	115	103.8		51.59
78.49		41	127.5	97.5	92.24		97.03
48.4		43.6	67.5	75	74.24		30.26
120.9		30.93	57.5	80	22.31		84.36
130.4		38.3	57.5	100	29.58		80.18
70.6		41.7	39.66	94.8	57.2		78.2
187.4		26.9	28.16	113.5	58.9		49.38
177.8		44.7	40.79	113.5	48.8		70.64
127.5		50.6	49.86	115.8	52.86		95.46
42.9		28.9	74.59	143	60		57.69
58.4		24.1	52.26	93.4	45.7		80.7
90.5		61.2	37.48	86.2	39.4		85
75.4		132.12	63.71	112	31.3		100.4
129.4		54.18	31.5	142.9	17.9		62.5

D9.091.1	D9.011.2	D9.128.3	D9.130.1	D9.157.3
65	52.5	145.9	40	110
90	50	107.7	52.5	75
75	55	52.7	62.5	105
82.5	85	67.2	62.5	100
67.5	60	61	62.5	95
65	55	61	50	75
75	65	22.96	85	85
50	55	21	100	55
95	35	21	80	165
100	225	16.9	50	125
85	117.5	160.8	75	65
90	150	82.5	85	50
82.5	30	23.11	70	90
60	40	50	75	60
90	225	123	52.5	85
85	247	80	100	80
80	205	50	75	95
80	240	42.5	40	62.5
90	80	25	65	45
75	65	40	85	55
65	50	75	75	90
60	140	75	95	80
90	40	62.5	70	75
80	50	65	80	75
90	130	60	65	75

D9.091.1	D9.011.2	D9.128.3	D9.130.1	D9.157.3
78.7	50	32.5	80	55
88.5	60	70	65	75
81.1	75	27.5	80	75
80.4	145	25	67.5	75
62.8	40	45	95	100
73.9	60	20	90	55
64.7	55	50	67.5	70
71.31	145	50	57.5	55
65.46	70	55	70	110
86.9	55	60	40	42.5
72.5	55	55	80	62.5
71.21	25	47.5	50	100
91.71	35	27.5	50	75
78.5	115	30	40	95
73.9	212	20	70	75
58.7	140	25	65	90
53.3	120	45	65	75
83.7	25	15	62.5	90
58.9	40	105	60	100
43.6	45	102.5	60	95
33.4	30	80	85	130
43.02	50	77.5	100	60
44.73	65	70	62.5	75
35.9	130	40	65	105
62.8	40	30	95	100

Appendix c

Growth ring conifers

	D9.019.2	D9.036.1	D9.112.1	D9.059.1	D9.193	D9.111	D9.098	D9.153.1	D9.022
1	1060	1170	800	340	N/A due to preservation	1100	1800	860	620
2	2500	1800	600	410		920	1842	800	360
3	850	1080	520	300		920	1460	450	570
4	550	980	700	240		400	1340	600	420
5	850	1460	900	430		360	1360	340	400
6	400	1060	1040	250		520	860	300	280
7	380	1290	1300	150		260	1118	240	260
8	400	1460	1160	150		360	940	250	400
9	260	1400	1500	530		320	1240	250	600
10	220	1140	780	150		240	800	220	450
11	265	1760	1400	120		160	465	370	460
12	260	1580	1120	370		100	300	250	300
13	400	1800	1700	170		80	280	200	330
14	540		1320	190		160	460	270	X
15	500		800	440		140	920	300	230
16	620		1500	310		160	720	200	230
17	360		1500	160		280	810	300	280
18	560		1600	390		240	820	420	210
19	745		1400	230		320	640	400	450
20	700		900	220		160	610	440	200
21	820		760	220		160	1140	310	250
22	880		1000	140		220	940	210	380
23	700		440	360		360	1540	200	300
24	720		1600	370		200	1420	140	100
25	680		1100	340		120	1600	500	190
26	450		720	510		60	1840	450	300
27	680		900	380		120	1000	310	700
28	600		640	320		160	1500	350	
29	760		570	260		360	1800	680	
30	690		680	350		380	1500	370	
31	1100		620	220		120	2180	420	
32	1140		700	200		220	1300	500	

D9.094.1	D9.161.1	D9.139.1	D9.050.1	D9.118.1	D9.092.1	D9.109.1
1085	2300	870	1050	3350	2000	300
820	x	620	600	3700	1190	300
1450	2170	1000	800	3990	1250 p	690
2300	1530	1000	840	4080	x	250
1520	x	1450	f	3050	1240	700
1350	1830	950	1500	3200	1220	260
1710	2200	520	1610	3820	1250	230
1450	1720	600	1450	3235	1300	650
1360	1600	730	x	2000	1620	160
1620	1970	1200	200	1800	1400	260
1530	2500	700	450	2560	1600	300
1160	1780	1450	560	2180	2000	400
1330	2050	640	590	1500	2030	240
1630		1400	540	1000	1700	1200
1520		490	470	1130	1600	520
1500		1300	500	1650	2030	780
1350		920	500	1500	2150	x
1140		1500	220	2500	1500	1100
1150		740	540	2830		780
770		230	460	1900		bad preservation
840		870	630	1700		506.6666667
850		620	300	2020		
930		500	500	1600		
1110		760	280	2300		
1600		510	250	2100		
1650		800	190			
		400	x			
		410	150			
		100	250			

D9.094.1	D9.161.1	D9.139.1	D9.050.1	D9.118.1	D9.092.1	D9.109.1
		720	120			
		450	200			
			280			
			290			
			100			
			110			
			110			
			x			
			200			
			180			
			260			
			210			
			x			
			x			
			x			
			200			
			400			
			400			
			420			
			340			
			140			
			250			
			200			
			140			
			230			
			200			
			270			
			120			
			100			
			250			

D9.050.1	D9.050.1	D9.118.1	D9.092.1	D9.109.1	D9.168.1	D9.038.1
170	100	3350	2000	300	800	5650
240	240	3700	1190	300	1400	3430
340	390	3990	1250 p	690	780	2000
290	160	4080	x	250	350	1330
420	450	3050	1240	700	x	1450
350	450	3200	1220	260	350	2160
1305	330	3820	1250	230	900	1380
600	510	3235	1300	650	700	1450
780	550	2000	1620	160	1400	1020
900	290	1800	1400	260	2400	380
600	840	2560	1600	300	400	
830	250	2180	2000	400	900	
x	560	1500	2030	240	1850	
560	480	1000	1700	1200	1250	
260	500	1130	1600	520	250	
350	200	1650	2030	780	1250	
510	230	1500	2150	x	750	
670	200	2500	1500	1100	430	
670	260	2830		780	x	
x	270	1900		bad preservation	x	
280	370	1700			1120	
270	400	2020			950	
400	430	1600			280	
300		2300			850	
400		2100			600	
360					x	
x						
250						
110						
130						
240						
240						
250						
200						
240						
220						
240						
100						

D9.093.1	D9.044.1	D9.090.1	D9.181.1
1280	2800	n/a	x
1180	3200		620
790	4650		550
1570	5230		550
1270	3700		a number of rings couldn't be measured
1400	2200		300
1540	1100		300
690	1650		400
870			
1030			
700			
590			
500			
330			
470			
240			
400			
420			
370			
530			
400			
320			
450			
400			
410			
370p			
240			
170			
260			
250			
preservation			

D9.128.2	D9.110.1	D9.054.1	D9.040.1	D9.041.1	D9.021.1	D9.011.2	D9.128.3	D9.012.1	D9.96.1	D9.105.1
n/a preservation	1290	7950	4870	n/a	n/a	2450	7800	1810	2600	4100
	1940	7600	2850			2600	n/a	1440	4400	4190
	1700	5650	3400			n/a		1600	4100	n/a
	2710	6500	900					1250	x	
	1200	bad preservation	1500					1290	4690	
	1150		850					2020	3450	
	1560							1650	5950	
	1050							1700	5900	
	1250							1800		
	880							1950		
	1370							5050		
	1850							1600		
	2500							1240		
	2480							2040		
	1590							1800		
	1000							1700		
	1100							3850		
	980							1750		

Vessel groups

D9.012.1	D9.128.2	D9.096.1	D9.016.1	D9.053.1	D9.020.1	D9.018.1	D9.021.1	D9.091.1	d9.011.2
2	2	8	4	5	1	1	1	1	2
3	1	2	1	4	1	2	1	1	2
2	1	1	1	3	1	1	2	1	1
1	1	1	2	1	1	1	2	1	1
1	1	1	3	1	1	1	2	1	3
2	1	2	5	1	1	1	1	1	1
2	1	2	3	1	1	1	3	1	1
1	1	3	2	1	1	1	3	2	1
1	1	1	1	2	1	1	2	1	2
1	1	1	1	2	1	2	1	1	1
3	2	1	1	4	1	2	1	1	1
3	1	2	1	3	1	2	3	2	1
1	1	2	1	2	1	1	1	2	1
1	1	4	2	3	1	1	1	2	2
1	1	2	1	1	2	1	1	2	2
2	2	1	1	1	2	1	2	2	3
2	1	4	1	1	1	2	2	1	1
4	1	1	2	1	1	2	1	1	3
2	1	1	1	1	1	1	1	1	4
3	1	2	1	1	1	2	1	1	1
3	1	2	3	2	3	2	2	1	1
1	1	1	4	2	3	1	1	1	2
2	1	1	1	4	2	1	1	3	1
1	1	1	3	5	2	1	2	3	3
2	1	2	2	3	1	2	1	1	1

D9.027.1	D9.023.1	D9.019.1	D9.095.1	D9.089.1	D9.107.1	D9.105.1	D9.110.1
5	1	1	2	4	1	1	2
3	1	1	2	4	1	1	2
2	1	1	5	4	1	1	1
2	1	2	3	2	2	1	1
1	1	2	3	2	3	1	1
1	1	1	2	1	5	6	1
1	2	1	1	1	2	3	1
1	3	1	1	1	2	2	1
4	5	1	1	2	1	3	1
2	3	1	1	1	1	2	1
3	3	2	1	1	1	1	1
1	3	2	4	1	1	1	2
1	1	3	3	1	2	1	2
1	1	1	1	2	1	2	3
1	1	1	1	2	1	2	1
3	1	2	1	2	3	2	1
4	1	4	1	4	1	4	1
3	6	2	1	3	1	1	1
2	4	2	2	3	1	1	4
2	3	2	2	3	1	3	2
2	5	2	2	2	2	2	2
2	1	2	2	2	3	1	2
2	1	1	2	1	1	1	4
3	1	1	1	1	1	1	2
3	2	1	1	1	1	1	1

D9.054.1	D9.040.1	D9.128.1	D9.130.1	D9.157.3
1	3		6	2
1	3		5	2
1	2		4	1
2	5		4	1
3	5		1	2
2	4		1	1
1	7		1	1
1	2		1	2
1	3		2	1
1	4		2	3
1	5		4	3
1	5		1	2
2	6		1	1
2	8		3	1
2	5		1	1
2	3		1	1
1	5		1	1
1	5		1	1
1	2		1	3
1	3		1	3
1	5		2	2
1	5		5	1
1	5		2	2
1	3		2	1
1	7		1	1

Specific Gravity

Specimen number	SG1	SG2	SG3	SG4	SG5	SG6	SG7	Mean	
D9.012.1 (a)	0.672	0.4725	0.63	0.378	0.64	0.5775	0.4935	0.551929	0.56
D9.018.1	0.6405	0.357	0.4305	0.4935	0.5355	0.4725	0.567	0.4995	0.5
D9.020.1	0.651	0.756	0.4935	0.651	0.525	0.63	0.693	0.6285	0.63
D9.036.1	0.7455	0.7665	0.8085	0.861	0.7875	0.714	0.6825	0.7665	0.77
D9.050.1	0.9555	0.651	0.63	0.525	0.6615	0.567	0.6405	0.6615	0.67
D9.059.1	0.6405	0.63	0.714	0.714	0.693	0.588	0.735	0.6735	0.68
D9.096.1	0.609	0.7035	0.7035	0.6405	0.525	0.567	0.63	0.6255	0.63
D9.098.1	0.8295	0.777	0.7035	0.525	0.5985	0.819	0.777	0.7185	0.72
D9.111.1	0.7665	0.798	0.756	0.7875	0.7665	0.714	0.651	0.7485	0.75
D9.112.1	0.672	0.8715	0.84	0.819	0.8925	0.798	0.7035	0.7995	0.8
D9.019.1	0.546	0.3675	0.798	0.651	0.3885	0.357	0.4095	0.5025	0.51
D9.022.1	0.5775	0.7665	0.5565	0.63	0.84	0.7455	0.6195	0.6765	0.68
D9.019.2	0.693	0.7455	0.6825	0.819	0.8295	0.6615	0.7875	0.7455	0.75
D9.023.1	0.7245	0.5145	0.6195	0.609	0.5775	0.483	0.588	0.588	0.59
D9.027.1	0.525	0.651	0.7455	0.546	n/a	0.616875	0.62	0.617396	0.62
D9.038.1	0.63	0.9135	0.798	0.798	0.7245	0.651	0.9135	0.7755	0.78
D9.090.1	0.5985	0.588	0.4095	0.777	0.693	0.6195	0.693	0.6255	0.63
D9.091.1	0.588	0.546	0.672	0.651	0.672	0.525	0.5985	0.6075	0.61
D9.093.1	0.735	0.7455	0.735	0.7245	0.714	0.714	0.8925	0.7515	0.76
D9.094.1	0.8085	0.903	0.882	0.693	0.819	0.7455	0.7035	0.7935	0.8
D9.105	0.7665	0.672	0.8505	0.7875	0.693	0.63	0.504	0.7005	0.71
D9.110.1	0.5775	0.504	0.525	0.6405	0.567	0.609	0.651	0.582	0.59
D9.118.1	0.63	0.84	0.4935	0.8715	0.567	0.651	0.588	0.663	0.67
D9.153.1	0.6615	0.5775	0.735	0.4725	0.777	0.4515	0.462	0.591	0.6
D9.043.1	0.6405	0.4305	0.4305	0.567	0.546	0.693	0.55125	0.56	

